U.S. NAVAL TEST PILOT SCHOOL
FLIGHT TEST MANUAL

USNTPS-FTM-NO. 108
(PRELIMINARY)

FIXED WING PERFORMANCE

Written By:

GERALD L. GALLAGHER, LARRY B. HIGGINS,

LEROY A. KHINOO, and PETER W. PIERCE

Provided By:

Veda Incorporated
Contract N00421-90-C-0022

30 September 1992

TABLE OF CONTENTS

CHAPTER 1

INTRODUCTION

CHAPTER 1

TABLES

CHAPTER 1

INTRODUCTION

1.1 WHY PERFORMANCE FLIGHT TESTING

Aircraft performance generally can be defined as the flight maneuvers an aircraft must execute for successful mission accomplishment. Expected performance parameters must be an integral part of the aircraft design process. Given the user's performance expectations, the designer makes decisions regarding wing loading, power plant selection, airfoil selection, planform configuration, and other design considerations. All of these help tailor the design to give the aircraft the desired performance characteristics.

Actual aircraft performance characteristics are not always the same as the design or the predicted performance characteristics. Therefore, there is a need for performance flight testing to determine the actual performance. Performance flight testing is defined as the process of determining aircraft performance characteristics, or evaluating the energy gaining and losing capability of the aircraft. Determining aircraft performance depends upon fundamental knowledge in several disciplines including: atmospheric science; fluid dynamics; thermodynamics; subsonic aerodynamics; and supersonic aerodynamics. Performance measurement requires knowledge of the propulsion system characteristics of the aircraft. The flight test team must be familiar with the theory and operation of turbine engines, reciprocating engines, and propeller theory. They must understand the basic measurements, instrumentation techniques, and equipment to gather the data needed to determine the various elements of an aircraft's performance. The team uses these disciplines to form the basis for the flight test methods and techniques for performance flight testing.

Using appropriate test methods and techniques, the flight test team begins to answer questions about the aircraft's predicted or actual performance such as:

1. How fast will the aircraft fly?
2. How high will the aircraft fly?
3. How far and/or how long will the aircraft fly on a load of fuel?
4. How much payload can the aircraft carry?
5. How long a runway is required for takeoff and landing?

6. How fast will the aircraft climb?
7. How expensive is the aircraft to operate?
8. What is the aircraft's maximum sustained turn rate?

The results of performance flight testing are used for several purposes:

1. Determine mission suitability of the aircraft.
2. Determine if the aircraft meets specific contractual performance guarantees, or performance requirements as specified in the user generated requirements.
3. Provide data to construct aircraft flight manuals for use by operational aircrews.
4. Determine techniques and procedures for use by operational aircrews to attain optimum aircraft performance.
5. Determine an aircraft’s agility as measured by specific excess power and maneuverability.
6. Obtain research information to advance aeronautical science or to develop new flight test techniques.

1.2 FLIGHT TEST MANUAL OBJECTIVE

The objective of the Fixed Wing Performance Flight Test Manual (FTM) is to serve as a practical reference guide for planning, executing, and reporting fixed wing performance flight testing. The FTM is intended for use as a primary instructional tool at the U.S. Naval Test Pilot School (USNTPS) and as a reference document for those conducting fixed wing flight testing at the Naval Air Warfare Center Aircraft Division Center (NAVAIRWARCENACDIV) or similar organizations interested in fixed wing flight testing. It is not a substitute for fixed wing performance textbooks. Rather, the FTM summarizes applicable theory to facilitate an understanding of the concepts, techniques, and procedures involved in successful flight testing. The FTM is directed to test pilots and flight test engineers (FTE); it deals with the more practical and prominent aspects of performance issues, sometimes sacrificing exactness or completeness in the interest of clarity and brevity.

The FTM does not replace the Naval Air Test Center *Report Writing Handbook*. The FTM contains examples of performance parameters discussed in narrative and graphic format. It contains discussions of the effect various performance parameters have on mission performance and suitability, and a discussion of specification compliance where applicable. The examples in this manual show trends extracted from current aircraft and are in the format used at USNTPS.

Since this FTM is a text for USNTPS, it contains information relative to operations at USNTPS and NAVAIRWARCENACDIV; however, it does not contain information relative to the scope of a particular USNTPS syllabus exercise or to the reporting requirements for a particular exercise. Details of each flight exercise vary from time to time as resources and personnel change and are briefed separately to each class.

1.3 FLIGHT TEST MANUAL ORGANIZATION

1.3.1 MANUAL ORGANIZATION

The FTM is organized to simplify access to desired information. Although there is some cross referencing, in general, each chapter stands as a distinct unit. Discussions of flight test techniques are presented together with pertinent background analytic presentations. Most of the discussion applies to fixed wing aircraft in general; with specific examples given where appropriate. The contents are organized in a classical grouping and follow the chronology of the performance syllabus at USNTPS.

Chapter 1, Introduction, is an overview of the FTM including the objectives of performance testing, flight test conditions and pilot technique, and use of confidence levels.

Chapter 2, Pitot Static System Performance, deals with determining true airspeed (V_T), calibrated pressure altitude (H_{P_c}), airspeed position error (ΔV_{pos}), altimeter position error (ΔH_{pos}), Mach number (M), and probe temperature recovery factor (K_T). Tower fly-by, paced, measured course, space positioning, smoke trail, trailing source, and radar altimeter test methods are discussed.

Chapter 3, Stall Speed Determination, deals with determining stall speed in the takeoff and landing configurations. The variation in indicated stall speed as a function of gross weight is discussed. Determining calibrated stall speed is discussed.

Chapter 4, Level Flight Performance, examines the concepts of thrust and fuel flow required for jet aircraft, and power required for propeller driven aircraft. Range and endurance are determined. The constant weight to pressure ratio method (W/δ) is emphasized.

Chapter 5, Excess Power Characteristics, deals with determining the specific excess power (P_S) characteristics of an aircraft. The level acceleration method is emphasized.

Chapter 6, Turn Performance and Agility, is concerned with sustained and instantaneous turning performance as measures of maneuverability. Sustained turning performance load factors, turn rates, and turn radii are discussed as well as instantaneous turning performance at onset, tracking, and limit buffet levels. Steady turns, windup turns, and loaded level acceleration methods are discussed.

Chapter 7, Climb Performance, examines verification of climb schedules and combat ceiling requirements. Determining climb schedules from acceleration data and the sawtooth climb method are discussed.

Chapter 8, Descent Performance, discusses verification of descent performance in relation to airspeed, angle of attack, time and fuel used for minimum rate of descent from altitude. The sawtooth descent method is emphasized.

Chapter 9, Takeoff And Landing Performance, is concerned with takeoff performance, landing performance, and short takeoff and landing (STOL) performance. Corrections to standard conditions for wind, runway slope, thrust, weight, and density are considered, as well as pilot technique.

Chapter 10, Standard Mission Profiles, presents aircraft standard mission profiles for use in evaluating performance characteristics in a simulated mission environment.

1.3.2 CHAPTER ORGANIZATION

Each chapter has the same internal organization where possible. Following the chapter introduction, the second section gives the purpose of the test. The third section is a review of the applicable theory. The fourth discusses the test methods and techniques, data requirements, and safety precautions applicable to those methods. The fifth section discusses data reduction and the sixth pertains to data analysis. The seventh section covers relevant mission suitability aspects of the performance parameters. The eighth section discusses specification compliance. The ninth is a glossary of terms used in the chapter. Finally, the tenth section lists applicable references.

1.4 EFFECTIVE TEST PLANNING

To plan a test program effectively, sound understanding of the theoretical background for the tests being performed is necessary. This knowledge helps the test team establish the optimum scope of tests, choose appropriate test techniques and data reduction methods, and present the test results effectively. Because time and money are scarce resources, test data should be obtained with a minimum expenditure of both. Proper application of theory ensures the tests are performed at the proper conditions, with appropriate techniques, and using efficient data reduction methods.

1.5 RESPONSIBILITIES OF TEST PILOT AND FLIGHT TEST ENGINEER

Almost every flight test team is composed of one or more test pilots and one or more project engineers. Team members bring together the necessary expertise in qualitative testing and quantitative evaluation. To perform the necessary tests and evaluations, the test pilot must know the applicable theory, test methods, data requirements, data analysis, instrumentation, and specifications. The flight test engineer must possess a thorough knowledge of the pilot tasks required for mission performance in order to participate fully in the planning and execution of the test program.

1.5.1 THE TEST PILOT

The test pilot is proficient in the required flight skills to obtain accurate data. The pilot has well developed observation and perception powers to recognize problems and adverse characteristics. The pilot has the ability to analyze test results, understand them, and explain the significance of the findings. To fulfill these expectations, the pilot must possess a sound knowledge of:

1. The test aircraft and fixed wing aircraft in general.
2. The total mission of the aircraft and the individual tasks required to accomplish the mission.
3. Theory and associated test techniques required for qualitative and quantitative testing.
4. Specifications relevant to the test program.
5. Technical report writing.

The test pilot understands the test aircraft in detail. The pilot considers the effects of external configuration on aircraft performance. The test pilot should have flight experience in many different types of aircraft. By observing diverse characteristics exhibited by a variety of aircraft, the test pilot can make accurate and precise assessments of design concepts. Further, by flying many different types, the pilot develops adaptability. When flight test time is limited by monetary and time considerations, the ability to adapt is invaluable.

The test pilot clearly understands the aircraft mission. The test pilot knows the specific operational requirements the design was based on, the detail specification, and other planning documents. Knowledge of the individual pilot tasks required for total mission accomplishment is derived from recent operational experience. Additionally, the pilot can gain knowledge of the individual pilot tasks from talking with other pilots, studying operational and tactical manuals, and visiting replacement pilot training squadrons.

An engineering test pilot executes a flight test task and evaluates the validity of the results to determine whether the test needs to be repeated. Often the test pilot is the best judge of an invalid test point and can save the test team wasted effort. The test pilot's knowledge of theory, test techniques, relevant specifications, and technical report writing may be gained through formal education or practical experience. An effective and efficient method is through formal study with practical application at an established test pilot school. This education provides a common ground for the test pilot and FTE to converse in technical terms concerning aircraft performance and its impact on mission suitability.

1.5.2 THE FLIGHT TEST ENGINEER

The FTE has general knowledge of the same items for which the test pilot is mainly responsible. Additionally, the FTE possesses sound knowledge of:

1. Instrumentation requirements.
2. Planning and coordination aspects of the flight test program.
3. Data acquisition, reduction, and presentation.
4. Technical report writing.

These skills are necessary for the FTE to form an efficient team with the test pilot for the planning, executing, analyzing, and reporting process.

Normally, the FTE is responsible for determining the test instrumentation. This involves determining the ranges, sensitivities, frequency response required, and developing an instrumentation specification or planning document. The FTE coordinates the instrumentation requirements with the instrumentation engineers who are responsible for the design, fabrication, installation, calibration, and maintenance of the flight test instrumentation.

The FTE is in the best position to coordinate all aspects of the program because he or she does not fly in the test aircraft often and is available in the project office. The coordination involves aiding in the preparation and revision of the test plan and coordinating the order of the flights. Normally, the FTE prepares all test flight cards and participates in all flight briefings and debriefings.

A great deal of the engineer's time is spent working with flight and ground test data. The FTE reviews preliminary data from wind tunnel studies and existing flight tests. From this data, critical areas may be determined prior to military flight testing. During the flight tests, the engineer monitors and aids in the acquisition of data through telemetry facilities and radio, or by flying in the test aircraft. Following completion of flight tests, the engineer coordinates data reduction, data analysis, and data presentation.

The FTE uses knowledge of technical report writing to participate in the preparation of the report. Usually, the FTE and the test pilot proofread the entire manuscript.

1.6 PERFORMANCE SYLLABUS

1.6.1 OVERVIEW

The performance syllabus at USNTPS consists of academic instruction, flight briefings, demonstration flights, practice flights, exercise flights, flight reports, and evaluation flights. The performance phase of instruction concludes with an individual evaluation flight and a group Navy Technical Evaluation (NTE) formal oral presentation. The final exercise at USNTPS is a simulated Navy Developmental Test IIA (DT IIA). This exercise incorporates all the performance, stability, control, flying qualities, and airborne systems instruction into the total evaluation of an airborne weapon system.

The performance syllabus includes exercises in performance demonstration; performance practice; pitot static system performance; range and endurance performance; specific excess energy; climb, descent, takeoff, and landing performance; and turn performance. The syllabus is presented in a step-by-step, building block approach allowing concentration on specific objectives and fundamentals. This approach focuses on individual flight characteristics at the expense of evaluating the total weapon system. Progress through the syllabus is toward the end objective, the evaluation of the aircraft as a weapon system in the mission environment. The details of the current syllabus are contained in *U.S. Naval Test Pilot School Notice 1542*.

1.6.2 USNTPS APPROACH TO PERFORMANCE TESTING

The USNTPS provides an in-service aircraft for performance testing; and although the aircraft is not a new one, the USNTPS assumes it has not been evaluated by the Navy. The syllabus assumes a DT IIA was not conducted and USNTPS is designated to conduct a Navy Technical Evaluation for aircraft performance. The aircraft is assumed designated for present day use. Stability and control, weapons delivery, and other testing is assumed to be assigned to other directorates of NAVAIRWARCENACDIV. The student is charged with the responsibility of testing and reporting on the engine and airframe performance characteristics of the syllabus aircraft.

Mission suitability is an important phrase at NAVAIRWARCENACDIV, and its importance is reflected in the theme of flight testing at USNTPS. The fact an aircraft meets the requirements of pertinent Military Specifications is of secondary importance if any performance characteristic degrades the airplane's operational capability. The mission of each aircraft is discussed and students conclude whether or not the performance characteristics they evaluate are suitable for the intended mission. This conclusion is supported by a logical discussion and analysis of qualitative and quantitative observations, drawing on recent fleet experience.

The evaluation of aircraft performance for comparison to specification requirements, contract guarantees, or other airplanes require accurate quantitative data. At USNTPS, every effort is made to test under ideal weather conditions with all sensitive instrumentation operational; however, problems may arise occasionally which cause errors in the data. If bad weather, instrumentation failure, or other factors result in large errors or excessive data scatter, the student critiques the data; and if warranted, the flight is reflown. Precisely accurate data are not required before the data are presented in a student report. However, it is important to know if errors in the data exist and their effect on the results. The primary purpose of the performance syllabus at USNTPS is learning proper flight test techniques and the basic supporting theory.

1.6.3 FLIGHT BRIEFINGS

Printed and oral flight briefings are presented by the principal instructor for each exercise. The flight briefing gives specific details of the exercise and covers the objective, purpose, references, scope of test, method of test, test planning, and report requirements. The briefing also covers the applicable safety requirements for the exercise as well as administrative and support requirements.

1.6.4 DEMONSTRATION FLIGHTS

Demonstration flights are preceded by thorough briefings including: theory, test techniques, analysis of test results in terms of mission accomplishment and specification requirements, and data presentation methods. In flight, the instructor demonstrates test techniques, use of special instrumentation, and data recording procedures. After observing each technique, the student has the opportunity to practice until attaining reasonable proficiency. Throughout the demonstration flight, the instructor discusses the significance of each test, implications of results, and variations in the test techniques appropriate for other type aircraft. Students are encouraged to ask questions during the flight as many points are explained or demonstrated easier in flight than on the ground. A thorough post flight discussion between instructor and students completes the demonstration flight. During the debrief, the data obtained in flight are plotted and analyzed.

1.6.5 PRACTICE FLIGHTS

Each student is afforded the opportunity to practice the test methods and techniques in flight after the demonstration flight and prior to the exercise or data flight. The purpose of the practice flight is to gain proficiency in the test techniques, data acquisition, and crew coordination necessary for safe and efficient flight testing.

1.6.6 EXERCISE FLIGHTS

Each student usually flies one flight as part of each exercise. The student plans the flight, has the plan approved, and flies the flight in accordance with the plan. The purpose of the flight is to gather qualitative and quantitative data as part of an overall performance evaluation. The primary in flight objective is safe and efficient flight testing. Under no circumstances is flight safety compromised.

1.6.7 REPORTS

A fundamental purpose of USNTPS is to assist the test pilot/FTE team to develop their ability to report test results in clear, concise, unambiguous technical terms. After completing the exercise flight, the student reduces the data, and analyzes the data for mission suitability and specification compliance. The data are presented in the proper format and a report is prepared. The report process combines factual data gathered from ground and flight tests and analysis of its effect on mission suitability. The report conclusions answers the questions implicit in the purpose of the test.

1.6.8 PROGRESS EVALUATION FLIGHT

The progress evaluation flight is an evaluation exercise and an instructional flight. It is a graded check flight on the phase of study just completed. The flight crew consists of one student and one instructor. The student develops a flight plan considering a real or simulated aircraft mission and appropriate specification requirements. The student conducts the flight briefing, including the mission, discussion of test techniques, and specification requirements.

As the student demonstrates knowledge of test techniques in flight, the student is expected to comment on the impact of the results on the real or simulated mission. The instructor may comment on validity of the results obtained, errors or omissions in test procedures, and demonstrate variations in test techniques not introduced previously.

During the debrief the student presents, analyzes, and discusses the test results. The discussion includes the influence of the results on aircraft mission suitability.

1.7 PERFORMANCE FLIGHT TEST CONDITIONS AND PILOT TECHNIQUES

1.7.1 ATTITUDE FLYING

In flight test, attitude flying is absolutely essential. Under a given set of conditions (altitude, power setting, center of gravity), the aircraft airspeed is entirely dependent upon its attitude. The pilot's ability to fly the aircraft accurately depends upon the ability to see and interpret small attitude changes. This is best done by reference to the outside horizon. Any change in aircraft attitude is noticed by reference to the visual horizon long before the aircraft instruments show a change. Thus, it is often possible to change the attitude of the aircraft from a disturbed position back to the required position before the airspeed has changed. The outside horizon is useful as a rate instrument. For example if a stabilized point is required, the pilot holds zero pitch rate by holding aircraft attitude fixed in relation to an outside reference. If, as in acceleration run, the airspeed is continuously increasing or decreasing, the pilot makes a steady, smooth, and slow change in aircraft attitude.

The method of lining up a particular spot on the aircraft with an outside reference can be useful, but may waste time. Often, a general impression is all that is necessary. The pilot can see the pitch rate is zero by using peripheral vision while also glancing at the airspeed indicator or other cockpit instruments. As soon a pitch rate is noted, the pilot can make proper control movements to correct the aircraft attitude. The pilot must maintain situational awareness at all times during the flight.

If necessary to stabilize on an airspeed several knots from the existing airspeed, time can be saved by overshooting the required pitch attitude and using the rate of airspeed change as an indication of when to raise or lower the nose to the required position. A little practice allows the pilot to stabilize at a new airspeed with a minimum amount of airspeed overshoot in the least time.

1.7.2 TRIM SHOTS

Hands off, zero control force, steady trim conditions are required for stable test points. The point where all forces and moments are stabilized with a zero control force is a trim shot or trim point.

Normal attitude flying techniques are used for coarse adjustments to stabilize and trim at a particular speed or Mach number at a constant altitude. Stable equilibrium or unstable equilibrium techniques are then employed to establish precisely the desired airspeed and altitude. Once the proper attitude and power setting are established, the force is trimmed to zero while holding the required control position. The control is released to check for a change in pitch attitude. If the attitude changes, the pilot puts the attitude back at the trim position and retrims. Lateral and directional controls are used to hold the wings level and maintain constant heading and coordinated flight. The control forces are held in order to accomplish this, then the forces are relieved by proper trim actuation. The method of moving the trim device and allowing the aircraft to seek a new attitude hands off is very time consuming and inaccurate. The pilot should hold the aircraft attitude fixed and then relieve the existing control forces by trimming.

1.7.3 TEST CONDITIONS

There are three basic test conditions at which a pilot operates an aircraft while conducting performance testing. Each test condition requires specific flight techniques and uses different primary flight instruments for pilot reference. These conditions are stable equilibrium, unstable equilibrium, and nonequilibrium. Equilibrium test conditions are present when the aircraft is stabilized at a constant attitude, airspeed and altitude. A stable equilibrium condition is a condition in which the aircraft, if disturbed, returns to its initial condition. An unstable equilibrium test point is a point from which the aircraft, if disturbed, continues to diverge. A nonequilibrium condition is a condition during which there is a change in airspeed and/or altitude.

1.7.4 STABLE EQUILIBRIUM CONDITIONS

Stable equilibrium data points are obtained in both level and turning flight when operating at airspeeds greater than the airspeed for minimum drag (stable portion of the thrust or power required curve). The test technique for obtaining stable equilibrium data is to adjust altitude first, power second, and then wait until the aircraft stabilizes at the equilibrium flight airspeed. Altitude must be maintained precisely and thrust/power must not be changed once set. If this technique is followed, a time history of airspeed is used to determine when the equilibrium data point is obtained. For most tests, when the airspeed has changed less than 2 kn in the preceding 1 minute period, an equilibrium data point is achieved. Stable equilibrium test conditions are obtained best by approaching them with excess airspeed. This approach ensures convergence, whereas an accelerating approach may converge only after fuel exhaustion. The flight test technique used in obtaining stable equilibrium conditions is called the constant altitude or front side method.

The primary parameters for pilot reference when obtaining data points under stable equilibrium conditions are altitude, vertical speed, heading for straight flight, and bank angle for turning flight. There is no substitute for a good visual horizon. In airplanes equipped with automatic flight control systems (AFCS) which incorporate attitude, altitude, and heading hold modes, stable equilibrium data points can be obtained by using these modes provided the AFCS sensitivity is adequate for the test. In straight flight, stable equilibrium conditions can be achieved by using altitude and heading hold modes. In turning flight, stable equilibrium conditions can be achieved by using altitude and attitude hold modes.

1.7.5 UNSTABLE EQUILIBRIUM CONDITIONS

Unstable equilibrium data points are more difficult to obtain and require proper technique. For the unstable equilibrium data points, indicated airspeed is held constant. Altitude, engine speed, or bank angle is adjusted as required by the test being conducted. Unstable equilibrium data points are associated with the unstable portion of the thrust or power required curve. To obtain data points under these conditions, the desired test airspeed is established first, then the throttle is adjusted to climb or descend to the desired test altitude. The vertical speed indicator is an important instrument in achieving equilibrium conditions. With throttle set, the vertical speed is stabilized while maintaining the desired test airspeed. A throttle correction is made and the new stabilized vertical speed is observed. The approximate engine speed required for level flight can be determined by correlating the values. For example, while attempting to obtain a level flight data point at 135 KIAS, the pilot determined 88% produced an 800 ft/min climb in the vicinity of the desired test altitude and 80% produced a 200 ft/min descent. The test pilot determined a 1% change represented a 125 ft/min change in vertical speed. By adjusting throttle to 81.6%, equilibrium level flight conditions are achieved. Normal pilot technique usually enables the engine to be set to within 1% or 2% of the proper engine speed, then the averaging technique is useful. A variation of this technique must be used in turning flight when the throttle is set at MIL and cannot be used as the adjustable variable. In this case, bank angle (or load factor) is related to vertical speed in the same manner engine speed was related to vertical speed in the straight flight conditions. The flight test technique used in obtaining unstable equilibrium conditions is called the constant airspeed or back side method.

The primary parameters for pilot reference when obtaining data points under unstable equilibrium conditions are airspeed, vertical speed, heading for straight flight, and bank angle for turning flight. For tests in which rate of climb can be corrected to thrust or power required, achieving equilibrium at zero vertical speed is not necessary. A small altitude change over a short time period can be used to correct the test results to level conditions. In other tests, achieving zero vertical speed is necessary. Sufficient practice usually results in a satisfactory ability to obtain zero vertical speed at the desired test altitude in less time than it takes to determine an average rate of climb correction. The constant airspeed technique can be used to obtain test data under stable equilibrium conditions as well. Normally, automatic flight control systems offer little advantage over manual control in obtaining unstable equilibrium data points.

1.7.6 NONEQUILIBRIUM TEST POINTS

Nonequilibrium test points are usually the most difficult to obtain. They preclude stable conditions or the ability to trim to maintain constant conditions. The pilot does, however, have some schedule to follow in achieving a satisfactory flight path or flight test condition. Some nonequilibrium tests such as acceleration runs are performed at a constant altitude. Others, such as climbs and descents, are performed according to an airspeed schedule. Nonequilibrium test points require smoothly capturing, transitioning between data points, and maintaining a schedule.

The primary reference parameters for nonequilibrium tests is dictated by the specific test being performed. An AFCS can be an aid in obtaining nonequilibrium data. The degree it can be employed depends upon the specific test and the capability of the modes. Good heading hold and altitude hold modes can be valuable in obtaining level acceleration test data. Climb and descent tests can be performed using Mach or indicated airspeed hold modes if they have sufficiently high gain to maintain the desired schedule accuracy.

1.7.7 ENERGY MANAGEMENT

Proper energy management is critical to effective use of scarce flight test resources. Energy conservation when progressing from one test point or condition to another allows acquisition of a greater quantity of data.

The test pilot is mentally ahead of the aircraft and flight profile. The pilot is aware of the next test point and effects a smooth energy conserving transition from point to point. A smooth transition between points might include trading airspeed for an airspeed/ altitude entry condition for a succeeding test point.

The test should be planned to make maximum use of the entire flight profile. Takeoff, climb, descent, and landing tests can be combined with tests conducted at altitude.

1.8 CONFIDENCE LEVELS

The quality of a data point, whether it meets test requirements and test conditions, is determined by the test pilot/test team at the time the data are gathered. Confidence levels (CL) are a quantitative data rating scheme used to relate information about the quality of the data. The assignment of a CL to a data point is important to provide the test team and other future users of the data assistance in:

1. Determining how strong a conclusion can be based upon the data point.
2. Weighing of data when curve fitting.
3. Prioritizing further tests.

Low CLs can result from several causes. The following are some of the primary factors affecting CLs:

1. Atmospheric conditions (turbulence, wind shear).
2. Aircraft condition (marginal or degraded engine performance).
3. Pilot technique.

The following quantitative scale is used to quantify confidence levels.

Table 1.1
CONFIDENCE LEVELS

LEVEL	DESCRIPTOR	DESCRIPTION
1	Poor	Use only for order of magnitude assessment.
2	Marginal	Pilot technique/environmental conditions slightly outside of desired tolerances; accuracy sufficient to give good idea of the actual value, but not to support conclusion regarding specification compliance.
3	Acceptable	Tolerances just within the limits of acceptability as defined in the method of test. Useable for specification compliance.
4	Good	Tolerance well within the defined limits for the test.
5	Excellent	Tolerance limited only by the accuracy of the instrumentation used.

Levels 2, 3 and 4 have specific definitions in terms of established test standards. Most of the student test data falls into one of these categories. The meaning of the confidence level assignment should be unambiguous once the test standards are defined.

Some examples of using CLs are presented below.

1. A level acceleration is flown with +300 ft altitude deviation and +0.l g n_z excursion. The confidence level is 3.
2. A climb schedule is flown in smooth air with +2 KIAS airspeed deviation without noticeable n_z excursion. The confidence level is 4.

3. A sawtooth climb is flown smoothly with an airspeed deviation of ±5 kn. Confidence level is 2.

The use of confidence levels is encouraged throughout the performance syllabus. With experience, confidence levels are of significant value when used during the flying qualities syllabus.

1.9 FLIGHT SAFETY

1.9.1 INCREMENTAL BUILD-UP

The concept of incremental build-up is one of the most important aspects of flight testing. Build-up is the process of proceeding from the known to the unknown in an incremental, methodical pattern. Flight tests are structured in this manner. Testing begins with the best documented, least hazardous data points and proceeds toward the desired end points always conscious of the aircraft, pilot, and evaluation limits. There should be no surprises in flight test. In the event a data point yields an unexpected result or a series of data points creates an unexpected trend, evaluation stops until the results are analyzed and explained.

1.10 GLOSSARY

1.10.1 NOTATIONS

AFCS	Automatic flight control system	
CL	Confidence level	
ΔH_{pos}	Altimeter position error	ft
DT IIA	Developmental Test IIA	
ΔV_{pos}	Airspeed position error	kn
FTE	Flight test engineer	
FTM	Flight Test Manual	
g	Gravitational acceleration	ft/s^2
H_{P_c}	Calibrated pressure altitude	ft
K_T	Temperature recovery factor	
M	Mach number	
MIL	Military power	

NAVAIRWARCENACDIV	Naval Air Warfare Center Aircraft Division	
NTE	Navy Technical Evaluation	
n_z	Normal acceleration	g
P_s	Specific excess power	ft/s
STOL	Short takeoff and landing	
USNTPS	U.S. Naval Test Pilot School	
V_T	True airspeed	
W/δ	Weight to pressure ratio	

1.11 REFERENCES

1. NAVAIRTESTCEN Instruction 5213.3F, *Report Writing Handbook*, NAVAIRTESTCEN, Patuxent River, MD, 16 August 1984.

2. Naval Test Pilot School Flight Test Manual, *Fixed Wing Performance, Theory and Flight Test Techniques*, USNTPS-FTM-No.104, U. S. Naval Test Pilot School, Patuxent River, MD, July, 1977.

3. *U.S. Naval Test Pilot School Notice 1542*, Subj: Academic, Flight and Report Curriculum for Class --, U.S. Naval Test Pilot School, Patuxent River, MD.

4. USAF Test Pilot School, *Performance Phase Textbook Volume I*, USAF-TPS-CUR-86-01, USAF, Edwards AFB, CA, April, 1986.

CHAPTER 2

PITOT STATIC SYSTEM PERFORMANCE

CHAPTER 2

FIGURES

CHAPTER 2

TABLES

CHAPTER 2

EQUATIONS

Equation		PAGE
$P = \rho\ g_c\ R\ T$	(Eq 2.1)	2.4
$dP_a = -\ \rho\ g\ dh$	(Eq 2.2)	2.4
$g_{ssl}\ dH = g\ dh$	(Eq 2.3)	2.4
$\theta = \frac{T_a}{T_{ssl}} = \left(1 - 6.8755856 \times 10^{-6}\ H\right)$	(Eq 2.4)	2.5
$\delta = \frac{P_a}{P_{ssl}} = \left(1 - 6.8755856 \times 10^{-6}\ H\right)^{5.255863}$	(Eq 2.5)	2.5
$\sigma = \frac{\rho_a}{\rho_{ssl}} = \left(1 - 6.8755856 \times 10^{-6}\ H\right)^{4.255863}$	(Eq 2.6)	2.6
$P_a = P_{ssl}\left(1 - 6.8755856 \times 10^{-6}\ H_P\right)^{5.255863}$	(Eq 2.7)	2.6
$T_a = -56.50^\circ C = 216.65^\circ K$	(Eq 2.8)	2.6
$\delta = \frac{P_a}{P_{ssl}} = 0.223358\ e^{-4.80614 \times 10^{-5}\ (H - 36089)}$	(Eq 2.9)	2.6
$\sigma = \frac{\rho_a}{\rho_{ssl}} = 0.297069\ e^{-4.80614 \times 10^{-5}\ (H - 36089)}$	(Eq 2.10)	2.6
$P_a = P_{ssl}\left(0.223358\ e^{-4.80614 \times 10^{-5}\left(H_P - 36089\right)}\right)$	(Eq 2.11)	2.6
$V_T = \sqrt{\frac{2}{\rho_a}\left(P_T - P_a\right)} = \sqrt{\frac{2q}{\rho_a}}$	(Eq 2.12)	2.10

$$V_e = \sqrt{\frac{2q}{\rho_{ssl}}} = \sqrt{\frac{\sigma\, 2q}{\rho_a}} = \sqrt{\sigma}\, V_T$$ (Eq 2.13) 2.11

$$V_{e_{Test}} = V_{e_{Std}}$$ (Eq 2.14) 2.12

$$V_T^2 = \frac{2\gamma}{\gamma - 1} \frac{P_a}{\rho_a} \left[\left(\frac{P_T - P_a}{P_a} + 1 \right)^{\frac{\gamma - 1}{\gamma}} - 1 \right]$$ (Eq 2.15) 2.13

$$V_T = \sqrt{\frac{2\gamma}{\gamma - 1} \frac{P_a}{\rho_a} \left[\left(\frac{q_c}{P_a} + 1 \right)^{\frac{\gamma - 1}{\gamma}} - 1 \right]}$$ (Eq 2.16) 2.13

$$q_c = q \left(1 + \frac{M^2}{4} + \frac{M^4}{40} + \frac{M^6}{1600} + \ldots \right)$$ (Eq 2.17) 2.13

$$V_c^2 = \frac{2\gamma}{\gamma - 1} \frac{P_{ssl}}{\rho_{ssl}} \left[\left(\frac{P_T - P_a}{P_{ssl}} + 1 \right)^{\frac{\gamma - 1}{\gamma}} - 1 \right]$$ (Eq 2.18) 2.14

$$V_c = \sqrt{\frac{2\gamma}{\gamma - 1} \frac{P_{ssl}}{\rho_{ssl}} \left[\left(\frac{q_c}{P_{ssl}} + 1 \right)^{\frac{\gamma - 1}{\gamma}} - 1 \right]}$$ (Eq 2.19) 2.14

$$V_c = f \left(P_T - P_a \right) = f \left(q_c \right)$$ (Eq 2.20) 2.14

$$V_{c_{Test}} = V_{c_{Std}}$$ (Eq 2.21) 2.14

$$\frac{P'_T}{P_a} = \left[\frac{\gamma + 1}{2} \left(\frac{V}{a} \right)^2 \right]^{\frac{\gamma}{\gamma - 1}} \left[\frac{1}{\frac{2\gamma}{\gamma + 1} \left(\frac{V}{a} \right)^2 - \frac{\gamma - 1}{\gamma + 1}} \right]^{\frac{1}{\gamma - 1}}$$ (Eq 2.22) 2.15

$$\frac{q_c}{P_{ssl}} = \left[1 + 0.2\left(\frac{V_c}{a_{ssl}}\right)^2\right]^{3.5} - 1$$

(For $V_c \le a_{ssl}$) (Eq 2.23) 2.15

$$\frac{q_c}{P_{ssl}} = \left[\frac{166.921\left(\frac{V_c}{a_{ssl}}\right)^7}{\left[7\left(\frac{V_c}{a_{ssl}}\right)^2 - 1\right]^{2.5}}\right] - 1$$

(For $V_c \ge a_{ssl}$) (Eq 2.24) 2.15

$$V_e = \sqrt{\frac{2\gamma}{\gamma - 1}\frac{P_a}{\rho_{ssl}}\left[\left(\frac{q_c}{P_a} + 1\right)^{\frac{\gamma - 1}{\gamma}} - 1\right]}$$

(Eq 2.25) 2.17

$$V_e = V_T\sqrt{\sigma}$$

(Eq 2.26) 2.17

$$M = \frac{V_T}{a} = \frac{V_T}{\sqrt{\gamma g_c R T}} = \frac{V_T}{\sqrt{\gamma \frac{P}{\rho}}}$$

(Eq 2.27) 2.17

$$M = \sqrt{\frac{2}{\gamma - 1}\left[\left(\frac{P_T - P_a}{P_a} + 1\right)^{\frac{\gamma - 1}{\gamma}} - 1\right]}$$

(Eq 2.28) 2.17

$$\frac{P_T}{P_a} = \left(1 + \frac{\gamma - 1}{2}M^2\right)^{\frac{\gamma}{\gamma - 1}}$$

(Eq 2.29) 2.18

$$\frac{q_c}{P_a} = \left(1 + 0.2\,M^2\right)^{3.5} - 1$$

for $M < 1$ (Eq 2.30) 2.18

$$\frac{q_c}{P_a} = \left[\frac{166.921\,M^7}{\left(7M^2 - 1\right)^{2.5}}\right] - 1$$

for $M > 1$ (Eq 2.31) 2.18

$M = f\left(P_T - P_a, P_a\right) = f\left(V_c, H_P\right)$	(Eq 2.32)	2.19
$M_{Test} = M$	(Eq 2.33)	2.19
$\Delta H_{P_{ic}} = H_{P_i} - H_{P_o}$	(Eq 2.34)	2.22
$\Delta V_{ic} = V_i - V_o$	(Eq 2.35)	2.22
$H_{P_i} = H_{P_o} + \Delta H_{P_{ic}}$	(Eq 2.36)	2.22
$V_i = V_o + \Delta V_{ic}$	(Eq 2.37)	2.22
$\Delta P = P_s - P_a$	(Eq 2.38)	2.27
$\Delta V_{pos} = V_c - V_i$	(Eq 2.39)	2.27
$\Delta H_{pos} = H_{P_c} - H_{P_i}$	(Eq 2.40)	2.27
$\Delta M_{pos} = M - M_i$	(Eq 2.41)	2.27
$\frac{P_s}{P_a} = f_1\left(M, \alpha, \beta, R_e\right)$	(Eq 2.42)	2.28
$\frac{P_s}{P_a} = f_2\left(M, \alpha\right)$	(Eq 2.43)	2.28
$\frac{\Delta P}{q_c} = f_3\left(M, \alpha\right)$	(Eq 2.44)	2.28
$\frac{\Delta P}{q_c} = f_4\left(M\right)$ (High speed)	(Eq 2.45)	2.28
$\frac{\Delta P}{q_c} = f_5\left(C_L\right)$ (Low speed)	(Eq 2.46)	2.28
$\frac{\Delta P}{q_{c_i}} = f_6\left(M_i\right)$ (High speed)	(Eq 2.47)	2.29

$\frac{\Delta P}{q_c} = f_7 \left(W, V_c \right)$ (Low speed)	(Eq 2.48)	2.29
$V_{c_W} = V_{c_{Test}} \sqrt{\frac{W_{Std}}{W_{Test}}}$	(Eq 2.49)	2.30
$\frac{\Delta P}{q_c} = f_8 \left(V_{c_W} \right)$ (Low speed)	(Eq 2.50)	2.30
$V_{i_W} = V_{i_{Test}} \sqrt{\frac{W_{Std}}{W_{Test}}}$	(Eq 2.51)	2.30
$\frac{\Delta P}{q_{c_i}} = f_9 \left(V_{i_W} \right)$ (Low speed)	(Eq 2.52)	2.30
$\frac{T_T}{T} = 1 + \frac{\gamma - 1}{2} M^2$	(Eq 2.53)	2.32
$\frac{T_T}{T} = 1 + \frac{\gamma - 1}{2} \frac{V_T^2}{\gamma g_c R T}$	(Eq 2.54)	2.32
$\frac{T_T}{T} = 1 + \frac{K_T (\gamma - 1)}{2} M^2$	(Eq 2.55)	2.33
$\frac{T_T}{T} = 1 + \frac{K_T (\gamma - 1)}{2} \frac{V_T^2}{\gamma g_c R T}$	(Eq 2.56)	2.33
$\frac{T_T}{T_a} = \frac{T_i}{T_a} = 1 + \frac{K_T M^2}{5}$	(Eq 2.57)	2.33
$T_T = T_i = T_a + \frac{K_T V_T^2}{7592}$	(Eq 2.58)	2.33
$T_i = T_o + \Delta T_{ic}$	(Eq 2.59)	2.35

$$K_T = \left(\frac{T_i\ (^\circ K)}{T_a\ (^\circ K)} - 1 \right) \frac{5}{M^2}$$ (Eq 2.60) 2.35

$$V_{G_1} = 3600 \left(\frac{D}{\Delta t_1} \right)$$ (Eq 2.61) 2.50

$$V_{G_2} = 3600 \left(\frac{D}{\Delta t_2} \right)$$ (Eq 2.62) 2.50

$$V_T = \frac{V_{G_1} + V_{G_2}}{2}$$ (Eq 2.63) 2.50

$$\rho_a = \frac{P_a}{g_c\ R\ T_{a_{ref}}\ (^\circ K)}$$ (Eq 2.64) 2.50

$$\sigma = \frac{\rho_a}{\rho_{ssl}}$$ (Eq 2.65) 2.51

$$V_c = V_e - \Delta V_c$$ (Eq 2.66) 2.51

$$M = \frac{V_T}{38.9678 \sqrt{T_{a_{ref}}\ (^\circ K)}}$$ (Eq 2.67) 2.51

$$q_c = P_{ssl} \left\{ \left[1 + 0.2 \left(\frac{V_c}{a_{ssl}} \right)^2 \right]^{3.5} - 1 \right\}$$ (Eq 2.68) 2.51

$$q_{c_i} = P_{ssl} \left\{ \left[1 + 0.2 \left(\frac{V_i}{a_{ssl}} \right)^2 \right]^{3.5} - 1 \right\}$$ (Eq 2.69) 2.51

$$\Delta P = q_c - q_{c_i}$$ (Eq 2.70) 2.51

$$V_{i_W} = V_i \sqrt{\frac{W_{Std}}{W_{Test}}}$$ (Eq 2.71) 2.51

$$H_{P_{i_{ref}}} = H_{P_{o_{ref}}} + \Delta H_{P_{ic_{ref}}}$$ (Eq 2.72) 2.54

$$H_{P_i} = \frac{T_{ssl}}{a_{ssl}} \left[1 - \left(\frac{P_s}{P_{ssl}} \right)^{\frac{1}{\left(\frac{g_{ssl}}{g_c\, a_{ssl}\, R} \right)}} \right]$$ (Eq 2.73) 2.54

$$H_{P_{i_{ref}}} = \frac{T_{ssl}}{a_{ssl}} \left[1 - \left(\frac{P_a}{P_{ssl}} \right)^{\frac{1}{\left(\frac{g_{ssl}}{g_c\, a_{ssl}\, R} \right)}} \right]$$ (Eq 2.74) 2.55

$$\Delta h = d \tan\theta$$ (Eq 2.75) 2.57

$$\Delta h = L_{a/c} \frac{y}{x}$$ (Eq 2.76) 2.57

$$H_{P_c} = H_{P_{c_{twr}}} + \Delta h \frac{T_{Std}\ (^\circ K)}{T_{Test}\ (^\circ K)}$$ (Eq 2.77) 2.57

$$P_s = P_{ssl} \left(1 - 6.8755856 \times 10^{-6} H_{P_i} \right)^{5.255863}$$ (Eq 2.78) 2.57

$$P_a = P_{ssl} \left(1 - 6.8755856 \times 10^{-6} H_{P_c} \right)^{5.255863}$$ (Eq 2.79) 2.58

$$\text{Curve slope} = K_T \frac{\gamma - 1}{\gamma} T_a = 0.2\ K_T\ T_a\ (^\circ K)\ \text{(High speed)}$$ (Eq 2.80) 2.60

$$\text{Curve slope} = K_T \frac{0.2\ T_a\ (^\circ K)}{a_{ssl}^2}\ \text{(Low speed)}$$ (Eq 2.81) 2.60

$$K_T = \frac{\text{slope}}{0.2\ T_a\ (^\circ K)}\ \text{(High speed)}$$ (Eq 2.82) 2.60

$$K_T = \frac{\text{slope}\ a^2_{ssl}}{0.2\ T_a\ (^\circ K)}\ \text{(Low speed)}$$ (Eq 2.83) 2.61

$$M_i = \sqrt{\frac{2}{\gamma - 1}\left[\left(\frac{q_{c_i}}{P_s} + 1\right)^{\frac{\gamma - 1}{\gamma}} - 1\right]}$$ (Eq 2.84) 2.62

$$\Delta P = \left(\frac{\Delta P}{q_{c_i}}\right) q_{c_i}$$ (Eq 2.85) 2.62

$$q_c = q_{c_i} + \Delta P$$ (Eq 2.86) 2.62

$$\Delta V_{pos} = V_c - V_{i_W}$$ (Eq 2.87) 2.63

$$P_a = P_s - \Delta P$$ (Eq 2.88) 2.63

$$H_{P_c} = \frac{T_{ssl}}{a_{ssl}}\left[1 - \left(\frac{P_a}{P_{ssl}}\right)^{\frac{1}{\left(\frac{g_{ssl}}{g_c\ a_{ssl}\ R}\right)}}\right]$$ (Eq 2.89) 2.63

CHAPTER 2

PITOT STATIC SYSTEM PERFORMANCE

2.1 INTRODUCTION

The initial step in any flight test is to measure the pressure and temperature of the atmosphere and the velocity of the vehicle at the particular time of the test. There are restrictions in what can be measured accurately, and there are inaccuracies within each measuring system. This phase of flight testing is very important. Performance data and most stability and control data are worthless if pitot static and temperature errors are not corrected. Consequently, calibration tests of the pitot static and temperature systems comprise the first flights in any test program.

This chapter presents a discussion of pitot static system performance testing. The theoretical aspects of these flight tests are included. Test methods and techniques applicable to aircraft pitot static testing are discussed in some detail. Data reduction techniques and some important factors in the analysis of the data are also included. Mission suitability factors are discussed. The chapter concludes with a glossary of terms used in these tests and the references which were used in constructing this chapter.

2.2 PURPOSE OF TEST

The purpose of pitot static system testing is to investigate the characteristics of the aircraft pressure sensing systems to achieve the following objectives:

1. Determine the airspeed and altimeter correction data required for flight test data reduction.
2. Determine the temperature recovery factor, K_T.
3. Evaluate mission suitability problem areas.
4. Evaluate the requirements of pertinent Military Specifications.

2.3 THEORY

2.3.1 THE ATMOSPHERE

The forces acting on an aircraft in flight are a function of the temperature, density, pressure, and viscosity of the fluid in which the vehicle is operating. Because of this, the flight test team needs a means for determining the atmospheric properties. Measurements reveal the atmospheric properties have a daily, seasonal, and geographic dependence; and are in a constant state of change. Solar radiation, water vapor, winds, clouds, turbulence, and human activity cause local variations in the atmosphere. The flight test team cannot control these natural variances, so a standard atmosphere was constructed to describe the static variation of the atmospheric properties. With this standard atmosphere, calculations are made of the standard properties. When variations from this standard occur, the variations are used as a method for calculating or predicting aircraft performance.

2.3.2 DIVISIONS OF THE ATMOSPHERE

The atmosphere is divided into four major divisions which are associated with physical characteristics. The division closest to the earth's surface is the troposphere. Its upper limit varies from approximately 28,000 feet and -46°C at the poles to 56,000 feet and -79°C at the equator. These temperatures vary daily and seasonally. In the troposphere, the temperature decreases with height. A large portion of the sun's radiation is transmitted to and absorbed by the earth's surface. The portion of the atmosphere next to the earth is heated from below by radiation from the earth's surface. This radiation in turn heats the rest of the troposphere. Practically all weather phenomenon are contained in this division.

The second major division of the atmosphere is the stratosphere. This layer extends from the troposphere outward to a distance of approximately 50 miles. The original definition of the stratosphere included constant temperature with height. Recent data show the temperature is constant at 216.66°K between about 7 and 14 miles, increases to approximately 270°K at 30 miles, and decreases to approximately 180°K at 50 miles. Since the temperature variation between 14 and 50 miles destroys one of the basic definitions of the stratosphere, some authors divide this area into two divisions: stratosphere, 7 to 14 miles, and mesosphere, 15 to 50 miles. The boundary between the troposphere and the stratosphere is the tropopause.

The third major division, the ionosphere, extends from approximately 50 miles to 300 miles. Large numbers of free ions are present in this layer, and a number of different electrical phenomenon take place in this division. The temperature increases with height to 1500˚K at 300 miles.

The fourth major division is the exosphere. It is the outermost layer of the atmosphere. It starts at 300 miles and is characterized by a large number of free ions. Molecular temperature increases with height.

2.3.3 STANDARD ATMOSPHERE

The physical characteristics of the atmosphere change daily and seasonally. Since aircraft performance is a function of the physical characteristics of the air mass through which it flies, performance varies as the air mass characteristics vary. Thus, standard air mass conditions are established so performance data has meaning when used for comparison purposes. In the case of the altimeter, the standard allows for design of an instrument for measuring altitude.

At the present time there are several established atmosphere standards. One commonly used is the Arnold Research and Development Center (ARDC) 1959 model atmosphere. A more recent one is the U.S. Standard Atmosphere, 1962. These standard atmospheres were developed to approximate the standard average day conditions at 40˚ to 45˚N latitude.

These two standard atmospheres are basically the same up to an altitude of approximately 66,000 feet. Both the 1959 ARDC and the 1962 U.S. Standard Atmosphere are defined to an upper limit of approximately 440 miles. At higher levels there are some marked differences between the 1959 and 1962 atmospheres. The standard atmosphere used by the U.S. Naval Test Pilot School (USNTPS) is the 1962 atmosphere. Appendix VI gives the 1962 atmosphere in tabular form.

The U.S. Standard Atmosphere, 1962 assumes:

1. The atmosphere is a perfect gas which obeys the equation of state:

$$P = \rho\, g_c\, R\, T \qquad \text{(Eq 2.1)}$$

2. The air is dry.
3. The standard sea level conditions:

a_{ssl}	Standard sea level speed of sound	661.483 kn
g_{ssl}	Standard sea level gravitational acceleration	32.174049 ft/s^2
P_{ssl}	Standard sea level pressure	2116.217 psf
		29.9212 inHg
ρ_{ssl}	Standard sea level air density	0.0023769 slugs/ft^3
T_{ssl}	Standard sea level temperature	15˚C or 288.15˚K.

4. The gravitational field decreases with altitude.
5. Hydrostatic equilibrium exists such that:

$$dP_a = -\,\rho\, g\, dh \qquad \text{(Eq 2.2)}$$

6. Vertical displacement is measured in geopotential feet. Geopotential is a measure of the gravitational potential energy of a unit mass at a point relative to mean sea level and is defined in differential form by the equation:

$$g_{ssl}\, dH = g\, dh \qquad \text{(Eq 2.3)}$$

Where:

g	Gravitational acceleration (Varies with altitude)	ft/s
g_c	Conversion constant	32.17 lb_m/slug
g_{ssl}	Standard sea level gravitational acceleration	32.174049 ft/s^2
H	Geopotential (At the point)	ft
h	Tapeline altitude	ft
P	Pressure	psf

P_a	Ambient pressure	psf
R	Engineering gas constant for air	96.93 ft-lb_f/lb_m - °K
ρ	Air density	$slug/ft^3$
T	Temperature	°K.

Each point in the atmosphere has a definite geopotential, since g is a function of latitude and altitude. Geopotential is equivalent to the work done in elevating a unit mass from sea level to a tapeline altitude expressed in feet. For most purposes, errors introduced by letting h = H in the troposphere are insignificant. Making this assumption, there is slightly more than a 2% error at 400,000 feet.

7. Temperature variation with geopotential is expressed as a series of straight line segments:

a. The temperature lapse rate (a) in the troposphere (sea level to 36,089 geopotential feet) is 0.0019812°C/geopotential feet.

b. The temperature above 36,089 geopotential feet and below 65,600 geopotential feet is constant -56.50°C.

2.3.3.1 STANDARD ATMOSPHERE EQUATIONS

From the basic assumptions for the standard atmosphere listed above, the relationships for temperature, pressure, and density as functions of geopotential are derived.

Below 36,089 geopotential feet, the equations for the standard atmosphere are:

$$\theta = \frac{T_a}{T_{ssl}} = \left(1 - 6.8755856 \times 10^{-6}\, H\right) \qquad \text{(Eq 2.4)}$$

$$\delta = \frac{P_a}{P_{ssl}} = \left(1 - 6.8755856 \times 10^{-6}\, H\right)^{5.255863} \qquad \text{(Eq 2.5)}$$

$$\sigma = \frac{\rho_a}{\rho_{ssl}} = \left(1 - 6.8755856 \times 10^{-6}\, H\right)^{4.255863} \qquad \text{(Eq 2.6)}$$

$$P_a = P_{ssl}\left(1 - 6.8755856 \times 10^{-6}\, H_P\right)^{5.255863} \qquad \text{(Eq 2.7)}$$

Above 36,089 geopotential feet and below 82,021 geopotential feet the equations for the standard atmosphere are:

$$T_a = -56.50^\circ\mathrm{C} = 216.65^\circ\mathrm{K} \qquad \text{(Eq 2.8)}$$

$$\delta = \frac{P_a}{P_{ssl}} = 0.223358\, e^{-4.80614 \times 10^{-5}\,(H - 36089)} \qquad \text{(Eq 2.9)}$$

$$\sigma = \frac{\rho_a}{\rho_{ssl}} = 0.297069\, e^{-4.80614 \times 10^{-5}\,(H - 36089)} \qquad \text{(Eq 2.10)}$$

$$P_a = P_{ssl}\left(0.223358\, e^{-4.80614 \times 10^{-5}\left(H_P - 36089\right)}\right) \qquad \text{(Eq 2.11)}$$

Where:

δ	Pressure ratio	
e	Base of natural logarithm	
H	Geopotential	ft
H_P	Pressure altitude	ft
P_a	Ambient pressure	psf
P_{ssl}	Standard sea level pressure	2116.217 psf
θ	Temperature ratio	
ρ_a	Ambient air density	slug/ft^3
ρ_{ssl}	Standard sea level air density	0.0023769 slug/ft^3
σ	Density ratio	
T_a	Ambient temperature	˚C or ˚K

T_{ssl}	Standard sea level temperature	15˚C or 288.15˚K.

2.3.3.2 ALTITUDE MEASUREMENT

With the establishment of a set of standards for the atmosphere, there are several different means to determine altitude above the ground. The means used defines the type of altitude. Tapeline altitude, or true altitude, is the linear distance above sea level and is determined by triangulation or radar.

A temperature altitude can be obtained by modifying a temperature gauge to read in feet for a corresponding temperature, determined from standard tables. However, since inversions and nonstandard lapse rates exist, and temperature changes daily, seasonally, and with latitude, such a technique is not useful.

If an instrument were available to measure density, the same type of technique could be employed, and density altitude could be determined.

If a highly sensitive accelerometer could be developed to measure gravitational acceleration, geopotential altitude could be measured. This device would give the correct reading in level, unaccelerated flight.

A practical fourth technique, is based on pressure measurement. A pressure gauge is used to sense the ambient pressure. Instead of reading pounds per square foot, it indicates the corresponding standard altitude for the pressure sensed. This altitude is pressure altitude, H_P, and is the parameter on which flight testing is based.

2.3.3.3 PRESSURE VARIATION WITH ALTITUDE

The pressure altitude technique is the basis for present day altimeters. The instrument only gives a true reading when the pressure at altitude is the same as standard day. In most cases, pressure altitude does not agree with the geopotential or tapeline altitude.

Most present day altimeters are designed to follow Eq 2.5. This equation is used to determine standard variation of pressure with altitude below the tropopause. An example of the variation described by Eq 2.5 is presented in figure 2.1.

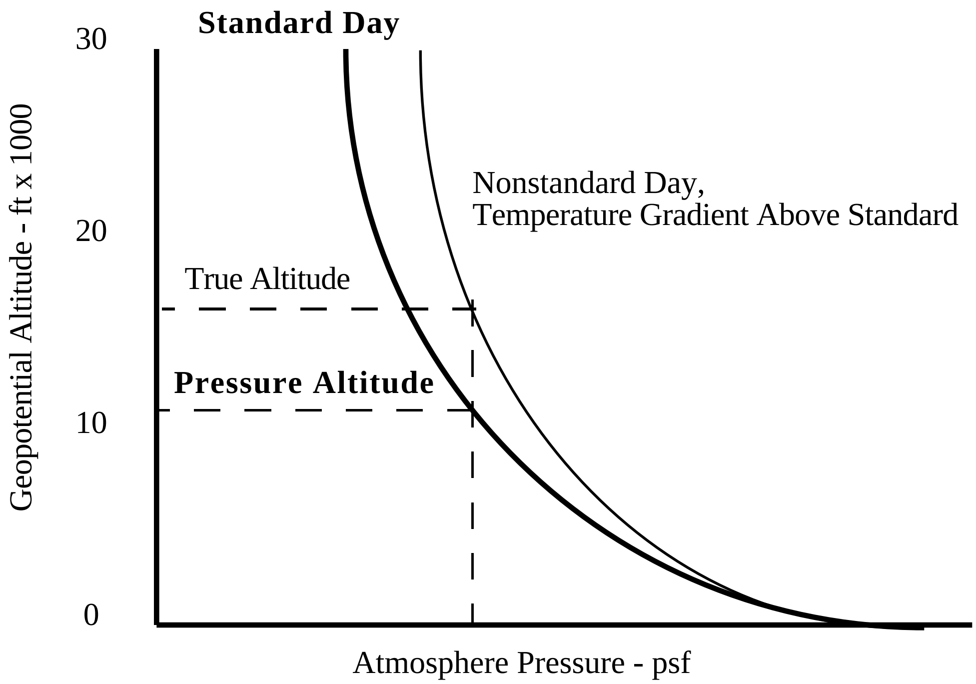

Figure 2.1
PRESSURE VARIATION WITH ALTITUDE

The altimeter presents the standard pressure variation in figure 2.1 as observed pressure altitude, H_{P_o}. If the pressure does not vary as described by this curve, the altimeter indication will be erroneous. The altimeter setting, a provision made in the construction of the altimeter, is used to adjust the scale reading up or down so the altimeter reads true elevation if the aircraft is on deck.

Figure 2.1 shows the pressure variation with altitude for a standard and non-standard day or test day. For every constant pressure (Figure 2.1), the slope of the test day curve is greater than the standard day curve. Thus, the test day temperature is warmer than the standard day temperature. This variance between true altitude and pressure altitude is important for climb performance. A technique is available to correct pressure altitude to true altitude.

The forces acting on an aircraft in flight are directly dependent upon air density. Density altitude is the independent variable which should be used for aircraft performance comparisons. However, density altitude is determined by pressure and temperature through the equation of state relationship. Therefore, pressure altitude is used as the independent variable with test day data corrected for non-standard temperature. This greatly facilitates flight testing since the test pilot can maintain a given pressure altitude regardless of the test day conditions. By applying a correction for non-standard temperature to flight test data, the data is corrected to a standard condition.

2.3.4 ALTIMETER SYSTEMS

Most altitude measurements are made with a sensitive absolute pressure gauge, an altimeter, scaled so a pressure decrease indicates an altitude increase in accordance with the U.S. Standard Atmosphere. If the altimeter setting is 29.92, the altimeter reads pressure altitude, H_P, whether in a standard or non-standard atmosphere. An altimeter setting other than 29.92 moves the scale so the altimeter indicates field elevation with the aircraft on deck. In this case, the altimeter indication is adjusted to show tapeline altitude at one elevation. In flight testing, 29.92 is used as the altimeter setting to read pressure altitude. Pressure altitude is not dependent on temperature. The only parameter which varies the altimeter indication is atmospheric pressure.

The altimeter is constructed and calibrated according to Eq 2.7 and 2.11 which define the standard atmosphere. The heart of the altimeter is an evacuated metal bellows which expands or contracts with changes in outside pressure. The bellows is connected to a series of gears and levers which cause a pointer to move. The whole mechanism is placed in an airtight case which is vented to a static source. The indicator reads the pressure supplied to the case. Altimeter construction is shown in figure 2.2. The altimeter senses the change in static pressure, P_S, through the static source.

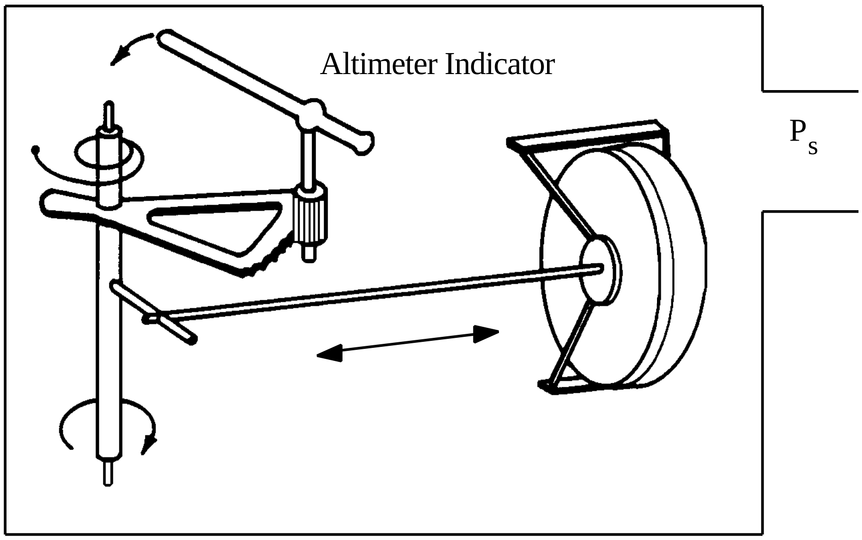

Figure 2.2
ALTIMETER SCHEMATIC

2.3.5 AIRSPEED SYSTEMS

Airspeed system theory was first developed with the assumption of incompressible flow. This assumption is only useful for low speeds of 250 knots or less at relatively low altitudes. Various concepts and nomenclature of incompressible flow are in use and provide a step toward understanding compressible flow relations.

2.3.5.1 INCOMPRESSIBLE AIRSPEED

True airspeed, in the incompressible case, is defined as:

$$V_T = \sqrt{\frac{2}{\rho_a}\left(P_T - P_a\right)} = \sqrt{\frac{2q}{\rho_a}} \qquad \text{(Eq 2.12)}$$

It is possible to use a pitot static system and build an airspeed indicator to conform to this equation. However, there are disadvantages:

1. Density requires measurement of ambient temperature, which is difficult in flight.

2. The instrument would be complex. In addition to the bellows in figure 2.3, ambient temperature and pressure would have to be measured, converted to density, and used to modify the output of the bellows.

3. Except for navigation, the instrument would not give the required pilot information. For landing, the aircraft is flown at a constant lift coefficient, C_L. Thus, the pilot would compute a different landing speed for each combination of weight, pressure altitude, and temperature.

4. Because of its complexity, the instrument would be inaccurate and difficult to calibrate.

Density is the variable which causes the problem in a true airspeed indicator. A solution is to assume a constant value for density. If ρ_a is replaced by ρ_{ssl} in Eq 2.12, the resultant velocity is termed equivalent airspeed, V_e:

$$V_e = \sqrt{\frac{2q}{\rho_{ssl}}} = \sqrt{\frac{\sigma\, 2q}{\rho_a}} = \sqrt{\sigma}\, V_T \qquad \text{(Eq 2.13)}$$

A simple airspeed indicator could be built which measures the quantity $(P_T - P_a)$. Such a system requires only the bellows system shown in figure 2.3 and has the following advantages:

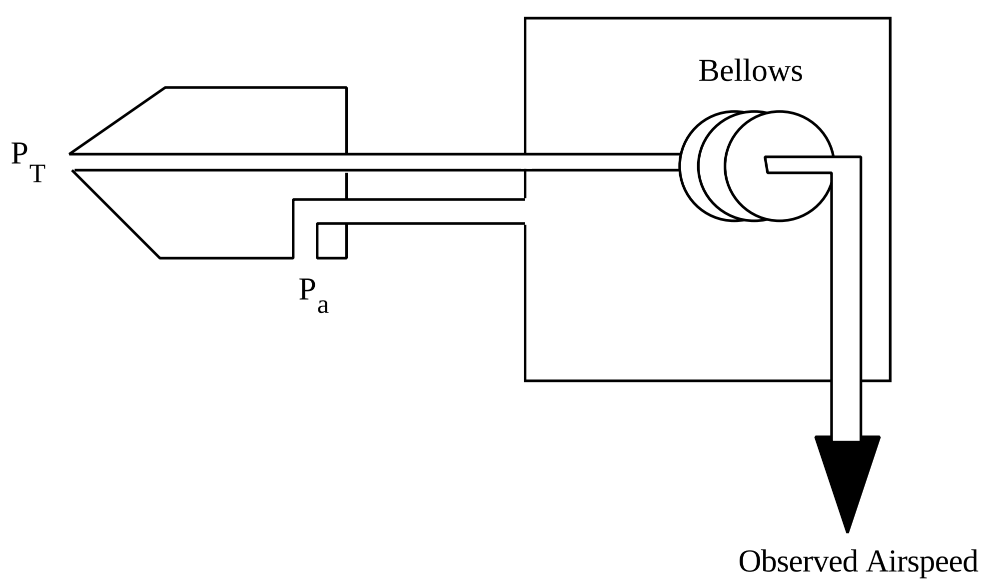

Figure 2.3
PITOT STATIC SYSTEM SCHEMATIC

1. Because of its simplicity, it has a high degree of accuracy.

2. The indicator is easy to calibrate and has only one error due to airspeed instrument correction (ΔV_{ic}).

3. The pilot can use V_e. In computing either landing or stall speed, the pilot only considers weight.

4. Since $V_e = f\ (P_T - P_a)$, it does not vary with temperature or density. Thus for a given value of $P_T - P_a$:

$$V_{e_{Test}} = V_{e_{Std}} \qquad \text{(Eq 2.14)}$$

Where:

P_a	Ambient pressure	psf
P_T	Total pressure	psf
q	Dynamic pressure	psf
ρ_a	Ambient air density	slug/ft^3
ρ_{ssl}	Standard sea level air density	0.0023769 slug/ft^3
σ	Density ratio	
V_e	Equivalent airspeed	ft/s
$V_{e_{Std}}$	Standard equivalent airspeed	ft/s
$V_{e_{Test}}$	Test equivalent airspeed	ft/s
V_T	True airspeed	ft/s.

V_e derived for the incompressible case was the airspeed primarily used before World War II. However, as aircraft speed and altitude capabilities increased, the error resulting from the assumption that density remains constant became significant. Airspeed indicators for today’s aircraft are built to consider compressibility.

2.3.5.2 COMPRESSIBLE TRUE AIRSPEED

The airspeed indicator operates on the principle of Bernoulli's compressible equation for isentropic flow in which airspeed is a function of the difference between total and static pressure. At subsonic speeds Bernoulli's equation is applicable, giving the following expression for V_T:

$$V_T^2 = \frac{2\gamma}{\gamma - 1} \frac{P_a}{\rho_a} \left[\left(\frac{P_T - P_a}{P_a} + 1 \right)^{\frac{\gamma - 1}{\gamma}} - 1 \right] \qquad \text{(Eq 2.15)}$$

Or:

$$V_T = \sqrt{\frac{2\gamma}{\gamma - 1} \frac{P_a}{\rho_a} \left[\left(\frac{q_c}{P_a} + 1 \right)^{\frac{\gamma - 1}{\gamma}} - 1 \right]} \qquad \text{(Eq 2.16)}$$

Dynamic pressure, q, and impact pressure, q_c, are not the same. However, at low altitude and low speed they are approximately the same. The relationship between dynamic pressure and impact pressure converges as Mach becomes small as follows:

$$q_c = q \left(1 + \frac{M^2}{4} + \frac{M^4}{40} + \frac{M^6}{1600} + \ldots \right) \qquad \text{(Eq 2.17)}$$

Where:

γ	Ratio of specific heats	
M	Mach number	
P_a	Ambient pressure	psf
P_T	Total pressure	psf
q	Dynamic pressure	psf
q_c	Impact pressure	psf
ρ_a	Ambient air density	slug/ft^3
V_T	True airspeed	ft/s.

2.3.5.3 CALIBRATED AIRSPEED

The compressible flow true airspeed equation (Eq 2.16) has the same disadvantages as the incompressible flow true airspeed case. Additionally, a bellows would have to be added to measure P_a. The simple pitot static system in figure 2.3 only measures P_T - P_a. To modify Eq 2.16 for measuring the quantity P_T - P_a, both ρ_a and P_a are replaced by the constant ρ_{ssl} and P_{ssl}. The resulting airspeed is defined as calibrated airspeed, V_c:

$$V_c^2 = \frac{2\gamma}{\gamma - 1}\frac{P_{ssl}}{\rho_{ssl}}\left[\left(\frac{P_T - P_a}{P_{ssl}} + 1\right)^{\frac{\gamma - 1}{\gamma}} - 1\right] \quad \text{(Eq 2.18)}$$

Or:

$$V_c = \sqrt{\frac{2\gamma}{\gamma - 1}\frac{P_{ssl}}{\rho_{ssl}}\left[\left(\frac{q_c}{P_{ssl}} + 1\right)^{\frac{\gamma - 1}{\gamma}} - 1\right]} \quad \text{(Eq 2.19)}$$

Or:

$$V_c = f\left(P_T - P_a\right) = f\left(q_c\right) \quad \text{(Eq 2.20)}$$

An instrument designed to follow Eq 2.19 has the following advantages:

1. The indicator is simple, accurate, and easy to calibrate.
2. V_c is useful to the pilot. The quantity V_c is analogous to V_e in the incompressible case, since at low airspeeds and moderate altitudes $V_e \cong V_c$. The aircraft stall speed, landing speed, and handling characteristics are proportional to calibrated airspeed for a given gross weight.
3. Since temperature or density is not present in the equation for calibrated airspeed, a given value of $(P_T - P_a)$ has the same significance on all days and:

$$V_{c_{Test}} = V_{c_{Std}} \quad \text{(Eq 2.21)}$$

Eq 2.19 is limited to subsonic flow. If the flow is supersonic, it must pass through a shock wave in order to slow to stagnation conditions. There is a loss of total pressure when the flow passes through the shock wave. Thus, the indicator does not measure the total pressure of the supersonic flow. The solution for supersonic flight is derived by considering a normal shock compression in front of the total pressure tube and an isentropic compression in the subsonic region aft of the shock. The normal shock assumption is good since the pitot tube has a small frontal area. Consequently, the radius of the shock in front of the hole may be considered infinite. The resulting equation is known as the Rayleigh Supersonic Pitot Equation. It relates the total pressure behind the shock P_T' to the free stream ambient pressure P_a and free stream Mach:

$$\frac{P'_T}{P_a} = \left[\frac{\gamma+1}{2}\left(\frac{V}{a}\right)^2\right]^{\frac{\gamma}{\gamma-1}} \left[\frac{1}{\frac{2\gamma}{\gamma+1}\left(\frac{V}{a}\right)^2 - \frac{\gamma-1}{\gamma+1}}\right]^{\frac{1}{\gamma-1}} \qquad \text{(Eq 2.22)}$$

Eq 2.22 is used to calculate the ratio of dynamic pressure to standard sea level pressure for super and subsonic flow. The resulting calibrated airspeed equations are as follows:

$$\frac{q_c}{P_{ssl}} = \left[1 + 0.2\left(\frac{V_c}{a_{ssl}}\right)^2\right]^{3.5} - 1 \qquad (\text{For } V_c \le a_{ssl}) \qquad \text{(Eq 2.23)}$$

Or:

$$\frac{q_c}{P_{ssl}} = \left[\frac{166.921\left(\frac{V_c}{a_{ssl}}\right)^7}{\left[7\left(\frac{V_c}{a_{ssl}}\right)^2 - 1\right]^{2.5}}\right] - 1 \qquad (\text{For } V_c \ge a_{ssl}) \qquad \text{(Eq 2.24)}$$

Where:

a	Speed of sound	ft/s or kn
a_{ssl}	Standard sea level speed of sound	661.483 kn
γ	Ratio of specific heats	
P_a	Ambient pressure	psf
P_{ssl}	Standard sea level pressure	2116.217 psf
P_T	Total pressure	psf
P_T'	Total pressure at total pressure source	psf
q_c	Impact pressure	psf

ρ_{ssl}	Standard sea level air density	0.0023769 slug/ft^3
V	Velocity	ft/s
V_c	Calibrated airspeed	ft/s
$V_{c_{Std}}$	Standard calibrated airspeed	ft/s
$V_{c_{Test}}$	Test calibrated airspeed	ft/s.

Airspeed indicators are constructed and calibrated according to Eq 2.23 and 2.24. In operation, the airspeed indicator is similar to the altimeter, but instead of being evacuated, the inside of the capsule is connected to the total pressure source, and the case to the static pressure source. The instrument then senses total pressure (P_T) within the capsule and static pressure (P_s) outside it as shown in figure 2.4.

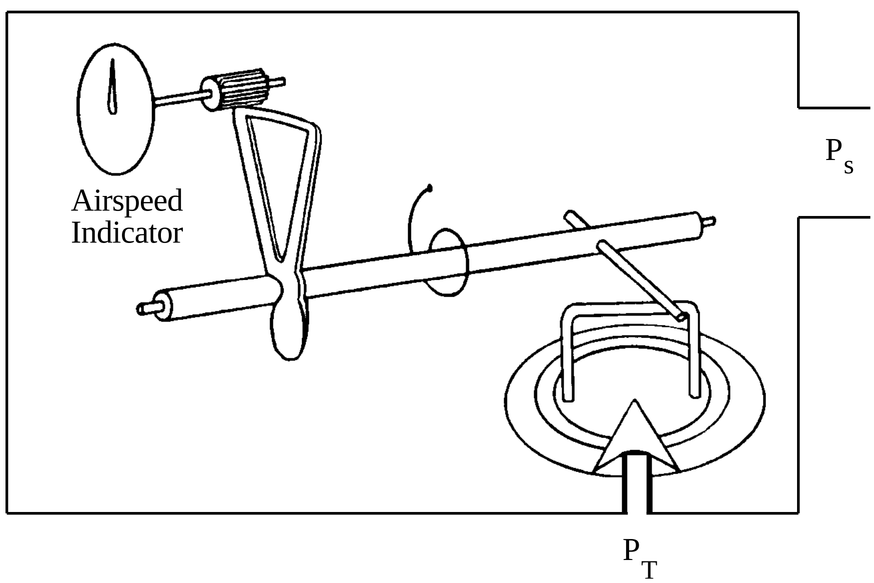

Figure 2.4
AIRSPEED SCHEMATIC

2.3.5.4 EQUIVALENT AIRSPEED

Equivalent airspeed (V_e) was derived from incompressible flow theory and has no real meaning for compressible flow. However, V_e is an important parameter in analyzing certain performance and stability and control parameters since they are functions of equivalent airspeed. The definition of equivalent airspeed is:

$$V_e = \sqrt{\frac{2\gamma}{\gamma - 1}\,\frac{P_a}{\rho_{ssl}}\left[\left(\frac{q_c}{P_a} + 1\right)^{\frac{\gamma - 1}{\gamma}} - 1\right]} \tag{Eq 2.25}$$

$$V_e = V_T\sqrt{\sigma} \tag{Eq 2.26}$$

Where:

γ	Ratio of specific heats	
P_a	Ambient pressure	psf
q_c	Impact pressure	psf
ρ_{ssl}	Standard sea level air density	0.0023769 slugs/ft^3
σ	Density ratio	
V_e	Equivalent airspeed	ft/s
V_T	True airspeed	ft/s.

2.3.6 MACHMETERS

Mach or Mach number, M, is defined as the ratio of the true airspeed to the local atmospheric speed of sound.

$$M = \frac{V_T}{a} = \frac{V_T}{\sqrt{\gamma\, g_c\, R\, T}} = \frac{V_T}{\sqrt{\gamma \frac{P}{\rho}}} \tag{Eq 2.27}$$

Substituting this relationship in the equation for V_T yields:

$$M = \sqrt{\frac{2}{\gamma - 1}\left[\left(\frac{P_T - P_a}{P_a} + 1\right)^{\frac{\gamma - 1}{\gamma}} - 1\right]} \tag{Eq 2.28}$$

Or:

$$\frac{P_T}{P_a} = \left(1 + \frac{\gamma - 1}{2} M^2\right)^{\frac{\gamma}{\gamma - 1}} \qquad \text{(Eq 2.29)}$$

This equation, which relates Mach to the free stream total and ambient pressures, is good for supersonic as well as subsonic flight. However, P_T' rather than P_T is measured in supersonic flight. By using the Rayleigh pitot equation and substituting for the constants, we obtain the following expressions:

$$\frac{q_c}{P_a} = \left(1 + 0.2\, M^2\right)^{3.5} - 1 \qquad \text{for } M < 1 \qquad \text{(Eq 2.30)}$$

$$\frac{q_c}{P_a} = \left[\frac{166.921\, M^7}{\left(7M^2 - 1\right)^{2.5}}\right] - 1 \qquad \text{for } M > 1 \qquad \text{(Eq 2.31)}$$

The Machmeter is essentially a combination altimeter and airspeed indicator designed to solve these equations. An altimeter capsule and an airspeed capsule simultaneously supply inputs to a series of gears and levers to produce the indicated Mach. A Machmeter schematic is presented in figure 2.5. Since the construction of the Machmeter requires two bellows, one for impact pressure (q_c) and another for ambient pressure (P_a), the meter is complex, difficult to calibrate, and inaccurate. As a result, the Machmeter is not used in flight test work except as a reference instrument.

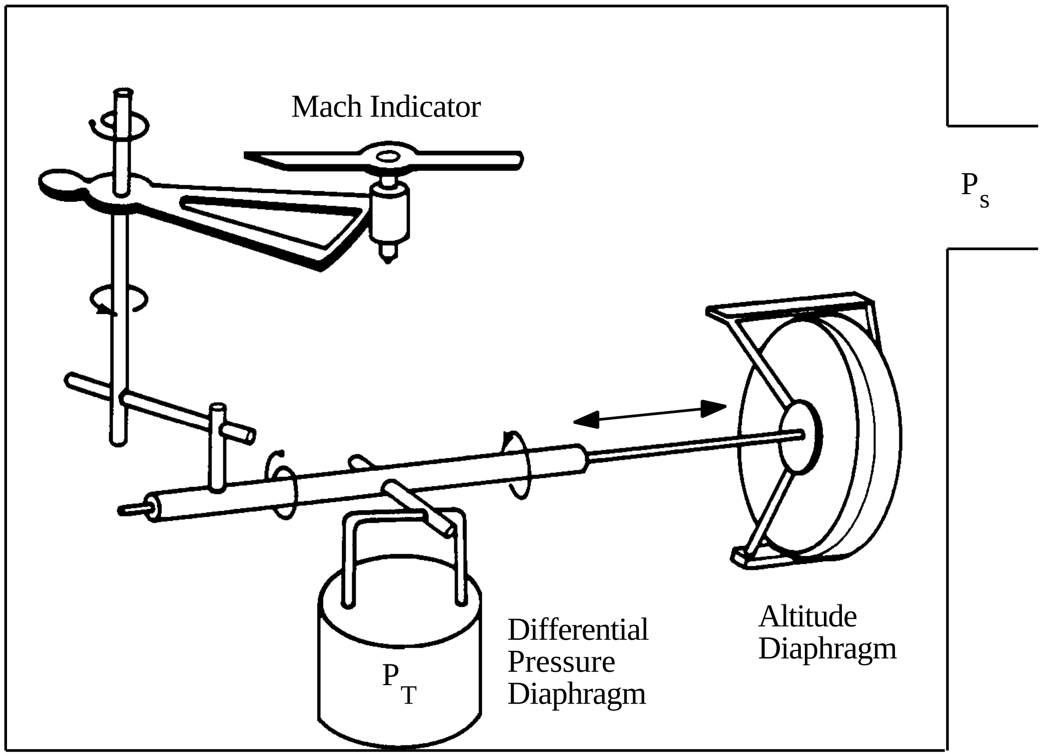

Figure 2.5
MACHMETER SCHEMATIC

Of importance in flight test is the fact:

$$M = f\left(P_T - P_a\,,\, P_a\right) = f\left(V_c, H_P\right) \quad \text{(Eq 2.32)}$$

As a result, Mach is independent of temperature, and flying at a given pressure altitude (H_P) and calibrated airspeed (V_c), the Mach on the test day equals Mach on a standard day. Since many aerodynamic effects are functions of Mach, particularly in jet engine-airframe performance analysis, this fact plays a major role in flight testing.

$$M_{Test} = M \quad \text{(Eq 2.33)}$$

Where:

a	Speed of sound	ft/s or kn
g_c	Conversion constant	32.17 lb_m/slug

γ	Ratio of specific heats	
H_P	Pressure altitude	ft
M	Mach number	
M_{Test}	Test Mach number	
P	Pressure	psf
P_a	Ambient pressure	psf
P_T	Total pressure	psf
q_c	Impact pressure	psf
R	Engineering gas constant for air	96.93 ft-lb_f/lb_m-˚K
ρ	Air density	slug/ft^3
T	Temperature	˚K
V_c	Calibrated airspeed	ft/s
V_T	True airspeed	ft/s.

2.3.7 ERRORS AND CALIBRATION

The altimeter, airspeed, Mach indicator, and vertical rate of climb indicators are universal flight instruments which require total and/or static pressure inputs to function. The indicated values of these instruments are often incorrect because of the effects of three general categories of errors: instrument errors, lag errors, and position errors.

Several corrections are applied to the observed pressure altitude and airspeed indicator readings (H_{P_o}, V_o) before calibrated pressure altitude and calibrated airspeed (H_{P_c}, V_c) are determined. The observed readings must be corrected for instrument error, lag error, and position error.

2.3.7.1 INSTRUMENT ERROR

The altimeter and airspeed indicator are sensitive to pressure and pressure differential respectively, and the dials are calibrated to read altitude and airspeed according to Eq 2.7, 2.11 and 2.23, and 2.24. Perfecting an instrument which represents such nonlinear functions under all flight conditions is not possible. As a result, an error exists called instrument error. Instrument error is the result of several factors:

1. Scale error and manufacturing discrepancies due to an imperfect mechanization of the controlling equations.
2. Magnetic Fields.
3. Temperature changes.
4. Friction.
5. Inertia.
6. Hysteresis.

The instrument calibration of an altimeter and airspeed indicator for instrument error is conducted in an instrument laboratory. A known pressure or pressure differential is applied to the instrument. The instrument error is determined as the difference between this known pressure and the observed instrument reading. As an instrument wears, its calibration changes. Therefore, an instrument is calibrated periodically. The repeatability of the instrument is determined from the instrument calibration history and must be good for a meaningful instrument calibration.

Data are taken in both directions so the hysteresis is determined. An instrument with a large hysteresis is rejected, since accounting for this effect in flight is difficult. An instrument vibrator can be of some assistance in reducing instrument error. Additionally, the instruments are calibrated in a static situation. The hysteresis under a dynamic situation may be different, but calibrating instruments for such conditions is not feasible.

When the readings of two pressure altimeters are used to determine the error in a pressure sensing system, a precautionary check of calibration correlations is advisable. A problem arises from the fact that two calibrated instruments placed side by side with their readings corrected by use of calibration charts do not always provide the same calibrated value. Tests such as the tower fly-by, or the trailing source, require an altimeter to provide a reference pressure altitude. These tests require placing the reference altimeter next to the aircraft altimeter prior to and after each flight. Each altimeter reading should be recorded and, if after calibration corrections are applied, a discrepancy still exists between the two readings, the discrepancy should be incorporated in the data reduction.

Instrument corrections ($\Delta H_{P_{ic}}$, ΔV_{ic}) are determined as the differences between the indicated values (H_{P_i}, V_i) and the observed values (H_{P_o}, V_o):

$$\Delta H_{P_{ic}} = H_{P_i} - H_{P_o} \qquad \text{(Eq 2.34)}$$

$$\Delta V_{ic} = V_i - V_o \qquad \text{(Eq 2.35)}$$

To correct the observed values:

$$H_{P_i} = H_{P_o} + \Delta H_{P_{ic}} \qquad \text{(Eq 2.36)}$$

$$V_i = V_o + \Delta V_{ic} \qquad \text{(Eq 2.37)}$$

Where:

$\Delta H_{P_{ic}}$	Altimeter instrument correction	ft
ΔV_{ic}	Airspeed instrument correction	kn
H_{P_i}	Indicated pressure altitude	ft
H_{P_o}	Observed pressure altitude	ft
V_i	Indicated airspeed	kn
V_o	Observed airspeed	kn.

2.3.7.2 PRESSURE LAG ERROR

The presence of lag error in pressure measurements is associated generally with climbing/descending or accelerating/decelerating flight and is more evident in static systems. When changing ambient pressures are involved, as in climbing and descending flight, the speed of pressure propagation and the pressure drop associated with flow through a tube introduces lag between the indicated and actual pressure. The pressure lag error is basically a result of:

1. Pressure drop in the tubing due to viscous friction.
2. Inertia of the air mass in the tubing.
3. Volume of the system.
4. Instrument inertia and viscous and kinetic friction.
5. The finite speed of pressure propagation.

Over a small pressure range the pressure lag is small and can be determined as a constant. Once a lag error constant is determined, a correction can be applied. Another approach, which is suitable for flight testing, is to balance the pressure systems by equalizing their volumes. Balancing minimizes or removes lag error as a factor in airspeed data reduction for flight at a constant dynamic pressure.

2.3.7.2.1 LAG CONSTANT TEST

The pitot static pressure systems of a given aircraft supply pressures to a number of different instruments and require different lengths of tubing for pressure transmission. The volume of the instrument cases plus the volume in the tubing, when added together for each pressure system, results in a volume mismatch between systems. Figure 2.6 illustrates a configuration where both the length of tubing and total instrument case volumes are unequal. If an increment of pressure is applied simultaneously across the total and static sources of figure 2.6, the two systems require different lengths of time to stabilize at the new pressure level and a momentary error in indicated airspeed results.

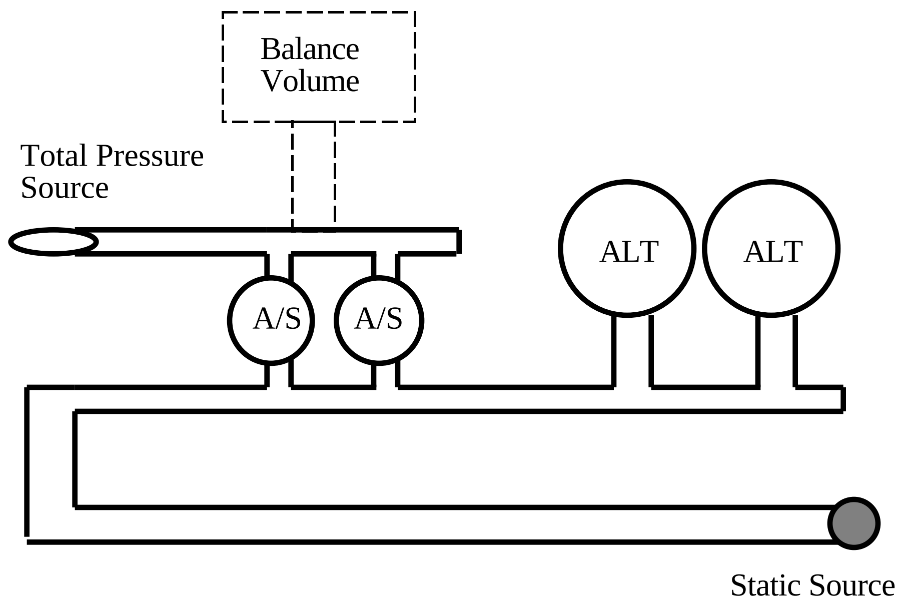

System	Length of 3/16 Inch Inside Diameter Tube	Total Volume of Instrument Cases
Static	18 ft	370×10^{-4} ft^3
Pitot	6 ft	20×10^{-4} ft^3

Figure 2.6

ANALYSIS OF PITOT AND STATIC SYSTEMS CONSTRUCTION

The lag error constant (λ) represents the time (assuming a first order dynamic response) required for the pressure of each system to reach a value equal to 63.2 percent of the applied pressure increment as shown in figure 2.7(a). This test is accomplished on the ground by applying a suction sufficient to develop a change in pressure altitude equal to 500 feet or an indicated airspeed of 100 knots. Removal of the suction and timing the pressure drop to 184 feet or 37 knots results in the determination of λ_S, the static pressure lag error constant (Figures 2.7(b) and 2.7(c)). If a positive pressure is applied to the total pressure pickup (drain holes closed) to produce a 100 knot indication, the total pressure lag error constant (λ_T) can be determined by measuring the time required for the indicator to drop to 37 knots when the pressure is removed. Generally the λ_T will be much smaller than the λ_S because of the smaller volume of the airspeed instrument case.

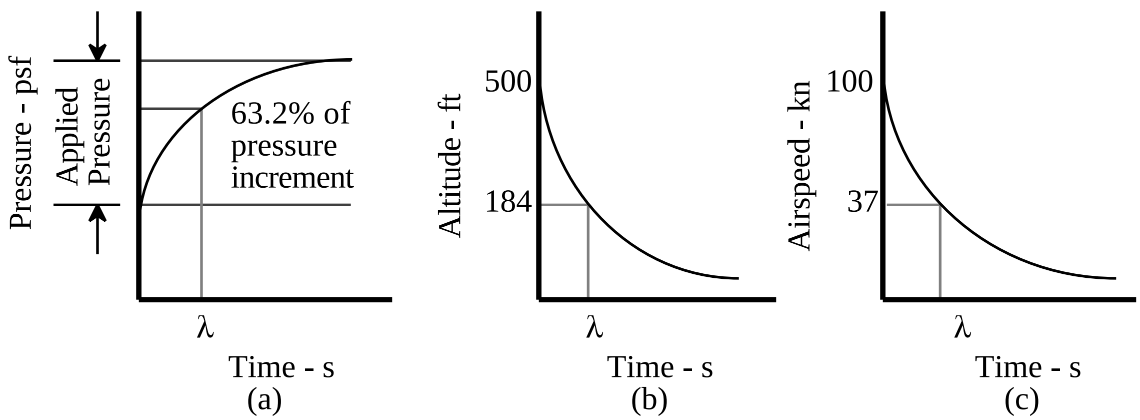

Figure 2.7
PITOT STATIC SYSTEM LAG ERROR CONSTANT

2.3.7.2.2 SYSTEM BALANCING

The practical approach to lag error testing is to determine if a serious lag error exists, and to eliminate it where possible. To test for airspeed system balance, a small increment of pressure (0.1 inch water) is applied simultaneously to both the pitot and static systems. If the airspeed indicator does not fluctuate, the combined systems are balanced and no lag error exists in indicated airspeed data because the lag constants are matched. Movement of the airspeed pointer indicates additional volume is required in one of the systems. The addition of a balance volume (Figure 2.6) generally provides satisfactory airspeed indications. Balancing does not help the lag in the altimeter, as this difficulty is due to the length of the static system tubing. For instrumentation purposes, lag can be eliminated from the altimeter by remotely locating a static pressure recorder at the static port. The use of balanced airspeed systems and remote static pressure sensors is useful for flight testing.

2.3.7.3 POSITION ERROR

Determination of the pressure altitude and calibrated airspeed at which an aircraft is operating is dependent upon the measurement of free stream total pressure, P_T, and free stream ambient pressure, P_a, by the aircraft pitot static system. Generally, the pressures registered by the pitot static system differ from free stream pressures as a result of:

1. The existence of other than free stream pressures at the pressure source.
2. Error in the local pressure at the source caused by the pressure sensors.

The resulting error is called position error. In the general case, position error may result from errors at both the total and static pressure sources.

2.3.7.3.1 TOTAL PRESSURE ERROR

As an aircraft moves through the air, a static pressure disturbance is generated in the air, producing a static pressure field around the aircraft. At subsonic speeds, the flow perturbations due to the aircraft static pressure field are nearly isentropic and do not affect the total pressure. As long as the total pressure source is not located behind a propeller, in the wing wake, in a boundary layer, or in a region of localized supersonic flow, the pressure errors due to the position of the total pressure source are usually negligible. Normally, the total pressure source can be located to avoid total pressure error.

An aircraft capable of supersonic speeds should be equipped with a noseboom pitot static system so the total pressure source is located ahead of any shock waves formed by the aircraft. A noseboom is essential, since correcting for total pressure errors which result when oblique shock waves exist ahead of the pickup is difficult. The shock wave due to the pickup itself is considered in the calibration equation.

Failure of the total pressure sensor to register the local pressure may result from the shape of the pitot static head, inclination to the flow due to angle of attack, α, or sideslip angle, β, or a combination of both. Pitot static tubes are designed in varied shapes. Some are suitable only for relatively low speeds while others are designed to operate in supersonic flight. If a proper design is selected and the pitot tube is not damaged, there should be no error in total pressure due to the shape of the probe. Errors in total pressure caused by the angle of incidence of a probe to the relative wind are negligible for most flight conditions. Commonly used probes produce no significant errors at angles of attack or sideslip up to approximately 20˚. With proper placement, design, and good leak checks of the pitot probe, zero total pressure error is assumed.

2.3.7.3.2 STATIC PRESSURE ERROR

The static pressure field surrounding an aircraft in flight is a function of speed and altitude as well as the secondary parameters, angle of attack, Mach, and Reynold's number. Finding a location for the static pressure source where free stream ambient pressure is sensed under all flight conditions is seldom possible. Therefore, an error generally exists in the measurement of the static pressure due to the position of the static pressure source.

At subsonic speeds, finding some location on the fuselage where the static pressure error is small under all flight conditions is often possible. Aircraft limited to subsonic speeds are instrumented with a flush static pressure ports in such a location.

On supersonic aircraft a noseboom installation is advantageous for measuring static pressure. At supersonic speeds, when the bow wave is located downstream of the static pressure sources, there is no error due to the aircraft pressure field. Any error which may exist is a result of the probe itself. Empirical data suggests free stream static pressure is sensed if the static ports are located more than 8 to 10 tube diameters behind the nose of the pitot static tube and 4 to 6 diameters in front of the shoulder of the pitot tube.

In addition to the static pressure error introduced by the position of the static pressure sources in the pressure field of the aircraft, there may be error in sensing the local static pressure due to flow inclination. Error due to sideslip is minimized by locating flush mounted static ports on opposite sides of the fuselage. For nosebooms, circumferential location of the static pressure ports reduces the adverse effect of sideslip and angle of attack.

2.3.7.3.3 DEFINITION OF POSITION ERROR

The pressure error at the static source has the symbol, ΔP, and is defined as:

$$\Delta P = P_s - P_a \tag{Eq 2.38}$$

The errors associated with ΔP are the position errors. Airspeed position error, ΔV_{pos}, is:

$$\Delta V_{pos} = V_c - V_i \tag{Eq 2.39}$$

Altimeter position error, ΔH_{pos}, is:

$$\Delta H_{pos} = H_{P_c} - H_{P_i} \tag{Eq 2.40}$$

Mach position error, ΔM_{pos}, is:

$$\Delta M_{pos} = M - M_i \tag{Eq 2.41}$$

Where:

ΔH_{pos}	Altimeter position error	ft
ΔM_{pos}	Mach position error	
ΔP	Static pressure error	psf
ΔV_{pos}	Airspeed position error	kn
H_{P_c}	Calibrated pressure altitude	ft
H_{P_i}	Indicated pressure altitude	ft
M	Mach number	
M_i	Indicated Mach number	
P_a	Ambient pressure	psf
P_s	Static pressure	psf
V_c	Calibrated airspeed	kn
V_i	Indicated airspeed	kn.

The definitions result in the position error having the same sign as ΔP. If P_s is greater than P_a, the airspeed indicator indicates a lower than actual value. Therefore, ΔP and ΔV_{pos} are positive in order to correct V_i to V_c. The correction is similar for ΔH_{pos} and ΔM_{pos}.

2.3.7.3.4 STATIC PRESSURE ERROR COEFFICIENT

Dimensional analysis shows the relation of static pressure (P_s) at any point in an aircraft pressure field to the free stream ambient pressure (P_a) depends on Mach (M), angle of attack (α), sideslip angle (β), and Reynold's number (R_e):

$$\frac{P_s}{P_a} = f_1 \left(M, \alpha, \beta, R_e \right) \qquad \text{(Eq 2.42)}$$

Reynold's number effects are negligible as the static source is not located in a thick boundary layer, and small sideslip angles are assumed. The relation simplifies to:

$$\frac{P_s}{P_a} = f_2 \left(M, \alpha \right) \qquad \text{(Eq 2.43)}$$

This equation can be generalized as follows:

$$\frac{\Delta P}{q_c} = f_3 \left(M, \alpha \right) \qquad \text{(Eq 2.44)}$$

The term $\frac{\Delta P}{q_c}$ is the static pressure error coefficient and is used in position error data reduction. Position error data presented as $\frac{\Delta P}{q_c}$ define a single curve for all altitudes.

For flight test purposes the static pressure error coefficient is approximated as:

$$\frac{\Delta P}{q_c} = f_4 \left(M \right) \text{ (High speed)} \qquad \text{(Eq 2.45)}$$

$$\frac{\Delta P}{q_c} = f_5 \left(C_L \right) \text{ (Low speed)} \qquad \text{(Eq 2.46)}$$

For the high speed case, the indicated relationship is:

$$\frac{\Delta P}{q_{c_i}} = f_6\left(M_i\right) \text{ (High speed)} \tag{Eq 2.47}$$

The high speed indicated static pressure error coefficient is presented as a function of indicated Mach number in figure 2.8.

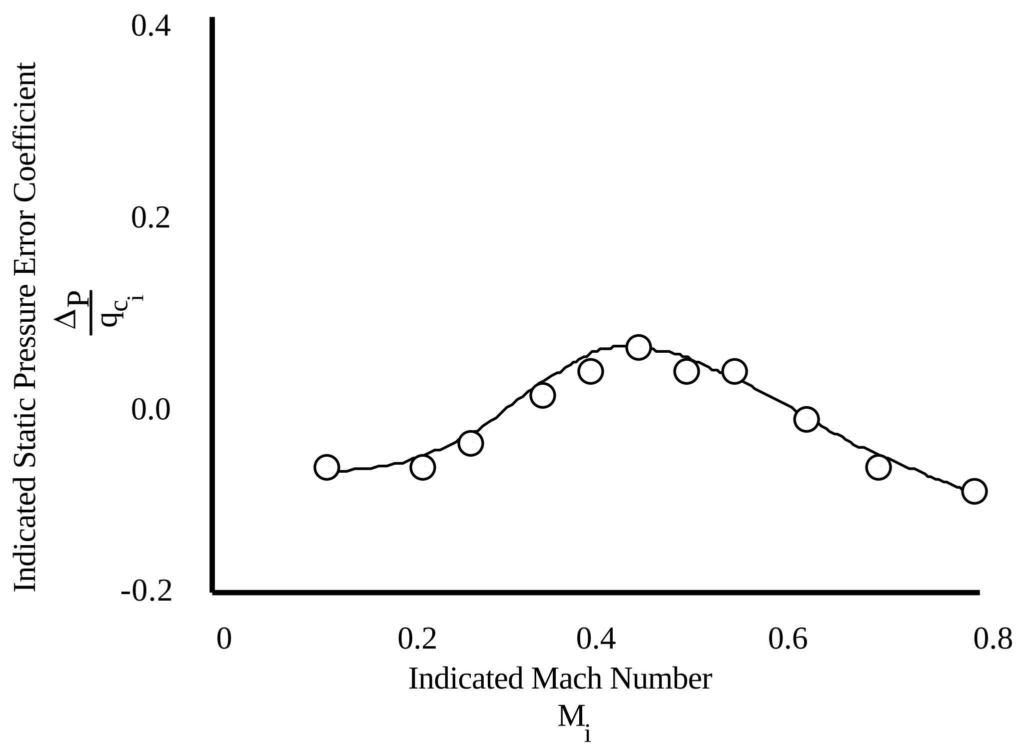

Figure 2.8
HIGH SPEED INDICATED STATIC PRESSURE ERROR COEFFICIENT

For the low speed case, where $C_L = f\ (W,\ n_z,\ V_e)$; and assuming $n_z = 1$ and $V_e \cong V_c$ then:

$$\frac{\Delta P}{q_c} = f_7\left(W, V_c\right) \text{ (Low speed)} \tag{Eq 2.48}$$

The number of independent variables is reduced by relating test weight, W_{Test}, to standard weight, W_{Std}, as follows:

$$V_{c_W} = V_{c_{Test}} \sqrt{\frac{W_{Std}}{W_{Test}}} \qquad \text{(Eq 2.49)}$$

Therefore, the expression for the static pressure error coefficient is:

$$\frac{\Delta P}{q_c} = f_8 \left(V_{c_W} \right) \text{ (Low speed)} \qquad \text{(Eq 2.50)}$$

For the indicated variables, the low speed relationships are:

$$V_{i_W} = V_{i_{Test}} \sqrt{\frac{W_{Std}}{W_{Test}}} \qquad \text{(Eq 2.51)}$$

$$\frac{\Delta P}{q_{c_i}} = f_9 \left(V_{i_W} \right) \text{ (Low speed)} \qquad \text{(Eq 2.52)}$$

Where:

α	Angle of attack	deg
β	Sideslip angle	deg
C_L	Lift coefficient	
ΔP	Static pressure error	psf
$\frac{\Delta P}{q_c}$	Static pressure error coefficient	
$\frac{\Delta P}{q_{c_i}}$	Indicated static pressure error coefficient	
M	Mach number	
M_i	Indicated Mach number	
n_z	Normal acceleration	g
P_a	Ambient pressure	psf
P_s	Static pressure	psf
q_c	Impact pressure	psf
q_{c_i}	Indicated impact pressure	psf

R_e	Reynold's number	
V_c	Calibrated airspeed	kn
$V_{c_{Test}}$	Test calibrated airspeed	kn
V_{c_W}	Calibrated airspeed corrected to standard weight	kn
V_e	Equivalent airspeed	kn
$V_{i_{Test}}$	Test indicated airspeed	kn
V_{i_W}	Indicated airspeed corrected to standard weight	kn
W	Weight	lb
W_{Std}	Standard weight	lb
W_{Test}	Test weight	lb.

The low speed indicated static pressure error coefficient is presented as a function of indicated airspeed corrected to standard weight in figure 2.9.

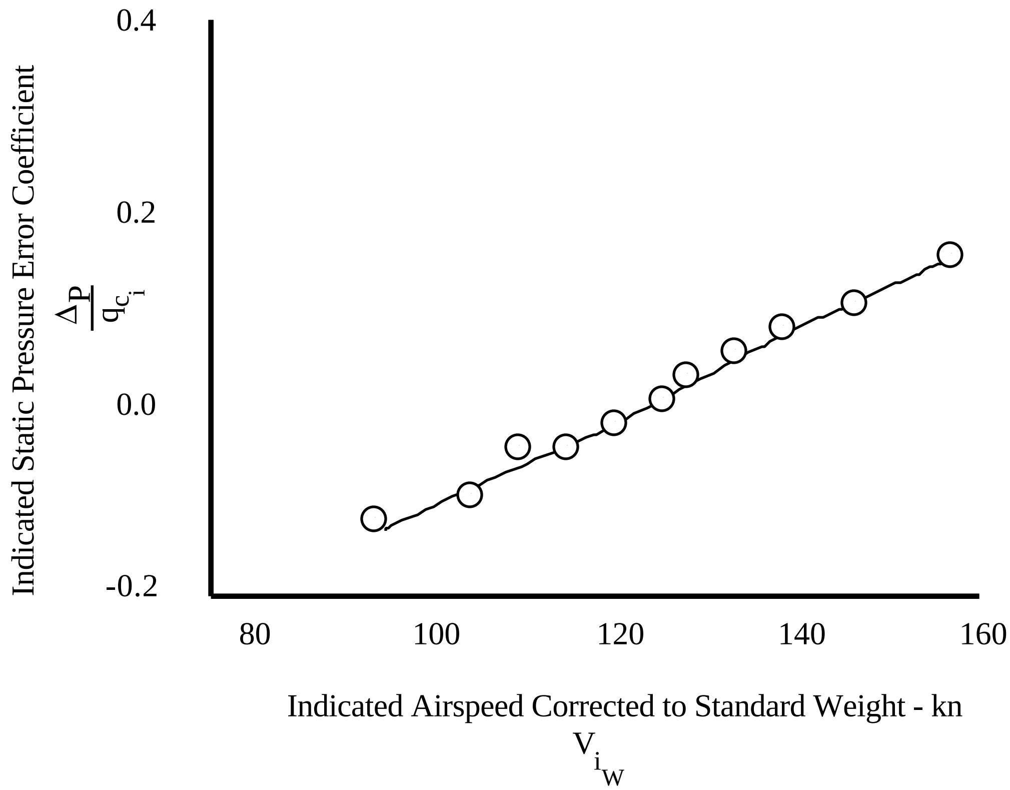

Figure 2.9
LOW SPEED INDICATED STATIC PRESSURE ERROR COEFFICIENT

2.3.8 PITOT TUBE DESIGN

The part of the total pressure not sensed through the pitot tube is referred to as pressure defect, and is a function of angle of attack. However, pressure defect is also a function of Mach number and orifice diameter. As explained in reference 4, the total pressure defect increases as the angle of attack or sideslip angle increases from zero; decreases as Mach number increases subsonically; and decreases as the ratio of orifice diameter to tube outside diameter increases. In general, if the ratio of orifice diameter to tube diameter is equal to one, the total pressure defect is zero up to angles of attack of 25 degrees. As the diameter ratio decreases to 0.74, the defect is still insignificant. But as the ratio of diameters decreases to 0.3, there is approximately a 5 percent total pressure defect at 15 degrees angle of attack, 12 percent at 20 degrees, and 22 percent at 25 degrees. For given values of orifice diameter and tube diameter, with an elongated nose shape, the elongation is equivalent to an effective increase in the ratio of diameters and the magnitude of the total pressure defect will be less than is indicated above for a hemispherical head. These pitot tube design guidelines are general rules for accurate sensing of total pressure. All systems must be evaluated in flight test, but departure from these proven design parameters should prompt particular interest.

2.3.9 FREE AIR TEMPERATURE MEASUREMENT

Knowledge of ambient temperature in flight is essential for true airspeed measurement. Accurate temperature measurement is needed for engine control systems, fire control systems, and weapon release computations.

From the equations derived for flow stagnation conditions, total temperature, T_T, is expressed as:

$$\frac{T_T}{T} = 1 + \frac{\gamma - 1}{2} M^2 \tag{Eq 2.53}$$

Expressed in terms of true airspeed:

$$\frac{T_T}{T} = 1 + \frac{\gamma - 1}{2} \frac{V_T^2}{\gamma\, g_c\, R\, T} \tag{Eq 2.54}$$

These temperature relations assume adiabatic flow or no addition or loss of heat while bringing the flow to stagnation. Isentropic flow is not required. Therefore, Eq 2.53 and 2.54 are valid for supersonic and subsonic flows. If the flow is not perfectly adiabatic, a temperature recovery factor, K_T, is used to modify the kinetic term as follows:

$$\frac{T_T}{T} = 1 + \frac{K_T\left(\gamma - 1\right)}{2} M^2 \qquad \text{(Eq 2.55)}$$

$$\frac{T_T}{T} = 1 + \frac{K_T\left(\gamma - 1\right)}{2} \frac{V_T^2}{\gamma\, g_c\, R\, T} \qquad \text{(Eq 2.56)}$$

If the subscripts are changed for the case of an aircraft and the appropriate constants are used:

$$\frac{T_T}{T_a} = \frac{T_i}{T_a} = 1 + \frac{K_T M^2}{5} \qquad \text{(Eq 2.57)}$$

$$T_T = T_i = T_a + \frac{K_T V_T^2}{7592} \qquad \text{(Eq 2.58)}$$

Where:

g_c	Conversion constant	32.17 lb_m/slug
γ	Ratio of specific heats	
K_T	Temperature recovery factor	
M	Mach number	
R	Engineering gas constant for air	96.93 ft-lb_f/lb_m-˚K
T	Temperature	˚K
T_a	Ambient temperature	˚K
T_i	Indicated temperature	˚K
T_T	Total temperature	˚K
V_T	True airspeed	kn.

The temperature recovery factor, K_T, indicates how closely the total temperature sensor observes the total temperature. The value of K_T varies from 0.7 to 1.0. For test systems a range of 0.95 to 1.0 is common. There are a number of errors possible in a temperature indicating system. In certain installations, these may cause the recovery factor to vary with airspeed. Generally, the recovery factor is a constant value. The following are the more significant errors:

1. Resistance - Temperature Calibration. Generally, building a resistance temperature sensing element which exactly matches the prescribed resistance - temperature curve is not possible. A full calibration of each probe is made, and the instrument correction, ΔT_{ic}, applied to the data.

2. Conduction Error. A clear separation between recovery errors and errors caused by heat flow from the temperature sensing element to the surrounding structure is difficult to make. This error can be reduced by insulating the probe. Data shows this error is small.

3. Radiation Error. When the total temperature is relatively high, heat is radiated from the sensing element, resulting in a reduced temperature indication. This effect is increased at very high altitude. Radiation error is usually negligible for well designed sensors when Mach is less than 3.0 and altitude is below 40,000 feet.

4. Time Constant. The time constant is defined as the time required for a certain percentage of the response to an instantaneous change in temperature to be indicated on the instrument. When the temperature is not changing or is changing at an extremely slow rate, the time constant introduces no error. Practical application of a time constant in flight is extremely difficult because of the rate of change of temperature with respect to time. The practical solution is to use steady state testing.

2.3.9.1 TEMPERATURE RECOVERY FACTOR

The temperature recovery system has two errors which must be accounted for, instrument correction, ΔT_{ic}, and temperature recovery factor, K_T. Although ΔT_{ic} is called instrument correction, it accounts for many system errors collectively from the indicator to the temperature probe. The ΔT_{ic} correction is obtained under controlled laboratory conditions.

The temperature recovery factor, K_T, measures the temperature recovery process adiabatically. A value of 1.0 for K_T is ideal, but values greater than 1.0 are observed when heat is added to the sensors by conduction (hot material around the sensor) or radiation (exposure to direct sunlight). The test conditions must be selected to minimize this type of interference.

Normally, temperature probe calibration can be done simultaneously with pitot static calibration. Indicated temperature, instrument correction, aircraft true Mach, and an accurate ambient temperature are the necessary data. The ambient temperature is obtained from a reference source such as a pacer aircraft, weather balloon, or tower thermometer. Accurate ambient temperature may be difficult to obtain on a tower fly-by test because of steep temperature gradients near the surface.

The temperature recovery factor at a given Mach may be computed as follows:

$$T_i = T_o + \Delta T_{ic} \tag{Eq 2.59}$$

$$K_T = \left(\frac{T_i\ (^\circ K)}{T_a\ (^\circ K)} - 1 \right) \frac{5}{M^2} \tag{Eq 2.60}$$

Where:

ΔT_{ic}	Temperature instrument correction	˚C
K_T	Temperature recovery factor	
M	Mach number	
T_a	Ambient temperature	˚C or ˚K
T_i	Indicated temperature	˚C or ˚K
T_o	Observed temperature	˚C.

2.4 TEST METHODS AND TECHNIQUES

The objective of pitot static calibration test is to determine position error in the form of the static pressure error coefficient. From the static pressure error coefficient, ΔV_{pos} and ΔH_{pos} are determined. The test is designed to produce an accurate calibrated pressure altitude (H_{P_c}), calibrated velocity (V_c), or Mach (M), for the test aircraft. Position error is sensitive to Mach, configuration, and perhaps angle of attack depending upon the type of static source. Choose the test method to take advantage of the capability of the instrumentation. Altimeter position error (ΔH_{pos}) is usually evaluated because H_{P_c} is fairly easy to determine, and the error can be read more accurately on the altimeter.

The test methods for calibrating pitot and static systems are numerous and often a test is known by several different titles within the aviation industry. Often, more than one system requires calibration, such as separate pilot, copilot, and flight test systems. Understanding the particular system plumbing is important for calibrating the required systems. The most common calibration techniques are presented and discussed briefly. Do not overlook individual instrument calibration in these tests. Leak check pitot static systems prior to calibration test programs.

One important part of planning for any flight test is the data card. Organize the card to assist the crew during the flight and emphasize the most important flight parameters. Match the inputs for a computer data reduction program to the order of test parameters. H_{P_o} is read first because it is the critical parameter, and the other parameters are listed in order of decreasing sensitivity. The tower operator's data card includes the tower elevation and the same run numbers with columns for theodolite reading, time, temperature, and tower pressure altitude. The time entry allows correlation between tower and flight data points. Include space on both cards for repeated or additional data points.

There are a few considerations for pilot technique during pitot static calibration flights. During stabilized points, fly the aircraft in coordinated flight, with the altitude and angle of attack held steady. Pitch bobbling or sideslip induce error, so resist making last second corrections. A slight climb or descent may cause the pilot to read the wrong altitude, particularly if there is any delay in reading the instrument. When evaluating altimeter position error, read the altimeter first. A slight error in the airspeed reading will not have much effect.

2.4.1 MEASURED COURSE

The measured course method is an airspeed calibration which requires flying the aircraft over a course of known length to determine true airspeed (V_T) from time and distance data. Calibrated airspeed, calculated from true airspeed, is compared to the indicated airspeed to obtain the airspeed position error. The conversion of true airspeed to calibrated airspeed requires accurate ambient temperature data. The validity of this test method is predicated on several important parameters:

1. Accuracy of elapsed time determination.
2. Accuracy of course measurement and course length.
3. A constant airspeed over the course.
4. Wind conditions.
5. Accurate temperature data.

Measurement of elapsed time is important and is one of the first considerations when preparing for a test. Elapsed time can be measured with extremely accurate electronic devices. On the other end of the spectrum is the human observer with a stopwatch.

Flying a measured course requires considerable pilot effort to maintain a stabilized airspeed for a prolonged period of time in close proximity to the ground. The problems involved in this test are a function of the overall aircraft flying qualities and vary with different aircraft. Averaging or integrating airspeed fluctuations is not conducive to accurate results. The pilot must maintain flight with small airspeed variations for some finite period of time at a given airspeed. This period of time is generally short on the backside of the level flight power polar. An estimate of the maximum time which stable airspeeds can be maintained for the particular aircraft is made to establish the optimum course length for the different airspeeds to be evaluated.

Ideally, winds should be calm when using the measured course. Data taken with winds can be corrected, provided wind direction and speed are constant. Wind data is collected for each data point using calibrated sensitive equipment located close to the ground speed course. In order to determine the no wind curve, runs are made in both directions (reciprocal headings). All runs must be flown on the course heading, allowing the aircraft to drift with the wind as shown in figure 2.10.

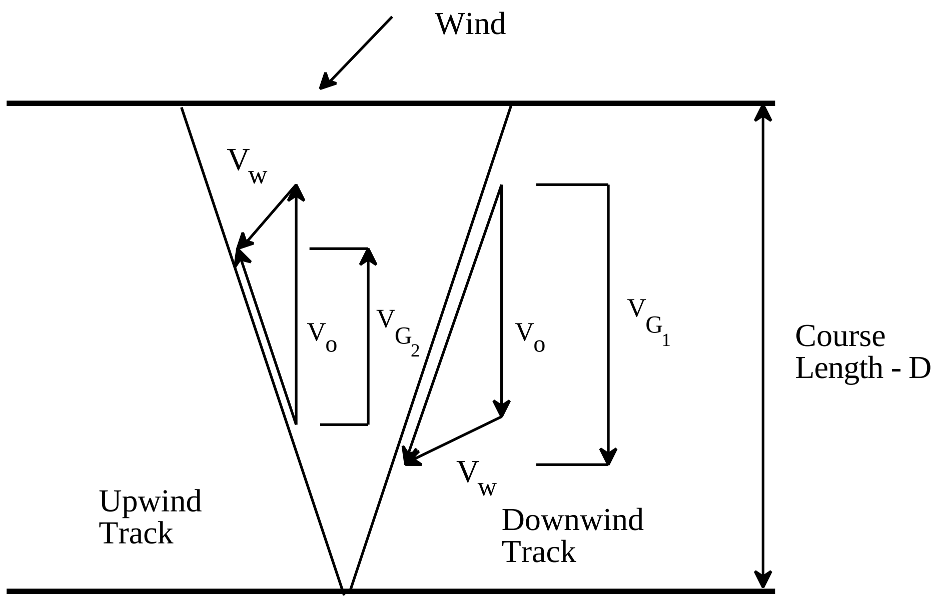

Figure 2.10
WIND EFFECT

True airspeed is determined by averaging the ground speeds. Calibrated airspeed is calculated using standard atmosphere relationships. This method of airspeed and altimeter system calibration is limited to level flight data point calibrations.

The speed course may vary in sophistication from low and slow along a runway or similarly marked course to high and fast when speed is computed by radar or optical tracking.

2.4.1.1 DATA REQUIRED

D, Δt, V_o, H_{P_o}, T_o, GW, $T_{a\ ref}$, $H_{P\ ref}$

Configuration

Wind data.

2.4.1.2 TEST CRITERIA

1. Coordinated, wings level flight.
2. Constant aircraft heading.
3. Constant airspeed.

4. Constant altitude.
5. Constant wind speed and direction.

2.4.1.3 DATA REQUIREMENTS

1. Stabilize 10 s prior to course start.
2. Record data during course length.
3. $V_o \pm 0.5$ kn.
4. $H_{P_o} \pm 20$ ft over course length.

2.4.1.4 SAFETY CONSIDERATIONS

Since these tests are conducted in close ground proximity, the flight crew must maintain frequent visual ground contact. The concentration required to fly accurate data points sometimes distracts the pilot from proper situational awareness. Often these tests are conducted over highly uniform surfaces (water or dry lake bed courses), producing significant depth perception hazards.

2.4.2 TRAILING SOURCE

Static pressure can be measured by suspending a static source on a cable and comparing the results directly with the static systems installed in the test aircraft. The trailing source static pressure is transmitted through tubes to the aircraft where it is converted to accurate pressure altitude by sensitive, calibrated instruments. Since the pressure from the source is transmitted through tubes to the aircraft for conversion to altitude, no error is introduced by trailing the source below the aircraft. The altimeter position error for a given flight condition can be determined directly by subtracting the trailing source altitude from the altitude indicated by the aircraft system. The trailing source cable should be a minimum of 2 wing spans in length, with as small an outside diameter as practical, and a rough exterior finish. The maximum speed of this test method may be limited to the speed at which the trailing source becomes unstable. Depending upon the frequency of the cable oscillation and the resultant maximum displacement of the towed source, large errors may be introduced into the towed source measurements. These errors are reflected as scatter. In addition to the errors induced by the tube oscillations, a fin stabilized source, once disturbed, tends to fly by itself and may move up into the downwash or wing vortices.

The test aircraft is stabilized prior to recording a data point; however, the trailing source may or may not be stable when the data is recorded. Therefore, a means must be provided to monitor the trailing source. When using a trailing source, record data when the aircraft and source are both stabilized in smooth air.

Since there is no method of predicting the point of instability of these trailing systems, monitor the trailing source continuously and plan the flight to accomplish moderate speed data points first and progress in a build-up fashion toward the higher speed points. Trailing source systems are known to exhibit instabilities at both very low speeds and high speeds. There are two main types of trailing sources, the trailing bomb and the trailing cone.

2.4.2.1 TRAILING BOMB

The aircraft static pressure, P_s, is compared directly with the ambient pressure, P_a, measured by a static source on a bomb shaped body suspended on a long length of pressure tubing below the aircraft. The trailing bomb, like the aircraft, may have a static source error. This error is determined by calibration in a wind tunnel.

The length of tubing required to place the bomb in a region where local static pressure approximates free stream pressure is at least twice the aircraft wing span. Since the bomb is below the aircraft, the static pressure is higher, but the pressure lapse in the tubing is the same as the free stream atmospheric pressure lapse. Thus, if the static source in the bomb is attached to an altimeter next to the aircraft, it indicates free stream pressure at altimeter level.

Accuracy depends upon the calibration of the bomb and the accuracy of the pressure gauge or altimeter used to read the trailing bomb's static pressure. Stability of the bomb at speeds above 0.5 Mach must also be considered.

2.4.2.2 TRAILING CONE

With the trailing cone method, the aircraft's static pressure, P_s, is compared to the ambient pressure, P_a, measured by a static source trailing behind the aircraft. A light weight cone is attached to the tube to stabilize it and keep the pressure tube taut.

The accuracy depends on the location of the static ports which should be at least six diameters ahead of the cone. The distance behind the aircraft is also important. The aircraft's pitot static instruments are calibrated with the trailing cone in place by tower fly-by or pace methods. These results are used to calibrate the cone installation. The cone can be used with good results as a calibration check of that aircraft's instruments or primary calibration of an aircraft of the same model.

2.4.2.3 DATA REQUIRED

V_o, H_{P_o}, $H_{P_{o\ ref}}$, T_o, GW, Configuration.

Note: Velocity and altitude data must be recorded for each system to be calibrated as well as the trailing source system (reference data).

2.4.2.4 TEST CRITERIA

1. Coordinated, wings level flight.
2. Constant aircraft heading.
3. Constant airspeed.
4. Constant altitude.
5. Steady indications on airspeed and altimeter systems.

2.4.2.5 DATA REQUIREMENTS

1. Stabilize 30 s prior to data record.
2. Record data for 15 s.
3. $V_o \pm 0.5$ kn.
4. $H_{P_o} \pm 10$ ft.

2.4.2.6 SAFETY CONSIDERATIONS

Considerable flight crew or flight and ground crew coordination is required to deploy and recover a trailing source system safely. Thorough planning and detailed pre-flight briefing are essential to ensure that each individual knows the proper procedure.

Trailing source instability stories are numerous. When these devices will exhibit unstable tendencies is difficult to predict. Factors such as probe design, cable length, airspeed, aircraft vibration levels, and atmospheric turbulence influence the onset of these instabilities. Monitor trailing source devices at all times. Chase aircraft normally accomplish this function. Under most circumstances, the onset of the instability is of sufficiently low frequency and amplitude so that corrective action can be taken. In the event the probe starts to exhibit unstable behavior, return to a flight condition which was previously satisfactory. If the instability grows to hazardous proportions, jettison the probe. Jettison devices vary in complexity and must be ground checked by the flight crew to ensure complete familiarity with procedures and proper operation.

2.4.3 TOWER FLY-BY

This method is a simple and excellent way to determine accurately static system error. A tall tower of known height is required as an observation point. The free stream static pressure can be established in any number of ways (such as a sensitive calibrated altimeter in the tower) and is recorded for each pass of the test aircraft. The test aircraft is flown down a predetermined track passing at a known distance (d) from the tower (Figure 2.11). Any deviation in the height of the aircraft above the tower (Δh) is determined by visual observation and simple geometry. The simplicity of this method allows a large number of accurate data points to be recorded quickly and inexpensively.

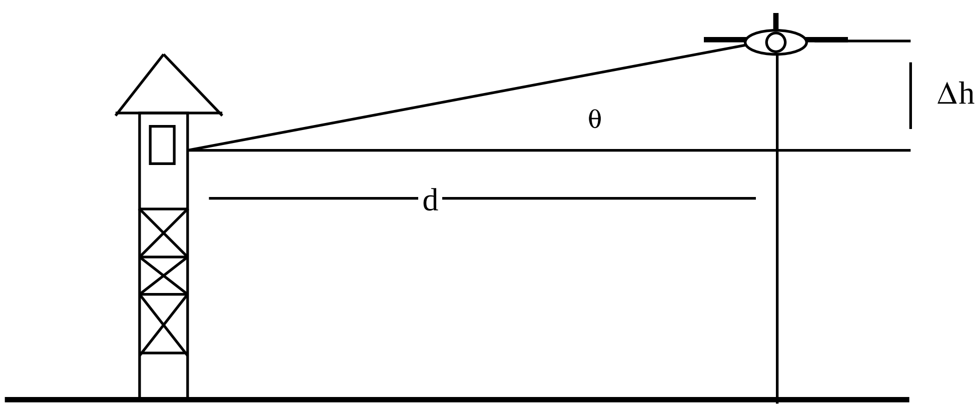

Figure 2.11
TOWER FLY-BY

It is important to ensure there is no false position error introduced during this test as a result of instrument calibration errors. Prior to the flight, with the test aircraft in a static condition, the reference instrument, used to establish the ambient pressure in the tower, is placed next to the aircraft test instrumentation. With both of these instruments in the same environment (and with their respective instrument corrections applied), the indications should be the same. If there is a discrepancy, the difference in readings is included in the data reduction.

The tower fly-by produces a fairly accurate calibrated pressure altitude, H_{P_c}, by triangulation. The aircraft is sighted through a theodolite and the readings are recorded along with tower pressure altitude on each pass.

An alternate method to determine the height of the aircraft above the tower (Δh) is to obtain a grid Polaroid photograph similar to the one in figure 2.12. The height of the aircraft above the tower is determined from the scaled length of the aircraft (x), scaled height of the aircraft above the tower (y), and the known length of the aircraft ($L_{a/c}$). Any convenient units of measure can be used for x and y. This photographic method of determining Δh has the advantage of not requiring the pilot to fly precisely over the predetermined track, thereby compensating for errors in (d) from figure 2.11.

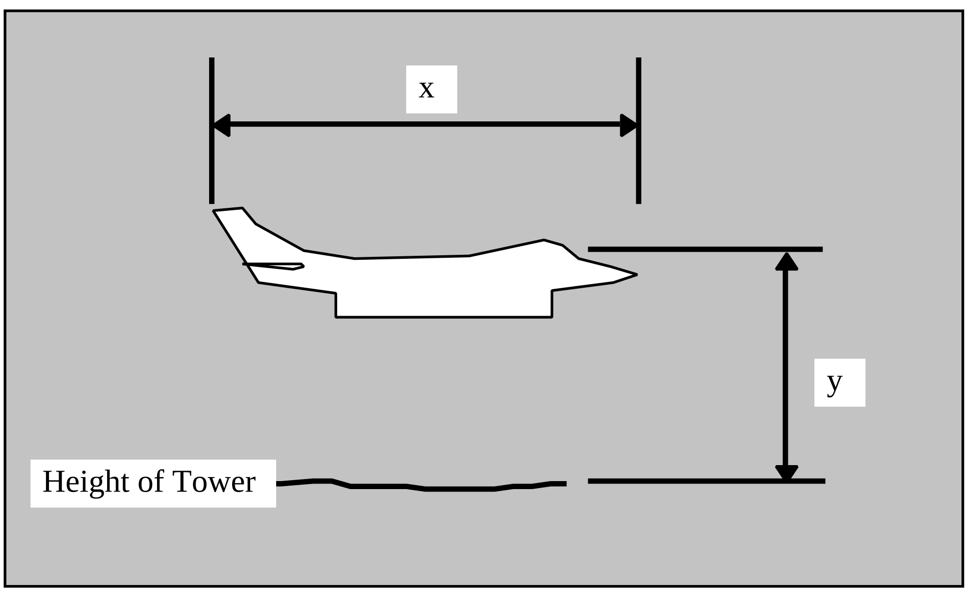

Figure 2.12
SAMPLE TOWER PHOTOGRAPH

The calibrated altitude of the aircraft is the sum of the pressure altitude of the theodolite at the time the point was flown plus the tapeline height above the tower corrected for nonstandard temperature.

Although the tower fly-by method is simple, accurate, and requires no sophisticated equipment, it has some disadvantages. It does not produce an accurate calibrated velocity, it is limited to subsonic flight, and angle of attack changes due to decreasing gross weight may affect the data. Angle of attack effects are most prevalent at low speeds, and all low speed points are flown as close to the same gross weight as possible. Make runs at least one wing span above the ground to remain out of ground effect.

2.4.3.1 DATA REQUIRED

V_o, H_{P_o}, $H_{P_{c\,twr}}$, T_o, $T_{a\,ref}$, GW, Configuration.

Note: Velocity and altitude data must be recorded for each system to be calibrated as well as tower reference pressure altitude, temperature, and aircraft geometric height data (d,θ).

2.4.3.2 TEST CRITERIA

1. Coordinated, wings level flight.
2. Constant heading and track over predetermined path.
3. Constant airspeed.
4. Constant altitude.

2.4.3.3 DATA REQUIREMENTS

1. Stabilize 15 s prior to abeam tower.
2. $V_o \pm 0.5$ kn.
3. $H_{P_o} \pm 10$ ft.
5. Ground track ± 1% of stand-off distance.

2.4.3.4 SAFETY CONSIDERATIONS

This test procedure requires considerable pilot concentration. Maintain situational awareness. Complete familiarity with normal and emergency aircraft procedures prevent excessive pilot distractions. Team work and well briefed/rehearsed data collection procedures also minimize distractions.

Most courses of this type are over highly uniform terrain such as water or dry lake beds, contributing to poor depth perception. A second crew member or ground safety observer can share backup altitude monitoring duties.

2.4.4 SPACE POSITIONING

Space positioning systems vary with respect to principle of operation. Automatic or manual optical tracking systems, radar tracking, and radio ranging systems fall into this category. A space positioning arrangement generally employs at least three tracking stations. These tracking stations track the test aircraft by radar lock or by a manual/visual sight arrangement. Depending upon the configuration, angular and linear displacements are recorded. Through a system of triangulation a computer solution of tapeline altitude and ground speed is obtained. The accuracy of the data can be increased by compensating for tracking errors developed as a result of the random drift away from a prearranged target point on the aircraft. Accuracy can be improved by using an on-board transponder to enhance the tracking process. Regardless of the tracking method, raw data is reduced using computer programs to provide position, velocity, and acceleration information. Normally the test aircraft is flown over a prearranged course to provide the station with a good target and the optimum tracking angles.

Depending on the accuracy desired and the existing wind conditions, balloons can be released and tracked to determine wind velocity and direction. Wind information can be fed into the solution for each data point and true airspeed determined. The true airspeed is used to determine calibrated airspeed and position error.

The use of space positioning systems requires detailed planning and coordination. Exact correlation between onboard and ground recording systems is essential. These systems are generally in high demand by programs competing for resource availability and priority. Due to the inherent complexities of hardware and software, this technique is expensive. The great value of this method is that large amounts of data can be obtained in a short time. Another aspect which makes these systems attractive is the wide variety of flight conditions which can be calibrated, such as climbs and descents. Accelerating and decelerating maneuvers can be time correlated if the data systems are synchronized.

The space positioning radar method is used primarily for calibrations at airspeeds unsuitable for tower fly-by or pacer techniques (i.e., transonic and supersonic speeds). The procedure requires an accurate radar-theodolite system and a pacer aircraft. If a pacer is unavailable, then the position error of the test aircraft must be known for one value of airspeed at the test altitude.

An important aspect of this method is the pressure survey required before the test calibration can be done. To do this, the pace aircraft flies at constant airspeed and altitude through the air mass to be used by the test aircraft. The radar continuously measures the pacer's tapeline altitude from start to finish of the survey. Since the altimeter position error of the pacer is known, the actual pressure altitude flown is known. The pressure altitude of the test aircraft is the tapeline difference between the test and pace aircraft corrected for non-standard temperature.

As soon as possible after completion of the pressure survey, the test aircraft follows the pacer aircraft through the air mass along the same ground track. A tracking beacon is required in the test aircraft, for both accurate radar ranging and to allow ground controllers to provide course corrections when necessary.

Because this method is used for transonic and supersonic portions of the calibration test, an accurate time correlation is necessary to properly relate radar data to aircraft instrumentation data.

2.4.4.1 DATA REQUIRED

V_o, H_{P_o}, T_o, GW, Configuration.

2.4.4.2 TEST CRITERIA

1. Coordinated, wings level flight.
2. Constant aircraft heading.
3. Constant airspeed.
4. Constant altitude.
5. Constant wind speed and direction.

2.4.4.3 DATA REQUIREMENTS

1. Stabilized 30 s prior to data record.
2. Record data for 15 s.
3. $V_o \pm 0.5$ kn.
4. $H_{P_o} \pm 10$ ft.

2.4.4.4 SAFETY CONSIDERATIONS

Knowledge of and adherence to normal and emergency operating procedures, limitations, and range safety requirements.

2.4.5 RADAR ALTIMETER

A calibrated radar altimeter can be used to determine altimeter position errors present in level flight at low altitude. A level runway or surface is required to establish a reference altitude for the test. A sensitive pressure altimeter is placed at the runway elevation during test runs. To determine position errors, the radar height is added to the runway pressure altitude and compared with the aircraft altimeter system indication. The aircraft altimeter may be used as the reference altimeter if the aircraft is landed on the runway reference point. The service system altimeter reading before and after the test runs can be used to establish a base pressure altitude to which the radar height is added. This method is recommended only for rough approximation of gross altimeter position errors. Flight above the level surface is conducted low enough to provide accurate height information with the radar altimeter, but not so low the pressure field around the aircraft is affected by ground proximity. A good guideline is generally one wing span.

2.4.5.1 DATA REQUIRED

Surface pressure altitude, V_o, H_{P_o}, T_o, GW, radar altitude. Configuration.

2.4.5.2 TEST CRITERIA

1. Coordinated, wings level flight.
2. Constant aircraft heading.
3. Constant airspeed.

4. Constant radar altimeter altitude.

2.4.5.3 DATA REQUIREMENTS

1. Stabilized flight for 15 s.
2. $V_o \pm 0.5$ kn.
3. $H_{P_o} \pm 10$ ft.
4. Radar altimeter altitude ± 3 ft.

2.4.5.4 SAFETY CONSIDERATIONS

The safety considerations relevant to this test are similar to those discussed for the measured course method.

2.4.6 PACED

The use of a pace calibration system offers many advantages and is used frequently in obtaining position error calibrations. Specially outfitted and calibrated pace aircraft are used for this purpose. These pace aircraft generally have expensive, specially designed, separate pitot static systems which are extensively calibrated. These calibrations are kept current and periodically cross-checked on speed courses or with space positioning equipment. These pace calibration aircraft systems, when properly maintained and documented, offer the tester a method of obtaining accurate position error information in a short period of time.

The test method requires precise formation flying. The pace aircraft can be lead or trail, depending on individual preference. The lead aircraft establishes the test point by stabilizing on the desired data point. The trail aircraft must stay close enough to the lead aircraft to detect minor relative speed differences but far enough away to prevent pitot static interference between aircraft systems and/or compromising flight safety. Experience shows good results are obtained by flying one wing span abeam, placing the two aircraft out of each others pressure field. Formation flight is used so the airspeed and altimeter instruments of both aircraft are at the same elevation.

Leak checks of all pitot static systems including the pace aircraft systems, is required prior to and following calibration flights. Many pace systems provide two separate calibration systems to further guarantee data accuracy.

The pacer aircraft provides the test aircraft with calibrated pressure altitude, H_{P_c}, and calibrated airspeed, V_c, at each test point. This method of calibration takes less flight time and can cover any altitude and airspeed as long as the two aircraft are compatible.

2.4.6.1 DATA REQUIRED

V_o, H_{P_o}, T_o, $V_{o\ ref}$, $H_{P_{o\ ref}}$, $T_{o\ ref}$, GW, Configuration.

Note: Velocity and altitude data must be recorded for each system to be calibrated as well as pace aircraft data.

2.4.6.2 TEST CRITERIA

1. Coordinated, wings level flight.
2. Constant heading.
3. Constant airspeed.
4. Constant altitude (or stable rate of change during climbs and descents).
5. No relative motion between the test and pace aircraft.

2.4.6.3 DATA REQUIREMENTS

1. Stabilize 30 s prior to data collection.
2. Record data for 15 s.
3. $V_o \pm 0.5$ kn.
4. $H_{P_o} \pm 10$ ft.

2.4.6.4 SAFETY CONSIDERATIONS

All the hazards of close formation flying are present with the pace calibration method. To reduce this risk, practice and teamwork are required. In addition to the workload present with formation flying, considerable attention must be directed toward accurately reading altimeter, airspeed, and other instruments. These increased risk factors may be mitigated by providing automatic data collection and/or an additional crew member to collect the necessary information while the pilot directs his attention to safe formation flight. Again, careful planning, a good mission briefing, and professional execution significantly decrease the inherent risks associated with these tests. Minimum safe calibration altitudes provide sufficient allowance for ejection/bailout. Be alert to the potential for mid-air collision and have a flight break-up procedure established. Minimum visual flight conditions are established in the planning phase (such as, 3 miles visibility and 1000 foot cloud clearance), and inadvertent instrument meteorological condition break-up procedures are established. Pilots of both aircraft must be aware of the minimum control airspeeds for their particular aircraft in each of the various configurations required during the test and some margin provided for formation maneuvering. As in all flight tests, normal and emergency operating procedures and limitations must be known. Upon completion of tests, a method of flight break-up or section recovery is used. At no time during these tests should there be a question in anyone's mind who is responsible for providing safe separation distance between aircraft.

2.5 DATA REDUCTION

2.5.1 MEASURED COURSE

The following equations are used for measured course data reduction:

$$V_i = V_o + \Delta V_{ic} \qquad \text{(Eq 2.37)}$$

$$V_{G_1} = 3600 \left(\frac{D}{\Delta t_1} \right) \qquad \text{(Eq 2.61)}$$

$$V_{G_2} = 3600 \left(\frac{D}{\Delta t_2} \right) \qquad \text{(Eq 2.62)}$$

$$V_T = \frac{V_{G_1} + V_{G_2}}{2} \qquad \text{(Eq 2.63)}$$

$$\rho_a = \frac{P_a}{g_c \, R \, T_{a_{ref}} \ (^\circ K)} \qquad \text{(Eq 2.64)}$$

$$\sigma = \frac{\rho_a}{\rho_{ssl}} \qquad \text{(Eq 2.65)}$$

$$V_e = V_T \sqrt{\sigma} \qquad \text{(Eq 2.26)}$$

$$V_c = V_e - \Delta V_c \qquad \text{(Eq 2.66)}$$

$$\Delta V_{pos} = V_c - V_i \qquad \text{(Eq 2.39)}$$

$$M = \frac{V_T}{38.9678 \sqrt{T_{a_{ref}} \; (^\circ K)}} \qquad \text{(Eq 2.67)}$$

$$T_i = T_o + \Delta T_{ic} \qquad \text{(Eq 2.59)}$$

$$K_T = \left(\frac{T_i \; (^\circ K)}{T_{a_{ref}} \; (^\circ K)} - 1 \right) \frac{5}{M^2} \qquad \text{(Eq 2.60)}$$

$$q_c = P_{ssl} \left\{ \left[1 + 0.2 \left(\frac{V_c}{a_{ssl}} \right)^2 \right]^{3.5} - 1 \right\} \qquad \text{(Eq 2.68)}$$

$$q_{c_i} = P_{ssl} \left\{ \left[1 + 0.2 \left(\frac{V_i}{a_{ssl}} \right)^2 \right]^{3.5} - 1 \right\} \qquad \text{(Eq 2.69)}$$

$$\Delta P = q_c - q_{c_i} \qquad \text{(Eq 2.70)}$$

$$V_{i_W} = V_i \sqrt{\frac{W_{Std}}{W_{Test}}} \qquad \text{(Eq 2.71)}$$

Where:

a_{ssl}	Standard sea level speed of sound	661.483 kn
D	Course length	nmi
ΔP	Static pressure error	psf
Δt	Elapsed time	s
ΔT_{ic}	Temperature instrument correction	˚C
ΔV_c	Compressibility correction	kn
ΔV_{ic}	Airspeed instrument correction	kn
ΔV_{pos}	Airspeed position error	kn
g_c	Conversion constant	32.17 lb_m/slug
K_T	Temperature recovery factor	
M	Mach number	
P_a	Ambient pressure	psf
P_{ssl}	Standard sea level pressure	2116.217 psf
q_c	Impact pressure	psf
q_{c_i}	Indicated impact pressure	psf
R	Engineering gas constant for air	96.93 ft-lb_f/lb_m ˚K
ρ_a	Ambient air density	slug/ft^3
ρ_{ssl}	Standard sea level air density	0.0023769 slugs/ft^3
σ	Density ratio	
T_a	Ambient temperature	˚C
$T_{a\ ref}$	Reference ambient temperature	˚C or ˚K
T_i	Indicated temperature	˚C
T_o	Observed temperature	˚C
V_c	Calibrated airspeed	kn
V_e	Equivalent airspeed	kn
V_G	Ground speed	kn
V_i	Indicated airspeed	kn
V_{i_W}	Indicated airspeed corrected to standard weight	kn
V_o	Observed airspeed	kn
V_T	True airspeed.	kn
W_{Std}	Standard weight	lb
W_{Test}	Test weight	lb.

From the observed and reference airspeed, altitude, and temperature data, compute V_{i_W}, ΔV_{pos}, K_T, $\frac{\Delta P}{q_{c_i}}$ as follows:

Step	Parameter	Notation	Formula	Units	Remarks
1	Observed airspeed	V_o		kn	
2	Airspeed instrument correction	ΔV_{ic}		kn	Lab calibration
3	Indicated airspeed	V_i	Eq 2.37	kn	
4	Elapsed time$_1$	Δt_1		s	One direction
5	Elapsed time$_2$	Δt_2		s	Reciprocal direction
6	Course length	D		nmi	Known distance
7	Ground speed$_1$	V_{G_1}	Eq 2.61	kn	One direction
8	Ground speed$_2$	V_{G_2}	Eq 2.62	kn	Reciprocal direction
9	True airspeed	V_T	Eq 2.63	kn	
10	Reference pressure altitude	$H_{P\ ref}$		ft	Reference altimeter at ground course, corrections applied
11	Ambient pressure	P_a		psf	From Appendix VI or calculated using 10
12	Ambient air density	ρ_a	Eq 2.64	slug/ft^3	
13	Density ratio	σ	Eq 2.65		
14	Equivalent airspeed	V_e	Eq 2.26	kn	
15	Compressibility correction	ΔVc		kn	From Appendix VII, or assumed 0 for low altitude/airspeed
16	Calibrated airspeed	V_c	Eq 2.66	kn	
17	Airspeed position error	ΔV_{pos}	Eq 2.39	kn	
18	Mach number	M	Eq 2.67		
19	Observed temperature	T_o		˚C	
20	Temperature instrument correction	ΔT_{ic}		˚C	Lab calibration

21	Indicated temperature	T_i	Eq 2.59	˚C
22	Temperature recovery factor	K_T	Eq 2.60	
23	Impact pressure	q_c	Eq 2.68	psf
24	Indicated impact pressure	q_{c_i}	Eq 2.69	psf
25	Static pressure error	ΔP	Eq 2.70	psf
26	Indicated airspeed corrected to standard weight	V_{i_W}	Eq 2.71	kn

Plot indicated static pressure error coefficient, $\frac{\Delta P}{q_{c_i}}$, as a function of indicated airspeed corrected to standard weight, V_{i_W}, as shown in figure 2.9.

Plot airspeed position error, ΔV_{pos}, versus indicated airspeed corrected to standard weight, V_{i_W}, as shown in figure 2.13.

2.5.2 TRAILING SOURCE/PACED

The following equations are used in the trailing source/paced data reduction:

$$H_{P_i} = H_{P_o} + \Delta H_{P_{ic}} \quad \text{(Eq 2.36)}$$

$$H_{P_{i_{ref}}} = H_{P_{o_{ref}}} + \Delta H_{P_{ic_{ref}}} \quad \text{(Eq 2.72)}$$

$$H_{P_i} = \frac{T_{ssl}}{a_{ssl}}\left[1 - \left(\frac{P_s}{P_{ssl}}\right)^{\frac{1}{\left(\frac{g_{ssl}}{g_c\, a_{ssl}\, R}\right)}}\right] \quad \text{(Eq 2.73)}$$

$$H_{P_{i_{ref}}} = \frac{T_{ssl}}{a_{ssl}} \left[1 - \left(\frac{P_a}{P_{ssl}} \right)^{\frac{1}{\left(\frac{g_{ssl}}{g_c \, a_{ssl} \, R} \right)}} \right] \tag{Eq 2.74}$$

$$\Delta P = P_s - P_a \tag{Eq 2.38}$$

$$V_i = V_o + \Delta V_{ic} \tag{Eq 2.37}$$

$$q_{c_i} = P_{ssl} \left\{ \left[1 + 0.2 \left(\frac{V_i}{a_{ssl}} \right)^2 \right]^{3.5} - 1 \right\} \tag{Eq 2.69}$$

$$V_{i_W} = V_i \sqrt{\frac{W_{Std}}{W_{Test}}} \tag{Eq 2.71}$$

Where:

a_{ssl}	Standard sea level speed of sound	661.483 kn
a_{ssl}	Standard sea level temperature lapse rate	0.0019812 ˚K/ft
$\Delta H_{P_{ic}}$	Altimeter instrument correction	ft
$\Delta H_{P_{ic\ ref}}$	Reference altimeter instrument correction	ft
ΔP	Static pressure error	psf
ΔV_{ic}	Airspeed instrument correction	kn
g_c	Conversion constant	32.17 lb_m/slug
g_{ssl}	Standard sea level gravitational acceleration	32.174049 ft/s^2
H_{P_i}	Indicated pressure altitude	ft
$H_{P_{i\ ref}}$	Reference indicated pressure altitude	ft
H_{P_o}	Observed pressure altitude	ft
$H_{P_{o\ ref}}$	Reference observed pressure altitude	ft
P_a	Ambient pressure	psf

P_s	Static pressure	psf
P_{ssl}	Standard sea level pressure altitude	2116.217 psf
q_{c_i}	Indicated impact pressure	psf
R	Engineering gas constant for air	96.93 ft-lb_f/lb_m-˚K
T_{ssl}	Standard sea level temperature	15˚C or 288.15˚K
V_i	Indicated airspeed	kn
V_{i_W}	Indicated airspeed corrected to standard weight	kn
V_o	Observed airspeed	kn
W_{Std}	Standard weight	lb
W_{Test}	Test weight	lb.

From the observed and reference airspeed and altitude data, compute V_{i_W} and $\frac{\Delta P}{q_{c_i}}$ as follows:

Step	Parameter	Notation	Formula	Units	Remarks
1	Observed pressure altitude	H_{P_o}		ft	
2	Altimeter instrument correction	$\Delta H_{P_{ic}}$		ft	Lab calibration
3	Indicated pressure altitude	H_{P_i}	Eq 2.36	ft	
4	Reference observed pressure altitude	$H_{P_{o\ ref}}$		ft	From reference source
5	Reference altimeter instrument correction	$\Delta H_{P_{ic\ ref}}$		ft	Lab calibration
6	Reference indicated pressure altitude	$H_{P_{i\ ref}}$	Eq 2.72	ft	
7	Static pressure	P_s	Eq 2.73	psf	Calculated, or from Appendix VI using H_{P_i}
8	Ambient pressure	P_a	Eq 2.74	psf	Calculated, or from Appendix VI using $H_{P_{i\ ref}}$
9	Static pressure error	ΔP	Eq 2.38	psf	
10	Observed airspeed	V_o		kn	

11	Airspeed instrument correction	ΔV_{ic}		kn	Lab calibration
12	Indicated airspeed	V_i	Eq 2.37	kn	
13	Indicated impact pressure	q_{c_i}	Eq 2.69	psf	
14	Standard weight	W_{Std}		lb	Specification weight or mission relevant weight
15	Test weight	W_{Test}		lb	
16	Indicated airspeed corrected to standard weight	V_{i_W}	Eq 2.71	kn	

Plot indicated static pressure error coefficient, $\frac{\Delta P}{q_{c_i}}$, as a function of indicated airspeed corrected to standard weight, V_{i_W}, as shown in figure 2.9.

2.5.3 TOWER FLY-BY

The following equations are used in the tower fly-by data reduction:

$$V_i = V_o + \Delta V_{ic} \qquad \text{(Eq 2.37)}$$

$$H_{P_i} = H_{P_o} + \Delta H_{P_{ic}} \qquad \text{(Eq 2.36)}$$

$$\Delta h = d \tan\theta \qquad \text{(Eq 2.75)}$$

$$\Delta h = L_{a/c} \frac{y}{x} \qquad \text{(Eq 2.76)}$$

$$H_{P_c} = H_{P_{c_{twr}}} + \Delta h \frac{T_{Std}\ (^\circ K)}{T_{Test}\ (^\circ K)} \qquad \text{(Eq 2.77)}$$

$$P_s = P_{ssl} \left(1 - 6.8755856 \times 10^{-6} H_{P_i} \right)^{5.255863} \qquad \text{(Eq 2.78)}$$

$$P_a = P_{ssl}\left(1 - 6.8755856 \times 10^{-6}\, H_{P_c}\right)^{5.255863} \qquad \text{(Eq 2.79)}$$

$$\Delta P = P_s - P_a \qquad \text{(Eq 2.38)}$$

$$q_{c_i} = P_{ssl}\left\{\left[1 + 0.2\left(\frac{V_i}{a_{ssl}}\right)^2\right]^{3.5} - 1\right\} \qquad \text{(Eq 2.69)}$$

$$V_{i_W} = V_i \sqrt{\frac{W_{Std}}{W_{Test}}} \qquad \text{(Eq 2.71)}$$

Where:

a_{ssl}	Standard sea level speed of sound	661.483 kn
d	Horizontal distance (Tower to aircraft)	ft
Δh	Aircraft height above tower	ft
$\Delta H_{P_{ic}}$	Altimeter instrument correction	ft
ΔP	Static pressure error	psf
ΔV_{ic}	Airspeed instrument correction	kn
H_{P_c}	Calibrated pressure altitude	ft
$H_{P_{c\,twr}}$	Tower calibrated pressure altitude	ft
H_{P_i}	Indicated pressure altitude	ft
H_{P_o}	Observed pressure altitude	ft
$L_{a/c}$	Length of aircraft	ft
P_a	Ambient pressure	psf
P_s	Static pressure	psf
P_{ssl}	Standard sea level pressure	2116.217 psf
θ	Angle (Aircraft above tower reference line)	deg
q_{c_i}	Indicated impact pressure	psf
T_{Std}	Standard temperature (At tower)	˚K
T_{Test}	Test temperature (At tower)	˚K
V_i	Indicated airspeed	kn
V_{i_W}	Indicated airspeed corrected to standard weight	kn

V_o	Observed airspeed	kn
W_{Std}	Standard weight	lb
W_{Test}	Test weight	lb
x	Scaled length of aircraft	
y	Scaled height of aircraft above tower.	

From the observed airspeed, pressure altitude, and tower data, compute $\frac{\Delta P}{q_{c_i}}$ and V_{iW} as follows:

Step	Parameter	Notation	Formula	Units	Remarks
1	Observed airspeed	V_o		kn	
2	Airspeed instrument correction	ΔV_{ic}		kn	Lab calibration
3	Indicated airspeed	V_i	Eq 2.37	kn	
4	Observed pressure altitude	H_{P_o}		ft	
5	Altimeter instrument correction	$\Delta H_{P_{ic}}$		ft	Lab calibration
6	Indicated pressure altitude	H_{P_i}	Eq 2.36	ft	
7	Horizontal distance	d		ft	Tower to aircraft
8	Angle	θ		deg	Aircraft above tower reference line
9 a	Aircraft height above tower	Δh	Eq 2.75	ft	Tapeline altitude
9 b	Aircraft height above tower	Δh	Eq 2.76	ft	Tapeline altitude
10	Tower calibrated pressure altitude	$H_{P_{c\,twr}}$		ft	Tower calibrated altitude, corrections applied
11	Standard temperature	T_{Std}		˚K	Standard temperature at tower altitude
12	Test temperature	T_{Test}		˚K	Test temperature at tower attitude

13	Calibrated pressure altitude	H_{P_c}	Eq 2.77	ft	Tower calibrated pressure altitude plus temperature corrected tapeline altitude
14	Static pressure	P_s	Eq 2.78	psf	
15	Ambient pressure	P_a	Eq 2.79	psf	
16	Static pressure error	ΔP	Eq 2.38	psf	
17	Indicated impact pressure	q_{c_i}	Eq 2.69	psf	
18	Standard weight	W_{Std}		lb	
19	Test weight	W_{Test}		lb	
20	Indicated airspeed corrected to standard weight	V_{i_W}	Eq 2.71	kn	

Plot indicated static pressure error coefficient, $\frac{\Delta P}{q_{c_i}}$ as a function of indicated airspeed corrected to standard weight, V_{i_W}, as shown in figure 2.9.

2.5.4 TEMPERATURE RECOVERY FACTOR

Temperature recovery factor, K_T, can be determined as presented in Section 2.5.1 using Eq 2.60 when a reference ambient temperature is available or by using the following equations and method:

$$T_i = T_o + \Delta T_{ic} \quad \text{(Eq 2.59)}$$

$$\text{Curve slope} = K_T \frac{\gamma - 1}{\gamma} T_a = 0.2\ K_T\ T_a\ (^\circ K)\ \text{(High speed)} \quad \text{(Eq 2.80)}$$

$$\text{Curve slope} = K_T \frac{0.2\ T_a\ (^\circ K)}{a_{ssl}^2}\ \text{(Low speed)} \quad \text{(Eq 2.81)}$$

$$K_T = \frac{\text{slope}}{0.2\ T_a\ (^\circ K)}\ \text{(High speed)} \quad \text{(Eq 2.82)}$$

$$K_T = \frac{\text{slope } a_{ssl}^2}{0.2\, T_a\, (^\circ K)} \text{ (Low speed)} \qquad \text{(Eq 2.83)}$$

Where:

a_{ssl}	Standard sea level speed of sound	661.483 kn
ΔT_{ic}	Temperature instrument correction	˚C or ˚K
γ	Ratio of specific heats	
K_T	Temperature recovery factor	
T_a	Ambient temperature	˚C or ˚K.
T_i	Indicated temperature	˚C or ˚K
T_o	Observed temperature	˚C or ˚K.

Step	Parameter	Notation	Formula	Units	Remarks
1	Observed temperature	T_o		˚C or ˚K	
2	Temperature instrument correction	ΔT_{ic}		˚C or ˚K	Lab calibration
3	Indicated temperature	T_i	Eq 2.59	˚C or ˚K	
4	Mach	M			From tables for M versus V_c, H_{P_c}
5	Plot T_i versus M^2				High speed
5 a	Plot T_i versus V_c^2/δ				Low speed
6	Curve slope		Eq 2.80		High speed
6 a	Curve slope		Eq 2.81		Low speed
7	Ambient tempeature	T_a		˚K	T_a is the curve intercept
8	Temperature recovery factor	K_T	Eq 2.82		High speed
8 a	Temperature recovery factor	K_T	Eq 2.83		Low speed

2.6 DATA ANALYSIS

Once the indicated static pressure error coefficient, $\frac{\Delta P}{q_{c_i}}$ as a function of indicated airspeed corrected to standard weight, V_{i_W}, or M is determined by one of the test methods, airspeed position error, ΔV_{pos}, and altimeter position error, ΔH_{pos}, as a function of indicated airspeed corrected to standard weight, V_{i_W}, or M_i can be determined. The following equations are used:

$$P_s = P_{ssl}\left(1 - 6.8755856 \times 10^{-6} H_{P_i}\right)^{5.255863} \qquad \text{(Eq 2.78)}$$

$$q_{c_i} = P_{ssl}\left\{\left[1 + 0.2\left(\frac{V_i}{a_{ssl}}\right)^2\right]^{3.5} - 1\right\} \qquad \text{(Eq 2.69)}$$

$$M_i = \sqrt{\frac{2}{\gamma - 1}\left[\left(\frac{q_{c_i}}{P_s} + 1\right)^{\frac{\gamma - 1}{\gamma}} - 1\right]} \qquad \text{(Eq 2.84)}$$

$$V_{i_W} = V_i\sqrt{\frac{W_{Std}}{W_{Test}}} \qquad \text{(Eq 2.71)}$$

$$\Delta P = \left(\frac{\Delta P}{q_{c_i}}\right) q_{c_i} \qquad \text{(Eq 2.85)}$$

$$q_c = q_{c_i} + \Delta P \qquad \text{(Eq 2.86)}$$

$$V_c = \sqrt{\frac{2}{\gamma - 1}\frac{P_{ssl}}{\rho_{ssl}}\left[\left(\frac{q_c}{P_{ssl}} + 1\right)^{\frac{\gamma - 1}{\gamma}} - 1\right]} \qquad \text{(Eq 2.19)}$$

$$\Delta V_{pos} = V_c - V_{i_W} \quad \text{(Eq 2.87)}$$

$$P_a = P_s - \Delta P \quad \text{(Eq 2.88)}$$

$$H_{P_c} = \frac{T_{ssl}}{a_{ssl}} \left[1 - \left(\frac{P_a}{P_{ssl}} \right)^{\frac{1}{\left(\frac{g_{ssl}}{g_c\, a_{ssl}\, R} \right)}} \right] \quad \text{(Eq 2.89)}$$

$$\Delta H_{pos} = H_{P_c} - H_{P_i} \quad \text{(Eq 2.40)}$$

Where:

a_{ssl}	Standard sea level speed of sound	661.483 kn
a_{ssl}	Standard sea level temperature lapse rate	0.0019812 ˚K/ft
ΔH_{pos}	Altimeter position error	ft
ΔP	Static pressure error	psf
ΔV_{pos}	Airspeed position error	kn
γ	Ratio of specific heats	
g_c	Conversion constant	32.17 lb_m/slug
g_{ssl}	Standard sea level gravitational acceleration	32.174049 ft/s^2
H_{P_c}	Calibrated pressure altitude	ft
H_{P_i}	Indicated pressure altitude	ft
M_i	Indicated Mach	
P_a	Ambient pressure	psf
P_s	Static pressure	psf
P_{ssl}	Standard sea level pressure	2116.217 psf
q_c	Impact pressure	psf
q_{c_i}	Indicated impact pressure	Psf

R	Engineering gas constant for air	96.93 ft-lb_f/lb_m-˚K
ρ_{ssl}	Standard sea level air density	0.0023769 slug/ft^3
T_{ssl}	Standard sea level temperature	288.15 ˚K
V_c	Calibrated airspeed	kn
V_i	Indicated airspeed	kn
V_{i_W}	Indicated airspeed corrected to standard weight	kn
W_{Std}	Standard weight	lb
W_{Test}	Test weight	lb.

Airspeed position error, ΔV_{pos}, and altimeter position error, ΔH_{pos}, as a function of indicated Mach, M_i, or indicated airspeed, V_i, are determined from indicated static pressure error coefficient, $\frac{\Delta P}{q_{c_i}}$, as follows:

Step	Parameter	Notation	Formula	Units	Remarks
1	Indicated pressure altitude	H_{P_i}		ft	Select H_{P_i} of interest
2	Static pressure	P_s	Eq 2.78	psf	
3	Indicated airspeed	V_i		kn	Select V_i of interest
4	Indicated impact pressure	q_{c_i}	Eq 2.69	psf	
5	Indicated Mach	M_i	Eq 2.84		High speed case
5 a	Indicated airspeed corrected to standard weight	V_{i_W}	Eq 2.71	kn	Low speed case
6	Static pressure error coefficient	$\frac{\Delta P}{q_{c_i}}$			From figure 2.8, High speed case
6 a	Static pressure error coefficient	$\frac{\Delta P}{q_{c_i}}$			From figure 2.9, Low speed case
7	Static pressure error	ΔP	Eq 2.85	psf	
8	Impact pressure	q_c	Eq 2.86	psf	
9	Calibrated airspeed	V_c	Eq 2.19	kn	
10	Airspeed position error	ΔV_{pos}	Eq 2.87	kn	

11	Ambient pressure	P_a	Eq 2.88	psf	
12	Calibrated pressure altitude	H_{P_c}	Eq 2.89	ft	
13	Altimeter position error	ΔH_{pos}	Eq 2.40	ft	
14	Return to 3 and vary V_i				Repeat for a series of V_i at same H_{P_i}
15	Return to 1 and choose new H_{P_i}				Repeat for a series of V_i for new H_{P_i}

Plot ΔV_{pos} versus M_i (high speed case) or V_i (low speed case) and ΔH_{pos} versus M_i or V_i as shown in figures 2.13 and 2.14.

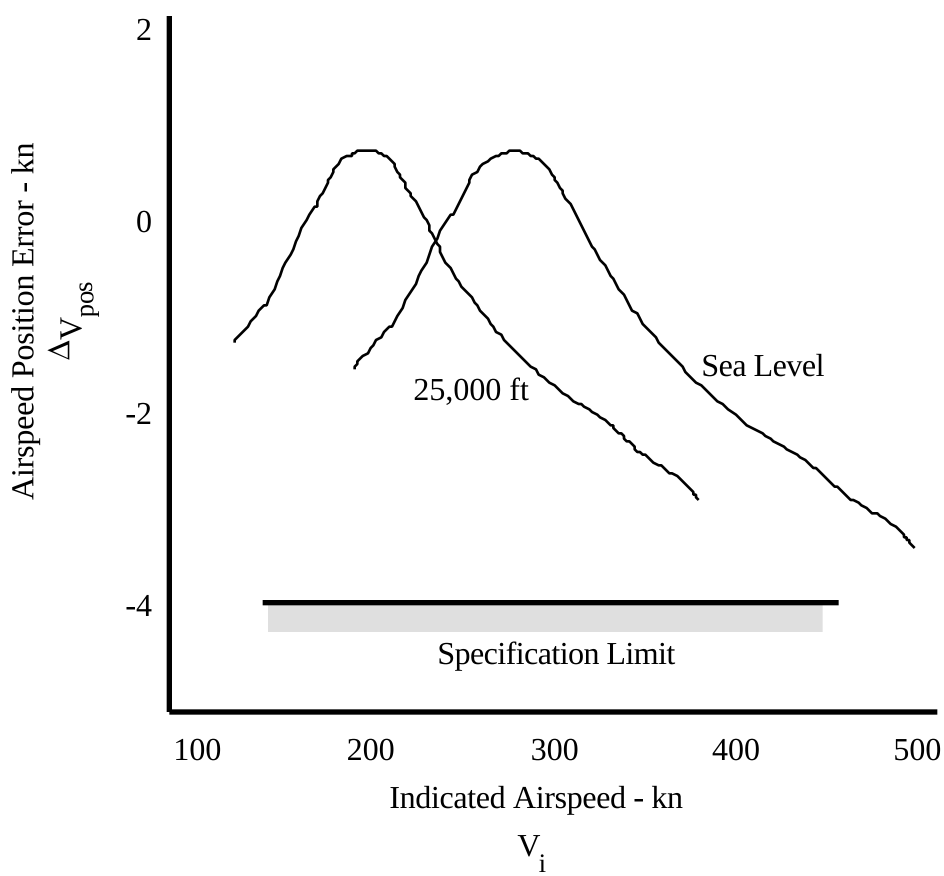

Figure 2.13
AIRSPEED POSITION ERROR

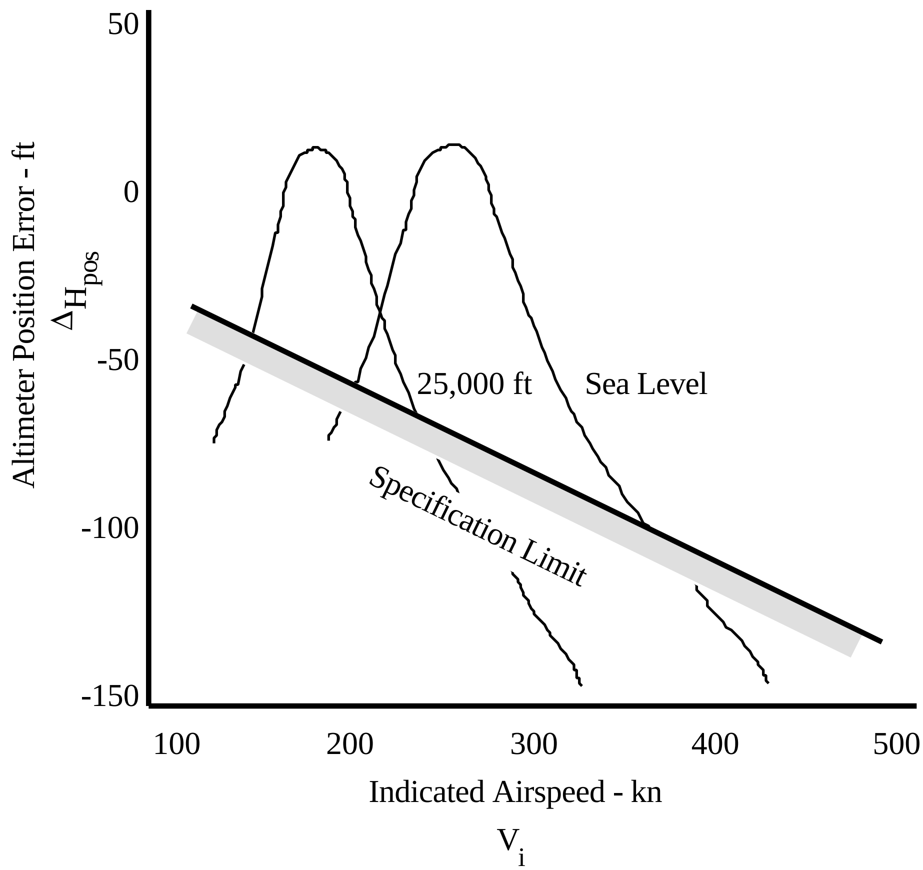

Figure 2.14
ALTIMETER POSITION ERROR

Analysis of pitot static system performance is done graphically. Superposition of the specification limits (Paragraph 2.8) on the data plots presented above identifies problems with system performance. Alternate configurations are evaluated when applicable. For each airspeed and altimeter calibration curve, be alert for discontinuities, large errors, and trends. Discontinuities, as in any primary flight instrument presentation, are not desirable.

Unbalanced pitot and static systems, large lag errors, indicator oscillations, and poor system performance at extreme flight conditions frequently are identified first with pilot qualitative comments. Unfavorable qualitative comments or unexplained difficulty in performing the airspeed calibration tasks can be an indication of pitot static system problems. Collection of quantitative data provides the opportunity to analyze qualitatively system performance.

2.7 MISSION SUITABILITY

The flight calibration of aircraft pitot and static systems is a very necessary and important test. A large measure of the accuracy of all performance and flying qualities evaluations depends on the validity of these calibration tests. Errors in the pitot static pressure systems may have serious implications considered with extreme speeds (high/low), maneuvering flight, and instrument flight rules (IFR) missions. The seriousness of the problem is compounded if pressure errors are transmitted to automatic flight control systems such as altitude retention systems or stability augmentation systems (SAS).

2.7.1 SCOPE OF TEST

The requirements of military specifications and the intended mission of the aircraft initially define the scope of the pitot and static system evaluation. The scope of the performance and flying qualities investigation may dictate an increase in the scope beyond that required above. This increase in scope may require flights at various external configurations and some testing may be required for calibration of the flight test instrumentation system alone. Generally, a flight check of the requirements of the specifications for maneuvering flight may be accomplished concurrently with the standard test.

The test pilot is responsible for observing and reporting undesirable characteristics in the pitot static system before they produce adverse results or degrade mission performance. When evaluating a pitot static system, the test team must consider the mission of the aircraft. Results of a pitot static system calibration attained at sea level may indicate satisfactory performance and specification compliance. However, operations at altitude may not be satisfactory.

2.8 SPECIFICATION COMPLIANCE

There are two military specifications which cover the requirements for pressure sensing systems in military aircraft. MIL-I-5072-1 covers all types of pitot static tube operated instrument systems (Figure 2.15) while MIL-I-6115A deals with instrument systems operated by a pitot tube and a flush static port (Figure 2.16). Both specifications describe in detail the requirements for construction and testing of these systems and state that one of the following methods of test will be used to determine "installation error" (position error):

1. "The speed course method."
2. "The suspended head or trailing tube method."
3. "The altimeter method."
4. "Pacer airplane method."

Federal Aviation Regulations (FAR) are directly applicable to ensure safe operation on the federal airways. These requirements are found in FAR Parts 27.1323 and 27.1335.

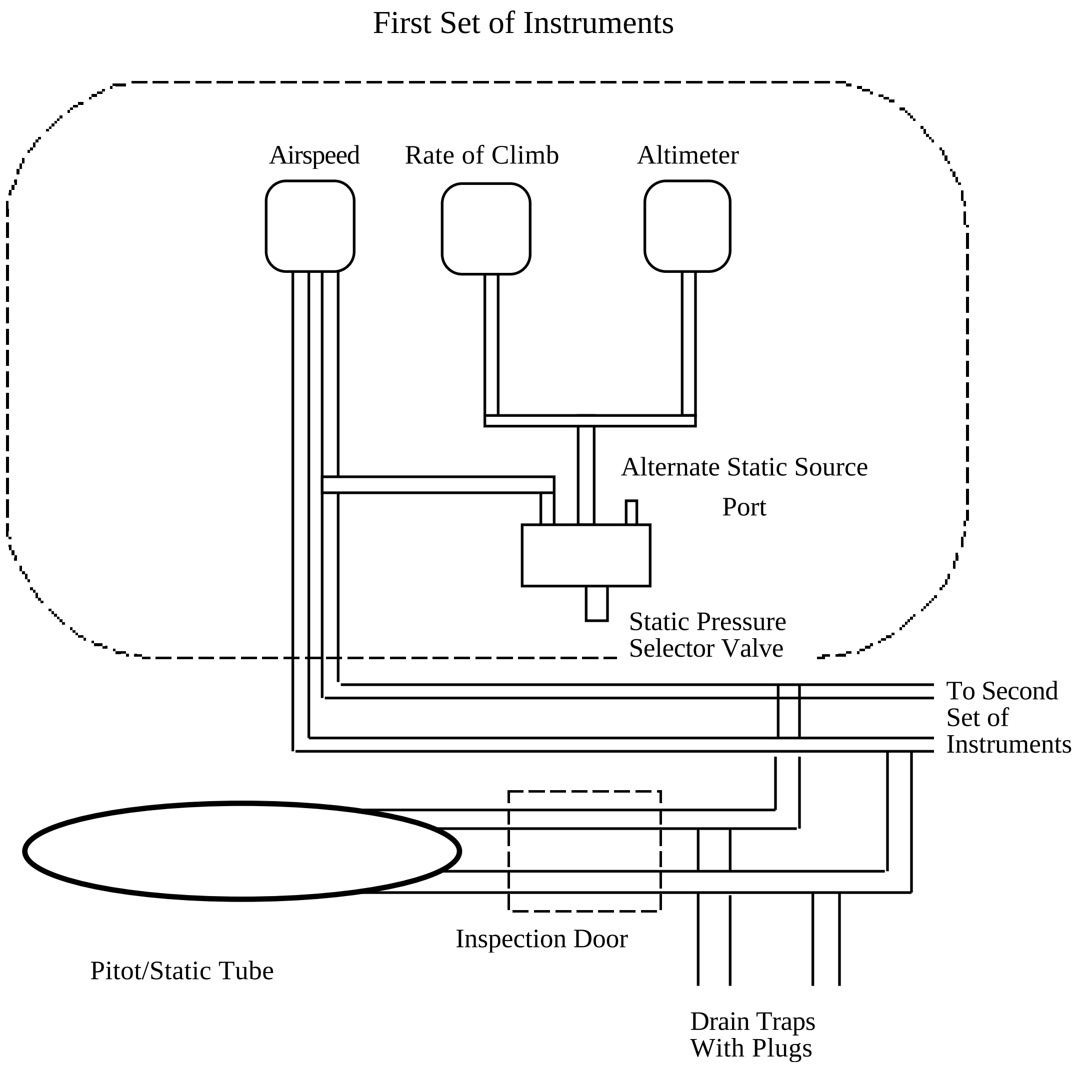

Figure 2.15

PITOT STATIC SYSTEM AS REFERRED TO IN MIL-I-5072-1

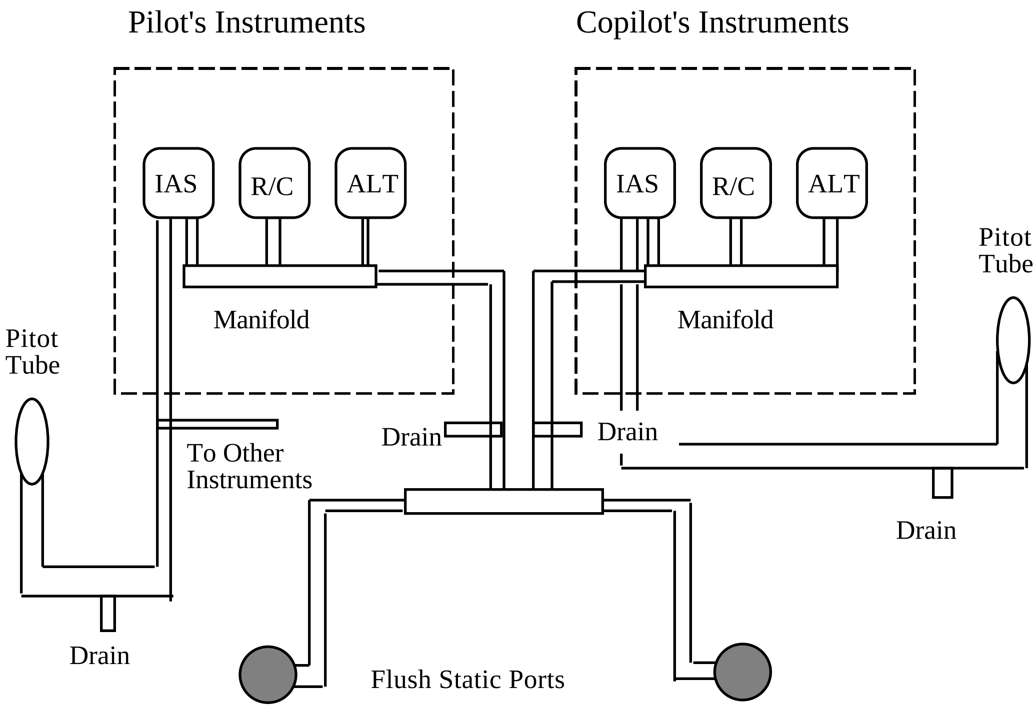

Figure 2.16
PITOT STATIC SYSTEM AS REFERRED TO IN MIL-I-6115A

2.8.1 TOLERANCES

Table 2.1, extracted from MIL-I-6115A, states the tolerance allowed on airspeed indicator and altimeter readings for five aircraft flight configurations, when corrected to standard sea level conditions.

Table 2.1

TOLERANCE ON AIRSPEED INDICATOR AND ALTIMETER READINGS

(Corrected to standard sea level condition 29.92 inHg and 15˚C)

Configuration	Speed Range	Gross Weight	Tolerances	
			Airspeed Indicator	Altimeter
Approach [1]	Stalling to 50 kn (58 mph) above stalling	Landing	± 4 kn ± 4.5 mph	25 ft per 100 KIAS
Approach [1]	Stalling to 50 kn (58 mph) above stalling	Normal	± 4 kn ± 4.5 mph	25 ft per 100 KIAS
Clean	Speed for maximum range to speed at normal rated power	Normal	± 1/2 % of indicated airspeed	25 ft per 100 KIAS
Clean	Stalling to maximum	Normal	± 4 kn ± 4.5 mph	25 ft per 100 KIAS
Clean	Stalling to maximum	Overload	± 4 kn ± 4.5 mph	25 ft per 100 KIAS
Dive	Maximum speed with brakes full open	Normal	± 6 kn ± 7 mph	50 ft per 100 KIAS

[1] The approach configuration shall include (in addition to wing flaps and landing gear down) such conditions as “canopy open”, “tail hook down”, etc., which may vary with or be peculiar to certain model airplanes.

2.8.2 MANEUVERS

There are four additional tests required by both military specifications which deal with the effect of maneuvers on pressure system operations. These tests are quite important and the descriptions of the test requirements are reprinted below as they appear in MIL-I-6115A.

2.8.2.1 PULLUP

“A rate of climb indicator shall be connected to the static pressure system of each pitot static tube (the pilot's and copilot's instruments may be used). The variation of static pressure during pullups from straight and level flight shall be determined at a safe altitude above the ground and at least three widely separated indicated airspeeds. During an abrupt “pullup” from level flight, the rate of climb indicator shall indicate “Up” without excessive hesitation and shall not indicate “Down” before it indicates “Up”.”

2.8.2.2 PUSHOVER

"A rate of climb indicator shall be connected to the static pressure system of each pitot static tube (the pilot's and copilot's instruments may be used). The variation of static pressure during pushover from straight and level flight shall be determined at a safe altitude above the ground and at least three widely separated indicated airspeeds. During an abrupt "pushover" from level flight, the rate of climb indicator shall indicate "Down" without excessive hesitation and shall not indicate "Up" before it indicates "Down"."

2.8.2.3 YAWING

"Sufficient maneuvering shall be done in flight to determine that the installation of the pitot static tube shall provide accurate static pressure to the flight instruments during yawing maneuvers of the airplane."

2.8.2.4 ROUGH AIR

"Sufficient maneuvering shall be done in flight to determine that the installation of the pitot static tube shall produce no objectionable instrument pointer oscillation in rough air. Pointer oscillation of the airspeed indicator shall not exceed 3 knots (4 mph)."

2.9 GLOSSARY

2.9.1 NOTATIONS

a	Speed of sound	kn
a	Temperature lapse rate	˚/ft
ARDC	Arnold Research and Development Center	
a_{ssl}	Standard sea level speed of sound	661.483 kn
a_{ssl}	Standard sea level temperature lapse rate	0.0019812 ˚K/ft
C_L	Lift coefficient	
D	Course length	nmi
d	Horizontal distance (Tower to aircraft)	ft
Δh	Aircraft height above tower	ft
$\Delta H_{P_{ic}}$	Altimeter instrument correction	ft

$\Delta H_{P_{ic\ ref}}$	Reference altimeter instrument correction	ft
ΔH_{pos}	Altimeter position error	ft
ΔM_{pos}	Mach position error	
ΔP	Static pressure error	psf
$\frac{\Delta P}{q_c}$	Static pressure error coefficient	
$\frac{\Delta P}{q_{c_i}}$	Indicated static pressure error coefficient	
Δt	Elapsed time	s
ΔT_{ic}	Temperature instrument correction	˚C
ΔV_c	Compressibility correction	kn
ΔV_{ic}	Airspeed instrument correction	kn
ΔV_{pos}	Airspeed position error	kn
e	Base of natural logarithm	
FAR	Federal Aviation Regulations	
g	Gravitational acceleration	ft/s^2
g_c	Conversion constant	32.17 $lb_m/slug$
g_{ssl}	Standard sea level gravitational acceleration	32.174049 ft/s^2
GW	Gross weight	lb
H	Geopotential	ft
h	Tapeline altitude	ft
H_P	Pressure altitude	ft
$H_{P\ ref}$	Reference pressure altitude	ft
H_{P_c}	Calibrated pressure altitude	ft
$H_{P_{c\ twr}}$	Tower calibrated pressure altitude	ft
H_{P_i}	Indicated pressure altitude	ft
$H_{P_{i\ ref}}$	Reference indicated pressure altitude	ft
H_{P_o}	Observed pressure altitude	ft
$H_{P_{o\ ref}}$	Reference observed pressure altitude	ft
IFR	Instrument flight rules	
K_T	Temperature recovery factor	
$L_{a/c}$	Length of aircraft	ft
M	Mach number	
M_i	Indicated Mach number	

M_{Test}	Test Mach number	
NACA	National Advisory Committee on Aeronautics	
n_z	Normal acceleration	g
P	Pressure	psf
P_a	Ambient pressure	psf
P_s	Static pressure	psf
P_{ssl}	Standard sea level pressure	2116.217 psf 29.9212 inHg
P_T	Total pressure	psf
P_T'	Total pressure at total pressure source	psf
q	Dynamic pressure	psf
q_c	Impact pressure	psf
q_{c_i}	Indicated impact pressure	psf
R	Engineering gas constant for air	96.93 ft-lb_f/lb_m-˚K
R_e	Reynold’s number	
SAS	Stability augmentation system	
T	Temperature	˚C or ˚K
T_a	Ambient temperature	˚C or ˚K
$T_{a\ ref}$	Reference ambient temperature	˚C or ˚K
T_i	Indicated temperature	˚C or ˚K
T_o	Observed temperature	˚C
T_{ssl}	Standard sea level temperature	15˚C or 288.15˚K
T_{Std}	Standard temperature (At tower)	˚K
T_T	Total temperature	˚K
T_{Test}	Test temperature (At tower)	˚K
USNTPS	U.S. Naval Test Pilot School	
V	Velocity	kn
V_c	Calibrated airspeed	kn
$V_{c_{Std}}$	Standard calibrated airspeed	kn
$V_{c_{Test}}$	Test calibrated airspeed	kn
V_{c_W}	Calibrated airspeed corrected to standard weight	kn
V_e	Equivalent airspeed	kn
$V_{e_{Std}}$	Standard equivalent airspeed	kn

$V_{e_{Test}}$	Test equivalent airspeed	kn
V_G	Ground speed	kn
V_i	Indicated airspeed	kn
$V_{i_{Test}}$	Test indicated airspeed	kn
V_{i_W}	Indicated airspeed corrected to standard weight	kn
V_o	Observed airspeed	kn
$V_{o\ ref}$	Reference observed airspeed	kn
V_T	True airspeed	kn
V_w	Wind velocity	kn
W	Weight	lb
W_{Std}	Standard weight	lb
W_{Test}	Test weight	lb
x	Scaled length of aircraft	
y	Scaled height of aircraft above tower	

2.9.2 GREEK SYMBOLS

α (alpha)	Angle of attack	deg
β (beta)	Sideslip angle	deg
δ (delta)	Pressure ratio	
γ (gamma)	Ratio of specific heats	
λ (lambda)	Lag error constant	
λ_S	Static pressure lag error constant	
λ_T	Total pressure lag error constant	
θ (theta)	Angle, Temperature ratio	deg
ρ (rho)	Air density	slug/ ft^3
ρ_a	Ambient air density	slug/ ft^3
ρ_{ssl}	Standard sea level air density	0.0023769 slug/ ft^3
σ (sigma)	Density ratio	

2.10 REFERENCES

1. Dommasch, Daniel O. et al, *Airplane Aerodynamics*, 4th Edition, Pitman Publishing Corp., New York, NY, 1967.

2. Gracey, William, *Measurement of Aircraft Speed and Altitude*, A Wiley-Interscience Publication, New York, NY, 1981.

3. Gracey, William, *Measurement of Aircraft Speed and Altitude*, NASA Reference Publication 1046, May, 1980.

4. Houston, *Accuracy of Airspeed Measurements and Flight Calibration Procedures*, NACA Report No. 919, 1984.

5. McCue, J.J., *Pitot-Static Systems*, USNTPS Class Notes, USNTPS, Patuxent River, MD., June, 1982.

6. Military Specification, “Instrument Systems, Pitot Tube and Flush Static Port Operated, Installation of”, MIL-I-6115A, 31 December 1960.

7. Military Specification, MIL-I-5072-1, “Instrument Systems; Pitot Static Tube Operated, Installation of”, 17 October 1949.

8. Naval Test Pilot School Flight Test Manual, *Fixed Wing Performance, Theory and Flight Test Techniques*, USNTPS-FTM-No.104, U. S. Naval Test Pilot School, Patuxent River, MD, July, 1977.

9. USAF Test Pilot School, *Performance Phase Textbook Volume I*, USAF-TPS-CUR-86-01, USAF, Edwards AFB, CA, April, 1986.

CHAPTER 3

STALL SPEED DETERMINATION

CHAPTER 3

FIGURES

CHAPTER 3

EQUATIONS

$$C_L = C_{L_{aero}} + \frac{T_G \sin \alpha_j}{q\,S}$$ (Eq 3.12) 3.17

$$C_L = C_{L_{aero}} + \frac{T_G \sin \alpha_j}{\frac{n_z W}{C_L}}$$ (Eq 3.13) 3.18

$$C_L = C_{L_{aero}} + C_L \left(\frac{T_G}{W} \frac{\sin \alpha_j}{n_z} \right)$$ (Eq 3.14) 3.18

$$C_L \left(1 - \frac{T_G}{W} \frac{\sin \alpha_j}{n_z} \right) = C_{L_{aero}}$$ (Eq 3.15) 3.18

$$C_L = \frac{C_{L_{aero}}}{\left(1 - \frac{T_G}{W} \frac{\sin \alpha_j}{n_z} \right)}$$ (Eq 3.16) 3.18

$$C_L = f\left(C_{L_{aero}}, \frac{T_G}{W}, \sin \alpha_j, n_z \right)$$ (Eq 3.17) 3.18

$$C_{L_{aero}} = f\left(\alpha, M, R_e \right)$$ (Eq 3.18) 3.19

$$C_{L_{aero}} = \frac{n_z W}{q\,S} = \frac{n_z W}{\frac{\gamma}{2} P_{ssl}\, S\, \delta\, M^2}$$ (Eq 3.19) 3.19

$$C_{L_{aero}} = \frac{n_z \left(\frac{W}{\delta} \right)}{\left(\frac{\gamma}{2} P_{ssl}\, S \right) M^2}$$ (Eq 3.20) 3.19

$$V_s = V_{s_{Test}} \sqrt{\frac{R + 2}{R + 1}}$$ (For decelerations) (Eq 3.21) 3.21

$$C_{L_s} = C_{L_{Test}} \left(\frac{R + 1}{R + 2} \right)$$ (For decelerations) (Eq 3.22) 3.21

$V_s = V_{s_{Test}} \sqrt{\dfrac{R+1}{R+2}}$ (For accelerations)	(Eq 3.23)	3.21
$R = \dfrac{V_{s_{Test}}}{\frac{c}{2}\dot{V}}$	(Eq 3.24)	3.21
$C_{L_{max_{Std\,\dot{V}}}} = C_{L_{max}} + K_d\left(\dot{V}_{Std} - \dot{V}_{Test}\right)$	(Eq 3.25)	3.22
$C_{L_{max_{Std\,\dot{V},\,CG}}} = C_{L_{max_{Std\,\dot{V}}}} + K_c\left(CG_{Std} - CG_{Test}\right)$	(Eq 3.26)	3.25
$\Delta L_t\left(l_t\right) = T_G\,(Z) - D_R\,(Y)$	(Eq 3.27)	3.26
$\Delta C_{L_t} = \dfrac{T_G}{q\,S}\left(\dfrac{Z}{l_t}\right) - \dfrac{D_R}{q\,S}\left(\dfrac{Y}{l_t}\right)$	(Eq 3.28)	3.26
$R_e = \dfrac{\rho\,V\,c}{\mu} = V_e\sqrt{\rho}\left(\dfrac{\sqrt{\rho_{ssl}}\;\;c}{\mu}\right)$	(Eq 3.29)	3.27
$C_{T_G} = \dfrac{T_G \sin \alpha_j}{q\,S}$	(Eq 3.30)	3.29
$C_{L_{max_{Std\,\dot{V},\,CG,\,W}}} = C_{L_{max_{Std\,\dot{V},\,CG}}} + K_W\left(W_{Std} - W_{Test}\right)$	(Eq 3.31)	3.31
$V_i = V_o + \Delta V_{ic}$	(Eq 3.32)	3.36
$V_c = V_i + \Delta V_{pos}$	(Eq 3.33)	3.36
$H_{P_i} = H_{P_o} + \Delta H_{P_{ic}}$	(Eq 3.34)	3.36
$H_{P_c} = H_{P_i} + \Delta H_{pos}$	(Eq 3.35)	3.36
$n_{z_i} = n_{z_o} + \Delta n_{z_{ic}}$	(Eq 3.36)	3.36

$n_z = n_{z_i} + \Delta n_{z_{tare}}$	(Eq 3.37)	3.36
$C_{L_{max_{Test}}} = \dfrac{n_z \, W_{Test}}{0.7 \, P_{ssl} \, \delta_{Test} \, M^2 \, S}$	(Eq 3.38)	3.37
$R = \dfrac{V_c}{\frac{c}{2} \dot{V}_{Test}}$	(Eq 3.39)	3.37
$C_{L_{max_{Std\,\dot{V}}}} = C_{L_{max_{Test}}} \left(\dfrac{R + 1}{R + 2} \right)$	(Eq 3.40)	3.37
$\left(C_{L_{aero_{Std\,\dot{V},\,CG,\,W}}} \right)_{Pwr\,ON} = \left(C_{L_{max_{Std\,\dot{V},\,CG,\,W}}} \right)_{Pwr\,ON} - C_{T_G}$	(Eq 3.41)	3.42
$\left(C_{L_{aero_{Std\,\dot{V},\,CG,\,W}}} \right)_{Pwr\,OFF} = \left(C_{L_{aero_{Std\,\dot{V},\,CG,\,W}}} \right)_{Pwr\,ON} - \Delta C_{L_t} - \Delta C_{L_E}$	(Eq 3.42)	3.42
$V_{e_s} = \sqrt{\dfrac{841.5 \, n_z \, W}{C_{L_{max}} \, S}}$	(Eq 3.43)	3.44

CHAPTER 3

STALL SPEED DETERMINATION

3.1 INTRODUCTION

This chapter deals with determining the stall airspeed of an airplane with emphasis on the takeoff and landing configurations. The stall is defined and factors which affect the stall speed are identified. Techniques to measure the stall airspeed are presented and data corrections for the test results are explained.

3.2 PURPOSE OF TEST

The purpose of this test is to determine the stall airspeed of the airplane in the takeoff and landing configuration, with the following objectives:

1. Determine the 1 g stall speed for an airplane at altitude and at sea level.
2. Apply corrections to obtain the stall speed for standard conditions to check compliance with performance guarantees.
3. Define mission suitability issues.

3.3 THEORY

The stall speed investigation documents the low speed boundary of the steady flight envelope of an airplane. In the classic stall, the angle of attack (α) is increased until the airflow over the wing surface can no longer remain attached and separates. The resulting abrupt loss of lift causes a loss of altitude and, in extreme cases, a loss of control. The operational requirement for low takeoff and landing airspeeds places these speeds very near the stall speed. Since the stall speed represents an important envelope limitation, it is a critical design goal and performance guarantee for aircraft procurement and certification trials. Verifying the guaranteed stall speed is a high priority early in the initial testing phases of an airplane. The significance of this measurement justifies the attention paid to the factors which affect the stall speed.

3.3.1 LOW SPEED LIMITING FACTORS

While defining the boundaries of the performance envelope, it is not uncommon to face degraded flying qualities near the limits. The reduced dynamic pressure near the stall airspeed produces a degradation in the effectiveness of the flight controls in addition to a lift reduction. Maintaining lift at these low speeds requires high α, which results in high drag and, frequently, handling difficulties. At some point in the deceleration, a minimum steady speed is reached which is ultimately defined by one of the following limiting factors:

1. Loss of lift. The separated flow is unable to produce sufficient lift.
2. Drag. Large increases in induced drag may cause high sink rates, compromising flight path control.
3. Uncommanded aircraft motions. These undesirable motions can range from a slight pitch over to a severe nose slice and departure.
4. Undesirable flying qualities. These characteristics include intolerable buffet level, shaking of the controls, wing rock, aileron reversal, and degraded stability.
5. Control effectiveness. Full nose up pitch control limits may be reached before any of the above conditions occurs.

From a test pilot's perspective, the task is to investigate how much lift potential can be exploited for operational use, without compromising aircraft control in the process. The definition of stall speed comes from that investigation. The 1 g stall case is discussed in this chapter and the accelerated stall case is covered in Chapter 6.

3.3.1.1 MAXIMUM LIFT COEFFICIENT

The discussion of minimum speed includes the notion of maximum lift coefficient ($C_{L_{max}}$). To maintain lift in a controlled deceleration at 1 g, the lift coefficient (C_L) increases as the dynamic pressure decreases (as a function of velocity squared). This increase in lift coefficient is provided by the steadily increasing α during the deceleration. At some point in the deceleration the airflow over the wing separates, causing a reduction of lift. The lift coefficient is a maximum at this point, and the corresponding speed at these conditions represents the minimum flying speed.

A high maximum lift coefficient is necessary for a low minimum speed. Wings designed for high speed are not well suited for high lift coefficients. Therefore, $C_{L_{max}}$ is typically enhanced for the takeoff and landing configurations by employing high lift devices, such as flaps, slats, or other forms of boundary layer control (BLC). The determination of stall airspeed for the takeoff or landing configuration invariably involves some of these high lift devices.

While the wing is normally a predominant factor in determining minimum speed capability, the maximum lift capability frequently depends upon thrust and center of gravity (CG) location. Thrust may make significant contributions to lift through both direct and indirect effects. The location of the CG affects pitch control effectiveness, pitch stability, and corresponding tail lift (positive or negative lift) required to balance pitching moments. These effects can be significant for airplanes with high thrust to weight ratios or close coupled control configurations (short moment arm for tail lift).

3.3.1.2 MINIMUM USEABLE SPEED

The speed corresponding to $C_{L_{max}}$ may not be a reasonable limit. Any of the other potential limitations from paragraph 3.3.1 may prescribe a minimum useable speed which is higher than the speed corresponding to $C_{L_{max}}$. The higher speed may be appropriate due to high sink rate, undesirable motions, flying qualities, or control effectiveness limits. Influence of the separated flow on the empennage may cause instabilities, loss of control, or intolerable buffeting. Any of these factors could present a practical minimum airspeed limit at a lift coefficient less than the $C_{L_{max}}$ potential of the airplane. In this case, the classic stall is not reached and a minimum useable speed is defined by another factor.

3.3.2 DEFINITION OF STALL SPEED

The definition of stall airspeed is linked to the practical concept of minimum useable airspeed. Useable means controllable in the context of a mission task. The stall speed might be defined by the aerodynamic stall, or it might be defined by a qualitative controllability threshold. The particular controllability issue may be defined precisely, as in an abrupt g-break, or loosely, as in a gradual increase in wing rock to an unacceptable level. Regardless of the particular controllability characteristic in question, the stall definition must be as precise as possible so the stall speed measurement is consistent and repeatable. Throughout the aerospace industry the definition of stall embraces the same concept of minimum useable speed. Two examples are presented below:

"The stalling speed, if obtainable, or the minimum steady speed, in knots (CAS), at which the airplane is controllable with.... (the words that follow describe the required configuration)."

- FAR Part 23.45

"The stall speed (equivalent airspeed) at 1 g normal to the flight path is the highest of the following:

1. The speed for steady straight flight at $C_{L_{max}}$ (the first local maximum of lift coefficient versus α which occurs as C_L is increased from zero).
2. The speed at which uncommanded pitching, rolling, or yawing occurs.
3. The speed at which intolerable buffet or structural vibration is encountered."

- MIL-STD-1797A

If a subjective interpretation is required for the stall definition, the potential exists for disagreement, particularly between the manufacturer and the procuring agency. In cases where the stall definition rests on a qualitative opinion, it is important to be as precise as possible for consistent test results. For example, if the dominant characteristic is a progressively increasing wing rock, the stall might be defined by a particular amplitude of oscillation for consistency (perhaps ± 10 deg bank). The stall may also be defined by a minimum permissible airspeed based upon an excessive sinking speed, or the inability to perform altitude corrections or execute a waveoff. If the stall is based on a criteria other than decreased lift, the minimum speed is usually specified as a specific α limit. This α limit, with approval by the procuring agency, is used as the stall speed definition for all specification requirements.

The important point is the definitions of controllable and useable are made by the user. The test pilot should be aware of the contractual significance of his interpretations in defining the stall, but must base his stall definition solely on mission suitability requirements.

3.3.3 AERODYNAMIC STALL

3.3.3.1 FLOW SEPARATION

In the classic stall, the lift coefficient increases steadily until airflow separation occurs, resulting in a loss of lift. The separation may occur at various locations on the wing and propagate in different patterns to influence the stall characteristics. Good characteristics generally result when the separation begins on the trailing edge of the wing root and progresses gradually forward and outboard. Separation at the wing tips is undesirable due to the loss of lateral control effectiveness and the tendency for large bank angle deviations when one tip stalls before the other. Separation at the leading edge is invariably abrupt, precipitating a dangerous loss of lift with little or no warning. Some wing characteristics which cause these variations in stall behavior are wing section, aspect ratio, taper ratio, and wing sweep.

3.3.3.2 WING SECTION

The relevant wing section design characteristics are airfoil thickness, thickness distribution, camber, and leading edge radius. To produce high maximum lift coefficients while maintaining the desirable separation at the trailing edge, the wing section must be designed to keep the flow attached at high α. Separation characteristics of two classes of wing section are shown in figure 3.1.

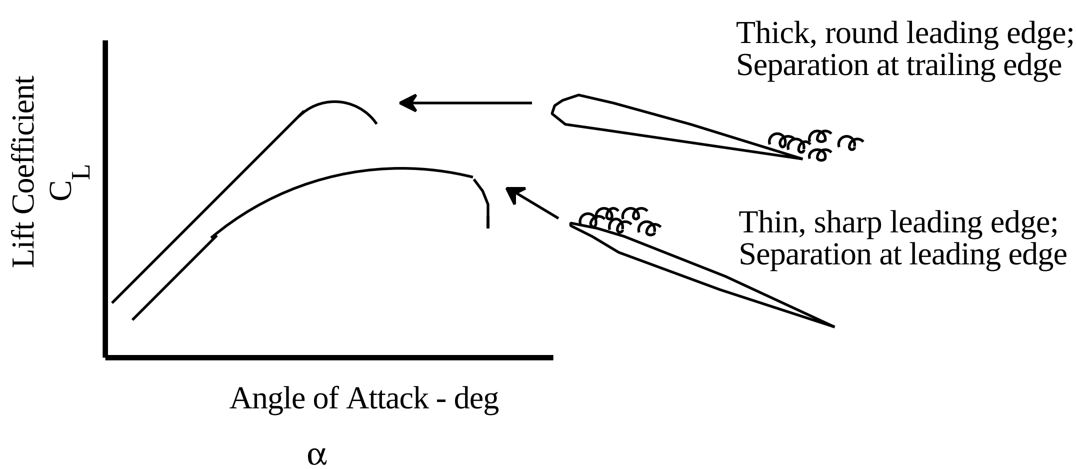

Figure 3.1
SAMPLE AIRFLOW SEPARATION CHARACTERISTICS

The classic airfoil shape features a relatively large leading edge radius and smoothly varying thickness along the chord line. This section is capable of producing large lift coefficients and promotes favorable airflow separation beginning at the trailing edge. The decrease in lift coefficient beyond $C_{L_{max}}$ is relatively gradual. Alternately, thin airfoils, particularly those with a small leading edge radius, typically have lower maximum lift coefficients. Airflow separation is less predictable, often beginning at the wing leading edge. Lift coefficient can decrease abruptly near $C_{L_{max}}$, even for small increases in α, and may precipitate unusual attitudes if the flow separates unevenly from both wings. High drag approaching $C_{L_{max}}$ can result in insidious and potentially high sink rates.

3.3.3.2.1 ASPECT RATIO

Aspect ratio (AR) is defined as the wing span divided by the average chord, or alternately, the square of the wing span divided by the wing area. The effect of increasing aspect ratio is to increase $C_{L_{max}}$ and steepen the lift curve slope as shown in figure 3.2.

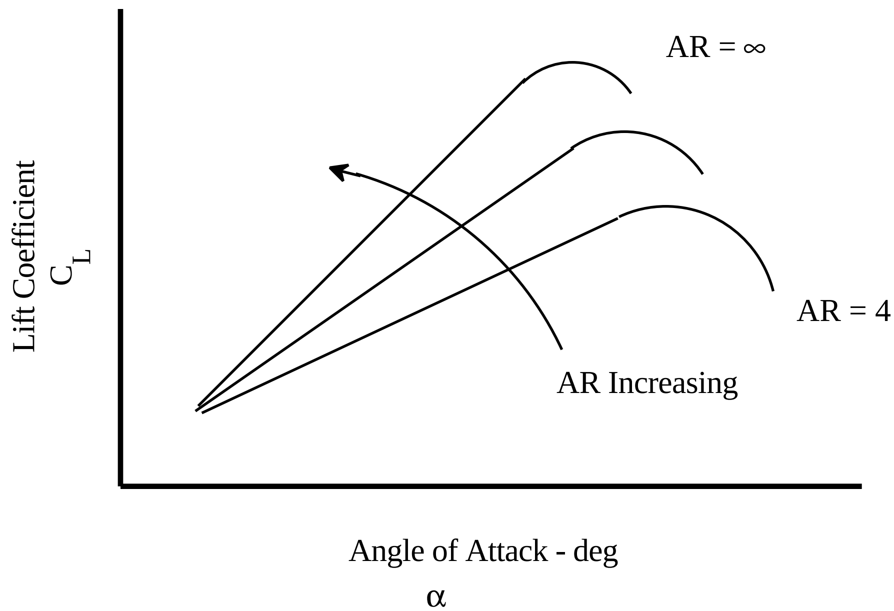

Figure 3.2
EFFECTS OF ASPECT RATIO

$C_{L_{max}}$ for a high aspect ratio wing occurs at a relatively low α, and corresponding low drag coefficient. Low aspect ratio wings, on the other hand, typically have shallow lift curve slopes and a relatively gradual variation of lift coefficient near $C_{L_{max}}$. The α for $C_{L_{max}}$ is higher, and the drag at these conditions is correspondingly higher.

3.3.3.2.2 TAPER RATIO

Taper ratio (λ) is the the chord length at the wing tip divided by the chord length at the wing root. For a rectangular wing ($\lambda = 1$), strong tip vortices reduce the lift loading at the tips. As the tip chord dimension is reduced, the tip loading increases, causing the adverse tendency for the wing tip to stall before the root. The tip stall typically causes a wing drop with little or no warning. The loss of lift is usually abrupt and controllability suffers with decreased aileron effectiveness.

3.3.3.2.3 WING SWEEP

The effect of increasing wing sweep angle (Λ) is to decrease the lift curve slope and $C_{L_{max}}$ as depicted in figure 3.3.

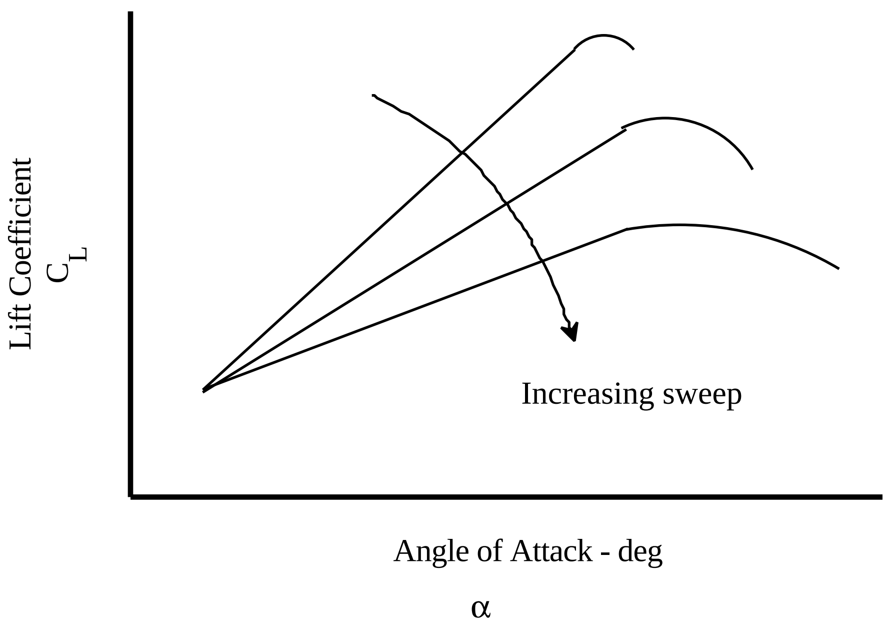

Figure 3.3
EFFECTS OF WING SWEEP

While the swept wing offers dramatic transonic drag reduction, the lift penalty at high α is substantial. As a wing is swept, $C_{L_{max}}$ decreases, according to the formula:

$$C_{L_{max\ (\Lambda)}} = C_{L_{max\ (\Lambda = 0)}} \cos(\Lambda) \quad \text{(Eq 3.1)}$$

Where:

$C_{L_{max\,(\Lambda)}}$	Maximum lift coefficient at Λ wing sweep	
$C_{L_{max\,(\Lambda = 0)}}$	Maximum lift coefficient at $\Lambda = 0$	
Λ	Wing sweep angle	deg.

Wing sweep causes a spanwise flow and a tendency for the boundary layer to thicken, inducing a tip stall. Besides the lateral control problem caused by tip stall, the loss of lift at the wing tips causes the center of pressure to move forward, resulting in a tendency to pitch up at the stall. Delta wing configurations are particularly susceptible to this pitch up tendency. The tip stall is often prevented by blocking the spanwise flow, using stall fences (MiG-21) or induced vortices from a leading edge notch at mid-span (F-4). Forward sweep, as in the X-29, exhibits the characteristic spanwise flow, but the tendency in this case is for root stall, and a resulting pitch down tendency at the stall.

3.3.3.3 IMPROVING SEPARATION CHARACTERISTICS

The tip stall caused by adverse flow separation characteristics of wings with low AR, low λ, or high Λ is usually avoided in the design phase by inducing a root stall through geometric wing twist, varying the airfoil section along the span, or employing leading edge devices at the tips. If problems show up in the flight test phase, fixes are usually employed such as stall strips or some similar device to trip the boundary layer at the root as shown in figure 3.4.

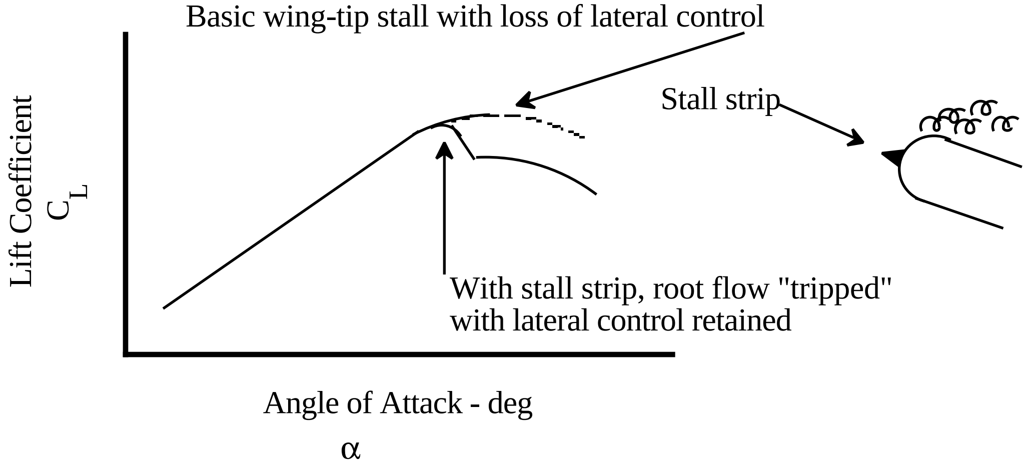

Figure 3.4
USE OF STALL STRIP AT WING ROOT

3.3.4 MAXIMUM LIFT

The previous section discussed factors which affect the shape of the lift curve at $C_{L_{max}}$ and the airflow separation characteristics at high α. These factors influence the airplane handling characteristics near $C_{L_{max}}$ and may prevent full use of the airplane's lift potential. Apart from handling qualities issues, low minimum speeds are achieved by designing for high maximum lift capability. The maximum lift characteristics of various airfoil sections are shown in figure 3.5.

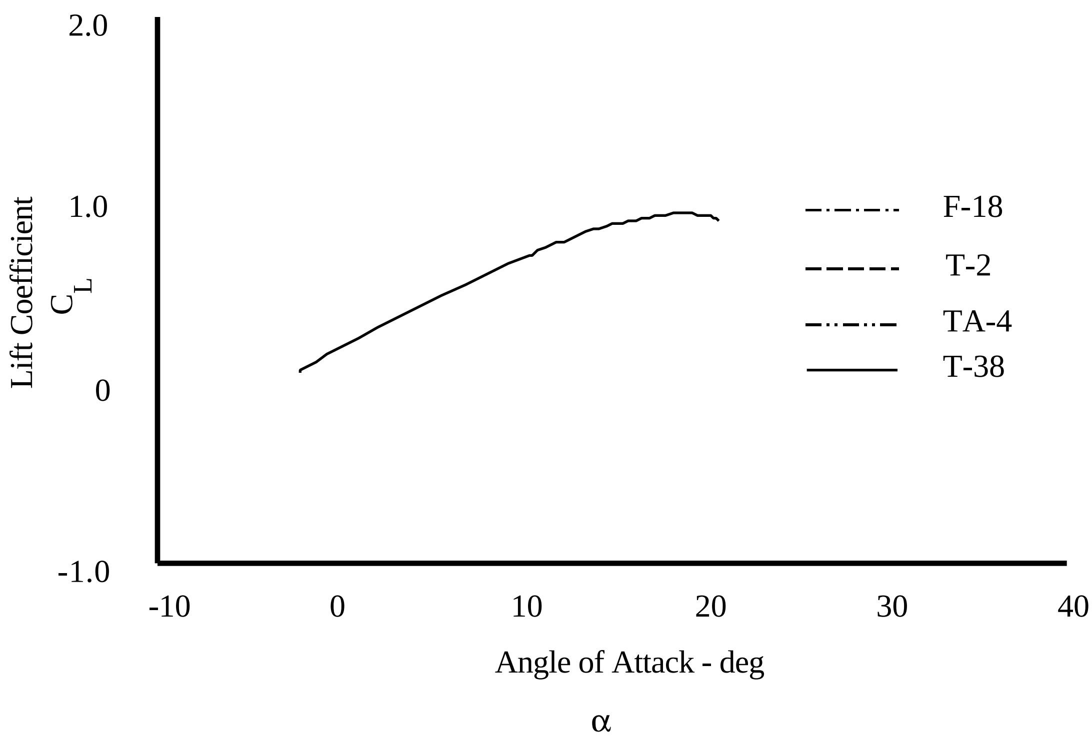

Figure 3.5
AIRFOIL SECTION LIFT CHARACTERISTICS

All of the airfoil sections displayed have roughly the same lift curve slope for low α, about 0.1 per deg. The theoretical maximum value is 2π per radian, or 0.11 per deg. The airfoil sections differ, however, at high α. The maximum value of lift coefficient and α where the maximum is reached determine the suitability of the airfoil for takeoff and landing tasks.

The desired low takeoff and landing speeds require high lift coefficients. The following expression illustrates the relationship between airspeed and lift coefficient:

$$V_{e_s} = \sqrt{\frac{n_z\,W}{C_{L_s}\,q\,S}} \qquad \text{(Eq 3.2)}$$

The potential benefit in stall speed reduction through increased lift coefficient can be seen in the following expression:

$$\frac{V_{e_{s_1}}}{V_{e_{s_2}}} = \sqrt{\frac{C_{L_{s_2}}}{C_{L_{s_1}}}} \qquad \text{(Eq 3.3)}$$

Large changes in lift coefficient are required in order to change equivalent airspeed (V_e) appreciably. Notice for a nominal 20% decrease in stall speed, over 50% increase in lift coefficient is required:

$$\text{If} \quad \frac{V_{e_{s_1}}}{V_{e_{s_2}}} = 0.8\,, \quad \text{then} \quad \frac{C_{L_{s_2}}}{C_{L_{s_1}}} = 0.64 \qquad \text{(Eq 3.4)}$$

And,

$$\frac{C_{L_{s_1}}}{C_{L_{s_2}}} = 1.56 \qquad \text{(Eq 3.5)}$$

Where:

C_{L_s}	Stall lift coefficient	
n_z	Normal acceleration	g
q	Dynamic pressure	psf
S	Wing area	ft^2
V_{e_s}	Stall equivalent airspeed	ft/s
W	Weight	lb.

Large lift coefficient increases are required to make effective decreases in stall speed. Since the wing design characteristics for high speed tasks are not compatible with those for high lift coefficient, the airplane designer must use high lift devices.

3.3.5 HIGH LIFT DEVICES

3.3.5.1 GENERATING EXTRA LIFT

Wing lift can be increased by using these techniques:

1. Increasing the wing area.
2. Increasing the wing camber.
3. Delaying the flow separation.

Various combinations of these techniques are employed to produce the high lift coefficients required for takeoff and landing tasks. Typical lift augmentation designs employ leading and trailing edge flaps and a variety of BLC schemes including slots, slats, suction and blowing, and the use of vortices. The relative benefit of each particular technique depends upon the lift characteristics of the wing on which it's used. For example, a trailing edge flap on a propeller airplane with a straight wing might increase $C_{L_{max}}$ three times as much as the same flap on a jet with a swept wing.

3.3.5.2 TRAILING EDGE FLAPS

Trailing edge flaps are employed to change the effective wing camber. They normally affect the aft 15% to 20% of the chord. The most common types of trailing edge flaps are shown in figure 3.6.

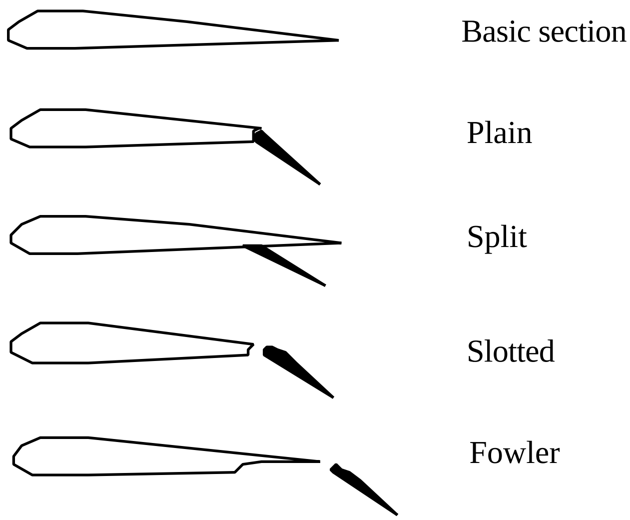

Figure 3.6
COMMON TRAILING EDGE FLAPS

The wing-flap combination behaves like a different wing, with characteristics dependent upon the design of the flap system. The plain flap is simply a hinged aft portion of the cross section of the wing, as used in the T-38. The split flap is a flat plate deflected from the lower surface of the wing, as in the TA-4. Slotted flaps direct high energy air over the upper flap surfaces to delay separation, as in the F-18 and U-21. Fowler flaps are slotted flaps which translate aft as they deflect to increase both the area of the wing and the camber, as in the T-2 and P-3. The relative effectiveness of the various types of trailing edge flaps is shown in figure 3.7.

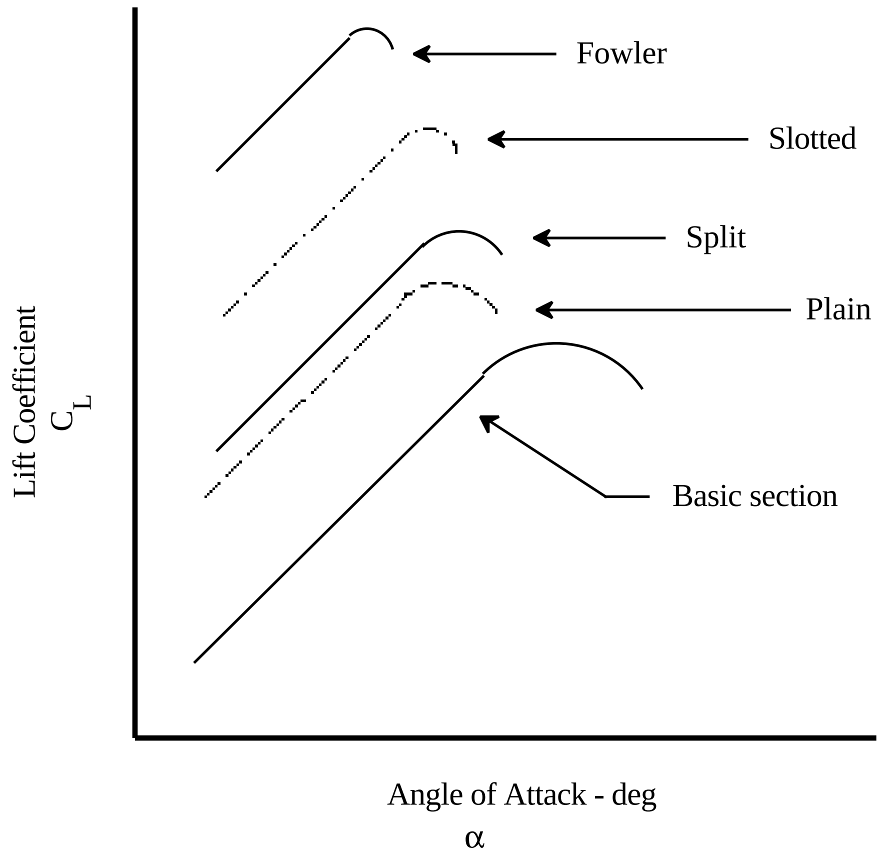

Figure 3.7
LIFT CHARACTERISTICS OF TRAILING EDGE FLAPS

All types provide a significant increase in $C_{L_{max}}$, without altering the lift curve slope. An added benefit is the reduction in the α for $C_{L_{max}}$, which helps the field of view over the nose at high lift conditions and reduces the potential for geometric limitations due to excessive α during takeoff and landing.

3.3.5.3 BOUNDARY LAYER CONTROL

Lift enhancement can be achieved by delaying the airflow separation over the wing surface. The boundary layer can be manipulated by airfoils or other surfaces installed along the wing leading edge. In addition, suction or blowing techniques can be employed at various locations on the wing to control or energize the boundary layer. Vortices are also employed to energize the boundary layer and delay airflow separation until a higher α. Different types of BLC are discussed in the following sections.

3.3.5.3.1 LEADING EDGE DEVICES

Leading edge devices are designed primarily to delay the flow separation until a higher α is reached. Some common leading edge devices are shown in figure 3.8.

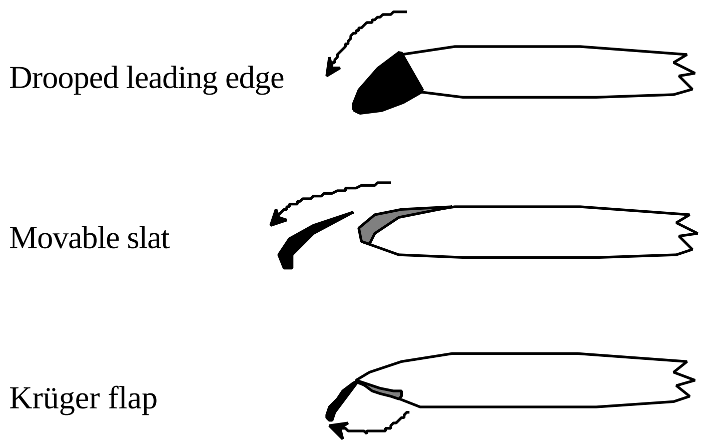

Figure 3.8
SAMPLE LEADING EDGE DEVICES

The lift provided from the leading edge surface is negligible; however, by helping the flow stay attached to the wing, flight at higher α is possible. An increase in $C_{L_{max}}$ is realized, corresponding to the lift resulting from the additional α available as shown in figure 3.9.

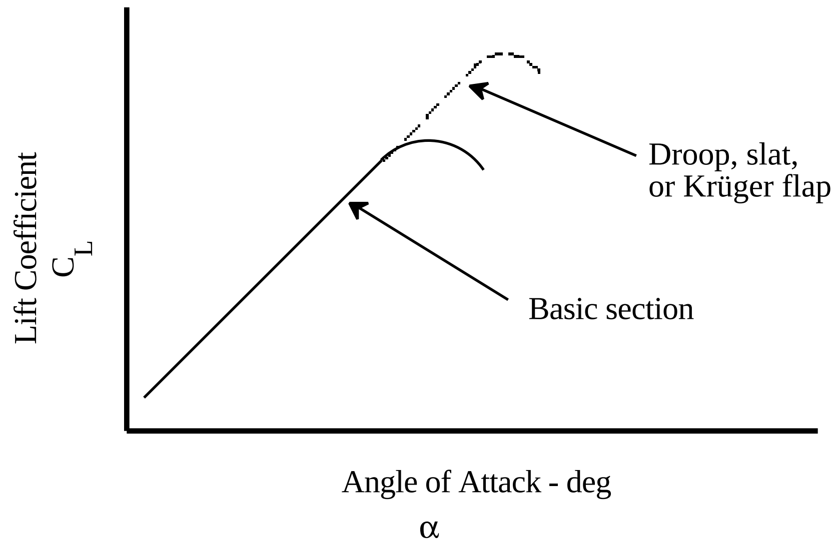

Figure 3.9
LEADING EDGE DEVICE EFFECTS

Since the α for $C_{L_{max}}$ may be excessively high, leading edge devices and slots are invariably used in conjunction with trailing edge flaps (except in delta wings) in order to reduce the α to values acceptable for takeoff and landing tasks.

3.3.5.3.2 BLOWING AND SUCTION

BLC can also involve various blowing or suction techniques. The concept is to prevent the stagnation of the boundary layer by either sucking it from the upper surface or energizing it, usually with engine bleed air. If BLC is employed on the leading edge, the effect is similar to a leading edge device. The energized flow keeps the boundary layer attached, allowing flight at higher α. If the high energy air is directed over the main part of the wing or a trailing edge flap (a blown wing or flap), the effect is similar to adding a trailing edge device. In either application if engine bleed air is used, the increase in lift is proportional to thrust.

3.3.5.3.3 VORTEX LIFT

Vortices can be used to keep the flow attached at extremely high α. Strakes in the F-16 and leading edge extensions in the F-18 are used to generate powerful vortices at high α. These vortices maintain high energy flow over the wing and make dramatic lift improvements. Canard surfaces can be used to produce powerful vortices for lift as well as pitching moments for control, as in the Gripen, Rafale, European fighter aircraft, and X-31 designs.

3.3.6 FACTORS AFFECTING $C_{L_{MAX}}$

3.3.6.1 LIFT FORCES

To specify the airplane's maximum lift coefficient, it is necessary to examine the forces which contribute to lift. Consider the airplane in a glide as depicted in figure 3.10.

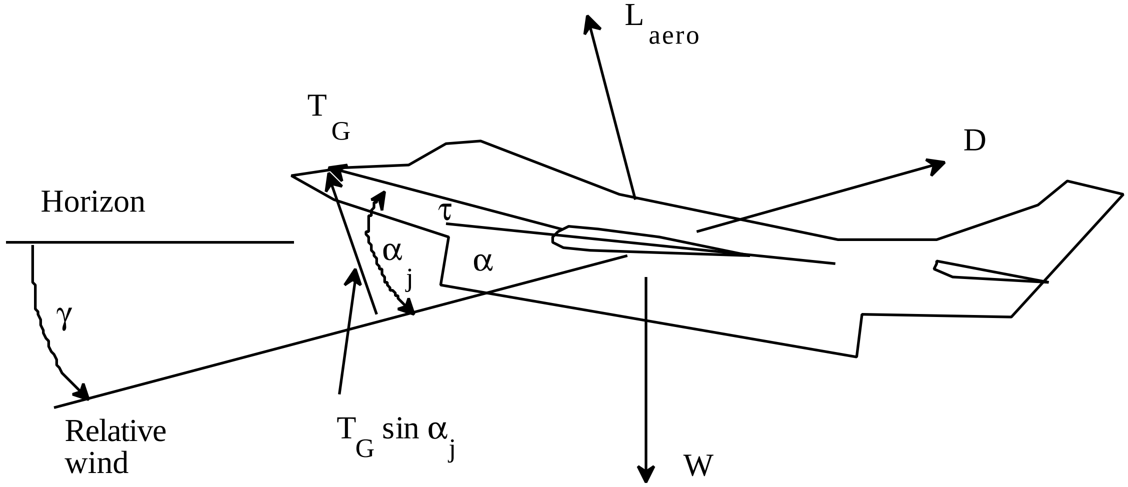

Figure 3.10
AIRPLANE IN STEADY GLIDE

Where:

α	Angle of attack	deg
α_j	Thrust angle	deg
D	Drag	lb
γ	Flight path angle	deg
L_{aero}	Aerodynamic lift	lb
τ	Inclination of the thrust axis with respect to the chord line	deg
T_G	Gross thrust	lb
W	Weight	lb.

Notice α_j can be expressed as:

$$\alpha_j = \alpha + \tau \quad \text{(Eq 3.6)}$$

The total lift of the airplane is composed of aerodynamic lift (L_{aero}) and thrust lift (L_{Thrust}):

$$L = L_{aero} + L_{Thrust} \quad \text{(Eq 3.7)}$$

Substituting the following expressions:

$$L = n_z W \quad \text{(Eq 3.8)}$$

$$L_{Thrust} = T_G \sin \alpha_j \quad \text{(Eq 3.9)}$$

The total lift is written:

$$L = n_z W = L_{aero} + T_G \sin \alpha_j \quad \text{(Eq 3.10)}$$

Dividing by the product of dynamic pressure and wing area, qS, we get the expression for lift coefficient:

$$C_L = \frac{L}{q\,S} = \frac{n_z W}{q\,S} = \frac{L_{aero}}{q\,S} + \frac{T_G \sin \alpha_j}{q\,S} \quad \text{(Eq 3.11)}$$

Or:

$$C_L = C_{L_{aero}} + \frac{T_G \sin \alpha_j}{q\,S} \quad \text{(Eq 3.12)}$$

Substituting the following into Eq 3.12:

$$q\,S = \frac{n_z W}{C_L}$$

Results in:

$$C_L = C_{L_{aero}} + \frac{T_G \sin \alpha_j}{\frac{n_z W}{C_L}} \qquad \text{(Eq 3.13)}$$

Rearranging:

$$C_L = C_{L_{aero}} + C_L\left(\frac{T_G}{W}\frac{\sin \alpha_j}{n_z}\right) \qquad \text{(Eq 3.14)}$$

$$C_L\left(1 - \frac{T_G}{W}\frac{\sin \alpha_j}{n_z}\right) = C_{L_{aero}} \qquad \text{(Eq 3.15)}$$

Finally:

$$C_L = \frac{C_{L_{aero}}}{\left(1 - \frac{T_G}{W}\frac{\sin \alpha_j}{n_z}\right)} \qquad \text{(Eq 3.16)}$$

Eq 3.16 can be expressed functionally:

$$C_L = f\left(C_{L_{aero}}, \frac{T_G}{W}, \sin \alpha_j, n_z\right) \qquad \text{(Eq 3.17)}$$

Where:

α	Angle of attack	deg
α_j	Thrust angle	deg
C_L	Lift coefficient	
$C_{L_{aero}}$	Aerodynamic lift coefficient	
L	Lift	lb
L_{aero}	Aerodynamic lift	lb
L_{Thrust}	Thrust lift	lb
n_z	Normal acceleration	g
q	Dynamic pressure	psf

S	Wing area	ft^2
T_G	Gross thrust	lb
τ	Inclination of the thrust axis with respect to the chord line	deg
W	Weight	lb.

C_L changes in any of the above factors affect the total lift coefficient and must be accounted for in the determination of stall speed. The effects of each of these factors are developed in the following sections.

3.3.6.2 AERODYNAMIC LIFT COEFFICIENT

3.3.6.2.1 BASIC FACTORS

The aerodynamic lift coefficient is affected by many factors. From dimensional analysis we get the result:

$$C_{L_{aero}} = f\left(\alpha,\ M,\ R_e\right) \qquad \text{(Eq 3.18)}$$

As long as the thrust contributions are negligible and the airplane is in steady flight, the lift coefficient is specified by α, Mach, and R_e. The expression for $C_{L_{aero}}$ is:

$$C_{L_{aero}} = \frac{n_z W}{q\,S} = \frac{n_z W}{\frac{\gamma}{2} P_{ssl}\, S\, \delta\, M^2} \qquad \text{(Eq 3.19)}$$

Rearranging:

$$C_{L_{aero}} = \frac{n_z\left(\frac{W}{\delta}\right)}{\left(\frac{\gamma}{2} P_{ssl}\, S\right) M^2} \qquad \text{(Eq 3.20)}$$

Where:

α	Angle of attack	deg
$C_{L_{aero}}$	Aerodynamic lift coefficient	
δ	Pressure ratio	

γ	Ratio of specific heats	
M	Mach number	
n_z	Normal acceleration	g
$n_z \frac{W}{\delta}$	Referred normal acceleration	g-lb
P_{ssl}	Standard sea level pressure	2116.217 psf
q	Dynamic pressure	psf
R_e	Reynold's number	
S	Wing area	ft^2
W	Weight	lb.

Eq 3.20 shows $C_{L_{aero}}$ is a function of just $n_z \frac{W}{\delta}$ and Mach, if thrust and R_e effects are neglected. For power-off or partial power stalls at 10,000 ft and below, these assumptions are reasonable and there is good correlation when plotting $n_z \frac{W}{\delta}$ versus Mach.

However, significant contributions can come from deceleration rate, CG position, and indirect power effects, to alter the apparent value of $C_{L_{aero}}$. These effects, plus the influence of R_e, are discussed in the following sections.

3.3.6.2.2 DECELERATION RATE

Deceleration rate has a pronounced affect on lift coefficient. Changes to the flow pattern within 25 chord lengths of an airfoil have been shown to produce significant non-steady flow effects. The lift producing flow around the airfoil (vorticity) does not change instantaneously. During rapid decelerations the wing continues to produce lift for some finite time after the airspeed has decreased below the steady state stall speed. The measured stall speed for these conditions is lower than the steady state stall speed. For this reason, a deceleration rate not to exceed 1/2 kn/s normally is specified when determining steady state stall speed for performance guarantees.

To correct the test data for deceleration rate, an expression is used which relates the observed stall speed, the actual steady state stall speed, and R, a parameter which represents the number of chord lengths ahead of the wing the airflow change is affecting. The equation comes from reference 7, and pertains to the deceleration case alone:

$$V_s = V_{s_{Test}} \sqrt{\frac{R + 2}{R + 1}} \text{ (For decelerations)} \qquad \text{(Eq 3.21)}$$

If the deceleration rate is low, it takes a long time to make a velocity change, during which time the wing travels many semi-chord lengths. R is a large number, and V_s and $V_{s_{Test}}$ are nearly equal. High deceleration rates make R a small number, so V_s could be significantly larger then the test value. In terms of C_L, the deceleration correction is:

$$C_{L_s} = C_{L_{Test}} \left(\frac{R + 1}{R + 2}\right) \text{ (For decelerations)} \qquad \text{(Eq 3.22)}$$

A similar analysis holds for errors due to accelerations, except the measured stall speeds are higher than steady state values. This case is applicable to the takeoff phase, and especially for catapult launches. The expression for accelerations is similar to Eq 3.22:

$$V_s = V_{s_{Test}} \sqrt{\frac{R + 1}{R + 2}} \text{ (For accelerations)} \qquad \text{(Eq 3.23)}$$

The R parameter came from wind tunnel tests, and is hard to relate to flight tests. However, experimental results lend credibility to the following empirical expression for R from reference 7:

$$R = \frac{V_{s_{Test}}}{\frac{c}{2}\dot{V}} \qquad \text{(Eq 3.24)}$$

Where:

$\frac{c}{2}$	Semi-chord length	ft
C_{L_s}	Stall lift coefficient	
$C_{L_{Test}}$	Test lift coefficient	
$\dot{V}$	Acceleration/deceleration rate	kn/s
R	Number of semi-chord lengths	
V_s	Stall speed	kn
$V_{s_{Test}}$	Test stall speed	kn.

An alternate approach to the deceleration correction involves plotting the test data for several values of deceleration rate. The steady state value, or the value at a specification deceleration rate, can be obtained by extrapolation or interpolation of the test results. Figure 3.11 illustrates the technique.

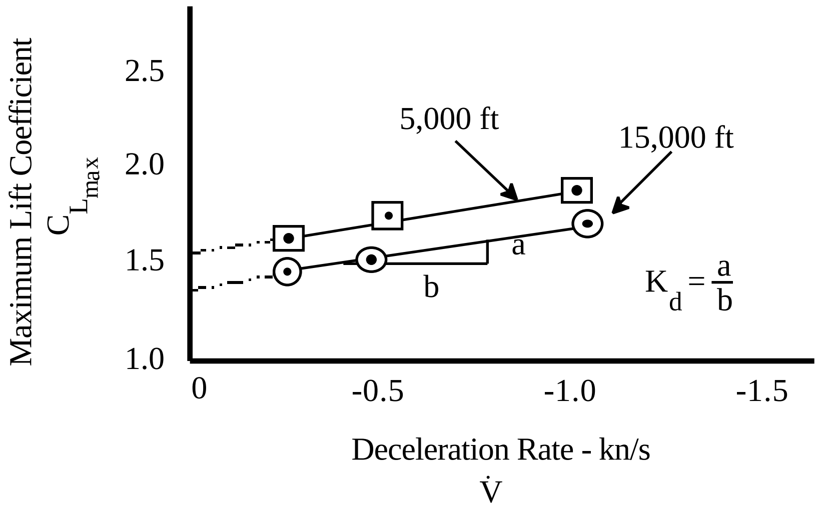

Figure 3.11
VARIATION OF $C_{L_{max}}$ WITH DECELERATION RATE

The data are faired to obtain the general correction represented by the slope of the line. Data can be corrected using the expression:

$$C_{L_{max_{Std\,\dot{V}}}} = C_{L_{max}} + K_d\left(\dot{V}_{Std} - \dot{V}_{Test}\right) \qquad \text{(Eq 3.25)}$$

Where:

$C_{L_{max}}$	Maximum lift coefficient	
$C_{L_{max\ Std\ \dot{V}}}$	Maximum lift coefficient at standard deceleration rate	
K_d	Slope of $C_{L_{max}}$ vs $\dot{V}$ (a negative number)	
$\dot{V}_{Std}$	Standard acceleration/deceleration rate	kn/s
$\dot{V}_{Test}$	Test acceleration/deceleration rate	kn/s.

If data using several deceleration rates are plotted, the corrections have a relatively high confidence level since no empirical expressions (as in the expression for R) are introduced.

3.3.6.2.3 CENTER OF GRAVITY EFFECTS

The CG affects the aerodynamic lift by altering the tail lift component. Consider the typical stable conditions where the CG is ahead of the aerodynamic center and the horizontal tail is producing a download. Moving the CG forward produces a nose down pitching moment, requiring more download to balance as shown in figure 3.12.

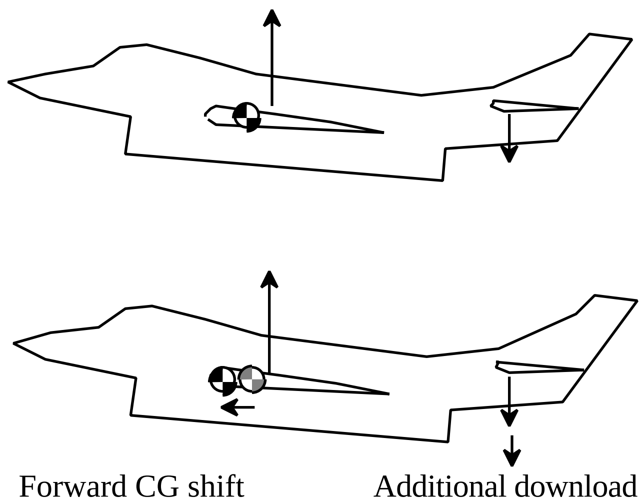

Figure 3.12
ADDITIONAL DOWNLOAD WITH FORWARD CG

The increased download to balance forward CG locations requires more nose up pitch control. In some cases, full aft stick (or yoke) is insufficient to reach the α for $C_{L_{max}}$, and a flight control deflection limit sets the minimum speed. Even if the tail is producing positive lift, as is the case with a negative static margin, the same effect prevails. In such cases, a forward CG shift would produce a decrease in the upload at the tail as shown in figure 3.13.

Thus, relatively aft CG locations have higher aerodynamic lift potential, resulting in lower airspeeds for any particular α. Forward CG locations have correspondingly higher speeds. The CG effect can be sizeable, particularly in designs with close-coupled, large horizontal control surfaces, like the Tornado or the F-14. For this reason, the stall speed requirement is frequently specified at the forward CG limit.

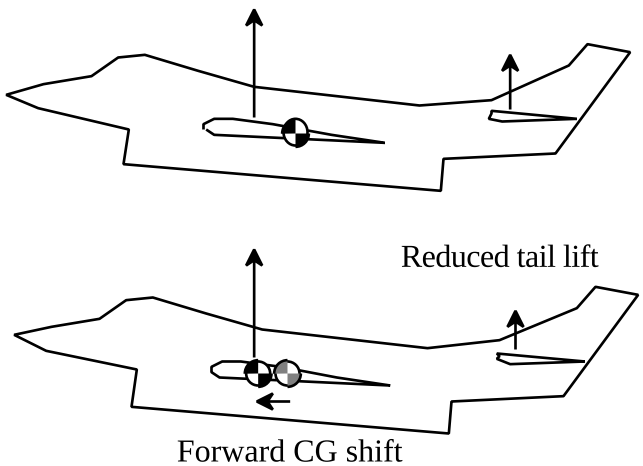

Figure 3.13
REDUCED LIFT WITH FORWARD CG SHIFT

To correct test data for the CG effects, plot $C_{L_{max}\ Std\ \dot{V}}$ versus CG_{Test} as in figure 3.14.

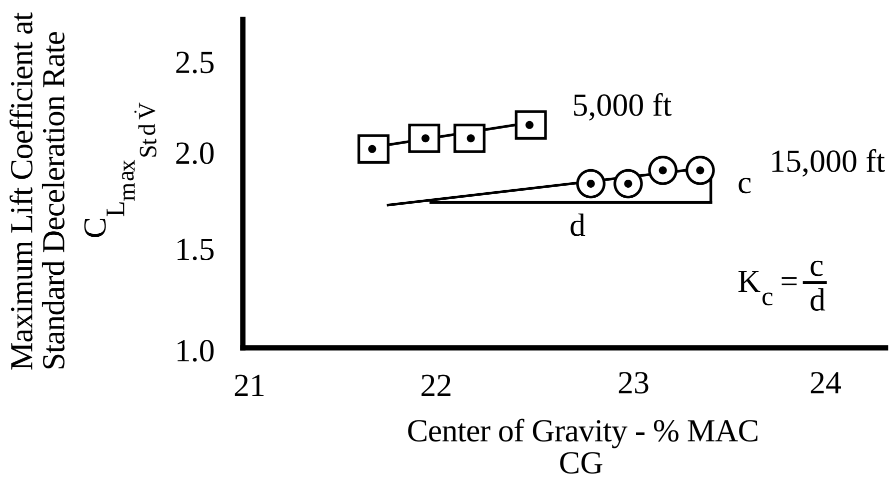

Figure 3.14
VARIATION OF $C_{L_{max}}$ WITH CG

$C_{L_{max}}$ increases as CG position increases in % MAC (CG moves aft). The correction is applied as follows:

$$C_{L_{max_{Std\,\dot{V},\,CG}}} = C_{L_{max_{Std\,\dot{V}}}} + K_c\left(CG_{Std} - CG_{Test}\right) \qquad \text{(Eq 3.26)}$$

Where:

CG_{Std}	Standard CG	% MAC
CG_{Test}	Test CG	% MAC
$C_{L_{max\ Std\ \dot{V}}}$	Maximum lift coefficient at standard deceleration rate	
$C_{L_{max\ Std\ \dot{V},\ CG}}$	Maximum lift coefficient at standard deceleration rate and CG	
K_c	Slope of $C_{L_{max\ Std\ \dot{V}}}$ vs CG (positive number).	

3.3.6.2.4 INDIRECT POWER EFFECTS

There are two indirect power effects to consider: trim lift from thrust-induced pitching moments, and induced lift from flow entrainment. Both are straightforward to visualize, but difficult to measure. The calculations require data from the aircraft contractor.

<u>Pitching Moment</u>

Pitching moments are produced from ram drag (D_R) at the engine inlet and from gross thrust (T_G) where the thrust axis is inclined to the flight path as depicted in figure 3.15.

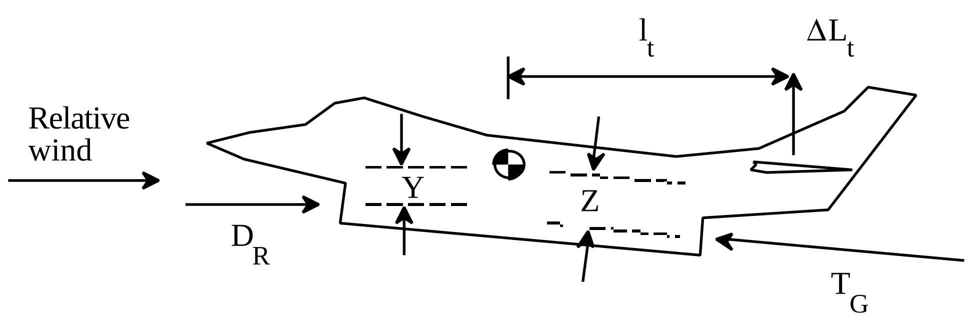

Figure 3.15
PITCHING MOMENTS FROM THRUST

Where:

ΔL_t	Tail lift increment	lb
D_R	Ram drag	lb
l_t	Moment arm for tail lift	ft
T_G	Gross thrust	lb
Y	Height of CG above ram drag	ft
Z	Height of CG above gross thrust	ft.

For this case, the moments from D_R and T_G require a balancing tail lift increment (ΔL_t), according to the expression:

$$\Delta L_t \left(l_t\right) = T_G\ (Z) - D_R\ (Y) \tag{Eq 3.27}$$

The effect of ΔL_t on the aerodynamic lift coefficient is expressed as:

$$\Delta C_{L_t} = \frac{T_G}{q\,S}\left(\frac{Z}{l_t}\right) - \frac{D_R}{q\,S}\left(\frac{Y}{l_t}\right) \tag{Eq 3.28}$$

Where:

ΔC_{L_t}	Incremental tail lift coefficient	
ΔL_t	Tail lift increment	lb
D_R	Ram drag	lb
l_t	Moment arm for tail lift	ft
q	Dynamic pressure	psf
S	Wing area	ft^2
T_G	Gross thrust	lb
Y	Height of CG above ram drag	ft
Z	Height of CG above gross thrust	ft.

This thrust effect is similar to the CG effect, except that the tail lift component is changed. The thrust axis component, T_G (Z), varies with thrust and CG location (especially vertical position), but is independent of α. The ram drag term, D_R (Y), varies with thrust, CG location, and α.

Thrust Induced Lift

If the nozzle is positioned so the exhaust induces additional airflow over a lifting surface, then an incremental lift is produced as a function of power setting. This effect is noticeable in designs where the nozzle is placed near the trailing edge of the wing, as in the A-6. At high thrust settings, and low airspeeds in particular, the jet exhaust causes increased flow over the wing, which raises the lift coefficient.

3.3.6.2.5 ALTITUDE

The effect of altitude on lift coefficient is due primarily to Reynold's number (R_e), which is defined below:

$$R_e = \frac{\rho\ V\ c}{\mu} = V_e \sqrt{\rho} \left(\frac{\sqrt{\rho_{ssl}}\ \ c}{\mu} \right) \qquad \text{(Eq 3.29)}$$

Where:

c	Chord length	ft
μ	Viscosity	lb-s/ft^2
ρ	Air density	slug/ft^3
R_e	Reynold's number	
ρ_{ssl}	Standard sea level air density	0.0023769 slug/ft^3
V	Velocity	kn
V_e	Equivalent airspeed	kn.

For the same V_e, R_e decreases with altitude. Results show as R_e decreases, the boundary layer has typically less energy and separates from the airfoil earlier than it would at lower altitude. Values of lift coefficient for α beyond this separation point are less than would be experienced at lower altitudes. R_e effects are depicted in figure 3.16.

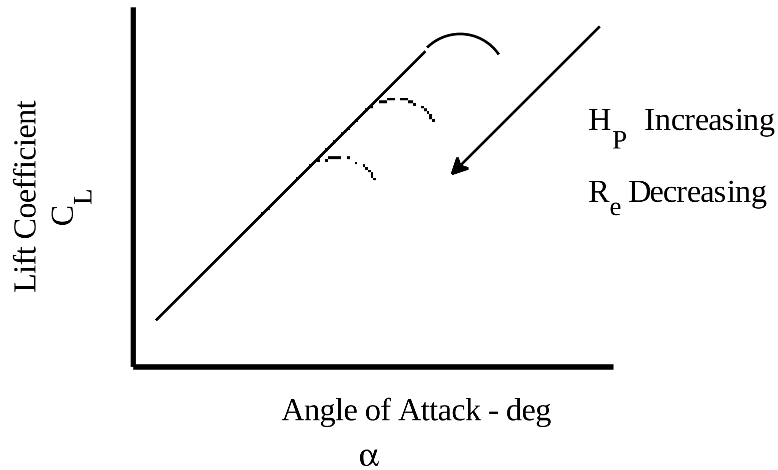

Figure 3.16
REYNOLD'S NUMBER EFFECT

The R_e effect of altitude on stall speed is on the order of 2 kn per 5,000 ft. To correct test data, or to refer test results to another altitude, the usual procedure is to plot $C_{L_{max}}$ versus H_{P_c}, using at least two different altitudes. Corrections to $C_{L_{max}}$ for standard deceleration rate, CG, and gross weight are made before plotting the variation with altitude. A typical plot is shown in figure 3.17.

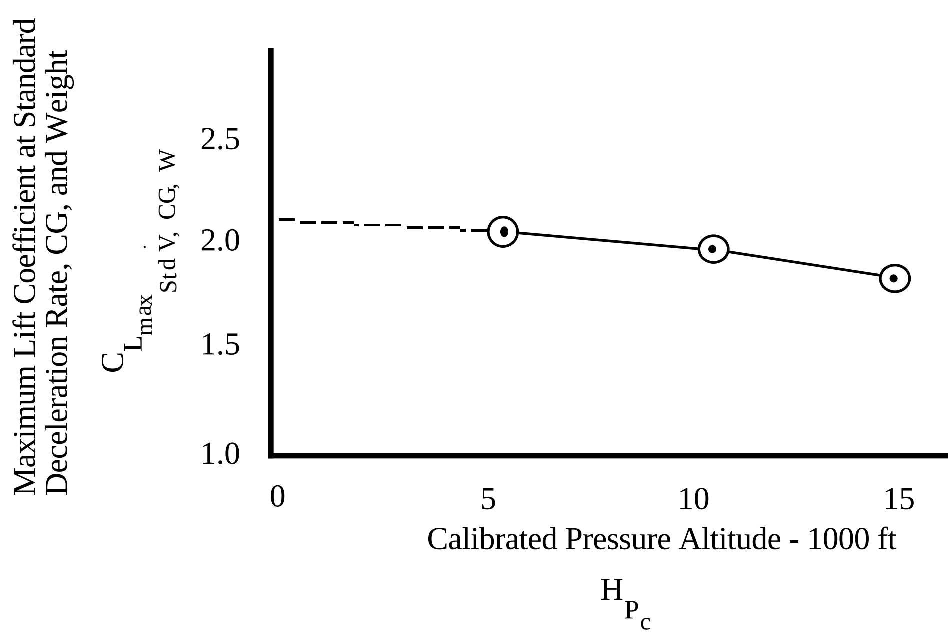

Figure 3.17
VARIATION OF $C_{L_{max}}$ WITH ALTITUDE

Figure 3.17 defines $C_{L_{max}}$ corrected to specific conditions of deceleration rate, CG, and weight for the standard altitude of interest. For extrapolations to sea level, data from three altitudes are recommended, since the variation is typically nonlinear.

3.3.6.3 THRUST AXIS INCIDENCE

The next factor to be developed in the lift equation is the component of thrust perpendicular to the flight path. Recall from Eq 3.7 direct thrust lift was accounted for in the development of the expression for total lift. Figure 3.18 highlights the thrust component of lift.

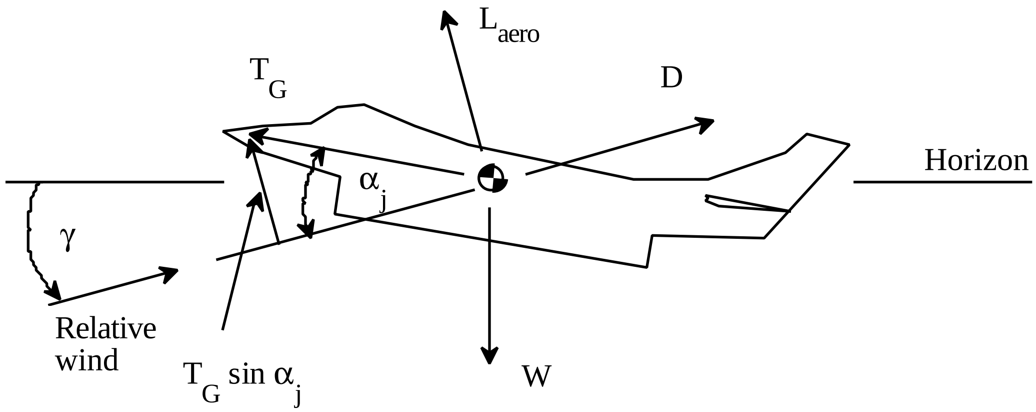

Figure 3.18
THRUST COMPONENT OF LIFT

The coefficient of thrust lift is denoted by the term C_{T_G} and is defined as:

$$C_{T_G} = \frac{T_G \sin \alpha_j}{q\,S} \qquad \text{(Eq 3.30)}$$

Where:

α_j	Thrust angle	deg
C_{T_G}	Coefficient of gross thrust lift	
q	Dynamic pressure	psf
S	Wing area	ft^2
T_G	Gross thrust	lb.

At high α and high thrust the thrust component of lift can be significant and must be accounted for in determining $C_{L_{max}}$ for minimum airspeed. The incidence of the nozzles may be fixed, as in conventional airplanes, or variable as in the Harrier or the YF-22. For aircraft designed to produce a large amount of thrust lift, the nozzle incidence angle is large, as is the thrust level. The thrust component is negligible, however, when the thrust is low or the incidence angle is small.

3.3.6.4 THRUST TO WEIGHT RATIO

The inclination of the thrust axis makes the actual thrust level significant in the measurement of airplane lift coefficient. Eq 3.16, repeated here for convenience, shows the thrust-to-weight term in the denominator, multiplied by the sine of the thrust axis inclination angle.

$$C_L = \frac{C_{L_{aero}}}{\left(1 - \frac{T_G}{W}\frac{\sin\alpha_j}{n_z}\right)} \qquad \text{(Eq 3.16)}$$

If the angle is large, then the test thrust-to-weight ratio can have a pronounced affect upon the results. This term is significant in power-on stalls for designs with high α capability, notably delta wing configurations where trailing edge flaps are not feasible. Corrections to test data for the effects of weight are significant only when the thrust-to-weight ratio at the test conditions is high, as in the takeoff or waveoff configurations. Plot $C_{L_{max}}$ versus gross weight to determine if a correction is necessary, as in figure 3.19.

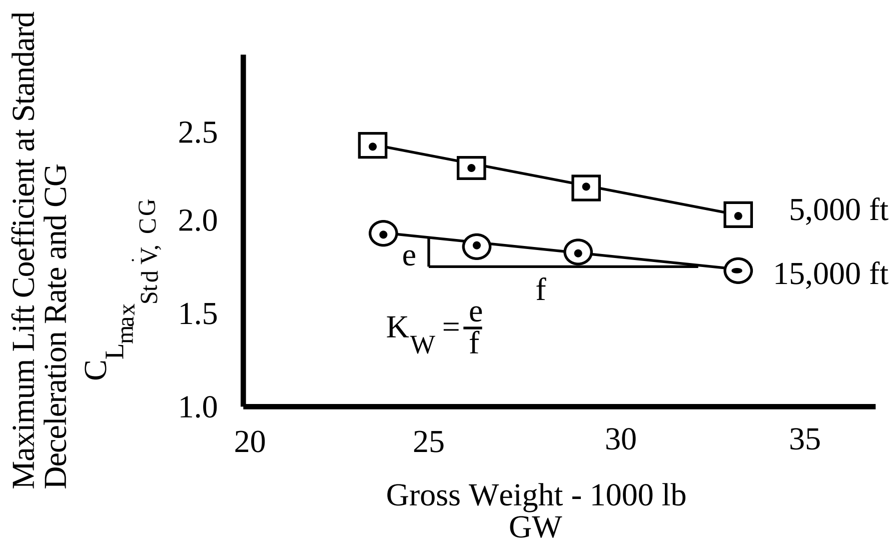

Figure 3.19
VARIATION OF $C_{L_{max}}$ WITH GROSS WEIGHT

If the graph has an appreciable slope, apply a gross weight correction as follows:

$$C_{L_{max}}{}_{Std\ \dot{V},\ CG,\ W} = C_{L_{max}}{}_{Std\ \dot{V},\ CG} + K_W\left(W_{Std} - W_{Test}\right) \qquad \text{(Eq 3.31)}$$

Where:

α_j	Thrust angle	deg
C_L	Lift coefficient	
$C_{L_{aero}}$	Aerodynamic lift coefficient	
$C_{L_{max}\ Std\ \dot{V},\ CG}$	Maximum lift coefficient at standard deceleration rate and CG	
$C_{L_{max}\ Std\ \dot{V},\ CG,\ W}$	Maximum lift coefficient at standard deceleration rate, CG, and weight	
K_W	Slope of $C_{L_{max}\ Std\ \dot{V},\ CG}$ vs GW (negative number)	lb^{-1}
n_z	Normal acceleration	g
T_G	Gross thrust	lb
W	Weight	lb
W_{Std}	Standard weight	lb
W_{Test}	Test weight	lb.

3.4 TEST METHODS AND TECHNIQUES

3.4.1 GRADUAL DECELERATION TECHNIQUE

For this technique a steady, gradual deceleration is maintained using the pitch control to modulate the deceleration rate until a stall occurs. Normally, the stall is indicated by a pitch down or a wing drop. A typical scope of test contains gradual decelerations for two CG locations using at least two test altitudes.

3.4.1.1 TEST PLANNING CONSIDERATIONS

While developing the test plan to determine the stall speed, consider the following issues:

1. Configuration. Define the precise configuration for the test, normally in accordance with a specification. Specify the following:

    a. Position of all high lift or drag devices.
    b. Trim setting.
    c. Thrust setting.
    d. Automatic flight control system (AFCS) status.

2. Weight and CG. Identify critical CG locations for the tests. Normally, the forward CG limit is critical if the stall is determined by $C_{L_{max}}$. Plan to get data at the specification gross weight, or use gross weight representative of mission conditions.

3. Loadings. Specify external stores loading. Stall speeds normally increase if external stores are loaded. Stores loading may have an adverse effect on stall and recovery characteristics.

4. Stall Characteristics. Consider the stall characteristics of the the test airplane. Plan build up tests if the stall characteristics are unknown or the pilot has no recent experience with stalls in the test airplane. Consider build up tests to determine the altitude required to recover from the stall. Employ appropriate safety measures to avoid inadvertent departures or post-stall gyrations. Specify recovery procedures for these cases.

5. Altitudes. Plan to get data at two or more test altitudes to allow for extrapolation of test results to sea level. Choose the lowest altitude based upon any adverse stall characteristics and predicted altitude lost during recoveries. Document the stall at an altitude approximately ten thousand feet above this minimum, and follow with tests at the lower altitude.

3.4.1.2 INSTRUMENTATION REQUIREMENTS

Precise accelerometers are necessary for accurate stall speed measurements. Twin-axis accelerometers for n_Z and n_X are ideal, but it is impractical to align the accelerometers with the flight path at the stall. An n_X accelerometer could be used to measure deceleration rate accurately, except n_X is extremely sensitive to pitch attitude (θ) changes through the weight component, W $\sin\theta$. Record the n_Z instrument error at 1 g for the test airplane to use in determining the tare correction. These tests are at essentially 1 g, but the changing θ and γ during the deceleration make the actual acceleration normal to the flight path difficult to determine. The precise n_Z is determined by correcting the observed n_Z using the alignment angle of the accelerometer with the fuselage reference line and the corrected α.

Angle of attack is normally obtained from a boom installation, to place the α vane in the free stream. Even with boom installations, however, corrections are required due to the upwash effect. These calibrations require comparisons of stabilized θ and flight path. Inertial navigation systems can be used for these measurements.

The measurement of airspeed is the biggest challenge. A calibrated trailing cone is a good source of airspeed data and can be used to calibrate the test airplane pitot static system. A pacer aircraft with a calibrated airspeed system is another option. The least accurate alternative is the pitot static system of the test airplane, since position error calibrations normally don’t include the stall speed region.

If possible, obtain time histories of airspeed, n_Z, θ, α, and pitch control position for analysis. Real time observations of flight parameters are not nearly as accurate. Buffet makes the gauges hard to read at a glance and it is difficult to time-correlate the critical readings to the actual stall event.

Reliable fuel weight at each test point is required. Normally, a precise fuel gauge calibration or fuel counter is used.

If power-on stalls are required and thrust effects are anticipated, maintenance personnel should trim the engine(s) prior to the tests.

Perform a weight and balance calibration for the test airplane after all test instrumentation is installed.

3.4.1.3 FLIGHT PROCEDURES

3.4.1.3.1 BUILD UP

Plan a build up sequence consisting of approaches to stall and recoveries using the standard recovery procedures. If telemetry is used or a pacer airplane is employed, an additional build up is recommended to practice the data retrieval procedures and identify any equipment, instrumentation, or coordination problems. Perform these build up procedures at a safe altitude prior to any performance tests.

3.4.1.3.2 DATA RUNS

Trim for approximately 1.2 times the predicted stall speed, which is typically very close to predicted optimum α for takeoffs and landings. Set the thrust appropriate for the configuration. Record the trim conditions, including trim settings. If applicable, position the pacer aircraft and have telemetry personnel ready.

From the trim speed, begin a steady 1/2 kn/s deceleration by increasing the pitch attitude. Control deceleration rate throughout the run by adjusting the pitch attitude. Attempt to fly a steady flight path, making all corrections smoothly to minimize n_z variations. When the stall is reached, record the data.

If telemetry is being used, make an appropriate “standby” call a few seconds before marking the stall. For tests involving a pacer airplane, the pacer stays with the test airplane throughout the deceleration. If the pacer tends to overrun the test airplane during the run, the pacer maintains fore-and-aft position by climbing slightly. The pacer stabilizes relative motion at the “standby” call. If there is any apparent relative motion when “mark” is called, the pacer notes it on the data card. The pacer keeps his eyes on the test airplane throughout the stall and recovery to maintain a safe distance and to facilitate the join up following the test run.

Exercise care to recover from the stall in a timely manner, using the recommended recovery procedures. The perishable data are the airspeed and altitude at the stall. These numbers can be memorized and recorded after the recovery, together with the remaining less perishable entries.

3.4.1.4 DATA REQUIRED

Run number, Configuration, V_o, H_{P_o}, n_{z_o}, W, and α, Fuel used or fuel remaining. For power-on stalls, add N, OAT, and fuel flow.

3.4.1.5 TEST CRITERIA

1. Constant trim and thrust.
2. Coordinated, wings level flight.
3. Constant normal acceleration.
4. Less than 1 kn/s deceleration rate (1/2 kn/s is the normal target deceleration rate).

3.4.1.6 DATA REQUIREMENTS

1. If automatic data recording is available, record the 30 s prior to stall.
2. Steady deceleration rate for 10 s prior to stall.
3. $V_o \pm 1/2$ kn.
4. H_{P_o} as required for 2% accuracy for $\frac{W}{\delta}$.
5. $n_{z_o} \pm 0.05$ g, (nearest tenth).

3.4.1.7 SAFETY CONSIDERATIONS

Exercise due care and vigilance since all stall tests are potentially dangerous. Carefully consider crew coordination while planning recoveries and procedures for all contingencies, including:

1. Inadvertent departure.
2. Unintentional spin.
3. Engine flameout and air start.
4. Asymmetric power at high α.

Make appropriate weather limitations for the tests. List all necessary equipment for the tests and set go/no-go criteria. Identify critical airplane systems and make data card entries to prompt the aircrew to monitor these systems during the tests. Assign data taking and recording responsibilities for the flight. Stress lookout doctrine and consider using reserved airspace for high workload tests. Plan to initiate recovery at the stall, and record hand-held data after the recovery is complete.

3.5 DATA REDUCTION

3.5.1 POWER-OFF STALLS

Test results are normally presented as the variation of stall speed with gross weight. Another useful presentation is the variation of referred normal acceleration $\left(n_z \frac{W}{\delta}\right)$ with Mach. The following equations are used for power-off stall data reduction:

$$V_i = V_o + \Delta V_{ic} \quad \text{(Eq 3.32)}$$

$$V_c = V_i + \Delta V_{pos} \quad \text{(Eq 3.33)}$$

$$H_{P_i} = H_{P_o} + \Delta H_{P_{ic}} \quad \text{(Eq 3.34)}$$

$$H_{P_c} = H_{P_i} + \Delta H_{pos} \quad \text{(Eq 3.35)}$$

$$n_{z_i} = n_{z_o} + \Delta n_{z_{ic}} \quad \text{(Eq 3.36)}$$

$$n_z = n_{z_i} + \Delta n_{z_{tare}} \quad \text{(Eq 3.37)}$$

$$C_{L_{max_{Test}}} = \frac{n_z \; W_{Test}}{0.7 \; P_{ssl} \; \delta_{Test} \; M^2 \; S} \tag{Eq 3.38}$$

$$R = \frac{V_c}{\frac{c}{2} \; \dot{V}_{Test}} \tag{Eq 3.39}$$

$$C_{L_{max_{Std \; \dot{V}}}} = C_{L_{max_{Test}}} \left(\frac{R + 1}{R + 2} \right) \tag{Eq 3.40}$$

$$C_{L_{max_{Std \; \dot{V}}}} = C_{L_{max}} + K_d \left[\dot{V}_{Std} - \dot{V}_{Test} \right] \tag{Eq 3.25}$$

$$C_{L_{max_{Std \; \dot{V}, \; CG}}} = C_{L_{max_{Std \; \dot{V}}}} + K_c \left(CG_{Std} - CG_{Test} \right) \tag{Eq 3.26}$$

$$C_{L_{max_{Std \; \dot{V}, \; CG, \; W}}} = C_{L_{max_{Std \; \dot{V}, \; CG}}} + K_W \left(W_{Std} - W_{Test} \right) \tag{Eq 3.31}$$

Where:

$\frac{c}{2}$	Semi-chord length	ft
CG_{Std}	Standard CG	% MAC
CG_{Test}	Test CG	% MAC
$C_{L_{max}}$	Maximum lift coefficient	
$C_{L_{max \; Std \; \dot{V}}}$	Maximum lift coefficient at standard deceleration rate	
$C_{L_{max \; Std \; \dot{V}, \; CG}}$	Maximum lift coefficient at standard deceleration rate and CG	
$C_{L_{max \; Std \; \dot{V}, \; CG, \; W}}$	Maximum lift coefficient at standard deceleration rate, CG, and weight	
$C_{L_{max_{Test}}}$	Test maximum lift coefficient	
$\Delta H_{P_{ic}}$	Altimeter instrument correction	ft
ΔH_{pos}	Altimeter position error	ft
$\Delta n_{z_{ic}}$	Normal acceleration instrument correction	g
$\Delta n_{z_{tare}}$	Accelerometer tare correction	g

δ_{Test}	Test pressure ratio	
ΔV_{ic}	Airspeed instrument correction	kn
ΔV_{pos}	Airspeed position error	kn
H_{P_c}	Calibrated pressure altitude	ft
H_{P_i}	Indicated pressure altitude	ft
H_{P_o}	Observed pressure altitude	ft
K_d	Slope of $C_{L_{max}}$ vs $\dot{V}$	
K_W	Slope of $C_{L_{max}}{}_{Std\,\dot{V}\,,\,CG}$ vs GW	lb^{-1}
M	Mach number	
n_z	Normal acceleration	g
n_{z_i}	Indicated normal acceleration	g
n_{z_o}	Observed normal acceleration	g
P_{ssl}	Standard sea level pressure	2116.217 psf
R	Number of semi-chord lengths	
S	Wing area	ft^2
V_c	Calibrated airspeed	kn
V_i	Indicated airspeed	kn
V_o	Observed airspeed	kn
$\dot{V}_{Test}$	Test acceleration/deceleration rate	kn/s
W_{Std}	Standard weight	lb
W_{Test}	Test Weight	lb.

From the observed airspeed, pressure altitude, normal acceleration, fuel weight, and deceleration rate, compute C_L as follows:

Step	Parameter	Notation	Formula	Units	Remarks
1	Observed airspeed	Vo		kn	
2	Airspeed instrument correction	ΔV_{ic}		kn	Lab calibration
3	Indicated airspeed	V_i	Eq 3.32	kn	
4	Airspeed position error	ΔV_{pos}		kn	Not required for trailing cone, May not be available for the test airplane

5	Calibrated airspeed	V_c	Eq 3.33	kn	
6	Observed pressure altitude	H_{P_o}		ft	
7	Altimeter instrument correction	$\Delta H_{P_{ic}}$		ft	Lab calibration
8	Indicated pressure altitude	H_{P_i}	Eq 3.34	ft	
9	Altimeter position error	ΔH_{pos}		ft	Not required for trailing cone, May not be available for the test airplane
10	Calibrated pressure altitude	H_{P_c}	Eq 3.35	ft	
11	Mach number	M			From Appendix VIII, using H_{P_c} and V_c
12	Observed normal acceleration	n_{z_o}		g	
13	Normal acceleration instrument correction	$\Delta n_{z_{ic}}$		g	Lab calibration
14	Indicated normal acceleration	n_{z_i}	Eq 3.36	g	
15	Normal acceleration tare correction	$\Delta n_{z_{tare}}$		g	Flight observation
16	Normal acceleration	n_z	Eq 3.37	g	
17	Test weight	W_{Test}		lb	
18	Test pressure ratio	δ_{Test}			From Appendix VI, using H_{P_c}
19	Standard sea level pressure	P_{ssl}		psf	2116.217 psf
20	Wing area	S		ft^2	
21	Test maximum lift coefficient	$C_{L_{max_{Test}}}$	Eq 3.38		
22	Chord length	c		ft	

23	Test deceleration rate	$\dot{V}_{Test}$		kn/s	From airspeed trace, if available; otherwise use the observed value
24	Standard deceleration rate	$\dot{V}_{Std}$		kn/s	From specification; otherwise 1/2 kn/s
25	R parameter	R	Eq 3.39		
26	Slope of $C_{L_{max}}$ vs $\dot{V}$	K_d		kn/s	From graph
27 a	Maximum lift coefficient at standard deceleration rate	$C_{L_{max}\ Std\ \dot{V}}$	Eq 3.40		Empirical correction
27 b	Maximum lift coefficient at standard deceleration rate	$C_{L_{max}\ Std\ \dot{V}}$	Eq 3.25		Graphical correction
28	Test CG	CG_{Test}		% MAC	
29	Standard CG	CG_{Std}		% MAC	From specification
30	Slope of $C_{L_{max}\ Std\ \dot{V}}$ vs CG	K_c			
31	Maximum lift coefficient at standard deceleration rate and CG	$C_{L_{max}\ Std\ \dot{V},\ CG}$	Eq 3.26		Graphical correction.
32	Standard weight	W_{Std}		lb	From specification
33	Slope of $C_{L_{max}\ Std\ \dot{V},\ CG}$ vs GW	K_W		lb^{-1}	
34	Maximum lift coefficient at standard deceleration rate, CG, and weight	$C_{L_{max}\ Std\ \dot{V},\ CG,\ W}$	Eq 3.31		Graphical correction.
35	Maximum lift coefficient at standard deceleration rate, CG, weight, and altitude	$C_{L_{max}\ Std\ \dot{V},\ CG,\ W,\ H_P}$			From $C_{L_{max}}$ versus H_P plot
36	Referred normal acceleration	$n_z \frac{W}{\delta}$		g-lb	Calculation for data presentation

Finally, plot $n_z \frac{W}{\delta}$ versus Mach as shown in figure 3.20 and $C_{L_{max}}$ $_{Std\ \dot{V},\ CG,\ W}$ versus H_{P_c} as shown in figure 3.17

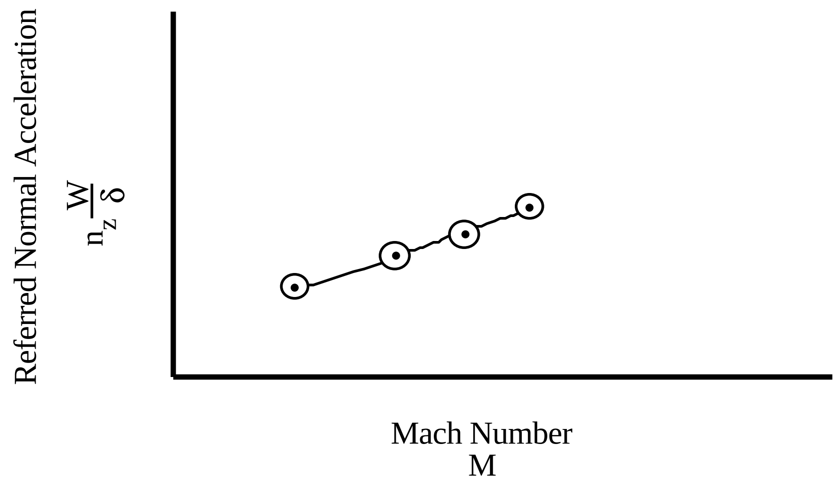

Figure 3.20
REFERRED NORMAL ACCELERATION VERSUS MACH NUMBER

3.5.2 POWER-ON STALLS

The procedure to calculate the lift coefficient for power-on stalls is the same as for power-off stalls. Power effects can be documented when measurements of gross thrust and ram drag are available. The lift from the inclined thrust axis can be accounted for directly. However, the indirect effects of thrust (i.e., flow entrainment and trim lift) are contained in the aerodynamic lift term and can be isolated only by subtracting the aerodynamic lift measured with the power-off. The following procedure is used to calculate the power effects.

Data reduction for power-on stalls is similar to section 3.5.1. The following additional equations are needed:

$$C_{T_G} = \frac{T_G \sin \alpha_j}{q\ S} \tag{Eq 3.30}$$

$$\left(C_{L_{aero}}{}_{Std\,\dot{V},\,CG,\,W}\right)_{Pwr\,ON} = \left(C_{L_{max}}{}_{Std\,\dot{V},\,CG,\,W}\right)_{Pwr\,ON} - C_{T_G} \qquad \text{(Eq 3.41)}$$

$$\Delta C_{L_t} = \frac{T_G}{q\,S}\left(\frac{Z}{l_t}\right) - \frac{D_R}{q\,S}\left(\frac{Y}{l_t}\right) \qquad \text{(Eq 3.28)}$$

$$\left(C_{L_{aero}}{}_{Std\,\dot{V},\,CG,\,W}\right)_{Pwr\,OFF} = \left(C_{L_{aero}}{}_{Std\,\dot{V},\,CG,\,W}\right)_{Pwr\,ON} - \Delta C_{L_t} - \Delta C_{L_E} \qquad \text{(Eq 3.42)}$$

Where:

α_j	Thrust angle	deg
C_{D_R}	Coefficient of ram drag	
$\left(C_{L_{aero}}{}_{Std\,\dot{V},\,CG,\,W}\right)_{Pwr\,OFF}$	Aerodynamic lift coefficient at standard deceleration rate, CG, and weight, power-off	
$\left(C_{L_{aero}}{}_{Std\,\dot{V},\,CG,\,W}\right)_{Pwr\,ON}$	Aerodynamic lift coefficient at standard deceleration rate, CG, and weight, power-on	
$\left(C_{L_{max}}{}_{Std\,\dot{V},\,CG,\,W}\right)_{Pwr\,ON}$	Maximum lift coefficient at standard deceleration rate, CG, and weight, power-on	
C_{T_G}	Coefficient of gross thrust lift	
ΔC_{L_E}	Coefficient of thrust-entrainment lift	
ΔC_{L_t}	Incremental tail lift coefficient	
l_t	Moment arm for tail lift	ft
q	Dynamic pressure	psf
S	Wing area	ft^2
T_G	Gross thrust	lb
Y	Height of CG above ram drag	ft
Z	Height of CG above gross thrust.	ft

To calculate the aerodynamic lift coefficient at standard deceleration rate, CG, and weight power-off proceed as follows:

Step	Parameter	Notation	Formula	Units	Remarks
1	Maximum lift coefficient at standard deceleration rate, CG, and weight, power-on	$\left(C_{L_{max}\ Std\ \dot{V},\ CG,\ W}\right)_{Pwr\ ON}$			As for power-off
2	Gross thrust	T_G		lb	From contractor
2	Coefficient of gross thrust lift	C_{T_G}	Eq 3.30		
3	Aerodynamic lift coefficient at standard deceleration rate, CG, and weight, power-on	$\left(C_{L_{aero}\ Std\ \dot{V},\ CG,\ W}\right)_{Pwr\ ON}$	Eq 3.41		
4	Incremental tail lift coefficient	ΔC_{L_t}	Eq 3.28		
5	Coefficient of thrust-entrainment lift	ΔC_{L_E}			From contractor
6	Aerodynamic lift coefficient at standard deceleration rate, CG, and weight, power-off	$\left(C_{L_{aero}\ Std\ \dot{V},\ CG,\ W}\right)_{Pwr\ OFF}$	Eq 3.42		

3.6 DATA ANALYSIS

3.6.1 CALCULATING $C_{L_{MAX}}$ FOR STANDARD CONDITIONS

3.6.1.1 POWER-OFF STALLS

After the data reduction is complete, the corrected values of $C_{L_{max}}$ for standard conditions are known. Values of $C_{L_{max}}$ for other conditions of deceleration rate, gross weight, CG position, or altitude can be calculated using the correction factors determined from the test results, plus the altitude variation graph.

3.6.1.2 POWER-ON STALLS

The procedure recommended to determine the power-on lift coefficient for standard conditions is the following:

1. Calculate $C_{L_{max}}$ with power-off and correct for $\dot{V}$, CG, and W to obtain $\left(C_{L_{max}\ Std\ \dot{V},\ CG,\ W}\right)_{Pwr\ OFF}$.
2. Subtract the thrust effects (C_{T_G}, ΔC_{L_t}, and ΔC_{L_E}) to get $\left(C_{L_{aero}\ Std\ \dot{V},\ CG,\ W}\right)_{Pwr\ OFF}$.
3. Obtain the standard thrust and calculate the corresponding C_{T_G}, ΔC_{L_t}, and ΔC_{L_E}.
4. Add the corrections to $\left(C_{L_{max}\ Std\ \dot{V},\ CG,\ W}\right)_{Pwr\ OFF}$ to get $\left(C_{L_{max}\ Std\ \dot{V},\ CG,\ W}\right)_{Pwr\ ON}$.
5. Plot versus H_{P_c} for the extrapolation to sea level, if required.

3.6.2 CALCULATING STALL SPEED FROM $C_{L_{MAX}}$

Once $C_{L_{max}}$ is determined, the equivalent airspeed of interest can be calculated using Eq 3.43 to solve for V_{e_s}.

$$V_{e_s} = \sqrt{\frac{841.5\ n_z\ W}{C_{L_{max}}\ S}} \qquad \text{(Eq 3.43)}$$

Where:

$C_{L_{max}}$	Maximum lift coefficient	
n_z	Normal acceleration	g
S	Wing area	ft^2
V_{e_s}	Stall equivalent airspeed	kn
W	Weight	lb.

3.7 MISSION SUITABILITY

The stall speed represents the absolute minimum useable speed for an airplane in steady conditions. For takeoff and landing phases, recommended speeds are chosen a safe margin above the stall speeds. For takeoffs the margin depends upon:

1. The stall speed.
2. The speed required for positive rotation.
3. The speed at which thrust available equals thrust required after liftoff.
4. The minimum control speed after engine failure for multi-engine airplanes.

For catapult launches, the minimum speed also depends upon a 20 ft maximum sink limit off the bow. The minimum end speed for launches is intended to give at least a 4 kn margin above the absolute minimum speed. For landing tasks, similar considerations are given to the approach and potential waveoff scenarios. Normally a twenty percent margin over the stall speed (however determined) is used, making the recommended approach speed 1.2 times the stall speed.

From the pilot’s perspective, low takeoff speeds are desirable for several reasons. With a low takeoff speed the airplane can accelerate to takeoff speed quickly, using relatively little runway to get airborne. Safety is enhanced since relatively more runway is available for aborting the takeoff in emergencies. Operationally, the short takeoff distance provides flexibility for alternate runway takeoffs (off-duty, downwind, etc.) and allows the airplane to operate from fields with short runways. For shipboard operations, the low takeoff speed is less stressful on the airframe and the ship’s catapult systems, and makes it easier to launch in conditions of little natural wind.

Low approach speeds provide relatively more time to assess the approach parameters and make appropriate corrections. The airplane is also more maneuverable at low speeds, since tight turns are possible. Low approach speeds also make the airplane easier to handle from an air traffic control perspective. The air traffic controller can exploit the airplane’s speed flexibility for aircraft sequencing and its enhanced maneuverability for vectoring in and around the airfield for departures, circling approaches, and missed approaches.

Low landing speeds give the pilot relatively more time to react to potential adverse runway conditions after touchdown. Less runway is used during the time it takes the pilot to react to a problem and decide to go-around. Low landing speeds also help to reduce the kinetic energy which has to be absorbed during the rollout by the airplane's braking system or by the ship's arresting gear. Low landing speeds promote short stopping distances, leaving more runway ahead and a safety margin in case of problems during the rollout. The reduced runway requirements also give the airplane operational flexibility, as in the takeoff case.

3.8 SPECIFICATION COMPLIANCE

The stall speed is used to verify compliance with performance guarantees of the detailed specification. The specified minimum takeoff and landing speeds are determined using the stall speed as a reference. For example, the minimum approach speed might be specified to be below a certain airspeed for a prescribed set of conditions. The specified approach speed (V_{APR}) may be referenced to a minimum speed in the approach configuration ($V_{PA_{min}}$), with $V_{PA_{min}}$ defined as a multiple of the stall speed (V_S). That is, $V_{APR} = 1.05\ V_{PA_{min}}$, where $V_{PA_{min}} = 1.1\ V_S$. The minimum approach speed, equal to $(1.1)(1.05)V_S$, would meet the specification requirement only if the stall speed was low enough for the identical conditions. Similarly, the takeoff speed specifications depend upon the stall speed in the takeoff configuration.

3.9 GLOSSARY

3.9.1 NOTATIONS

AFCS	Automatic flight control system	
AR	Aspect ratio	
BLC	Boundary layer control	
c	Chord length	ft
$\frac{c}{2}$	Semi-chord length	ft
CAS	Calibrated airspeed	kn
C_{D_R}	Coefficient of ram drag	
CG	Center of gravity	% MAC
CG_{Std}	Standard CG	% MAC

CG_{Test}	Test CG	% MAC
C_L	Lift coefficient	
$C_{L_{aero}}$	Aerodynamic lift coefficient	
$\left(C_{L_{aero\ Std\ \dot{V},\ CG,\ W}}\right)_{Pwr\ OFF}$	Aerodynamic lift coefficient at standard deceleration rate, CG, and weight, power-off	
$\left(C_{L_{aero\ Std\ \dot{V},\ CG,\ W}}\right)_{Pwr\ ON}$	Aerodynamic lift coefficient at standard deceleration rate, CG, and weight, power-on	
$C_{L_{max}}$	Maximum lift coefficient	
$C_{L_{max\ (\Lambda = 0)}}$	Maximum lift coefficient at $\Lambda = 0$	
$C_{L_{max\ (\Lambda)}}$	Maximum lift coefficient at Λ wing sweep	
$C_{L_{max\ Std\ \dot{V}}}$	Maximum lift coefficient at standard deceleration rate	
$C_{L_{max\ Std\ \dot{V},\ CG}}$	Maximum lift coefficient at standard deceleration rate and CG	
$C_{L_{max\ Std\ \dot{V},\ CG,\ W}}$	Maximum lift coefficient at standard deceleration rate, CG, and weight	
$\left(C_{L_{max\ Std\ \dot{V},\ CG,\ W}}\right)_{Pwr\ ON}$	Maximum lift coefficient at standard deceleration rate, CG, and weight, power-on	
$C_{L_{max\ Std\ \dot{V},\ CG,\ W,\ Hp}}$	Maximum lift coefficient at standard deceleration rate, CG, weight,and altitude	
$C_{L_{max_{Test}}}$	Test maximum lift coefficient	
C_{L_s}	Stall lift coefficient	
$C_{L_{Test}}$	Test lift coefficient	
C_{T_G}	Coefficient of gross thrust lift	
D	Drag	lb
ΔC_{L_E}	Coefficient of thrust-entrainment lift	
ΔC_{L_t}	Incremental tail lift coefficient	
$\Delta H_{P_{ic}}$	Altimeter instrument correction	ft
ΔH_{pos}	Altimeter position error	ft
ΔL_t	Tail lift increment	lb
$\Delta n_{z_{ic}}$	Normal acceleration instrument correction	g
$\Delta n_{z_{tare}}$	Accelerometer tare correction	g

D_R	Ram drag	lb
ΔV_{ic}	Airspeed instrument correction	kn
ΔV_{pos}	Airspeed position error	kn
H_P	Pressure altitude	ft
H_{P_c}	Calibrated pressure altitude	ft
H_{P_i}	Indicated pressure altitude	ft
H_{P_o}	Observed pressure altitude	ft
K_c	Slope of $C_{L_{max}}$ $_{Std\ \dot{V}}$ vs CG	
K_d	Slope of $C_{L_{max}}$ vs $\dot{V}$	
K_W	Slope of $C_{L_{max}}$ $_{Std\ \dot{V}\ ,\ CG}$ vs GW	lb^{-1}
L	Lift	lb
l	Length	ft
L_{aero}	Aerodynamic lift	lb
l_t	Moment arm for tail lift	ft
L_{Thrust}	Thrust lift	lb
M	Mach number	
MAC	Mean aerodynamic chord	
N	Engine speed	RPM
n_x	Acceleration along the X axis	g
n_z	Normal acceleration	g
$n_z \frac{W}{\delta}$	Referred normal acceleration	g-lb
n_{z_i}	Indicated normal acceleration	g
n_{z_o}	Observed normal acceleration	g
OAT	Outside air temperature	˚C or ˚K
P_{ssl}	Standard sea level pressure	2116.217 psf
q	Dynamic pressure	psf
R	Number of semi-chord lengths	
R_e	Reynold's number	
S	Wing area	ft^2
T	Thrust	lb
T_G	Gross thrust	lb
V	Velocity	kn
V_{APR}	Approach speed	kn
V_c	Calibrated airspeed	kn
V_e	Equivalent airspeed	kn

V_{e_s}	Stall equivalent airspeed	ft/s or kn
V_i	Indicated airspeed	kn
V_o	Observed airspeed	kn
$V_{PA_{min}}$	Minimum speed in the approach configuration	kn
V_s	Stall speed	kn
$V_{s_{Test}}$	Test stall speed	kn
$\dot{V}$	Acceleration/deceleration rate	kn/s
$\dot{V}_{Std}$	Standard acceleration/deceleration rate	kn/s
$\dot{V}_{Test}$	Test acceleration/deceleration rate	kn/s
W	Weight	lb
W_{Std}	Standard weight	lb
W_{Test}	Test weight	lb
Y	Height of CG above ram drag	ft
Z	Height of CG above gross thrust	ft

3.9.2 GREEK SYMBOLS

α (alpha)	Angle of attack	deg
α_j	Thrust angle	deg
δ (delta)	Pressure ratio	
δ_{Test}	Test pressure ratio	
γ (gamma)	Flight path angle,	
	Ratio of specific heats	deg
Λ (Lambda)	Wing sweep angle	deg
λ (lambda)	Taper ratio	
μ (mu)	Viscosity	lb-s/ft^2
θ (theta)	Pitch attitude	deg
ρ (rho)	Air density	slug/ft^3
ρ_{ssl}	Standard sea level air density	0.0023769 slug/ft^3
τ (tau)	Inclination of the thrust axis with respect to the chord line	deg

3.10 REFERENCES

1. Branch, M., *Determination of Stall Airspeed at Altitude and Sea Level*, Flight Test Division Technical Memorandum, FTTM No. 3-72, Naval Air Test Center, Patuxent River, MD, November, 1972.

2. Federal Aviation Regulations, Part 23, *Airworthiness Standards: Normal, Utility, and Acrobatic Category Airplanes*, June 1974.

3. Lan, C. E., and Roskam, J., *Airplane Aerodynamics and Performance*, Roskam Aviation and Engineering Corp.,Ottawa, Kansas, 1981.

4. Lean, D., *Stalling and the Measurement of Maximum Lift*, AGARD Flight Test Manual, Vol II, Chap 7, Pergamon Press, Inc., New York, NY., 1959.

5. McCue, J.J., *Pitot-Static Systems*, USNTPS Class Notes, USNTPS, Patuxent River, MD., June, 1982.

6. Military Standard, “Flying Qualities of Piloted Aircraft”, MIL-STD-1797A, 30 January, 1990.

7. Naval Test Pilot School Flight Test Manual, *Fixed Wing Performance, Theory and Flight Test Techniques*, USNTPS-FTM-No.104, U. S. Naval Test Pilot School, Patuxent River, MD, July, 1977.

8. Powell, J., *Airplane Performance*, USNTPS Classroom Notes, USNTPS, Patuxent River, MD.

9. Strike Aircraft Test Directorate Flight Test Manual, *Carrier Suitability Testing Manual*, SA FTM-01, Strike Aircraft Test Directorate, Patuxent River, MD, March,1991.

10. USAF Test Pilot School, *Performance Phase Textbook Volume I*, USAF-TPS-CUR-86-01, USAF, Edwards AFB, CA, April, 1986.

CHAPTER 4

LEVEL FLIGHT PERFORMANCE

CHAPTER 4

FIGURES

CHAPTER 4

EQUATIONS

$L - W + T_G \sin \alpha_j = 0$	(Eq 4.13)	4.9
$L = W - T_G \sin \alpha_j$	(Eq 4.14)	4.9
$C_L = \frac{L}{qS}$	(Eq 4.15)	4.9
$C_L = \frac{W - T_G \sin \alpha_j}{qS}$	(Eq 4.16)	4.9
$D = C_{D_P} qS + \frac{\left(W - T_G \sin \alpha_j\right)^2}{\pi\, e\, AR\, qS}$	(Eq 4.17)	4.9
$D = C_{D_P} qS + \frac{W^2}{\pi\, e\, AR\, qS}$	(Eq 4.18)	4.9
$q = \frac{1}{2} \rho_{ssl} V_e^2$	(Eq 4.19)	4.9
$q = \frac{1}{2} \rho_a V_T^2$	(Eq 4.20)	4.9
$q = \frac{1}{2} \gamma P_a M^2$	(Eq 4.21)	4.10
$D = \frac{C_{D_p} \rho_{ssl} V_e^2 S}{2} + \frac{2 W^2}{\pi\, e\, AR\, S \rho_{ssl} V_e^2}$	(Eq 4.22)	4.10
$D = \frac{C_{D_p} \rho_a V_T^2 S}{2} + \frac{2 W^2}{\pi\, e\, AR\, S \rho_a V_T^2}$	(Eq 4.23)	4.10
$D = \frac{C_{D_p} \gamma P_a M^2 S}{2} + \frac{2W^2}{\pi\, e\, AR\, S \gamma P_a M^2}$	(Eq 4.24)	4.10

$$D = \frac{C_{D_{p\,(M)}} \gamma P_a M^2 S}{2} + \frac{2W^2}{\pi e_{(M)} AR\, S \gamma P_a M^2}$$

(Eq 4.25) 4.12

$$\frac{D}{\delta} = \frac{C_{D_{P(M)}} \gamma P_{ssl} M^2 S}{2} + \frac{2\left(W/\delta\right)^2}{\pi e_{(M)} AR\, S \gamma P_{ssl} M^2}$$

(Eq 4.26) 4.12

$$\frac{D}{\delta} = f\left(M, \frac{W}{\delta}\right)$$

(Eq 4.27) 4.13

$$\dot{W}_f = f\left(P, \rho, \mu, V, L, N\right)$$

(Eq 4.28) 4.14

$$\frac{\dot{W}_f}{\delta\sqrt{\theta}} = f\left(M, \frac{N}{\sqrt{\theta}}, R_e\right)$$

(Eq 4.29) 4.14

$$\frac{\dot{W}_f}{\delta\sqrt{\theta}} = f\left(M, \frac{N}{\sqrt{\theta}}\right)$$

(Eq 4.30) 4.15

$$\frac{T_{N_x}}{\delta} = f\left(M, \frac{N}{\sqrt{\theta}}\right)$$

(Eq 4.31) 4.15

$$\frac{\dot{W}_f}{\delta\sqrt{\theta}} = f\left(M, \frac{T_{N_x}}{\delta}\right)$$

(Eq 4.32) 4.15

$$T_{N_x} = T_G \cos\alpha_j - T_R$$

(Eq 4.33) 4.15

$$T_{N_x} = D \text{ (For small } \alpha_j\text{, where } \cos\alpha_j \cong 1\text{)}$$

(Eq 4.34) 4.15

$$\frac{T_{N_x}}{\delta} = \frac{D}{\delta}$$

(Eq 4.35) 4.15

$$\frac{\dot{W}_f}{\delta\sqrt{\theta}} = f\left(M, \frac{D}{\delta}\right)$$

(Eq 4.36) 4.15

$$\frac{\dot{W}_f}{\delta\sqrt{\theta}} = f\left(M, \frac{W}{\delta}\right)$$ (Eq 4.37) 4.16

$$\theta = \frac{T_a}{T_{ssl}}$$ (Eq 4.38) 4.21

$$\theta_T = \frac{T_T}{T_{ssl}} = \frac{OAT}{T_{ssl}}$$ (Eq 4.39) 4.21

$$\frac{\dot{W}_f}{\delta\sqrt{\theta}} = f\,(M, OAT)$$ (Eq 4.40) 4.22

$$T_T = T_a\left(1 + \frac{\gamma - 1}{2}\ M^2\right)$$ (Eq 4.41) 4.22

$$P_T = P_a\left(1 + \frac{\gamma - 1}{2}\ M^2\right)^{\frac{\gamma}{\gamma - 1}}$$ (Eq 4.42) 4.22

$$\delta = \frac{P_a}{P_{ssl}}$$ (Eq 4.43) 4.23

$$\delta_T = \frac{P_T}{P_{ssl}}$$ (Eq 4.44) 4.23

$$\frac{\theta_T}{\theta} = \left(1 + 0.2\ M^2\right)$$ (Eq 4.45) 4.23

$$\frac{\delta_T}{\delta} = \left(1 + 0.2\ M^2\right)^{3.5}$$ (Eq 4.46) 4.23

$$\frac{\dot{W}_f}{\delta_T\sqrt{\theta_T}} = f\,(M, OAT)$$ (Eq 4.47) 4.23

$$TSFC = \frac{\dot{W}_f}{T_{N_x}}$$ (Eq 4.48) 4.25

$T_{N_x} = D$	(Eq 4.49)	4.26
$\dot{W}_f \approx D$	(Eq 4.50)	4.26
$S.R. = \dfrac{nmi}{W_f}$	(Eq 4.51)	4.28
$S.R. = \dfrac{V_T}{\dot{W}_f}$	(Eq 4.52)	4.28
$S.E. = \dfrac{t}{W_{f_{Used}}}$	(Eq 4.53)	4.28
$S.E. = \dfrac{1}{\dot{W}_f}$	(Eq 4.54)	4.29
$Range = \left(S.R._{avg}\right)\left(Fuel\ Used\right)$	(Eq 4.55)	4.31
$nmi = \dfrac{nmi}{lb} \times lb$	(Eq 4.56)	4.31
$THP = \dfrac{T\,V_T}{550} = \dfrac{D\,V_T}{550}$	(Eq 4.57)	4.33
$THP = \dfrac{C_{D_P}\,\rho_a\,V_T^3\,S}{1100} + \dfrac{W^2}{275\,\pi\,e\,AR\,S\,\rho_a\,V_T}$	(Eq 4.58)	4.33
$THP = THP_p + THP_i$	(Eq 4.59)	4.34
$D = \dfrac{C_D}{C_L}\,W$	(Eq 4.60)	4.35
$THP = \dfrac{C_D\,W\,V_T}{C_L\,550}$	(Eq 4.61)	4.35
$L = W = C_L\,\dfrac{1}{2}\,\rho_a\,V_T^2\,S$	(Eq 4.62)	4.35

$THP = \dfrac{\left(\frac{2}{S}\right)^{\frac{1}{2}} W^{\frac{3}{2}} C_D}{\rho_a^{\frac{1}{2}} C_L^{\frac{3}{2}}\ 550}$	(Eq 4.63)	4.35
$\rho_a = \rho_{ssl}\ \sigma$	(Eq 4.64)	4.35
$THP = \dfrac{\sqrt{2}\, W^{\frac{3}{2}} C_D}{\left(S\ \rho_{ssl}\right)^{\frac{1}{2}} \sqrt{\sigma}\ C_L^{\frac{3}{2}}\ 550}$	(Eq 4.65)	4.35
$THP_e = THP\ \sqrt{\sigma}$	(Eq 4.66)	4.35
$THP_e = \dfrac{\sqrt{2}\, W^{\frac{3}{2}} C_D}{\left(S\ \rho_{ssl}\right)^{\frac{1}{2}} C_L^{\frac{3}{2}}\ 550}$	(Eq 4.67)	4.36
$THP = K_1 V_T^3 + K_2\ V_T^{-1}$	(Eq 4.68)	4.37
$3\ K_1 V_T^2 - K_2\ V_T^{-2} = 0$	(Eq 4.69)	4.37
$3\ K_1 V_T^3 = K_2\ V_T^{-1}$	(Eq 4.70)	4.37
$3\ THP_p = THP_i$	(Eq 4.71)	4.37
$3\ D_p = D_i$	(Eq 4.72)	4.37
$3\ C_{D_p} = C_{D_i}$	(Eq 4.73)	4.37

$$THP = K_o \frac{C_D}{C_L^{\frac{3}{2}}}$$ (Eq 4.74) 4.38

$$V_T = \frac{V_e}{\sqrt{\sigma}}$$ (Eq 4.75) 4.39

$$THP = \frac{THP_e}{\sqrt{\sigma}}$$ (Eq 4.76) 4.39

$$\sigma = \frac{\rho_a}{\rho_{ssl}}$$ (Eq 4.77) 4.40

$$THP_e \, V_e = \frac{C_{D_P} \rho_{ssl} \, V_e^4 \, S}{1100} + \frac{W^2}{275 \, \pi \, e \, AR \, S \, \rho_{ssl}}$$ (Eq 4.78) 4.40

$$\eta_P = \frac{THP}{SHP}$$ (Eq 4.79) 4.41

$$THP = \eta_P \, SHP$$ (Eq 4.80) 4.41

$$THPSFC = \frac{\dot{W}_f}{THP}$$ (Eq 4.81) 4.41

$$SHPSFC = \frac{\dot{W}_f}{SHP}$$ (Eq 4.82) 4.42

$$\dot{W}_f = \frac{THP}{\eta_P} \, SHPSFC$$ (Eq 4.83) 4.42

$$\left(\frac{W}{\delta}\right)_{Target} = \frac{W + W_f}{\delta}$$ (Eq 4.84) 4.47

$$\left(\frac{W}{\delta}\right)_{Target} = \frac{W_{aircraft} + W_f}{\delta}$$ (Eq 4.85) 4.48

$$\delta = \frac{W_{aircraft}}{\left(\frac{W}{\delta}\right)_{Target}} + \frac{1}{\left(\frac{W}{\delta}\right)_{Target}} W_f$$ (Eq 4.86) 4.48

$$OAT = T_a \left(1 + \frac{\gamma - 1}{2} K_T M^2\right)$$ (Eq 4.87) 4.48

$$H_{P_c} = H_{P_o} + \Delta H_{P_{ic}} + \Delta H_{pos}$$ (Eq 4.88) 4.59

$$T_a = T_o + \Delta T_{ic}$$ (Eq 4.89) 4.59

$$V_c = V_o + \Delta V_{ic} + \Delta V_{pos}$$ (Eq 4.90) 4.59

$$V_T = \frac{V_c}{\sqrt{\sigma}}$$ (Eq 4.91) 4.60

$$M = \frac{V_T}{a_{ssl}\sqrt{\theta}}$$ (Eq 4.92) 4.60

$$\dot{W}_{f_{ref}} = \frac{\dot{W}_f}{\delta\sqrt{\theta}}$$ (Eq 4.93) 4.60

$$W_{ref} = \frac{W}{\delta}$$ (Eq 4.94) 4.60

$$R_{Test} = \sum_{j=1}^{n} V_j \, \Delta t_j$$ (Eq 4.95) 4.63

$$R.F._{Test} = \frac{t_T}{\ln\left(\frac{W_1}{W_2}\right)}$$ (Eq 4.96) 4.63

$$R_{Std} = R.F._{Test} \ln\left(\frac{W_{Std_1}}{W_{Std_2}}\right)$$ (Eq 4.97) 4.63

$M = f\left(V_c, H_{P_c}\right)$	(Eq 4.98)	4.66
$\delta = f\left(H_{P_c}\right)$	(Eq 4.99)	4.67
$\frac{W + W_f}{\delta} = \frac{W}{\delta}$	(Eq 4.100)	4.67
$\frac{W}{\delta}\text{ (error)} = \frac{100\left[\frac{W}{\delta}\text{ (test)} - \frac{W}{\delta}\text{ (target)}\right]}{\frac{W}{\delta}\text{ (target)}}$	(Eq 4.101)	4.67
$^{\circ}C = {}^{\circ}K - 273.15$	(Eq 4.102)	4.67
$OAT = f\left(T_a, M\right)$	(Eq 4.103)	4.67
$T_a = f\left(OAT, M\right)$	(Eq 4.104)	4.67
$S.R.\ \delta = \frac{661.483M}{\left(\frac{\dot{w}_f}{\delta\sqrt{\theta}}\right)}$	(Eq 4.105)	4.68
$V_e = \sqrt{\frac{2q}{\rho_{ssl}}} = \sqrt{\frac{\sigma 2q}{\rho_a}} = \sqrt{\sigma}\ V_T$	(Eq 4.106)	4.73
$SHP_e = SHP\sqrt{\sigma}$	(Eq 4.107)	4.73
$T_a = T_{a_{Std}} + \Delta T_a$	(Eq 4.108)	4.78
$S.R. = \frac{a_{ssl}\ M}{\left(\frac{\dot{W}_f}{\delta\sqrt{\theta}}\right)\delta}$	(Eq 4.109)	4.78
$V_{T_{Hot\ day}} = 661.483\ M\sqrt{\theta_{Std}}\left(\frac{\sqrt{\theta_{Hot\ day}}}{\sqrt{\theta_{Std}}}\right)$	(Eq 4.110)	4.81

$$\dot{W}_{f_{\text{Hot day}}} = \dot{W}_{f_{\text{Std}}} \left(\frac{\sqrt{\theta_{\text{Hot day}}}}{\sqrt{\theta_{\text{Std}}}} \right)$$ (Eq 4.111) 4.82

$$\frac{\dot{W}_f}{\sqrt{\theta}} = ¢$$ (Eq 4.112) 4.82

$$\text{Range} = \int_0^{W_{f_{\text{Used}}}} (\text{S.R.})\, dW_f$$ (Eq 4.113) 4.86

$$\text{Range} = \int_{W_1}^{W_2} (\text{S.R.})\, dW$$ (Eq 4.114) 4.87

$$\text{Range} = \int_{W_1}^{W_2} (\text{S.R. } \delta) \left(\frac{W}{\delta} \right) \frac{1}{W}\, dW$$ (Eq 4.115) 4.87

$$\text{Range} = \int_{W_1}^{W_2} \left[\frac{661.483\, M}{\left(\frac{\dot{W}_f}{\delta \sqrt{\theta}} \right)} \frac{W}{\delta} \right] \frac{dW}{W}$$ (Eq 4.116) 4.87

$$\frac{D}{\delta} = K_3 + K_4 \left(\frac{W}{\delta} \right)^2$$ (Eq 4.117) 4.88

$$\text{R.F.} = \left[(\text{S.R. } \delta) \frac{W}{\delta} \right]$$ (Eq 4.118) 4.90

$$\text{R.F.} = \left[\frac{661.483\, M}{\left(\frac{\dot{W}_f}{\delta \sqrt{\theta}} \right)} \left(\frac{W}{\delta} \right) \right]$$ (Eq 4.119) 4.90

$$\text{Range} = \int_{W_1}^{W_2} (\text{R.F.}) \frac{dW}{W}$$ (Eq 4.120) 4.90

$$C_L = \frac{2\,W}{\gamma\,P_a\,M^2\,S} = \frac{2\,\frac{W}{\delta}}{\gamma\,M^2\,S\,P_{ssl}}$$

(Eq 4.121) 4.101

$$C_L = f\left(\frac{W}{\delta}, M^2\right)$$

(Eq 4.122) 4.101

$$\frac{\frac{W}{\delta}}{\frac{D}{\delta}} = \frac{W}{D} = \text{Constant}$$

(Eq 4.123) 4.101

$$\frac{661.483\,M}{\left(\frac{\dot{W}_f}{\delta\sqrt{\theta}}\right)} = \text{Constant}$$

(Eq 4.124) 4.102

$$\frac{TSFC}{\sqrt{\theta}} = \text{Constant}$$

(Eq 4.125) 4.102

$$\text{Range} = \text{R.F.}\ \ln\frac{W_1}{W_2}$$

(Eq 4.126) 4.105

CHAPTER 4

LEVEL FLIGHT PERFORMANCE

4.1 INTRODUCTION

This chapter examines the theory and flight tests to determine aircraft level flight performance. Of specific interest are range and endurance. Aerodynamic forces acting on the aircraft, lift and drag, and engine parameters are presented as functions of easily measured parameters. These engine and aerodynamic functions are combined to complete the analysis. The final result provides a method to determine engine and airplane performance characteristics with minimum flight testing. Only those aircraft and engine characteristics pertaining to level, unaccelerated flight are investigated. By definition, the aircraft is in level, unaccelerated flight when the sum of the forces and moments acting upon it equal zero. Therefore, lift equals aircraft weight, and the net thrust parallel flight path equals the aircraft drag.

4.2 PURPOSE OF TEST

The purpose of this test is to investigate aircraft performance characteristics in level flight to achieve the following objectives:

1. Determine significant performance parameters: maximum range and optimum range, maximum endurance and optimum endurance, and long range or ferry range.
2. Evaluate pertinent requirements of the specification.

4.3 THEORY

Aircraft level flight performance analysis is the process of determining standard day level flight characteristics from data obtained during nonstandard conditions. Until the advent of high speed aircraft and the accompanying compressibility effects, most flight test data were reduced by the density altitude method. The density altitude method can be used in the speed range where the assumption of constant drag for constant true speed and density altitude is valid. However, where effects of compressibility are not negligible this method results in erroneous standard day data. With jet powered aircraft came the necessity of standardizing data for constant compressibility conditions, thus avoiding compressibility corrections. This type of data reduction is the pressure altitude method. The pressure altitude method is based on the concept of maintaining a constant pressure altitude and indicated air speed, and correcting data only for temperature to obtain standard day performance. With identical test and standard day indicated airspeeds the test and standard day Mach numbers are the same.

Aerodynamic theory shows total drag is a function only of Mach number if weight and altitude are fixed. Reynold's number effects are generally ignored in flight test work. This is the basis for the simplicity and effectiveness of the pressure altitude method of flight test data reduction. Using this method, only a temperature correction to test day data is needed. Compressibility effects are automatically held constant.

4.3.1 DRAG

If a vehicle is to sustain flight, it must overcome the resistance to its motion through the air. The resistive force, acting in a direction opposing the direction of flight, is called aerodynamic drag.

A propulsion system, either propeller driven or jet, produces thrust to overcome the drag force on the vehicle. If the propulsive force or thrust is just equal and in opposite direction to the drag force on the vehicle in flight, the vehicle is in steady or equilibrium flight. If the thrust exceeds the drag, the vehicle accelerates.

The total drag on an aircraft is the sum of many component drags, such as the drag caused by the wings, fuselage, or tail. The aircraft manufacturer is interested in component drags when estimating the total drag of a proposed aircraft. The wind tunnel engineer is also interested in component drags, values he can measure experimentally on models in a wind tunnel. From these measurements, he attempts to predict the drag of a proposed or actual aircraft.

The flight test engineer is more interested in the total drag of an aircraft configuration, or in changes in total drag with changes in configuration. Total aircraft drag, rather than component drag, is the major consideration in aircraft performance determination. Total drag is determined normally from flight test measurements and is made up of many components.

4.3.1.1 SKIN FRICTION DRAG

Skin friction drag is caused by the viscosity of air flowing over the aircraft and is proportional to the shear stress on the aircraft surface caused by the airflow. Skin friction drag is created on all of the airframe surfaces exposed to the air stream such as wing, fuselage, and tail.

4.3.1.2 PRESSURE DRAG

Pressure drag arises because of the overall pressure distribution on an object. The difference between the forces caused by the high pressures on the forward portion and low pressures on the aft portion of the object is pressure drag. This drag is also know as wake or form drag because its magnitude is proportional to the size of the wake produced behind the object. Pressure drag always occurs since the total pressure is never completely recovered at the aft stagnation point, and there is always at least a small wake of separated flow behind any aerodynamic shape.

4.3.1.3 PROFILE DRAG

Profile drag is a measure of the resistance to flight caused by the viscous action of the air on the profile of the aircraft. The resistance to flight is the sum of skin friction and pressure drag. Profile drag is sometimes called boundary layer or viscous drag since neither skin friction nor pressure drag would occur if air were nonviscous. Equivalent flat plate area is accepted as a standard by which values of profile drag for aerodynamic shapes are compared.

4.3.1.4 INTERFERENCE DRAG

Interference drag is generated when several objects are placed in the same air stream creating eddy currents, turbulence, or restrictions to smooth flow. Any time two parts of an aircraft are joined or any object is placed on or in close proximity to an aircraft, interference drag is created. Fuselage-wing root junction and external stores hung on a wing are examples which produce this drag.

4.3.1.5 PARASITE DRAG

Parasite drag is the sum of profile and interference drag. It can be described as the drag which is not caused by lift or compressibility effects. Aircraft parasite drag is independent of angle of attack. Parasite drag is the total of each increment of drag caused by parts of the aircraft and its stores. A major source of parasite drag on reciprocating air cooled engine aircraft is called cooling drag where energy is lost as air is forced past cylinders of those piston powered propeller aircraft. The parasite drag equation is:

$$D_p = C_{D_p} qS \qquad \text{(Eq 4.1)}$$

Where:

C_{D_p}	Parasite drag coefficient	
D_p	Parasite drag	lb
q	Dynamic pressure	psf
S	Wing area	ft^2.

4.3.1.6 INDUCED DRAG

The portion of the total drag force due to the production of lift is defined as induced drag. Since the function of lift is to overcome weight, induced drag can be correctly described as drag due to lift. Fortunately, the thrust or power required to overcome induced drag is not excessive, especially at high speeds.

As a wing produces lift, the vortices impart a final vertical velocity, V_v, to the air stream. Figure 4.1 depicts the airflow.

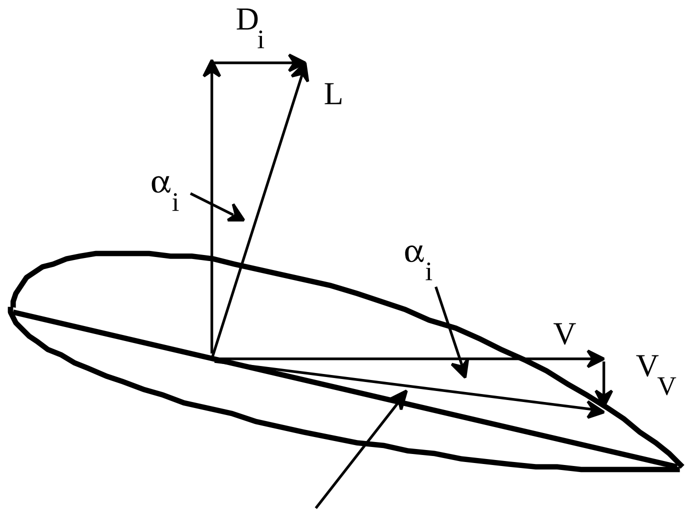

Figure 4.1
INDUCED FLOW FIELD

The term α_i is defined as the induced angle of attack in radians, and is the angle between the free stream relative wind and the average relative wind at the wing aerodynamic center. From the geometry of the lift and drag on an airfoil, the induced drag for small angles ($\sin \alpha_i \cong \alpha_i$) is:

$$D_i = L\,\alpha_i = C_L\, q\, S\, \alpha_i \qquad \text{(Eq 4.2)}$$

$$L = C_L\, qS \qquad \text{(Eq 4.3)}$$

$$D_i = C_{D_i}\, qS \qquad \text{(Eq 4.4)}$$

Prandtl found if the wing has an elliptical planform, the induced angle of attack is constant across the span. In addition to the planform, the induced drag is dependent upon the aspect ratio (AR). The smaller the aspect ratio, the larger the induced angle of attack and the greater the downwash. Induced angle of attack (α_i) is a function of AR as follows:

$$\alpha_i = \frac{C_L}{\pi\, AR} \qquad \text{(Eq 4.5)}$$

Substituting into Eq 4.2 and 4.4 for an elliptical airfoil:

$$C_{D_i} = \frac{C_L^2}{\pi\, AR} \qquad \text{(Eq 4.6)}$$

An induced drag coefficient can be defined for any given planform by inserting a constant, Oswald's efficiency factor, (e). The constant can be determined for any given aircraft configuration from flight test data and is used in the total drag coefficient equation for any wing planform or for an entire aircraft. Eq 4.6 becomes:

$$C_{D_i} = \frac{C_L^2}{\pi\, e\, AR} \qquad \text{(Eq 4.7)}$$

Where:

α_i	Induced angle of attack	deg
AR	Aspect ratio	
C_{D_i}	Induced drag coefficient	
C_L	Lift coefficient	
D_i	Induced drag	lb
e	Oswald's efficiency factor	
L	Lift	lb
π	Constant	
q	Dynamic pressure	psf
S	Wing area	ft^2.

4.3.1.7 WAVE DRAG

Wave drag, often called compressibility or Mach drag, is the drag resulting when flow over the surfaces of an aircraft exceeds Mach 1.0. Supersonic flow over aircraft surfaces results in the formation of shock waves, causing a sizeable increase in drag due to the large pressure changes across the shock. Behind the shock wave, the flow field operates in an adverse pressure gradient due to the large increase in static pressure as the velocity is slowed to a lower supersonic or subsonic value. The net drag due to this higher pressure behind a shock wave is the wave drag.

4.3.1.8 RAM DRAG

Ram drag is drag due to ram compression aft of the compressor prior to the combustion section in the diffuser of a turbojet or turbofan engine. This term is widely used in propulsion. Net thrust is usually defined as gross thrust minus ram drag.

4.3.1.9 TRIM DRAG

Trim drag is an additional drag force resulting from the use of the horizontal tail in trimming the aircraft. The tail may carry a download for which the wing must provide additional lift. The increase in angle of attack required for this additional lift also increases the drag and reduces the critical Mach. The trim drag is significant at high altitudes particularly in designs with a short tail moment arm. The download requirements can be reduced by reducing the static margin (moving the CG aft). Canard configurations produce an upload for trim which is equivalent to providing negative trim drag.

4.3.1.10 TOTAL DRAG

For flight test, a detailed breakdown of all drag components is not necessary. Conventionally, all drag which is not a function of lift is called parasite drag, and all drag which is a function of lift is called induced drag. If the aircraft velocity is greater than the critical Mach, wave drag accounts for the losses due to shock waves. Total drag may be written as the sum of the major component drags or sum of the drag coefficients using definitions similar to Eq 4.1.

$$D = D_P + D_i + D_M \tag{Eq 4.8}$$

$$C_D = C_{D_P} + C_{D_i} + C_{D_M} \tag{Eq 4.9}$$

Where:

C_D	Drag coefficient
C_{D_i}	Induced drag coefficient
C_{D_M}	Mach drag coefficient
C_{D_p}	Parasite drag coefficient

D	Drag	lb
D_i	Induced drag	lb
D_M	Mach drag	lb
D_p	Parasite drag	lb.

4.3.1.11 LOW SPEED DRAG CHARACTERISTICS

An equation for low speed total drag, ignoring Mach effects, is presented below using Eq 4.8 and assuming a parabolic drag polar (C_{D_i} is proportional to C_L^2).

$$D = C_D \, qS \qquad \text{(Eq 4.10)}$$

$$C_D = C_{D_p} + \frac{C_L^2}{\pi \, e \, AR} \qquad \text{(Eq 4.11)}$$

$$D = C_{D_P} \, q \, S + \frac{C_L^2}{\pi \, e \, AR} \, qS \qquad \text{(Eq 4.12)}$$

An expression for C_L is developed to quantify the drag. The forces acting on an airplane in level flight are given in figure 4.2.

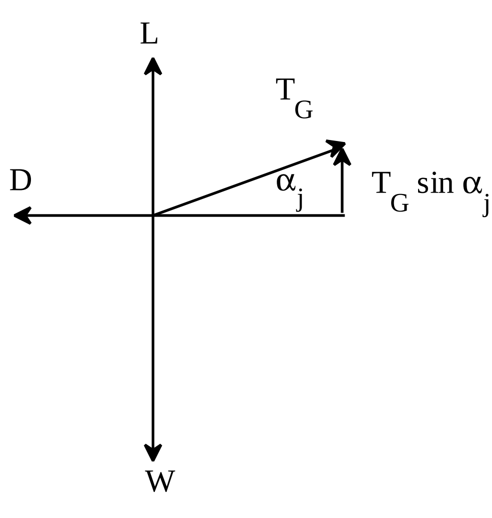

Figure 4.2
FORCES IN LEVEL FLIGHT

To maintain level unaccelerated flight the sum of the forces in the z axis equals zero:

$$L - W + T_G \sin \alpha_j = 0 \qquad \text{(Eq 4.13)}$$

$$L = W - T_G \sin \alpha_j \qquad \text{(Eq 4.14)}$$

The lift coefficient is defined and substituted into Eq 4.12.

$$C_L = \frac{L}{qS} \qquad \text{(Eq 4.15)}$$

$$C_L = \frac{W - T_G \sin \alpha_j}{qS} \qquad \text{(Eq 4.16)}$$

$$D = C_{D_P}\, qS + \frac{\left(W - T_G \sin \alpha_j\right)^2}{\pi\, e\, AR\, qS} \qquad \text{(Eq 4.17)}$$

To simplify the above equation, assume weight (W) is much larger than the vertical thrust component ($T \sin \alpha_j$). This is a valid assumption for airplanes in cruise where α_j is small. At low speed, large α_j and high thrust setting may introduce sizeable error. Eq 4.17 reduces to:

$$D = C_{D_P}\, qS + \frac{W^2}{\pi\, e\, AR\, qS} \qquad \text{(Eq 4.18)}$$

Dynamic pressure (q) can be expressed in any of the following forms:

$$q = \frac{1}{2}\, \rho_{ssl}\, V_e^2 \qquad \text{(Eq 4.19)}$$

$$q = \frac{1}{2}\, \rho_a\, V_T^2 \qquad \text{(Eq 4.20)}$$

$$q = \frac{1}{2} \gamma P_a M^2 \qquad \text{(Eq 4.21)}$$

The level flight drag Eq 4.18 can then become:

$$D = \frac{C_{D_p} \rho_{ssl} V_e^2 S}{2} + \frac{2 W^2}{\pi e AR S \rho_{ssl} V_e^2} \qquad \text{(Eq 4.22)}$$

$$D = \frac{C_{D_p} \rho_a V_T^2 S}{2} + \frac{2 W^2}{\pi e AR S \rho_a V_T^2} \qquad \text{(Eq 4.23)}$$

$$D = \frac{C_{D_p} \gamma P_a M^2 S}{2} + \frac{2W^2}{\pi e AR S \gamma P_a M^2} \qquad \text{(Eq 4.24)}$$

Where:

α_j	Thrust angle	deg
AR	Aspect ratio	
C_D	Drag coefficient	
C_{D_p}	Parasite drag coefficient	
C_L	Lift coefficient	
D	Drag	lb
e	Oswald's efficiency factor	
γ	Ratio of specific heats	
L	Lift	lb
M	Mach number	
π	Constant	
P_a	Ambient pressure	psf
q	Dynamic Pressure	psf
ρ_a	Ambient air density	slugs/ft^3
ρ_{ssl}	Standard sea level air density	0.0023769 slugs/ft^3
S	Wing area	ft^2

T_G	Gross thrust	lb
V_e	Equivalent airspeed	kn
V_T	True airspeed	kn
W	Weight	lb.

A sketch of the drag equations in general form is shown in figure 4.3.

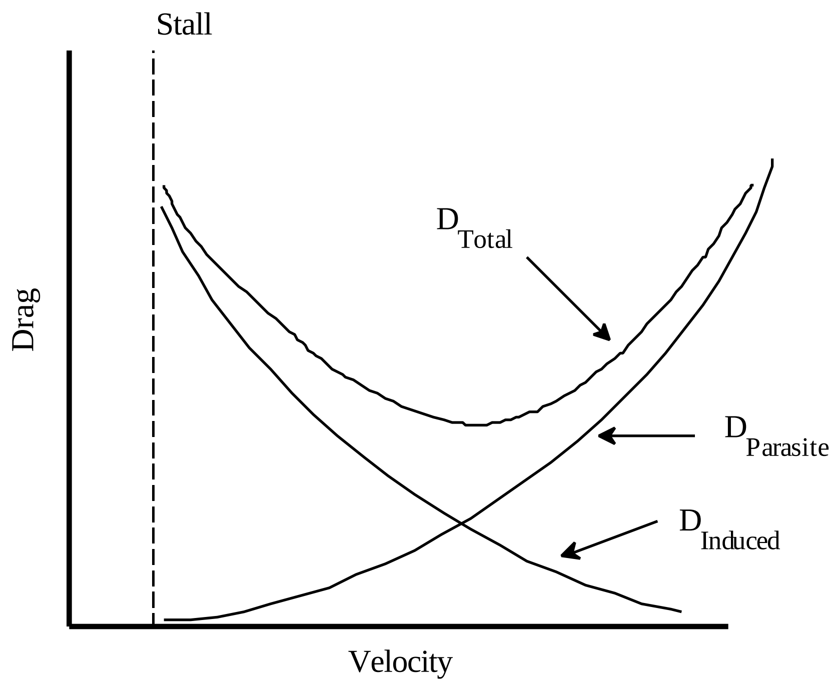

Figure 4.3
DRAG CURVES

The general features of the total drag curve are:

1. Positive sloped segment often called the front side.
2. Negative sloped segment called the back side.
3. Minimum drag point called the bucket.

4.3.1.12 HIGH MACH DRAG

At high transonic Mach numbers, the drag polar parameters (C_{D_p} and e) start to vary. Eq 4.24 is the level flight drag equation expressed as a function of Mach. For the low speed case C_{D_p} and e are constant. This simplification is not possible in the high Mach case since C_{D_p} and e vary. Figure 4.4 is a sketch showing typical C_{D_p} and e variations with Mach.

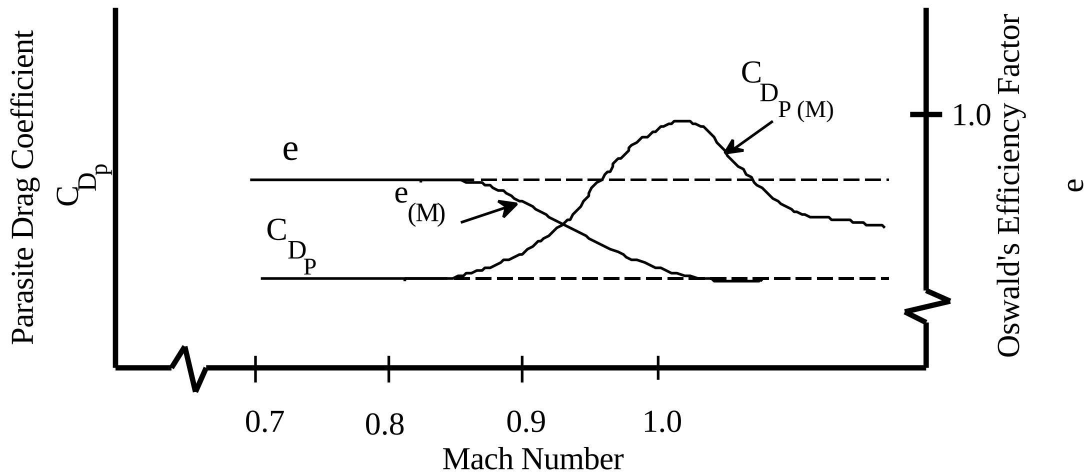

Figure 4.4
MACH EFFECT ON DRAG

A generalized form of drag equation at high Mach is:

$$D = \frac{C_{D_{p\,(M)}} \gamma P_a M^2 S}{2} + \frac{2W^2}{\pi\, e_{(M)}\, AR\, S\, \gamma\, P_a M^2} \qquad \text{(Eq 4.25)}$$

Mach drag is accounted for in the parasite and induced drag terms. There are three independent variables (M, W, P_a) in Eq 4.25. To document the airplane, drag in level flight at various Mach numbers would be measured. At each altitude the weight would be varied over its allowable range. This approach would be a major undertaking. To simplify the analysis, the independent variables are reduced to two by multiplying both sides of Eq 4.25 by $\frac{P_{ssl}}{P_a}$ and the induced drag term by $\frac{P_{ssl}}{P_{ssl}}$. Substituting $\delta = \frac{P_a}{P_{ssl}}$ and simplifying:

$$\frac{D}{\delta} = \frac{C_{D_{P(M)}} \gamma P_{ssl} M^2 S}{2} + \frac{2\left(W/\delta\right)^2}{\pi\, e_{(M)}\, AR\, S\, \gamma\, P_{ssl} M^2} \qquad \text{(Eq 4.26)}$$

Eq 4.26 in functional notation is:

$$\frac{D}{\delta} = f\left(M, \frac{W}{\delta}\right) \qquad \text{(Eq 4.27)}$$

Where:

AR	Aspect ratio	
$C_{D_{p\,(M)}}$	Parasite drag coefficient at high Mach	
D	Drag	lb
δ	Pressure ratio	
$e_{(M)}$	Oswald's efficiency factor at high Mach	
γ	Ratio of specific heats	
M	Mach number	
π	Constant	
P_a	Ambient pressure	psf
P_{ssl}	Standard sea level pressure	2116.217 psf
S	Wing area	ft^2
W	Weight	lb.

This grouping of terms allows drag data to be correlated and corrected, or referred to other weights and altitudes. Documenting the airplane operating envelope (M, W, H_P) can be efficiently accomplished. Graphically this relationship looks like figure 4.5.

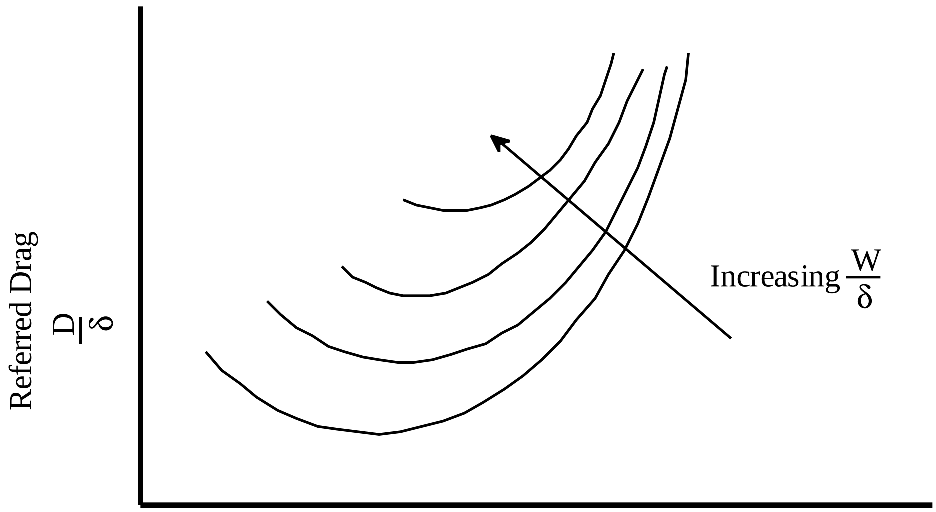

Figure 4.5
LEVEL FLIGHT DRAG

4.3.2 JET THRUST REQUIRED

Fuel flow, $\dot{W}_f$, is a function of both fluid properties and engine variables. Dimensional analysis shows:

$$\dot{W}_f = f\left(P, \rho, \mu, V, L, N\right) \tag{Eq 4.28}$$

A parameter called referred fuel flow, $\frac{\dot{W}_f}{\delta\sqrt{\theta}}$, is functionally expressed as follows:

$$\frac{\dot{W}_f}{\delta\sqrt{\theta}} = f\left(M, \frac{N}{\sqrt{\theta}}, R_e\right) \tag{Eq 4.29}$$

Referred fuel flow and referred engine speed, $\frac{N}{\sqrt{\theta}}$, are not the only referred engine parameters. The complete list includes six others. These parameters can be derived mathematically from the Buckingham Pi Theorem, or related to the physical phenomena occurring in the engine. Neglecting Reynold's number, Eq 4.29 becomes:

$$\frac{\dot{W}_f}{\delta\sqrt{\theta}} = f\left(M, \frac{N}{\sqrt{\theta}}\right) \tag{Eq 4.30}$$

Referred net thrust parallel flight path can be defined as $\frac{T_{N_x}}{\delta}$ and is a function of the same parameters as fuel flow:

$$\frac{T_{N_x}}{\delta} = f\left(M, \frac{N}{\sqrt{\theta}}\right) \tag{Eq 4.31}$$

Referred fuel flow can be expressed functionally:

$$\frac{\dot{W}_f}{\delta\sqrt{\theta}} = f\left(M, \frac{T_{N_x}}{\delta}\right) \tag{Eq 4.32}$$

In unaccelerated flight, net thrust parallel flight path is equal to net or total drag:

$$T_{N_x} = T_G \cos\alpha_j - T_R \tag{Eq 4.33}$$

$$T_{N_x} = D \text{ (For small } \alpha_j\text{, where } \cos\alpha_j \cong 1) \tag{Eq 4.34}$$

$$\frac{T_{N_x}}{\delta} = \frac{D}{\delta} \tag{Eq 4.35}$$

Eq 4.32 becomes:

$$\frac{\dot{W}_f}{\delta\sqrt{\theta}} = f\left(M, \frac{D}{\delta}\right) \tag{Eq 4.36}$$

From Eq 4.27, referred fuel flow and referred gross weight are functionally related as follows:

$$\frac{\dot{W}_f}{\delta\sqrt{\theta}} = f\left(M, \frac{W}{\delta}\right) \qquad \text{(Eq 4.37)}$$

Where:

α_j	Thrust angle	deg
D	Drag	lb
δ	Pressure ratio	
H_P	Pressure altitude	ft
L	Lift	lb
M	Mach number	
μ	Viscosity	lb-s/ft^2
N	Engine speed	RPM
P	Pressure	psf
θ	Temperature ratio	
ρ	Air density	slugs/ft^3
R_e	Reynold's number	
T_G	Gross thrust	lb
T_{N_x}	Net thrust parallel flight path	lb
T_R	Ram drag	lb
V	Velocity	kn
W	Weight	lb
$\dot{W}_f$	Fuel flow	lb/h.

The relationship expressed in Eq 4.37 is presented in figure 4.6.

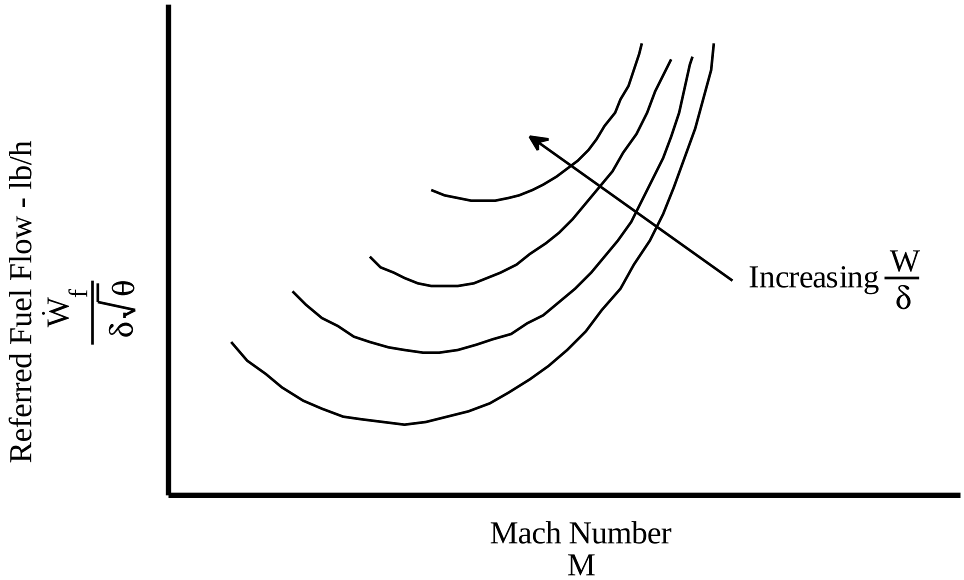

Figure 4.6
REFERRED FUEL FLOW

All variables affecting range and endurance are contained in figure 4.6, including velocity, fuel flow, gross weight, altitude, and ambient temperature. Range and endurance can be determined without directly measuring thrust or drag.

4.3.3 JET THRUST AVAILABLE

In level flight, thrust available determines maximum level flight airspeed, V_H, as shown in figure 4.7. For a turbojet, V_H takes the following forms:

M_{mrt}	Mach number at military rated thrust
M_{max}	Mach number at maximum thrust

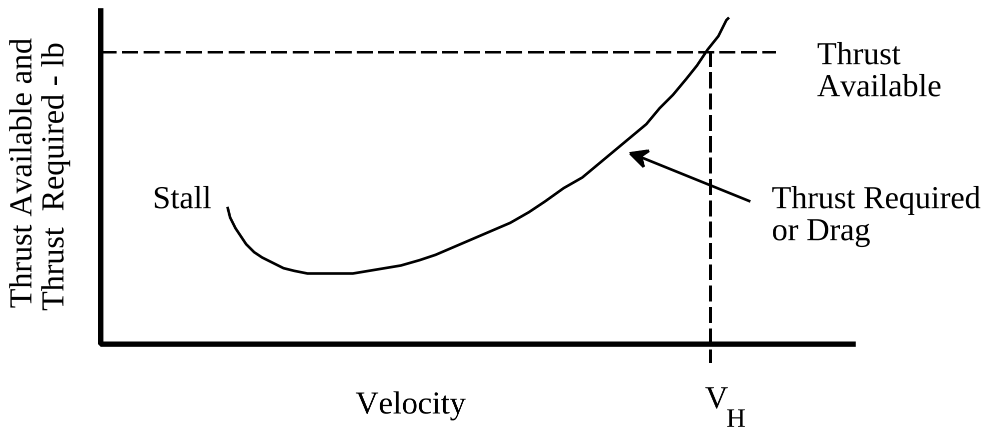

Figure 4.7
MAXIMUM LEVEL FLIGHT AIRSPEED

In performance testing, the aircraft is flown to a stabilized maximum level flight airspeed (V_H) where thrust equals drag. A second condition satisfied at this point is fuel flow required equals fuel flow available as depicted in figure 4.8.

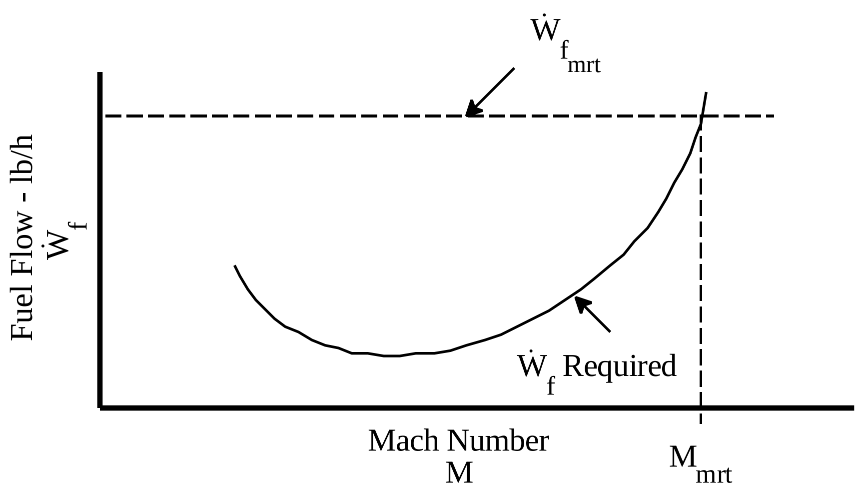

Figure 4.8
FUEL FLOW VERSUS MACH NUMBER

4.3.3.1 FUEL FLOW CORRECTION

Thrust required depends on, gross weight, pressure altitude, and Mach number as far as drag is concerned. Thrust available depends on power setting, pressure altitude, Mach, and ambient temperature. Test day M_{mrt} occurs at the point where test condition fuel flow required equals the test condition fuel flow available at military power. Evaluating the aircraft to other conditions requires referring the test conditions to standard conditions and then adjusting M_{mrt} (test) to M_{mrt} (standard). The technique determines M_{mrt} for specified conditions by determining the intersection of referred fuel flow required and referred fuel flow available. These parameters are calculated separately and combined to find the intersection.

4.3.3.1.1 REFERRED FUEL FLOW REQUIRED

The test results for a given configuration, gross weight, and pressure altitude can be plotted as in figure 4.6. From the figure, fuel flow is independent of ambient temperature. The same curve applies for cold day, standard day, or hot day.

4.3.3.1.2 REFERRED FUEL FLOW AVAILABLE

Referred fuel flow available is not independent of ambient temperature. From engine propulsion studies, variables affecting referred fuel flow available are: power setting, pressure altitude, Mach number, and ambient temperature. The temperature effect is illustrated by 5 power available curves presented in figure 4.9. M_{mrt} increases as the ambient temperature decreases.

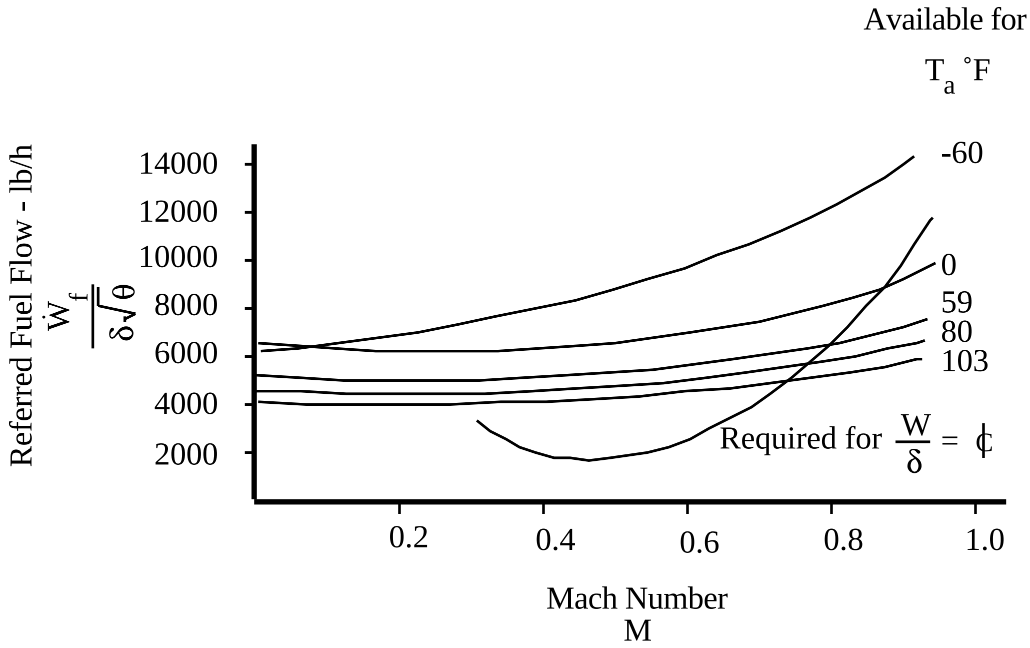

Figure 4.9
REFERRED FUEL FLOW AVAILABLE

For a fixed geometry turbojet and ignoring Reynold's number, referred fuel flow depends upon Mach and $\frac{N}{\sqrt{\theta}}$. The engine fuel control schedules engine speed, N, as a function of the inlet total temperature (at engine compressor face),T_{T_2}, in a manner similar to figure 4.10.

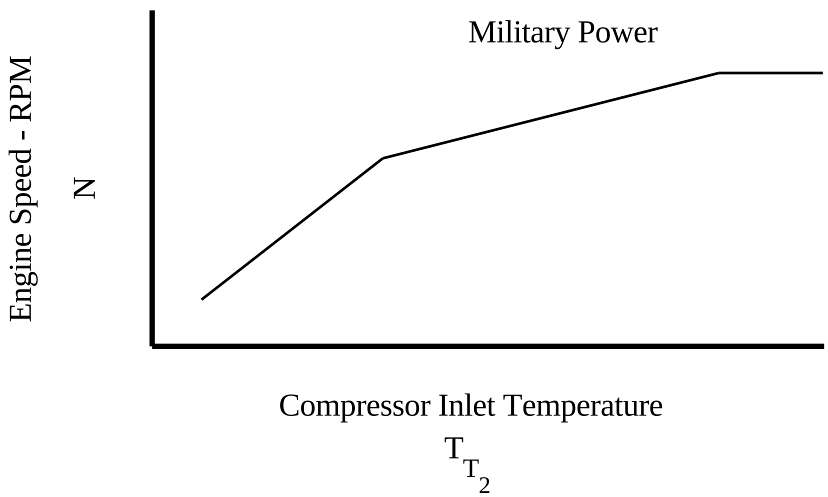

Figure 4.10
ENGINE SCHEDULING

The temperature at the compressor face is equal to the ambient temperature or outside air temperature. The temperature ratio, θ, and total temperature ratio, θ_T, are defined as:

$$\theta = \frac{T_a}{T_{ssl}} \qquad \text{(Eq 4.38)}$$

$$\theta_T = \frac{T_T}{T_{ssl}} = \frac{OAT}{T_{ssl}} \qquad \text{(Eq 4.39)}$$

The outside air temperature can be related to the total temperature ratio and referred engine speed as shown in figure 4.11.

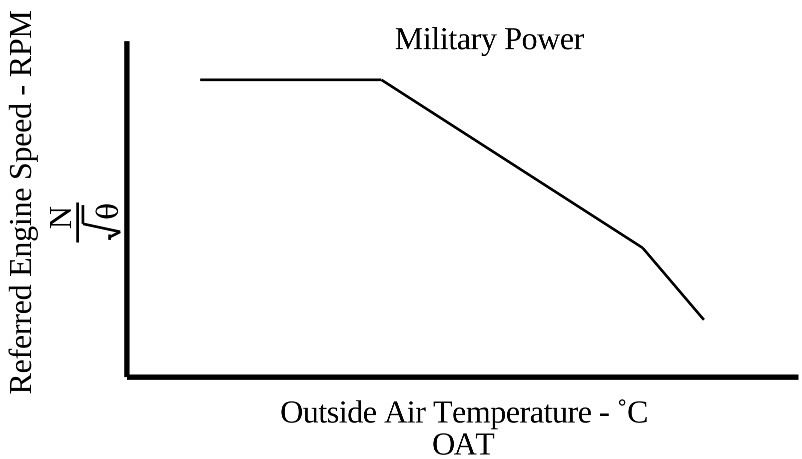

Figure 4.11
REFERRED ENGINE SCHEDULING

The referred engine speed is fairly linear over certain ranges of OAT with break points in the schedules. These break points occur because the engine switches modes of control as the OAT increases. At low temperatures it may be running to a maximum airflow schedule, and at hotter temperatures it runs to maximum turbine temperature or maximum physical speed. To calculate M_{mrt} for one power setting Eq 4.30 can be rewritten as:

$$\frac{\dot{W}_f}{\delta\sqrt{\theta}} = f\left(M, OAT\right) \quad \text{(Eq 4.40)}$$

The function plotted over the range of flight test data appears as in figure 4.12.

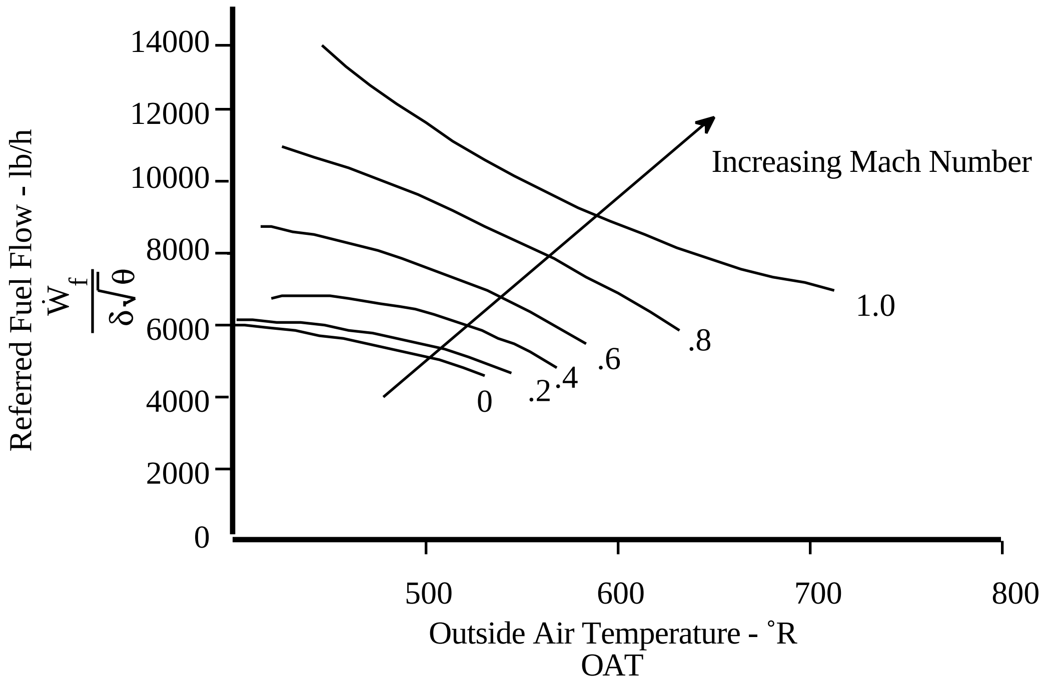

Figure 4.12
REFERRED FUEL FLOW AND OAT

Figure 4.12 can be simplified for analysis by defining a referred fuel flow which accounts for Mach effects. From total properties:

$$T_T = T_a\left(1 + \frac{\gamma - 1}{2} M^2\right) \quad \text{(Eq 4.41)}$$

$$P_T = P_a\left(1 + \frac{\gamma - 1}{2} M^2\right)^{\frac{\gamma}{\gamma - 1}} \quad \text{(Eq 4.42)}$$

$$\theta = \frac{T_a}{T_{ssl}} \quad \text{(Eq 4.38)}$$

$$\delta = \frac{P_a}{P_{ssl}} \qquad \text{(Eq 4.43)}$$

$$\theta_T = \frac{T_T}{T_{ssl}} = \frac{OAT}{T_{ssl}} \qquad \text{(Eq 4.39)}$$

$$\delta_T = \frac{P_T}{P_{ssl}} \qquad \text{(Eq 4.44)}$$

Letting γ equal 1.4 for the temperatures normally encountered, Eq 4.41 and 4.42 simplify to:

$$\frac{\theta_T}{\theta} = \left(1 + 0.2\ M^2\right) \qquad \text{(Eq 4.45)}$$

$$\frac{\delta_T}{\delta} = \left(1 + 0.2\ M^2\right)^{3.5} \qquad \text{(Eq 4.46)}$$

Since $\theta_T = f\ (\theta, M)$ and $\delta_T = f\ (\delta, M)$ a parameter is defined as fuel flow referred to total conditions and figure 4.12 is replotted as figure 4.13.

$$\frac{\dot{W}_f}{\delta_T \sqrt{\theta_T}} = f\left(M, OAT\right) \qquad \text{(Eq 4.47)}$$

Where:

δ	Pressure ratio	
δ_T	Total pressure ratio	
γ	Ratio of specific heats	
M	Mach number	
OAT	Outside air temperature	˚C or ˚K
P_a	Ambient pressure	psf
P_{ssl}	Standard sea level pressure	2116.217 psf
P_T	Total pressure	psf
θ	Temperature ratio	

θ_T	Total temperature ratio	
T_a	Ambient temperature	˚C or ˚K
T_{ssl}	Standard sea level temperature	15˚C, 288.15˚K
T_T	Total temperature	˚C,˚K
$\dot{W}_f$	Fuel flow	lb/h.

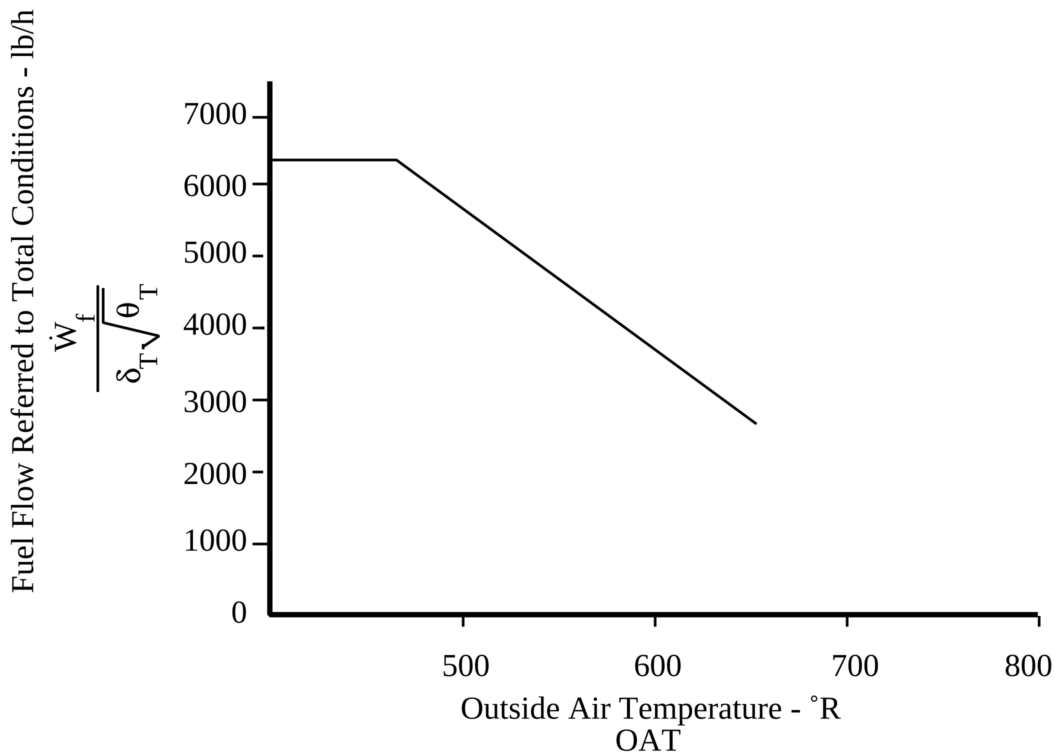

Figure 4.13
REFERRED FUEL FLOW AT TOTAL CONDITIONS

In figure 4.13, fuel flow is not dependent on Mach. The data for figure 4.13 can come from any military power condition, regardless of pressure altitude or ambient temperature. The aircraft need not be in equilibrium, allowing the data points to be taken during military power climbs and accelerations. A sufficient number of points from the W/δ flights can be obtained by including a M_{mrt} point for each W/δ. After all of the W/δ flights are complete, a curve similar to figure 4.14 is plotted. The curve should be fairly linear and can be extrapolated over a small range of OAT. Using figures 4.6 and 4.14, fuel flow can be unreferred to calculate M_{mrt} for any condition.

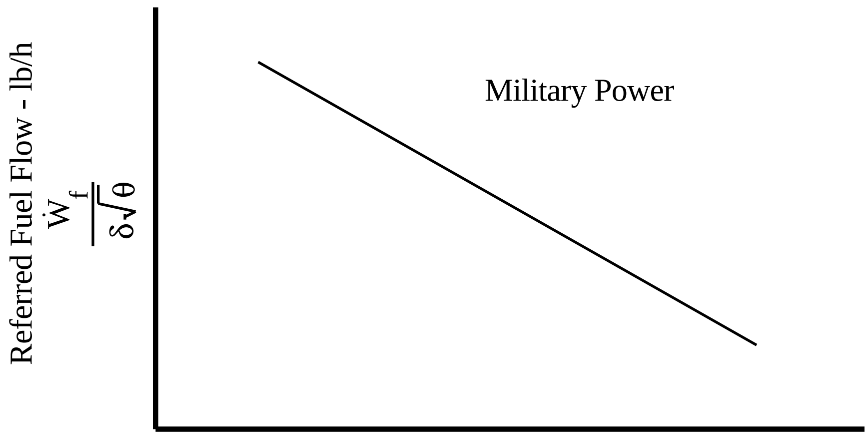

Figure 4.14
LINEARIZED REFERRED FUEL FLOW AVAILABLE

4.3.4 JET RANGE AND ENDURANCE

The ability of an airplane to convert fuel energy into flying distance is a high priority performance item. Efficient range characteristics are specified in either of two general forms:

1. To extract the maximum flying distance from a given fuel load.
2. To fly a specified distance with minimum expenditure of fuel.

The common denominator for each is the specific range (S.R.) or nautical miles per pound of fuel. For a jet, fuel flow is approximately proportional to the thrust produced. Thrust Specific Fuel Consumption (TSFC) can be defined as the ratio of fuel flow to net thrust parallel flight path and is shown in figure 4.15.

$$TSFC = \frac{\dot{W}_f}{T_{N_x}} \qquad \text{(Eq 4.48)}$$

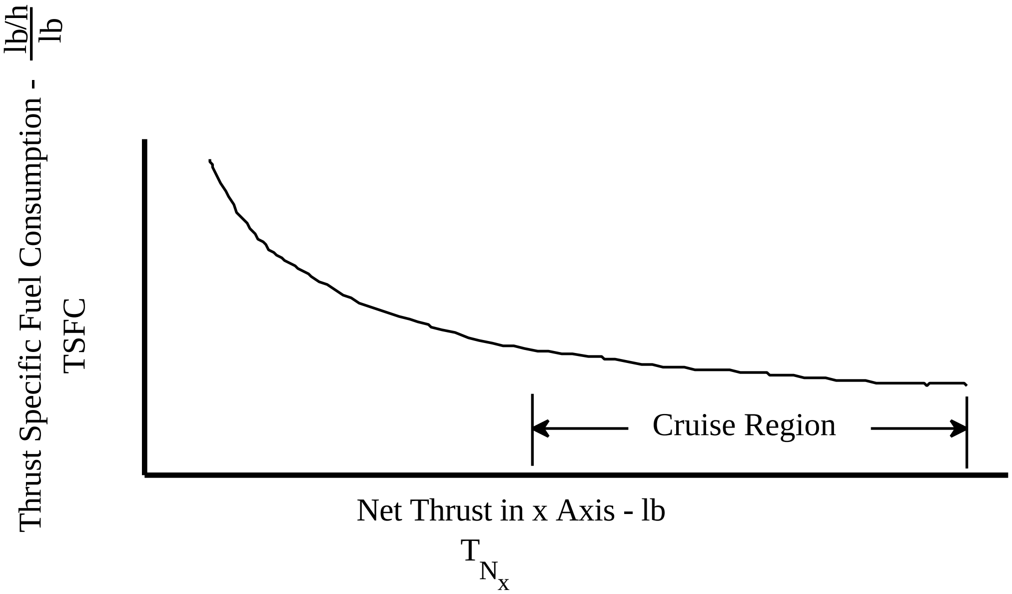

Figure 4.15
THRUST SPECIFIC FUEL CONSUMPTION

In the cruise region, TSFC is essentially constant. Therefore, the drag curve and the fuel flow required curve are similar. This can be shown by letting net thrust parallel flight path equal drag then fuel flow would be proportional to drag.

$$T_{N_x} = D \tag{Eq 4.49}$$

$$\dot{W}_f \approx D \tag{Eq 4.50}$$

A graph of fuel flow and drag characteristics, assuming constant TSFC, is shown in figure 4.16.

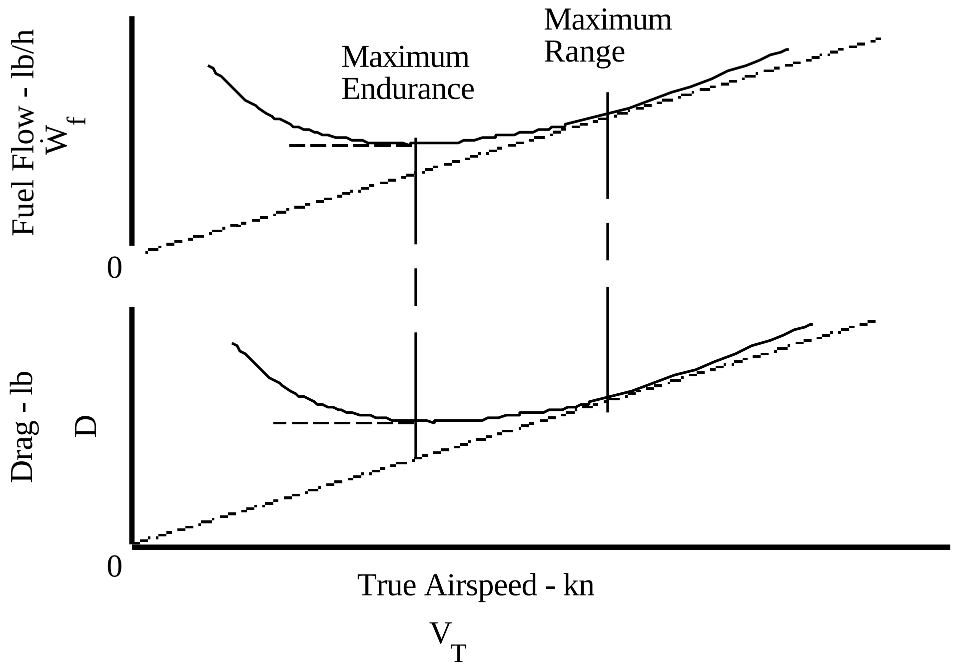

Figure 4.16
JET RANGE AND ENDURANCE

Maximum range occurs at the tangent to the drag curve, and maximum endurance occurs at minimum drag.

The thrust specific fuel consumption is not constant but is a function of many engine propulsion variables. In general, engine efficiency increases with increasing engine speed and decreasing inlet temperature. Specific range increases with increasing altitude. Likewise, endurance is not constant with increasing altitude. Minimum fuel flow decreases with increasing altitude until the optimum altitude is reached, then begins to increase again. The decrease in fuel flow is due to increasing engine efficiency as speed increases and temperature decreases. Eventually, decreased Reynold's number and increased Mach negate the positive effects of increasing altitude and an optimum altitude is reached.

Range must be distinguished from endurance. Range involves flying distance while endurance involves flying time. The appropriate definition of the latter is specific endurance (S.E). Endurance equates to flying the maximum amount of time for the least amount of fuel.

To determine aircraft range and endurance, the thrust or power required must be put in terms of actual aircraft fuel flow required. Figure 4.17 depicts where the maximum range and endurance occur.

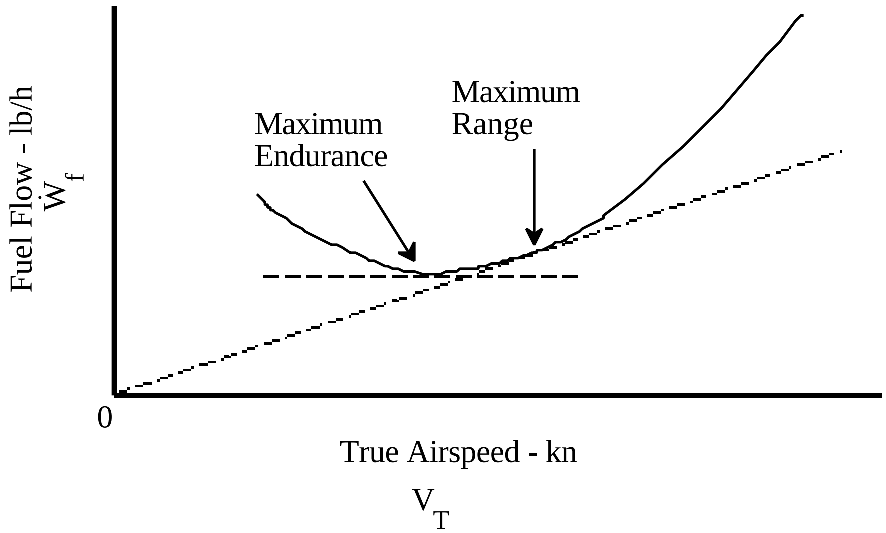

Figure 4.17
FUEL FLOW REQUIRED

Specific Range can be defined and calculated by dividing true airspeed by the actual fuel flow.

$$\text{S.R.} = \frac{\text{nmi}}{W_f} \qquad \text{(Eq 4.51)}$$

$$\text{S.R.} = \frac{V_T}{\dot{W}_f} \qquad \text{(Eq 4.52)}$$

Maximum range airspeed is the speed at the tangent from the origin to the fuel flow curve (Figure 4.17). Maximum endurance airspeed is located where fuel flow is minimum (Figure 4.17). Specific endurance is calculated by dividing flight time by fuel used such that:

$$\text{S.E.} = \frac{t}{W_{f_{Used}}} \qquad \text{(Eq 4.53)}$$

$$S.E. = \frac{1}{\dot{W}_f} \tag{Eq 4.54}$$

Where:

D	Drag	lb
nmi	Nautical miles	
S.E.	Specific endurance	h/lb
S.R.	Specific range	nmi/lb
t	Time	s
T_{N_x}	Net thrust parallel flight path	lb
TSFC	Thrust specific fuel consumption	$\frac{lb/h}{lb}$
V_T	True airspeed	kn
$W_{f_{Used}}$	Fuel used	lb
$\dot{W}_f$	Fuel flow	lb/h.

An analysis of range performance can be obtained by plotting specific range versus velocity as shown in figure 4.18.

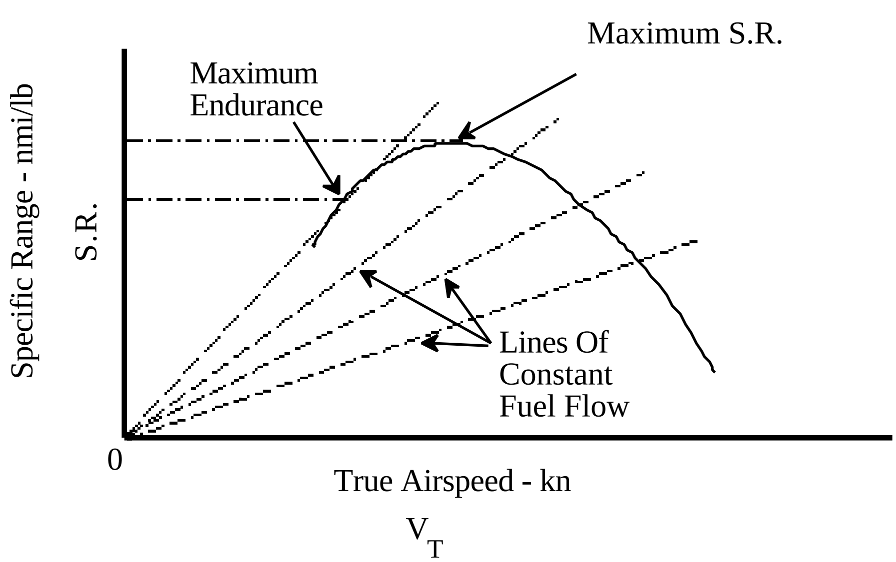

Figure 4.18
RANGE AND ENDURANCE

The maximum specific range is at the peak of the curve while maximum endurance is the tangent to the curve through the origin. Long range cruise operation is conducted generally at some airspeed slightly higher than the airspeed for maximum S.R. which does not significantly reduce range but does shorten enroute time.

The curves of specific range versus velocity are affected by three principal variables: airplane weight, the external aerodynamic configuration of the airplane, and altitude. These curves are the source of range and endurance operating data and are included in the operator's flight handbook.

4.3.4.1 WEIGHT EFFECTS

Total range is dependent on both the fuel available and the specific range. A typical variation of specific range with weight for a particular cruise operation is given in figure 4.19.

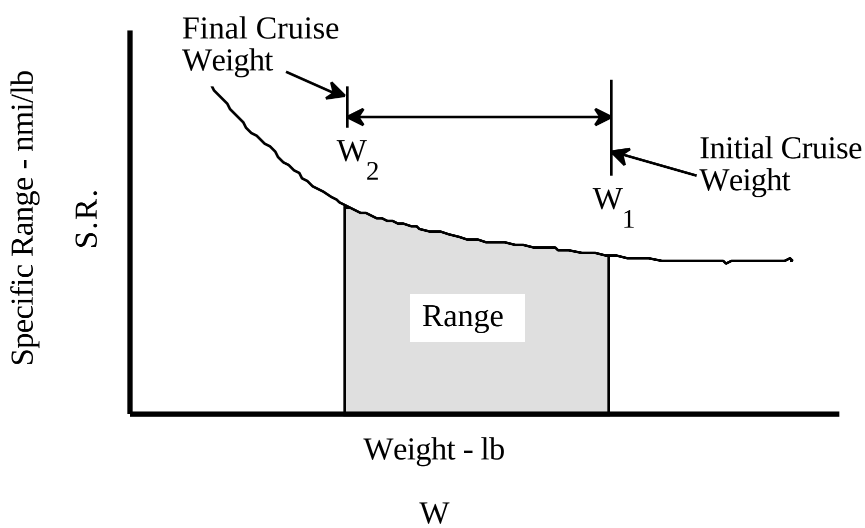

Figure 4.19
SPECIFIC RANGE VARIATION WITH WEIGHT

Range obtained by the expenditure of fuel can be related to the crosshatched area between the weights at the beginning and end of cruise. The actual range is computed by multiplying the average specific range by the pounds of fuel expended.

$$\text{Range} = \left(S.R._{avg}\right)\left(\text{Fuel Used}\right) \qquad \text{(Eq 4.55)}$$

$$\text{nmi} = \frac{\text{nmi}}{\text{lb}} \times \text{lb} \qquad \text{(Eq 4.56)}$$

Where:

nmi	Nautical miles	
S.R.	Specific range	nmi/lb.

From drag aerodynamic theory, weight is found only in the induced part of the drag equation. Therefore, total drag must change since it is the sum of parasite and induced drag. As weight increases, the specific range and endurance decreases. The speed for optimum range and endurance also increases. The effects are depicted in figure 4.20.

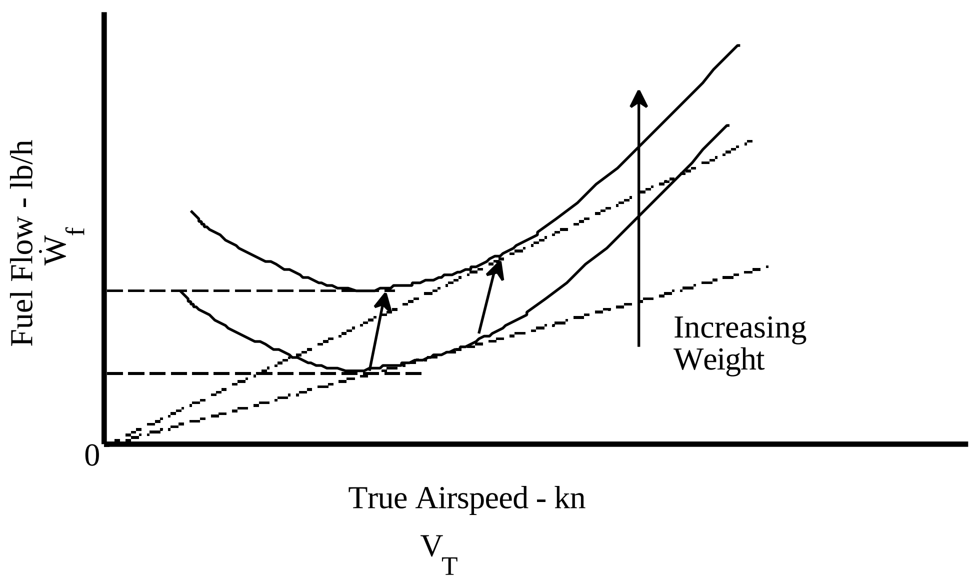

Figure 4.20
JET RANGE AND ENDURANCE WEIGHT EFFECTS

4.3.4.2 AERODYNAMIC EFFECTS

The external configuration determines the amount of parasite drag contribution to total drag. In this case, only the D_p of the drag curve is affected. Figure 4.21 depicts the parasite drag effects. For higher drag, the specific range and endurance time decrease. The speed for optimum range and endurance also decreases.

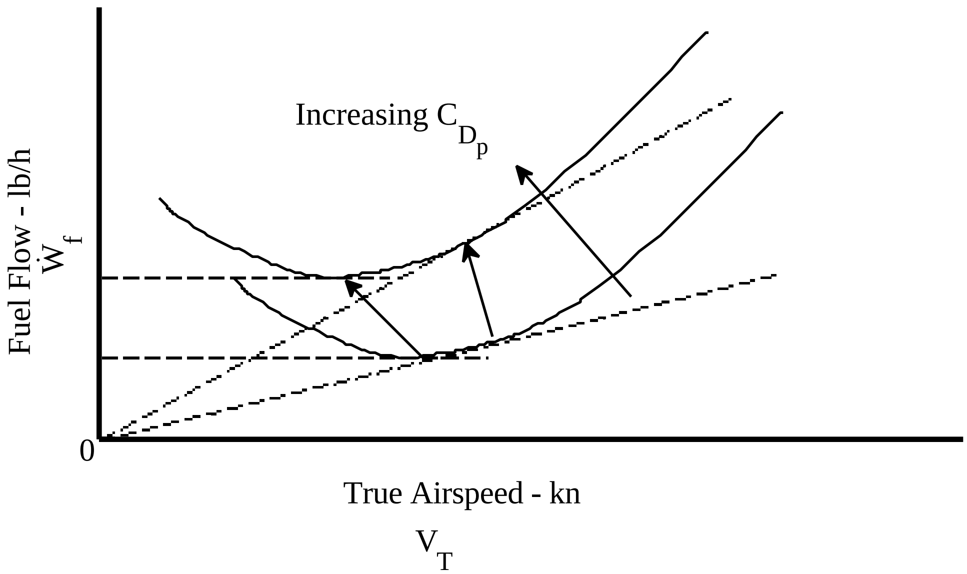

Figure 4.21
JET RANGE AND ENDURANCE PARASITE DRAG EFFECTS

4.3.4.3 ALTITUDE EFFECTS

The low speed drag equation does not contain altitude dependent variables; therefore, changes in altitude do not affect the drag curve. Minimum drag occurs at higher airspeed as altitude is increased. So long as TSFC does not increase markedly, a continuous gain of range is experienced as altitude is gained. Actually, up to the stratosphere, TSFC tends to decrease for most engines so greater gains in range are obtained than would be found if TSFC is assumed constant. At low altitudes, inefficient part throttle operation further increases the obtainable TSFC, producing an additional decrease in range. At high altitudes (above 35,000 to 40,000 feet) TSFC starts to increase so test data reveal a leveling off in range for stratospheric conditions. As airplanes fly higher, this leveling off results in an optimum best range altitude for any given gross weight, above which altitude, decreases in range are encountered. Figure 4.22 shows specific range has sizeable increases with altitude while endurance performance remains constant. A limiting factor on increased altitude would be transonic drag.

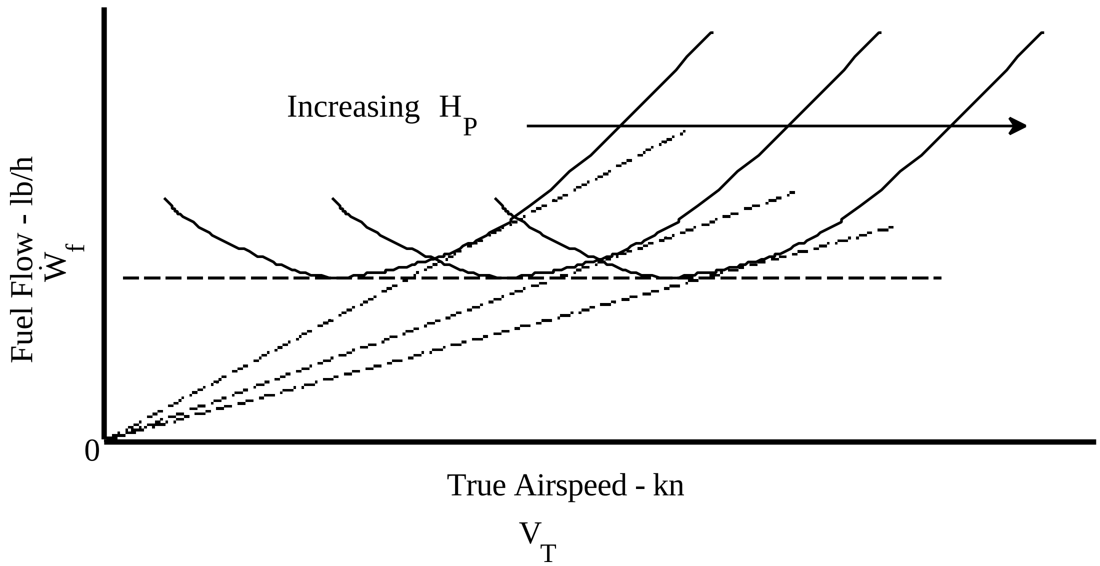

Figure 4.22
JET RANGE AND ENDURANCE ALTITUDE EFFECTS

4.3.5 TURBOPROP THRUST REQUIRED

Power requirements for turboprops deal with thrust horsepower rather than engine thrust as in the turbojet. The thrust horsepower required depends upon drag (thrust) and true airspeed. Thrust horsepower can be defined as:

$$THP = \frac{T\ V_T}{550} = \frac{D\ V_T}{550} \qquad \text{(Eq 4.57)}$$

The drag equation was given in Eq 4.23. Substituting for drag in Eq 4.57:

$$THP = \frac{C_{D_P}\ \rho_a\ V_T^3\ S}{1100} + \frac{W^2}{275\ \pi\ e\ AR\ S\ \rho_a\ V_T} \qquad \text{(Eq 4.58)}$$

Assumptions for Eq 4.58 are the same as for the drag equation:

1. Coefficient of drag is a function of lift and not a function of Mach number or Reynold's number.
2. A parabolic polar as in Eq 4.11.

3. Level flight with no thrust lift (L = W).

Eq 4.58 can be analyzed by making the following assumptions:

1. Fixed configuration and gross weight.
2. Constant altitude.
3. Low Mach.
4. S, C_{D_p}, and $\frac{1}{\pi eAR}$ are constants.

Thrust horsepower required can be expressed as:

$$THP = THP_p + THP_i \tag{Eq 4.59}$$

and graphically depicted as in figure 4.23.

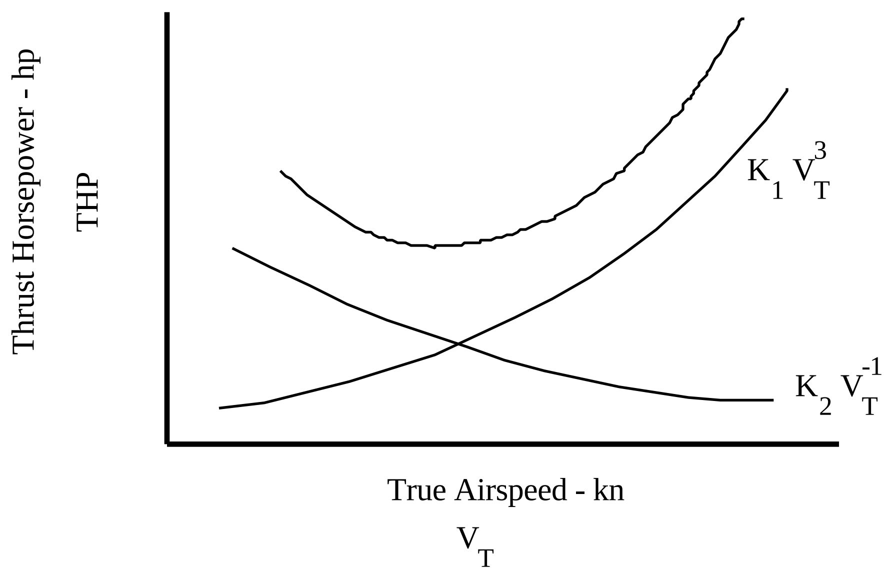

Figure 4.23
THRUST HORSEPOWER REQUIRED

A general form of the power required equation, not analytically based on a drag polar, can be developed. It starts with level flight horsepower required as given in Eq 4.57. In level flight, drag can be expressed as:

$$D = \frac{C_D}{C_L} W \tag{Eq 4.60}$$

Substituting Eq 4.60 into Eq 4.57 for D, and assuming no vertical thrust:

$$THP = \frac{C_D \, W \, V_T}{C_L \, 550} \tag{Eq 4.61}$$

$$L = W = C_L \frac{1}{2} \rho_a V_T^2 S \tag{Eq 4.62}$$

$$THP = \frac{\left(\frac{2}{S}\right)^{\frac{1}{2}} W^{\frac{3}{2}} C_D}{\rho_a^{\frac{1}{2}} C_L^{\frac{3}{2}} \, 550} \tag{Eq 4.63}$$

A general form of the level flight power required can be obtained by converting ambient density and substituting into Eq 4.63:

$$\rho_a = \rho_{ssl} \, \sigma \tag{Eq 4.64}$$

$$THP = \frac{\sqrt{2} \, W^{\frac{3}{2}} C_D}{\left(S \, \rho_{ssl}\right)^{\frac{1}{2}} \sqrt{\sigma} \, C_L^{\frac{3}{2}} \, 550} \tag{Eq 4.65}$$

The resultant equation shows THP as a function of C_L, W, σ. The effects of density (H_P and T_a) can be removed by defining a new term called equivalent thrust horsepower (THP_e) and substituting into Eq 4.65. THP_e is a function of C_L and W.

$$THP_e = THP \sqrt{\sigma} \tag{Eq 4.66}$$

$$THP_e = \frac{\sqrt{2}\, W^{\frac{3}{2}}\, C_D}{\left(S\,\rho_{ssl}\right)^{\frac{1}{2}} C_L^{\frac{3}{2}}\; 550} \tag{Eq 4.67}$$

Where:

550	Conversion factor	$550\,\frac{\text{ft-lb}}{\text{s}} = 1$ horsepower
AR	Aspect ratio	
C_D	Drag coefficient	
C_{D_p}	Parasite drag coefficient	
C_L	Lift coefficient	
D	Drag	lb
e	Oswald's efficiency factor	
L	Lift	lb
π	Constant	
ρ_a	Ambient air density	slugs/ft^3
ρ_{ssl}	Standard sea level air density	0.0023769 slugs/ft^3
S	Wing area	ft^2
σ	Density ratio	
T	Thrust	lb
THP	Thrust horsepower	hp
THP_e	Equivalent thrust horsepower	hp
THP_i	Induced thrust horsepower	hp
THP_p	Parasite thrust horsepower	hp
V_T	True airspeed	kn
W	Weight	lb.

4.3.5.1 MINIMUM THRUST HORSEPOWER REQUIRED

Two methods exist to determine conditions for minimum power required in level flight. One is used for an airplane with a parabolic polar as in Eq 4.58. Substituting constants for the parasite and induced drag constants in Eq 4.58 yields:

$$THP = K_1 V_T^3 + K_2 V_T^{-1} \qquad \text{(Eq 4.68)}$$

Taking the derivative and setting it to zero for minimum power gives:

$$3 K_1 V_T^2 - K_2 V_T^{-2} = 0 \qquad \text{(Eq 4.69)}$$

Minimum power required can be found by multiplying Eq 4.69 by V_T and rearranging:

$$3 K_1 V_T^3 = K_2 V_T^{-1} \qquad \text{(Eq 4.70)}$$

$$3 \, THP_p = THP_i \qquad \text{(Eq 4.71)}$$

Multiplying by $\frac{550}{V_T}$ and dividing both sides by qS:

$$3 D_p = D_i \qquad \text{(Eq 4.72)}$$

$$3 C_{D_p} = C_{D_i} \qquad \text{(Eq 4.73)}$$

Eq 4.73 relates directly to the parabolic drag polar and identifies a unique point on the drag polar producing the minimum power required in level flight. In figure 4.24 there is an optimal C_L to fly for minimum power required similar to the optimal C_L to fly for minimum drag. Also the minimum power point occurs at higher C_L than the minimum drag point.

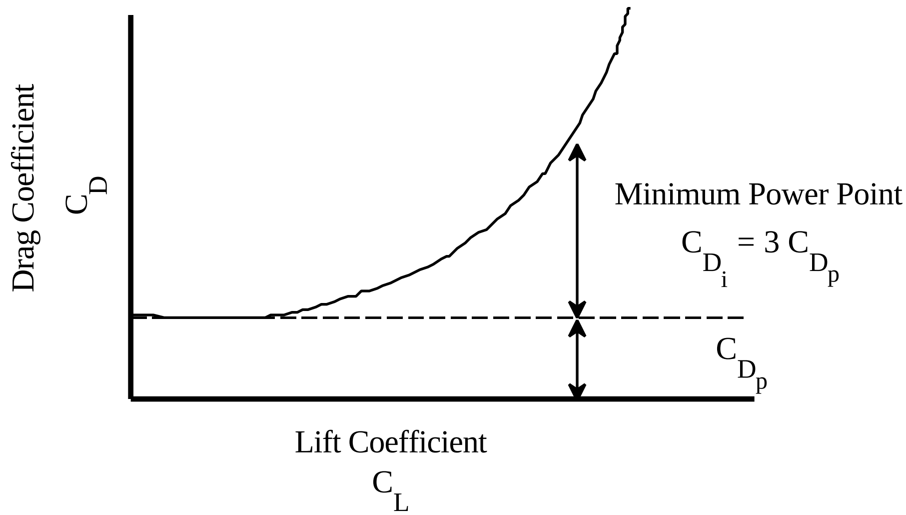

Figure 4.24
PARABOLIC DRAG POLAR

The second method to determine minimum power required involves using general conditions. By using the general form of the power required equation, Eq 4.65 reduces to a constant, K_o, and a relationship between lift and drag coefficients for a given weight and density altitude:

$$THP = K_o \frac{C_D}{C_L^{\frac{3}{2}}} \quad \text{(Eq 4.74)}$$

If the point on the power polar is located which gives the maximum ratio of $\left.\frac{C_L^{3/2}}{C_D}\right|_{max}$, the power required is minimum as shown in figure 4.25.

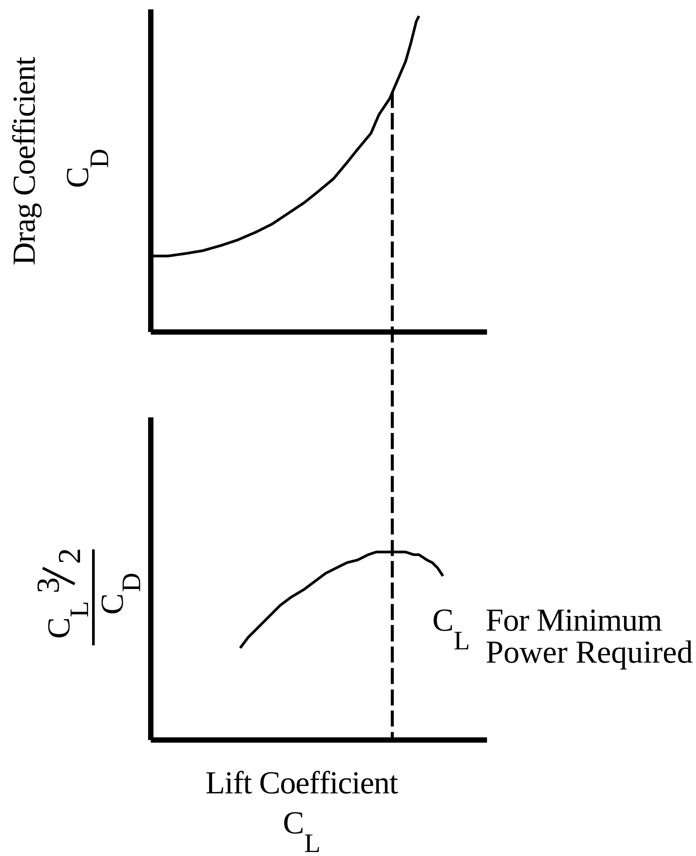

Figure 4.25
GENERAL POLAR

Power required data can be gathered without regard to altitude and generalized as THP_e versus V_e. There is also a method to determine the precise shape of the power required curve using only a small number of data points. Since most turboprops have thick wings, high AR, and little wing sweep; a parabolic drag polar is assumed. Further, if the following relationships are used, multiplying both sides of Eq 4.58 by V_e, and substituting, Eq 4.58 can be rewritten as Eq 4.78:

$$V_T = \frac{V_e}{\sqrt{\sigma}} \qquad \text{(Eq 4.75)}$$

$$THP = \frac{THP_e}{\sqrt{\sigma}} \qquad \text{(Eq 4.76)}$$

$$\sigma = \frac{\rho_a}{\rho_{ssl}} \qquad \text{(Eq 4.77)}$$

$$THP_e \, V_e = \frac{C_{D_P} \, \rho_{ssl} \, V_e^4 \, S}{1100} + \frac{W^2}{275 \, \pi \, e \, AR \, S \, \rho_{ssl}} \qquad \text{(Eq 4.78)}$$

Where:

AR	Aspect ratio	
C_D	Drag coefficient	
C_{D_i}	Induced drag coefficient	
C_{D_p}	Parasite drag coefficient	
C_L	Lift coefficient	
D_i	Induced drag	lb
D_p	Parasite drag	lb
e	Oswald's efficiency factor	
K_1	Parasite drag constant	
K_2	Induced drag constant	
K_o	Constant	
π	Constant	
ρ_a	Ambient air density	slugs/ft^3
ρ_{ssl}	Standard sea level density	slugs/ft^3
S	Wing area	ft^2
σ	Density ratio	
THP	Thrust horsepower	hp
THP_e	Equivalent thrust horsepower	hp
THP_i	Induced thrust horsepower	hp
THP_{min}	Minimum thrust horsepower	hp
THP_p	Parasite thrust horsepower	hp
V_e	Equivalent airspeed	kn
V_T	True airspeed	kn
W	Weight	lb.

Figure 4.26 shows flight data for one gross weight plotted in the form of Eq 4.78. Data provided in this manner allows for easy interpretation. Some correction for varying aircraft weight may be required.

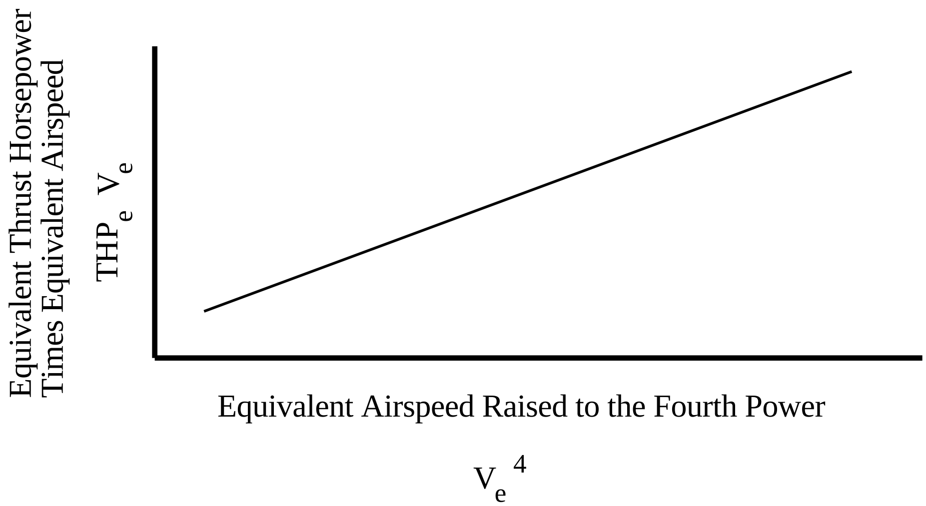

Figure 4.26
LINEARIZED THRUST HORSEPOWER REQUIRED

4.3.6 TURBOPROP RANGE AND ENDURANCE

For both a turboprop and reciprocating engine aircraft, the fuel flow is approximately proportional to the horsepower produced. This power is noted as either brake horsepower (BHP) or shaft horsepower (SHP). Additionally, shaft horsepower is related to thrust horsepower by propeller efficiency (η_P).

$$\eta_P = \frac{THP}{SHP} \qquad \text{(Eq 4.79)}$$

$$THP = \eta_P \, SHP \qquad \text{(Eq 4.80)}$$

Specific fuel consumption can be defined in either THP or SHP terms.

$$THPSFC = \frac{\dot{W}_f}{THP} \qquad \text{(Eq 4.81)}$$

$$SHPSFC = \frac{\dot{W}_f}{SHP} \qquad \text{(Eq 4.82)}$$

$$\dot{W}_f = \frac{THP}{\eta_P}\ SHPSFC \qquad \text{(Eq 4.83)}$$

Where:

η_P	Propeller efficiency	
SHP	Shaft horsepower	hp
SHPSFC	Shaft horsepower specific fuel consumption	$\frac{lb/h}{hp}$
THP	Thrust horsepower	hp
THPSFC	Thrust horsepower specific fuel consumption	$\frac{lb/h}{hp}$
$\dot{W}_f$	Fuel flow	lb/h.

The relationship is similar to the TSFC versus net thrust for a jet in figure 4.19 and is shown in figure 4.27.

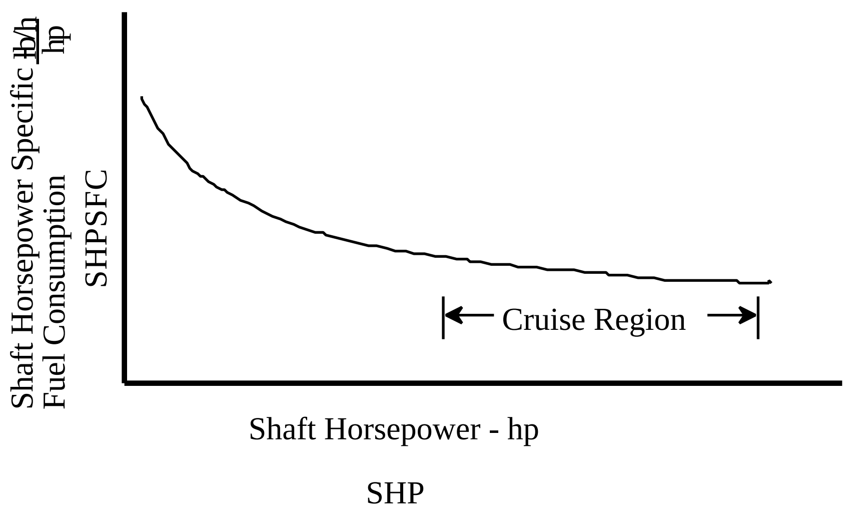

Figure 4.27
SHAFT HORSEPOWER SPECIFIC FUEL CONSUMPTION

Propeller efficiency varies with propeller advance ratio and pitch angle as shown in figure 4.28.

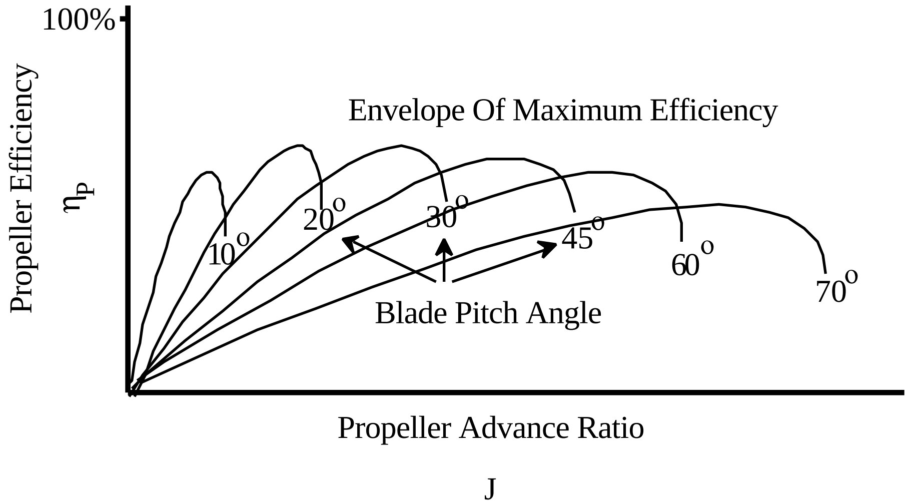

Figure 4.28
PROPELLER EFFICIENCY

If SHPSFC is fairly constant in the cruise region as in figure 4.27, and if η_P is held constant by changing blade pitch as in figure 4.28, then fuel flow is proportional to thrust horsepower and figure 4.29 can be developed.

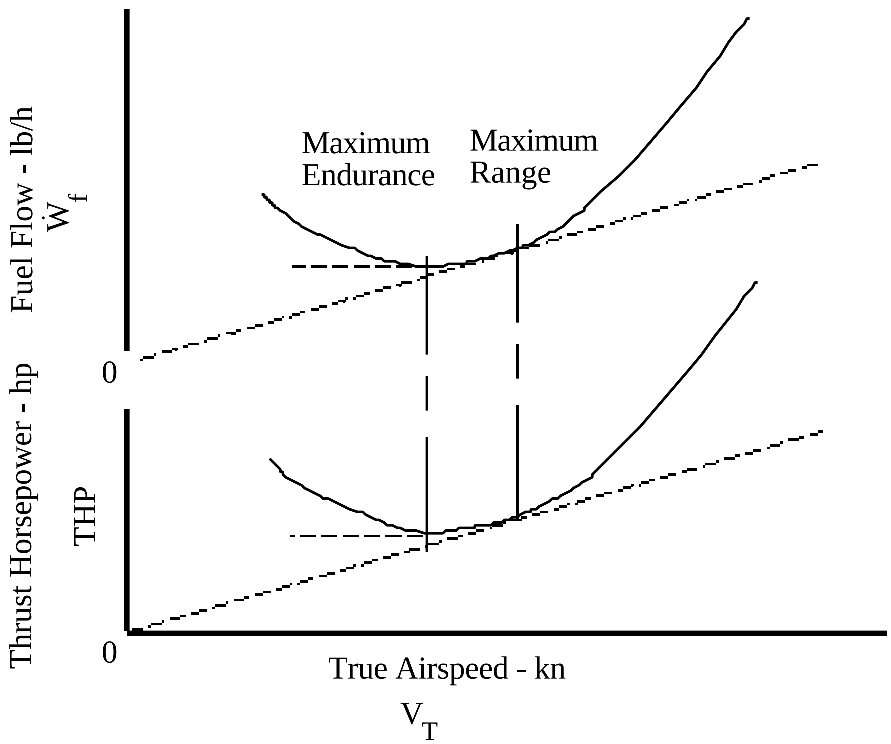

Figure 4.29
TURBOPROP RANGE AND ENDURANCE

Maximum range occurs at the tangent to the power required curve and maximum endurance occurs at the minimum power required point. This is very similar to the jet in figure 4.26.

4.3.6.1 WEIGHT AND AERODYNAMIC EFFECTS

As in the jet, power required changes with changes in aircraft weight or configuration as discussed in paragraphs 4.3.4.1 and 4.3.4.2.

4.3.6.2 ALTITUDE EFFECTS

In Eq 4.58, the density term (ρ_a) appears in both the parasite and induced terms. An increase in density altitude decreases parasite power required and increases induced power required. As in the jet, turboprop efficiency increases with engine speed as altitude is increased to an optimum then begins to decrease. Therefore, specific range is not constant, but increases with increasing altitude to an optimum. Endurance is not constant and increases to an optimum altitude. The results appear in figure 4.30.

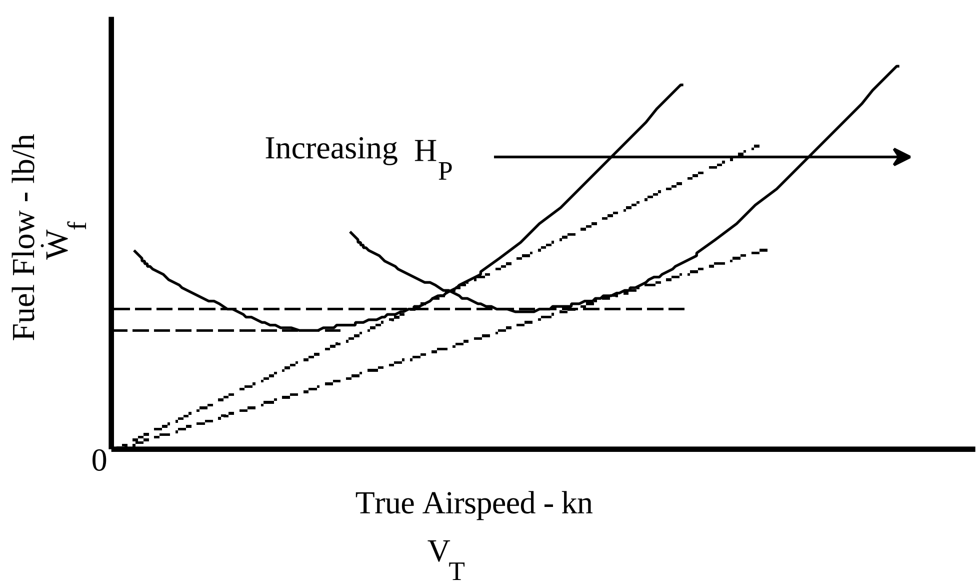

Figure 4.30
TURBOPROP RANGE AND ENDURANCE ALTITUDE EFFECTS

4.4 TEST METHODS AND TECHNIQUES

4.4.1 CONSTANT W/δ

The speed power flight test is a common method used to obtain the cruise performance of jet aircraft. This method allows determining maximum endurance, maximum range, and maximum airspeed in a minimum of flight sorties. The method involves gathering fuel flow data at various altitudes, gross weights, and airspeeds to define sufficiently the operating envelope of the aircraft. One W/δ is chosen for each set of data points, usually based on a nominal standard weight. The resulting curves do not represent all altitude and gross weight combinations which result in the particular W/δ of the curve. For example, an aircraft weighing 100,000 lb at an altitude of 18,000 ft has the same W/δ as a 200,000 lb aircraft at sea level. However, the fuel flow at 18,000 ft is much less than at sea level, resulting in a different fuel flow versus Mach curve. The Range Factor (specific range multiplied by the aircraft's weight) is the same in both of the cases above. Results appear as in figure 4.6.

The test techniques for the constant W/δ test are presented primarily for the single spool compressor, constant geometry engine. However, they apply equally well to twin spool compressor and variable geometry engines. The data reduction, on the other hand, applies only to fixed geometry engines. The power parameter used in this method is engine speed. The method is modified for more complex engines. Because of the variety of configurations existing, it is not practical, to describe methods for correcting engine data to standard conditions suitable for all types. The characteristics of each of the more complex engines may require different correction methods. Engine manufacturer's charts are a good source of data when making this analysis.

Target W/δ should cover the entire flight envelope. Data are gathered from M_{mrt} or V_{max} to V_{min} over a range of W/δ which covers the highest weight / highest altitude to lowest weight / lowest altitude. A rule of thumb for the altitude increments is to use 5,000 ft altitude intervals at standard gross weight. The actual number of flights is frequently limited by flight time or funding constraints. The interval may therefore need to be increased if flight tests are limited.

To gather data at a constant W/δ, a card is used to present target altitude as a function of fuel remaining. Values on the card would reflect instrument and position errors.

For example; W/δ is based on H_{P_c}, so altimeter position error and altimeter instrument correction must be subtracted to obtain the target H_{P_o} used when obtaining fuel flow data. The following data are required in preparing the W/δ card:

1. The empty weight of the aircraft.
2. Fuel density and fuel loading.
3. Altimeter calibrations relevant to altitude and airspeed of the test.
4. Airspeed calibrations (position and instrument errors).
5. Determine the target W/δ based upon standard gross weight and altitude range of interest.
6. Construct a plot of H_{P_c} versus weight as in figure 4.31. Given a weight, this plot can be used to determine altitude to fly to achieve the desired W/δ.
7. Convert gross weight into fuel remaining or used during the mission. Plot H_{P_c} versus fuel used as shown in figure 4.32. The dashed lines shown are the $\pm 2\%$ W/δ variation permitted. If fuel temperature changes throughout the flight, use an average value for determining fuel density.
8. Since the values read from the figure are H_{P_c}, apply altimeter position error and instrument corrections to H_{P_c} to obtain H_{P_o} values for the data card. Pay particular attention to the sign of the correction because the above procedure necessitates going from calibrated values to observed values.
9. Prepare a data card similar to figure 4.33.

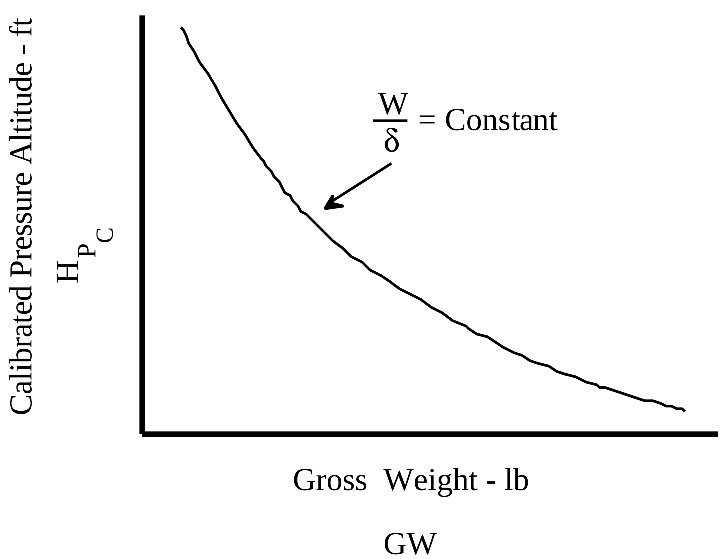

Figure 4.31
TEST ALTITUDE VERSUS GROSS WEIGHT

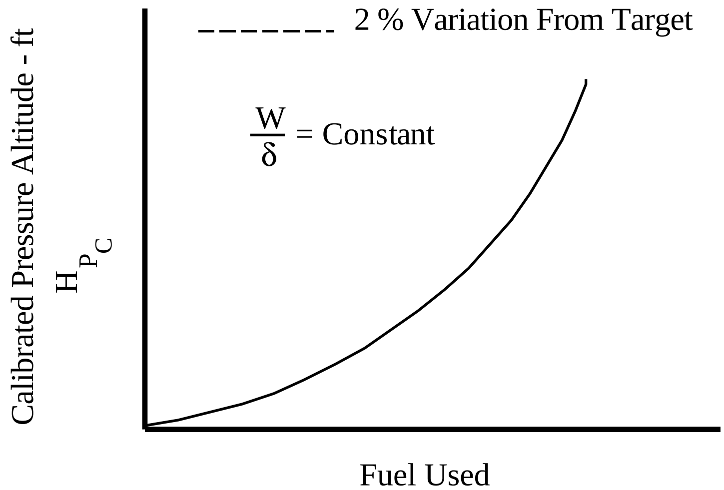

Figure 4.32
TEST ALTITUDE VERSUS FUEL USED

$V_{o\ tgt}$	$V_{o\ act}$	H_{P_c}	W_f start	W_f end	t	T_a	N	$\dot{W}_f$
kn	kn	ft	lb	lb	s	˚C	%	lb/h
V_{max}								

Figure 4.33
JET IN FLIGHT DATA CARD

As fuel weight changes, altitude changes to keep the target W/δ constant. The following equations show δ is directly related to fuel weight and is a linear function.

$$\left(\frac{W}{\delta}\right)_{Target} = \frac{W + W_f}{\delta} \qquad \text{(Eq 4.84)}$$

$$\left(\frac{W}{\delta}\right)_{Target} = \frac{W_{aircraft} + W_f}{\delta} \tag{Eq 4.85}$$

$$\delta = \frac{W_{aircraft}}{\left(\frac{W}{\delta}\right)_{Target}} + \frac{1}{\left(\frac{W}{\delta}\right)_{Target}} W_f \tag{Eq 4.86}$$

Ambient temperature (T_a) at altitude can be obtained in either of two ways:

1. Observed T_a from a balloon sounding, buddy system, etc.
2. Calculate T_a from measured OAT using the equation:

$$OAT = T_a \left(1 + \frac{\gamma - 1}{2} K_T M^2\right) \tag{Eq 4.87}$$

Where:

δ	Pressure ratio	
γ	Ratio of specific heats	
K_T	Temperature recovery factor	
M	Mach number	
OAT	Outside air temperature	˚C or ˚K
T_a	Ambient temperature	˚C or ˚K
W	Weight	lb
$W_{aircraft}$	Aircraft weight	lb
W_f	Fuel weight	lb.

There are no special calibrations to the aircraft fuel quantity system although special instrumentation measuring fuel used can be calibrated. The zero fuel gross weight is contained in the aircraft weight and balance forms. In any event, the known quantity of fuel at engine start is necessary and close tracking of fuel remaining is required. For aircraft fuel tanks without quantity measurement, further special planning is required. One technique is to keep these fuel tanks full until their entire contents can be transferred to internal tanks with fuel quantity readings.

The derivation of Eq 4.37 assumed constant aircraft and engine geometry and the effects of changing Reynold’s number were small. The effect of decreased Reynold’s number may in fact not be small. The test sequence must be planned so as not to hide or mask the effect. The Reynold’s number effects can be checked by going back later in the flight and repeating data points at the same W/δ and Mach, but now at a lighter weight and therefore higher altitude. Figure 4.34 shows the results.

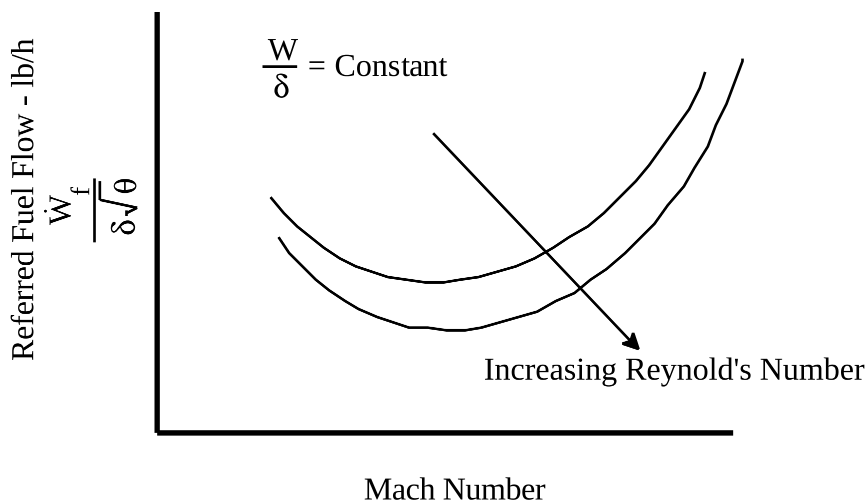

Figure 4.34
REYNOLD’S NUMBER EFFECT

The following is an efficient way for obtaining data at constant W/δ.

1. Technique:

a. The first point is flown at M_{mrt} or V_{max} with subsequent data taken in order of descending Mach or airspeed. Stabilization is quicker if the data point is approached from the fast side. If a point is required faster than the present speed, accelerate beyond the target speed and then decelerate again into the target point.

b. Ideally, the fuel remaining for the correct W/δ occurs midway through the timed period. For low fuel flow rates a longer stable point may be required.

c. The constant altitude technique can be used on the front side of the power curve, and the constant airspeed technique used on the back side. On the front side, fix the engine power, adjust attitude, then maintain altitude to obtain stabilized airspeed. On the back side, stabilize on airspeed by adjusting attitude then adjust power to maintain constant altitude. For the airspeeds near the airspeed for minimum power, a combination of the two techniques may be used although the back side technique is more useful if airspeed is the more difficult parameter to hold constant.

d. Stabilize the aircraft by proper trimming and control pitch by outside reference. Record data in an organized sequence to expedite the data point. Trim the aircraft for hands off flight when stabilized.

2. Procedure:

a. Before engine start, know the correct fuel loading.

b. When approaching within 2000 to 3000 feet of the test altitude, read the fuel remaining and extrapolate to account for the time required to stabilize on the data point. Determine the target altitude for the first data point.

c. Using the target airspeed from the flight data card, apply the altimeter position error and instrument correction to determine the H_{P_o}. Using the allowed fuel, establish a stable point at the target airspeed and correct altitude.

d. Obtain enough stabilized points to completely define the fuel flow versus velocity curve at the particular W/δ tested.

e. Record the fuel counter reading and start the stop watch when the speed is stabilized and the aircraft is within 2% of the desired W/δ. Fly the aircraft at the required altitude for a minimum of one minute, record the fuel counter reading and other data. If the airspeed changes more than 2 knots using the front side technique or the altitude change exceeds 50 ft using the back side technique, repeat the point.

f. Data are recorded in wings level, ball-centered, level (no vertical velocity), stabilized (unaccelerated) flight. Data are recorded starting with the most important first; fuel flow, pressure altitude, airspeed, ambient temperature, fuel weight/gross weight. Angle of attack is nice to have and, engine speed, EGT, EPR, etc., can provide correlating information. A minimum of six points are flown at each W/δ. Fly extra points where the minimum range and endurance area are expected from pre-flight planning.

4.4.1.1 W/δ FLIGHT PLANNING PROGRAM

A constant W/δ flight planning program generates a list of altitudes required to attain a desired W/δ in flight based on fuel remaining.

The program lists numerous performance routines including level flight. From the menu, select the appropriate name of the W/δ flight planning program. Instructions to proceed would be a series of questions to be answered. The following information is required as inputs:

1. Aircraft zero fuel weight (includes everything except fuel, pilots, stores, etc.).
2. Minimum and maximum fuel weight for calculations.
3. Fuel weight increment for calculations.
4. Desired referred weight (W/δ).

The program calculation includes:

1. Gross weight for each increment of fuel by adding the zero fuel weight to the fuel remaining.
2. Pressure ratio for each gross weight above by dividing the given gross weight by the target W/δ desired.
3. Selection of H_{P_c} for each δ as would be done manually from an atmospheric table.

Data can be output as a listing of the calibrated pressure altitude required to maintain the constant W/δ for each increment of fuel remaining. Instrument error and position error are unique to the installation and instrument; therefore, corrections must be made to the H_{P_c} in flight to determine the H_{P_o} required for the given W/δ. The program calculates the pressure altitude required to attain the target W/δ for each increment of fuel remaining. It should present the information on a monitor or in some form which can be printed. After review of the prepared information any desired changes would be made and the W/δ planning record would be printed for use in flight. An example W/δ planning record is presented in figure 4.35.

Aircraft:			W/δ:	42285	
Pilot:					
W_f	H_P	W_f	H_P	W_f	H_P
3200	31175				
3100	31359				
3000	31543				
2900	31729				
2800	31916				
2700	32105				
2600	32295				
2500	32486				
2400	32679				
2300	32873				
2200	33068				
2100	33265				
2000	33463				
Instrument Correction				Position Error	
H_P	$\Delta H_{P_{ic}}$			V_o, M_o	ΔH_{pos}

Figure 4.35
W/δ PLANNING CHART

4.4.1.2 DATA REQUIRED

H_P, V_o, T_a, and W_f or GW are necessary to complete the test results. Angle of attack is desired information and, engine speed, EGT, EPR, etc., can provide correlating information. A minimum of six points are flown at each W/δ with most of the points taken on the front side and bucket.

4.4.1.3 TEST CRITERIA

1. Balanced (ball centered), wings level, unaccelerated flight.
2. Engine bleed air systems off or operated in normal flight mode.
3. Stabilized engine power setting.
4. Altimeter set at 29.92.

4.4.1.4 DATA REQUIREMENTS

1. Stabilize 60 seconds prior to recording data.
2. Record stabilized data for 30 seconds.
3. W/δ within ± 2% of the target.
4. Airspeed change less than 2 kn in one minute for front side.
5. Altitude change less than 50 ft in one minute for back side.

4.4.2 RANGE CRUISE TEST

The range cruise test (ferry mission) is used to verify and refine the estimates of the range performance generated during the W/δ tests. Specifically, use it to check the optimum W/δ and the total ferry range. Usually a series of flights are flown at W/δ above and below the predicted optimum W/δ. The standard day range from each of these can be used to determine the actual optimum W/δ and are compared with the data predicted by W/δ testing.

Planning the time or distance flown accounts for all portions of the test including cruise as show in figure 4.36.

	Fuel used	Fuel remaining
Prior to engine start		
Engine start and taxi		
Takeoff and accelerate to climb schedule		
Climb		
Cruise		
Fuel reserve		

Figure 4.36
FUEL USED FOR CRUISE

Estimated fuel used for engine start, taxi, takeoff, and acceleration to climb schedule is obtained from manufacturer's charts. Fuel used in the climb is obtained from the prior climb tests. Fuel reserve is determined by Naval Air System Command Specification, AS-5263, reference 2. The total of these fuel increments subtracted from the total fuel available gives the amount of fuel available for the cruise portion of the test.

Plan fuel used during the climb corresponding to W/δ altitude. When on cruise schedule, record data often enough to obtain at least 10 points.

Figure 4.37 is a sample flight data card for use on the test flight.

Data Point	Time	F/C	V_o	H_{P_o}	T_a	N	$\dot{W}_f$
Prior eng start							
Start							
Taxi							
Takeoff							
Start climb							
End climb							
Start cruise							
Cruise increment							
Cruise increment							
End cruise							

Figure 4.37
CRUISE DATA CARD

A recommended procedure for performing the range cruise test is:

1. Prior to engine start, check that the correct amount of fuel is onboard and the fuel counter is set correctly.

2. Record data at each point planned, i.e., engine start, taxi etc.

3. Upon reaching the altitude corresponding to the fuel counter reading for the desired W/δ, set up the cruise climb at the desired Mach.

4. Increase altitude as the fuel counter is decreased to maintain a constant W/δ by performing a shallow climb. An alternate method is to hold a constant altitude and stair-step the aircraft in increments of 100 to 200 feet. Cruise begins in the stratosphere and the Mach and engine speed remain constant (using a constant velocity corresponding to the indicated Mach is preferred due to the accuracy of the instruments). If cruise begins below the tropopause, a slight decrease in engine speed is required initially. $\frac{N}{\sqrt{\theta}}$ is a function of W/δ and Mach. For a given W/δ and Mach, a constant $\frac{N}{\sqrt{\theta}}$ is required and therefore engine

speed is decreased as T_a decreases to hold $\frac{N}{\sqrt{\theta}}$ constant. During the cruise portion, minimize throttle movements. If turns are required, make them very shallow (less than 10˚ bank).

4.4.2.1 DATA REQUIRED

Obtain a sufficient number of data points enroute to minimize the effect of errors in reading the data. The data card suggested in paragraph 4.4.2 can be expanded to include incremental points along the cruise line. The following parameters are recorded:

H_{P_o}, V_o, T_o, Aircraft weight, time.

4.4.2.2 TEST CRITERIA

1. Balanced (ball centered), wings level, unaccelerated flight.
2. Engine bleed air systems off or operated in normal flight mode.
3. Stabilized engine power setting.
4. Altimeter set at 29.92 in.Hg.

4.4.2.3 DATA REQUIREMENTS

1. Stabilize 60 seconds prior to recording data.

then:

2. Airspeed change less than 2 kn for front side.
3. Altitude change less than 50 ft for back side.
4. W/δ within 2% of target.

4.4.3 TURBOPROP RANGE AND ENDURANCE

The turboprop level flight tests do not require the rigors associated with the W/δ method most often used for the turbojet (although the W/δ method can be used). Measurement of level flight parameters only require setting power for level flight and recording data. Power settings should be those recommended by the engine manufacturer for the altitude selected. An iterative computer program would be used to develop referred curves from which range and endurance for any altitude can be determined. Test day data would use power required plotted against airspeed to determine the range and endurance airspeeds for a given altitude. Test day data would only be useful for flights at the exact conditions from which the data was obtained and would not be of much use in determining the level flight performance under any other condition.

Shaft horsepower needs to be determined for each level flight point flown. Shaft horsepower is related to Thrust horsepower through propeller efficiency as stated in Eq 4.79.

$$\eta_P = \frac{THP}{SHP} \qquad \text{(Eq 4.79)}$$

Neither THP nor SHP are normally available from cockpit instruments but can be determined from engine curves developed by the engine manufacturer. Torque, rpm, fuel flow, and ambient temperature would be used to determine the SHP. Fuel flow would be provided by the engine curves, measured in flight, or determined by fuel remaining and time aloft.

To gather data, a card is used to list the data attainable from standard cockpit instruments or special performance instrumentation if installed. Prepare a data card similar to figure 4.38.

$V_{i\ tgt}$ kn	$V_{o\ act}$ kn	H_{P_c} ft	$W_{f\ start}$ lb	$W_{f\ end}$ lb	t s	T_a ˚C	Q ft-lb	N RPM	$\dot{W}_f$ lb/h

Figure 4.38
PROP IN FLIGHT DATA CARD

Ambient temperature can be determined the same way as described in section 4.4.1 if not available in the cockpit.

There are no special calibrations to the aircraft fuel quantity system although special instrumentation measuring fuel used can be calibrated. The zero fuel gross weight is contained in the aircraft weight and balance forms. In any event, the known quantity of fuel at engine start is necessary and close tracking of fuel remaining is required. If fuel used during each point is small, just record the fuel remaining as data is being recorded instead of fuel at the beginning and end of the data point. For aircraft fuel tanks without quantity measurement, further special planning is required. One technique is to keep these fuel tanks full until their entire contents can be transferred to internal tanks with fuel quantity readings.

The exact number of data points to fly is not important although a sufficient number of points should be flown over the airspeed range from V_{max} to near stall to lend confidence to the ensuing computer iterations when smoothing referred curves.

The constant altitude technique can be used on the front side of the power curve, and the constant airspeed technique used on the back side. On the front side, fix the engine power then adjust attitude, maintaining altitude, to obtain stabilized airspeed. On the back side, stabilize on airspeed by adjusting attitude then adjust power to maintain constant altitude. For the airspeeds near the airspeed for minimum power, a combination of the two techniques may be used although the back side technique is more useful if airspeed is most difficult to hold constant.

Using the target airspeed from the flight data card, apply the altimeter position error and instrument correction to determine the H_P. The corrections could be applied later since the test is not the W/δ technique. Stabilize the aircraft by proper trimming, control pitch by outside reference, and record data in an organized sequence to expedite the data point. Trim the aircraft for hands off flight when stabilized.

Data are recorded in wings level, ball-centered, level (no vertical velocity), stabilized (unaccelerated) flight. Data are recorded starting with the most important first; torque, engine speed, fuel flow if available, pressure altitude, airspeed, ambient temperature if available, fuel remaining / gross weight. Angle of attack is nice to have and, N_1, EGT, etc., can provide correlating information. Fly extra points where the bucket or maximum endurance area is expected from pre-flight planning since power changes for a given airspeed range might be quite small here.

4.4.3.1 DATA REQUIRED

$\dot{W}_f$, or fuel remaining and time of flight, torque, engine speed, T_a, V_o, H_{P_o} are necessary to complete the test results. Angle of attack, N_1, EGT, etc., can provide correlating information. The data points should be flown over the range of airspeeds attainable with emphasis taken on the front side and bucket.

4.4.3.2 TEST CRITERIA

1. Balanced (ball centered), wings level, unaccelerated flight.
2. Engine bleed air system off or operated in normal flight mode.
3. Stabilized engine power setting.
4. Altimeter set at 29.92.

4.4.3.3 DATA REQUIREMENTS

1. Stabilize 60 s prior to recording data.
2. Record stabilized data for 30 s.
3. Airspeed change less than 2 kn in one minute for front side.
4. Altitude change less than 50 ft in one minute for back side.

4.5 DATA REDUCTION

4.5.1 JET RANGE AND ENDURANCE

The following equations are used for referred range and endurance:

$$H_{P_c} = H_{P_o} + \Delta H_{P_{ic}} + \Delta H_{pos} \qquad \text{(Eq 4.88)}$$

$$T_a = T_o + \Delta T_{ic} \qquad \text{(Eq 4.89)}$$

$$V_c = V_o + \Delta V_{ic} + \Delta V_{pos} \qquad \text{(Eq 4.90)}$$

$$\sigma = \frac{\rho_a}{\rho_{ssl}} \qquad \text{(Eq 4.77)}$$

$$\delta = \frac{P_a}{P_{ssl}} \qquad \text{(Eq 4.43)}$$

$$\theta = \frac{T_a}{T_{ssl}} \qquad \text{(Eq 4.38)}$$

$$V_T = \frac{V_c}{\sqrt{\sigma}} \qquad \text{(Eq 4.91)}$$

$$M = \frac{V_T}{a_{ssl}\sqrt{\theta}} \qquad \text{(Eq 4.92)}$$

$$\dot{W}_{f_{ref}} = \frac{\dot{W}_f}{\delta\sqrt{\theta}} \qquad \text{(Eq 4.93)}$$

$$W_{ref} = \frac{W}{\delta} \qquad \text{(Eq 4.94)}$$

Where:

a_{ssl}	Standard sea level speed of sound	661.483 kn
δ	Pressure ratio	
$\Delta H_{P_{ic}}$	Altimeter instrument correction	ft
ΔH_{pos}	Altimeter position error	ft
ΔT_{ic}	Temperature instrument correction	˚C
ΔV_{ic}	Airspeed instrument correction	kn
ΔV_{pos}	Airspeed position error	kn
H_{P_c}	Calibrated pressure altitude	ft
H_{P_o}	Observed pressure altitude	ft
M	Mach number	
P_a	Ambient pressure	psf
P_{ssl}	Standard sea level pressure	2116.217 psf
θ	Temperature ratio	

ρ_a	Ambient air density	slugs/ft^3
ρ_{ssl}	Standard sea level air density	0.0023769 slugs/ft^3
σ	Density ratio	
T_a	Ambient temperature	˚C
T_o	Observed temperature	˚C
T_{ssl}	Standard sea level temperature	˚C
V_c	Calibrated airspeed	kn
V_o	Observed airspeed	kn
V_T	True airspeed	kn
W	Weight	lb
$\dot{W}_f$	Fuel flow	lb/h
$\dot{W}_{f\ ref}$	Referred fuel flow	lb/h
W_{ref}	Referred aircraft weight	lb.

From the observed airspeed, altitude, and temperature data, compute $\dot{W}_{f\ ref}$ and M as follows:

Step	Parameter	Notation	Formula	Units	Remarks
1	Observed altitude	H_{P_o}		ft	
2	Altitude instrument correction	$\Delta H_{P_{ic}}$		ft	Lab calibration
3	Altitude position error	ΔH_{pos}		ft	Airspeed calibration
4	Calibrated altitude	H_{P_c}	Eq 4.88	ft	
5	Observed temperature	T_o		˚C	
6	Temp instrument correction	ΔT_{ic}		˚C	Lab calibration
7	Ambient temperature	T_a	Eq 4.89	˚C	
8	Observed airspeed	V_o		kn	
9	Airspeed instrument correction	ΔV_{ic}		kn	Lab calibration
10	Airspeed position error	ΔV_{pos}		kn	Airspeed calibration

11	Calibrated airspeed	V_c	Eq 4.90	kn	
12	Ambient pressure	P_a		psf	From Appendix VI, or calculated from 4
13	Ambient air density	ρ_a		slugs/ft^3	From Appendix VI or calculated (see Chapter 2)
14	Density ratio	σ	Eq 4.77		Or from Appendix VI
15	Pressure ratio	δ	Eq 4.43		
16	Temperature ratio	θ	Eq 4.38		
17	True airspeed	V_T	Eq 4.91	kn	
18	Mach number	M	Eq 4.92		Or from Mach indicator with instrument correction
19	Referred fuel flow	$\dot{W}_{f\ ref}$	Eq 4.93	lb/h	
20	Referred weight	W_{ref}	Eq 4.94	lb	

Plot referred fuel flow as a function of Mach for each W/δ flown as shown in figure 4.39.

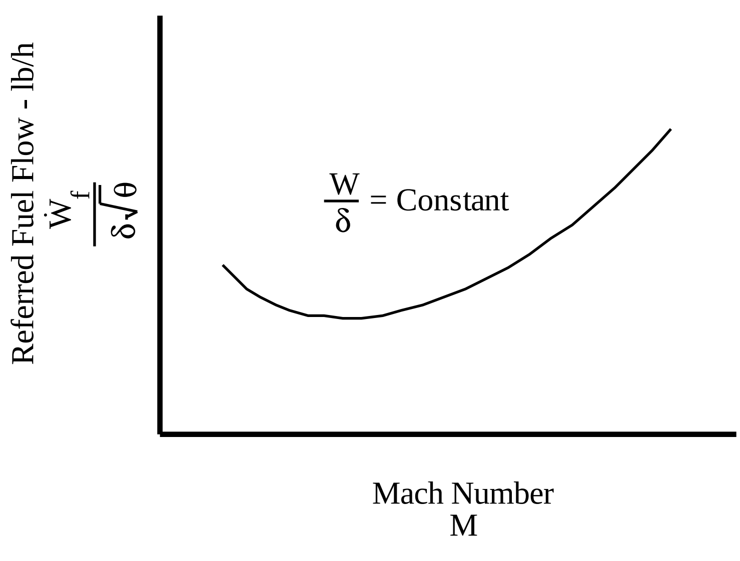

Figure 4.39
REFERRED LEVEL FLIGHT PERFORMANCE

4.5.2 JET FERRY RANGE

The following equations are used in determination of ferry range:

$$R_{Test} = \sum_{j=1}^{n} V_j \, \Delta t_j \qquad \text{(Eq 4.95)}$$

$$R.F._{Test} = \frac{t_T}{\ln\left(\frac{W_1}{W_2}\right)} \qquad \text{(Eq 4.96)}$$

$$R_{Std} = R.F._{Test} \ln\left(\frac{W_{Std_1}}{W_{Std_2}}\right) \qquad \text{(Eq 4.97)}$$

Where:

Δt_j	Time of each time interval	s
n	Number of time intervals	
$R.F._{Test}$	Test day average range factor	
R_{Std}	Standard day cruise range	nmi
R_{Test}	Test cruise range	nmi
t_T	Total cruise time	s
V_j	Avg true airspeed in time interval	kn
W_1	Initial cruise weight	lb
W_2	Final cruise weight	lb
W_{Std_1}	Standard initial cruise weight	lb
W_{Std_2}	Standard final cruise weight	lb.

Standard day cruise weight at the start and end of cruise is required to calculate ferry range. W_{Std_2} is the standard weight at the AS-5263 fuel reserve. Pitot static relationships are used to calculate true airspeed, V_T, and Mach. The test day W/δ for each set of data points is calculated to ensure the planned Mach and W/δ were flown. The test day total range (air miles) is found by numerically integrating the true airspeed with respect to time as in Eq 4.95. The test day average range factor is found from Eq 4.96. Standard day cruise range is then predicted using Eq 4.97.

The total range capability of the aircraft can be evaluated by adding the nautical air miles traveled during climb plus nautical air miles traveled during cruise. Range credit is not allowed for takeoff, acceleration to climb speed, and descent.

4.5.3 JET COMPUTER DATA REDUCTION

Various computer programs are in existence to assist in reduction of performance data. This section contains a brief summary of the assumptions and logic which might be used. The treatment is purposefully generic as programs change over time or new ones are acquired or developed. It is assumed detailed instructions on the use of the particular computer or program are available for the computer program to be used. In any event, the operating system would be invisible to the user.

4.5.3.1 BASIC DATA ENTRY

The purpose of the computer data reduction for range and endurance is to automatically calculate and generate referred range and endurance curves for data taken at one constant referred gross weight (W/δ). It would also combine curves for many W/δ flights into a composite curve. The program may be capable of predicting actual range and endurance performance at the specified W/δ for any temperature conditions.

From a menu selection the appropriate choice would be made to enter the W/δ Range and Endurance program. Data entry requirements for the program are cued as follows:

1. Basic Data:
    - a. Type of aircraft (T-2C, P-3C).
    - b. Bureau Number.
    - c. Standard gross weight.
    - d. Target altitude.
    - e. Method (W/δ).
    - f. Miscellaneous data (such as anti-ice on).
    - g. Date of tests.
    - h. Pilot(s) name(s).

2. For each data point:
   a. Point #.
   b. Observed airspeed (V_o).
   c. Observed pressure altitude (H_{P_o}).
   d. OAT or ambient temperature (T_a).
   e. Fuel flow.
   f. Gross weight.

Note the following:

1. Basic data is that common to all data points. Other data is entered for each point. Items 1.c and d are used for calculations. The rest of basic data is header information for the final plots.
2. V_o and H_{P_o} for each point are observed variables.
3. Temperature may be input as either ambient (degrees Kelvin) or as OAT (degrees Centigrade). This allows data from several different flights to be included in one file.
4. In multi-engine aircraft, fuel flow is the total of all engines.
5. Gross weight must be calculated from the fuel remaining plus the zero fuel weight of the aircraft. This allows data from more than one aircraft or flight to be included in the same file.
6. Edit and store data appropriately for future use or additions.
7. The process is repeated for each W/δ flown.
8. Data from a single W/δ curve are of limited usefulness until they are combined with data from other values of W/δ to cover the normal operating envelope of the aircraft. For example, a family of curves of referred fuel flow versus Mach for various values of constant W/δ may be used to calculate range and endurance for any flight conditions by interpolating between the curves.

One feature of the program calculates the variation between the actual W/δ and target W/δ as shown in figure 4.40. Any points falling outside of the allowed $\pm$ 2% band can be identified for future reference and editing or deletion.

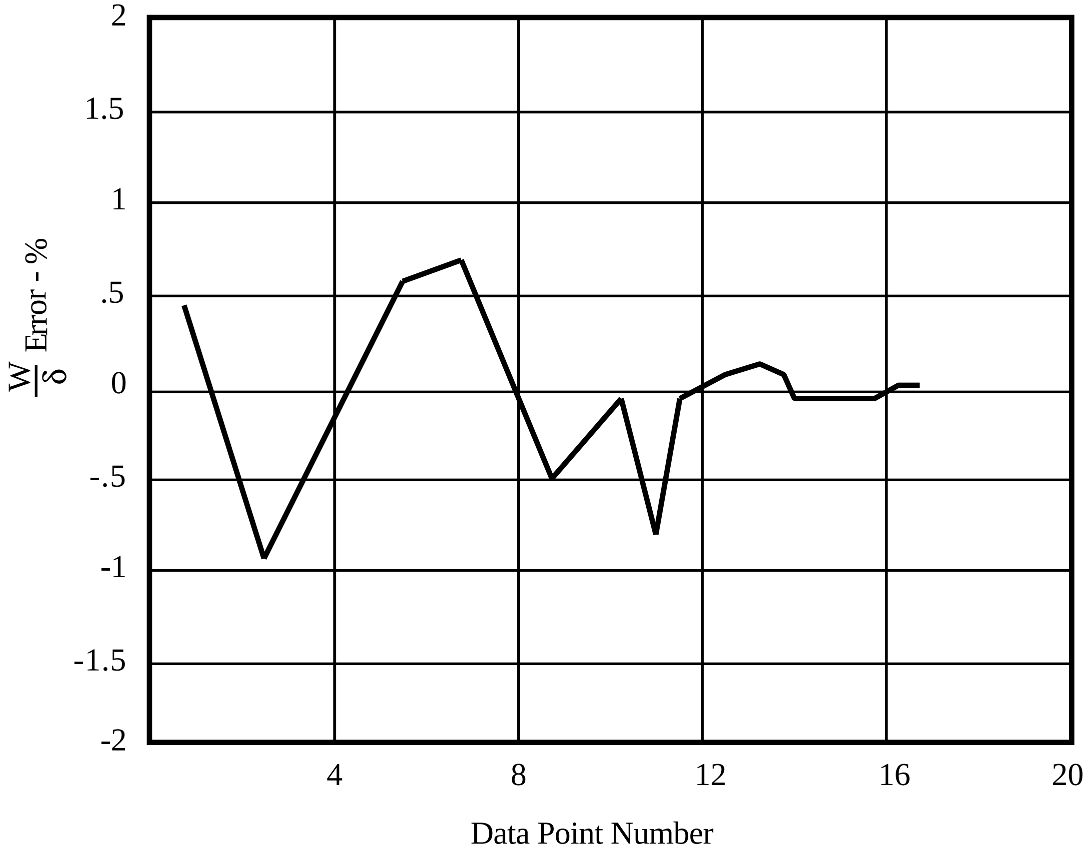

Figure 4.40
W/δ VARIATION

4.5.3.1.1 EQUATIONS USED

Position error calculations from calibrations:

$$H_{P_c} = H_{P_o} + \Delta H_{P_{ic}} + \Delta H_{pos} \qquad \text{(Eq 4.88)}$$

$$V_c = V_o + \Delta V_{ic} + \Delta V_{pos} \qquad \text{(Eq 4.90)}$$

True Mach:

$$M = f\left(V_c, H_{P_c}\right) \qquad \text{(Eq 4.98)}$$

Pressure ratio:

$$\delta = f\left(H_{P_c}\right) \qquad \text{(Eq 4.99)}$$

Test W/δ:

$$\frac{W + W_f}{\delta} = \frac{W}{\delta} \qquad \text{(Eq 4.100)}$$

% W/δ error from:

$$\frac{W}{\delta}\,(\text{error}) = \frac{100\left[\frac{W}{\delta}\,(\text{test}) - \frac{W}{\delta}\,(\text{target})\right]}{\frac{W}{\delta}\,(\text{target})} \qquad \text{(Eq 4.101)}$$

If ambient temperature (˚K) was entered:

$$^\circ C = {}^\circ K - 273.15 \qquad \text{(Eq 4.102)}$$

$$OAT = f\left(T_a, M\right) \qquad \text{(Eq 4.103)}$$

If OAT was entered:

$$T_a = f\left(OAT, M\right) \qquad \text{(Eq 4.104)}$$

Temperature ratio:

$$\theta = \frac{T_a}{T_{ssl}} \qquad \text{(Eq 4.38)}$$

Referred fuel flow:

$$\dot{W}_{f_{ref}} = \frac{\dot{W}_f}{\delta\sqrt{\theta}} \qquad \text{(Eq 4.93)}$$

Referred specific range:

$$S.R.\ \delta = \frac{661.483M}{\left(\frac{\dot{W}_f}{\delta\sqrt{\theta}}\right)} \qquad \text{(Eq 4.105)}$$

Where:

δ	Pressure ratio	
$\Delta H_{P_{ic}}$	Altimeter instrument correction	ft
ΔH_{pos}	Altimeter position error	ft
ΔV_{ic}	Airspeed instrument correction	kn
ΔV_{pos}	Airspeed position error	kn
H_{P_c}	Calibrated pressure altitude	ft
H_{P_o}	Observed pressure altitude	ft
M	Mach number	
OAT	Outside air temperature	˚C
θ	Temperature ratio	

S.R.Specific range nmi/lbT $_a$Ambient temperature˚C or ˚KT $_{ssl}$Standard seal level temperature˚C or ˚KV $_c$Calibrated airspeed knV $_o$Observed airspeed knWWeight lbW $_f$Fuel weight lb $\dot{W}_f$ Fuel flow lb/h $\dot{W}_{f\ ref}$Referred fuel flow lb/h.

4.5.3.2 referred curves

4.5.3.2.1 referred Fuel flow versus mach

The program produces a plot of only the referred data points first. It then fairs the curve through the points based on the order of fit selected. In general, the lowest order fit reasonably representing the shape of the curve (3 rd order is a good starting point) is used. If any data points are clearly suspect, the program presents opportunities to re-enter the data subroutine for editing. This referred curve (similar to figure 4.39) can be combined with different W/δ curves to plot a family of referred fuel flow curves similar to figure 4.49. Single curves for each W/δ would include the actual data points plotted on them.

4.5.3.2.2 REFERRED SPECIFIC RANGE VERSUS MACH

The program plots referred specific range ((S.R.(δ)) versus Mach, calculated from the faired referred fuel flow curve as developed in paragraph 4.5.3.2.1. A single curve is plotted for each W/δ. The program plots a family of these curves as shown in figure 4.50 at various W/δs. The optimum range factor and maximum range of the aircraft would be calculated. Since these curves are derived from the faired curves no data points are shown.

4.5.3.2.3 MAXIMUM VALUES

A list of the referred maximum range and endurance points from each W/δ curve in the previous graphs can be displayed. These values are valid only for the target W/δs. They are useful in precisely locating the points on the referred plots. The maximum referred specific range points is used to calculate range factor in another option of the program. Data for each W/δ may look like:

1.	W/δ	21,000 lb.
2.	Maximum endurance:	Referred fuel flow = 1400 lb/h
		Mach = 0.32
3.	Maximum range:	Referred specific range = 0.02 nmi/lb
		Mach = 0.52

4.5.3.2.4 REFERRED PARAMETERS

A list of referred parameters calculated for each data point for each W/δ curve is available in the program routine. A check of the program's accuracy can be accomplished by hand-calculating one or two points. The parameters displayed are each individual data point, not points on the faired curves. The display may appear as in figure 4.41.

Nominal	Altitude	30000 ft					
Point #	V_c kn	H_{P_c} ft	T_a $^\circ C$	Mach true	$\dot{W}_{f\ ref}$ lb/h	W/δ lb	S.R.(δ) nmi/lb
1	285.5	27431.4	-43.7	.718	9243.3	37811	.0513775
2	etc					37800	
3		etc				37790	
4			etc			37820	
5				etc		37810	
6					etc	37800	

Figure 4.41
REFERRED PARAMETERS

4.5.3.3 UNREFERRED CURVES

Unreferring data allows the calculation of actual specific range fuel flow required at the target W/δ for any temperature condition.

Since specific range is not dependent upon temperature, the program plots specific range versus Mach for standard gross weight at the nominal altitude. The program plots the data for each W/δ singularly, and is capable of combining data similar to figure 4.55.

To calculate actual fuel flow required, the temperature must be specified. The program asks for the temperature entry choice as standard day temperature, delta T_a from standard temperature, or as a specific ambient temperature (T_a). The program plots fuel flow required versus Mach singularly for each W/δ and is capable of combining data similar to figure 4.56.

4.5.3.4 MAXIMUM UNREFERRED VALUES

Maximum values can be selected as in the referred case in paragraph 4.5.3.2.3. Data may appear as:

1.	Pressure altitude	Given in ft MSL
2.	Maximum endurance	Specified at given ˚C, ΔT_a
		Fuel flow in lb/h
		Mach for maximum endurance
3.	Maximum range	Specific range in nmi/lb
		Mach for maximum range

4.5.4 TURBOPROP COMPUTER DATA REDUCTION

Computer programs for range and endurance data reduction for the turboprop are available. As in section 4.5.3, it is assumed detailed instructions on the use of the particular computer program are available. The purpose of the computer data reduction for range and endurance of the turboprop is to automatically calculate and generate referred range and endurance curves for data taken with power set for level flight at any altitude and airspeed. Unreferred curves would also be available given the specific altitude and gross weight desired.

4.5.4.1 DATA ENTRY

From a menu selection the appropriate choice would be made to enter the Range and Endurance program. Data entry requirements for the program would be cued as follows:

1. Basic data:
    a. Type of aircraft (U-21, T-34).
    b. Bureau Number.
    c. Standard gross weight.
    d. Date of tests.
    e. Pilot(s) name(s).
    f. Configuration.
    g. Engine type.
    h. Fuel type.

2. For each data point:
   a. Point number.
   b. Indicated airspeed (kn).
   c. OAT (˚C) or ambient temperature (˚K).
   d. Indicated pressure altitude (ft).
   e. Fuel flow (lb/h).
   f. Torque (psi or ft-lb).
   g. Engine speed.
   h. Gross weight (lb).
   i. Angle of attack (units) if desired and/or available.

Note the following:

1. Basic data is that common to all data points. Item 1.c is used for calculations. The rest of basic data is header information for the final plots.

2. V_o, H_{P_o} and OAT for each point are observed variables. The program would need to know instrument and position error corrections to determine V_c, H_{P_c}, and T_{ic}. The program may require the corrections be made before the data is input.

3. Temperature may be input as either ambient (degrees Kelvin) or OAT (degrees Celsius). The program would be able to use either.

4. In multi-engine aircraft, fuel flow and torque would normally be the total of all engines. The program might be capable of accepting individual engine torque if it is set up to recognize multiple engines.

5. Gross weight would be calculated from the fuel remaining plus the zero fuel weight of the aircraft.

4.5.4.1.1 EQUATIONS USED

Position error calculations from calibrations:

$$H_{P_c} = H_{P_o} + \Delta H_{P_{ic}} + \Delta H_{pos} \quad \text{(Eq 4.88)}$$

$$V_c = V_o + \Delta V_{ic} + \Delta V_{pos} \quad \text{(Eq 4.90)}$$

Equivalent airspeed:

$$V_e = \sqrt{\frac{2q}{\rho_{ssl}}} = \sqrt{\frac{\sigma 2q}{\rho_a}} = \sqrt{\sigma}\ V_T \qquad \text{(Eq 4.106)}$$

Pressure ratio:

$$\delta = f\left(H_{P_c}\right) \qquad \text{(Eq 4.99)}$$

If ambient temperature (˚K) was entered:

$$^\circ C = {}^\circ K - 273.15 \qquad \text{(Eq 4.102)}$$

If OAT was entered:

$$T_a = f\left(OAT\right) \qquad \text{(Eq 4.104)}$$

Temperature ratio:

$$\theta = \frac{T_a}{T_{ssl}} \qquad \text{(Eq 4.38)}$$

Referred fuel flow:

$$\dot{W}_{f_{ref}} = \frac{\dot{W}_f}{\delta\sqrt{\theta}} \qquad \text{(Eq 4.93)}$$

Equivalent shaft horsepower:

$$SHP_e = SHP\sqrt{\sigma} \qquad \text{(Eq 4.107)}$$

Specific fuel consumption::

$$SHPSFC = \frac{\dot{W}_f}{SHP} \qquad \text{(Eq 4.82)}$$

Where:

δ	Pressure ratio	
$\Delta H_{P_{ic}}$	Altimeter instrument correction	ft
ΔH_{pos}	Altimeter position error	ft
ΔV_{ic}	Airspeed instrument correction	kn
ΔV_{pos}	Airspeed position error	kn
H_{P_c}	Calibrated pressure altitude	ft
H_{P_o}	Observed pressure altitude	ft
OAT	Outside air temperature	˚C
P_a	Ambient pressure	psf
q	Dynamic pressure	psf
θ	Temperature ratio	
σ	Density ratio	
SHP	Shaft horsepower	hp
SHP_e	Equivalent shaft horsepower	hp
SHPSFC	Shaft horsepower specific fuel consumption	lb/h/hp
T_a	Ambient temperature	˚C or ˚K
T_{ssl}	Standard seal level temperature	˚C or ˚K
V_c	Calibrated airspeed	kn
V_e	Equivalent airspeed	kn
V_o	Observed airspeed	kn
V_T	True airspeed	kn
W	Weight	lb
W_f	Fuel weight	lb
$\dot{W}_{f\,ref}$	Referred fuel flow	lb/h
$\dot{W}_f$	Fuel flow	lb/h.

4.5.4.2 REFERRED CURVES

4.5.4.2.1 LINEARIZED SHAFT HORSEPOWER

The program produces a plot of equivalent shaft horsepower times equivalent airspeed as a function of equivalent airspeed to the fourth power for a standard gross weight. An essentially linearized plot of the data results for easier interpretation. Using a form of Eq 4.78, the plot appears similar to figure 4.26 with SHP_e replacing THP_e by assuming propeller efficiency (η_P) is 100%. Figure 4.42 illustrates.

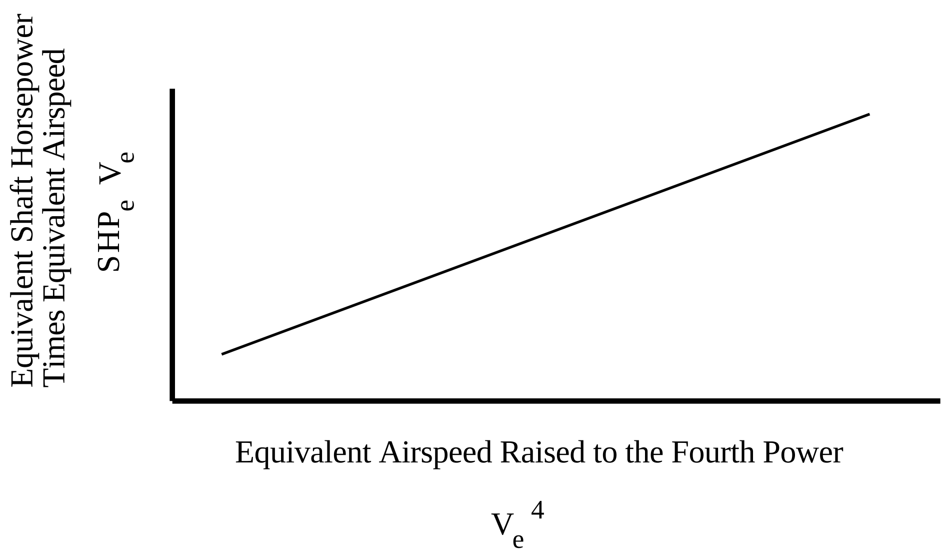

Figure 4.42
LINEARIZED SHAFT HORSEPOWER

4.5.4.2.2 EQUIVALENT SHP

Figure 4.42 is a working plot. Once the curve is fitted through the data points, equivalent SHP versus equivalent airspeed is determined. Fairly simple math converts figure 4.42 to figure 4.43.

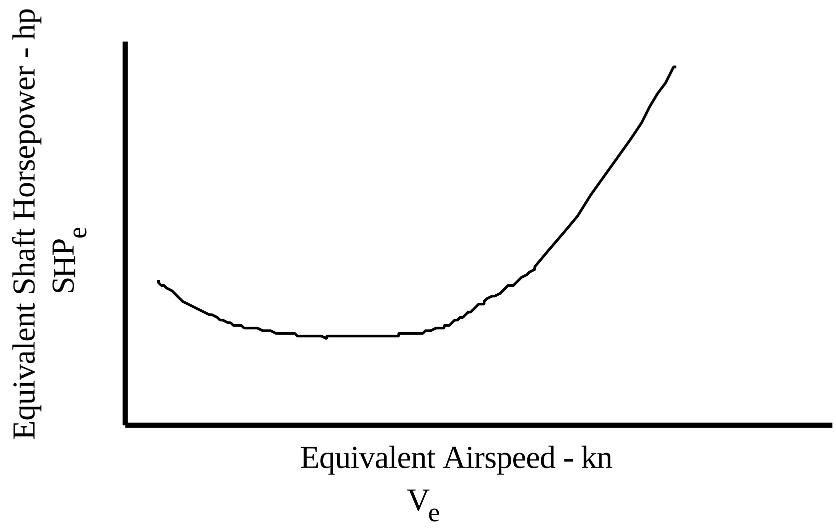

Figure 4.43
EQUIVALENT SHP

4.5.4.2.3 REFERRED FUEL FLOW

The program also calculates referred fuel flow for the data points entered and plots them against the referred shaft horsepower producing a plot similar to figure 4.44. The curve is used later when unreferring fuel flow and presenting the relationship to calibrated airspeed.

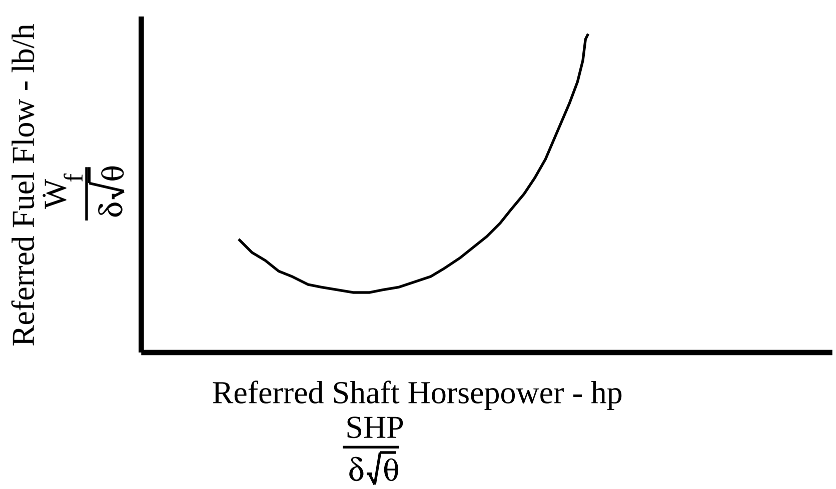

Figure 4.44
REFERRED FUEL FLOW AND SHP

4.5.4.2.4 SPECIFIC FUEL CONSUMPTION

Specific fuel consumption is defined in Eq 4.82 in terms of SHP, that is pounds per hour fuel flow per shaft horsepower.

$$SHPSFC = \frac{\dot{W}_f}{SHP} \tag{Eq 4.82}$$

The computer program uses the relationship to calculate and plot figure 4.45 from figure 4.44.

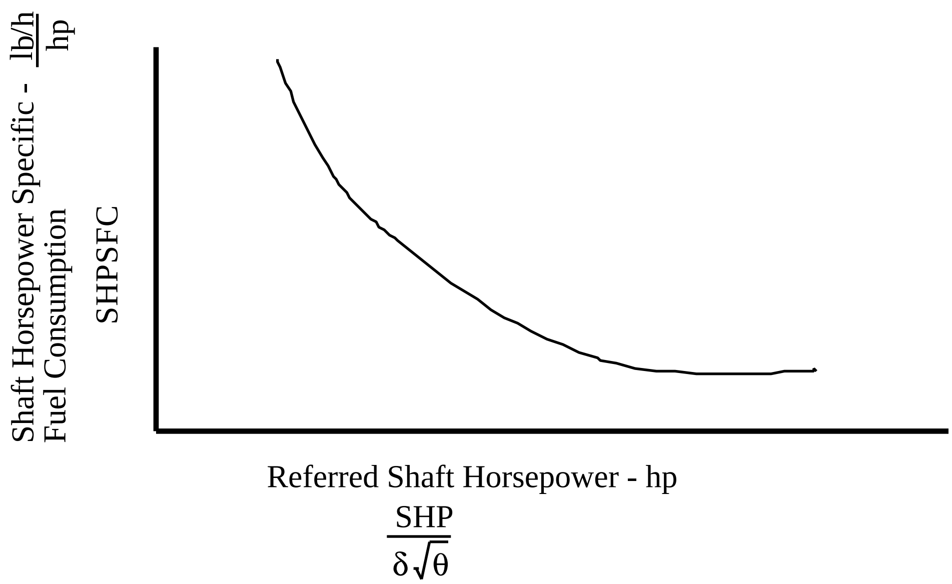

Figure 4.45
SPECIFIC FUEL CONSUMPTION

4.6 DATA ANALYSIS

4.6.1 JET RANGE AND ENDURANCE

Once the referred level flight data is developed, unreferred performance can be obtained for a specified weight, altitude and ambient temperature. The following equations are used.

$$T_a = T_{a_{Std}} + \Delta T_a \qquad \text{(Eq 4.108)}$$

$$\dot{W}_{f_{ref}} = \frac{\dot{W}_f}{\delta\sqrt{\theta}} \qquad \text{(Eq 4.93)}$$

$$S.R. = \frac{a_{ssl}\, M}{\left(\frac{\dot{W}_f}{\delta\sqrt{\theta}}\right)\delta} \qquad \text{(Eq 4.109)}$$

Where:

a_{ssl}	Standard sea level speed of sound	661.483 kn
δ	Pressure ratio	
ΔT_a	Temperature differential	˚C, ˚K
M	Mach number	
θ	Temperature ratio	
S.R.	Specific range	nmi/lb
T_a	Ambient temperature	˚C or ˚K
$T_{a_{Std}}$	Standard ambient temperature	˚C or ˚K
$\dot{W}_f$	Fuel flow	lb/h
$\dot{W}_{f\ ref}$	Referred fuel flow	lb/h.

From figure 4.39 the data is unreferred for a specified gross weight, altitude, and ambient temperature as follows:

Step	Parameter	Notation	Formula	Units	Remarks
1	Referred weight	W/δ		lb	Choose one
2	Weight	W		lb	Select one and H_P is defined
3	Pressure altitude	H_P		ft	Select one and W is defined
4	Ambient temperature	T_a	Eq 4.108	˚C	Standard day from Appendix VI for (3), or for non standard day, or specify
5	Referred fuel flow	$\dot{W}_{f\ ref}$	Eq 4.93	lb/h	From figure 4.39 at each M
6	Actual fuel flow	$\dot{W}_f$		lb/h	Unrefer for δ and θ at (1) or (2)
7	Specific Range	S.R.	Eq 4.109	nmi/lb	

Plot unreferred fuel flow, $\dot{W}_f$, versus M for a specified gross weight, altitude, and ambient temperature; and plot S.R. versus M for the same gross weight, altitude, and ambient temperature as in figure 4.46.

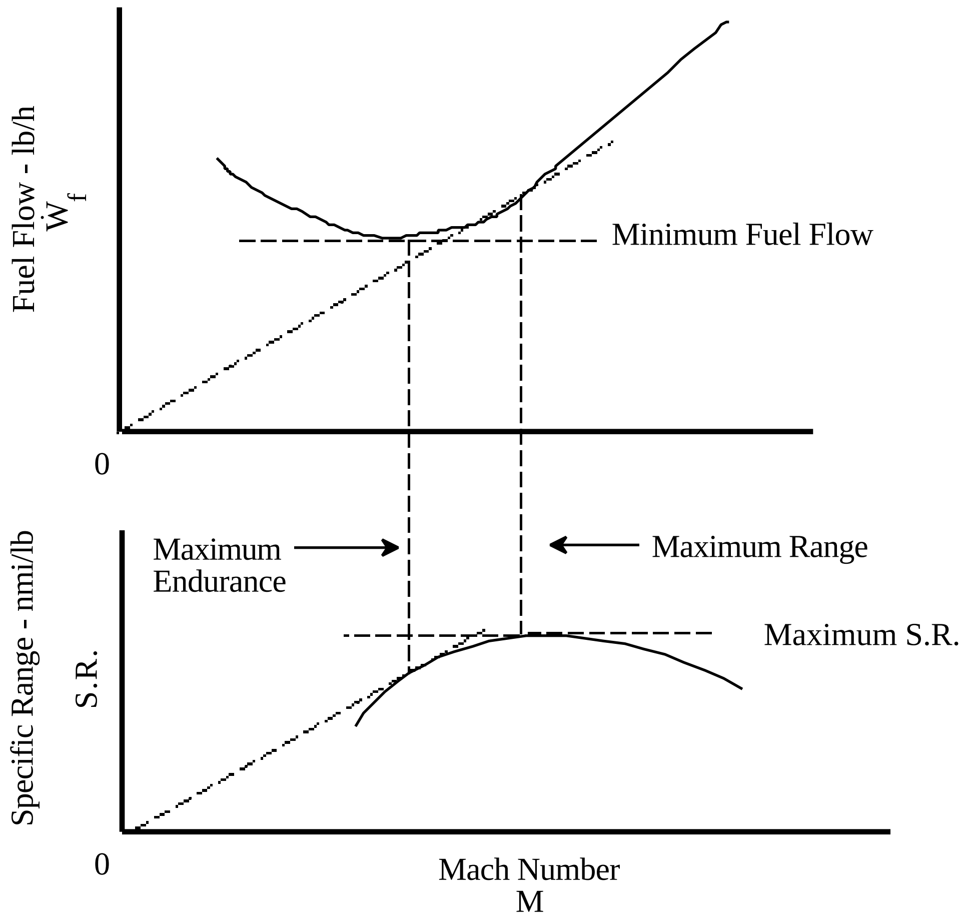

Figure 4.46
UNREFERRED LEVEL FLIGHT PERFORMANCE

As previously shown in figure 4.17, maximum specific range occurs at the tangent to the fuel flow versus V_T curve of a line drawn from the origin. Since V_T =K x M for a given T_a, the same conclusion applies to figure 4.46. Maximum endurance Mach (minimum fuel flow) occurs at the tangent to the specific range versus Mach curve of a line drawn from the origin in figure 4.46.

4.6.2 NON STANDARD DAY RANGE AND ENDURANCE

The referred data curve, figure 4.39, can be generated from test day data without regard to the ambient temperature. For a given altitude and gross weight, an increase in ambient temperature results in an increased actual fuel flow so the ratio $\frac{\dot{W}_f}{\sqrt{\theta}}$ remains constant. Figure 4.47 is figure 4.46 plotted versus V_T for standard and hot days.

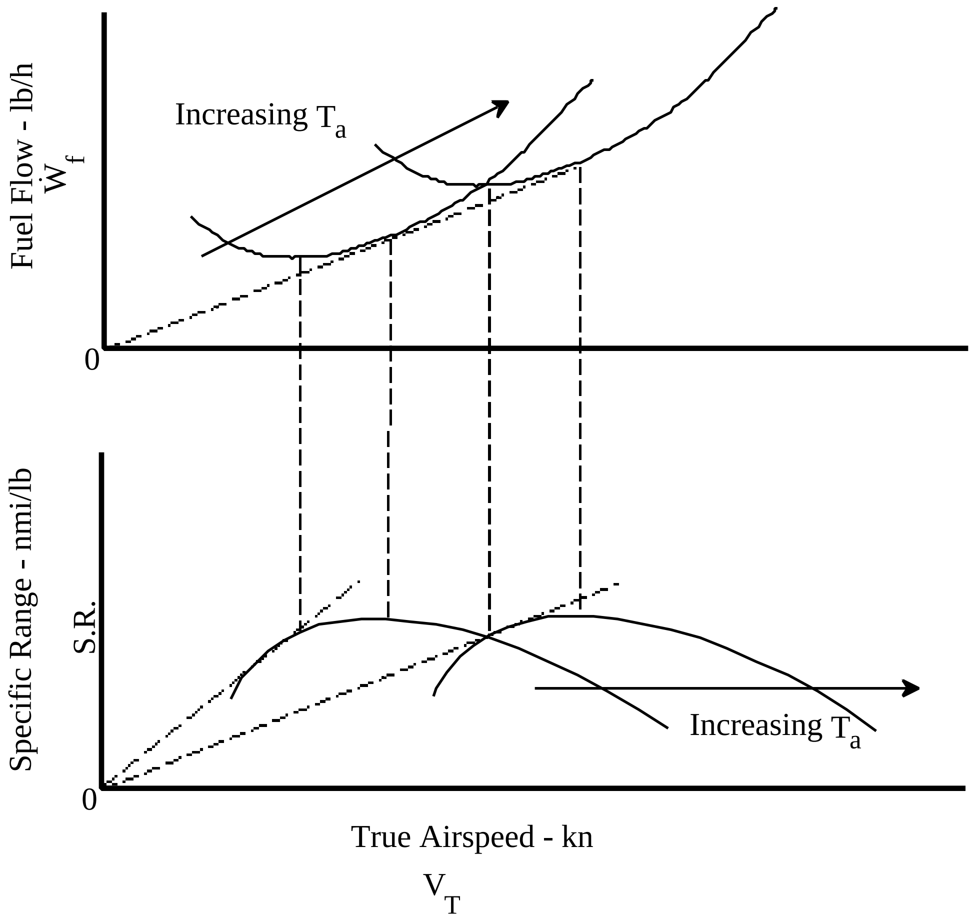

Figure 4.47
LEVEL FLIGHT NON STANDARD DAY

Regardless of ambient temperature, the aircraft specific range is constant. On a hot day the actual fuel flow increases so $\frac{\dot{W}_f}{\sqrt{\theta}}$ is constant. V_T is scaled up by the same factor. To illustrate:

$$V_{T_{\text{Hot day}}} = 661.483\ M\ \sqrt{\theta_{\text{Std}}}\left(\frac{\sqrt{\theta_{\text{Hot day}}}}{\sqrt{\theta_{\text{Std}}}}\right) \tag{Eq 4.110}$$

$$\dot{W}_{f_{\text{Hot day}}} = \dot{W}_{f_{\text{Std}}}\left(\frac{\sqrt{\theta_{\text{Hot day}}}}{\sqrt{\theta_{\text{Std}}}}\right) \tag{Eq 4.111}$$

from:

$$\frac{\dot{W}_f}{\sqrt{\theta}} = ¢ \tag{Eq 4.112}$$

Where:

M	Mach number	
θ	Temperature ratio	
V_T	True airspeed	kn
$\dot{W}_f$	Fuel flow	lb/h
¢	Constant.	

As ambient temperature increases, endurance time decreases since $\dot{W}_f$ increases to keep $\frac{\dot{W}_f}{\sqrt{\theta}}$ constant.

4.6.3 WIND EFFECTS ON RANGE AND ENDURANCE

The effect of wind on range is very important. A head wind reduces range and a tail wind increases range. Specific range for no wind was $\frac{V_T}{\dot{W}_f}$. For a head wind or tail wind, ground speed for the fuel flow needs to be maximized $\frac{GS}{\dot{W}_f}$. Figure 4.48 shows the variation with speed to maximize specific range in the presence of wind.

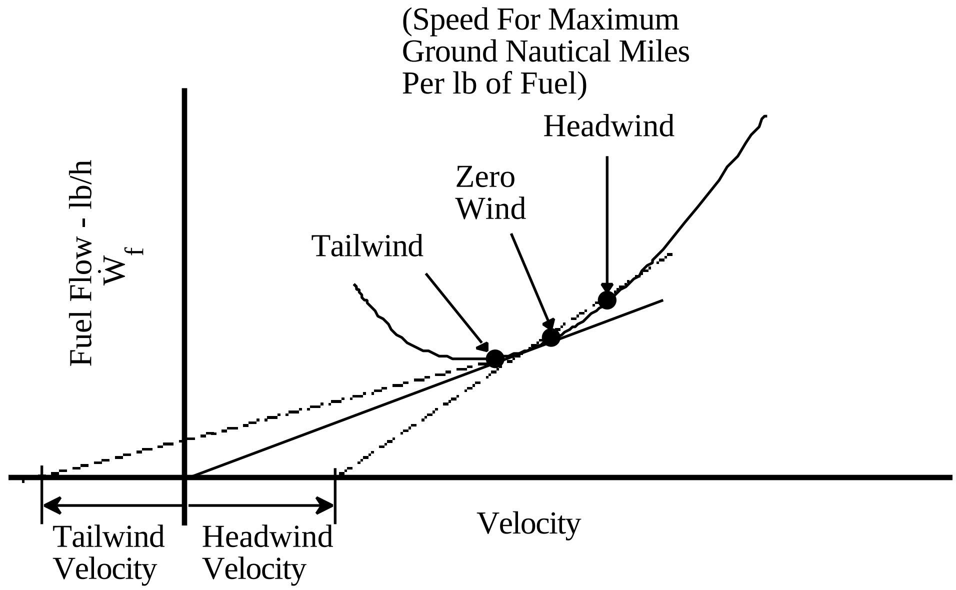

Figure 4.48
WIND EFFECT ON LEVEL FLIGHT RANGE

With zero wind, a line from the origin tangent to the curve locates the maximum range condition. With a head wind, the speed for maximum ground range is located by a line drawn tangent from a velocity offset equal to the head wind. The range is at some higher velocity and fuel flow. Although the range is less than when at zero wind, the higher velocity minimizes the range loss due to the head wind. The effect of a tail wind is the reverse. The correction in speed to account for wind becomes critical only when wind velocities exceed 25 percent of the true airspeed.

4.6.4 RANGE AND ENDURANCE PROFILES

The foregoing analysis presented the data for a single W/δ. To determine the actual range and endurance, data from all W/δ flights are combined.

4.6.4.1 REFERRED FUEL FLOW COMPOSITE

When all W/δ flights are combined, the results look like figure 4.49 for lines of constant W/δ from minimum to maximum.

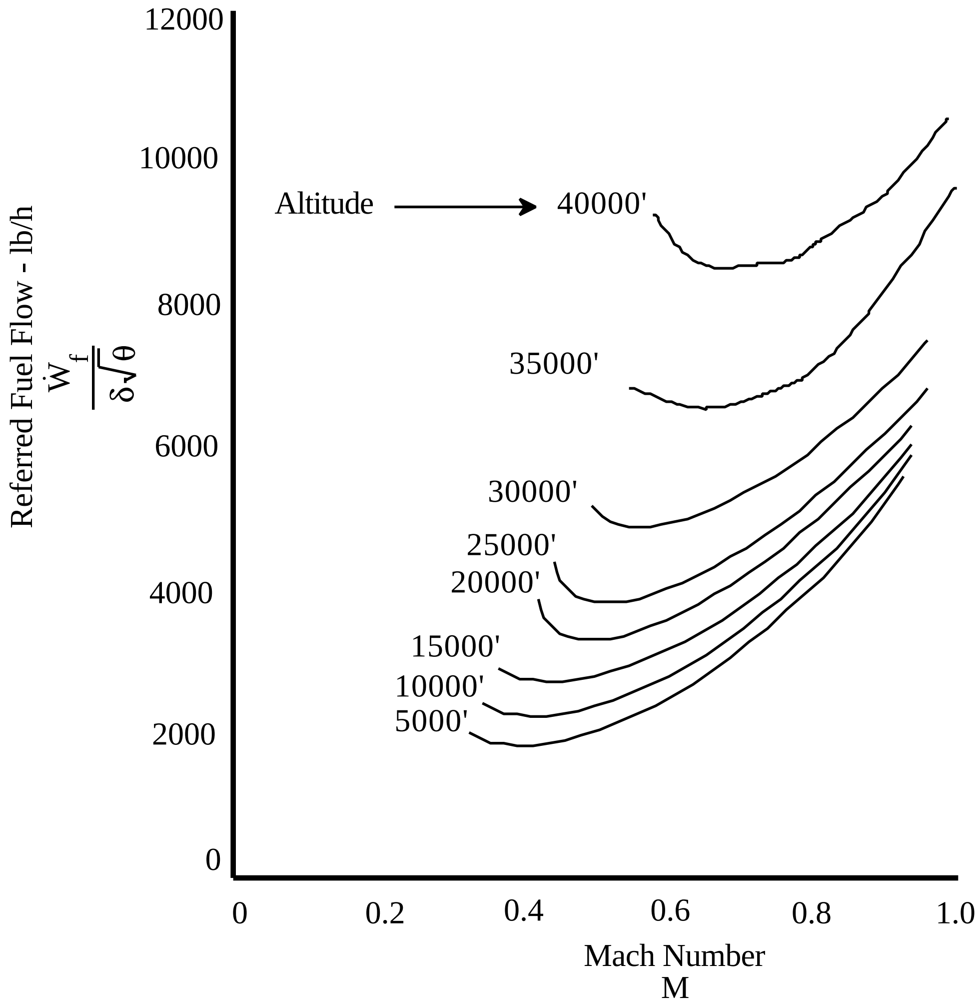

Figure 4.49
REFERRED FUEL FLOW COMPOSITE

4.6.4.2 REFERRED SPECIFIC RANGE COMPOSITE

Range performance can be determined by rearranging figure 4.49 into another referred composite curve called referred specific range as shown in figure 4.50.

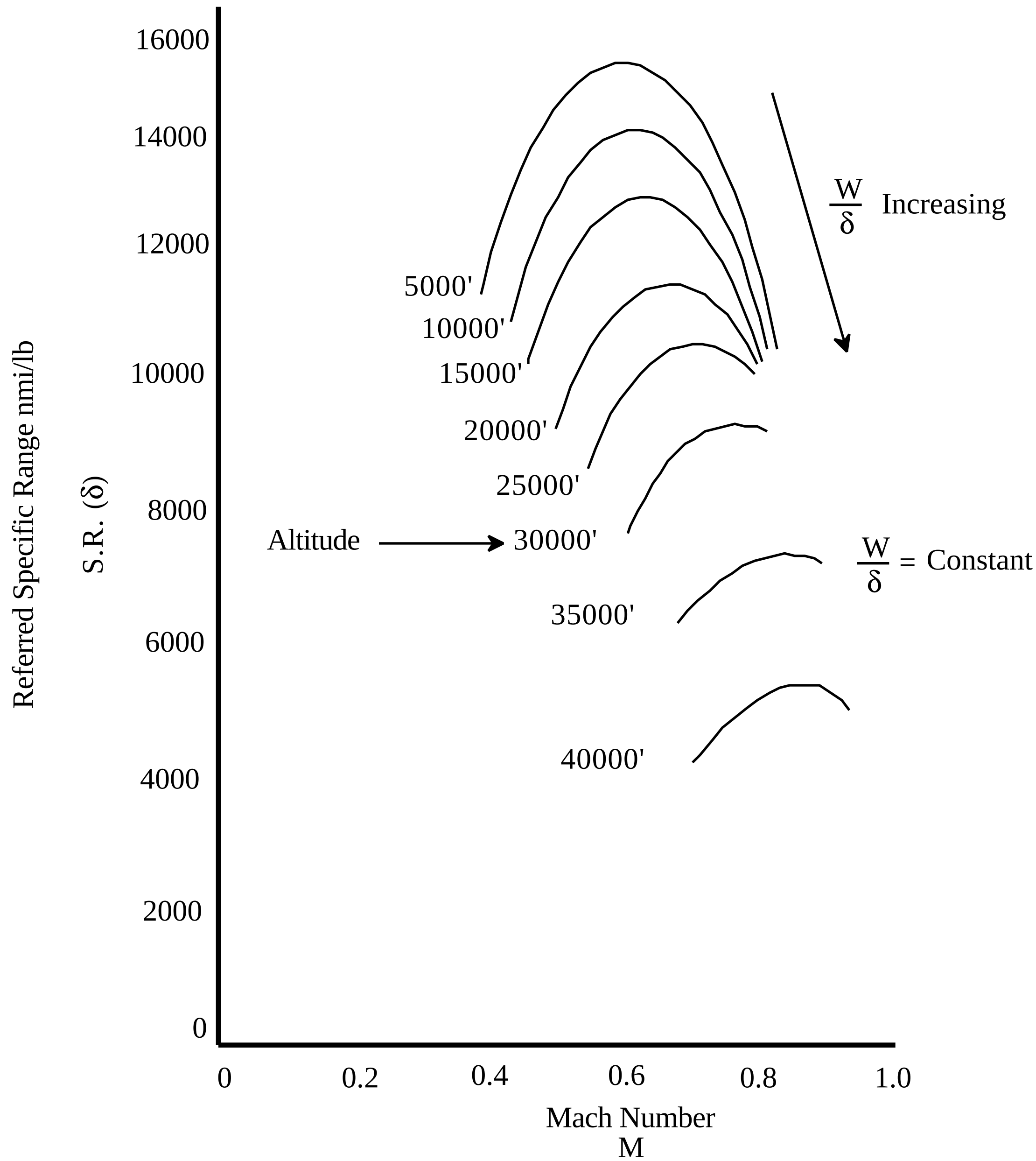

Figure 4.50
REFERRED SPECIFIC RANGE

Equations for the referred specific range determination are:

$$\text{S.R.} = \frac{a_{ssl}\, M}{\left(\dfrac{\dot{W}_f}{\delta\sqrt{\theta}}\right)\delta} \qquad \text{(Eq 4.109)}$$

where referred specific range is defined as the product of S.R. and δ.

$$\text{S.R. } \delta = \frac{661.483\text{M}}{\left(\frac{\dot{W}_f}{\delta \sqrt{\theta}}\right)}$$

(Eq 4.105)

Where:

a_{ssl}	Standard sea level speed of sound	661.483 kn
δ	Pressure ratio	
M	Mach number	
θ	Temperature ratio	
S.R.	Specific range	nmi/lb
$\dot{W}_f$	Fuel flow	lb/h.

Specific range is calculated by Eq 4.109 as in paragraph 4.6.1 for each W/δ line then multiplied by the pressure ratio δ corresponding to the altitudes chosen to obtain referred specific range.

4.6.4.2.1 RANGE CALCULATION

When the specific range is known, the actual range is found by integrating the specific range over the fuel burned. Since the gross weight decreases as fuel is consumed, the specific range is constantly changing. Evaluating how the specific range changes depends on the type of cruise control being used. The cruise may be flown at some schedule of altitude, Mach, fuel flow, engine speed, cruise climb, etc. with each type resulting in different range performance. Determining the optimum range profile is the goal.

The following equations show the development of the range equation in terms of the data actually measured in flight tests:

$$\text{Range} = \int_0^{W_{f_{Used}}} (\text{S.R.})\, dW_f$$

(Eq 4.113)

Fuel used is just the change in gross weight, so:

$$\text{Range} = \int_{W_1}^{W_2} (\text{S.R.})\, dW \tag{Eq 4.114}$$

Converting the quantities inside the integral into terms of referred parameters (S.R. x δ) and multiplying top and bottom by W, the range is a function of referred parameters (S.R. x δ) and (W/δ):

$$\text{Range} = \int_{W_1}^{W_2} (\text{S.R. } \delta) \left(\frac{W}{\delta}\right) \frac{1}{W}\, dW \tag{Eq 4.115}$$

In terms of measured data:

$$\text{Range} = \int_{W_1}^{W_2} \left[\frac{661.483\ M}{\left(\dfrac{\dot{W}_f}{\delta \sqrt{\theta}}\right)} \frac{W}{\delta} \right] \frac{dW}{W} \tag{Eq 4.116}$$

Where:

δ	Pressure ratio	
M	Mach number	
θ	Temperature ratio	
S.R.	Specific range	nmi/lb
W	Weight	lb
W_1	Initial cruise weight	lb
W_2	Final cruise weight	lb
W_f	Fuel weight	lb
$\dot{W}_f$	Fuel flow	lb/h.

4.6.4.2.2 INTERPOLATING THE REFERRED DATA CURVES

The W/δ flights were planned to include W/δ ranging from minimum to maximum values to make extrapolation of the referred curves unnecessary. Since the number of test flights are finite, interpolation is necessary. However, interpolation between the lines of constant W/δ is not linear. Interpolation uses the following equations and resultant figures:

$$\frac{D}{\delta} = f\left(M, \frac{W}{\delta}\right) \tag{Eq 4.27}$$

For a parabolic drag polar :

$$\frac{D}{\delta} = \frac{C_{D_{P(M)}} \gamma P_{ssl} M^2 S}{2} + \frac{2\left(W/\delta\right)^2}{\pi\, e_{(M)}\, AR\, S\, \gamma\, P_{ssl}\, M^2} \tag{Eq 4.26}$$

Interpolating between W/δ at constant M and substituting for all constants in Eq 4.26, Eq 4.117 results and figure 4.51 can be developed.

$$\frac{D}{\delta} = K_3 + K_4\left(\frac{W}{\delta}\right)^2 \tag{Eq 4.117}$$

Where:

AR	Aspect ratio	
$C_{D_{p\,(M)}}$	Parasite drag coefficient at high Mach	
D	Drag	lb
δ	Pressure ratio	
e	Oswald's efficiency factor	
γ	Ratio of specific heats	
K_3	Constant	
K_4	Constant	
M	Mach number	
π	Constant	
P_{ssl}	Standard sea level pressure	2116.217 psf
S	Wing area	ft^2
W	Weight	lb.

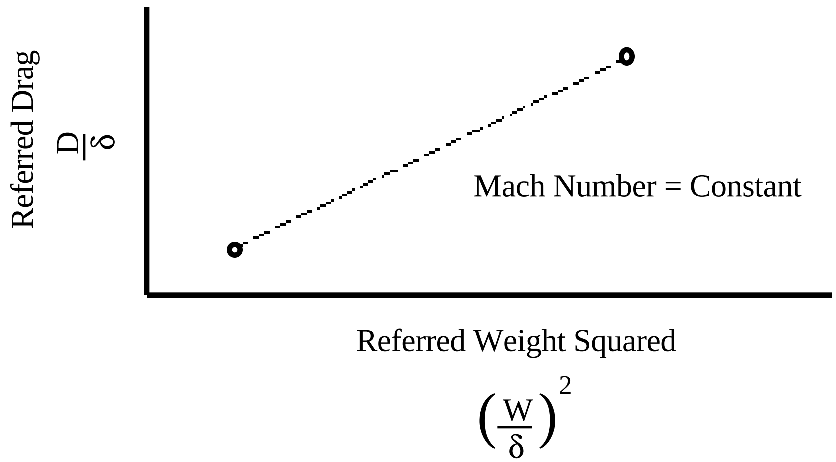

Figure 4.51
INTERPOLATED W/δ AT CONSTANT MACH

Since D/δ is proportional to referred fuel flow, $\frac{\dot{W}_f}{\delta\sqrt{\theta}}$, figure 4.52 can be develop in similar fashion.

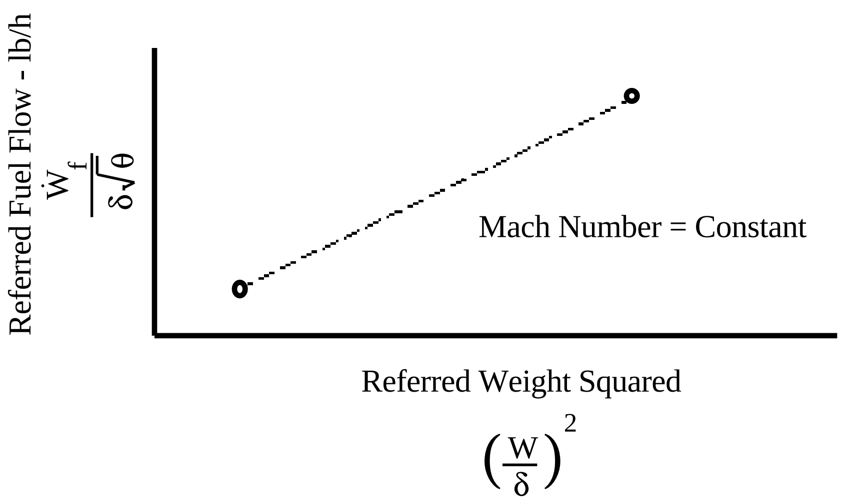

Figure 4.52
INTERPOLATED W/δ ALTERNATE AT CONSTANT MACH

For an aircraft exhibiting a cubic drag polar such as the T-38, figure 4.53 works for interpolation.

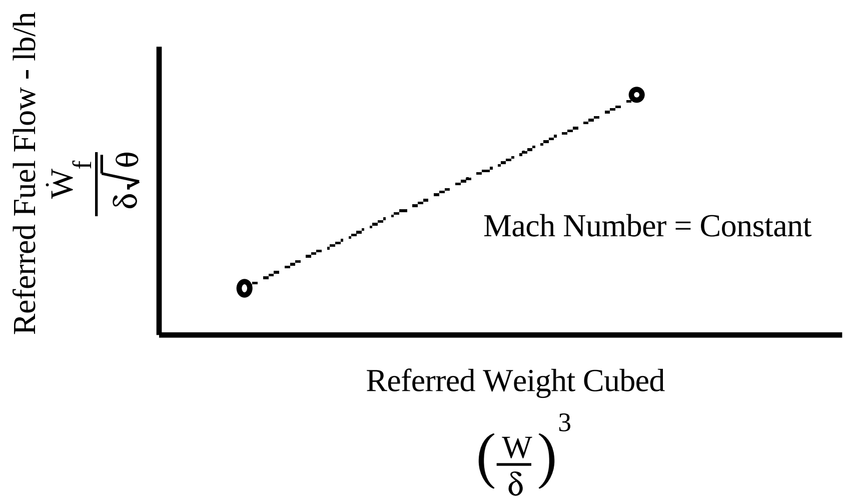

Figure 4.53
CUBIC DRAG POLAR INTERPOLATED W/δ AT CONSTANT MACH

4.6.4.3 OPTIMUM RANGE

From Eq 4.105, the product of referred specific range and referred weight is the range factor (R.F.) and is useful in determining optimum range.

$$R.F. = \left[(S.R.\ \delta) \frac{W}{\delta} \right] \tag{Eq 4.118}$$

Therefore:

$$R.F. = \left[\frac{661.483\ M}{\left(\frac{\dot{W}_f}{\delta \sqrt{\theta}} \right)} \left(\frac{W}{\delta} \right) \right] \tag{Eq 4.119}$$

$$\text{Range} = \int_{W_1}^{W_2} (R.F.) \frac{dW}{W} \tag{Eq 4.120}$$

Where:

δ	Pressure ratio	
M	Mach number	
θ	Temperature ratio	
R.F.	Range factor	
S.R.	Specific range	nmi/lb
W	Weight	lb
$\dot{W}_f$	Fuel flow	lb/h.

Optimum range performance then is achieved by maximizing the range factor. In other words, if the range factor is held at its maximum value, maximum aircraft range results.

4.6.4.3.1 CALCULATING MAXIMUM RANGE FACTOR AND OPTIMUM MACH

Maximum range factor is calculated from figure 4.50 by multiplying the maximum of each referred specific range curve by its associated W/δ. The calculated values result in the maximum range factor (Eq 4.118) and the Mach number for optimum range factor for each W/δ curve. These values can be plotted as in figure 4.54.

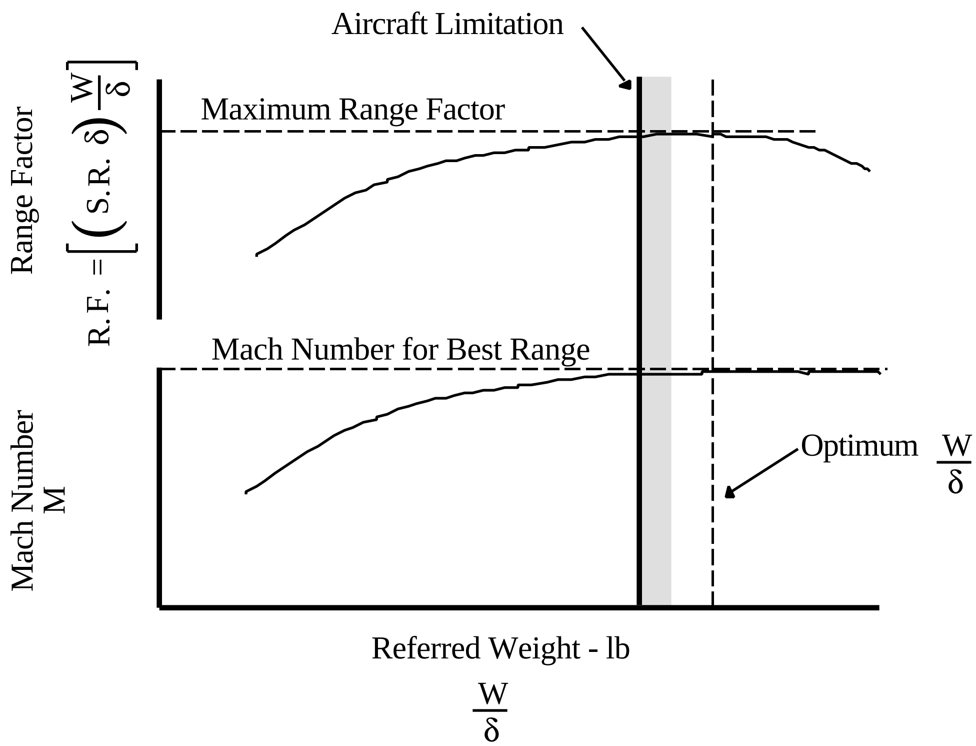

Figure 4.54
OPTIMUM RANGE

The peak range factor may be unobtainable if:

1. The optimum W/δ is in excess of the absolute ceiling of the aircraft.
2. Safety or operational considerations preclude ascending to these high altitudes.

In these cases the maximum range factor and optimum Mach occur at the highest W/δ tested.

If able to fly high enough, the results appear as in figure 4.55.

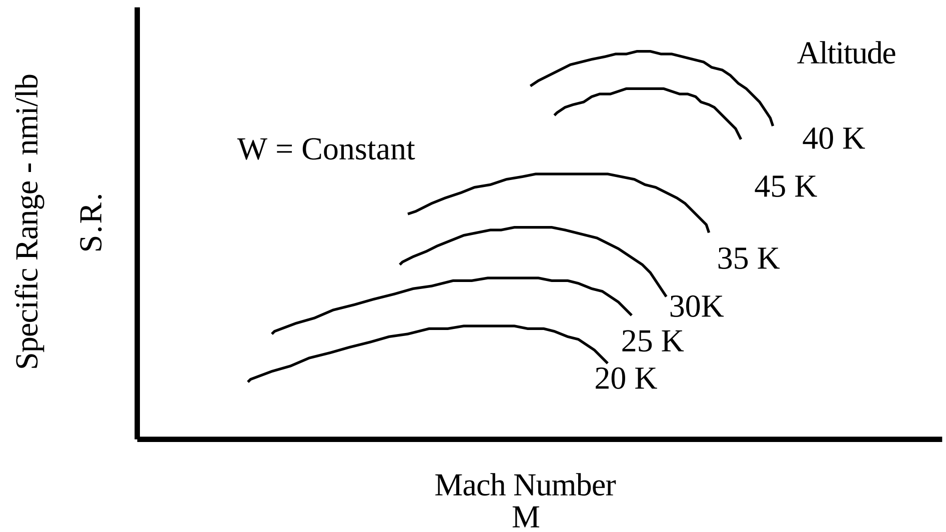

Figure 4.55
ACTUAL SPECIFIC RANGE

The range factor increases with increasing W/δ (altitude for a given weight) and ultimately reaches a maximum. In figure 4.55, the Mach number for best range is also determined once the optimum W/δ is known.

Actual specific range can be determined by unreferring figure 4.54 for a specific weight as a function of Mach number and pressure altitude as in figure 4.55. Figure 4.55 shows the particular airspeed and altitude to fly for maximum S.R.

4.6.4.4 OPTIMUM ENDURANCE FOR JETS

Fuel flow is proportional to the thrust. Therefore, a jet achieves maximum specific endurance when operated at minimum thrust required or where the lift to drag ratio is maximum, $\left.\frac{L}{D}\right|_{max}$. In subsonic flight below the drag rise Mach, $\left.\frac{L}{D}\right|_{max}$ occurs at a specific value of lift coefficient where the ratio of lift to drag coefficients is maximum, $\left.\frac{C_L}{C_D}\right|_{max}$. For a given aircraft this ratio is independent of weight or altitude. If the aircraft of a given weight and configuration is operated at various altitudes, the value of the minimum thrust required is unaffected as discussed in paragraph 4.3.4.3. Endurance is really only a function of engine performance.

Specific fuel consumption of the jet engine is strongly affected by operating engine speed and altitude. The jet engine generally operates more efficiently near normal rated engine speed and the low temperatures of the stratosphere to produce low specific fuel consumption. Increased altitude provides the favorable lower inlet air temperature and requires a greater engine speed to provide the thrust required at $\left.\frac{C_L}{C_D}\right|_{max}$. The typical jet experiences an increase in specific endurance with altitude with the peak values occurring at or near the tropopause. An example is the single engine jet with a maximum specific endurance at 35,000 feet which is at least 40% greater than the maximum value at sea level. If the jet is at low altitude and it is necessary to hold for a considerable time, maximum time in the air is obtained by beginning a climb to some optimum altitude dependent upon the fuel quantity available. The fuel expended during the climb may be offset by lower TSFC at the higher altitude providing greater total endurance.

The altitude where TSFC is minimum is called the critical altitude. At altitudes above critical, the TSFC increases resulting in decreased endurance performance. Decreasing engine component efficiencies caused by the reduced Reynold’s number and operating engine speed above the design value encountered at very high altitudes lead to the increased TSFC. For present day engines, the critical altitude usually occurs fairly close to the beginning of the isothermal layer near 36,000 feet.

Endurance considerations discussed above all depend upon steady level flight at a particular altitude. Fuel required to climb to the altitude for optimum level flight endurance must be considered in the overall endurance performance. Many times it is more advantageous for overall endurance to remain at a lower altitude than to expend fuel for climbing. By compiling climb fuel consumption data with level flight endurance data, guidelines can be established in making decisions to climb or maintain altitude.

4.6.4.4.1 UNREFERRED ENDURANCE

A referred fuel flow composite is presented in figure 4.49. The data can be unreferred and replotted as in figure 4.56 as actual fuel flow curves for various altitudes at a given weight and configuration. The calibrated airspeed for minimum fuel flow is found to increase some with increasing altitude. The figure is based on a specific temperature at each altitude. Hot day endurance requires higher fuel flow than on a standard day since for a given weight, altitude, and airspeed, $\frac{\dot{W}_f}{\sqrt{\theta}}$ is constant and not $\dot{W}_f$.

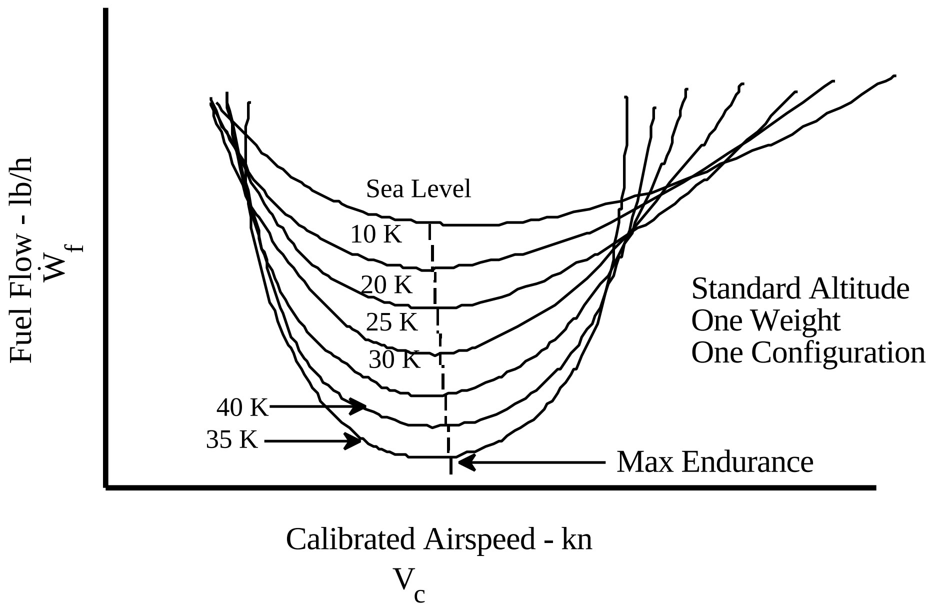

Figure 4.56
ACTUAL FUEL FLOW

Once the target airspeed for maximum endurance is known, the fuel flow and optimum altitude for a given gross weight can be found from a composite plot of minimum fuel flow points. Figure 4.57 illustrates.

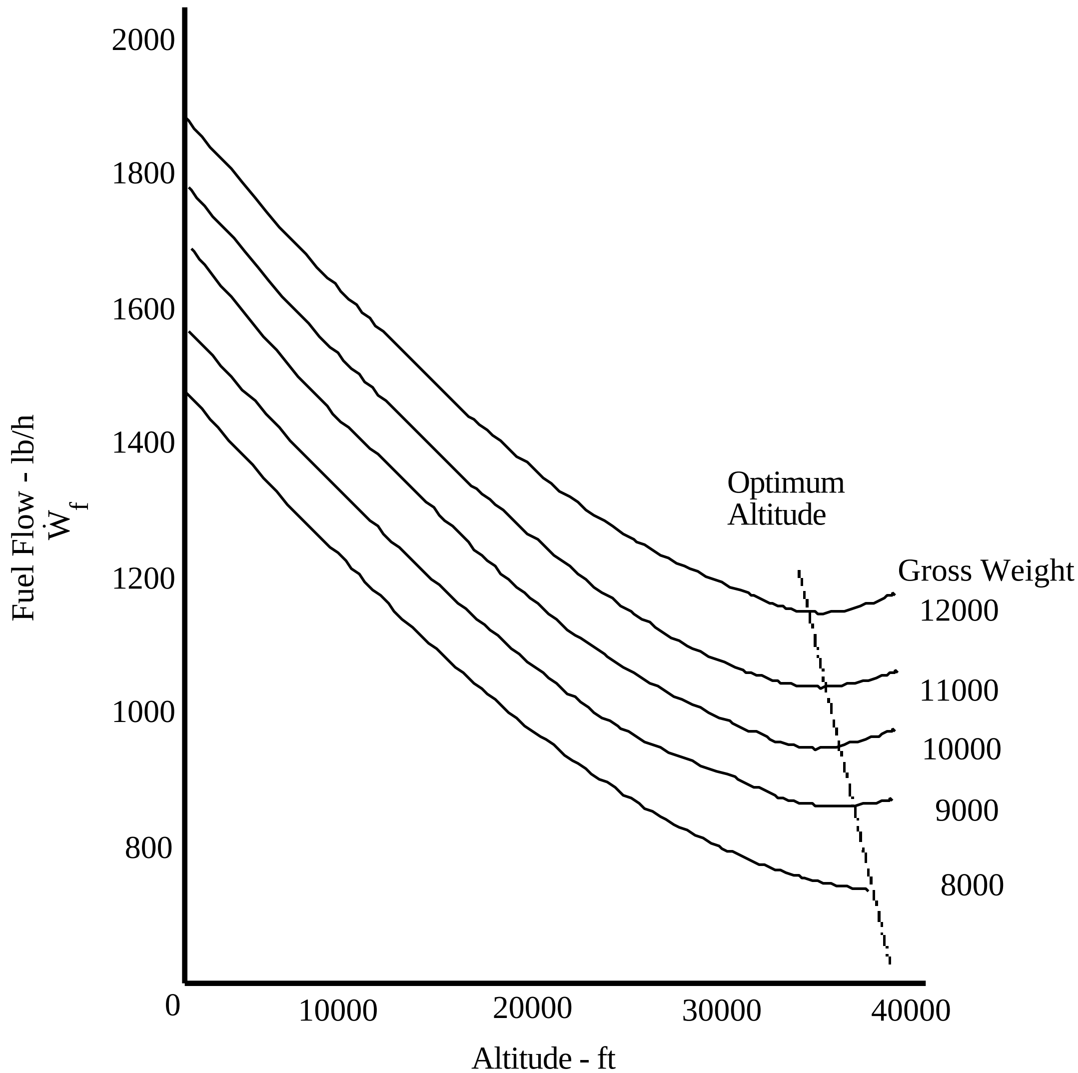

Figure 4.57
OPTIMUM ENDURANCE

4.6.5 FERRY RANGE

Total range capability was determined in paragraph 4.5.2. To summarize, the total range capability of the aircraft included distance traveled during climb plus distance traveled during cruise. Range credit is not allowed for takeoff, acceleration to climb speed, and descent. Distance traveled during the climb is obtained from the climb tests and distance traveled during cruise is computed by using the range factor and Eq 4.120 where W_1 was the initial cruise weight (end of climb) using fuel allowances for ground time and acceleration to climb speed and fuel for climb from the requirements. W_2 was the final cruise weight at the end of the cruise phase. At each test point, altitude, airspeed, weight, ambient temperature, engine speed, and Mach number were recorded while flying a pre-planned profile, including a slow climb to optimize range. Figure 4.58 presents typical format for ferry range data.

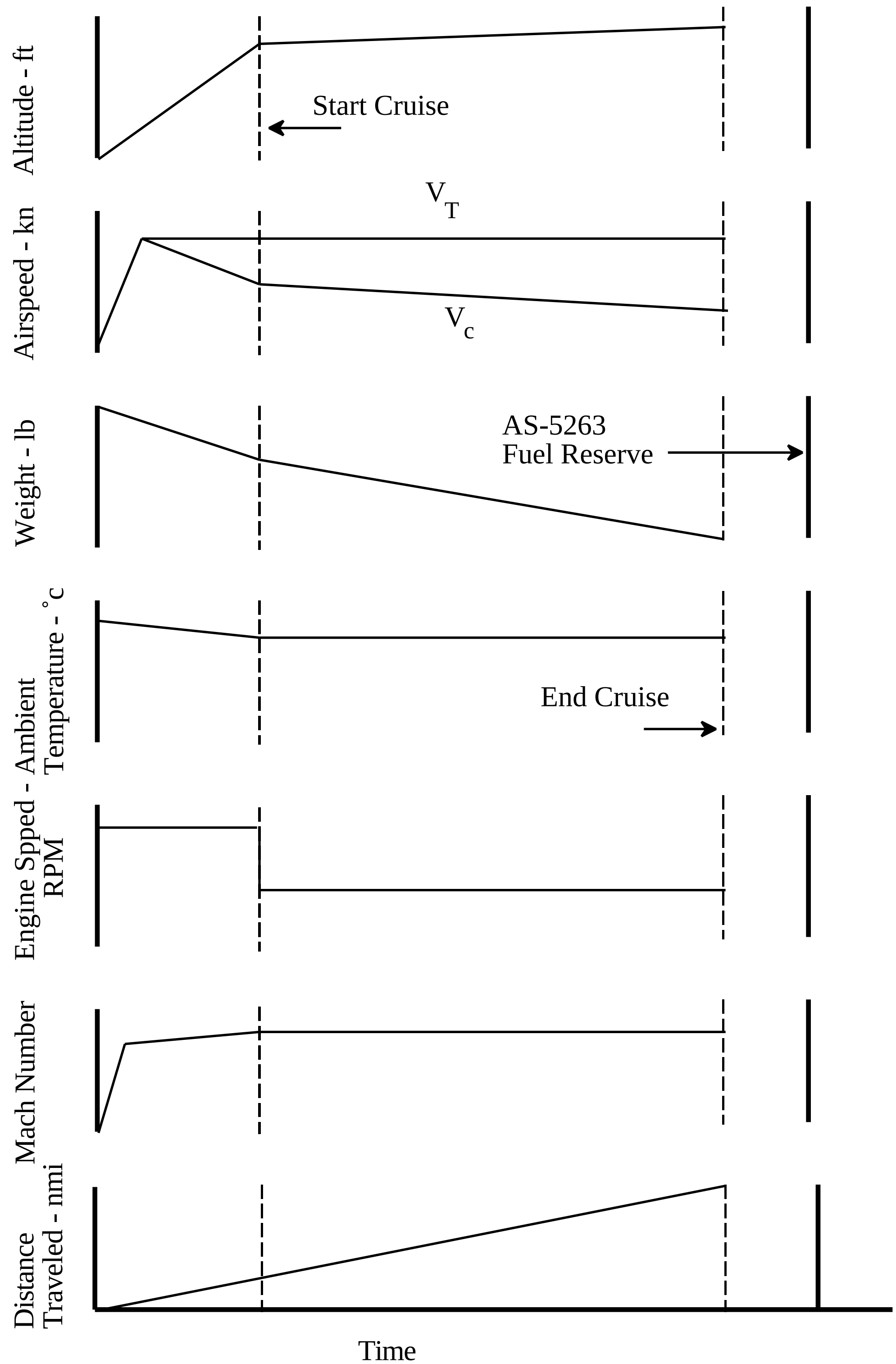

Figure 4.58
FERRY RANGE

4.6.6 CRUISE CLIMB AND CONTROL

Cruise climb and control implies that an airplane is operated to maintain the recommended long range cruise condition throughout the flight. Since fuel is consumed during cruise, the gross weight of the airplane will vary and optimum airspeed, altitude, and power setting can vary. Cruise control means the control of optimum airspeed, altitude, and power setting to maintain the maximum specific range condition. At the beginning of cruise, the high initial weight of the airplane will require specific values of airspeed, altitude, and power setting to produce the recommended cruise condition. As fuel is consumed and the airplane gross weight decreases, the optimum airspeed and power setting may decrease or the optimum altitude may increase. In addition, the optimum specific range will also increase. The pilot must use the proper cruise control technique to ensure that the optimum conditions are maintained.

Cruise altitude of the turbojet should be as high as possible within compressibility or thrust limits. In general, the optimum altitude to begin cruise is the highest altitude at which the maximum continuous thrust can provide the optimum aerodynamic conditions. The optimum altitude is determined mainly by the gross weight at the beginning of cruise. For the majority of jets this altitude will be at or above the tropopause for normal cruise configurations.

Most jets which have transonic or moderate supersonic performance will obtain maximum range with a high subsonic cruise. However, an airplane designed specifically for high supersonic performance will obtain maximum range with a supersonic cruise; subsonic operation will cause low lift to drag ratios, poor inlet and engine performance and reduce the range capability.

The cruise control of the jet is considerably different from that of the prop airplane. Since the specific range is so greatly affected by altitude, the optimum altitude for beginning of cruise should be attained as rapidly as is consistent with climb fuel requirements. The range climb schedule varies considerably between airplanes, and the performance section of the flight handbook will specify the appropriate procedure. The descent from cruise altitude will employ essentially the same procedure. A rapid descent is necessary to minimize the time at low altitudes where specific range is low and fuel flow is high for a given engine speed.

During cruise flight of the jet, the gross weight decrease by fuel used can result in two types of cruise control. During a constant altitude cruise, a reduction in gross weight will require a reduction of airspeed and engine thrust to maintain the optimum lift coefficient of subsonic cruise. While such a cruise may be necessary to conform to the flow of traffic, it constitutes a certain operational inefficiency. If the airplane were not restrained to a particular altitude, maintaining the same lift coefficient and engine speed would allow the airplane to climb as the gross weight decreases. Since altitude generally produces a beneficial effect on range, the climbing cruise implies a more efficient flight path.

The cruising flight of the jet will begin usually at or above the tropopause in order to provide optimum range conditions. If flight is conducted at $(C_L^{1/2}/C_D)_{max}$, optimum range will be obtained at specific values of lift coefficient and drag coefficient. When the airplane is fixed at these values of C_L and C_D, and V_T is held constant, both lift and drag are directly proportional to the density ratio σ. Also, above the tropopause, the thrust is proportional to σ when V_T and engine speed are constant. Then a reduction of gross weight by the use of fuel would allow the jet to climb but the jet would remain in equilibrium because lift, drag, and thrust all vary in the same fashion.

The relationship of lift, drag, and thrust is convenient since it justified the condition of a constant velocity. Above the tropopause, the speed of sound is constant and a constant velocity during the cruise climb would produce a constant Mach number. In this case, the optimum values of $(C_L^{1/2}/C_D)$, C_L, and C_D do not vary during the climb since the Mach number is constant. The specific fuel consumption is initially constant above the tropopause but begins to increase at altitudes much above the tropopause. If the specific fuel consumption is assumed to be constant during the cruise climb, a 10% decrease in gross weight from the consumption of fuel would create:

1. No change in Mach number or V_T.
2. A 5% decrease in V_e.
3. A 10% decrease in σ (higher altitude).
4. A 10% decrease in fuel flow.
5. An 11% increase in specific range.

4.6.6.1 CRUISE CLIMB AND CONTROL SCHEDULES

The term cruise climb applies to various types of flight programs designed to improve overall maximum range for a given fuel load. The example in this section refers to a flight programmed to maintain a constant M and W/δ.

To determine how a schedule of constant M and W/δ is flown, consider all factors which are constant when M and W/δ are constant. From the lift equation:

$$C_L = \frac{2\,W}{\gamma\,P_a\,M^2\,S} = \frac{2\,\frac{W}{\delta}}{\gamma\,M^2\,S\,P_{ssl}} \qquad \text{(Eq 4.121)}$$

Since γ, P_{ssl}, and S are constant:

$$C_L = f\left(\frac{W}{\delta}, M^2\right) \qquad \text{(Eq 4.122)}$$

If in a cruise climb, W/δ and M are constant then C_L = Constant.

For steady, level flight, neglecting viscosity:

$$\frac{D}{\delta} = f\left(M, \frac{W}{\delta}\right) \qquad \text{(Eq 4.27)}$$

Therefore D/δ must be constant. The ratio of two constants must also be constant so:

$$\frac{\frac{W}{\delta}}{\frac{D}{\delta}} = \frac{W}{D} = \text{Constant} \qquad \text{(Eq 4.123)}$$

Since W = L in steady level flight, L/D = Constant. Neglecting viscosity, for a constant area engine the following parameters are a function of Mach number and W/δ and are therefore constant:

1. $N/\sqrt{\theta}$ constant referred engine speed.
2. T_G/δ constant gross thrust/pressure ratio.
3. P_{T_6}/δ constant exit pressure/pressure ratio.
4. $\dot{W}_f/\delta\sqrt{\theta}$ constant referred fuel flow.

Previously, the specific range parameter was also constant therefore:

$$\frac{661.483\ M}{\left(\dfrac{\dot{W}_f}{\delta\sqrt{\theta}}\right)} = \text{Constant} \tag{Eq 4.124}$$

From Eq 4.48 and the fact that $\dot{W}_f/\delta\sqrt{\theta}$ and T_{N_x}/δ are constant it can be shown that:

$$\frac{TSFC}{\sqrt{\theta}} = \text{Constant} \tag{Eq 4.125}$$

Where:

C_L	Lift coefficient	
D	Drag	lb
δ	Pressure ratio	
γ	Ratio of specific heats	
M	Mach number	
P_a	Ambient pressure	psf
P_{ssl}	Standard sea level pressure	2116.217 psf
θ	Temperature ratio	
S	Wing area	ft^2
TSFC	Thrust specific fuel consumption	$\frac{lb/h}{lb}$
W	Weight	lb
$\dot{W}_f$	Referred fuel flow	lb/h.

The example can continue further but there are very few constant parameters which are easily measured or available to record. The Mach number, α, H_{P_i}, engine speed, fuel remaining, T_G, and T_G/δ can be read from cockpit instruments so a pilot would be able to fly the following type schedules:

1. Constant α and Mach.
2. Constant W/δ and Mach.
3. Constant T_G/δ and Mach.
4. Constant $N/\sqrt{\theta}$ and Mach.
5. Constant T_G and $N/\sqrt{\theta}$ in an isothermal layer.
6. Other variations or combinations of the above.

Flight testing has indicated that schedule 2 produces the best results with the instrumentation available. A slight modification of schedule 4 with schedule 2 was also recommended as suitable. For variable area engines schedule 3 appeared to have the greatest promise.

Increases in cruising ranges of from 5-6% can be realized using cruise climb techniques as compared to level flight procedures. Of the two factors, altitude and Mach, Mach is the most critical and must be maintained on the assigned value.

4.6.7 RANGE DETERMINATION FOR NON-OPTIMUM CRUISE

Various forms of cruise control appear on the referred specific range curve as shown in figure 4.59.

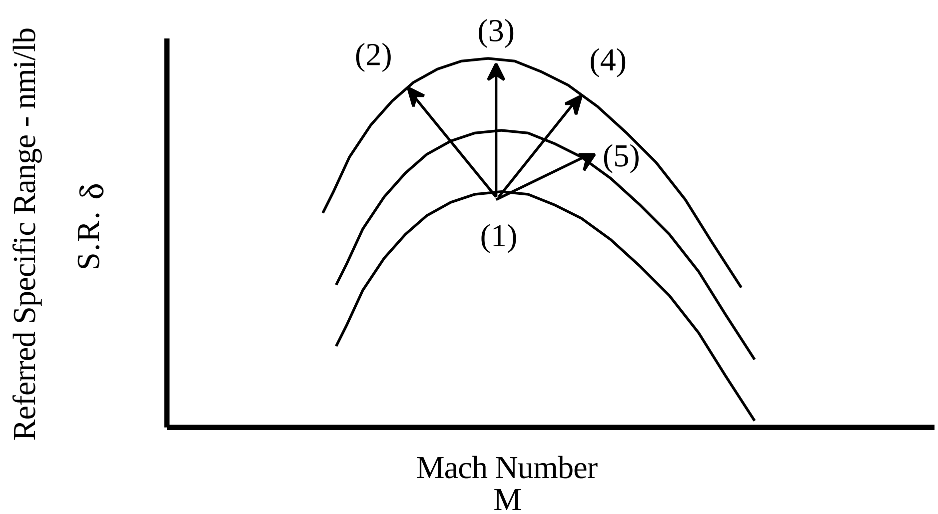

Figure 4.59

CRUISE CONTROL VARIATIONS ON REFERRED SPECIFIC RANGE

Schedule (1) is the cruise climb. The schedule is flown at constant W/δ and M and is characterized by an increase in S.R. and by always remaining at the optimum Mach number. The schedule is a single point on the figure.

Schedule (2) maintains constant altitude and decreases Mach as W/δ decreases to remain on the peaks of the W/δ curves. Mach is always optimum and S.R. increases but not to the same extent as in Schedule (1).

Schedule (3) maintains constant altitude and constant Mach, and as W/δ decreases, the Mach moves away from the optimum. This schedule may not be too far off from schedule (2).

Schedule (4) maintains constant altitude and power setting (either fuel flow or engine speed). A constant altitude W/δ will decrease as W decreases, and at constant power setting, M will increase as W decreases. Mach will not be optimum for max specific range even though S.R. may increase.

Schedule (5) holds constant power setting and calibrated airspeed. As W decreases it will be necessary to climb to maintain constant V_c. Climbing at constant V_c will yield an increase in Mach number which moves the point away from Mach as W/δ decreases. S.R. will increase with decreased W, but the increase will not be as great as the other schedules.

Some of these schedules are simpler than others to use. For example, it is easier to fly constant altitude and power setting than to climb at constant M and W/δ. However, experience has proven that savings in fuel or increase in range can be attained by executing an optimum climb covered in Chapter 7.

Regardless of the method of cruise control, the range is calculated by solving Eq 4.115.

$$\text{Range} = \int_{W_1}^{W_2} (\text{S.R. } \delta) \left(\frac{W}{\delta}\right) \frac{1}{W} \, dW \tag{Eq 4.115}$$

Since range factor was defined as:

$$\text{R.F.} = \left[(\text{S.R.}\ \delta) \frac{W}{\delta} \right] \qquad \text{(Eq 4.118)}$$

and Eq 4.118 resulted in an analytical solution to the range equation for a schedule (1) cruise for constant R.F.:

$$\text{Range} = \text{R.F.} \ln \frac{W_1}{W_2} \qquad \text{(Eq 4.126)}$$

Non optimum solutions can be obtained from a graphical solution to Eq 4.114.

$$\text{Range} = \int_{W_1}^{W2} (\text{S.R.})\, dW \qquad \text{(Eq 4.114)}$$

Where:

δ	Pressure ratio	
R.F.	Range factor	
S.R.	Specific range	nmi/lb
W	Weight	lb.

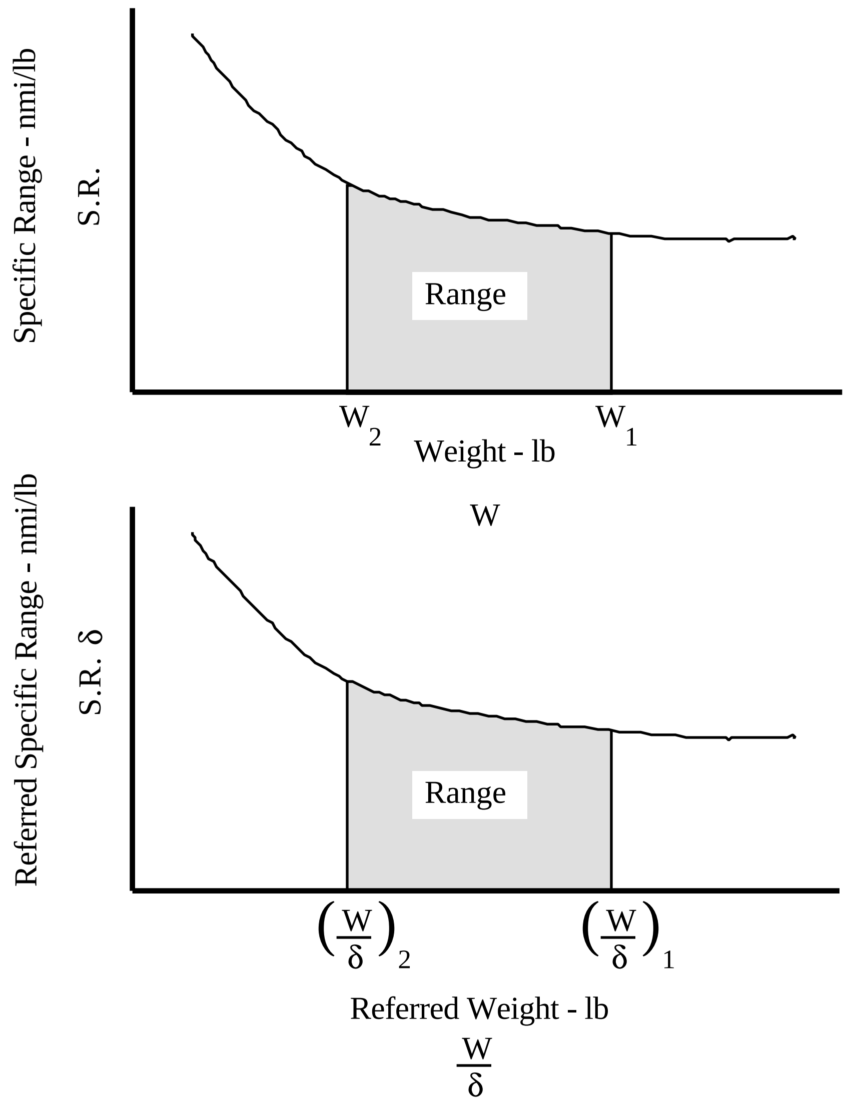

Figure 4.60
ACTUAL RANGE FROM NON OPTIMUM CRUISE

The shaded area in each of the curves of figure 4.60 represent the same thing. Both show the actual range. The problem can be solved from the referred data. Using schedule (2) or (3), the relationship of ((S.R.(δ)) and (W/δ) can be plotted as the fuel is burned (decreasing W/δ). The results would appear as in figure 4.61 and can be graphically integrated to get the range for various cruise schedules. Non-optimum cruise and the cruise climb can be compared to determine if the aircraft under test has any realistic benefit from the cruise climb.

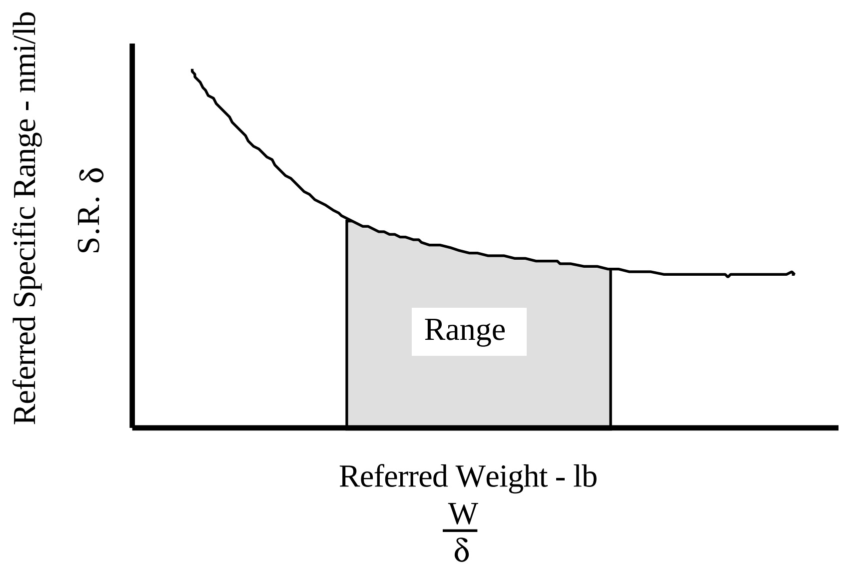

Figure 4.61
RANGE FOR VARIOUS CRUISE SCHEDULES

4.6.8 TURBOPROP RANGE AND ENDURANCE

Unreferring the data presented in section 4.5.4 allows the calculation of actual range and endurance for specified conditions. Input GW, altitude of interest and ambient temperature to the computer program. Curves of SHP, fuel flow, and specific range as functions of calibrated airspeed (V_c) can be produced. Combined curves for a series of set conditions define the range and endurance over the entire aircraft operating envelope. Typical unreferred curves are shown in figures 4.62, 4.63, and 4.64.

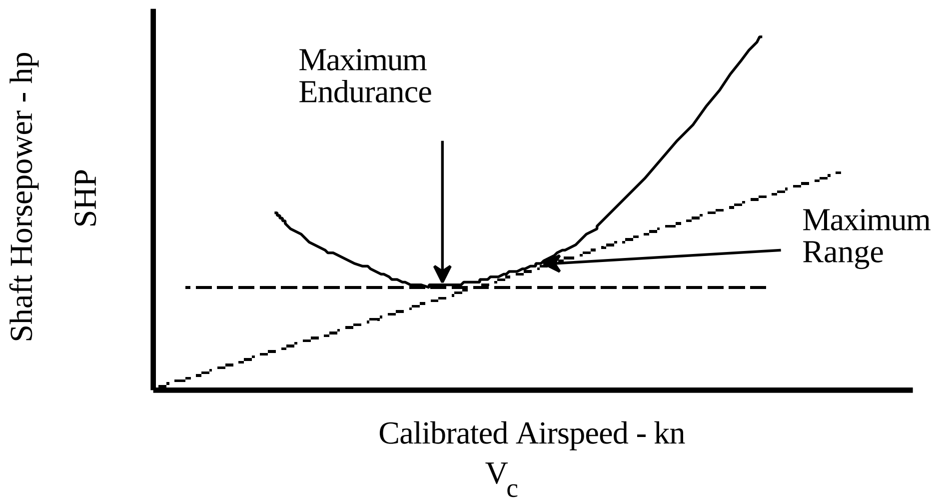

Figure 4.62

POWER REQUIRED

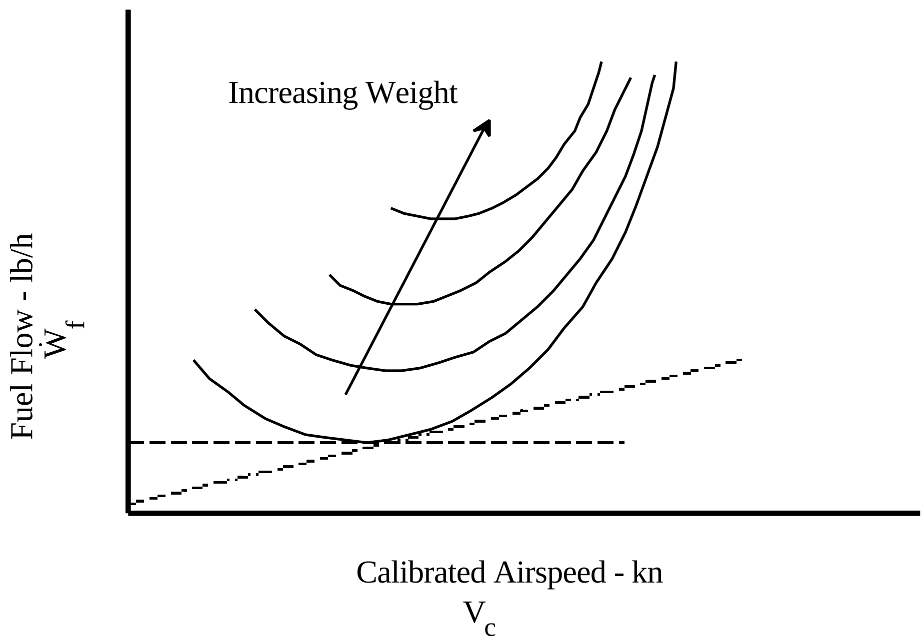

Figure 4.63

FUEL CONSUMPTION

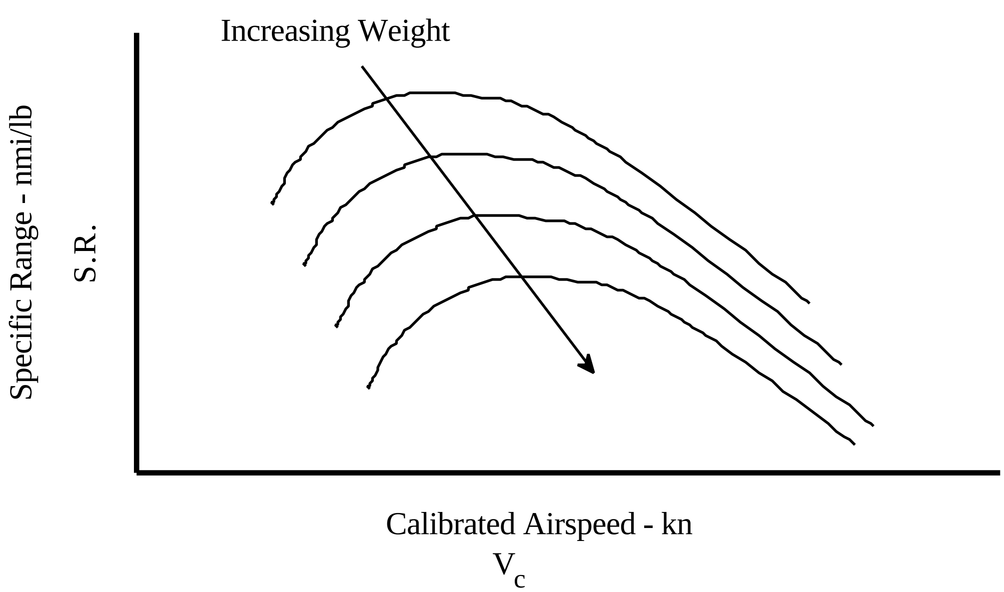

Figure 4.64

SPECIFIC RANGE

From these curves, range and endurance profiles can be determined as a function of fuel used for representative mission altitudes and ambient conditions expected.

4.6.8.1 MAXIMUM VALUES

Maximum values can be determined for a given set of conditions from the unreferred plots as follows:

1.	Maximum endurance	Specified at given ˚C, ΔT_a
		Fuel flow in lb/h
		Velocity for maximum endurance
		Maximum endurance in hours
2.	Maximum range	Specific range in nmi/lb
		Velocity for maximum range
		Maximum range in nmi

4.6.8.2 WIND EFFECTS

The effect of wind on range of the turboprop aircraft may be even more important than for the turbojet due to the lower airspeed. A head wind reduces range and a tail wind increases range. Specific range for no wind was $\frac{V_T}{\dot{W}_f}$. For a head wind or tail wind ground speed for the fuel flow needs to be maximized $\frac{GS}{\dot{W}_f}$. The variation with speed to maximize specific range in the presence of wind is similar to that shown for the turbojet in figure 4.48.

4.6.8.3 PROPELLER EFFICIENCY

The turbine of a turboprop is designed to absorb large amounts of energy from the expanding combustion gases in order to provide not only the power required to satisfy the compressor and other components of the engine, but to deliver the maximum torque possible to a propeller shaft as well. Propulsion is produced through the combined action of a propeller at the front and the thrust produced by the unbalanced forces created within the engine that result in the discharge of high-velocity gases through a nozzle at the rear. The propeller of a typical turboprop is responsible for roughly 90% of the total thrust under sea level, static conditions on a standard day. This percentage varies with airspeed, exhaust nozzle area and, to some degree temperature, barometric pressure and the power rating of the engine.

Section 4.6.7 assumes constant propeller efficiency. Test results would need to be spot checked at various conditions of weight and altitude to confirm results. If follow-on results show significant differences in propeller efficiency, a computer iteration with the additional results could determine the actual performance. In this case a combination test may have to be performed. W/δ type tests would be appropriate.

4.7 MISSION SUITABILITY

The mission requirements are the ultimate standard for level flight performance. Obviously, the requirements of a trainer, fighter or attack aircraft vary. Optimum range and endurance profiles are not feasible for every mission phase. However, the level flight performance must satisfy mission requirements. Often, aircraft roles change as they mature or the threat is changed. With this in mind, the level flight performance capability would ideally be greater than the procuring agency originally set as the goals. Level flight performance is only a part of the overall performance and the suitability of the aircraft for a particular role also depends on takeoff, excess energy, maneuvering, climb, descent, and landing performance.

The specifications set desired numbers the procuring agency is expecting of the final product. These specifications are important as measures for contract performance. They are important in determining whether or not to continue the acquisition process at various stages of aircraft development.

Mission suitability conclusions concerning level flight performance are not restricted to optimum performance test results and specification conformance. Test results reflect the performance capabilities of the aircraft, while mission suitability conclusions include the flying qualities associated with specific airspeeds and shipboard operations. Consideration of the following items is worthwhile when recommending airspeeds for maximum endurance and range:

1. Flight path stability.
2. Pitch attitude.
3. Field of view.
4. IFR/VFR holding.
5. Mission profile or requirements.
6. Overall performance including level flight.
7. Compatibility of airspeeds / altitudes with the mission and location restrictions.
8. Performance sensitivities for altitude or airspeed deviations.

4.8 SPECIFICATION COMPLIANCE

Level flight performance guarantees are stated in the detailed specification for the model and in Naval Air Systems Command Specification, AS-5263. The detail specification provides mission profiles to be expected and performance guarantees generically as follows:

1. Mission requirements.
    a. Land or sea based.
    b. Ferry capable.
    c. Instrument departure, transit, and recovery.
    d. Type of air combat maneuvering.
    e. Air to air combat (offensive and/or defensive) including weapons deployment.
    f. Low level navigation.
    g. Carrier suitability.

2. Performance guarantees are based on: type of day (ICAO standard atmosphere), empty gross weight, standard gross weight, drag index, fuel quantity and type at engine start, engine(s) type, loading, and configuration. Guarantees would likely include:
    a. Maximum Mach number specified in level flight at a specified gross weight and power setting at prescribed altitude.
    b. Maximum range at optimum cruise altitude, at specified Mach. Range specified as not less than, given the fuel allowed for start, taxi, maximum or military thrust take off to climb speed, power to be used in climb to optimum altitude, and fuel reserve requirements.
    c. Maximum specific range in nautical miles per pound of fuel at a prescribed altitude at standard gross weight.
    d. Maximum endurance fuel flow in pounds per hour at prescribed gross weight and airspeeds at given altitudes.

AS-5263 further defines requirements for, and methods of, presenting characteristics and performance data for U.S. Navy piloted aircraft. Deviations from this specification are permissible, but in all cases must be approved by the procuring activity. Generally level flight performance guarantees are stated for standard day conditions and mission or takeoff gross weight. The specification gives some general guidelines to performance guarantees. It states the following about level flight:

1. All speeds are in knots true airspeed unless otherwise noted.
2. Maximum speed is the highest speed obtainable in level flight. The maximum speed shall be within all operating restrictions.

3. Combat speed is the highest speed obtainable in level flight at combat weight with maximum power at combat altitude.

4. Average cruise speed is determined by dividing the total cruise distance by the time for cruise not including time and distance to climb.

5. Speed at specified altitude is the highest speed obtainable within all operating restrictions in level flight at combat weight and stated power. Except for interceptors, the altitude at which this speed is quoted shall not exceed either combat or cruise ceilings. For interceptors the altitude shall not exceed combat ceiling.

6. Airspeed for long range operation is the greater of the two speeds at which 99 percent of the maximum miles per pound of fuel are attainable at the momentary weight and altitude.

7. Airspeed for maximum endurance operation is the airspeed for minimum fuel flow attainable at momentary weight and altitude except as limited by acceptable handling characteristics of the aircraft.

8. Fuel consumption data shall be increased by 5% for all engine power conditions as a service tolerance to allow for practicable operation. Additionally, corrections or allowances shall be made for power plant installation losses such as accessory drives, ducts, fans, cabin pressure bleeds, tail-pipes, afterburners, ram-pressure recovery, etc.

9. Combat radius is the distance attainable on a practicable flight to the target and return a distance equal to that flown out carrying a specific load.

10. Combat range is the distance (including climb distance) attainable on a practicable one way flight carrying a specific load.

4.9 GLOSSARY

4.9.1 NOTATIONS

550	Conversion factor	$550 \frac{\text{ft-lb}}{\text{s}} = 1$ horsepower
AR	Aspect ratio	
a_{ssl}	Standard sea level speed of sound	661.483 kn
BHP	Brake horsepower	hp
C_D	Drag coefficient	
C_{D_i}	Induced drag coefficient	

C_{D_M}	Mach drag coefficient	
C_{D_p}	Parasite drag coefficient	
$C_{D_{p\,(M)}}$	Parasite drag coefficient at high Mach	
C_L	Lift coefficient	
D	Drag	lb
$\Delta H_{P_{ic}}$	Altimeter instrument correction	ft
ΔH_{pos}	Altimeter position error	ft
D_i	Induced drag	lb
D_M	Mach drag	lb
D_p	Parasite drag	lb
ΔT_a	Temperature differential	
ΔT_{ic}	Temperature instrument correction	˚C
Δt_j	Time of each time interval	s
ΔV_{ic}	Airspeed instrument correction	kn
ΔV_{pos}	Airspeed position error	kn
e	Oswald’s efficiency factor	
$e_{(M)}$	Oswald’s efficiency factor at high Mach	
EGT	Exhaust gas temperature	˚C
EPR	Engine pressure ratio	
F/C	Fuel counter	lb
GS	Ground speed	kn
H_P	Pressure altitude	ft
H_{P_c}	Calibrated pressure altitude	ft
H_{P_i}	Indicated altitude	ft
H_{P_o}	Observed pressure altitude	ft
ICAO	International Civil Aeronautics Organization	
J	Propeller advance ratio	
K	Constant	
K_1	Parasite drag constant	
K_2	Induced drag constant	
K_3	Constant	
K_4	Constant	
K_o	Constant	
K_T	Temperature recovery factor	
L	Lift	lb
M	Mach number	

M_{max}	Mach number at maximum thrust	
M_{mrt}	Mach number at military rated thrust	
M_o	Observed Mach number	
MSL	Mean sea level	
N	Engine speed	RPM
n	Number of time intervals	
nmi	Nautical miles	
$\frac{N}{\sqrt{\theta}}$	Referred engine speed	RPM
OAT	Outside air temperature	˚C or ˚K
P	Pressure	psf
P_a	Ambient pressure	psf
P_{ssl}	Standard sea level pressure	2116.217 psf
P_T	Total pressure	psf
q	Dynamic pressure	psf
R.F.	Range factor	
$R.F._{Test}$	Test day average range factor	
R_e	Reynold's number	
R_{Std}	Standard day cruise range	nmi
R_T	Total range	nmi
R_{Test}	Test cruise range	nmi
S	Wing area	ft^2
S.E.	Specific endurance	h/lb
S.R.	Specific range	nmi/lb
SHP	Shaft horsepower	hp
SHP_e	Equivalent shaft horsepower	hp
SHPSFC	Shaft horsepower specific fuel consumption	$\frac{lb/h}{hp}$
T	Thrust	lb
t	Time	s
T_a	Ambient temperature	˚C or ˚K
$T_{a_{Std}}$	Standard ambient temperature	˚K
T_G	Gross thrust	lb
THP	Thrust horsepower	hp
THP_e	Equivalent thrust horsepower	hp
THP_i	Induced thrust horsepower	Hp

THP_{min}	Minimum thrust horsepower	hp
THP_p	Parasite thrust horsepower	hp
THPSFC	Thrust horsepower specific fuel consumption	$\frac{lb/h}{hp}$
Time	Time at the start of each segment	s
T_{N_x}	Net thrust parallel flight path	lb
$\frac{T_{N_x}}{\delta}$	Referred net thrust parallel flight path	lb
T_o	Observed temperature	˚C
T_R	Ram drag	lb
TSFC	Thrust specific fuel consumption	$\frac{lb/h}{lb}$
T_{ssl}	Standard seal level temperature	15˚C, 288.15˚K
T_T	Total temperature	˚K
t_T	Total cruise time	s
T_{T_2}	Inlet total temperature (at engine compressor face)	˚K
V	Velocity	kn
V_c	Calibrated airspeed	kn
V_e	Equivalent airspeed	kn
V_H	Maximum level flight airspeed	kn
V_i	Indicated airspeed	kn
Vj	Avg true airspeed in time interval	kn
V_{max}	Maximum airspeed	kn
V_{min}	Minimum airspeed	kn
V_o	Observed airspeed	kn
V_T	True airspeed	kn
V_v	Vertical velocity	fpm
W	Weight	lb
W/δ	Weight to pressure ratio	lb
W_1	Initial cruise weight	lb
W_2	Final cruise weight	lb
$W_{aircraft}$	Aircraft weight	lb
W_f	Fuel weight	lb
$W_{f_{Used}}$	Fuel used	lb
$\dot{W}_f$	Fuel flow	lb/h

$\dot{W}_{f\ ref}$	Referred fuel flow	lb/h
W_{ref}	Referred aircraft weight	lb
W_{Std_1}	Standard initial cruise weight	lb
W_{Std_2}	Standard final cruise weight	lb
¢	Constant	

4.9.2 GREEK SYMBOLS

α (alpha)	Angle of attack	deg
α_i	Induced angle of attack	deg
α_j	Thrust angle	deg
δ (delta)	Pressure ratio	
γ (gamma)	Ratio of specific heats	
η_P (eta)	Propeller efficiency	
μ (mu)	Viscosity	lb-s/ft^2
π (pi)	Constant	
θ (theta)	Temperature ratio	
θ_T	Total temperature ratio	
ρ (rho)	Air density	slugs/ft^3
ρ_a	Ambient air density	slugs/ft^3
ρ_{ssl}	Standard sea level air density	0.0023769 slugs/ft^3
σ (sigma)	Density ratio	

4.10 REFERENCES

1. Department of the Army, *Operator's Manual for Army U-21A Aircraft*, TM 555-1510-209-10, Headquarters Department of the Army, Washington D.C., 26 September 1988.

2. Naval Air System Command Specification, *Guidelines For Preparation Of Standard Aircraft Characteristics Charts And Performance Data Piloted Aircraft (Fixed Wing)*, *AS-5263*, 23 October, 1986.

3. Naval Test Pilot School Flight Test Manual, *Fixed Wing Performance, Theory and Flight Test Techniques,* USNTPS-FTM-No.104, U.S. Naval Test Pilot School, Patuxent River, MD, July 1977.

4. Powell, J.W., *Airplane Performance*, *Fixed Wing Flight Mechanics*, USNTPS Class Notes, USNTPS, Patuxent River, MD., no date.

5. Roberts, S.C., *Light Aircraft Performance for Test Pilots and Flight Test Engineers*, Flight Research, Inc, Mojave, CA., 9 July 1982.

6. USAF Test Pilot School Flight Test Manual, *Performance Flight Testing Phase*, Volume I, Chapter 11, USAF Test Pilot School, Edwards AFB, CA, February 1987.

7. USAF Test Pilot School, *Performance Phase Textbook Volume I*, USAF TPS-CUR-86-01, USAF, Edwards AFB, CA, April, 1986.

8. USAF Test Pilot School, *Performance Planning Guide*, USAF Test Pilot School, Edwards AFB, CA.,July 1987.

CHAPTER 5

EXCESS POWER CHARACTERISTICS

CHAPTER 5

FIGURES

CHAPTER 5

EQUATIONS

Equation		PAGE
$TE = PE + KE$	(Eq 5.1)	5.2
$PE = \int_o^h W\, dh$	(Eq 5.2)	5.2
$PE = W \left(H_{P_c} + \Delta T \text{ correction} \right)$	(Eq 5.3)	5.2
$KE = \frac{1}{2} \frac{W}{g} V_T^2$	(Eq 5.4)	5.3
$TE = W\, h + \frac{1}{2} \frac{W}{g} V_T^2$	(Eq 5.5)	5.3
$\frac{TE}{W} = h + \frac{V_T^2}{2\, g}$	(Eq 5.6)	5.3
$E_h = h + \frac{V_T^2}{2\, g}$	(Eq 5.7)	5.3
$\frac{d}{dt} E_h = \frac{d}{dt} \left(h + \frac{V_T^2}{2\, g} \right)$	(Eq 5.8)	5.7
$\frac{d}{dt} E_h = \frac{dh}{dt} + \frac{V_T}{g} \frac{dV_T}{dt}$	(Eq 5.9)	5.7
$\sum F_x = \frac{W}{g} \frac{dV_T}{dt}$	(Eq 5.10)	5.8
$T_{N_x} = T_G \cos \alpha_j - T_R$	(Eq 5.11)	5.8
$T_{N_x} - D - W \sin \gamma = \frac{W}{g} \frac{dV_T}{dt}$	(Eq 5.12)	5.8

$$\sin\gamma = \frac{V_T \text{ (vertical)}}{V_T \text{ (flight path)}} = \frac{\frac{dh}{dt}}{V_T}$$ (Eq 5.13) 5.9

$$T_{N_x} - D - W\frac{dh}{dt}\frac{1}{V_T} = \frac{W}{g}\frac{dV_T}{dt}$$ (Eq 5.14) 5.9

$$\frac{V_T\left(T_{N_x} - D\right)}{W} - \frac{dh}{dt} = \frac{V_T}{g}\frac{dV_T}{dt}$$ (Eq 5.15) 5.9

$$\frac{V_T\left(T_{N_x} - D\right)}{W} = \frac{dE_h}{dt}$$ (Eq 5.16) 5.9

$$P_s = \frac{V_T\left(T_{N_x} - D\right)}{W}$$ (Eq 5.17) 5.9

$$P_s = \frac{dE_h}{dt}$$ (Eq 5.18) 5.10

$$P_s = \frac{dh}{dt} + \frac{V_T}{g}\frac{dV_T}{dt}$$ (Eq 5.19) 5.10

$$P_s = \frac{V_T\left(T_{N_x} - D - \Delta D_i\right)}{W}$$ (Eq 5.20) 5.13

$$P_s = \frac{V_T\left(T_{N_x} - D - \Delta D_i\right)}{W + \Delta W}$$ (Eq 5.21) 5.15

$$P_s = \frac{V_T\left(T_{N_x} - D - \Delta D_p\right)}{W}$$ (Eq 5.22) 5.16

$$P_s = \frac{V_T\,(T_{N_x} + \Delta T_{N_x} - D)}{W}$$ (Eq 5.23) 5.17

$$P_s = \frac{\left(P_A - \Delta P_A\right) - \left(P_{req} + \Delta P_{req}\right)}{W}$$ (Eq 5.24) 5.19

$$q_c = P_{ssl} \left\{ \left[1 + 0.2 \left(\frac{V_c}{a_{ssl}} \right)^2 \right]^{3.5} - 1 \right\}$$ (Eq 5.25) 5.28

$$P_a = P_{ssl} \left(1 - 6.8755856 \times 10^{-6} H_{P_c} \right)^{5.255863}$$ (Eq 5.26) 5.28

$$M = \sqrt{ \frac{2}{\gamma - 1} \left[\left(\frac{q_c}{P_a} + 1 \right)^{\frac{\gamma - 1}{\gamma}} - 1 \right] }$$ (Eq 5.27) 5.28

$$T_a = \frac{OAT + 273.15}{1 + \frac{\gamma - 1}{2} K_T M^2}$$ (Eq 5.28) 5.28

$$h = H_{P_c} \frac{T_{a_{Test}}}{T_{a_{Std}}}$$ (Eq 5.29) 5.28

$$V_T = M \sqrt{\gamma g_c R T_a}$$ (Eq 5.30) 5.28

$$\frac{W_{Test}}{W_{Std}}$$ (Eq 5.31) 5.31

$$\frac{V_{T_{Std}}}{V_{T_{Test}}} = \frac{M_{Std} \sqrt{\theta_{Std}}}{M_{Test} \sqrt{\theta_{Test}}}$$ (Eq 5.32) 5.32

$$\frac{V_{T_{Std}}}{V_{T_{Test}}} = \sqrt{\frac{T_{a_{Std}}}{T_{a_{Test}}}}$$ (Eq 5.33) 5.32

$$\Delta T = f \left(T_a \right)$$ (Eq 5.34) 5.32

$$\Delta D = D_{Std} - D_{Test} = \frac{2 \left(W_{Std}^2 - W_{Test}^2 \right)}{\pi \, e \, AR \, S \, \gamma \, P_a \, M^2}$$ (Eq 5.35) 5.32

$P_{s_{Std}} = P_{s_{Test}} \frac{W_{Test}}{W_{Std}} \sqrt{\frac{T_{a_{Std}}}{T_{a_{Test}}}} + \frac{V_{T_{Std}}}{W_{Std}} (\Delta T_{N_x} - \Delta D)$	(Eq 5.36)	5.32
$V_c = V_i + \Delta V_{pos}$	(Eq 5.37)	5.36
$H_{P_c} = H_{P_i} + \Delta H_{pos}$	(Eq 5.38)	5.36
$M = f\left(V_c , H_{P_c}\right)$	(Eq 5.39)	5.37
$W_{Test} = \text{Initial } W - \int \dot{W}_f \; dt$	(Eq 5.40)	5.37
$°C = °K - 273.15$	(Eq 5.41)	5.37
$OAT = f\left(T_a , M_T\right)$	(Eq 5.42)	5.37
$T_a = f\left(OAT, M \right)$	(Eq 5.43)	5.37
$V_{T_{Test}} = f\left(V_c , H_{P_c} , T_a\right)$	(Eq 5.44)	5.37
$V_{T_{Std}} = f\left(V_c, H_{p_c}, T_{Std}\right)$	(Eq 5.45)	5.37
$h = H_{P_{c_{ref}}} + \Delta H_{P_c} \left(\frac{T_a}{T_{Std}}\right)$	(Eq 5.46)	5.37
$E_h = h + \frac{V_{T_{Test}}^2}{2g}$	(Eq 5.47)	5.38
$P_{s_{Test}} = \frac{dE_h}{dt}$	(Eq 5.48)	5.38
$\gamma_{Test} = \sin^{-1}\left(\frac{dh/dt}{V_{T_{Test}}}\right)$	(Eq 5.49)	5.38

$$CCF = 1 + \left(\frac{V_{T_{Std}}}{g}\frac{dV}{dh}\right)$$ (Eq 5.50) 5.38

$$P_{s_{Std}} = P_{s_{Test}}\left(\frac{W_{Test}}{W_{Std}}\right)\left(\frac{V_{T_{Std}}}{V_{T_{Test}}}\right) + \left(\frac{V_{T_{Std}}}{W_{Std}}\right)(\Delta T_{N_x} - \Delta D)$$ (Eq 5.51) 5.38

$$\left(\frac{dh}{dt}\right)_{Std} = \frac{P_{s_{Std}}}{CCF}$$ (Eq 5.52) 5.38

$$\gamma_{Std} = \sin^{-1}\left(\frac{\left(\frac{dh}{dt}\right)_{Std}}{V_{T_{Std}}}\right)$$ (Eq 5.53) 5.39

$$\left|\gamma_{Test} - \gamma_{Std}\right| < 0.1$$ (Eq 5.54) 5.39

CHAPTER 5

EXCESS POWER CHARACTERISTICS

5.1 INTRODUCTION

This chapter deals with determining excess power characteristics using the total energy approach. Test techniques commonly used are presented with the associated methods of data reduction and analysis.

5.2 PURPOSE OF TEST

The purpose of these tests is to determine the aircraft excess power characteristics, with the following objectives:

1. Derive climb schedules to optimize time to height, energy gain, or to minimize fuel consumption (Chapter 7).
2. Predict sustained turn performance envelopes (Chapter 6).
3. Define mission suitability and enable operational comparisons to be made among different aircraft.

5.3 THEORY

Formerly, climb performance and level acceleration were treated as separate and distinct performance parameters, each with their own unique flight test requirements, data reduction, and analysis. In the 1950's it was realized climb performance and level acceleration were really different aspects of the same characteristic, and aircraft performance is based on “the balance that must exist between the kinetic and potential energy exchange of the aircraft, the energy dissipated against the drag, and the energy derived from the fuel” (Reference 1, pp 187-195). Excess power characteristics are tested and analyzed efficiently using the total energy concept rather than treating climbs and accelerations as separate entities.

5.3.1 TOTAL ENERGY

The total energy possessed by an aircraft inflight is the sum of its potential energy (energy of position) and its kinetic energy (energy of motion) and is expressed as:

$$TE = PE + KE \qquad \text{(Eq 5.1)}$$

Where:

KE	Kinetic energy	ft-lb
PE	Potential energy	ft-lb
TE	Total energy	ft-lb.

5.3.1.1 POTENTIAL ENERGY

Potential energy (PE) is the energy a body possesses by virtue of its displacement against a field from a reference energy level. The reference energy level is usually the lowest available; although, sometimes only a local minimum. An aircraft inflight is displaced against the earth’s gravitational field from a reference level, which is usually chosen as sea level. The aircraft's potential energy is equal to the work done in raising it to the displaced level, expressed as:

$$PE = \int_{o}^{h} W\, dh \qquad \text{(Eq 5.2)}$$

In terms of measurable flight test quantities, Eq 5.2 can be expressed as:

$$PE = W\left(H_{P_c} + \Delta T \text{ correction}\right) \qquad \text{(Eq 5.3)}$$

Where:

h	Tapeline altitude	ft
H_{P_c}	Calibrated pressure altitude	ft
PE	Potential energy	ft-lb
T	Temperature	˚C or ˚K
W	Weight	lb.

5.3.1.2 KINETIC ENERGY

The kinetic energy (KE) or translational energy along the flight path is expressed as:

$$KE = \frac{1}{2}\frac{W}{g}V_T^2 \qquad \text{(Eq 5.4)}$$

Where:

g	Gravitational acceleration	ft/s^2
KE	Kinetic energy	ft-lb
V_T	True airspeed	ft/s
W	Weight	lb.

5.3.2 SPECIFIC ENERGY

Using Eq 5.3 and 5.4, total energy (TE) can be expressed as:

$$TE = W\,h + \frac{1}{2}\frac{W}{g}V_T^2 \qquad \text{(Eq 5.5)}$$

Using standard American engineering units (velocity in ft/s, weight in lb, acceleration in ft/s^2), energy has units of ft-lb. To generalize the analysis and eliminate dependence on aircraft weight, Eq 5.5 is normalized by dividing by weight:

$$\frac{TE}{W} = h + \frac{V_T^2}{2\,g} \qquad \text{(Eq 5.6)}$$

Eq 5.6 is the specific energy state equation, and has units of feet. The aircraft's specific energy, or energy per unit weight, can be defined in terms of energy height (E_h):

$$E_h = h + \frac{V_T^2}{2\,g} \qquad \text{(Eq 5.7)}$$

Where:

E_h	Energy height	ft
g	Gravitational acceleration	ft/s^2
h	Tapeline altitude	ft
TE	Total energy	ft-lb
V_T	True airspeed	ft/s
W	Weight	lb.

Energy height is not an altitude, rather the sum of the aircraft's specific potential and kinetic energies. It represents the altitude which the aircraft theoretically would be capable of reaching in a zoom climb, if its kinetic energy were perfectly convertible to potential energy without loss of any kind, and if it arrived at that altitude at zero airspeed.

Energy paper, consisting of lines of constant E_h superposed on a height-velocity plot, is used commonly for analysis. The units on the horizontal axis may be either true airspeed or Mach number. The shape of the lines of constant E_h are parabolic for a true airspeed plot but not for a Mach number plot, because of the temperature dependent relationship between Mach number and true airspeed below the tropopause. Some examples of energy paper are shown in figures 5.1 and 5.2.

Figure 5.1

ENERGY HEIGHT VERSUS TRUE AIRSPEED

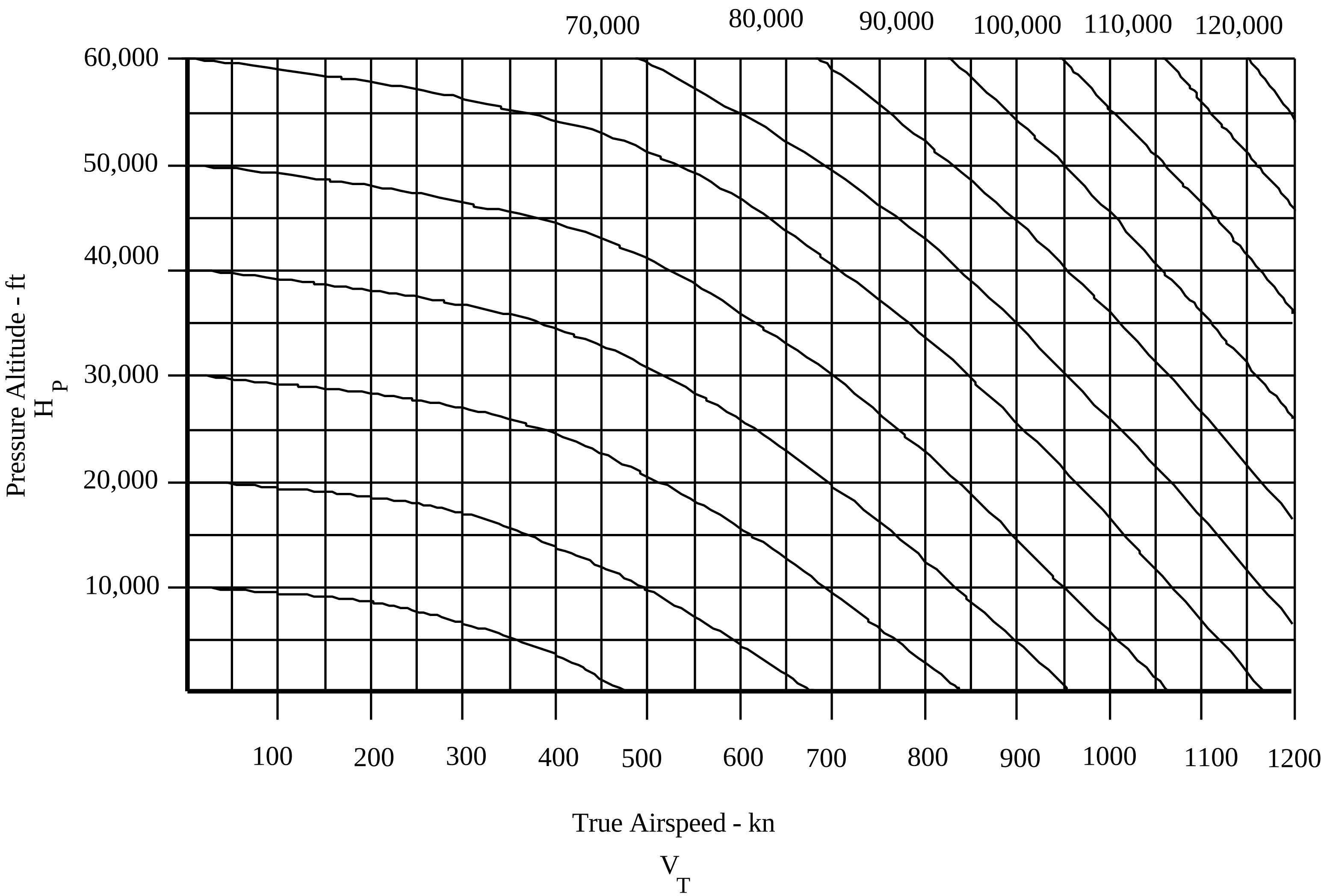

EXCESS POWER CHARACTERISTICS

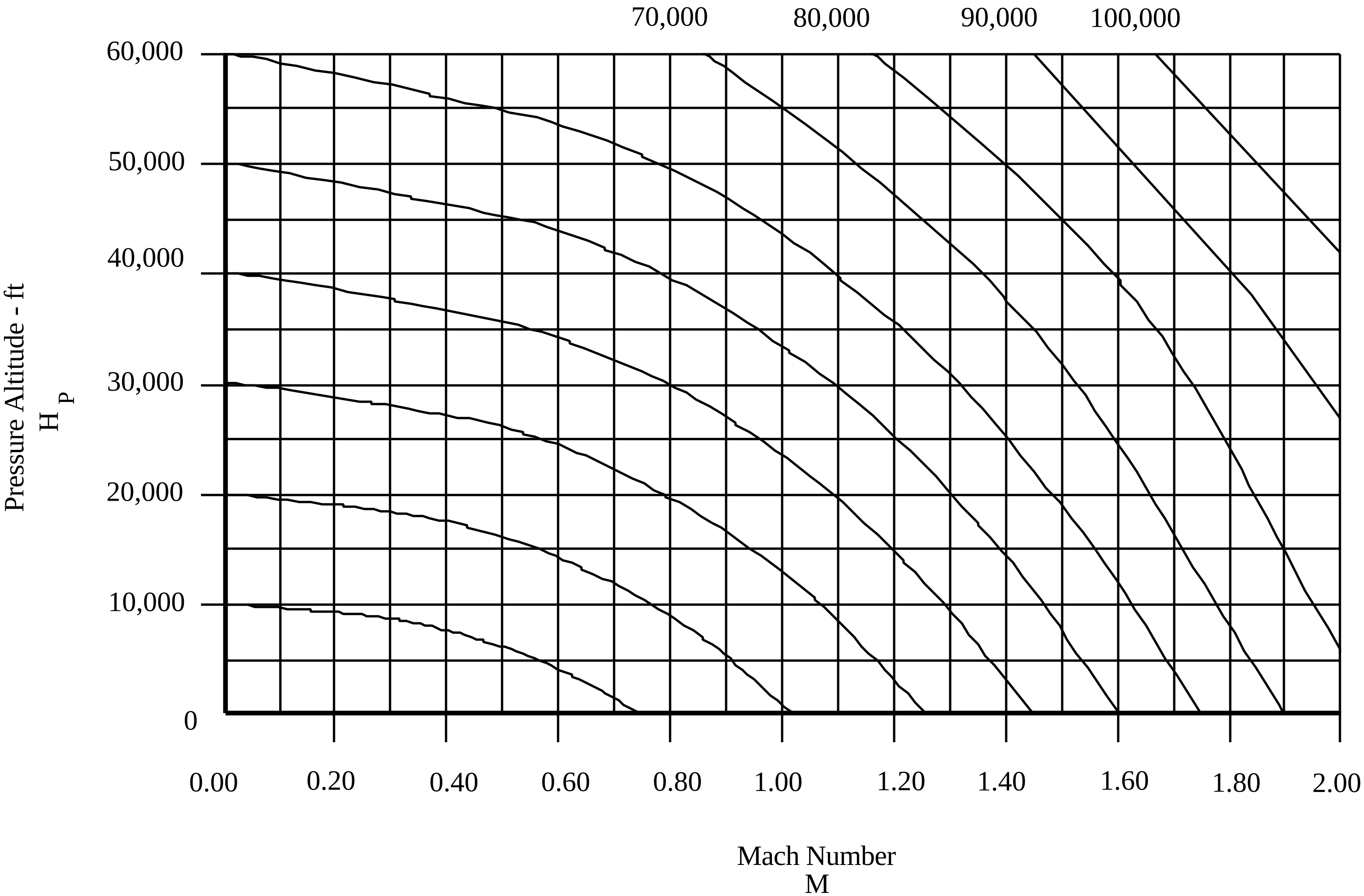

Figure 5.2
ENERGY HEIGHT VERSUS MACH NUMBER

5.3.3 SPECIFIC POWER

Power is defined as the rate of doing work, or the time rate of energy change. The specific power of an aircraft is obtained by taking the time derivative of the specific energy equation, Eq 5.7, which becomes:

$$\frac{d}{dt} E_h = \frac{d}{dt}\left(h + \frac{V_T^2}{2\,g}\right) \tag{Eq 5.8}$$

Or:

$$\frac{d}{dt} E_h = \frac{dh}{dt} + \frac{V_T}{g}\frac{dV_T}{dt} \tag{Eq 5.9}$$

Where:

E_h	Energy height	ft
g	Gravitational acceleration	ft/s^2
h	Tapeline altitude	ft
t	Time	s
V_T	True airspeed	ft/s.

The units are now ft/s, which does not denote a velocity but rather the specific energy rate in $\frac{\text{ft-lb}}{\text{lb-s}}$. Eq 5.9 contains terms for both rate of climb and flight path acceleration.

5.3.4 DERIVATION OF SPECIFIC EXCESS POWER

Consider an aircraft accelerating in a climbing left turn as shown in figure 5.3.

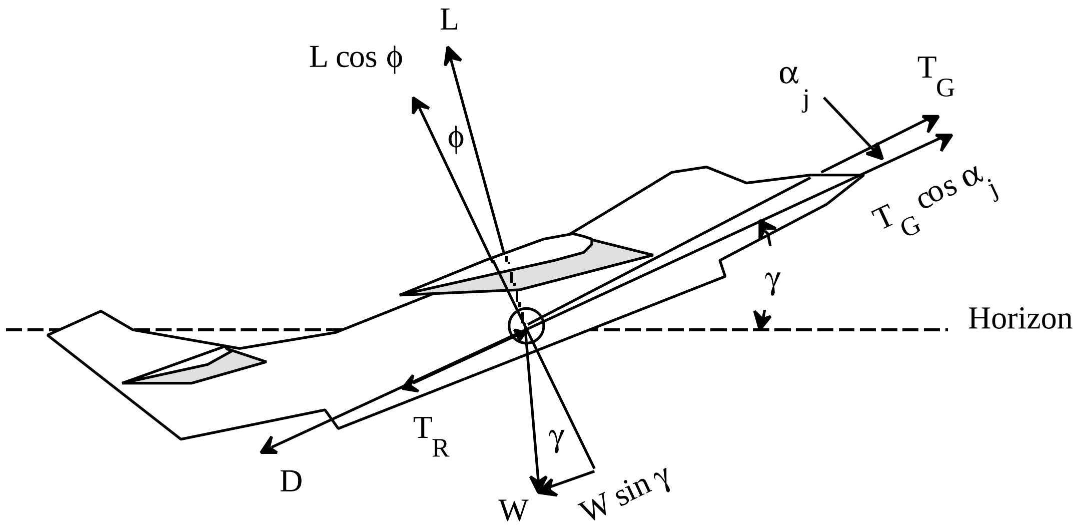

Figure 5.3

AIRCRAFT ACCELERATING IN CLIMBING LEFT TURN

Assuming constant mass ($\frac{V}{g}\frac{dW}{dt} = 0$), the forces parallel to flight path (F_x) are resolved as:

$$\sum F_x = \frac{W}{g}\frac{dV_T}{dt} \qquad \text{(Eq 5.10)}$$

Expanding the left hand side and noting the lift forces, L and L cos ϕ, act perpendicular to the flight path there is no component along the flight path:

$$T_{N_x} = T_G \cos \alpha_j - T_R \qquad \text{(Eq 5.11)}$$

$$T_{N_x} - D - W \sin\gamma = \frac{W}{g}\frac{dV_T}{dt} \qquad \text{(Eq 5.12)}$$

The flight path angle (γ) can be expressed in terms of the true vertical and true flight path velocities:

$$\sin \gamma = \frac{V_T \text{ (vertical)}}{V_T \text{ (flight path)}} = \frac{\frac{dh}{dt}}{V_T} \qquad \text{(Eq 5.13)}$$

Assuming the angle between the thrust vector and the flight path (α_j) is small (a good assumption for non-vectored thrust), then $\cos \alpha_j \approx 1$.

Substituting these results in Eq 5.12 yields:

$$T_{N_x} - D - W \frac{dh}{dt} \frac{1}{V_T} = \frac{W}{g} \frac{dV_T}{dt} \qquad \text{(Eq 5.14)}$$

Eq 5.14, normalized by dividing throughout by the aircraft weight, multiplied throughout by the true airspeed, and rearranged produces:

$$\frac{V_T \left(T_{N_x} - D\right)}{W} - \frac{dh}{dt} = \frac{V_T}{g} \frac{dV_T}{dt} \qquad \text{(Eq 5.15)}$$

From Eq 5.9:

$$\frac{V_T \left(T_{N_x} - D\right)}{W} = \frac{dE_h}{dt} \qquad \text{(Eq 5.16)}$$

The left hand side of Eq 5.16 represents the net force along the flight path (excess thrust, which may be positive or negative), which when multiplied by the velocity yields the excess power, and divided by the aircraft weight becomes the specific excess power of the aircraft (P_s):

$$P_s = \frac{V_T\left(T_{N_x} - D\right)}{W} \qquad \text{(Eq 5.17)}$$

Or:

$$P_s = \frac{dE_h}{dt} \qquad \text{(Eq 5.18)}$$

Which can be expressed as:

$$P_s = \frac{dh}{dt} + \frac{V_T}{g}\frac{dV_T}{dt} \qquad \text{(Eq 5.19)}$$

Where:

α_j	Thrust angle	
D	Drag	lb
E_h	Energy height	ft
F_x	Forces parallel to flight path	lb
γ	Flight path angle	deg
g	Gravitational acceleration	ft/s^2
h	Tapeline altitude	ft
P_s	Specific excess power	ft/s
t	Time	s
T_G	Gross thrust	lb
T_{N_x}	Net thrust parallel flight path	lb
T_R	Ram drag	lb
V_T	True airspeed	ft/s
W	Weight	lb.

The terms in Eq 5.19 all represent instantaneous quantities. P_s relates how quickly the airplane can change its energy state. P_s is a measure of what is known as energy maneuverability. When $P_s > 0$, the airplane is gaining energy. When $P_s < 0$, the airplane is losing energy. A typical P_s plot is shown in figure 5.4.

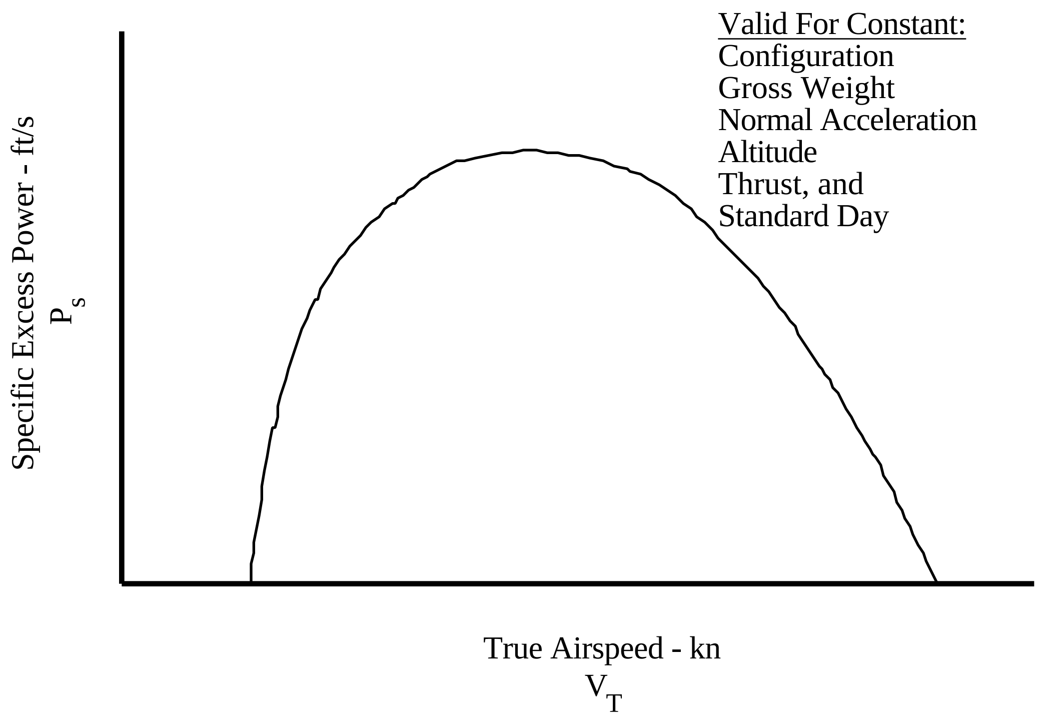

Figure 5.4
SPECIFIC EXCESS POWER VERSUS TRUE AIRSPEED

P_S is valid for a single flight condition (configuration, gross weight, normal acceleration, and altitude). A family of P_S plots at altitude intervals of approximately 5,000 ft is necessary to define the airplane's specific excess power envelope for each configuration. When presented as a family, P_S curves usually are plotted versus Mach number or calibrated airspeed (V_C) as shown in figure 5.5.

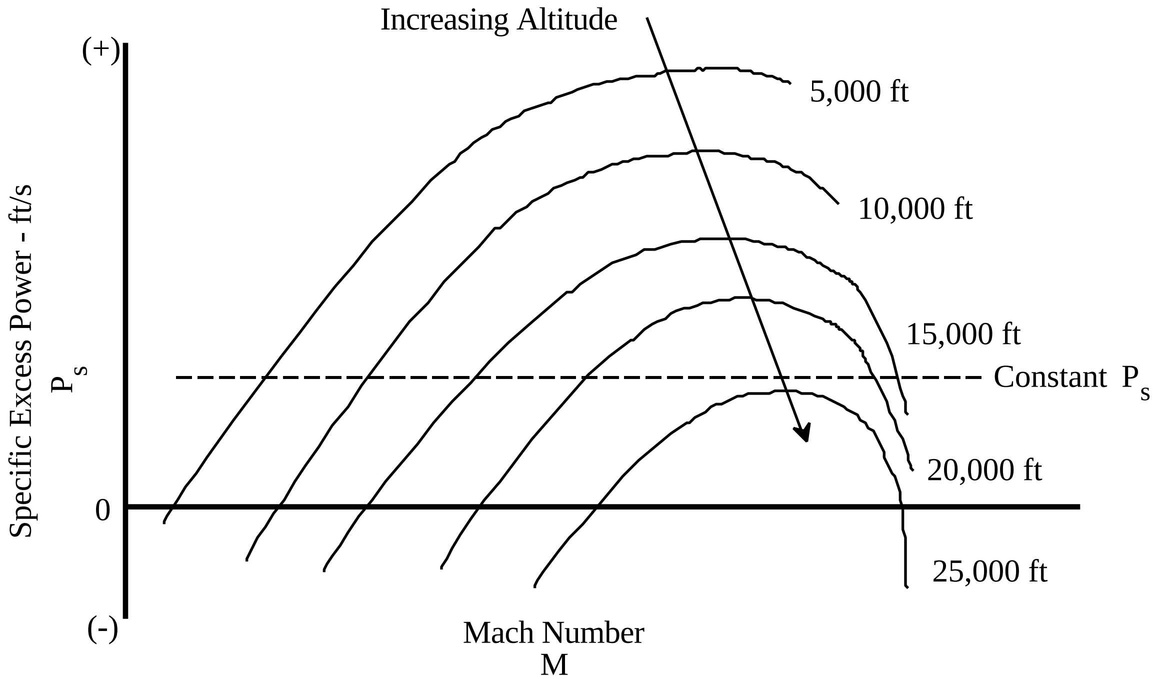

Figure 5.5
FAMILY OF SPECIFIC EXCESS POWER CURVES

Notice the P_S curves have a similar shape, but shift and decrease in magnitude with increasing altitude. Regions can be documented where the airplane is instantaneously losing energy, represented in figure 5.5 by the conditions where P_S is negative. The variation of P_S with Mach number and altitude are often displayed on a plot of energy height versus Mach number for climb performance analysis. For a given level of P_S, represented by a horizontal cut in figure 5.5, combinations of altitude and Mach number can be extracted to show the change in energy height. A plot containing several such P_S contours is used to determine climb profiles (Chapter 7). P_S is derived analytically from the airplane thrust available and thrust required curves (Reference 2, Chapter 10) which are multiplied by the velocity to obtain the power available and power required curves. The difference between power available and power required, divided by the aircraft weight, is the specific excess power, P_S. The graphical portrayal of typical P_S curves for jet and propeller aircraft is presented in figure 5.6.

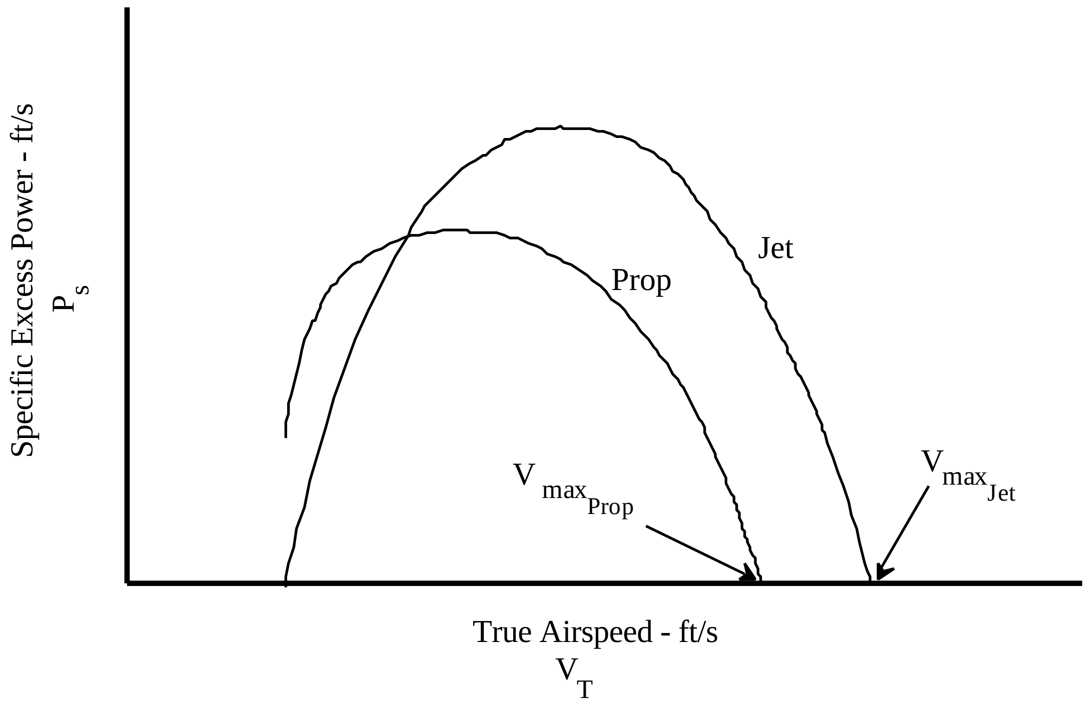

Figure 5.6
TYPICAL SPECIFIC EXCESS POWER CHARACTERISTICS

5.3.5 EFFECTS OF PARAMETER VARIATION ON SPECIFIC EXCESS POWER

The following discussion of the effect of variation in normal acceleration, gross weight, drag, thrust, and altitude is presented as it applies to jet airplanes.

5.3.5.1 INCREASED NORMAL ACCELERATION

Increased normal acceleration affects the P_S equation by increasing the induced drag and has most effect at low speeds (Figure 5.7):

$$P_s = \frac{V_T\left(T_{N_x} - D - \Delta D_i\right)}{W} \qquad \text{(Eq 5.20)}$$

Where:

D	Drag	lb
ΔD_i	Change in induced drag	lb
P_s	Specific excess power	ft/s
T_{N_x}	Net thrust parallel flight path	lb
V_T	True airspeed	ft/s
W	Weight	lb.

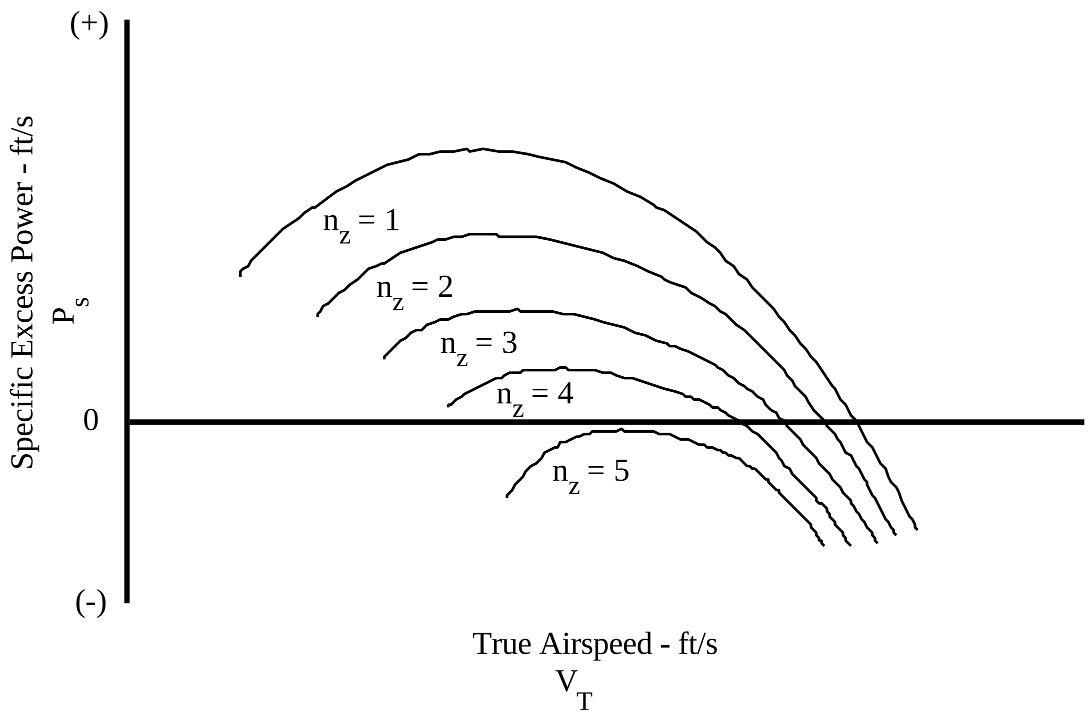

Figure 5.7
EFFECT OF INCREASED NORMAL ACCELERATION ON SPECIFIC EXCESS POWER

Chapter 6 contains a discussion of P_s for $n_z > 1$.

5.3.5.2 INCREASED GROSS WEIGHT

The effect of increasing gross weight is similar to that of increasing the normal acceleration, with the difference that both the numerator and denominator are affected rather than the numerator alone (Figure 5.8):

$$P_s = \frac{V_T\left(T_{N_x} - D - \Delta D_i\right)}{W + \Delta W} \qquad \text{(Eq 5.21)}$$

Where:

D	Drag	lb
ΔD_i	Change in induced drag	lb
P_S	Specific excess power	ft/s
T_{N_x}	Net thrust parallel flight path	lb
V_T	True airspeed	ft/s
W	Weight	lb.

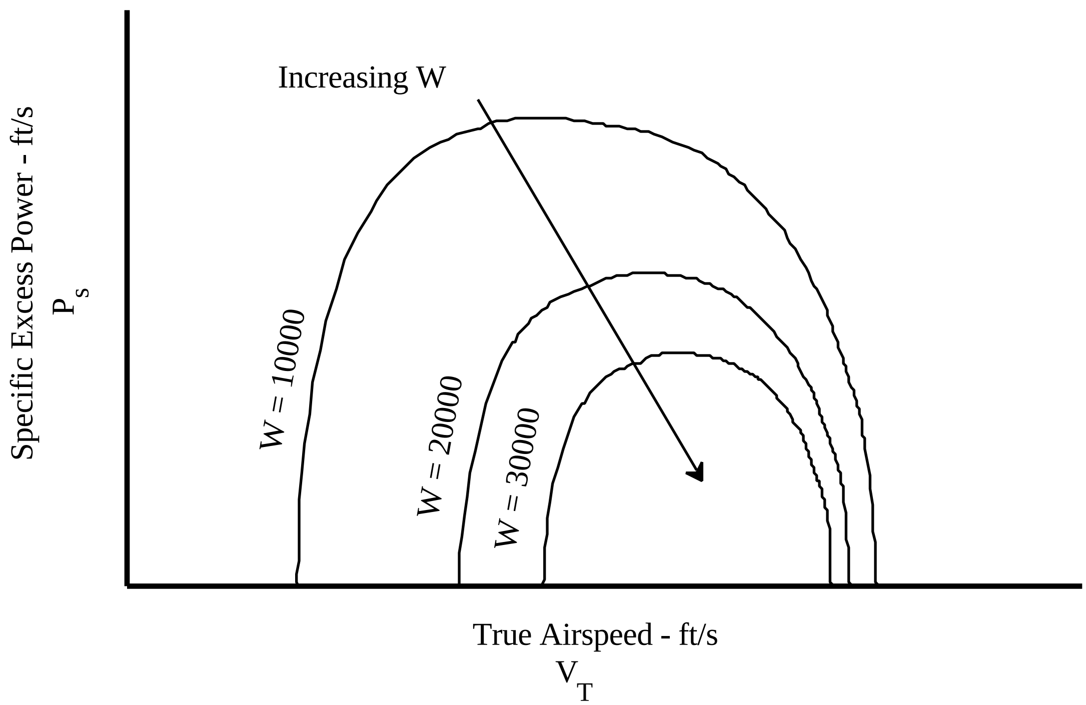

Figure 5.8

EFFECT OF INCREASED GROSS WEIGHT ON SPECIFIC EXCESS POWER

For example, compare the P_S curves for an airplane at 2 g with one at twice the standard weight shown in figure 5.9. At the maximum and minimum level flight speeds where $P_S = 0$, the additional induced drag is the same in both cases. The balance of thrust and drag is the same, resulting in identical minimum and maximum level flight speeds. At intermediate speeds where $P_S > 0$, the value of P_S for the high gross weight case is half that of the aircraft at 2 g even though the actual excess power may be the same (P_S is specific to the higher weight).

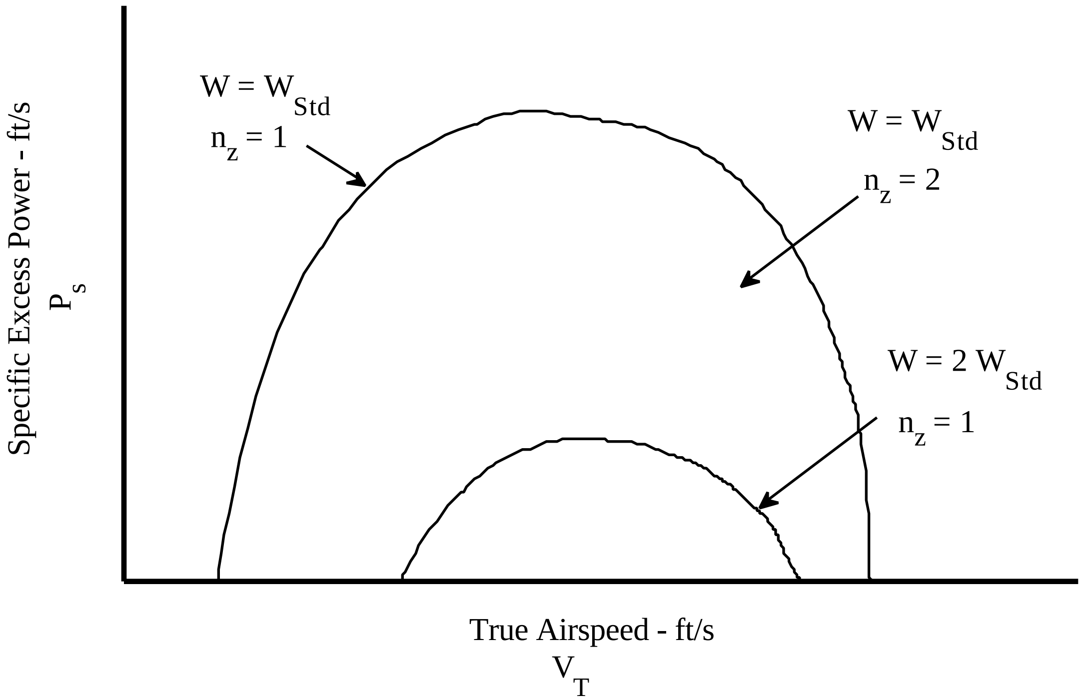

Figure 5.9
COMPARING EFFECT OF INCREASED GROSS WEIGHT WITH INCREASED NORMAL ACCELERATION

5.3.5.3 INCREASED PARASITE DRAG

Increasing the airplane's parasite drag has an effect which increases as airspeed increases. As drag is increased, both P_S and the speed for maximum P_S decrease (Figure 5.10):

$$P_s = \frac{V_T \left(T_{N_x} - D - \Delta D_p \right)}{W} \qquad \text{(Eq 5.22)}$$

Where:

D	Drag	lb
ΔD_p	Change in parasite drag	lb
P_S	Specific excess power	ft/s
T_{N_x}	Net thrust parallel flight path	lb
V_T	True airspeed	ft/s
W	Weight	lb.

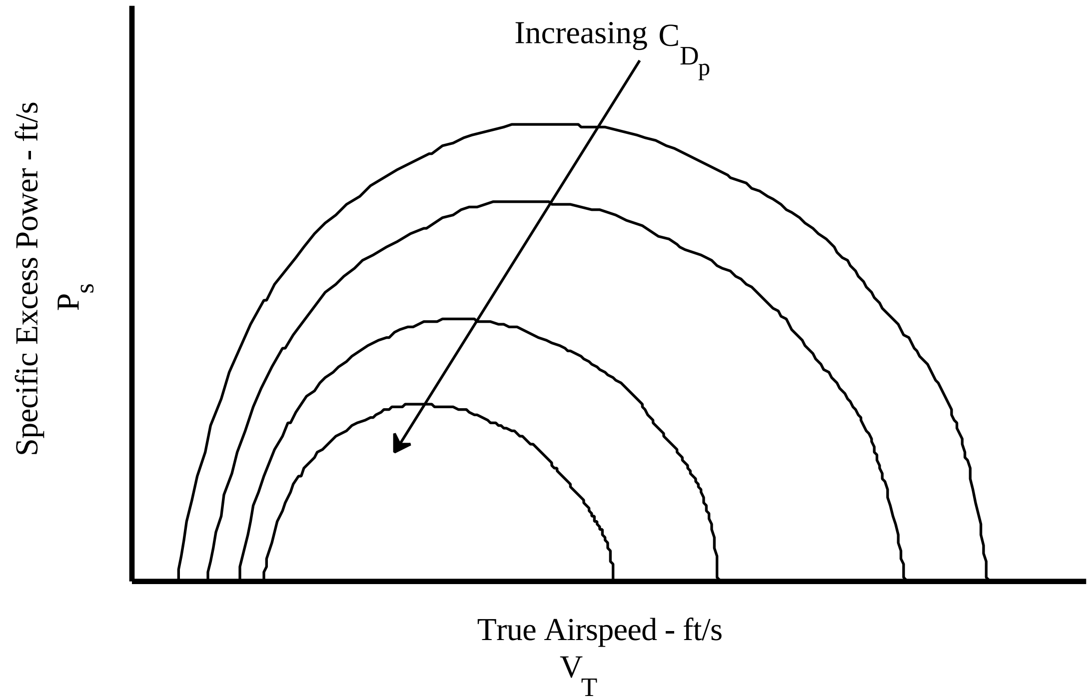

Figure 5.10
EFFECT OF INCREASED DRAG ON SPECIFIC EXCESS POWER

5.3.5.4 INCREASED THRUST

Increasing thrust increases P_S. As thrust is increased, both P_S and the speed for maximum P_S increase (Figure 5.11):

$$P_s = \frac{V_T \left(T_{N_x} + \Delta T_{N_x} - D\right)}{W} \qquad \text{(Eq 5.23)}$$

Where:

D	Drag	lb
P_S	Specific excess power	ft/s
T_{N_x}	Net thrust parallel flight path	lb
V_T	True airspeed	ft/s
W	Weight	lb.

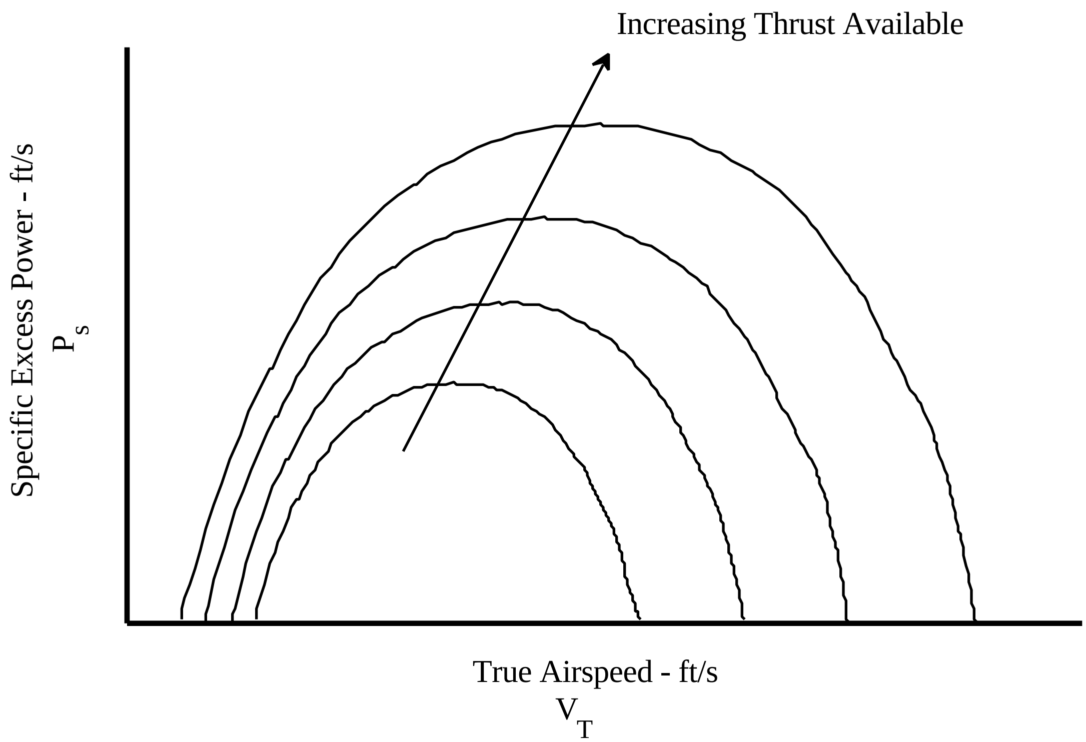

Figure 5.11
EFFECT OF INCREASED THRUST ON SPECIFIC EXCESS POWER

5.3.5.5 INCREASED ALTITUDE

The typical result of an increase in altitude is shown in figure 5.12.

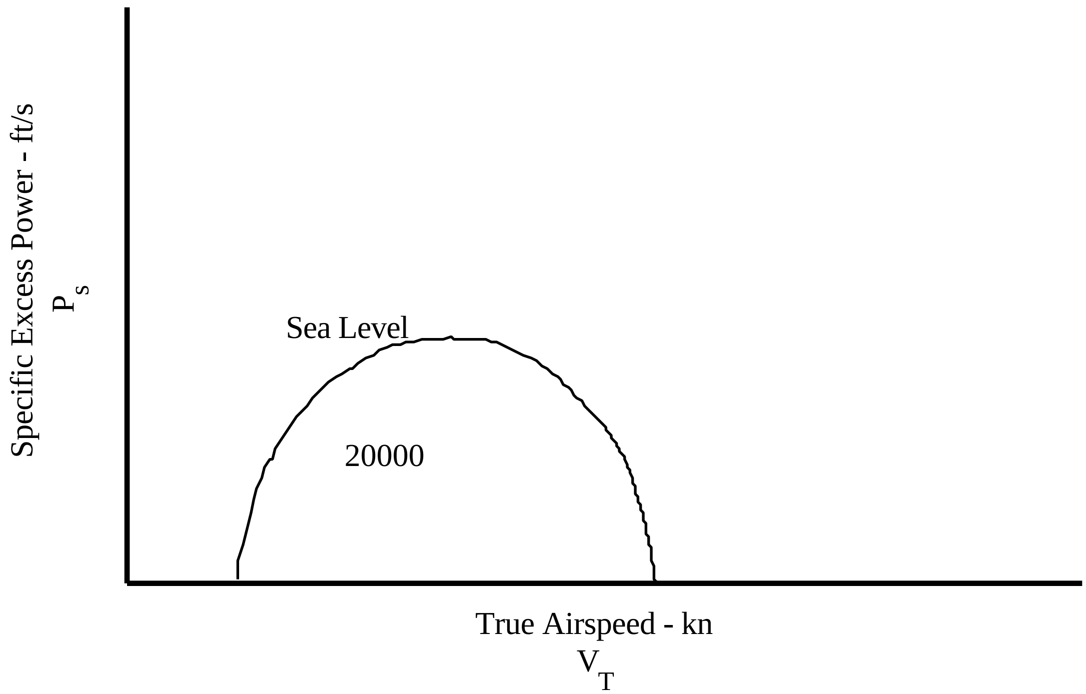

Figure 5.12
EFFECT OF INCREASED ALTITUDE ON SPECIFIC EXCESS POWER

As altitude is increased, both power available and power required are affected. The power required increases with increasing true airspeed. The power available decreases depending on the particular characteristics of the engine:

$$P_s = \frac{\left(P_A - \Delta P_A\right) - \left(P_{req} + \Delta P_{req}\right)}{W} \qquad \text{(Eq 5.24)}$$

Where:

P_A	Power available	ft-lb/s
P_{req}	Power required	ft-lb/s
P_S	Specific excess power	ft/s
W	Weight	lb.

5.3.5.6 SUBSONIC AIRCRAFT

The specific excess power characteristics for subsonic aircraft designs are generally dominated at high speeds by the transonic drag rise. At low altitudes, however, the high dynamic pressures for high subsonic speeds may impose a structural envelope limit which effectively prevents the airplane from reaching its performance potential. These aircraft have to be throttled back for those conditions to avoid damage to the airframe. In general, the transonic drag rise determines the high speed P_S characteristics as shown in figure 5.13.

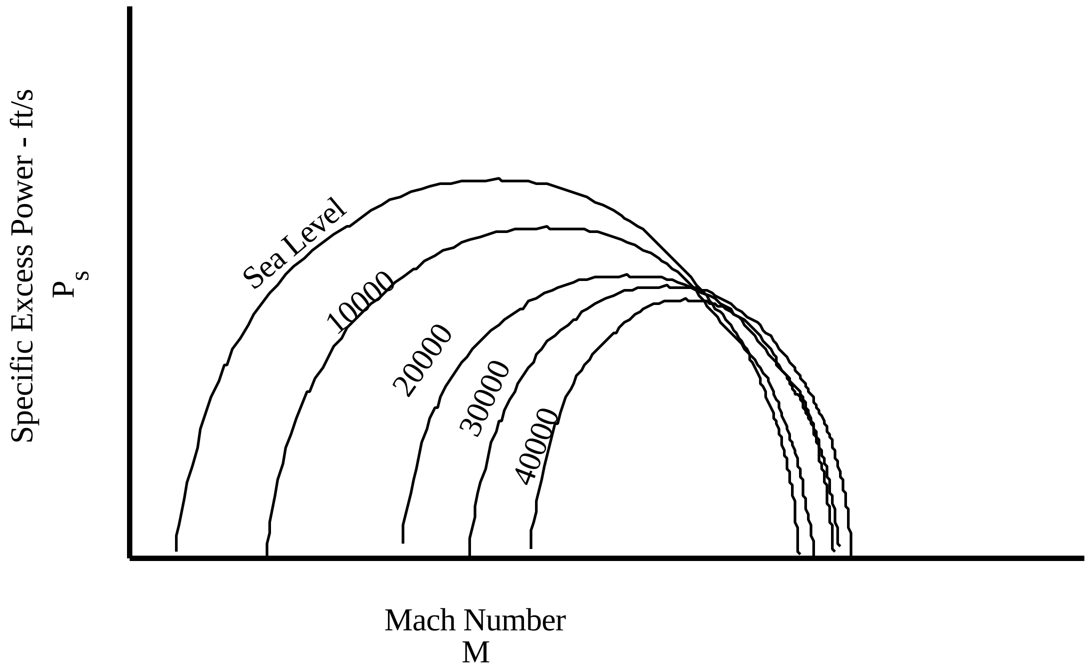

Figure 5.13
TYPICAL SPECIFIC EXCESS POWER FOR SUBSONIC AIRPLANE

5.3.5.7 SUPERSONIC AIRCRAFT

The specific excess power characteristics of a supersonic aircraft takes a form depending on the variation of net thrust and drag with Mach number. There is typically a reduction in P_S in the transonic region resulting from the compressibility drag rise. When P_S is substantially reduced in the transonic region, the level acceleration is slowed very noticeably. The aircraft may require afterburner to accelerate through the transonic drag rise but are then capable of sustaining supersonic flight in military power. The P_S plot for a typical supersonic aircraft is shown in figure 5.14.

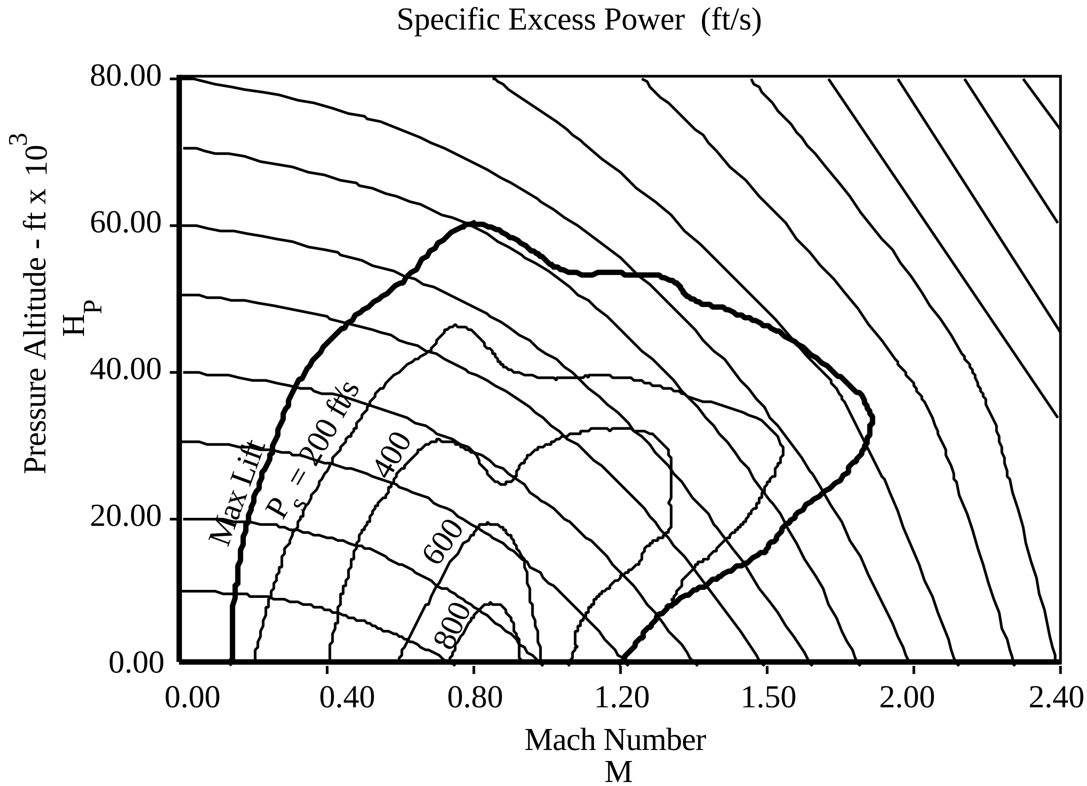

Figure 5.14

TYPICAL SPECIFIC EXCESS POWER SUPERSONIC AIRPLANE

5.4 TEST METHODS AND TECHNIQUES

The principal test method for obtaining P_S data is the level acceleration. The sawtooth climb method is used for cases when P_S is low or the aircraft is limited by gear or flap extension speed in the takeoff or landing configuration. Other methods include the use of extremely sensitive inertial platforms for dynamic test techniques.

Since the P_S analysis distinguishes between increased energy from a climb and increased energy from acceleration, any measurement errors in height (tapeline altitude) degrades the accuracy of the final results. Reliance on pitot static instrumentation, even when specially calibrated, does not produce results as good as can be obtained with more sophisticated, absolute space positioning equipment such as high resolution radar or laser tracking devices.

5.4.1 LEVEL ACCELERATION

The specific excess power characteristics for the entire flight envelope are determined from a series of level accelerations performed at different altitudes, usually separated by about 5,000 ft.

The acceleration run should be started at as low a speed as practicable with the engine(s) stabilized at the desired power setting (usually MIL or MAX). This requirement presents difficulties in flight technique when P_S is high. A commonly used method is to stabilize the aircraft in a climb at the desired speed sufficiently below the target altitude long enough to allow the engine(s) to reach normal operating temperatures. Speedbrakes, and sometimes flaps, are used to increase drag to reduce the rate of climb. As the target altitude is approached, speedbrakes and flaps are retracted and the airplane is pushed over into level flight. The first few seconds of data are discarded usually, but this technique enables a clean start with the least data loss.

If P_S is negative at the minimum airspeed, the start must be above the target altitude in a descending acceleration. The objective is to level at the target altitude at a speed where P_S is positive and the acceleration run can proceed normally.

During the acceleration run, maintain the target altitude as smoothly as possible. Altitude variations are taken into account in the data reduction process and only affect the results when they are large enough to produce measurable changes in engine performance. Changes in induced drag caused by variations in normal acceleration cannot be accounted for, or corrected, and generate significant errors. The altitude may be allowed to vary as much as ± 1000 ft around the target altitude without serious penalties in the accuracy of P_S data but the normal acceleration must be held within ± 0.1 g. Using normal piloting techniques, considerably tighter altitude tolerances are easily achievable without exceeding the g limits. The altitude tolerance is typically ± 300 ft. The normal acceleration tolerance of ± 0.1 g allows the pilot to make shallow turns for navigational purposes during the acceleration run. The g will remain within tolerance if the bank angle does not exceed 10˚, but the turn should be limited to no more than a 30˚ heading change to minimize the build up of errors.

Smoothness during the acceleration is helped by anticipation and attitude flying. If the mechanical characteristics of the longitudinal control system make small precise inputs around trim difficult, the airplane may be flown off trim so force reversals are not encountered during the acceleration. In some aircraft, trimming during the run is inadvisable because the smallest possible trim input can cause an unacceptably large variation in normal acceleration. Others may have trim system characteristics which permit their use. The test aircraft determines the appropriate technique.

Near the maximum level flight airspeed, the P_S approaches zero. The acceleration run is usually terminated when the acceleration drops below a given threshold, usually 2 kn/min. The P_S data are anchored by determining the $P_S = 0$ airspeed, using the front side technique presented in Chapter 4. When the acceleration drops below 2 kn/min, smoothly push over to gain 5 to 10 kn, then smoothly level off. Hold the resulting lower altitude until the airspeed decreases and stabilizes (less than 2 kn/min change) at the maximum level flight airspeed.

5.4.1.1 DATA REQUIRED

The following data are required at intervals throughout the acceleration run:

Time, H_{P_o}, V_o, $\dot{W}_f$, OAT, W_f.

The desired frequency of data recording depends on the acceleration rate. When the acceleration is low, acceptable results can be achieved using manual recording techniques and taking data every few seconds. As the acceleration increases, hand-held data-taking becomes more difficult. For anything more than moderate acceleration rates some form of automatic data recording is essential.

5.4.1.2 TEST CRITERIA

1. Coordinated, level flight during the acceleration run.
2. Engine(s) stabilized at normal operating temperatures.
3. Altimeter set to 29.92.

5.4.1.3 DATA REQUIREMENTS

1. H_{P_o} ± 300 ft.
2. Normal acceleration ± 0.1 g.
3. Bank angle ≤ 10˚.
4. Heading change ≤ 30˚.

5.4.1.4 SAFETY CONSIDERATIONS

There are no unique hazards or safety precautions associated with level acceleration runs. However, take care to observe airspeed limitations and retract flaps or speedbrakes if used to help control the entry to the run.

5.4.2 SAWTOOTH CLIMBS

Sawtooth climbs provide a useful alternative method of obtaining P_S data, especially when P_S is low or there are airspeed limits which must be observed, as in the takeoff, landing, wave-off or single engine configurations. The technique consists of making a series of short climbs (or descents, if P_S is negative at the test conditions) at constant V_o covering the desired range of airspeeds. The altitude band for the climbs is usually the lesser of 1000 ft either side of the target altitude or the height change corresponding to two minutes of climb (or descent).

The same altitude band should be used for each climb, until P_S becomes so low that the climbs are stopped after two minutes, in which case the starting and ending altitudes are noted. The target altitude must be contained within the climb band, preferably close to the middle. As P_S decreases, and time rather than altitude change becomes the test criterion, the climb band shrinks symmetrically about the target altitude.

As with the acceleration runs, sufficient altitude should be allowed for the engine(s) to reach normal operating temperatures and the airplane to be completely stabilized at the desired airspeed before entering the data band. Smoothness is just as important as in the acceleration runs and for the same reasons. The tolerance on airspeed is ± 1 kn, but this must not be achieved at the expense of smoothness. If a small airspeed error is made while establishing the climb, maintaining the incorrect speed as accurately as possible is preferred rather than trying to correct it and risk aborting the entire run. The speed should, of course, be noted. Sawtooth climb test techniques and data reduction are discussed further in Chapter 7.

5.4.3 DYNAMIC TEST METHODS

The modern techniques of performance testing use dynamic test methods. The crucial requirements for dynamic test methods are:

1. Accurate measure of installed thrust in flight.
2. Accelerometers of sufficient sensitivity and precision to enable highly accurate determination of rates and accelerations in all three axes.

The desired objective of dynamic performance testing is to generate accurate C_L/C_D plots similar to the one shown in figure 5.15.

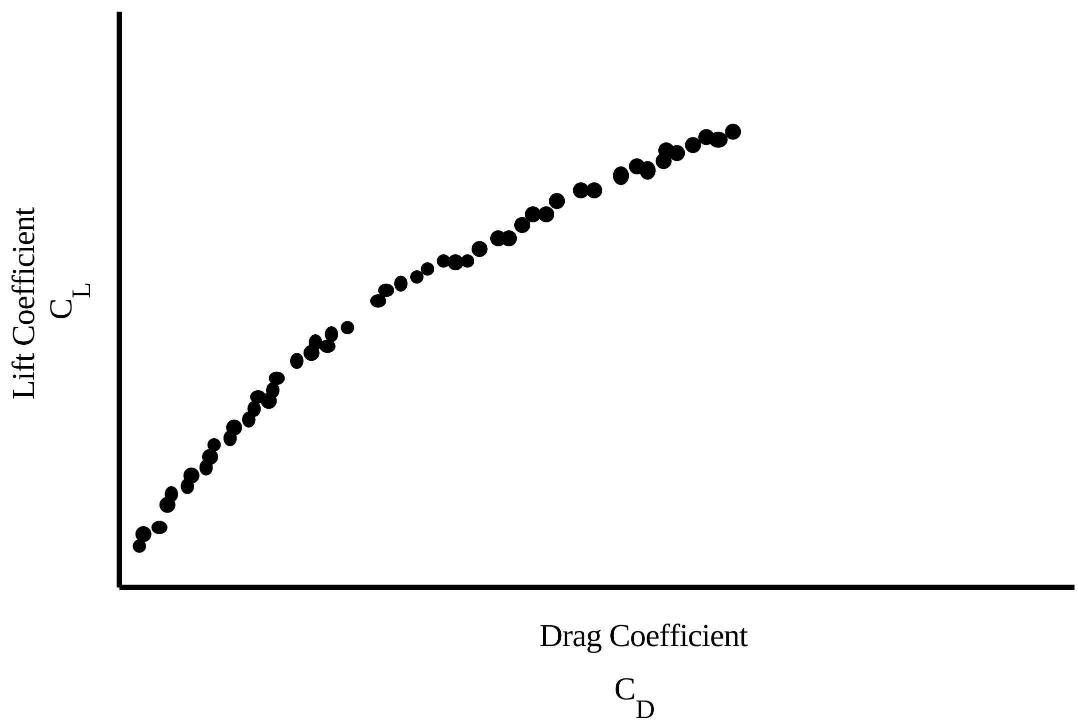

Figure 5.15
LIFT VERSUS DRAG COEFFICIENT DERIVED FROM DYNAMIC PERFORMANCE TESTS

Once these plots have been produced, cruise, turn, and acceleration performance can be modelled using the same validated thrust model used to generate the C_L/C_D plots.

The fundamental theory underlying the generation of these plots is to derive expressions for C_L and C_D in terms of known or measurable quantities (including thrust, weight, x, and z accelerations).

The Pressure Area method, or the Mass Flow method, enable inflight thrust measurements to be performed to accuracies of 3-5% as was demonstrated during the X-29 program, in which eight different telemetered pressure measurements allowed continuous, real-time determination of thrust.

There are three methods of measuring the x and z accelerations: CG (or body axis) accelerometers, flight path accelerometers (FPA) and inertial navigation systems (INS). CG accelerometers are strapped to the airframe and sense accelerations along the three orthogonal body axes. The FPA mounts on a gimballed platform at the end of a nose boom similar to a swivelling pitot head. Accelerations are measured relative to the flight path. Finally, INS may be used to record the accelerations. In this case the INS measurements are taken in the inertial reference frame.

In general, any of these methods generate the values of x and z accelerations required to calculate the values of C_L and C_D. However, various transformations and corrections must be performed depending upon the accelerometer configuration used. The test techniques used in dynamic performance testing include non-steady profiles such as the push-over, pull-up (POPU) (Figure 5.16), the wind-up-turn (WUT), or the split-S (SS).

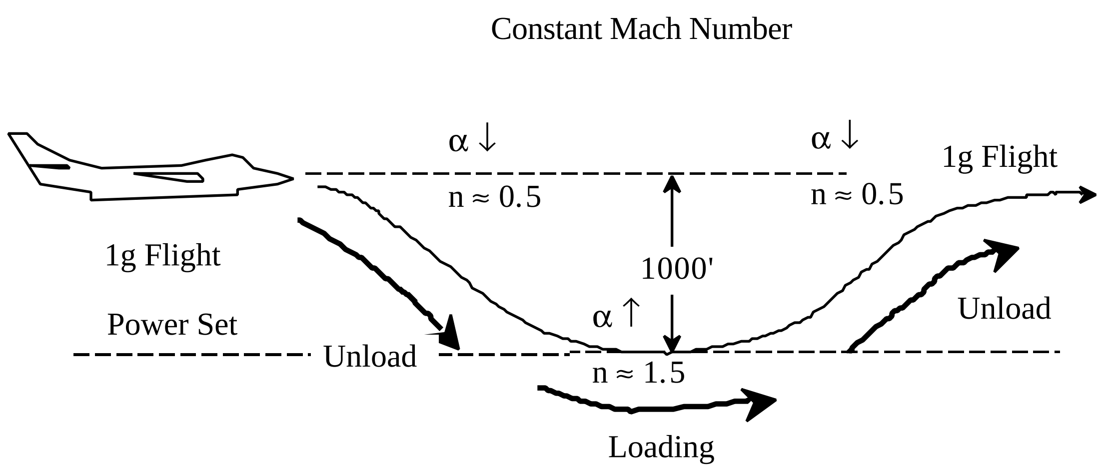

Figure 5.16
PUSH-OVER PULL-UP MANEUVER

The aircraft is flown through a sweep of angle of attack (α), and hence pitch rate, at constant Mach number. Because of the dynamics of the maneuver, some corrections are made. Examples of the type of corrections applied to this data include:

1. Pitch rate corrections to α. Because the aircraft is pitching, a FPA registers an error in the value of α (increase for nose-down pitch rates, decrease for nose-up pitch rates).
2. Accelerometer rate corrections. Placement of the accelerometers at the end of a nose boom means they measure not only the accelerations of the aircraft but accelerations due to the rotation of the aircraft about its CG, and accelerations due to angular accelerations of the aircraft.
3. Local flow corrections. Errors result from the immersion of an FPA in an upwash field ahead of the airplane.
4. Boom bending. An FPA mounted at the end of a boom is subjected to errors caused by bending of the boom under load.
5. Transformation of inertial velocities into accelerations relative to the wind, or stability axes.
6. Transformation of accelerations sensed by CG accelerometers from body axes to stability axes.

The significance of dynamic performance testing methods is the capability to acquire large quantities of data quickly from a single maneuver. A relatively small number of POPUs, WUTs or SSs may be flown instead of a large series of level accelerations, stabilized cruise points, and steady sustained turn performance points. In practice, a number of conventional tests are required to validate the performance model established by the results of the dynamic tests. However, this number is small and decreases as confidence in the technique is gained.

5.5 DATA REDUCTION

5.5.1 LEVEL ACCELERATION

The following equations are used to reduce level acceleration data.

$$q_c = P_{ssl}\left\{\left[1 + 0.2\left(\frac{V_c}{a_{ssl}}\right)^2\right]^{3.5} - 1\right\} \qquad \text{(Eq 5.25)}$$

$$P_a = P_{ssl}\left(1 - 6.8755856 \times 10^{-6}\, H_{P_c}\right)^{5.255863} \qquad \text{(Eq 5.26)}$$

$$M = \sqrt{\frac{2}{\gamma - 1}\left[\left(\frac{q_c}{P_a} + 1\right)^{\frac{\gamma - 1}{\gamma}} - 1\right]} \qquad \text{(Eq 5.27)}$$

$$T_a = \frac{OAT + 273.15}{1 + \frac{\gamma - 1}{2} K_T M^2} \qquad \text{(Eq 5.28)}$$

$$h = H_{P_c} \frac{T_{a_{Test}}}{T_{a_{Std}}} \qquad \text{(Eq 5.29)}$$

$$V_T = M \sqrt{\gamma\, g_c\, R\, T_a} \qquad \text{(Eq 5.30)}$$

$$E_h = h + \frac{V_T^2}{2\,g} \qquad \text{(Eq 5.7)}$$

Where:

a_{ssl}	Standard sea level speed of sound	661.483 kn
E_h	Energy height	ft
g	Gravitational acceleration	ft/s^2
γ	Ratio of specific heats	
g_c	Conversion constant	32.17 lb_m/slug
h	Tapeline altitude	ft
H_{P_c}	Calibrated pressure altitude	ft
K_T	Temperature recovery factor	
M	Mach number	
OAT	Outside air temperature	˚C
P_a	Ambient pressure	psf
P_{ssl}	Standard sea level pressure	2116.217 psf
q_c	Impact pressure	psf
R	Engineering gas constant for air	96.93ft-lb_f/lb_m-˚K
T_a	Ambient temperature	˚K
$T_{a_{Std}}$	Standard ambient temperature	˚K
$T_{a_{Test}}$	Test ambient temperature	˚K
V_c	Calibrated airspeed	kn
V_T	True airspeed	ft/s.

Correct observed altitude and airspeed data to calibrated altitude and airspeed. Using calibrated altitude, airspeed, and OAT compute E_h as follows:

Step	Parameter	Notation	Formula	Units	Remarks
1	Impact pressure	q_c	Eq 5.25	psf	
2	Ambient pressure	P_a	Eq 5.26	psf	
3	Mach number	M	Eq 5.27		
4	Ambient temperature	T_a	Eq 5.28	˚K	Or from reference source
5	Tapeline height	h	Eq 5.29	ft	
6	True airspeed	V_T	Eq 5.30	ft/s	
7	Energy height	E_h	Eq 5.7	ft	

Plot E_h as a function of elapsed time as shown in figure 5.17.

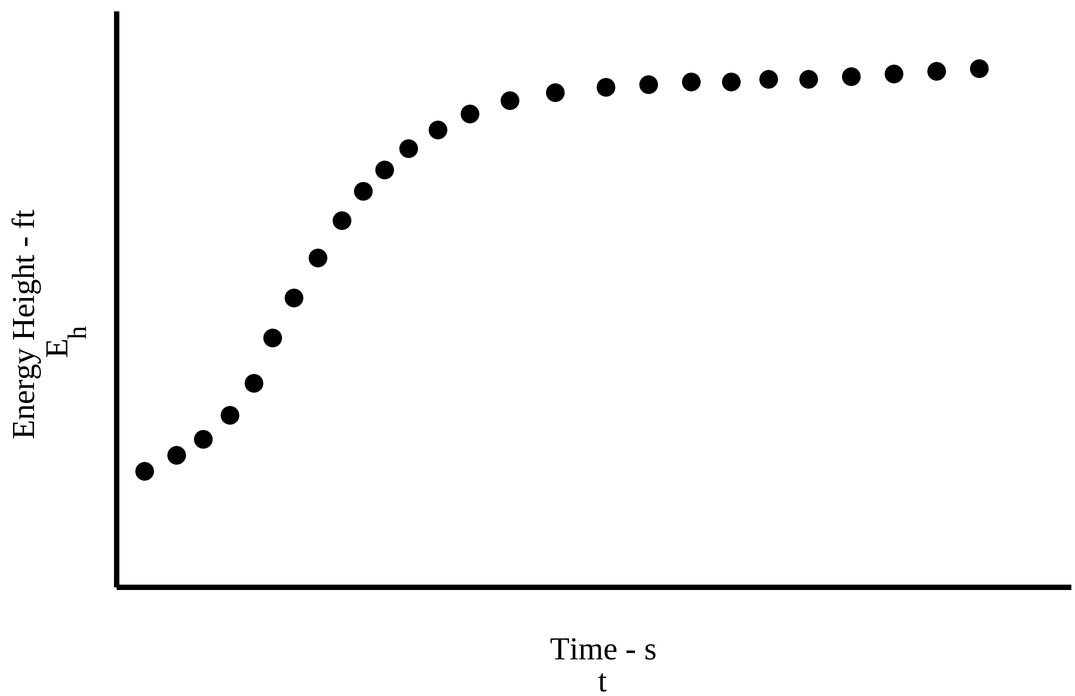

Figure 5.17

ENERGY HEIGHT VERSUS ELAPSED TIME

Fair a curve through the data points of figure 5.17 and find its derivative ($P_s = dE_h/dt$) at a sufficient number of points. Plot P_s against Mach number or true airspeed as in figure 5.18.

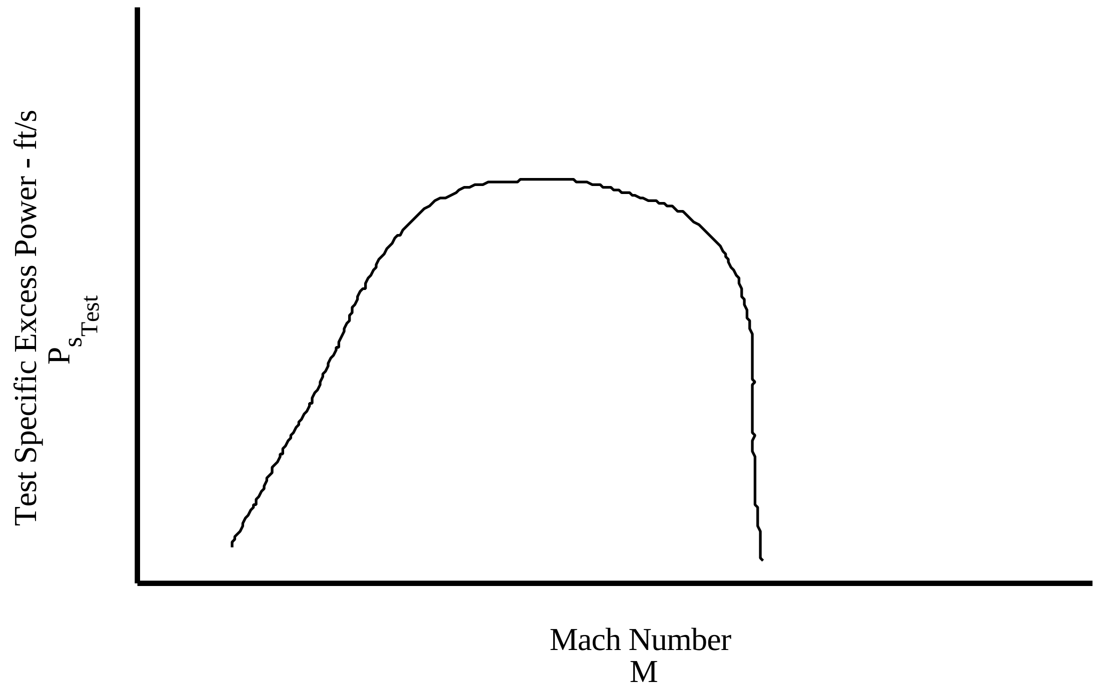

Figure 5.18
TEST SPECIFIC EXCESS POWER VERSUS MACH NUMBER

5.5.2 CORRECTING FOR NON-STANDARD CONDITIONS

P_S values obtained from the level acceleration method reflect the test day conditions and must be generalized to standard weight and standard atmospheric conditions. The following equations are used to correct for:

1. W for non-standard weight.
2. V_T for non-standard temperature.
3. T for temperature effect on thrust.
4. D for induced drag change resulting from the weight correction.

The weight ratio is calculated from the aircraft fuel state and fuel flow data ($\dot{W}_f$):

$$\frac{W_{Test}}{W_{Std}} \qquad \text{(Eq 5.31)}$$

The velocity ratio is determined from:

$$\frac{V_{T_{Std}}}{V_{T_{Test}}} = \frac{M_{Std}\sqrt{\theta_{Std}}}{M_{Test}\sqrt{\theta_{Test}}} \qquad \text{(Eq 5.32)}$$

For a constant Mach number correction, $M_{Std} = M_{Test}$ so:

$$\frac{V_{T_{Std}}}{V_{T_{Test}}} = \sqrt{\frac{T_{a_{Std}}}{T_{a_{Test}}}} \qquad \text{(Eq 5.33)}$$

The change in thrust with temperature at constant altitude and constant Mach number is computed from the engine thrust model:

$$\Delta T = f\left(T_a\right) \qquad \text{(Eq 5.34)}$$

The change in induced drag with gross weight is computed from the aircraft drag model (drag polar). For constant altitude and constant Mach number, parasite drag is constant and for a parabolic drag polar:

$$\Delta D = D_{Std} - D_{Test} = \frac{2\left(W_{Std}^2 - W_{Test}^2\right)}{\pi\, e\, AR\, S\, \gamma\, P_a\, M^2} \qquad \text{(Eq 5.35)}$$

Eq 5.36 is used to correct $P_{s_{Test}}$ to $P_{s_{Std}}$.

$$P_{s_{Std}} = P_{s_{Test}} \frac{W_{Test}}{W_{Std}} \sqrt{\frac{T_{a_{Std}}}{T_{a_{Test}}}} + \frac{V_{T_{Std}}}{W_{Std}} \left(\Delta T_{N_x} - \Delta D\right) \qquad \text{(Eq 5.36)}$$

Where:

AR	Aspect ratio	
D_{Std}	Standard drag	lb
D_{Test}	Test drag	lb
e	Oswald's efficiency factor	
M	Mach number	
M_{Std}	Standard Mach number	
M_{Test}	Test Mach number	
π	Constant	
P_a	Ambient pressure	psf
P_s	Specific excess power	ft/s
$P_{s_{Std}}$	Standard specific excess power	ft/s
$P_{s_{Test}}$	Test specific excess power	ft/s
θ_{Std}	Standard temperature ratio	
θ_{Test}	Test temperature ratio	
S	Wing area	ft^2
T_a	Ambient temperature	˚K
$T_{a_{Std}}$	Standard ambient temperature	˚K
$T_{a_{Test}}$	Test ambient temperature	˚K
T_{N_x}	Net thrust parallel flight path	lb
T_{Std}	Standard thrust	lb
T_{Test}	Test thrust	lb
$V_{T_{Std}}$	Standard true airspeed	ft/s
$V_{T_{Test}}$	Test true airspeed	ft/s
W_{Std}	Standard weight	lb
W_{Test}	Test weight	lb.

5.5.3 COMPUTER DATA REDUCTION

Various computer programs are in existence to assist in reduction of performance data. This section contains a brief summary of the assumptions and logic which might be used. The treatment is purposefully generic as programs change over time or new ones are acquired or developed. Detailed instructions for the particular computer or program are assumed to be available.

The purpose of the energy analysis data reduction program is to calculate standard day specific excess power for any maneuver performed at constant power setting (idle or military). For level accelerations, the program plots $P_{s_{Std}}$ versus Mach number for any n_z, and calculates the maximum sustained n_z available. Referred fuel flow available versus OAT is plotted. For climbs and descents, the program calculates fuel, time, and no-wind distance. This section deals with level acceleration runs.

Basic data such as aircraft type, standard gross weight, etc., is entered. For each data point the following information is input data.

1. Time (s).
2. Indicated airspeed (kn).
3. Indicated pressure altitude (ft) (29.92).
4. OAT (˚C) or ambient Temperature (˚K).
5. Fuel flow (lb/h).

The program calculates referred parameters for each data point, and plots energy height versus time as in figure 5.17.

The program calculates P_s by taking the derivative of energy height with respect to time. Therefore, a curve is fitted in some manner to the E_h versus time plot. Since P_s is calculated from the slope of this curve, any slight bends in the curve are magnified when the derivative (slope) is calculated. Care must be taken to fit a smooth, accurate curve through the data.

Following completion of the curve fitting, the program computes and plots standard day P_s versus Mach number as in figure 5.18.

The program calculates and plots fuel, time, and distance for the maneuver. Fuel flow is plotted first as referred fuel flow available versus OAT as in figure 5.19.

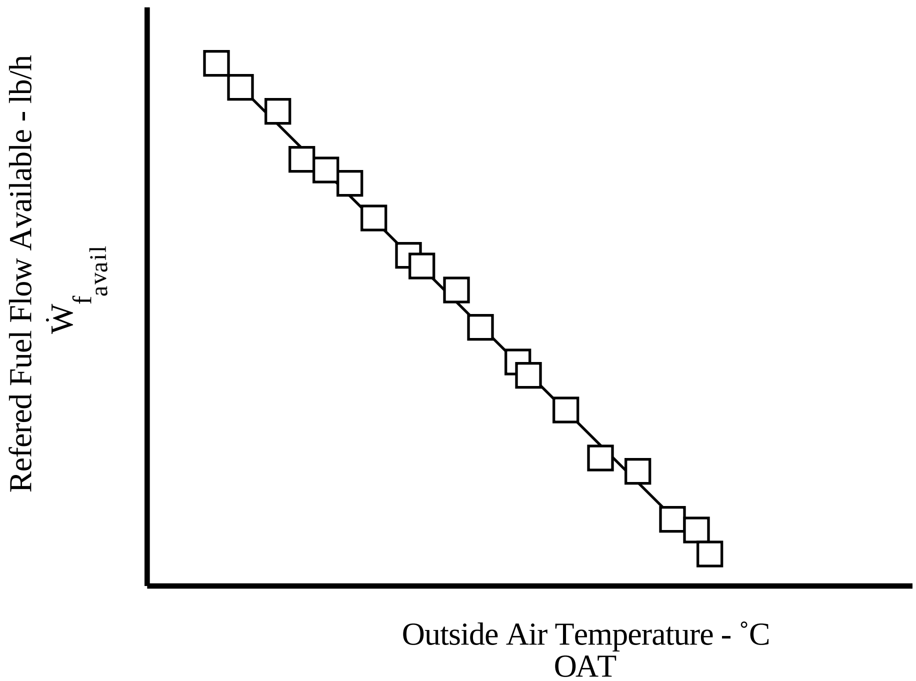

Figure 5.19
REFERRED FUEL FLOW VERSUS OAT

Since fuel flow is referred to total conditions, the curve may be used in combination with range and endurance data to calculate standard day V_H using the method described in Chapter 4.

The program next plots the ratio of $P_{s_{Std}}$ to fuel flow versus Mach number as in figure 5.20.

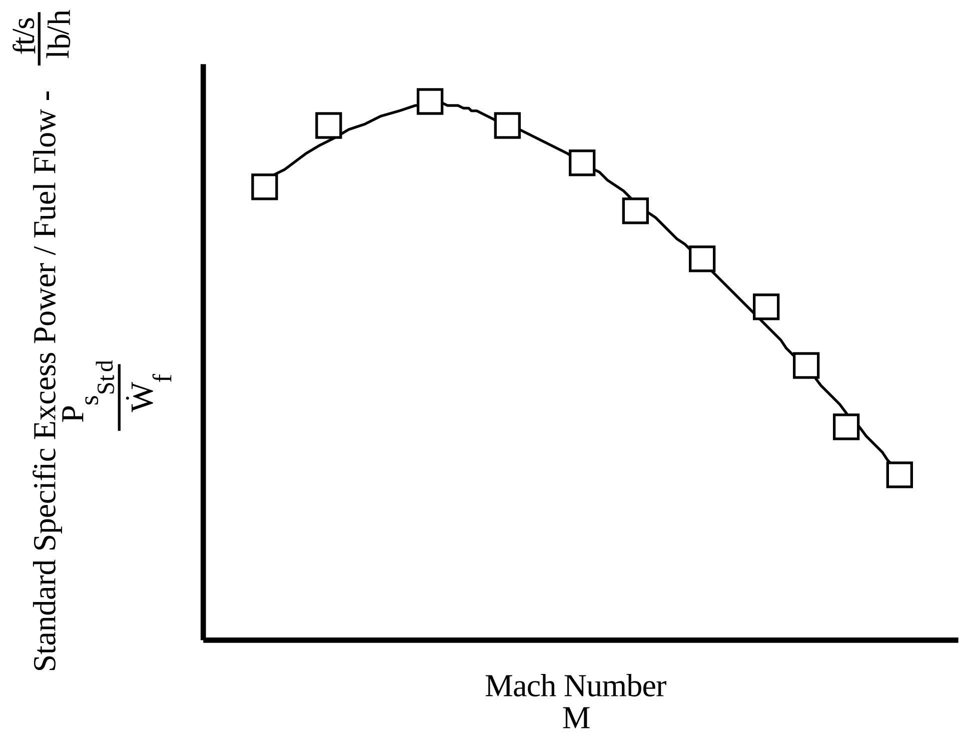

Figure 5.20
STANDARD SPECIFIC EXCESS POWER/FUEL FLOW RATIO VERSUS MACH NUMBER

A family of these plots from several altitudes may be cross-plotted on energy paper and used to determine climb schedules as discussed in Chapter 7.

For turn performance, the program plots $P_{s_{Std}}$ versus Mach number for any n_z, and predicts maximum sustained n_z. Excess power data can be related to turn performance as discussed in Chapter 6.

5.5.3.1 EQUATIONS USED BY THE COMPUTER ROUTINE

Position error:

$$V_c = V_i + \Delta V_{pos} \tag{Eq 5.37}$$

$$H_{P_c} = H_{P_i} + \Delta H_{pos} \tag{Eq 5.38}$$

Mach number:

$$M = f\left(V_c\,,\,H_{P_c}\right) \tag{Eq 5.39}$$

Weight:

$$W_{Test} = \text{Initial } W - \int \dot{W}_f \; dt \tag{Eq 5.40}$$

If ambient temperature (˚K) was entered:

$$°C = °K - 273.15 \tag{Eq 5.41}$$

$$OAT = f\left(T_a\,,\,M_T\right) \tag{Eq 5.42}$$

If OAT ˚C was entered:

$$T_a = f\left(OAT, M\right) \tag{Eq 5.43}$$

Test day true airspeed:

$$V_{T_{Test}} = f\left(V_c\,,\,H_{P_c}\,,\,T_a\right) \tag{Eq 5.44}$$

Standard day true airspeed:

$$V_{T_{Std}} = f\left(V_c, H_{P_c}, T_{Std}\right) \tag{Eq 5.45}$$

First data point as $H_{P_{c\,ref}}$:

$$h = H_{P_{c_{ref}}} + \Delta H_{P_c}\left(\frac{T_a}{T_{Std}}\right) \tag{Eq 5.46}$$

Energy height:

$$E_h = h + \frac{V_{T_{Test}}^2}{2g} \qquad \text{(Eq 5.47)}$$

Test day P_s from faired E_h versus time curve:

$$P_{s_{Test}} = \frac{dE_h}{dt} \qquad \text{(Eq 5.48)}$$

Test day flight path angle, dh/dt from the curve of h versus time:

$$\gamma_{Test} = \sin^{-1}\left(\frac{dh/dt}{V_{T_{Test}}}\right) \qquad \text{(Eq 5.49)}$$

Climb correction factor:

$$CCF = 1 + \left(\frac{V_{T_{Std}}}{g}\frac{dV}{dh}\right) \qquad \text{(Eq 5.50)}$$

Standard day P_s:

$$P_{s_{Std}} = P_{s_{Test}}\left(\frac{W_{Test}}{W_{Std}}\right)\left(\frac{V_{T_{Std}}}{V_{T_{Test}}}\right) + \left(\frac{V_{T_{Std}}}{W_{Std}}\right)(\Delta T_{N_x} - \Delta D) \qquad \text{(Eq 5.51)}$$

$$\left(\frac{dh}{dt}\right)_{Std} = \frac{P_{s_{Std}}}{CCF} \qquad \text{(Eq 5.52)}$$

Standard day flight path angle:

$$\gamma_{Std} = \sin^{-1}\left(\frac{\left(\frac{dh}{dt}\right)_{Std}}{V_{T_{Std}}}\right) \tag{Eq 5.53}$$

The program repeats the $P_{s_{Std}}$ calculation using the new standard until:

$$\left|\gamma_{Test} - \gamma_{Std}\right| < 0.1 \tag{Eq 5.54}$$

Where:

CCF	Climb correction factor	
D	Drag	lb
ΔH_{pos}	Altimeter position error	ft
ΔV_{pos}	Airspeed position error	kn
E_h	Energy height	ft
g	Gravitational acceleration	ft/s^2
γ_{Std}	Standard flight path angle	deg
γ_{Test}	Test flight path angle	deg
h	Tapeline altitude	ft
H_{P_c}	Calibrated pressure altitude	ft
$H_{P_{c\,ref}}$	Reference calibrated pressure altitude	ft
H_{P_i}	Indicated pressure altitude	ft
M	Mach number	
OAT	Outside air temperature	˚C
P_s	Specific excess power	ft/s
$P_{s_{Std}}$	Standard specific excess power	ft/s
$P_{s_{Test}}$	Test specific excess power	ft/s
T_a	Ambient temperature	˚K
T_{N_x}	Net thrust parallel flight path	lb
T_{Std}	Standard thrust	lb
T_{Test}	Test thrust	lb
V_c	Calibrated airspeed	kn
V_i	Indicated airspeed	kn
$V_{T_{Std}}$	Standard true airspeed	ft/s

$V_{T_{Test}}$	Test true airspeed	ft/s
W_{Std}	Standard weight	lb
W_{Test}	Test weight	lb
$\dot{W}_f$	Fuel flow	lb/h.

5.6 DATA ANALYSIS

The analysis of P_s data is directed towards two objectives. The first is that of determining the optimum climb schedules for the airplane which is discussed in Chapter 7. The second is the evaluation of the airplane's tactical strengths and weaknesses and comparison of those characteristics with potential threat aircraft for which similar data is known.

5.6.1 TACTICAL ANALYSIS

The development of total energy concepts has enabled great progress to be made in analyzing the tactical capability of aircraft. The analysis is especially powerful when flight tests of potential threat aircraft allow direct comparisons to be made between aircraft. Such analysis has been of tremendous help in deciding the most advantageous tactics to be used against different threat aircraft and has led to the inclusion of P_s plots (E-M plots) in tactical manuals. More recently, total energy analysis has played a major part in the development of current research programs in fighter agility.

5.7 MISSION SUITABILITY

Requirements for climb performance will be specified in the detail specification for the aircraft. The determination of mission suitability will depend largely on whether the aircraft meets these requirements, and on the type of analysis described in the previous section. The precise shape of the aircraft's P_s envelopes probably will not be specified, although the shape may be implicit in a requirement. Certain P_s values may be required over a range of speeds and altitudes. The final evaluation of mission suitability will depend on more specific flight tests such as rate of climb and agility testing.

5.8 SPECIFICATION COMPLIANCE

Specification compliance for P_s characteristics is concerned with meeting the requirements of the detailed specification for the aircraft. Published specifications, such as MIL-1797, have general applicability but only in the context of requiring that the flying qualities should allow the performance potential to be achieved by using normal piloting techniques.

5.9 GLOSSARY

5.9.1 NOTATIONS

AR	Aspect ratio	
a_{ssl}	Standard sea level speed of sound	661.483 kn
CCF	Climb correction factor	
CG	Center of gravity	
D	Drag	lb
ΔD_i	Change in induced drag	lb
ΔD_p	Change in parasite drag	lb
ΔH_{pos}	Altimeter position error	ft
D_{Std}	Standard drag	lb
D_{Test}	Test drag	lb
ΔV_{pos}	Airspeed position error	kn
e	Oswald’s efficiency factor	
E_h	Energy height	ft
FPA	Flight path accelerometer	
F_x	Forces parallel to flight path	lb
g	Gravitational acceleration	ft/s^2
g_c	Conversion constant	32.17 lb_m/slug
h	Tapeline altitude	ft
H_{P_c}	Calibrated pressure altitude	ft
$H_{P_{c\,ref}}$	Reference calibrated pressure altitude	ft
H_{P_i}	Indicated pressure altitude	ft
INS	Inertial navigation system	
KE	Kinetic energy	ft-lb

K_T	Temperature recovery factor	
M	Mach number	
MAX	Maximum power	
MIL	Military power	
M_{Std}	Standard Mach number	
M_{Test}	Test Mach number	
n_z	Normal acceleration	g
OAT	Outside air temperature	˚C
P_A	Power available	ft-lb/s
P_a	Ambient pressure	psf
PE	Potential energy	ft-lb
POPU	Push-over, pull-up	
P_{req}	Power required	ft-lb/s
P_s	Specific excess power	ft/s
P_{ssl}	Standard sea level pressure	2116.217 psf
$P_{s_{Std}}$	Standard specific excess power	ft/s
$P_{s_{Test}}$	Test specific excess power	ft/s
q_c	Impact pressure	psf
R	Engineering gas constant for air	96.93ft-lb_f/lb_m-˚K
S	Wing area	ft^2
SS	Split-S	
T	Temperature	˚C, or ˚K
	Thrust	lb
t	Time	s
T_a	Ambient temperature	˚K
$T_{a_{Std}}$	Standard ambient temperature	˚K
$T_{a_{Test}}$	Test ambient temperature	˚K
TE	Total energy	ft-lb
T_{N_x}	Net thrust parallel flight path	lb
T_{Std}	Standard thrust	lb
T_{Test}	Test thrust	lb
V	Velocity	ft/s
V_c	Calibrated airspeed	kn
V_i	Indicated airspeed	kn
V_o	Observed airspeed	kn

V_T	True airspeed	kn, ft/s
$V_{T_{Std}}$	Standard true airspeed	ft/s
$V_{T_{Test}}$	Test true airspeed	ft/s
W	Weight	lb
W_f	Fuel weight	lb
W_{Std}	Standard weight	lb
W_{Test}	Test weight	lb
WUT	Wind-up-turn	
$\dot{W}_f$	Fuel flow	lb/h

5.9.2 GREEK SYMBOLS

α (alpha)	Angle of attack	deg
α_j	Thrust angle	deg
γ (gamma)	Flight path angle	deg
	Ratio of specific heats	
γ_{Std}	Standard flight path angle	deg
γ_{Test}	Test flight path angle	deg
π (pi)	Constant	
θ_{Std} (theta)	Standard temperature ratio	
θ_{Test}	Test temperature ratio	

5.10 REFERENCES

1. Rutowski, E.S., *Energy Approach to the General Aircraft Maneuverability Problem*, Journal of the Aeronautical Sciences, Vol 21, No 3, March 1954.

2. Powell, J., *Airplane Performance*, USNTPS Classroom Notes, USNTPS, Patuxent River, MD.

3. USAF Test Pilot School, *Performance Phase Textbook Volume I*, USAF-TPS-CUR-86-01, USAF, Edwards AFB, CA, April, 1986.

CHAPTER 6

TURN PERFORMANCE AND AGILITY

CHAPTER 6

FIGURES

CHAPTER 6

EQUATIONS

$\omega = \frac{V_T}{R}$	(Eq 6.13)	6.6
$\omega = \frac{g}{V_T} \tan\phi$	(Eq 6.14)	6.6
$\omega = \frac{g}{V_T} \sqrt{\left(n_z^2 - 1\right)}$	(Eq 6.15)	6.6
$\phi = \tan^{-1}\left(\frac{F_Y}{W}\right)$	(Eq 6.16)	6.8
$L = \frac{W}{\cos\phi}$	(Eq 6.17)	6.8
$\Delta L = F_Y \tan\phi$	(Eq 6.18)	6.9
$F_R = W \tan\phi + \frac{F_Y}{\cos\phi}$	(Eq 6.19)	6.10
$n_R = \tan\phi + \frac{n_Y}{\cos\phi}$	(Eq 6.20)	6.10
$\phi_E = \tan^{-1}\left(\tan\phi + \frac{n_Y}{\cos\phi}\right)$	(Eq 6.21)	6.10
$R = \frac{V_T^2}{g\left(\tan\phi + \frac{n_Y}{\cos\phi}\right)}$	(Eq 6.22)	6.10
$\omega = \frac{g\left(\tan\phi + \frac{n_Y}{\cos\phi}\right)}{V_T}$	(Eq 6.23)	6.10
$\Delta\omega = \frac{g\, n_Y}{V_T \cos\phi}$	(Eq 6.24)	6.10
$n_R = n_z - \cos\gamma$	(Eq 6.25)	6.12

$$R_{(\text{wings level})} = \frac{V_T^2}{g\left(n_z - \cos\gamma\right)}$$ (Eq 6.26) 6.12

$$\omega_{(\text{wings level})} = \frac{g\left(n_z - \cos\gamma\right)}{V_T}$$ (Eq 6.27) 6.12

$$L = C_L q\, S + T_G \sin\alpha_j$$ (Eq 6.28) 6.16

$$n_z = \frac{C_L q}{W/S} + \frac{T_G}{W} \sin\alpha_j$$ (Eq 6.29) 6.16

$$n_{z_{max}} = \frac{C_{L_{max}}\, q}{(W/S)_{min}}$$ (Eq 6.30) 6.17

$$n_{z_{max}} = \frac{C_{L_{max}}}{(W/S)_{min}}\ 0.7\ P_a M^2$$ (Eq 6.31) 6.17

$$n_{z_{max}} = K M^2$$ (Eq 6.32) 6.17

$$K = \frac{0.7}{(W/S)}\ C_{L_{max}} P_a$$ (Eq 6.33) 6.17

$$\frac{1}{V_{s\,(1g)}^{\ 2}} = \frac{n_L}{V_A^{\ 2}}$$ (Eq 6.34) 6.18

$$V_A = V_{s\,(1g)} \sqrt{n_L}$$ (Eq 6.35) 6.18

$$R = \frac{a^2\ M^2}{g\sqrt{K^2 M^4 - 1}}$$ (Eq 6.36) 6.20

$$\omega = \frac{g\sqrt{K^2 M^4 - 1}}{a\, M}$$ (Eq 6.37) 6.21

$K = \frac{0.7}{(W/S)} \; C_{L_{max}} \; P_a$	(Eq 6.38)	6.21
$R_{min_{V>V_A}} = \left(\frac{a^2}{g \sqrt{n_L^2 - 1}} \right) M^2$	(Eq 6.39)	6.23
$\omega_{max_{V>V_A}} = \left(\frac{g \sqrt{n_L^2 - 1}}{a} \right) \frac{1}{M}$	(Eq 6.40)	6.23
$D = \frac{C_D}{C_L} \; L$	(Eq 6.41)	6.29
$T = \frac{C_D}{C_L} \; n_z W$	(Eq 6.42)	6.29
$n_z = \frac{T}{W} \frac{C_L}{C_D}$	(Eq 6.43)	6.29
$n_{z_{sust_{max}}} = \frac{T}{W} \left(\frac{C_L}{C_D} \right)_{max}$ (Jet)	(Eq 6.44)	6.29
$n_z = \frac{T\left(V_T\right)}{W} \; \frac{L}{D\left(V_T\right)}$	(Eq 6.45)	6.29
$n_{z_{sust_{max}}} = \frac{THP_{avail}}{W} \; \frac{L}{\left(THP_{req}\right)_{min}}$ (Propeller)	(Eq 6.46)	6.30
$\omega_{sust} = \frac{57.3 \, g}{V_T} \sqrt{n_{z_{sust}}^2 - 1}$ (deg/s)	(Eq 6.47)	6.30
$R_{sust} = \frac{V_T^{\;2}}{g \sqrt{n_{z_{sust}}^2 - 1}}$	(Eq 6.48)	6.30

$$\frac{T}{\delta} = f\left(M, \frac{\dot{W}_f}{\delta_T \sqrt{\theta_T}}\right)$$

(Eq 6.49) 6.32

$$\frac{\Delta D}{\delta} = \frac{\Delta T}{\delta}$$

(Eq 6.50) 6.33

$$\Delta D_{Std\text{-}Test} = \frac{1}{\pi e AR\ S\ (0.7)\ P_{ssl}\ \delta_{Test}\ M^2}\left[\left(n_z W\right)^2_{Std} - \left(n_z W\right)^2_{Test}\right]$$

(Eq 6.51) 6.34

$$n_{z_{Std}} = \sqrt{\frac{1}{W^2_{Std}}\left[\left(n_z W\right)^2_{Test} + \Delta T\,\pi\ e\ AR\,(0.7)\ S\ P_{ssl}\ \delta_{Test}\ M^2\right]}$$

(Eq 6.52) 6.34

$$n_{z_{Std}} = n_{z_{Test}}\left(\frac{W_{Test}}{W_{Std}}\right)$$

(Eq 6.53) 6.35

$$T_{ex} = T - D = \frac{W}{V_T}\frac{dh}{dt} + \frac{W}{g}\frac{dV_T}{dt}$$

(Eq 6.54) 6.38

$$\frac{dV_T}{dt} = \frac{11.3\ P_s}{V_T}$$

(Eq 6.55) 6.48

$$n_z = n_{z_o} + \Delta n_{ic} + \Delta n_{z\ tare}$$

(Eq 6.56) 6.57

$$V_i = V_o + \Delta V_{ic}$$

(Eq 6.57) 6.63

$$V_c = V_i + \Delta V_{pos}$$

(Eq 6.58) 6.63

$$H_{P_i} = H_{P_o} + \Delta H_{P_{ic}}$$

(Eq 6.59) 6.63

$$H_{P_c} = H_{P_i} + \Delta H_{pos}$$

(Eq 6.60) 6.63

$$n_{z_i} = n_{z_o} + \Delta n_{z_{ic}}$$

(Eq 6.61) 6.63

$n_{z_{Test}} = n_{z_i} + \Delta n_{z_{tare}}$	(Eq 6.62)	6.63
$C_{L_{max_{Test}}} = \dfrac{n_{z\ Test}\ W_{Test}}{0.7\ P_{ssl}\ \delta_{Test}\ M^2\ S}$	(Eq 6.63)	6.63
$V_T = a\ M$	(Eq 6.64)	6.64
$\Delta T = T_{Std} - T$	(Eq 6.65)	6.66
$n_{z_{sust}} = \sqrt{\dfrac{P_{s_{1g}}\ \pi\ e\ AR\ S\ \ 0.7\ P_{ssl}\delta\ M^2}{V_T W_{Std}} + 1}$	(Eq 6.66)	6.68
$T_{ex} = T - D = \dfrac{W_{Std}}{V_T}\ P_{s_{1g}}$	(Eq 6.67)	6.68
$n_{z_{sust}} = \sqrt{\left(\dfrac{n_z W_{Std}}{\delta\ M}\right)^2 \dfrac{\delta_h}{W_{Std}}\ M}$	(Eq 6.68)	6.68
$n_z = \left(\dfrac{\delta}{W}\right)\left(0.7\ P_{ssl}\ S\right)\ C_L\ M^2$	(Eq 6.69)	6.71
$\left(n_z \dfrac{W}{\delta}\right)_{Test} = \left(0.7\ P_{ssl}\ S\right) C_L\ M^2$	(Eq 6.70)	6.71

CHAPTER 6

TURN PERFORMANCE AND AGILITY

6.1 INTRODUCTION

This chapter covers airplane turning performance and agility characteristics. Sustained and instantaneous turn performance characteristics are developed, and measures of agility are presented. Test techniques are described for documenting turn rate, turn radius, and excess energy while maneuvering. Data reduction methods and analysis techniques are described for evaluating and comparing airplane turning performance and maneuvering characteristics.

6.2 PURPOSE OF TEST

The purpose of these tests is to determine the turning performance and maneuvering characteristics of the airplane, with the following objectives:

1. Measure sustained and instantaneous turn performance.
2. Measure maneuvering excess energy characteristics.
3. Present agility measures and airplane comparison methods.
4. Define mission suitability issues.

6.3 THEORY

6.3.1 MANEUVERING

An airplane inflight has a velocity vector which defines its speed and direction of flight. The capacity to change this vector is called maneuverability. Quantifying the maneuverability of an airplane involves documenting the acceleration, deceleration, and turning characteristics. These characteristics are not independent, as the analysis shows; however, they can be isolated for study with the help of specialized test techniques. The level acceleration testing, introduced in Chapter 5, isolated the acceleration characteristics from the increased drag of turning flight. In this chapter, turn performance is introduced at constant speed, to isolate the turning characteristics from flight path accelerations. Then, the combined characteristics of accelerations and turns are addressed using a total energy approach.

In maneuvering, the forces of lift, weight, thrust, and drag are altered to generate linear or radial accelerations. The radial acceleration causes a turn in the horizontal, in the vertical, or in an oblique plane. Forces which cause a radial acceleration include: weight, sideforce, lift, and thrust (although thrust is easily included in the lift and sideforce terms). Each of these forces can curve the flight path, turning the airplane. Visualizing how weight can turn the flight path is easy. For example, at zero g (though the resulting ballistic flight path is not generally thought of as a turn). Sideforce can cause the flight path to curve, allowing level turns to be performed at zero bank angle. The most common force used to turn, however, is the lift force. Lift variations at zero bank angle can cause the flight path to curve up or down, but most turns are performed by tilting the lift vector from the vertical. Generally, a turn has vertical and horizontal components, although the one easiest to analyze is the level turn.

6.3.2 LEVEL TURNS

All of the forces which can be used to alter the velocity vector contribute to maneuverability. For level turns the turning forces are lift, thrust, and sideforce. Lift is the primary force and is investigated first. Turn radius and turn rate expressions are developed, then the effects of sideforce and thrust are discussed.

6.3.2.1 FORCES IN A TURN

Consider an airplane in a steady, level turn which is coordinated in the sense sideforce is zero, as depicted in figure 6.1.

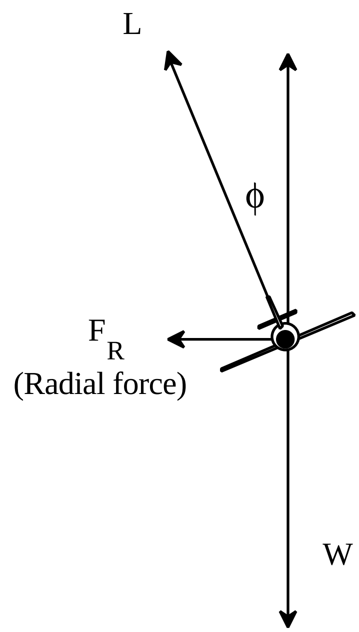

Figure 6.1

FORCES IN A STEADY LEVEL TURN

The turning force produces a radial acceleration which can be measured. The following steps derive an expression for the radial acceleration. Load factor, n_z, is defined by the expression:

$$n_z = \frac{L}{W} \tag{Eq 6.1}$$

From the right triangle of lift and its components:

$$L^2 = W^2 + (W \tan\phi)^2 \tag{Eq 6.2}$$

Dividing by W^2, gives:

$$n_z^2 = 1 + \tan^2\phi \tag{Eq 6.3}$$

Or:

$$\tan \phi = \sqrt{\left(n_z^2 - 1\right)} \qquad \text{(Eq 6.4)}$$

Summing the forces in the vertical yields:

$$L \cos \phi = W \qquad \text{(Eq 6.5)}$$

Substituting for W using Eq 6.1:

$$n_z = \frac{1}{\cos \phi} \qquad \text{(Eq 6.6)}$$

The horizontal summation yields:

$$W \tan \phi = \frac{W}{g} a_R \qquad \text{(Eq 6.7)}$$

Simplifying, and rearranging gives an expression for a_R:

$$a_R = g \tan \phi \qquad \text{(Eq 6.8)}$$

In terms of load factor:

$$a_R = g \sqrt{\left(n_z^2 - 1\right)} \qquad \text{(Eq 6.9)}$$

Where:

a_R	Radial acceleration	ft/s^2
ϕ	Bank angle	deg
g	Gravitational acceleration	ft/s^2
L	Lift	lb
n_z	Normal acceleration	g
W	Weight	lb.

6.3.2.2 TURN RADIUS AND TURN RATE

The primary characteristics which describe a turn are the turn radius and turn rate. Expressions for these characteristics are developed using the following depiction of an airplane in a steady, level turn (Figure 6.2).

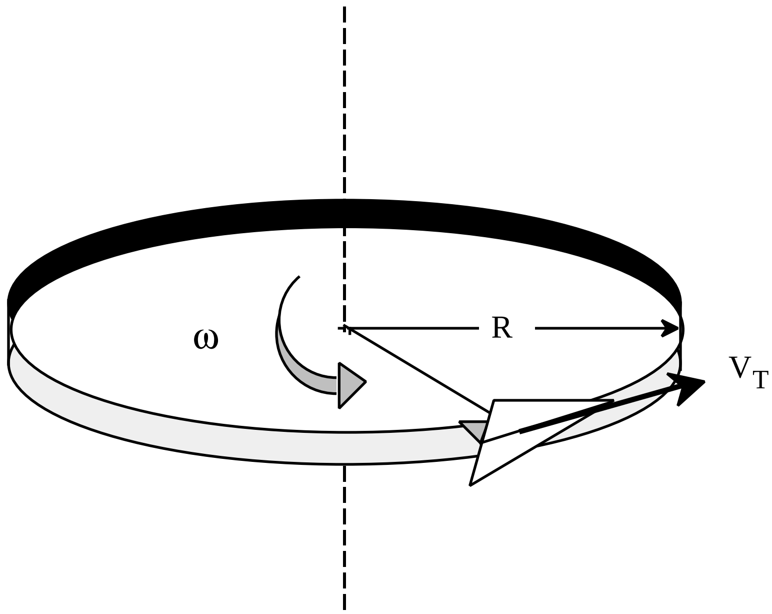

Figure 6.2
STEADY TURN DIAGRAM

The radius, R, of a level turn is calculated using the following relationship:

$$R = \frac{V_T^2}{a_R} \qquad \text{(Eq 6.10)}$$

Substituting for a_R, using Eq 6.8:

$$R = \frac{V_T^2}{g \tan \phi} \qquad \text{(Eq 6.11)}$$

Using Eq 6.9:

$$R = \frac{V_T^2}{g\sqrt{\left(n_z^2 - 1\right)}} \qquad \text{(Eq 6.12)}$$

Turn radius varies with true airspeed and load factor as depicted in figure 6.3.

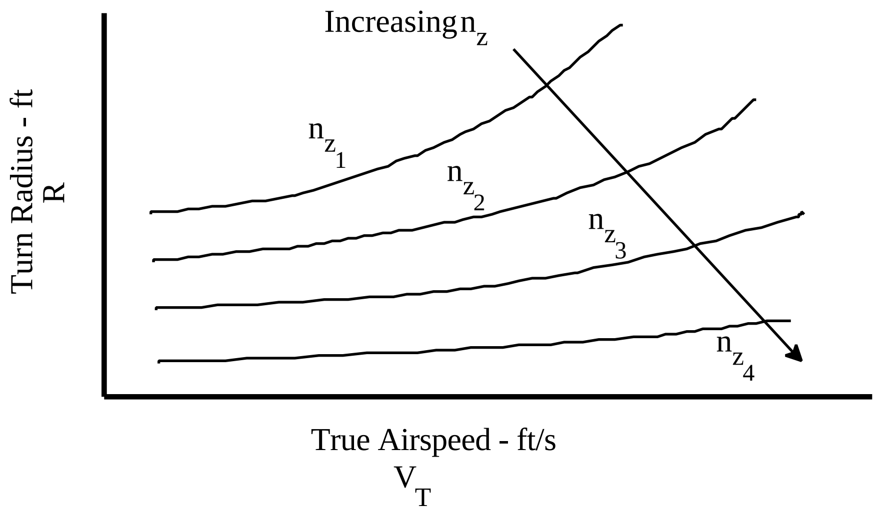

Figure 6.3
TURN RADIUS

Turn rate, ω, is expressed as:

$$\omega = \frac{V_T}{R} \qquad \text{(Eq 6.13)}$$

Eq 6.11 or 6.12 can be used to calculate turn rate as follows:

$$\omega = \frac{g}{V_T}\tan\phi \qquad \text{(Eq 6.14)}$$

$$\omega = \frac{g}{V_T}\sqrt{\left(n_z^2 - 1\right)} \qquad \text{(Eq 6.15)}$$

Where:

a_R	Radial acceleration	ft/s^2
ϕ	Bank angle	deg
g	Gravitational acceleration	ft/s^2
n_z	Normal acceleration	g
R	Turn radius	ft
V_T	True airspeed	ft/s
ω	Turn rate	rad/s.

Turn rate varies with true airspeed and load factor as depicted in figure 6.4. A line, from the origin, representing a constant $\frac{\omega}{V_T}$, relates to a particular turn radius.

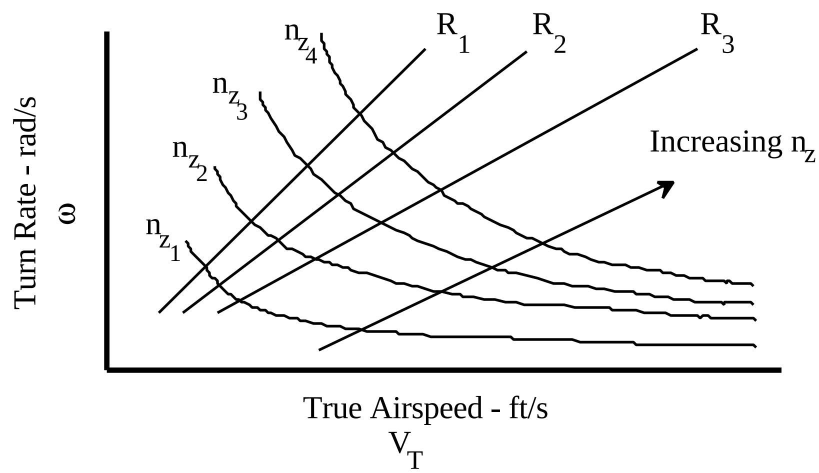

Figure 6.4
TURN RATE

6.3.2.3 SIDEFORCE EFFECTS

The preceding treatment of level turns dealt exclusively with coordinated turns, turns with no sideforce. To see the effects of non-zero sideforce, consider an airplane in a wings-level steady turn, as shown in figure 6.5(a).

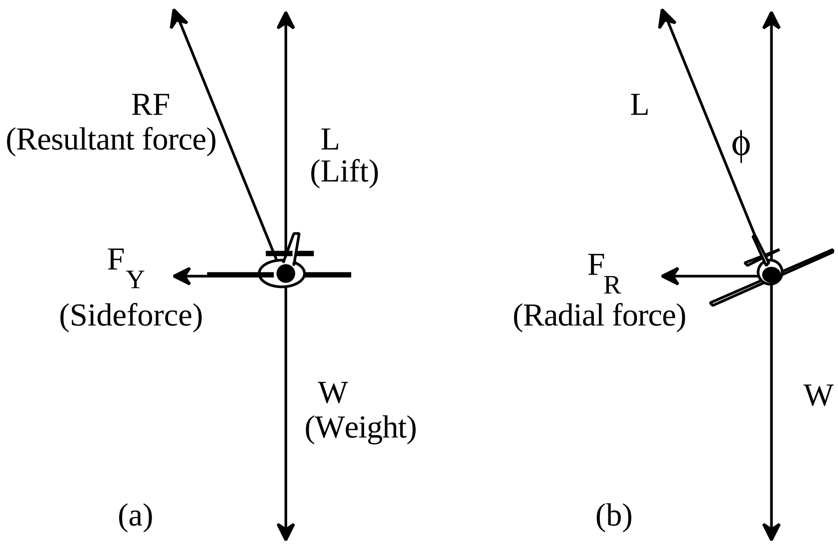

Figure 6.5

FLAT TURN AND COORDINATED TURN COMPARISON

For this example, the sideforce, F_Y, is a purely radial force which produces a flat turn (zero bank angle). An equivalent coordinated turn, shown in figure 6.5(b), results if the airplane is banked to an angle, ϕ:

$$\phi = \tan^{-1}\left(\frac{F_Y}{W}\right) \quad \text{(Eq 6.16)}$$

The lift, L, required in this case is:

$$L = \frac{W}{\cos\phi} \quad \text{(Eq 6.17)}$$

Next, consider the effect of sideforce in a steady uncoordinated turn, as shown in figure 6.6.

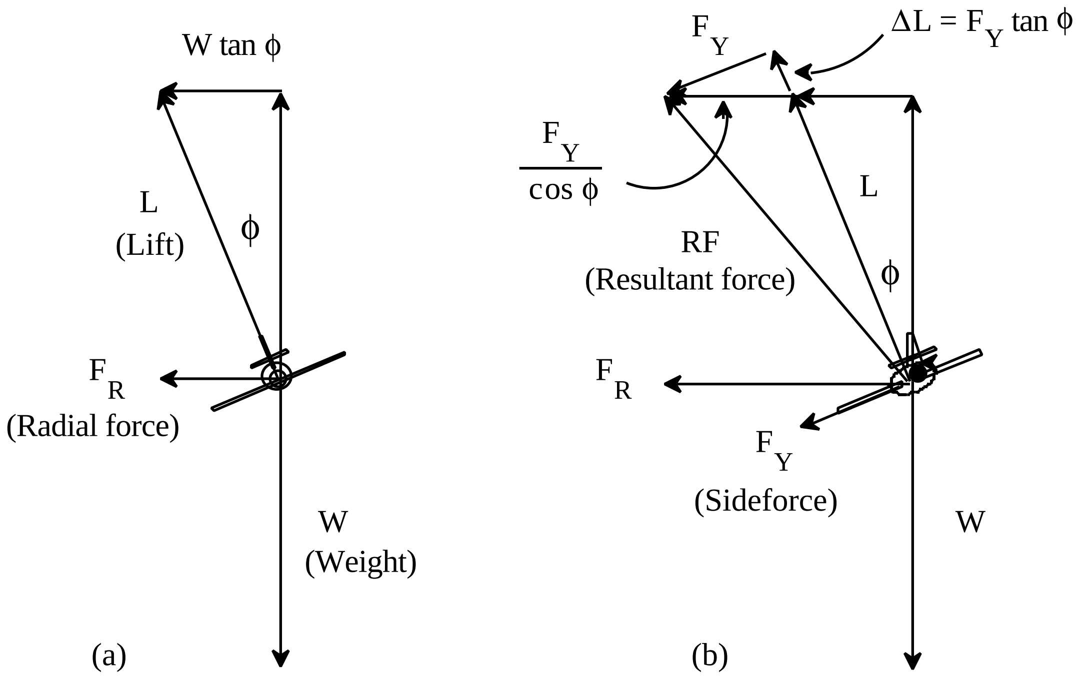

Figure 6.6

COORDINATED AND UNCOORDINATED TURN COMPARISON

Figure 6.6 (a) depicts the airplane in a steady turn of constant bank angle ϕ, with no sideforce. In this case, the resultant force and the lift are the same, and equal to $\frac{W}{\cos\phi}$. Figure 6.6 (b) shows the addition of sideforce in the direction of the turn, keeping the bank angle constant. Notice that the resultant force is no longer coincident with the lift, but its vertical component must remain equal to W. An increase in lift, ΔL, is required (at some drag penalty) to offset the negative lift from the sideforce. This extra lift requirement depends upon the amount of sideforce and the angle of bank, according to the expression:

$$\Delta L = F_Y \tan\phi \tag{Eq 6.18}$$

The radial force for this example is greater than for figure 6.6 (a) by the increment $\frac{F_Y}{\cos\phi}$, composed of the radial components of F_Y and ΔL. The total radial force is expressed as:

$$F_R = W \tan\phi + \frac{F_Y}{\cos\phi} \qquad \text{(Eq 6.19)}$$

Normalizing, to get load factor terms:

$$n_R = \tan\phi + \frac{n_Y}{\cos\phi} \qquad \text{(Eq 6.20)}$$

The resulting turn is equivalent to a coordinated turn at the equivalent bank angle, ϕ_E, as shown below:

$$\phi_E = \tan^{-1}\left(\tan\phi + \frac{n_Y}{\cos\phi}\right) \qquad \text{(Eq 6.21)}$$

Expressions for turn radius and turn rate which include a sideforce term are:

$$R = \frac{V_T^2}{g\left(\tan\phi + \frac{n_Y}{\cos\phi}\right)} \qquad \text{(Eq 6.22)}$$

And:

$$\omega = \frac{g\left(\tan\phi + \frac{n_Y}{\cos\phi}\right)}{V_T} \qquad \text{(Eq 6.23)}$$

Note if $n_Y = 0$, the above equations reduce to the form of Eq 6.11 and 6.14, for coordinated turns.

The presence of sideforce in a turn alters the turn rate and radius. The increase in turn rate with augmenting sideforce, $\Delta\omega$, is expressed by:

$$\Delta\omega = \frac{g\, n_Y}{V_T \cos\phi} \qquad \text{(Eq 6.24)}$$

Where:

ϕ	Bank angle	deg
ϕ_E	Equivalent bank angle	deg
F_R	Radial force	lb
F_Y	Sideforce	lb
g	Gravitational acceleration	ft/s^2
n_R	Radial load factor, $\frac{F_R}{W}$	g
n_Y	Sideforce load factor, $\frac{F_Y}{W}$	g
n_z	Normal acceleration	g
R	Turn radius	ft
V_T	True airspeed	ft/s
ω	Turn rate	rad/s.

Though it appears sideforce can be used to augment turning performance, in practice it is a relatively inefficient and uncomfortable means to turn. It may have potential uses, however, in decoupled control modes of fly-by-wire airplanes. For example, direct sideforce control can be used to turn without banking for course corrections in a weapons delivery mode.

6.3.2.4 THRUST EFFECTS

For this discussion, the thrust component of lift is assumed constant and is absorbed in the lift term. In practice, the thrust component may be significant if thrust lift is a large percentage of total lift. Later sections present the effects of thrust lift, particularly low speed effects with vectored thrust.

6.3.3 VERTICAL TURNS

Vertical turns highlight the influence of the weight vector on turns. In the level turn, weight does not contribute to the radial force. In the vertical turn, however, weight contributes directly to the radial force. The contribution depends upon the changing orientation of the lift and weight vectors in the vertical turn. Consider the variation of radial acceleration for a constant speed loop, with a constant 4 g indicated on the cockpit accelerometer, as shown in figure 6.7.

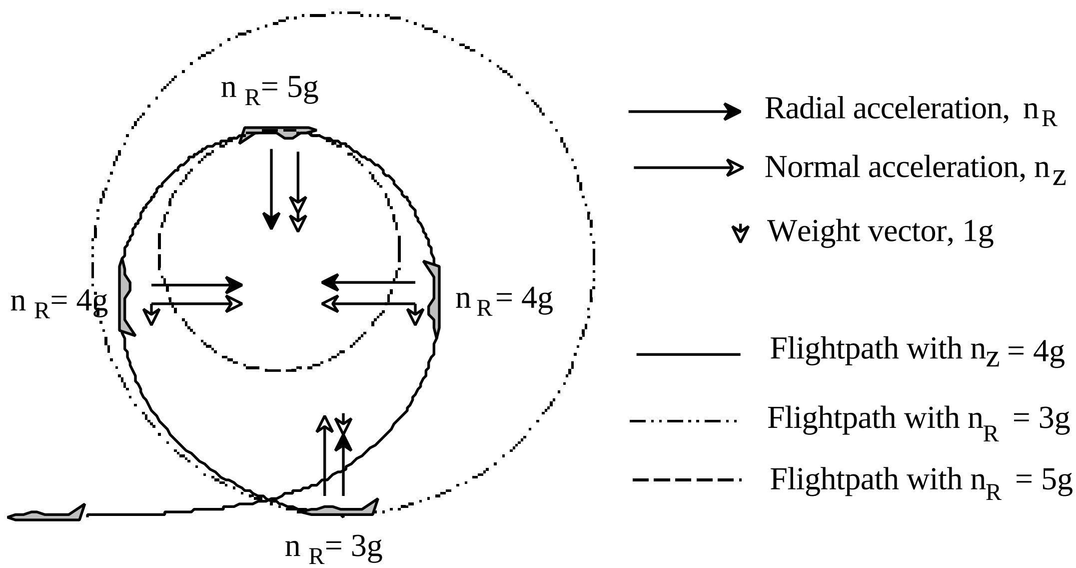

Figure 6.7

VARIATION OF RADIAL ACCELERATION IN A CONSTANT SPEED, 4 G LOOP

The radial load factor can be expressed as:

$$n_R = n_z - \cos\gamma \qquad \text{(Eq 6.25)}$$

The changing radial acceleration causes the turn radius and turn rate to vary, as well. The generalized expressions for turn radius and turn rate are:

$$R_{(\text{wings level})} = \frac{V_T^2}{g\left(n_z - \cos\gamma\right)} \qquad \text{(Eq 6.26)}$$

and,

$$\omega_{(\text{wings level})} = \frac{g\left(n_z - \cos\gamma\right)}{V_T} \qquad \text{(Eq 6.27)}$$

Where:

γ	Flight path angle	deg
g	Gravitational acceleration	ft/s^2
n_R	Radial load factor	g
n_z	Normal acceleration	g
R	Turn radius	ft
V_T	True airspeed	ft/s
ω	Turn rate	rad/s.

The orientation of the lift vector to the weight vector has a significant effect on turn performance, as shown in the following turn data from 15,000 ft. Figure 6.8 presents the turning capability of an airplane in different orientations. In this figure, the typical horizontal turn is compared to turns in the vertical plane. The pull-up and pull-down cases are similar to the bottom and the top of a loop, respectively. The straight up/down data refer to the cases where the pitch attitude is plus or minus 90 deg.

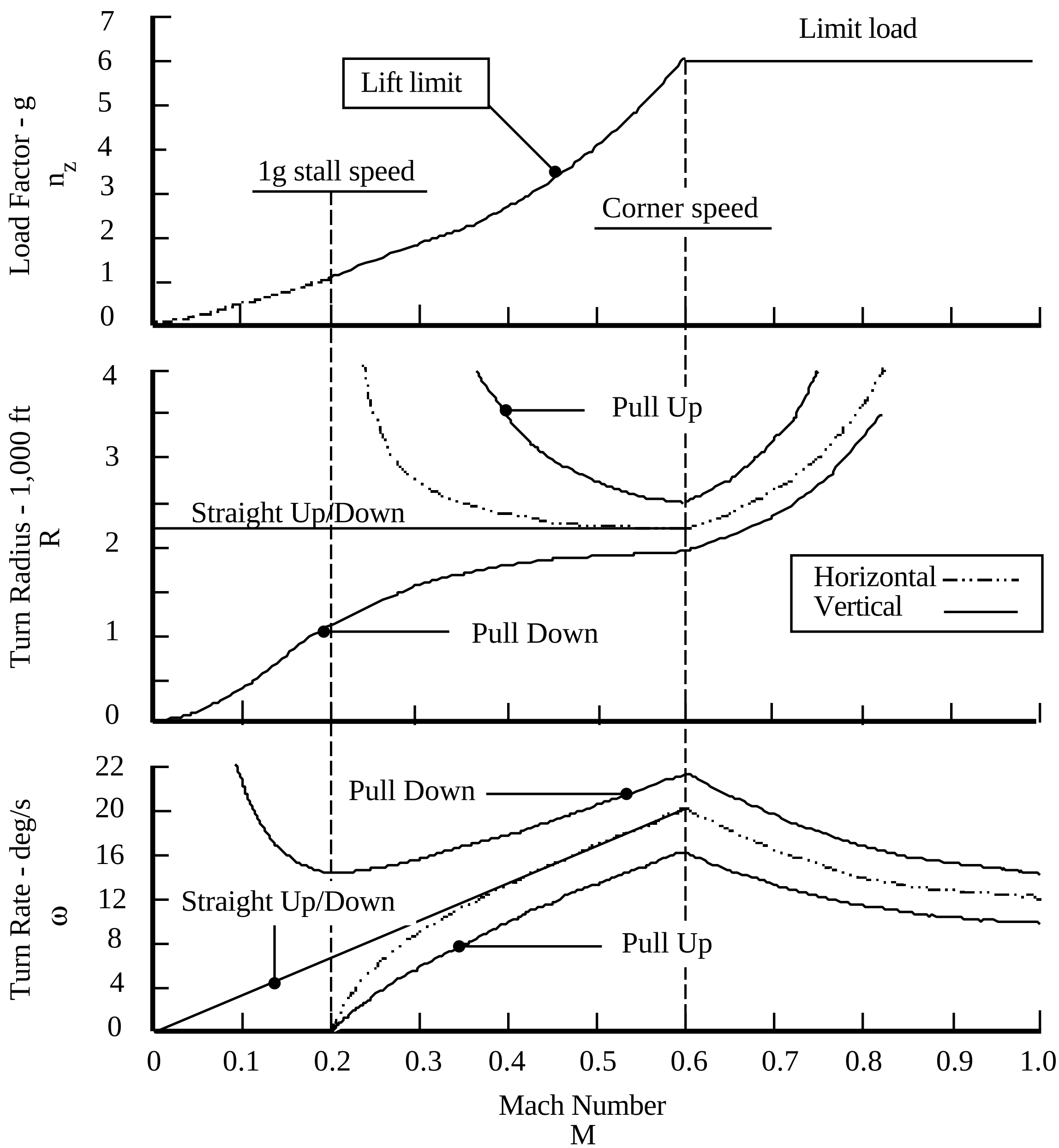

Figure 6.8
VERTICAL TURN PERFORMANCE

The weight vector can be used to tighten a turn, only if the lift vector is pointed below the horizon. Whenever the nose of the airplane is pulled up, the turn is hampered by the weight vector. The advantage of using the weight vector to tighten a turn is short-lived, but it can be exploited in a variety of tactical situations.

6.3.4 INSTANTANEOUS TURN PERFORMANCE

Instantaneous performance describes the capability of an airplane at a particular flight condition, at an instant in time. There is no consideration of the airplane’s ability to sustain the performance for any length of time, nor is there any consideration of the energy rate at these conditions. Energy loss rate may be high, and is manifested usually by rapid deceleration or altitude loss. The engine is capable of changing the energy loss rate at these conditions. The energy situation is covered in a later section. First, consider the maneuvering potential of the airframe alone. Instantaneous turn performance is a function of the lift capability and the structural strength of the airframe.

6.3.4.1 THE V-N DIAGRAM

The V-n diagram is a useful format for presenting airframe lift capabilities and structural strength limitations. On this plot, airplane operating envelopes are mapped on a grid of airspeed and load factor. Any set of criteria can be used to define envelope boundaries on a V-n diagram. For example, the operational, service, and permissible envelopes referred to in the fixed wing flying qualities specification are described by V-n diagrams. However, the most common V-n diagram describes maximum aerodynamic capabilities and strength limitations, as depicted in figure 6.9.

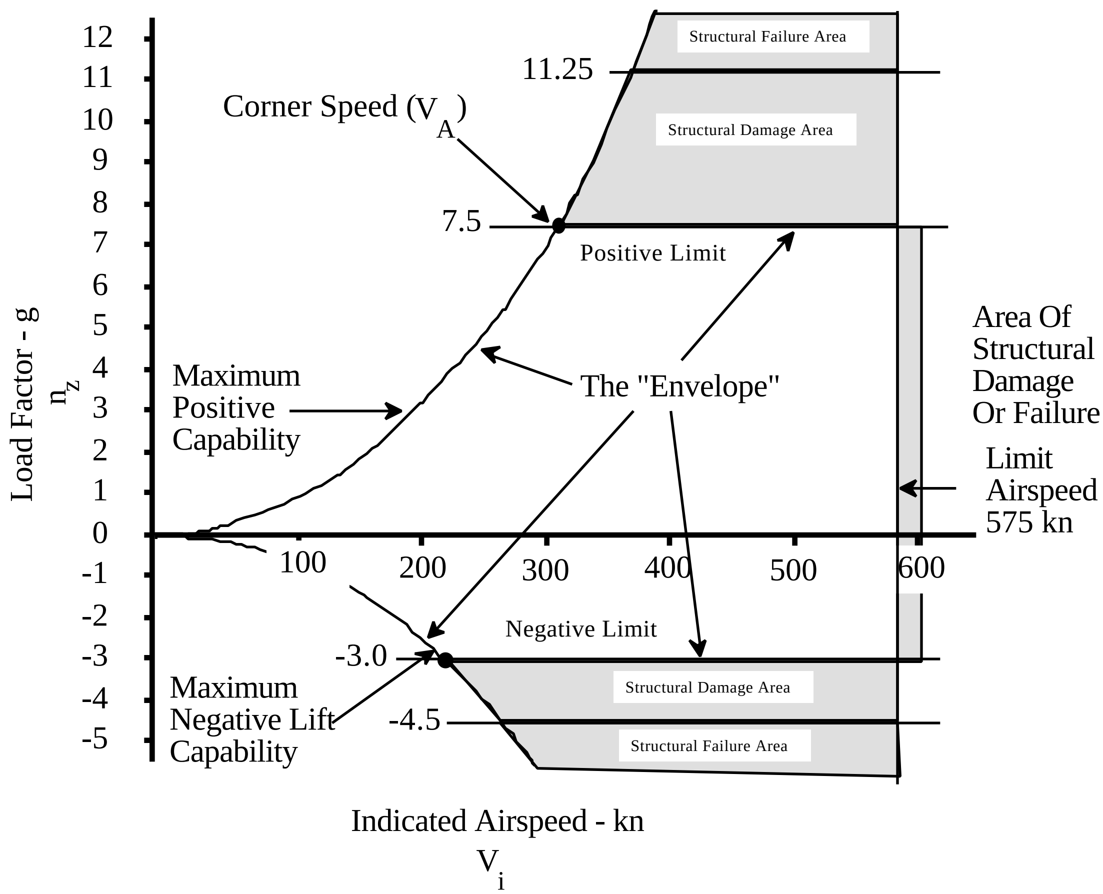

Figure 6.9
THE V-N DIAGRAM

Beginning at zero airspeed, two curves diverge to describe the maximum lift boundaries for positive and negative load factors. Since the lines represent stall, operations to the left of these curves are beyond the capability of the airplane, except in dynamic, unsteady maneuvers such as zoom climbs. From the example shown, steady flight is not attainable below 100 kn, the 1 g stall speed. At 200 kn, 4 g is attainable, and so on, with increasing load factor capability as speed is increased. At some speed, the load factor available is equal to the load limit of the airframe, n_L. This speed is called the corner speed or maneuvering speed, $V_{A.}$ The significance of V_A is developed in later sections. The same constraints define the negative load factor capabilities and negative g corner speed. Notice the negative g available at any particular speed is typically lower than the positive g available, due to the wing camber and control power effects. The envelope is bounded on the right for all load factors by the limit airspeed, V_L.

The lift boundary of the V-n diagram is the primary focus of flight test documentation. The airplane is able to develop n_L at all speeds above V_A, though it may be difficult to verify near V_L due to the deceleration experienced while pulling to n_L. For airspeeds above V_A, calculations of instantaneous turn performance parameters can be made without documentation, based on the constant n_L out to V_L. Flight tests are required, however, to document the boundary imposed by the lift limit, where the maximum load factor is diminished. The measure of instantaneous maneuverability is not only a high n_L, but also a low V_A.

6.3.4.2 LIFT LIMIT

The emphasis in this section is on the limitation to instantaneous turn performance imposed by the airplane lift capability. The forces contributing to lift are shown in figure 6.10.

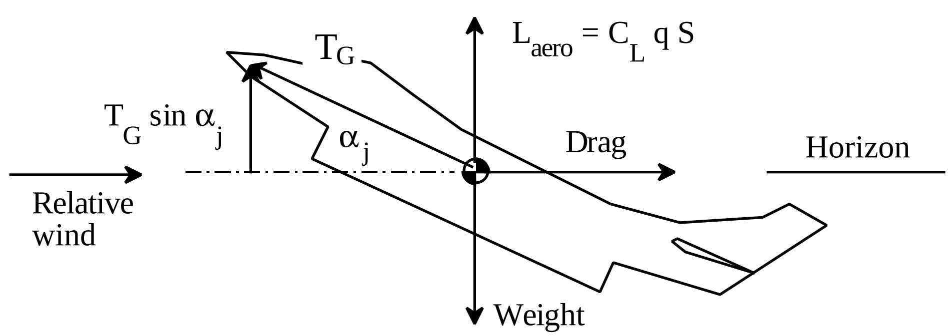

Figure 6.10
FORCES CONTRIBUTING TO LIFT

Total lift is expressed as the sum of aerodynamic lift and thrust lift.

$$L = C_L q\, S + T_G \sin \alpha_j \quad \text{(Eq 6.28)}$$

Normalizing, by dividing by weight,W:

$$n_z = \frac{C_L q}{W/S} + \frac{T_G}{W} \sin \alpha_j \quad \text{(Eq 6.29)}$$

Neglecting thrust effects, the load factor is a function of lift coefficient, dynamic pressure, and wing loading. For a given set of test conditions (altitude and Mach number), the maximum load factor is attained when C_L is maximum and W/S is a minimum:

$$n_{z_{max}} = \frac{C_{L_{max}} q}{(W/S)_{min}} \tag{Eq 6.30}$$

Instantaneous turn performance demands high $C_{L_{max}}$ and low wing loading for attaining high load factors. The maximum lift coefficient is limited by aerodynamic stall, maximum control deflection, or any of a number of adverse flying qualities (see Chapter 3 for additional discussion of stall). Wing loading is variable, since gross weight decreases with fuel depletion and the release of external stores. On some airplanes, variable wing sweep can change the effective wing surface area.

Expressing dynamic pressure in terms of Mach number gives:

$$n_{z_{max}} = \frac{C_{L_{max}}}{(W/S)_{min}} 0.7 \; P_a M^2 \tag{Eq 6.31}$$

Regrouping:

$$n_{z_{max}} = K M^2 \tag{Eq 6.32}$$

Where:

$$K = \frac{0.7}{(W/S)} C_{L_{max}} P_a \tag{Eq 6.33}$$

The following depicts the functional relationship:

$$n_{z_{max}} = f\left(C_{L_{max}}, \frac{W}{S}, H_p, M^2\right)$$

From Eq 6.32, the variation of $n_{z_{max}}$ with Mach number for a particular altitude is parabolic, if $C_{L_{max}}$ and W/S are constant, as shown in figure 6.11.

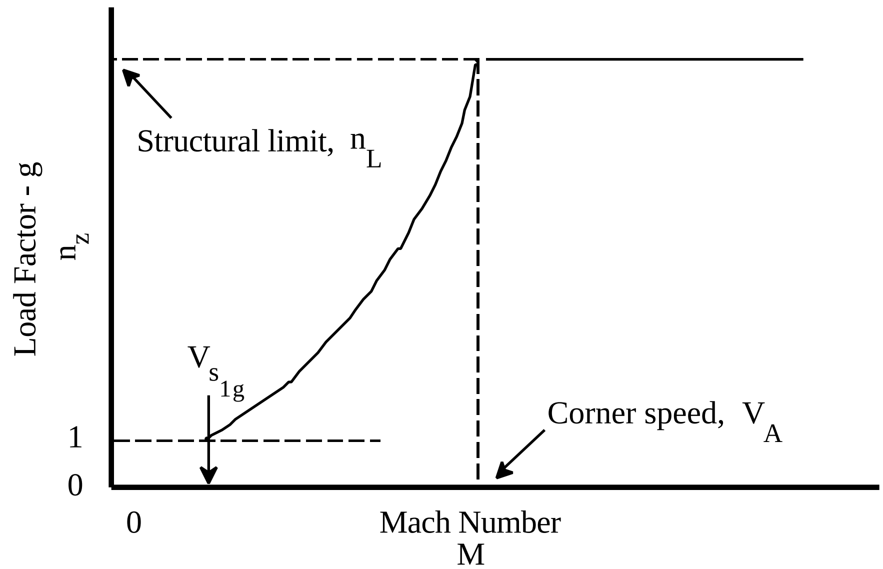

Figure 6.11
MAXIMUM INSTANTANEOUS LOAD FACTOR

This shape is characteristic for the lift boundary of the V-n diagram. If the 1 g stall speed is known, a simple calculation reveals the predicted corner speed, V_A. Since $\frac{n_{z_{max}}}{M^2}$ is constant along the curve, so is $\frac{n_{z_{max}}}{V^2}$. Thus:

$$\frac{1}{V_{s\,(1g)}^{2}} = \frac{n_L}{V_A^{2}} \tag{Eq 6.34}$$

And,

$$V_A = V_{s\,(1g)} \sqrt{n_L} \tag{Eq 6.35}$$

Where:

α_j	Thrust angle	deg
C_L	Lift coefficient	
$C_{L_{max}}$	Maximum lift coefficient	
H_P	Pressure altitude	ft
K	Constant	
L	Lift	lb
L_{aero}	Aerodynamic lift	lb

M	Mach number	
n_L	Limit normal acceleration	g
n_z	Normal acceleration	g
$n_{z_{max}}$	Maximum normal acceleration	g
P_a	Ambient pressure	psf
q	Dynamic pressure	psf
S	Wing area	ft^2
T_G	Gross thrust	lb
V_A	Maneuvering speed	kn, ft/s
V_s	Stall speed	kn or ft/s
W	Weight	lb.

In arriving at figure 6.11, a constant $C_{L_{max}}$ is assumed. This assumption is valid at low Mach number. At higher Mach number compressibility effects must be considered.

6.3.4.3 VARIATION OF MAXIMUM LIFT COEFFICIENT WITH MACH NUMBER

The typical variation of $C_{L_{max}}$ with Mach number for a constant altitude is depicted in figure 6.12.

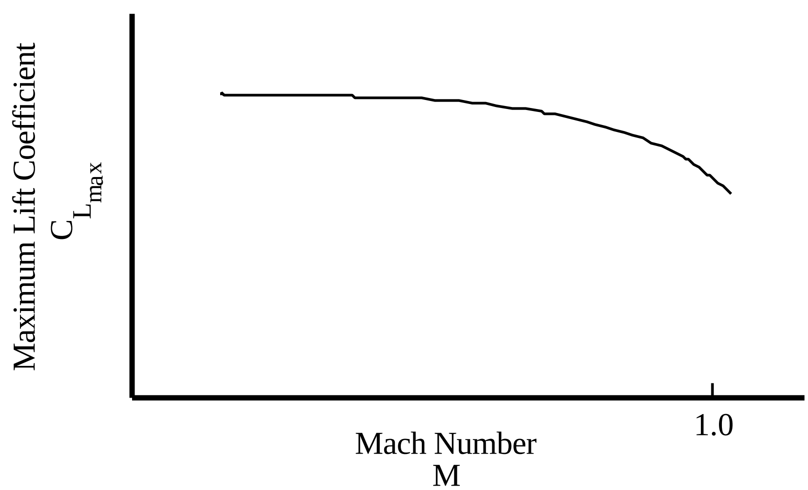

Figure 6.12
VARIATION OF MAXIMUM LIFT COEFFICIENT WITH MACH NUMBER

Up to about 0.7 Mach number, $C_{L_{max}}$ is essentially constant, even for a wing with a relatively thick airfoil section. At higher Mach number, a transonic reduction in $C_{L_{max}}$ is noted, which may begin below the corner speed. The expected reduction in $n_{z_{max}}$ is illustrated in figure 6.13.

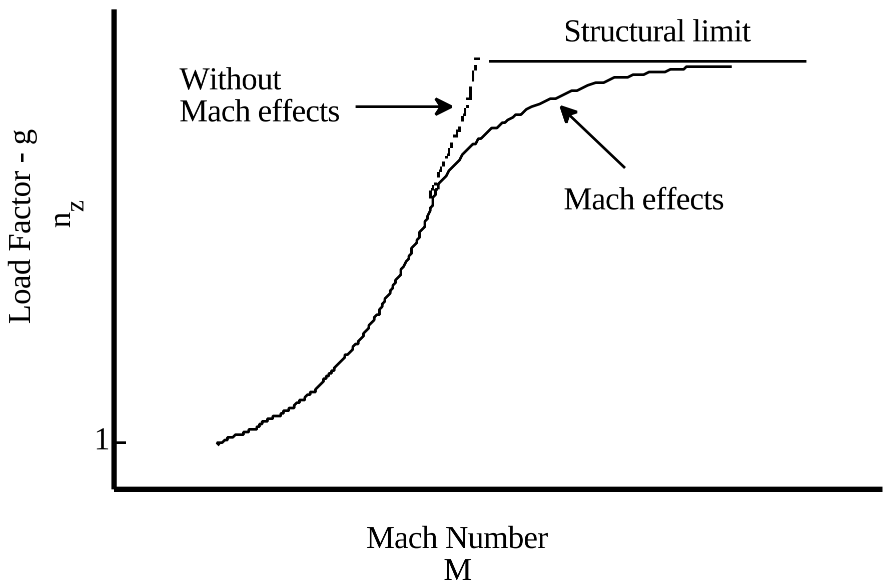

Figure 6.13
MAXIMUM INSTANTANEOUS LOAD FACTOR WITH COMPRESSIBILITY EFFECTS

High performance airplanes, particularly supersonic interceptors and fighters, exhibit this characteristic Mach number effect.

6.3.4.4 INSTANTANEOUS TURN RADIUS AND RATE

Instantaneous turn radius and turn rate vary with Mach number according to these relationships derived from Eq 6.12 and 6.15:

$$R = \frac{a^2 \ M^2}{g \sqrt{K^2 \ M^4 - 1}} \qquad \text{(Eq 6.36)}$$

And:

$$\omega = \frac{g\sqrt{K^2 M^4 - 1}}{a\,M} \qquad \text{(Eq 6.37)}$$

Where:

$$K = \frac{0.7}{(W/S)}\, C_{L_{max}}\, P_a \qquad \text{(Eq 6.38)}$$

Where:

a	Speed of sound	ft/s
$C_{L_{max}}$	Maximum lift coefficient	
g	Gravitational acceleration	ft/s^2
K	Constant	
M	Mach number	
P_a	Ambient pressure	psf
R	Turn radius	ft
S	Wing area	ft^2
ω	Turn rate	rad/s
W	Weight	lb.

For a range of speeds where $C_{L_{max}}$ is constant at a particular altitude, K is constant. Figure 6.14 depicts instantaneous turn performance with constant K.

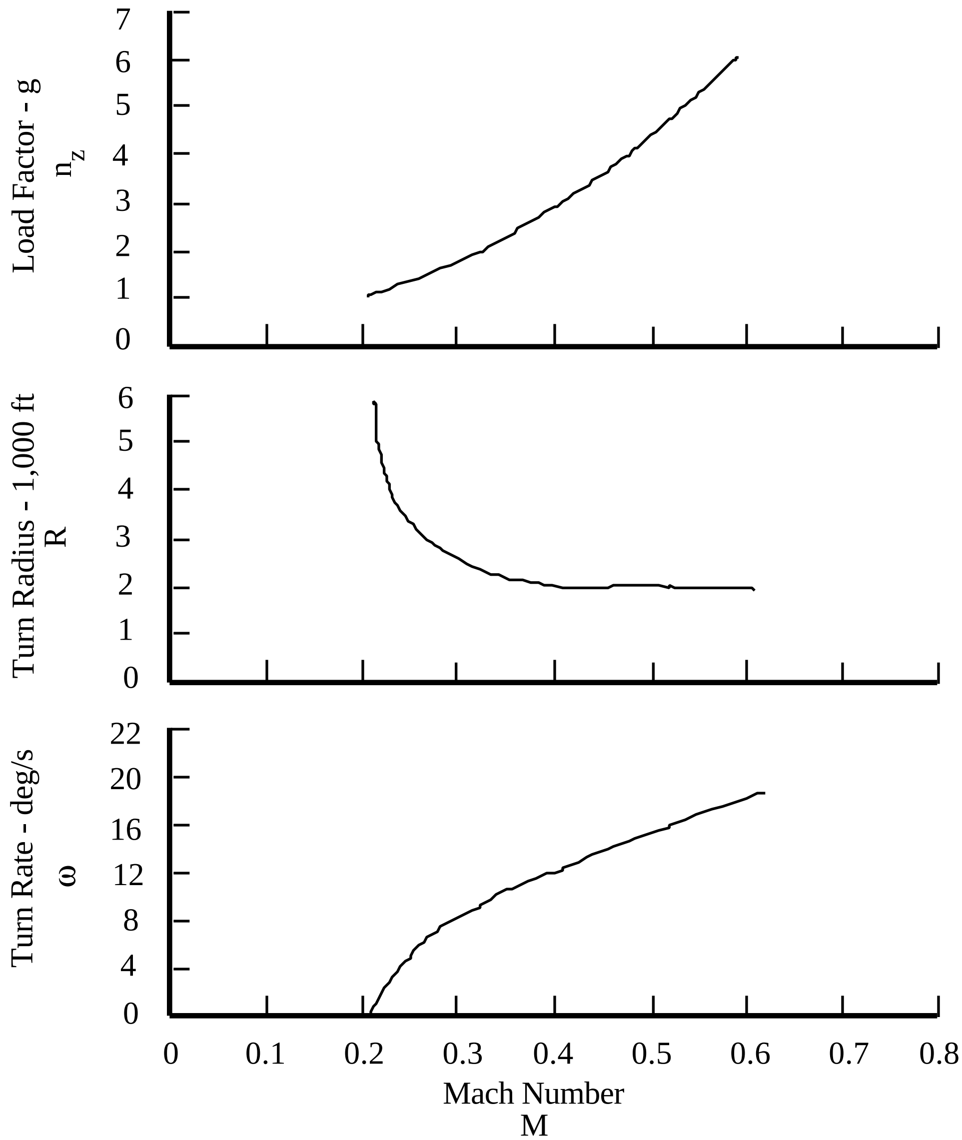

Figure 6.14
INSTANTANEOUS TURN PERFORMANCE USING CONSTANT MAXIMUM LIFT COEFFICIENT

At the 1 g stall speed, no turns can be made; turn radius is infinite and turn rate is zero. As airspeed is increased from the stall speed, turn radius rapidly diminishes, approaching a minimum at a relatively slow airspeed. Turn rate, on the other hand, continues to improve as speed is increased from the stall speed. Both curves become discontinuous at the corner speed, where the limit load factor forces a reduction in $C_{L_{max}}$ as speed increases (K is no longer constant).

6.3.4.5 STRUCTURAL LIMIT

Instantaneous turn performance improves with speed as long as load factor is allowed to increase. Beyond the corner speed, however, load factor is limited by structural strength. The decreases in instantaneous turn performance which result when load factor is limited are evident when examining the following relationships:

$$R_{min\ V>V_A} = \left(\frac{a^2}{g\sqrt{n_L^2 - 1}} \right) M^2 \qquad \text{(Eq 6.39)}$$

And,

$$\omega_{max\ V>V_A} = \left(\frac{g\sqrt{n_L^2 - 1}}{a} \right) \frac{1}{M} \qquad \text{(Eq 6.40)}$$

Where:

a	Speed of sound	ft/s
g	Gravitational acceleration	ft/s^2
M	Mach number	
n_L	Limit normal acceleration	g
$R_{min\ V>V_A}$	Minimum turn radius for $V > V_A$	ft
V_A	Maneuvering speed	ft/s
$\omega_{max\ V>V_A}$	Maximum turn rate for $V > V_A$	rad/s.

Since the quantities within the parentheses are constants, Eq 6.39 is a parabola, and Eq 6.40 is a hyperbola. Adding the segments representing the characteristics at speeds above V_A to figure 6.14, the following composite instantaneous turn performance graphs result (Figure 6.15).

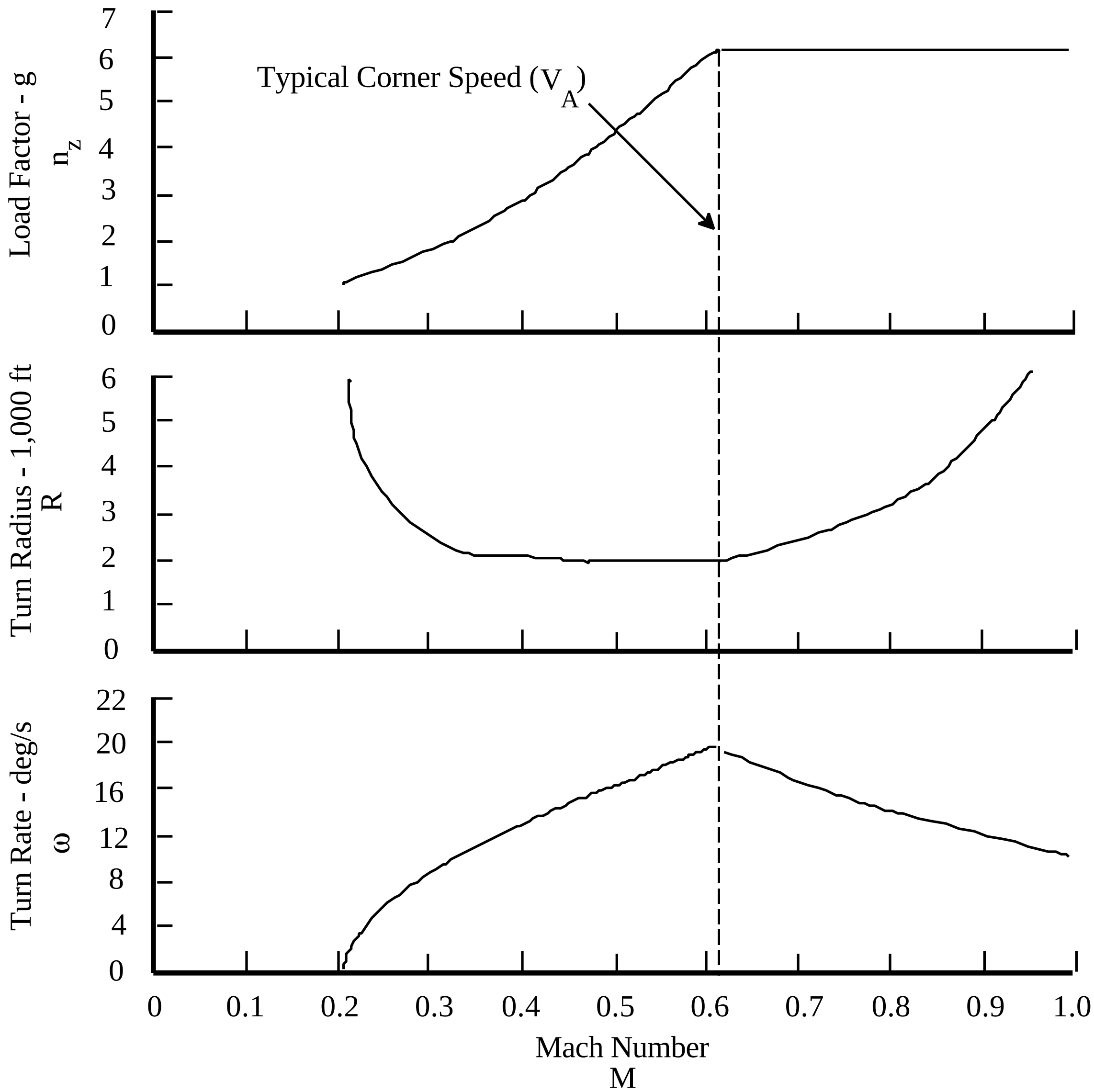

Figure 6.15
INSTANTANEOUS TURN PERFORMANCE

6.3.4.6 CORNER SPEED

The significance of the corner speed can be seen in figure 6.15. At the speed corresponding to the intersection of the lift boundary and the structural limit, the minimum instantaneous turn radius and maximum instantaneous turn rate are achieved. Thus, V_A is the speed for maximum turn performance when energy loss is not a consideration.

6.3.4.7 THRUST LIFT EFFECTS

In the previous discussions, thrust lift was neglected. Current technologies embracing high thrust-to-weight ratios and vectored thrust, however, make the thrust lift contribution significant. To investigate the effects of thrust lift on instantaneous turn performance, reexamine Eq 6.29, repeated here for convenience.

$$n_z = \frac{C_L q}{W/S} + \frac{T_G}{W} \sin \alpha_j \qquad \text{(Eq 6.29)}$$

Where:

α_j	Thrust angle	deg
C_L	Lift coefficient	
n_z	Normal acceleration	g
q	Dynamic pressure	psf
S	Wing area	ft^2
T_G	Gross thrust	lb
W	Weight	lb.

Considering an airplane with adjustable nozzles, like the Harrier, the thrust term in Eq 6.29 could approach unity. Thus, an incremental 1 g is provided by the thrust lift. The contribution from thrust lift is illustrated in figure 6.16, constructed by adding the incremental 1 g at all speeds to the curves in figure 6.15 (though still limited by n_L).

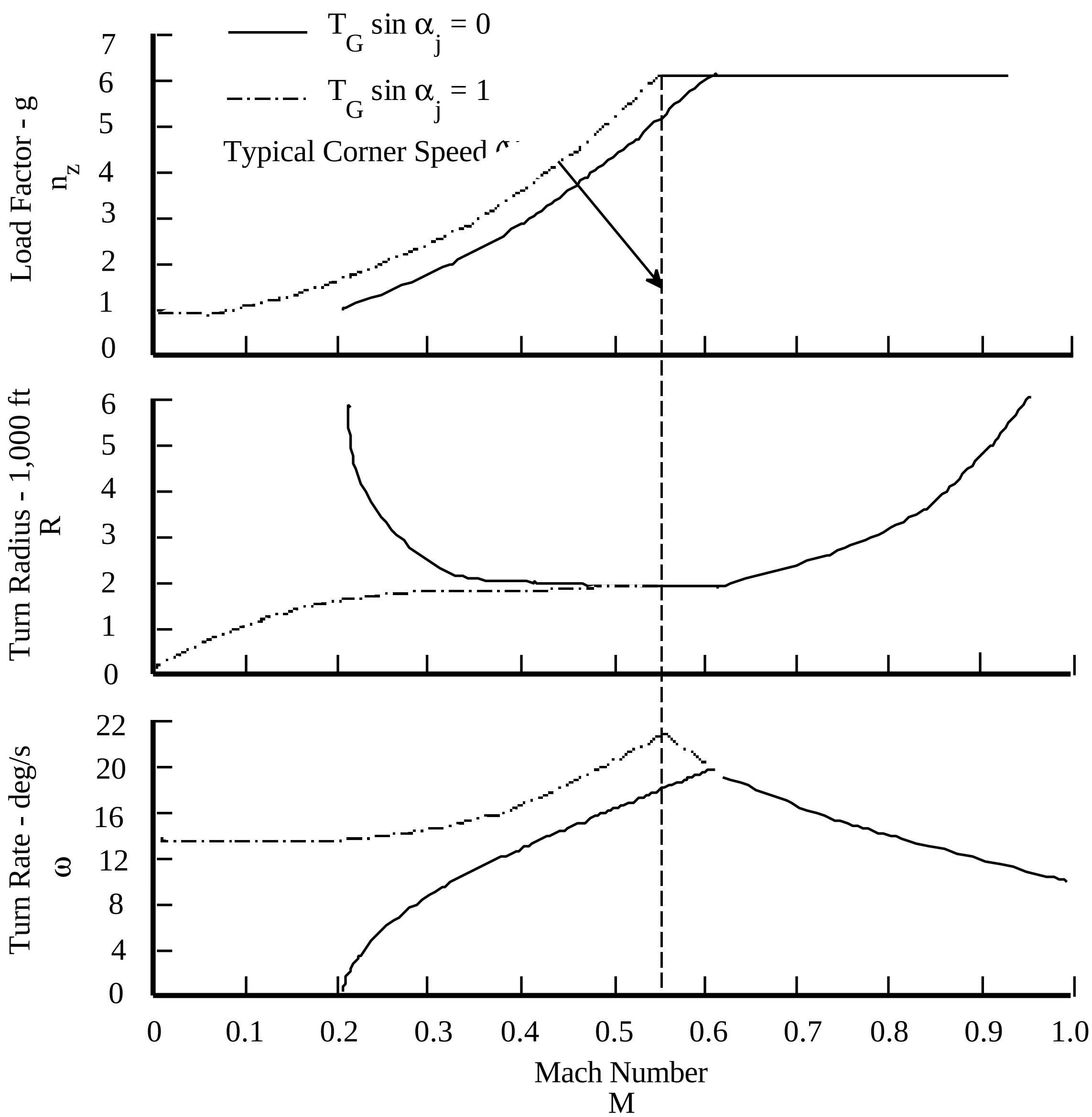

Figure 6.16
INSTANTANEOUS TURN PERFORMANCE WITH VECTORED THRUST

Significant improvements to instantaneous turn performance are realized at low airspeeds. At high airspeeds the vectored thrust contribution is small.

6.3.5 SUSTAINED TURN PERFORMANCE

The concept of sustained maneuverability is used to describe the airplane's ability to maneuver at constant altitude without losing energy and without decelerating. If the airplane is maintaining a level turn at constant airspeed and load factor, the forces along the flight path are balanced. Thrust equals drag for these conditions; therefore, the amount of maneuvering drag the airplane can balance is limited by the maximum thrust. Any changes in thrust available or drag will affect the sustained turning performance. The sustained turning capability may also be limited by airframe considerations.

For a level turn at a particular airspeed, the airplane uses excess thrust to counter the increased drag. Thrust available varies with ambient temperature, Mach number and altitude. Thrust required varies with Mach number and W/δ. Figure 6.17 depicts the difference between thrust available and thrust required.

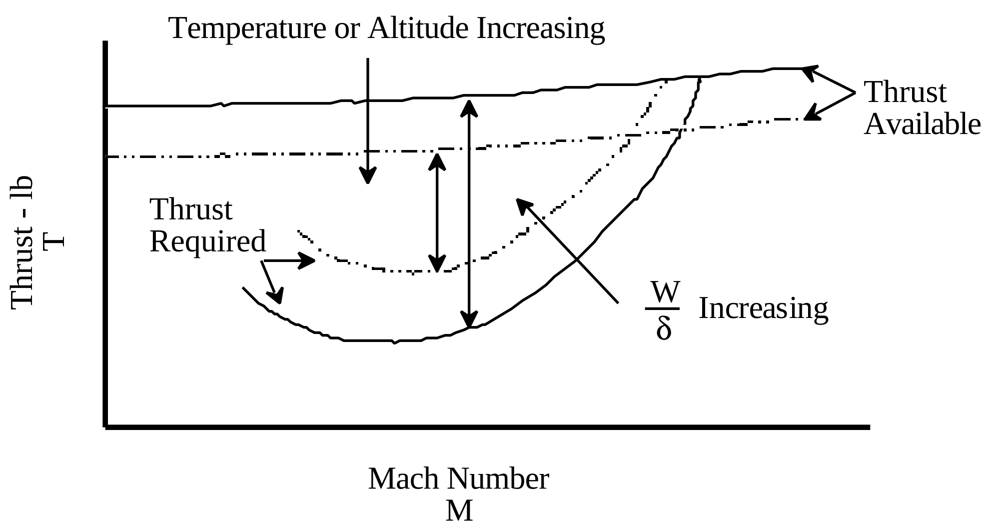

Figure 6.17
EXCESS THRUST

For stabilized level flight, thrust equals drag. At 1 g, the result is that thrust required varies with referred weight, W/δ, Mach number, and Reynold’s number. For the maneuvering case, since lift equals n_zW, the thrust required varies with n_zW/δ. Changes in W at 1 g are equivalent to changes in n_z at constant W. Figure 6.18 graphically depicts this relationship.

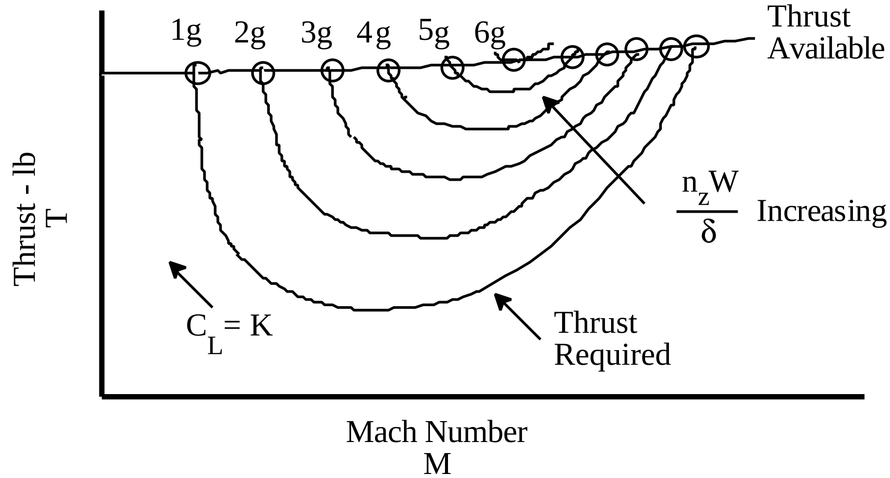

Figure 6.18
VARIATION OF EXCESS THRUST WITH LOAD FACTOR

This figure can be used to interpret the sustained turning performance. The intersections of the thrust required and available curves for various load factors indicate the airspeeds at which the airplane can sustain that load factor in a level turn. A crossplot of those intersections yields a sustained turn performance graph shown in figure 6.19.

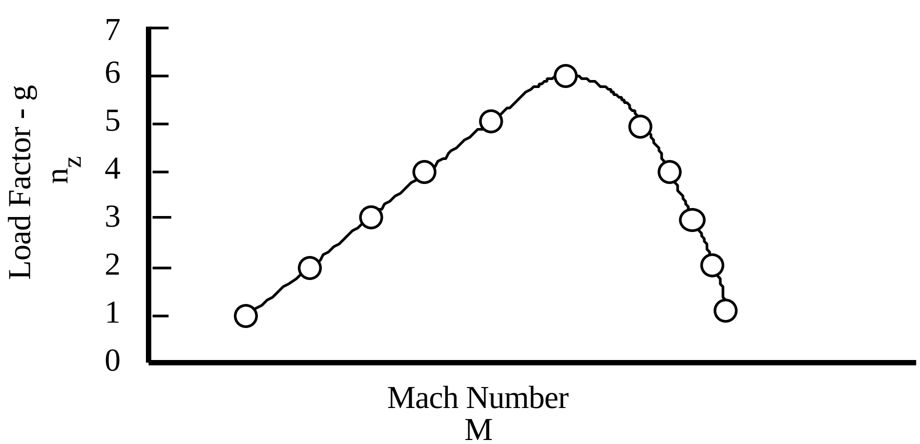

Figure 6.19
SUSTAINED TURN PERFORMANCE

6.3.5.1 SUSTAINED LOAD FACTOR

The conditions for maximum sustained load factor are found by observing in stabilized level turns, thrust equals drag. Using the general form of the drag equation:

$$D = \frac{C_D}{C_L} L \tag{Eq 6.41}$$

Substitute n_zW for L, and T for D:

$$T = \frac{C_D}{C_L} n_z W \tag{Eq 6.42}$$

Rearranging:

$$n_z = \frac{T}{W} \frac{C_L}{C_D} \tag{Eq 6.43}$$

The maximum load factor results when the product of thrust-to-weight and lift-to-drag ratios is maximized. For a jet, where thrust available is assumed to be constant with velocity, the result is:

$$n_{z_{sust_{max}}} = \frac{T}{W} \left(\frac{C_L}{C_D} \right)_{max} \quad \text{(Jet)} \tag{Eq 6.44}$$

The maximum sustained load factor occurs at the maximum lift-to-drag ratio for a jet airplane. For a propeller airplane, the result is:

$$n_z = \frac{T\left(V_T\right)}{W} \frac{L}{D\left(V_T\right)} \tag{Eq 6.45}$$

Substituting,

$$n_{z_{sust_{max}}} = \frac{THP_{avail}}{W} \frac{L}{\left(THP_{req}\right)_{min}} \qquad (\text{Propeller})$$

(Eq 6.46)

Where:

C_D	Drag coefficient	
C_L	Lift coefficient	
D	Drag	lb
L	Lift	lb
n_z	Normal acceleration	g
$n_{z\ sust\ max}$	Maximum sustained normal acceleration	g
T	Thrust	lb
THP_{avail}	Thrust horsepower available	hp
THP_{req}	Thrust horsepower required	hp
V_T	True airspeed	ft/s
W	Weight	lb.

Since thrust horsepower available is constant, the maximum sustained load factor occurs at minimum power required for a propeller airplane.

6.3.5.2 SUSTAINED TURN RADIUS AND TURN RATE

Sustained turn radius and turn rate are calculated using the following level turn equations:

$$\omega_{sust} = \frac{57.3\ g}{V_T} \sqrt{n_{z_{sust}}^2 - 1} \qquad (\text{deg/s})$$

(Eq 6.47)

And,

$$R_{sust} = \frac{V_T^{\ 2}}{g \sqrt{n_{z_{sust}}^2 - 1}}$$

(Eq 6.48)

Where:

g	Gravitational acceleration	ft/s^2
$n_{z\ sust}$	Sustained normal acceleration	g
R_{sust}	Sustained turn radius	ft
V_T	True airspeed	ft/s
ω_{sust}	Sustained turn rate	deg/s.

Typical curves for sustained turn performance are presented together with the results from instantaneous turn performance in figure 6.20.

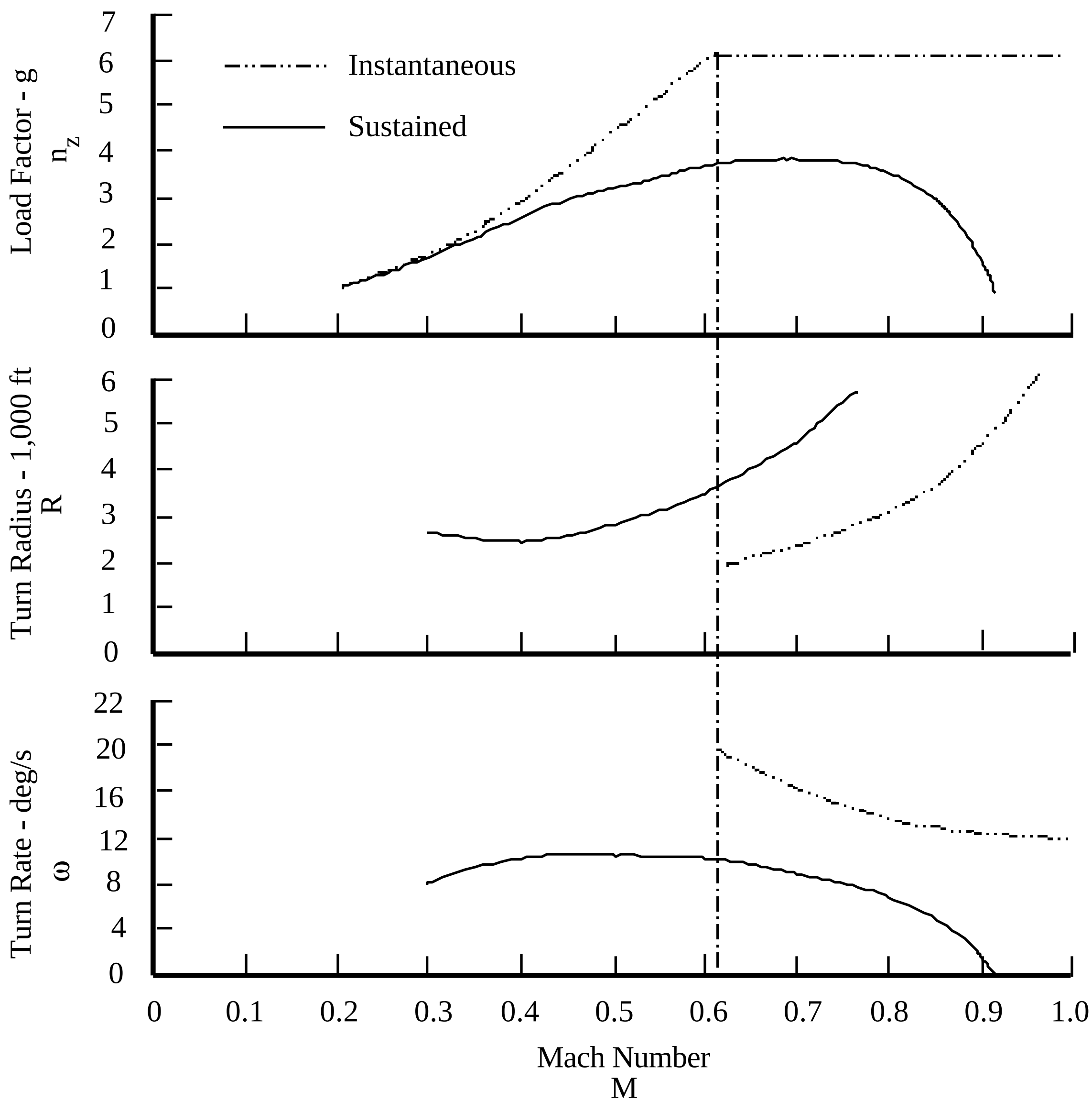

Figure 6.20
TURN PERFORMANCE CHARACTERISTICS

6.3.5.3 CORRECTIONS TO STANDARD DAY CONDITIONS

The maximum sustained load factor in a level turn is achieved when the drag balances the excess thrust at the particular flight conditions tested. Any variations in thrust available will alter the amount of drag which can be balanced. To correlate test data and refer it to standard conditions, the thrust characteristics of the engine must be known.

6.3.5.3.1 THRUST CORRECTION

Values of load factor obtained at test conditions must be corrected to account for variations in thrust from standard conditions. Measuring inflight thrust is not easy, but corrections to thrust are relatively straightforward. The procedure requires both an engine model and a drag model. Lacking either of these models, thrust correction cannot be made.

Thrust is a function of engine speed, altitude, Mach number, and ambient temperature, T_a. Analysis shows referred thrust, T/δ, has only two variables:

$$\frac{T}{\delta} = f\left(M, \frac{\dot{W}_f}{\delta_T \sqrt{\theta_T}}\right) \tag{Eq 6.49}$$

For a given airplane and engine, the maximum RPM is a constant; the thrust correction is for temperature variation alone. A typical plot of the variation of referred thrust with fuel flow referred to total conditions is presented as figure 6.21.

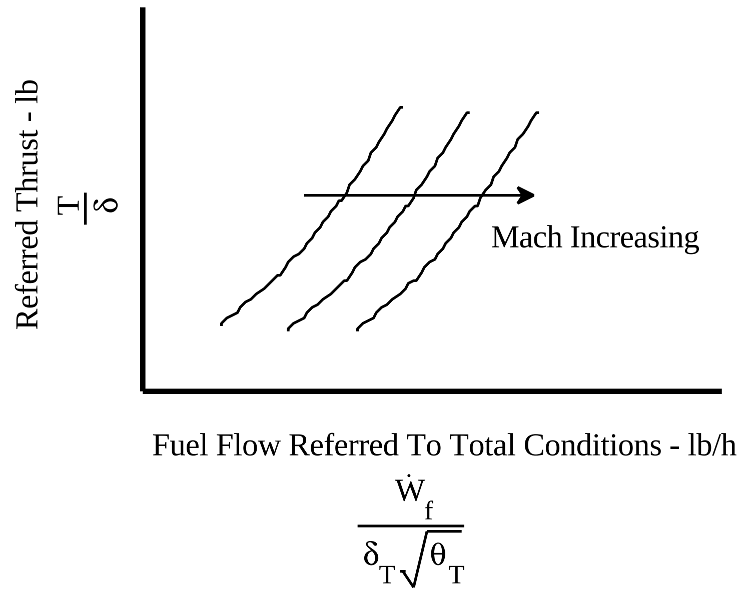

Figure 6.21
REFERRED THRUST REQUIRED

For any test Mach number, the thrust differential can be found by comparing the value of referred thrust obtained from test day referred engine speed, and referred thrust based upon the standard conditions. The difference is a function of temperature alone.

Since the thrust equals drag constraint applies to standard conditions, as well as test conditions, the difference in drag, ΔD, is identical to the thrust differential, ΔT.

$$\frac{\Delta D}{\delta} = \frac{\Delta T}{\delta} \tag{Eq 6.50}$$

To relate the drag differential to a sustained load factor correction, the corresponding lift differential must be found. The drag model is required for this step.

The drag polar is typically determined from level flight and acceleration tests. A parabolic drag polar is shown in figure 6.22 as an example.

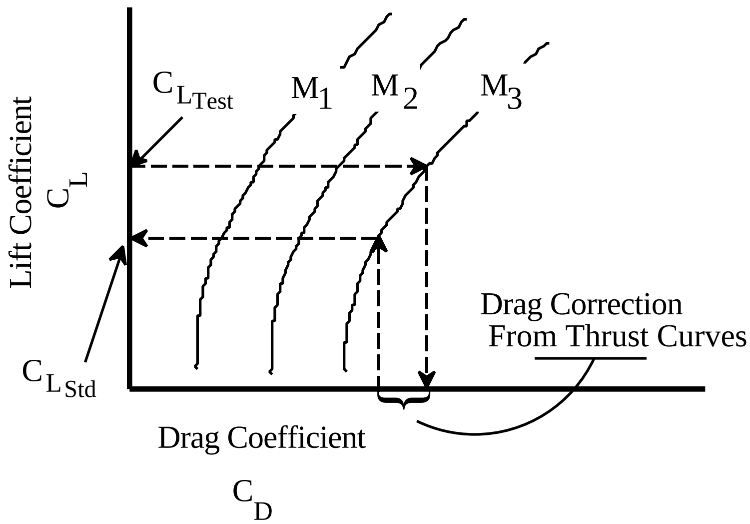

Figure 6.22
SAMPLE DRAG POLAR

For each test lift coefficient, a corresponding drag coefficient can be obtained from the drag polar. The drag differential (equal to the thrust differential) is added and the drag polar is used once again to obtain a corrected lift coefficient. Finally, the corrected lift coefficient is used to calculate the standard day load factor.

The drag correction can also be calculated if the equation for the polar is known. Given the thrust differential from the engine curves, the equivalent drag differential has this form for a parabolic drag polar:

$$\Delta D_{Std\text{-}Test} = \frac{1}{\pi e AR\, S\, (0.7)\, P_{ssl}\, \delta_{Test}\, M^2} \left[\left(n_z W\right)^2_{Std} - \left(n_z W\right)^2_{Test} \right] \quad \text{(Eq 6.51)}$$

Solving the above Eq for $n_{z\,Std}$ and substituting ΔT for ΔD,

$$n_{z_{Std}} = \sqrt{\frac{1}{W^2_{Std}} \left[\left(n_z W\right)^2_{Test} + \Delta T\, \pi\, e\, AR \left(0.7\right) S\, P_{ssl}\, \delta_{Test}\, M^2 \right]} \quad \text{(Eq 6.52)}$$

Where:

AR	Aspect ratio	
D	Drag	lb
δ	Pressure ratio	
D_{Std}	Standard drag	lb
D_{Test}	Test drag	lb
δ_{Test}	Test pressure ratio	
M	Mach number	
$\frac{N}{\sqrt{\theta}}$	Referred engine speed	RPM
n_z	Normal acceleration	g
π	Constant	
P_{ssl}	Standard sea level pressure	psf
S	Wing area	ft^2
T	Thrust	lb
W	Weight	lb.

6.3.5.3.2 GROSS WEIGHT CORRECTION

Lacking either the thrust model or the drag polar, thrust cannot be corrected. If the thrust correction to standard conditions is assumed to be zero, the drag correction and the lift differential must be zero as well. The correction to standard weight reflects the condition where lift (n_zW) is constant for the two conditions. Notice the weight correction is contained in thrust correction (in Eq 6.52, let $\Delta T = 0$):

$$n_{z_{Std}} = n_{z_{Test}} \left(\frac{W_{Test}}{W_{Std}} \right) \qquad \text{(Eq 6.53)}$$

Where:

$n_{z_{Std}}$	Standard normal acceleration	g
$n_{z_{Test}}$	Test normal acceleration	g
W_{Std}	Standard weight	lb
W_{Test}	Test weight	lb.

6.3.6 THE MANEUVERING DIAGRAM

The instantaneous and sustained performance characteristics are often displayed together on an energy maneuvering(E-M) diagram, also called a doghouse plot. Such a plot is shown in figure 6.23

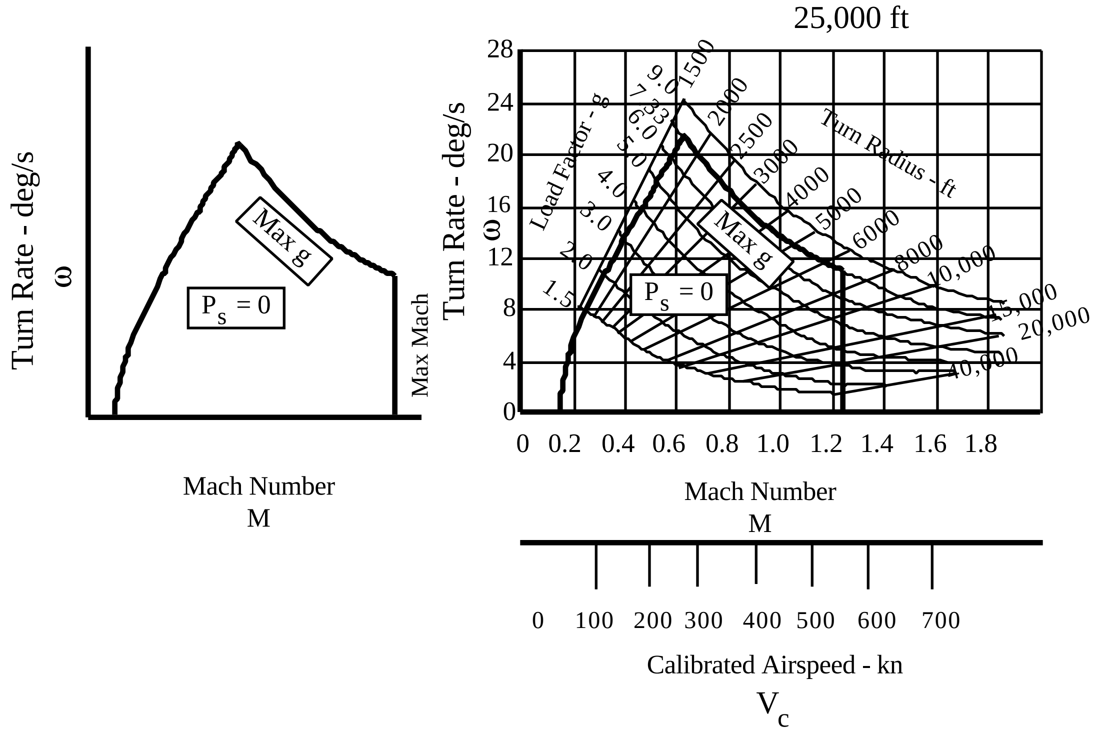

Figure 6.23
MANEUVERING DIAGRAM

In figure 6.23, the diagram grid refers to only one altitude and one weight, expressing the following relevant instantaneous and sustained turning parameters: load factor, turn radius, turn rate, Mach number, and airspeed. To plot the turn performance characteristics for another altitude, the maneuvering diagram for that altitude must be used. Notice data reduction in this format is minimal, since only one of the turn performance parameters (n_z, R, ω) is needed to specify all three.

This diagram is extremely useful in documenting and comparing airplanes. A major weakness in this depiction, however, is it doesn't indicate performance over a time interval (except for the $P_s = 0$ condition). It doesn't show, for example, how long the instantaneous performance can be maintained. To investigate these dynamic performance characteristics, a total energy analysis is made.

6.3.7 MANEUVERING ENERGY RATE

The previous sections define and describe maneuvering performance at a constant speed. To investigate maneuvering performance when speed is changing, it is necessary to describe the relationship between linear accelerations and radial accelerations. In Chapter 5, acceleration performance was covered in detail using an energy analysis. In this and subsequent sections, the energy analysis is applied to maneuvering performance and the results are combined with acceleration performance to provide a measure of airplane agility. A brief review of energy concepts follows.

As an airplane flies, propulsive energy from the fuel is added to the total energy state of the airplane in the form of an increase in either potential or kinetic energy. When the airplane maneuvers, energy is dissipated against drag. The relative energy gain and loss characteristics of an airplane during maneuvering are important measures of its dynamic performance.

As in the 1 g case, the excess thrust characteristics determine the actual energy rate. The energy rate is observable (and measurable) as a combined instantaneous rate of climb (or descent) and flight path acceleration (or deceleration).

The maneuvering energy rate is described by the specific excess power measured while turning. Turning increases the induced drag, which decreases the excess thrust and reduces P_S. This characteristic variation of P_S with load factor is depicted in figure 6.24.

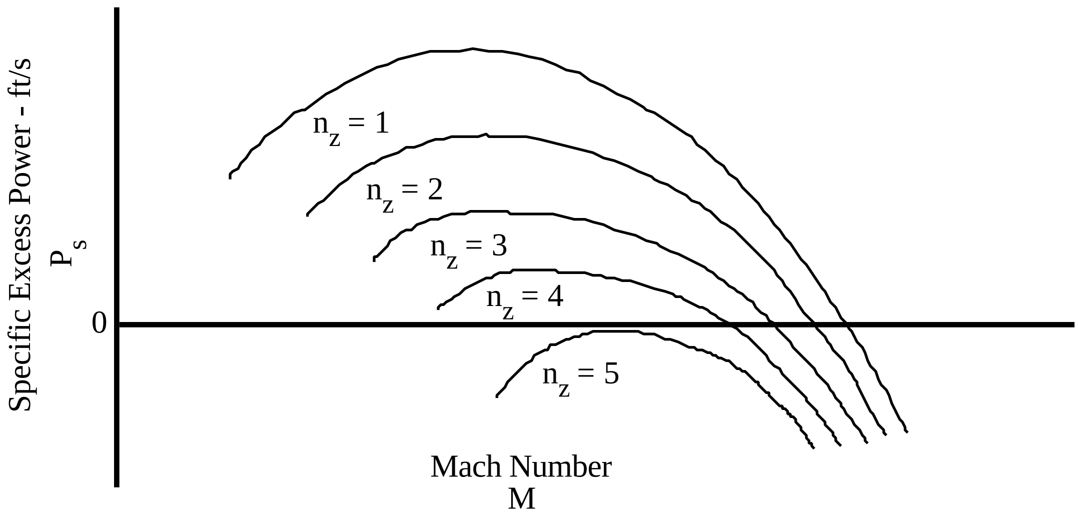

Figure 6.24
VARIATION OF SPECIFIC EXCESS POWER WITH LOAD FACTOR

Notice the similarity of figures 6.18 and 6.24. The former shows the excess thrust, while the latter shows the excess thrust times velocity divided by weight. Notice also the intercepts of the P_S curves with the horizontal axis, the points where $P_S = 0$. These points represent maximum sustained turning performance, since T = D. At all other points, there is either a thrust excess or a thrust deficit, manifested by a measurable energy rate.

6.3.8 PREDICTING TURN PERFORMANCE FROM SPECIFIC EXCESS POWER

Turning performance may be predicted from level acceleration data, using the relationship between specific excess power and the induced drag. Recall that corrections to sustained turn performance were made for thrust changes using the calculated thrust difference and the $P_S = 0$ condition (T = D) to calculate the drag differential. The differential lift was then obtained using the drag polar. Here, the excess thrust can be measured directly at each Mach number using the following:

$$T_{ex} = T - D = \frac{W}{V_T}\frac{dh}{dt} + \frac{W}{g}\frac{dV_T}{dt} \tag{Eq 6.54}$$

Where:

D	Drag	lb
g	Gravitational acceleration	ft/s^2
h	Tapeline altitude	ft
T	Thrust	lb
T_{ex}	Excess thrust	lb
V_T	True airspeed	ft/s
W	Weight	lb.

The correction for excess thrust can be made in the same manner previously described. For this application, the excess thrust at a particular Mach number can be interpreted as the increase in drag required to make $P_s = 0$. Entering the drag polar with this drag differential, the lift differential can be found. Eq 6.51 can be used for this calculation with a parabolic drag polar. From the lift increase, the predicted maximum sustained load factor at the Mach number in question is calculated.

To compile acceleration data at many different altitudes, excess thrust (from Eq 6.54) characteristics can be documented. For a fixed altitude, referred excess thrust, T_{ex}/δ, varies with Mach number as shown below.

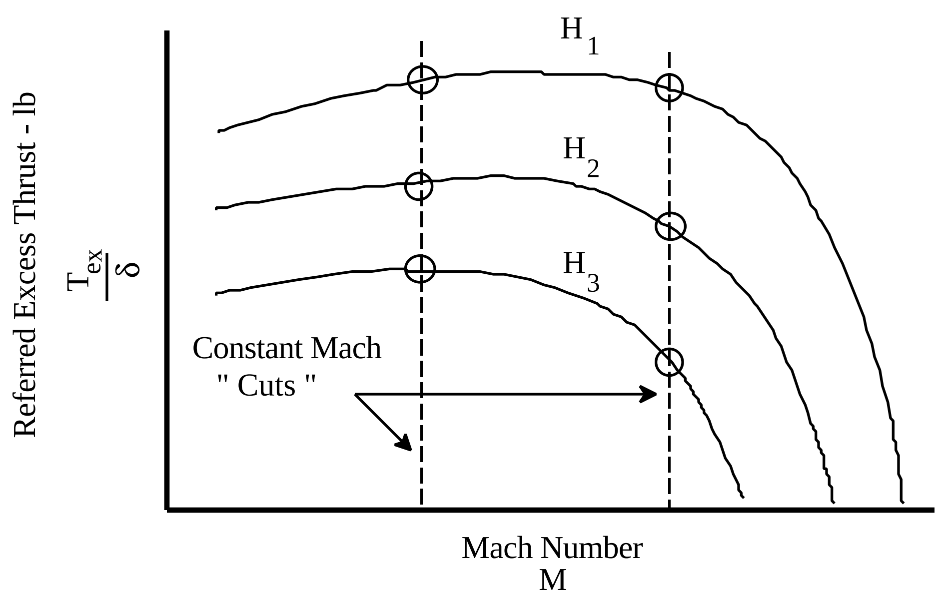

Figure 6.25

REFERRED EXCESS THRUST VERSUS MACH NUMBER

From the graph a vertical cut (at constant Mach number) yields the values representative of the drag differential at each test altitude. These values are different since the angle of attack varies across the altitude range. If the drag polar is available (or assumed of a certain order), the lift difference can be calculated, expressed as a function of referred load factor divided by Mach number times δ, all raised to the appropriate power. Figure 6.26 is a graphical depiction of this calculation.

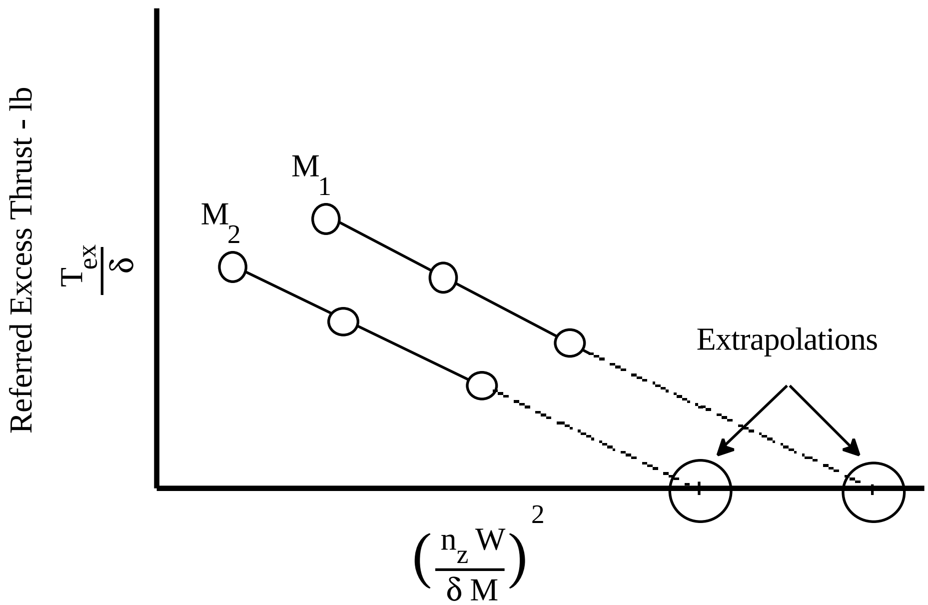

Figure 6.26
EXTRAPOLATIONS TO ZERO REFERRED EXCESS THRUST FOR A PARABOLIC DRAG POLAR

The above figure assumes a parabolic drag polar, so the data linearize to allow extrapolations to zero excess thrust, the area of interest. Each intercept defines maximum sustained load factor for a standard weight at a particular Mach number for different altitudes (because of the δ). A crossplot of sustained load factor at a standard weight versus Mach number for various altitudes can be made, as shown in figure 6.27.

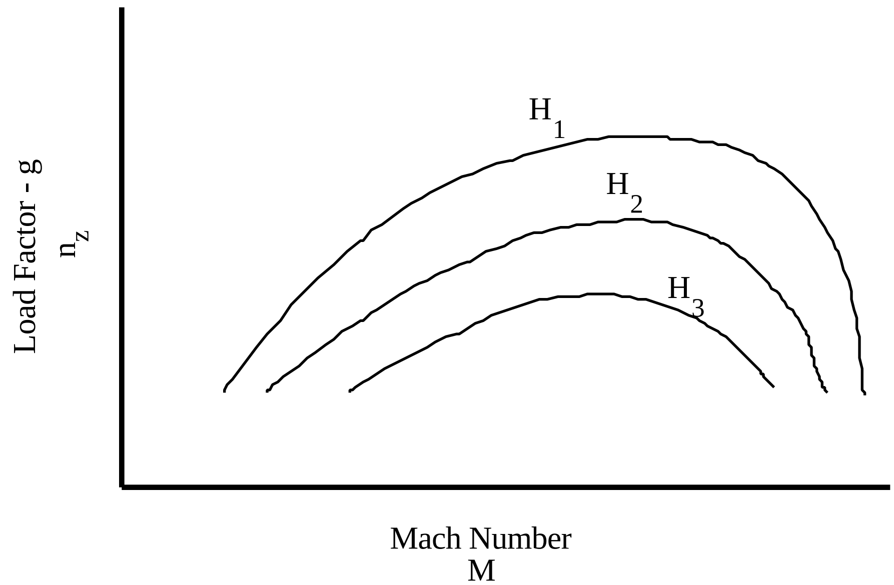

Figure 6.27
PREDICTED MAXIMUM SUSTAINED LOAD FACTOR VERSUS MACH NUMBER

6.3.9 AGILITY

Turn performance is but one aspect of an airplane's maneuvering performance. To describe the characteristics desirable in a tactical airplane, the term agility is often used. Agility is the ability to make rapid, controlled changes in airplane motion. Included within the scope of the term agility are the climb, acceleration, deceleration, and turn characteristics of the airplane. An agile airplane is capable of performing quick and precise changes in climb angle, speed, or direction of flight. The ability to make rapid changes describes maneuverability; the ability to precisely guide the airplane through such changes describes controllability. Thus, maneuverability and controllability are subsets of agility.

While it might seem reasonable to demand every airplane be agile, the concept is not practical. The cost of agility is prohibitively high, particularly for relatively large airplanes. From a design perspective, the problem is how to obtain enough thrust and control power to overcome the inertia and aerodynamic damping of the airplane. For large airplanes the problem is insurmountable with current technology. Virtually every agile airplane ever built was relatively small. Only the small airplanes are nimble at low speeds, since the control power requirements for large airplanes are so hard to meet at low speeds.

6.3.10 AGILITY COMPARISONS

Not every mission has a requirement for agility. In fact, turning performance flight tests are routinely omitted in the testing of transport and cargo category airplanes. The tactical combat airplanes are those which have a mission requirement for agility. For these airplanes, the task of specifying a particular level of agility is difficult. There is no consensus, but there are several popular ways to compare the agility of rival airplanes. Some figures of merit for these comparisons are characteristics already investigated in this and previous chapters. The formats for the comparisons differ, with each having its own advantages and disadvantages. Some of the common methods are presented in the following discussions.

6.3.10.1 SPECIFIC EXCESS POWER OVERLAYS

Using acceleration run data at various altitudes and a common load factor, contours of constant P_S can be shown on an H-V diagram. If the plots are overlaid for rival airplanes, the areas of relative P_S advantage for each are evident. An example of one such P_S overlay is shown as in figure 6.28.

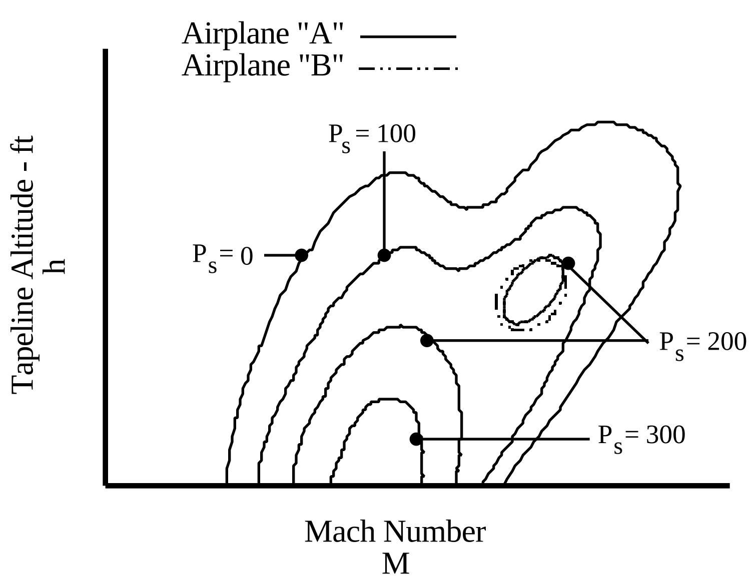

Figure 6.28
SPECIFIC EXCESS POWER OVERLAY

Careful inspection of the overlay reveals the areas of relative superiority and inferiority. But, the plot is difficult to study. If enough P_S contours are displayed to interpret the relative P_S envelopes, the plot becomes cluttered. If the relative differences are great, the plot is even harder to read. A cleaner presentation of the same data can be made by plotting only the P_S differential.

6.3.10.2 DELTA SPECIFIC EXCESS POWER PLOTS

Displaying the differential P_S of the two rival airplanes (A and B) on the H-V diagram can be a more useful format for comparing relative strengths. The delta P_S is obtained by subtracting the P_S of one airplane from the other at each energy state. Figure 6.29 is a sample delta P_S plot.

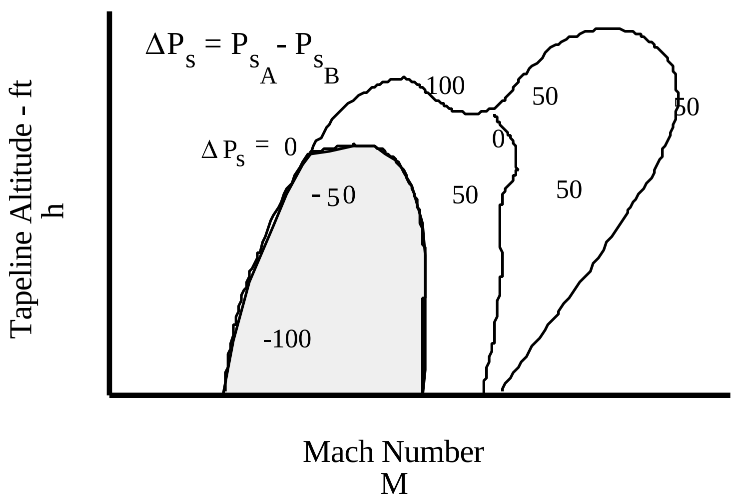

Figure 6.29
DELTA SPECIFIC EXCESS POWER CONTOURS

Areas of relative advantage are easily seen in this presentation format. For example, the shaded areas represent regions where the delta P_S is negative. For airplane A, operating in these shaded regions is discouraged, since the rival airplane (B) enjoys a P_S advantage there. Preferred energy conditions for engagements can be determined from this graph.

Unfortunately, the delta P_S plot is for one load factor. Once the airplane begins to turn, the delta P_S contours change. For a more complete representation of the tactical envelope, similar plots for other load factors are needed. These data come from loaded acceleration and deceleration tests. Composite overlays of different load factors can be used to indicate the delta P_S trends with load factor. The 2 g plot can overlay the 1 g plot, for example, to show the changing P_S situation when the airplanes begin to maneuver. A complete maneuvering picture requires overlays at regular intervals up to the limit g, but the presentation can become cluttered quickly. Another way to present the changing P_S as the airplane maneuvers uses the familiar maneuvering diagram.

6.3.10.3 DOGHOUSE PLOT

The doghouse plot maneuvering diagram, introduced in paragraph 6.3.6, is named for its characteristic shape. This diagram was used in the earlier discussion for a combined presentation of sustained and instantaneous turn performance data. The plot is also a useful display for data from loaded accelerations and decelerations. With these additional data, various P_S contours can be mapped, as figure 6.30 illustrates.

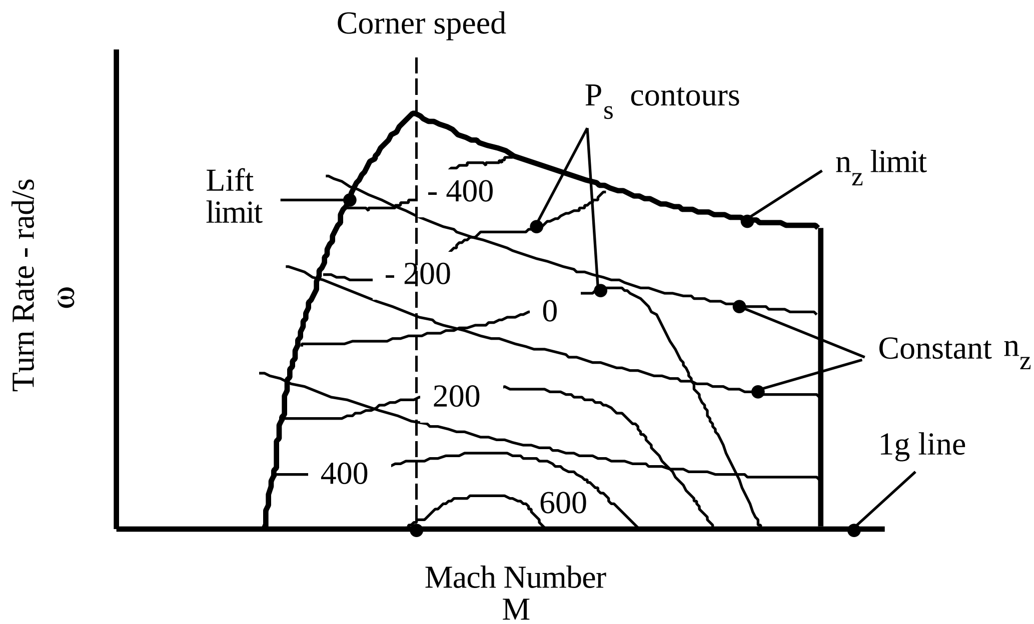

Figure 6.30
DOGHOUSE PLOT WITH SPECIFIC EXCESS POWER CONTOURS

Significant features shown on the plot include:

1. Maximum maneuver limits (stall, limit load, limit speed).
2. Corner speed.

3. Sustained turn line ($P_S = 0$).
4. Turn rate and energy loss for any speed and g.

Studying this diagram, the tactical pilot can plan his maneuvers based upon the conditions for best energy gain and energy conservation. For tactical comparisons, the diagrams for rival airplanes can be overlaid to show the areas of relative energy advantage. Like the P_S overlays, these plots can become extremely cluttered. Less cluttered versions of these displays use delta P_S contours, as in figure 6.29. A limitation of this comparison format is the reference to one altitude and weight. Many such diagrams, representing other operating conditions, must be correlated in order to put together a complete picture for tactical planning.

6.3.10.4 SPECIFIC EXCESS POWER VERSUS TURN RATE

If a vertical cut is made on a maneuvering diagram, the value of P_S can be plotted as a function of either load factor or turn rate for a constant Mach number and altitude, as shown in figure 6.31.

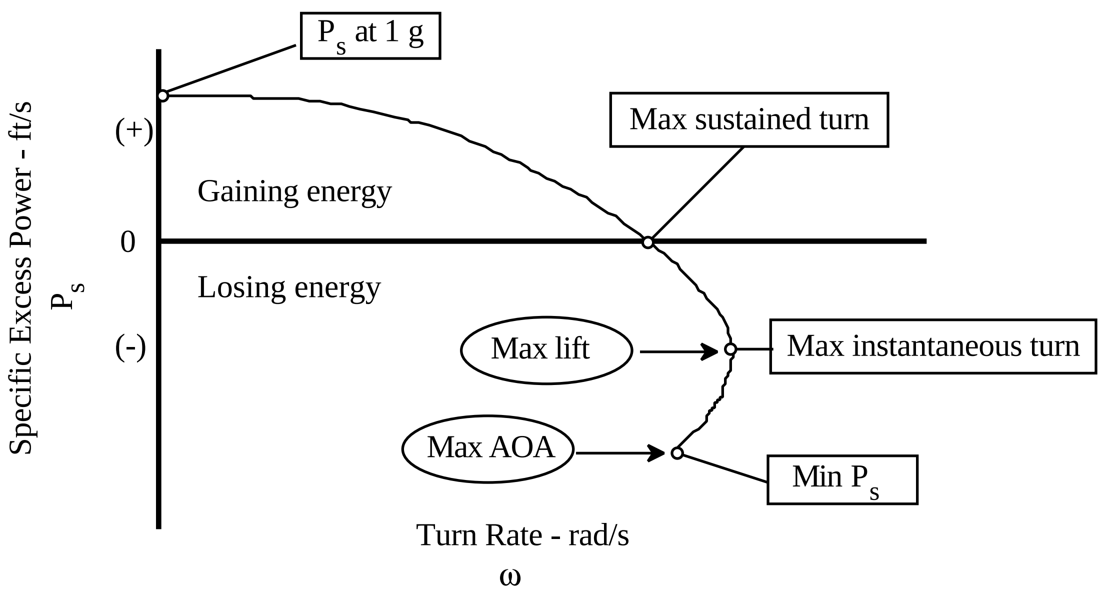

Figure 6.31
SPECIFIC EXCESS POWER VERSUS TURN RATE

This plot gives a better feel for the rate at which P_S changes as a turn is tightened. The maximum sustained turn is represented by the x axis intercept. The maximum instantaneous turn rate is an end point if the data come solely from a doghouse plot (since on a doghouse plot there is no way to show more than one value of P_S for any combination of Mach number and turn rate). However, if loaded deceleration runs are continued past the accelerated stall, the data can be used to continue this curve past the maximum instantaneous turn, to the limit angle of attack. In this case, the decreasing load factor beyond the maximum instantaneous performance point causes less turn rate, even as greater energy is sacrificed. Despite the diminished turn rate, these high energy loss conditions are tactically useful for maximum rate decelerations to force an overshoot or to take advantage of slow speed pointing ability. Inspecting the shape of the curve can reveal a point of diminishing returns, a turn rate beyond which the increase in performance does not justify the increased rate of energy loss.

The simplicity of these plots makes it relatively easy to interpret overlays for comparisons. Figure 6.32 is an example comparison using this data format.

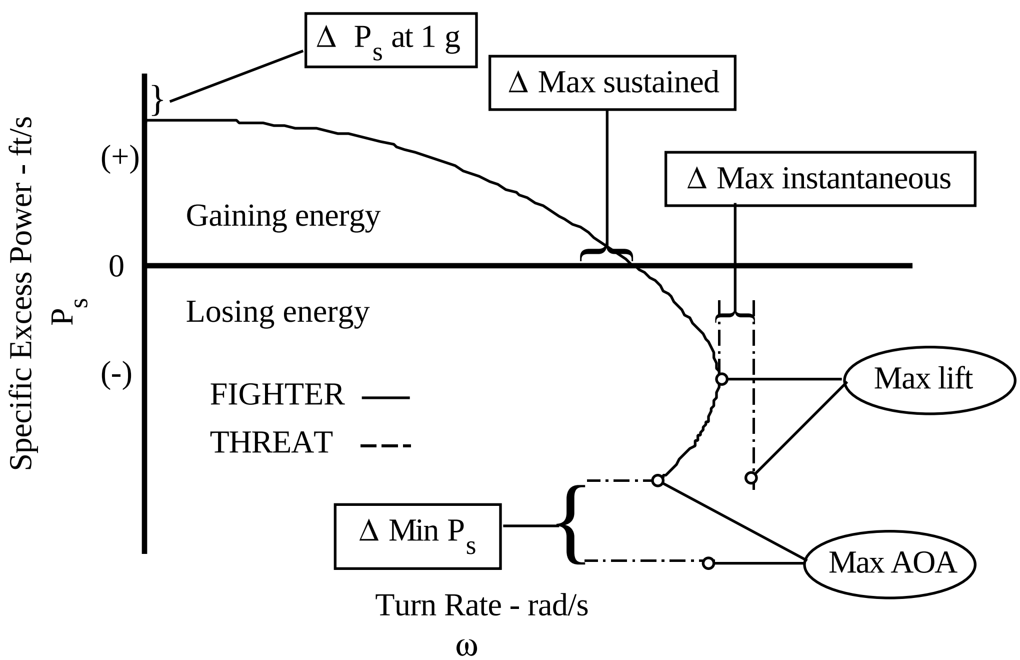

Figure 6.32
SPECIFIC EXCESS POWER VERSUS TURN RATE COMPARISON

The relative P_S advantage at any turn rate is the vertical distance between the curves. Alternately, for any P_S, the difference in turn rate capability is displayed as the horizontal spread. This presentation can be used to develop tactical maneuvers against specific rival or threat airplanes.

Still, this curve represents only one Mach number and altitude. To complete the maneuvering picture, several of these curves are required. Usually, either altitude or Mach number is fixed and the other is plotted in some carpet map format, with P_S and either turn rate or load factor. An example of such a plot is shown in figure 6.33.

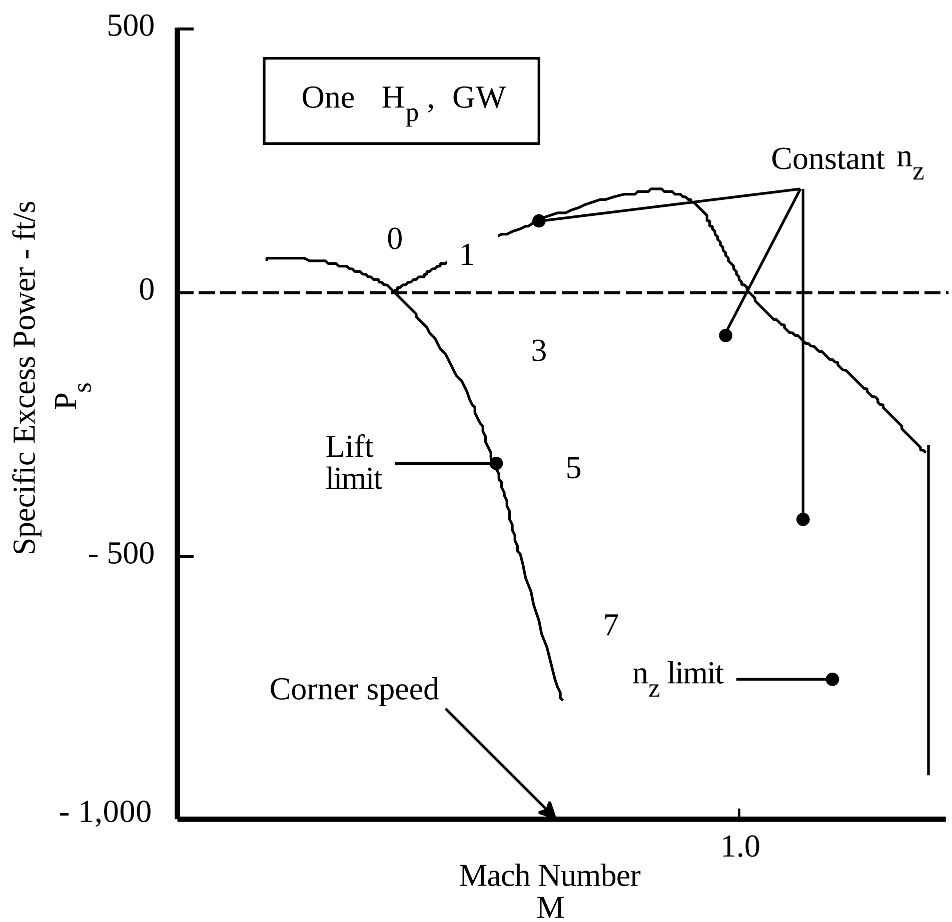

Figure 6.33
COMPOSITE MANEUVERING DIAGRAM

All of these presentations show the areas of relative P_S advantage for comparisons. They also provide data for the development of tactics against a particular rival airplane. The maneuvering environment is fluid and the airplanes don't stay on any one particular curve long enough to validate the analyses. Nevertheless, these formats serve well in the analysis of a tactical environment consisting of relatively prolonged engagements and rear-quarter attacks. In this scenario, the pilot who starts with the most energy and maintains an energy advantage throughout the engagement can wait for an opportunity to make a lethal attack, or can disengage at will.

The chief disadvantage of tactical analyses based upon these data presentations is they don't treat the quick fight. Neither do they address the capabilities of all-aspect missiles. If the opponent has the ability to make the quick kill, an analysis based upon a drawn-out energy duel is irrelevant. The quick turn at maximum performance becomes the critical parameter. While the relative energy loss rate for instantaneous maneuverability is displayed on the previously introduced plots, it's hard to visualize the overall effect of a P_S advantage or deficit. For example, using these diagrams it's difficult to interpret how fast airspeed is lost or how quickly it can be regained after a maximum performance maneuver. It also doesn't show how long a high turn rate can be maintained. One presentation which shows what happens over time is the dynamic speed turn plot.

6.3.10.5 DYNAMIC SPEED TURN PLOTS

The typical future combat confrontation will likely consist of rapid decelerations, maximum rate turning, quick shots, and maximum accelerations. In order to analyze these maximum maneuvers, a format is needed which retains the dynamic quality of the maneuvers. Dynamic speed turn plots, introduced in reference 2, are diagrams which show the potential to gain or lose airspeed in a maximum maneuver.

The first plot is constructed by converting the negative P_S values along the maximum instantaneous turn boundary into an airspeed deceleration in kn/s using Eq 6.55.

$$\frac{dV_T}{dt} = \frac{11.3\ P_s}{V_T}$$

(Eq 6.55)

Where:

P_S	Specific excess power	ft/s
V_T	True airspeed	ft/s.

Turn rate is plotted against the calculated deceleration rate, with airspeeds annotated along the resulting curve, as shown in figure 6.34.

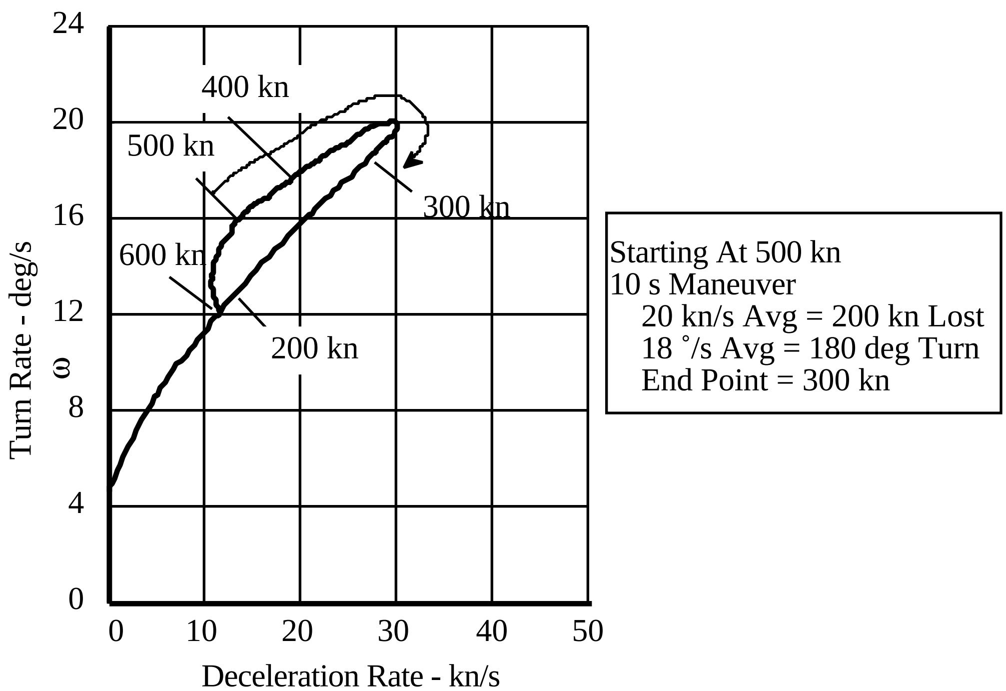

Figure 6.34
DYNAMIC TURN PLOT

This diagram can be used to visualize the dynamic performance in a maximum performance decelerating turn. The following example, extracted from reference 2, illustrates how the plot can be used. An airplane at 500 kn true airspeed begins a maximum performance turn. The average deceleration rate for the next 10 seconds is about 20 kn/s. Over the 10 second period, the airplane loses about 200 kn, while averaging about 18 deg/s turn rate. After the 180 deg turn the airplane is at 300 kn, with the capability for an instantaneous turn rate of about 18 deg/s.

The second is a plot of acceleration versus airspeed at 1 g. It can be constructed directly from 1 g acceleration run data. Accelerations are obtained from standard day data, using Eq 6.55. Acceleration is plotted against airspeed, or Mach number, as shown in figure 6.35.

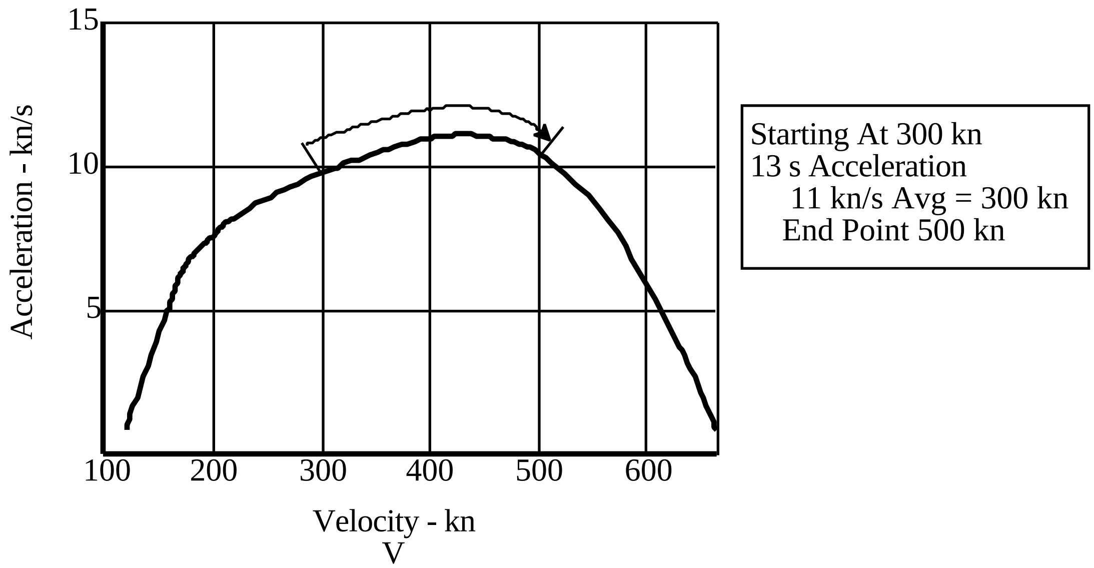

Figure 6.35
DYNAMIC SPEED PLOT

To continue the previous example, the same airplane begins a level acceleration from 300 kn to regain energy following its maximum performance turn. From 300 kn to 500 kn, the average acceleration is about 11 kn/s. The airplane is back at 500 kn after about 13 s.

The dynamic speed turn plots can be used to compare airplanes, by plotting the data of the rivals on the same graph. Quick-look analyses, as in the example above, can be made easily for a typical maneuver; computers can be used for precise analyses of capabilities.

6.4 TEST METHODS AND TECHNIQUES

The measures of maneuvering performance are turn rate, turn radius, load factor, Mach number, and altitude. All of these parameters are found on the maneuvering diagram, an example of which is presented as figure 6.36.

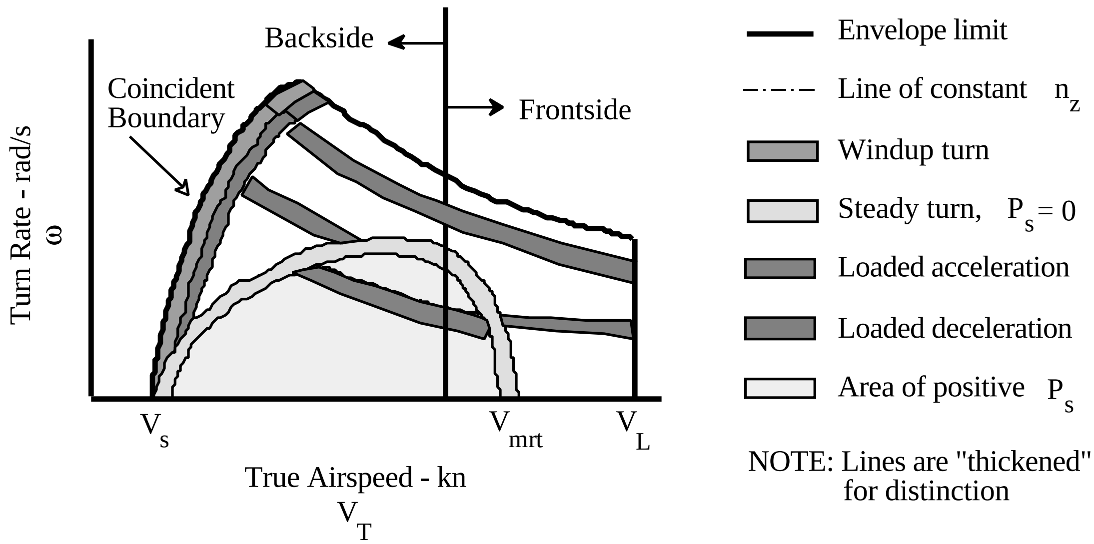

Figure 6.36
TURN PERFORMANCE CHARACTERISTICS

The diagram is helpful in describing the rationale for individual test techniques used to document maneuvering performance.

The first area of interest is the 1 g speed envelope for level flight. This is represented on the graph by the horizontal axis. The data for this boundary are normally obtained through level accelerations, as discussed in Chapter 5. Chief characteristics are the 1 g stall speed and the military rated thrust airspeed (V_{mrt}).

The boundary on the left is the lift limit. It represents accelerated stall conditions from just above the 1 g stall speed to the corner speed. Two techniques are used to document this area: windup turns and loaded decelerations. This boundary is typically a region of negative P_S.

Next, look at the sustained turn performance curve. The variation of maximum sustained load factor with Mach number is normally documented with steady turns**.** Two techniques are represented: the front side (or constant altitude) technique, and the backside (or constant airspeed) technique. Sustained turn performance can be calculated from level acceleration data. All along the sustained turn performance curve, $P_S = 0$. Above the curve P_S is negative; below it, P_S is positive.

To document the area of negative P_S between the sustained turn performance curve and the load factor limit, the loaded deceleration technique is used. The positive P_S area beneath the sustained turn performance curve is documented using the loaded acceleration technique.

6.4.1 WINDUP TURN

Instantaneous turn performance is documented usually with the windup turn technique. In this technique the load factor is smoothly and steadily increased with constant Mach number. The end point of the data run is the accelerated stall or the structural limit, whichever is reached first.

To perform the windup turn, momentarily stabilize at the desired Mach number. Set the thrust for the test as you roll into a turn and smoothly increase load factor. As load factor and drag increase, reduce the pitch attitude in order to keep Mach number constant. Use bank angle to adjust the pitch attitude. When the limit condition is reached, record the g level. Increase the load factor no faster than 1/2 g/s to minimize the effects of unsteady flow.

Buffet boundary data may be obtained using this technique. To document the buffet boundaries, the load factors at which certain levels of buffet occur are recorded. Typically, the buffet levels of interest are:

ONSET - The level of buffet first discernable is termed onset buffet. Buffet detection is easier if the load factor is applied gradually in the vicinity of the onset. Once buffet has begun, the shaking and vibrations compromise precise accelerometer readings.

TRACKING - The level of buffet beyond which no offensive tracking can reasonably be made is termed tracking buffet. Tracking limits are arbitrarily defined with respect to a particular weapon or weapon system. Defining this buffet level is difficult to standardize, since it depends largely upon opinion.

LIMIT - The buffet level which corresponds to accelerated stall is called limit buffet. The maximum load factor for the windup turn occurs at this point.

Not all airplanes have three distinct buffet levels. High lift devices, particularly leading edge devices, change the level of buffet when they are deployed. The position of all high lift devices must be noted for all data runs. Variable wing sweep also changes the buffet characteristics.

6.4.1.1 DATA REQUIRED

The windup turn data document the variations with Mach number of the lift coefficients corresponding to onset, tracking, and limit buffet levels. To investigate Reynold's number effects, data can be compared for a particular Mach number at different test altitudes. When correlating data from several altitudes, test values of n_z can be kept reasonable by taking low Mach number data at low altitude, and high Mach number data at a high test altitude. The following data are required for the windup turn:

H_{P_o}, V_o or M_o, n_{z_o}, W, α, OAT.

6.4.1.2 TEST CRITERIA

1. Steady Mach number.
2. Steady g onset, rate $\leq$ 1/2 g/s for onset buffet.

6.4.1.3 DATA REQUIREMENTS

Typical data accuracy tolerances are listed below; however, requirements may vary with available instrumentation.

1. $V_o \pm 1$ kn (most accurate method to calculate Mach number).
2. $M \pm 0.01$ M (alternate measurement).
3. $H_{P_o} \pm 100$ ft.
4. $n_{z_o} \pm 0.05$ g, or half the smallest display increment. Readings may be difficult while in buffet.
5. W nearest hundred pounds.
6. Angle of attack as required for operational correlation.
7. OAT $\pm$ 1 ˚C.

6.4.1.4 SAFETY CONSIDERATIONS

The windup turn is an intentional approach to a limiting condition. The consequences of exceeding the limit conditions during the runs must be considered in the planning stages. Contingencies such as inadvertent stall, departure, or spin must be anticipated. Review recovery procedures, particularly in cases where reconfiguring of the airplane is required during the recovery procedure.

Address the effects of sustained buffet and high angle of attack on critical airplane systems. Emphasize engine limits and handling characteristics.

6.4.2 STEADY TURN

Sustained turning performance is documented using steady turns. The maximum load factor which can be sustained in level flight at a particular Mach number is obtained using either a front side or a backside technique.

FRONT SIDE - For speed regions where the maximum sustained g decreases as speed increases, a front side, or constant altitude, technique can be used. If a constant load factor is maintained, the airplane converges to a unique airspeed. For example, if the speed deviates to a higher value, the excess power is negative at that load factor, resulting in a deceleration. Similarly, a lower airspeed causes an acceleration due to the positive excess power. Therefore, the airplane converges to the data point if the pilot holds altitude and load factor constant.

Typically, the first data point obtained using the front side technique is V_{mrt}. This point anchors the sustained turn performance curve in the same sense it anchors the P_s versus Mach number curve (at $P_{s\,=\,0}$) for an acceleration run. Perform a shallow dive to arrive at the test altitude at an airspeed higher than the predicted V_{mrt}. Allow the airplane to decelerate while maintaining level flight (constant load factor). The airspeed converges and stabilizes at V_{mrt}.

From V_{mrt} select a bank angle, normally from 30 to 45 degrees, and allow the airplane to decelerate at the corresponding constant load factor. Maintain level flight throughout this deceleration making all corrections smooth. Rough pitch control inputs changes the load factor and consequently the drag. Since convergence to the data point speed is decidedly slower from the low speed side, the drag from excessive pitch control activity could compromise the test results. Even though the airspeed eventually converges to the data point, it may be difficult to hold the altitude steady long enough for typical front side stabilization criteria (2 kn/min criteria from level flight performance tests). If the corrections for altitude variations are smooth, the interchange between potential and kinetic energies even out over the required time interval. A good visual horizon is required, unless the airplane is equipped with an inertial system and head-up display. The flight path vector and inertial horizon simplify this technique greatly. An autopilot with an altitude hold feature can be helpful for the front side points.

At higher bank angles, altitude is difficult to control using smooth pitch control inputs alone. Figure 6.37 illustrates the variation of normal acceleration with bank angle in a steady turn.

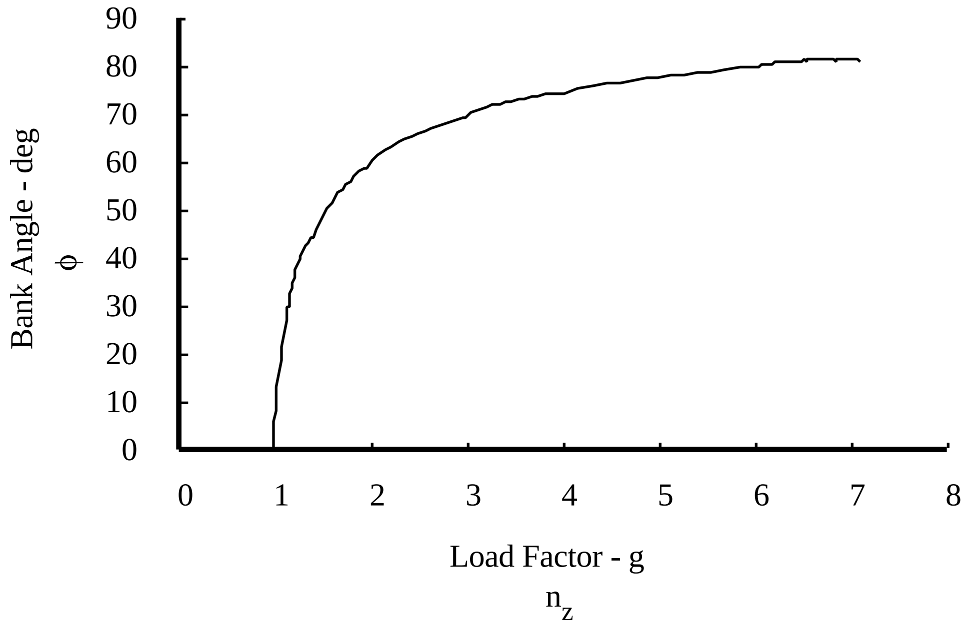

Figure 6.37
LEVEL TURN BANK ANGLE VERSUS LOAD FACTOR

Up to about 45 deg, the bank angle is a sensitive indicator of load factor. Most of the lift force is directed vertically, so small changes in load factor are effective in correcting rate of climb or descent. Above 60 deg, load factor is extremely sensitive to even small variations in bank angle. Since only a small component of the lift is directed vertically, flight path corrections with constant bank angle require excessive load factor deviations, compromising the data. For these conditions, it helps to trim to the desired load factor, using the accelerometer for reference. Bank angle can then be used to make the pitch attitude adjustments required to maintain level flight. The front side technique is practical to only about 3 g, above which the backside technique is normally used.

BACKSIDE - The backside technique is used above about 3 g, and wherever the maximum sustained g decreases as speed decreases. If a constant load factor is held in this region, the airspeed diverges from trim. For example, if the airplane gets slow, the excess power is negative and the airplane decelerates. Similarly, an airspeed faster than trim produces an acceleration. A constant airspeed technique is required since the test point is steady, but unstable.

To perform the backside technique, first stabilize at, or slightly slower than, the target airspeed. Roll into a turn and smoothly increase the thrust, while simultaneously increasing the load factor to prevent acceleration. Monitor the airspeed closely and correct deviations by adjusting the load factor. For increasing speed, apply more load factor. Fast deviations must be corrected immediately when stabilizing on the backside, since the amount of additional g required to decelerate increases with airspeed. If the airspeed deviation is too large for a comfortable correction, reduce thrust slightly to decelerate while holding the g, and then reset the thrust when the target airspeed is reached. Corrections for decreasing airspeed are easier, since accelerations can be made by a slight relaxation of load factor. While holding a steady load factor, maintain level flight by using bank angle to make fine adjustments to pitch attitude. Large pitch attitude corrections complicate or even prevent stabilization. Make a fine adjustment to the load factor when correcting for a rate of climb or descent. After the airspeed stabilizes, record the data when the airspeed, altitude, and load factor are steady for 5 seconds.

A modification of the above technique can be used for afterburner points. The rapid increase in airspeed which accompanies afterburner light off can be anticipated by initially stabilizing 20 to 30 kn slower than the desired test airspeed. After the burner lights off, the target airspeed can be intercepted with a smooth application of load factor.

As with the front side technique, a good visual horizon reference is required, but may be compensated for by a head-up display of inertial data.

6.4.2.1 DATA REQUIRED

Sustained turn performance is documented by performing level turns from V_{min} to V_{max} at constant test altitudes from near sea level to the combat ceiling of the airplane. The typical altitude interval is 5,000 ft. The following data are required for the steady turn.

H_{P_o}, V_o or M_o, n_{z_o}, W, α, OAT.

Data points should span the airspeed envelope, with a regular interval between data points. A rough plot of n_z versus airspeed or Mach number can be kept while obtaining the data as a guide to avoiding holes in the coverage.

The measurement of normal acceleration is critical for these tests. A sensitive g-meter is typically used. As discussed in previous chapters, the instrument correction is noted for 1.0 g. Then, at 1 g inflight, determine the tare correction as the difference between the actual reading and 1 g plus the instrument correction. This tare correction must be applied to each n_z reading after instrument corrections are applied.

$$n_z = n_{z_o} + \Delta n_{ic} + \Delta n_{z\ tare} \quad \text{(Eq 6.56)}$$

Where:

n_z	Normal acceleration	g
n_{z_o}	Observed normal acceleration	g
Δn_{ic}	Normal acceleration instrument correction	g
$\Delta n_{z\ tare}$	Normal acceleration tare correction	g.

6.4.2.2 TEST CRITERIA

1. Constant thrust.
2. Constant altitude ± 1,000 ft of target, and steady for 5 s.
3. Constant normal acceleration (bank angle).
4. Airspeed < 2 kn change over a one minute interval; steady for 5 s.

6.4.2.3 DATA REQUIREMENTS

Typical data accuracy tolerance are listed below; however, requirements may vary with available instrumentation.

1. H_{P_o} ± 100 ft.
2. V_o ± 1 kn.
3. n_{z_o} ± 0.05 g, or half the smallest display increment. Value can be calculated from the stabilized bank angle.
4. Weight ± 100 lb.
5. OAT ± 1˚ C.

6.4.2.4 SAFETY CONSIDERATIONS

There are no particular hazards associated with steady turns, apart from the case where the sustained and instantaneous boundaries coincide. Such conditions are covered in the previous sections. If many data points are planned, adverse effects of sustained high engine operating temperatures should be anticipated.

6.4.3 LOADED ACCELERATION

Level accelerations were introduced in Chapter 5 as a method to document the maximum thrust P_S characteristics of the airplane at 1 g. The airplane has excess thrust at higher load factors as well, but only within certain airspeed ranges, and only up to the maximum sustained load factor at the test altitude. Within these boundaries, acceleration tests can be performed while turning. The airspeed range for the loaded acceleration decreases from the 1 g envelope to a single point at the maximum sustained load factor at the test altitude. As in other dynamic test techniques, automatic data recording is necessary. Details of the 1 g level acceleration test technique are presented in Chapter 5. Loaded accelerations are performed slightly differently, as presented below.

Like the 1 g acceleration run, begin the loaded acceleration with the thrust stabilized at military or maximum thrust, depending upon the test. Choose a test load factor (half-g increments is a typical choice) and calculate the stall speed at that load factor. The initial airspeed should be 1.1 times the predicted stall speed, or higher as necessary, to ensure positive P_S for the acceleration. Begin the test below the test altitude by stabilizing the airspeed, thrust, and load factor in a slight climb. As in the 1 g acceleration, use a combination of drag devices, flaps, and climb angle as required to control the rate of climb. As the test altitude is approached, activate the test instrumentation, retract the drag devices and over-bank as necessary to intercept a level flight path. During the run, it is critical to keep the load factor constant. Small altitude variations can easily be accounted for in the data reduction, but load factor excursions compromise the data. A good way to minimize load factor excursions is to trim the pitch forces during the acceleration, provided the trim sensitivity is suitable. Adjust the bank angle to make pitch attitude corrections for level flight. Continue the acceleration until the airspeed stabilizes at the maximum sustained speed for the test load factor.

6.4.3.1 DATA REQUIRED

The following data are required from roughly 1.1 $V_{S(nz\ Test)}$ to $V_{mrt(nz\ Test)}$.

1. Pressure altitude versus time trace.
2. Airspeed versus time trace.
3. Load factor versus time trace.
4. Ambient temperature.
5. Fuel flow (integrated over elapsed time to compute change in weight).
6. Fuel weight.

6.4.3.2 TEST CRITERIA

1. Constant thrust.
2. Constant altitude ± 1,000 ft of target altitude.
3. Constant load factor ± 0.2 g.

6.4.3.3 DATA REQUIREMENTS

Typical data accuracy tolerances are listed below; however, requirements may vary with available instrumentation.

1. H_{P_o} ± 100 ft.
2. V_o ± 1 kn.
3. n_{z_o} ± 0.1 g.

4. OAT ± 1 ˚C.
5. Fuel flow ± 500 lb/h.
6. Weight ± 100 lb.

6.4.3.4 SAFETY CONSIDERATIONS

Loaded accelerations begin near the stall, so guard against the inadvertent stall while setting up the run. If speedbrakes or flaps are used prior to intercepting the acceleration profile, take care not to overspeed or over stress them.

6.4.4 LOADED DECELERATION

The loaded deceleration is used to document the region of negative P_S outside of the sustained performance curve. Decelerations can be performed from V_{Limit}, at various load factors from 1 up to the structural load limit. Decelerations performed at load factors below the maximum sustained g for the test altitude terminate on the sustained performance curve. For load factors above the maximum sustained g at the test altitude, the deceleration terminates at the lift limit. Once the lift limit is reached, the load factor is progressively relaxed so as to decelerate along the lift limit to 1 g.

If the full envelope is to be documented, begin the loaded deceleration from a shallow dive at V_{Limit} with the thrust stabilized at military (or maximum) thrust. As the test altitude is approached, activate the test instrumentation and smoothly level off, setting the target load factor and bank angle to maintain level flight. For low load factors, the deceleration will terminate on the sustained turn performance boundary. The final stages of this deceleration is precisely the front side technique used to define the sustained turn performance boundary. For load factors which exceed the sustained performance capability at the test conditions, the deceleration will continue to the accelerated stall. After the lift limit is reached, the test can be terminated. Alternately, the deceleration can be continued to document the lift limit boundary. The deceleration rate along the lift boundary is typically high, however, and the bank angle must be reduced as load factor decreases or else a high rate of descent will develop.

6.4.4.1 DATA REQUIRED

The following data are required from V_{Limit} (or, as desired) to $V_{s(n_{z\ test})}$.

1. Pressure altitude versus time trace.
2. Airspeed versus time trace.
3. Load factor versus time trace.
4. Ambient temperature.
5. Fuel flow (integrated over elapsed time to compute change in weight).
6. Fuel weight.

6.4.4.2 TEST CRITERIA

1. Constant thrust.
2. Constant altitude.
3. Constant load factor.

6.4.4.3 DATA REQUIREMENTS

Typical data accuracy tolerances are listed below; however, requirements may vary with available instrumentation.

1. $H_{P_o} \pm 100$ ft.
2. $V_o \pm 1$ kn.
3. $n_{z_o} \pm 0.1$ g.
4. OAT ± 1 ˚C.
5. Fuel flow ± 500 lb/h.
6. Weight ± 100 lb.

6.4.4.4 SAFETY CONSIDERATIONS

The loaded deceleration begins at high speed, where the pitch control may be sensitive and the limit load factor relatively easy to reach. Exercise care to avoid over stresses during the rapid onset of load factor at the start of the run.

The decelerations may take a relatively long time to complete, and the sustained high load factors become a physiological concern. Test planning for the high g events should address techniques to avoid the adverse effects of rapid g onset and sustained high g.

The high negative P_s near the end of the high g decelerations may result in rapid approaches to stalled conditions, so the possibility of inadvertent stalls or departures must be considered. Potential adverse effects on airplane systems from sustained buffet should be anticipated. High angle of attack engine characteristics should be studied for potential problem areas, such as compressor stall, over-temperature, and flameout.

6.4.5 AGILITY TESTS

Tests which highlight the agility of an airplane are those which document rapid transitions between states. The states include attitudes, rates, and flight path accelerations. Since agility includes the ability to precisely control these transitions, some agility test techniques are more flying qualities tests than performance tests. There is a distinction between: 1) the ability to generate a change, and 2) the ability to capture the desired final state. The distinction is between what is called transient agility and functional agility. The former describes the quickness from steady-state to a steady rate of change; the latter, from one steady state to another. The emphasis is strongly on time as a figure of merit. Evidence suggests the quickest time between states is not always accomplished with full deflection control inputs.

6.4.5.1 PITCH AGILITY

These tests highlight the nose-pointing capability of the airplane. Rapid pitch attitude changes are evaluated for 30, 60, 90, and 180 deg. The changes are made in the horizontal and vertical planes. Measures include time to maximum steady pitch rate and time to capture the final pitch angle. If automatic data recording is not available, the time to final state can be measured using a stopwatch.

6.4.5.2 LOAD FACTOR AGILITY

These tests are concerned with controlling the flight path. Wings-level roller coaster maneuvers are performed to capture prescribed load factors. The maneuvers may also be performed in the vertical plane, but energy loss rate complicates the technique. These g capture maneuvers have proved difficult to perform using digital normal acceleration displays. Digital displays can be read only when the normal acceleration is relatively steady, offering no trend information to help in the aggressive capture of precise g levels.

6.4.5.3 AXIAL AGILITY

Tests for axial agility include accelerations and decelerations using military and maximum thrust, speedbrakes, and thrust reversing. Engine spool-up time is included in the measurements. Relevant tests include decelerations from high supersonic speed to corner speed and accelerations to corner speed following a post-stall maneuver.

6.5 DATA REDUCTION

6.5.1 WINDUP TURN

The data reduction for windup turns uses the following equations:

$$V_i = V_o + \Delta V_{ic} \qquad \text{(Eq 6.57)}$$

$$V_c = V_i + \Delta V_{pos} \qquad \text{(Eq 6.58)}$$

$$H_{P_i} = H_{P_o} + \Delta H_{P_{ic}} \qquad \text{(Eq 6.59)}$$

$$H_{P_c} = H_{P_i} + \Delta H_{pos} \qquad \text{(Eq 6.60)}$$

$$n_{z_i} = n_{z_o} + \Delta n_{z_{ic}} \qquad \text{(Eq 6.61)}$$

$$n_{z_{Test}} = n_{z_i} + \Delta n_{z_{tare}} \qquad \text{(Eq 6.62)}$$

$$C_{L_{max_{Test}}} = \frac{n_{z_{Test}} W_{Test}}{0.7\, P_{ssl}\, \delta_{Test}\, M^2\, S} \qquad \text{(Eq 6.63)}$$

$$V_T = a\ M$$

(Eq 6.64)

$$R = \frac{V_T^2}{g\sqrt{\left(n_z^2 - 1\right)}}$$

(Eq 6.12)

$$\omega = \frac{V_T}{R}$$

(Eq 6.13)

Where:

a	Speed of sound	ft/s
$C_{L_{max_{Test}}}$	Test maximum lift coefficient	
$\Delta H_{P_{ic}}$	Altimeter instrument correction	ft
ΔH_{pos}	Altimeter position error	ft
$\Delta n_{z_{ic}}$	Normal acceleration instrument correction	g
$\Delta n_{z_{tare}}$	Accelerometer tare correction	g
δ_{Test}	Test pressure ratio	
ΔV_{ic}	Airspeed instrument correction	kn
ΔV_{pos}	Airspeed position error	kn
H_{P_c}	Calibrated pressure altitude	ft
H_{P_i}	Indicated pressure altitude	ft
H_{P_o}	Observed pressure altitude	ft
M	Mach number	
$n_{z\ Test}$	Test normal acceleration	g
n_{z_i}	Indicated normal acceleration	g
n_{z_o}	Observed normal acceleration	g
P_{ssl}	Standard sea level pressure	2116.217 psf
R	Turn radius	ft
S	Wing area	ft^2
V_c	Calibrated airspeed	kn
V_i	Indicated airspeed	kn
V_o	Observed airspeed	kn
V_T	True airspeed	ft/s
ω	Turn rate	rad/s
W_{Test}	Test Weight	lb.

For onset, tracking, and limit buffet levels compute C_L using the observed airspeed, pressure altitude, normal acceleration, and fuel weight. Calculate referred n_z for later analysis.

Step	Parameter	Notation	Formula	Units	Remarks
1	Observed airspeed	V_o		kn	
2	Airspeed instrument correction	ΔV_{ic}		kn	Lab calibration
3	Indicated airspeed	V_i	Eq 6.57	kn	
4	Airspeed position error	ΔV_{pos}		kn	Flight calibration
5	Calibrated airspeed	V_c	Eq 6.58	kn	
6	Observed pressure altitude	H_{P_o}		ft	
7	Altimeter instrument correction	$\Delta H_{P_{ic}}$		ft	Lab calibration
8	Indicated pressure altitude	H_{P_i}	Eq 6.59	ft	
9	Altimeter position error	ΔH_{pos}		ft	Flight calibration
10	Calibrated pressure altitude	H_{P_c}	Eq 6.60	ft	
11	Mach number	M			$f\,(H_{P_c}, V_c)$
12	Observed normal acceleration	n_{z_o}		g	
13	Normal acceleration instrument correction	$\Delta n_{z_{ic}}$		g	Lab calibration
14	Indicated normal acceleration	n_{z_i}	Eq 6.61	g	
15	Normal acceleration tare correction	$\Delta n_{z_{tare}}$		g	Flight observation
16	Test normal acceleration	$n_{z\ Test}$	Eq 6.62	g	
17	Test weight	W_{Test}		lb	
18	Test pressure ratio	δ_{Test}			$f\,(H_{P_c})$

19	Standard sea level pressure	P_{ssl}		psf	2116. psf
20	Wing area	S		ft^2	Airplane data
21	Test maximum lift coefficient	$C_{L_{max_{Test}}}$	Eq 6.63		
22	Test referred normal acceleration	$n_z \frac{W}{\delta}$		g-lb	
23	Speed of sound	a		ft/s	From Appendix VI
24	True airspeed	V_T	Eq.6.72	ft/s	
25	Turn radius	R	Eq.6.12	ft	
26	Turn rate	ω	Eq.6.13	rad/s	

6.5.2 STEADY TURN

6.5.2.1 STABILIZED TURN

Follow the data reduction in section 6.5.1 through step number 20. Corrections to standard conditions are illustrated for a parabolic drag polar, using the following equations:

$$\Delta T = T_{Std} - T$$

(Eq 6.65)

$$n_{z_{Std}} = \sqrt{\frac{1}{W^2_{Std}} \left[\left(n_z W\right)^2_{Test} + \Delta T \, \pi \, e \, AR \left(0.7\right) S \, P_{ssl} \, \delta_{Test} \, M^2 \right]}$$

(Eq 6.52)

$$V_T = a \; M$$

(Eq 6.64)

$$R = \frac{V_T^2}{g \sqrt{\left(n_z^2 - 1\right)}}$$

(Eq 6.12)

$$\omega = \frac{V_T}{R}$$

(Eq 6.13)

Where:

a	Speed of sound	ft/s
AR	Aspect ratio	
ΔT	Change in thrust	lb
e	Oswald's efficiency factor	
M	Mach number	
$n_{z\ Std}$	Standard normal load factor	g
R	Turn radius	ft
T	Thrust	lb
T_{Std}	Standard thrust	lb
V_T	True airspeed	ft/s
ω	Turn rate	rad/s
W_{Std}	Standard weight	lb.

The thrust correction is made according to the following steps. With the standard day n_z, the standard day turn radius and turn rate can be calculated.

Step	Parameter	Notation	Formula	Units	Remarks
1	Test temperature ratio	θ_{Test}			f (T_a)
2	Engine RPM	N		rpm	
3	Referred RPM	$\frac{N}{\sqrt{\theta}}$			
4	Thrust	T		lb	From engine curves
5	Standard temperature ratio	θ_{Std}			From Appendix VI
6	Standard referred RPM	$\frac{N}{\sqrt{\theta_{Std}}}$		rpm	
7	Standard thrust	T_{Std}		lb	From engine curves
8	Change in thrust	ΔT	Eq.6.73	lb	
9	Standard load factor	$n_{z\ Std}$	Eq.6.52		
10	Speed of sound	a		ft/s	From Appendix VI
11	True airspeed	V_T	Eq.6.72	ft/s	
12	Turn radius	R	Eq.6.12	ft	
13	Turn rate	ω	Eq.6.13	rad/s	

6.5.2.2 LEVEL ACCELERATION

The following equations are used to reduce acceleration data for the prediction of steady turn performance:

$$V_T = a\ M \tag{Eq 6.64}$$

$$n_{z_{sust}} = \sqrt{\frac{P_{s_{1g}}\ \pi\ e\ AR\ S\ \ 0.7\ P_{ssl}\delta\ M^2}{V_T W_{Std}} + 1} \tag{Eq 6.66}$$

$$T_{ex} = T - D = \frac{W_{Std}}{V_T}\ P_{s_{1g}} \tag{Eq 6.67}$$

$$n_{z_{sust}} = \sqrt{\left(\frac{n_z W_{Std}}{\delta\ M}\right)^2\ \ \frac{\delta_h}{W_{Std}}\ M} \tag{Eq 6.68}$$

Where:

a	Speed of sound	ft/s
AR	Aspect ratio	
D	Drag	lb
δ	Pressure ratio	
δ_h	Pressure ratio for selected altitude	
e	Oswald's efficiency factor	
M	Mach number	
n_z	Normal acceleration	g
$n_{z_{sust}}$	Sustained normal acceleration	g
$P_{s\ 1g}$	Specific excess energy at 1 g	ft/s
P_{ssl}	Standard sea level pressure	2116 psf
S	Wing area	ft^2
T	Thrust	lb
Tex	Excess thrust	lb
V_T	True airspeed	ft/s
W_{Std}	Standard weight	lb.

The data required from acceleration runs include P_S values for standard conditions, at specific Mach number for a given weight and altitude. Sustained normal acceleration can be calculated, or determined graphically if at least two altitudes are documented. One method to calculate $n_{z_{sust}}$ follows this sequence:

Step	Parameter	Notation	Formula	Units	Remarks
1	Specific excess power at 1 g	$P_{S\ 1\ g}$		ft/s	From acceleration run
2	Mach number	M			From acceleration run
3	True airspeed	V_T	Eq 6.64	ft/s	
4	Standard weight	W_{Std}		lb	
5	Sustained normal acceleration	$n_{z_{sust}}$	Eq 6.66	g	

For graphical data reduction, use $P_{S\ 1\ g}$ data for standard conditions at one altitude at a time. Perform steps 1 - 4 above, plus the following steps:

Step	Parameter	Notation	Formula	Units	Remarks
5	Excess thrust	T_{ex}	Eq 6.67	lb	
6	Pressure ratio	δ			$f\ (H_{P_c})$
7	Referred excess thrust	$\frac{T_{ex}}{\delta}$		lb	

Plot $\frac{T_{ex}}{\delta}$ versus Mach number for each altitude, on the same graph.

Make a vertical cut for several values of Mach number, and at each intersection record $\frac{T_{ex}}{\delta}$ and calculate $\left[\frac{n_z W_{Std}}{\delta M}\right]^2$ (here, $n_z = 1$). The exponent identifies a parabolic drag polar.

Construct a new graph of $\frac{T_{ex}}{\delta}$ versus $\left[\frac{n_z W_{Std}}{\delta M}\right]^2$ and plot the values for each Mach number chosen.

Each Mach number line can be extrapolated to the horizontal axis, representing T_{ex} = 0 at that Mach number. The value of $\left[\frac{n_z W_{Std}}{\delta M}\right]^2$ at the x axis intercept provides $n_{z_{sust}}$ data for any altitude chosen at that Mach number, as follows:

Step	Parameter	Notation	Formula	Units	Remarks
8	Pressure ratio	δ_h			For selected altitude
9	Sustained load factor	$n_{z_{sust}}$	Eq 6.68	g	

Finally, the values of $n_{z_{sust}}$ at each selected altitude can be plotted on a graph of n_z versus Mach number. The values of $n_{z_{sust}}$ at each altitude for different Mach numbers can be faired to complete the data reduction.

6.5.3 LOADED ACCELERATION

The data reduction for loaded accelerations is identical to the procedure described in Chapter 5. Final results include P_s measurements as a function of Mach number.

6.5.4 LOADED DECELERATION

Data reduction for loaded decelerations is the same as for accelerations, except the values of P_s are negative. Final results include P_s measurements as a function of Mach number.

6.5.5 AGILITY TESTS

Agility test data consists primarily of traces or simple time measurements. No standard data reduction procedure is currently specified.

6.6 DATA ANALYSIS

6.6.1 WINDUP TURN

Instantaneous turn performance parameters can be documented using the C_L data from the windup turns. Begin the analysis by plotting values of C_L for onset, tracking, and limit buffet versus Mach number. A typical plot is shown in figure 6.38.

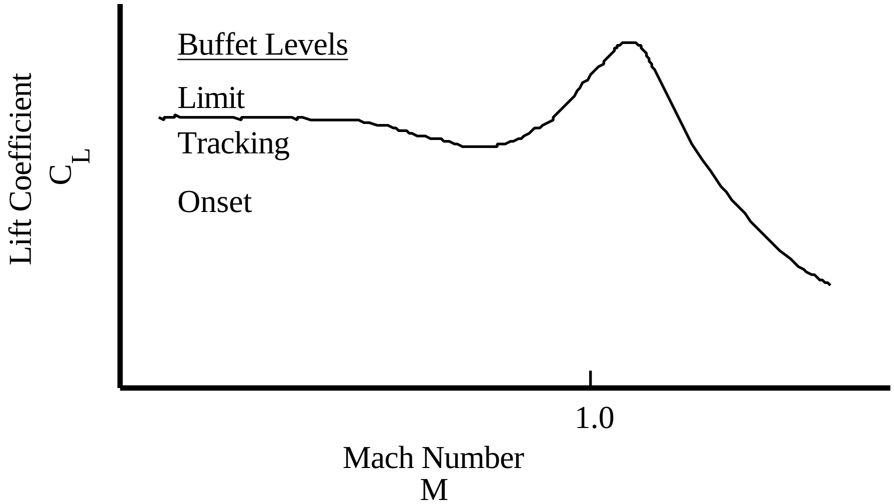

Figure 6.38
LIFT COEFFICIENT VERSUS MACH NUMBER CHARACTERISTICS

From the faired data, the instantaneous n_z versus Mach number for any particular altitude (δ) and weight (W) can be calculated using the expression:

$$n_z = \left(\frac{\delta}{W}\right)\left(0.7\ P_{ssl}\ S\right)\ C_L\ M^2 \tag{Eq 6.69}$$

Using these values of load factor, instantaneous turn radius, and turn rate can be determined (Section 6.5.2.1). Alternately, instantaneous n_z can be plotted directly on a maneuvering diagram for the altitude of interest.

Another way to obtain instantaneous turn parameters involves Eq 6.69 written in the following form:

$$\left(n_z \frac{W}{\delta}\right)_{Test} = \left(0.7\ P_{ssl}\ S\right) C_L\ M^2 \tag{Eq 6.70}$$

Where:

C_L	Lift coefficient	
δ	Pressure ratio	
M	Mach number	
n_z	Normal acceleration	g

P_{ssl}	Standard sea level pressure	psf
S	Wing area	ft^2
W	Weight	lb.

The left side of this equation is referred n_z; the right side is a function of Mach number. A plot of referred n_z versus Mach number holds data from tests at any weight or altitude. From the referred n_z curve, values of unreferred n_z can be obtained for any desired weight and altitude combination in order to plot instantaneous turn parameters for analysis.This procedure is similar to the other, except there's no need to calculate C_L directly.

6.6.2 STEADY TURN

The steady turn analysis begins with plots of standard day load factor versus Mach number for each test altitude. These plots can be faired to get a smooth variation for the calculation of turn radius and rate using V_T and $n_{z\ Std}$.

Alternately, the smoothed values of $n_{z\ Std}$ can be plotted directly on a maneuvering diagram for the altitude of interest. Values of turn radius and turn rate are simultaneously displayed on the plot.

Once plotted, the sustained turn data can be examined for compliance with mission standards or specifications. In addition, combined sustained and instantaneous turn performance data can be examined with respect to engine-airframe compatibility. Assessments can be made concerning the amount of the available maneuvering envelope beyond the sustained performance capability of the airplane. Areas for potential improvement are depicted in figure 6.39.

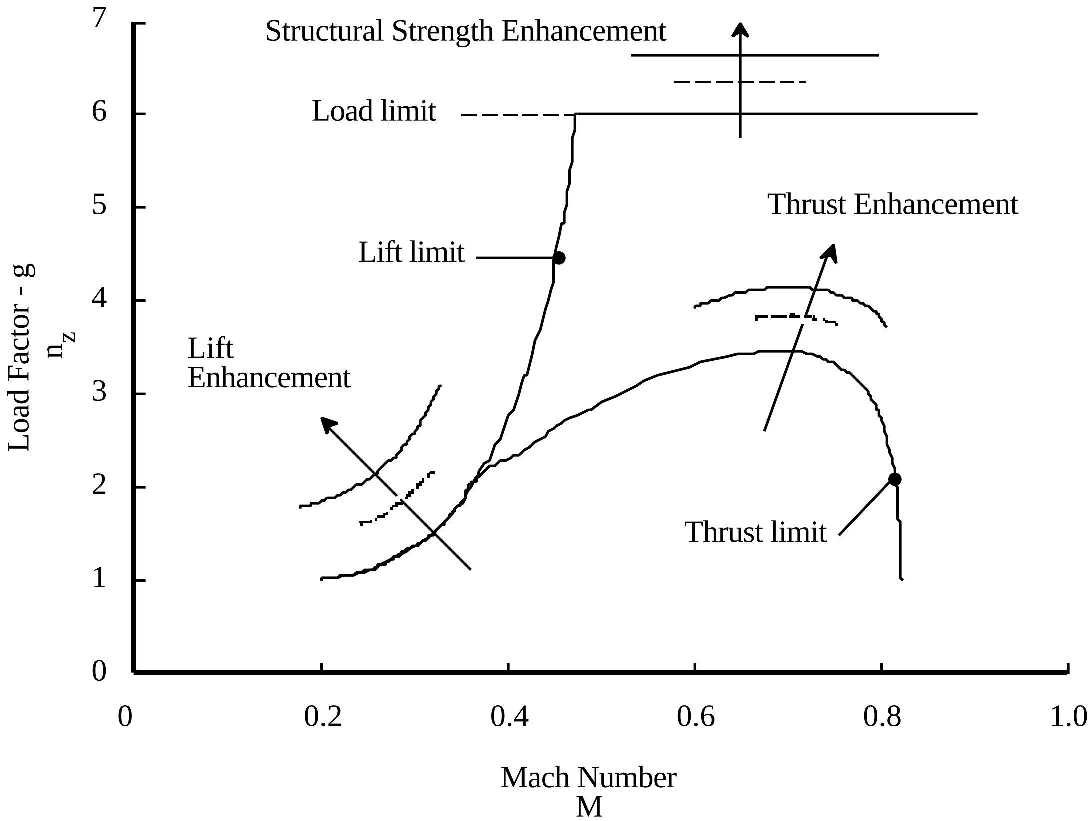

Figure 6.39
ENGINE-AIRFRAME COMPATIBILITY

6.6.3 LOADED ACCELERATION AND DECELERATION

Data from loaded accelerations and decelerations are compiled and added to 1 g acceleration data. These combined data can be plotted in a variety of formats. One example format is a family of curves showing P_S different load factors, as shown in figure 6.40

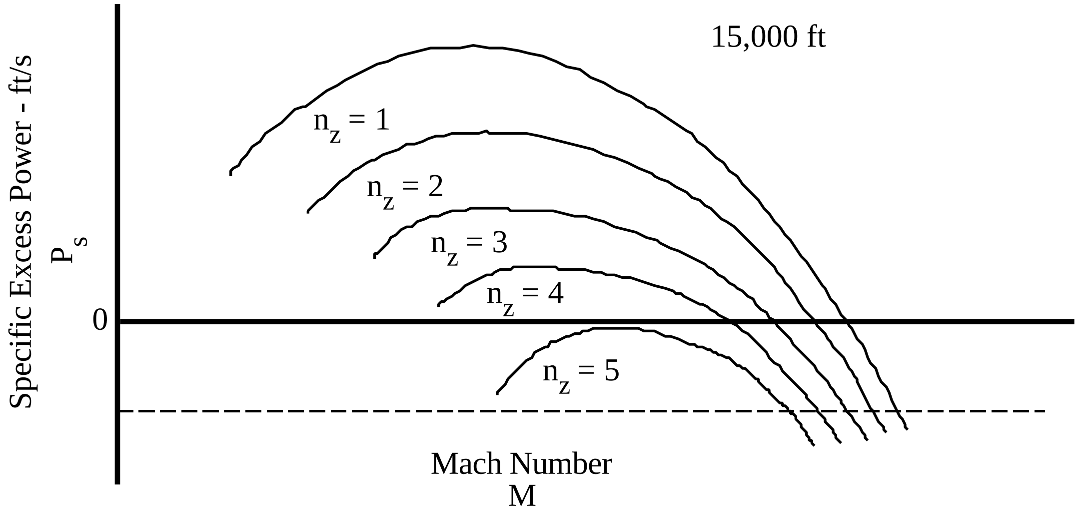

Figure 6.40
SPECIFIC EXCESS POWER VERSUS MACH NUMBER FOR VARIOUS LOAD FACTORS

Horizontal cuts in this plot indicate turn performance at specific values of P_S. For example, the horizontal axis ($P_S = 0$) represents the level sustained turn performance. A cut at a negative P_S can be interpreted as the turn performance that: 1) can be attained while passing through 15,000 ft in a corresponding rate of descent; or 2) will result in a deceleration equivalent to that energy loss rate.

6.6.4 AGILITY TESTS

The analysis for agility test results consists of tabulating the data. Time traces, if available, can provide insights into agility characteristics, but the analysis is largely covered in the flying qualities evaluation. Figure 6.41 show a typical data trace from one of these maneuvers.

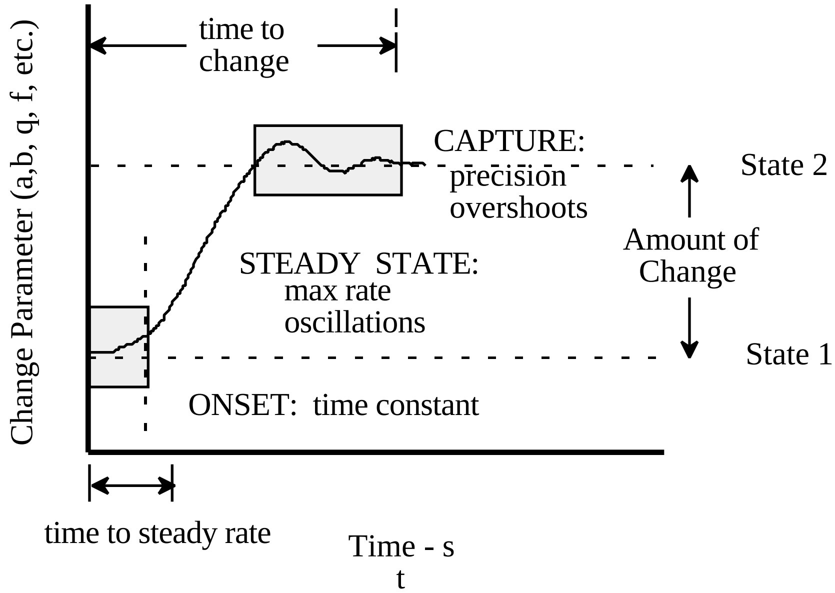

Figure 6.41
AGILITY TEST DATA TRACE

The time to steady rate of change and the time to capture the final steady state are seen in this data trace.

6.7 MISSION SUITABILITY

The mission suitability of the turning performance characteristics of an airplane depends upon its detailed mission requirements. For an airplane with a mission requirement for maneuverability, the turning performance characteristics are evaluated in light of the whole weapons system, in the predicted tactical scenario. The factors affecting the outcome of air-to-air combat are many, as illustrated in figure 6.42.

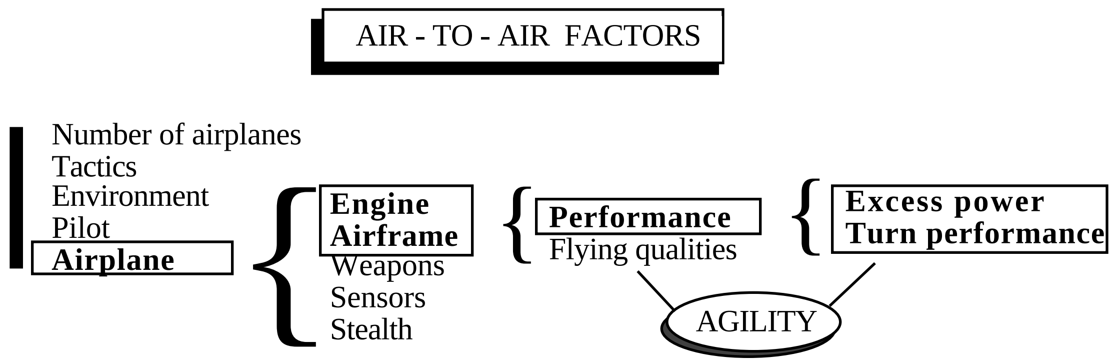

Figure 6.42
FACTORS AFFECTING AIR-TO-AIR COMBAT

Evaluation of each factor listed in the above figure provide data on relative strengths and weaknesses of airplanes, but no one factor guarantees mission success. The turn performance characteristics investigated in this chapter can be used to make comparisons and predictions, but superior performance in this category does not necessarily infer the airplane is better suited for the mission. Nevertheless, it's worthwhile to investigate the common turn performance and agility measures so relative advantages of the airplanes can be placed in the proper perspective.

The chief maneuvering characteristics presented in the previous sections were turn radius, turn rate, and excess energy. There are tradeoffs. High speeds mean high available energy for climbs and turns, giving more available options; however, turn rate and radius suffer, even at high load factors. The advantages of slow speeds are increased turn rate and decreased turn radius; however, at a relatively low energy state, the airplane become susceptible to attack. The relevance of turn performance parameters are discussed below with respect to basic tactical maneuvers.

6.7.1 LOAD FACTOR

While load factor alone does not prescribe turn rate or radius, it describes an airplane limit which is a potential maneuvering restriction. The freedom to use high load factors allows the pilot to maneuver at g levels which may be denied to some adversaries. Specifically, a higher limit load factor is a significant advantage, producing a higher turn rate and forcing an opponent to slow down to match your turn.

While current technology has produced combat airplanes capable of very high load factors and rapid g onset rates, the value of this maneuvering capability depends upon the ability of the pilot to cope with the high g environment. Physiological problems associated with this strenuous high g environment include g-induced loss of situational awareness and g loss of consciousness (G-LOC). These debilitating conditions, the results of rapid onset rates to high load factors, leave the pilot either unable to keep up with the tactical situation or, in extreme cases, unconscious. New anti-g flight equipment is under development to give the pilot the freedom to use the full maneuvering potential of the airplane.

6.7.2 TURN RADIUS

Maximum performance turn radius is largely a function of speed. The really tight turns are made only at low speeds. At the same speed, two opposing airplanes have different turn radii only if they're at different load factors. In that case, their turn rates are different as well and it's difficult to isolate the advantage of a small turn radius. If one of the airplanes is at a lower speed, with equal turn rates, it enjoys a position advantage if both airplanes continue the turn. Consider the one-circle fight depicted in figure 6.43.

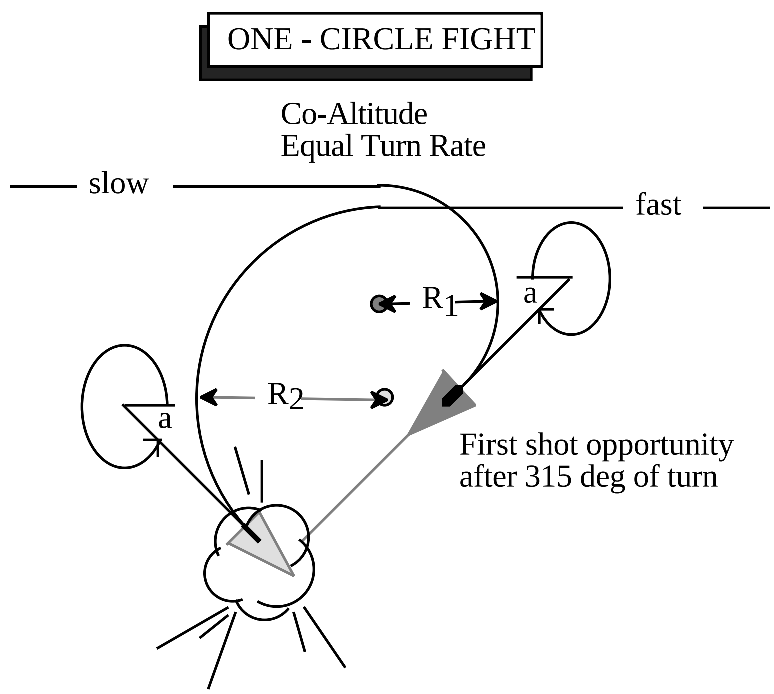

Figure 6.43
TURN RADIUS ADVANTAGE

To employ a forward-firing weapon against an adversary, it is necessary to put the enemy in your forward field of view (also, the weapon's). In the situation depicted above, the smaller turn radius (R_1) forces the opponent out in front. Even if the opponent has turned more degrees, it is still in the slower airplane's field of view due to the geometry of the engagement. If the slow airplane were able to turn as tightly at a faster engaging speed, the shot opportunity comes sooner. The type of weapon employed in this situation affects the outcome, since the fast airplane may have extended beyond the maximum range of the weapon, or may have rotated his nozzles out of the detection envelope of a heat-seeking missile. Still, the position advantage from a small turn radius is seen as the ability to put the opponent in your gun sight first.

Small turn radius confines the maneuvering to a relatively small area, making it easier to maintain visual contact with other airplanes. Formation tactics are enhanced, since it's easier for tactical elements to provide mutual support and to maneuver within the formation.

Turn radius is also relatable to ground attack missions. For straight attacks, the pilot has to be on track, there's no time to search for the target and no flexibility in the attack course. If turns in the target area are permissible, they must be tight turns to allow the pilot to acquire the target and maintain contact with it while prosecuting the attack. If high speeds are warranted in order to maintain a defensive posture while maneuvering in the target area, the required tight turns can be made only with high load factors, complicating the pilot's task.

6.7.3 TURN RATE

The heart of turn performance mission relation is the consideration of turn rate. In almost every tactical situation, turn rate is the measure of maneuvering advantage. When opposing fighters pass head on, the entire focus is on “getting angles”, the process by which a turn rate advantage is exploited to gain an offensive position. The significance of turn rate can be seen in the following depiction of a two-circle fight (Figure 6.44).

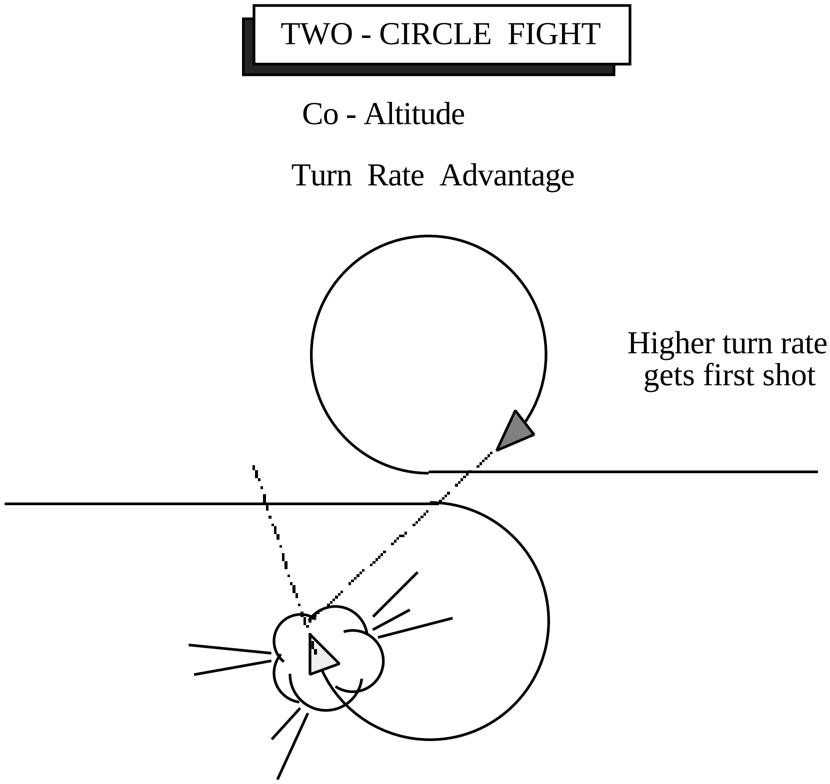

Figure 6.44
TURN RATE ADVANTAGE

A sustained turn rate advantage allows the pilot to put continual pressure on the adversary, eventually producing a shot opportunity or forcing the opponent to make a mistake. The importance of turning quicker encourages pilots to use the vertical plane of maneuvering to take advantage of the increased turn rate during a pull-down from a high relative position. The pilot exploits the tactical egg (Figure 6.7) by using gravity to enhance his turn rate over the top. An instantaneous turn rate advantage can produce the opportunity for a shot, which may justify the high energy loss, as long as it ends the engagement. In these tactical situations, time is critical to both offensive advantage and survivability. Turn rate is the one turn parameter which describes performance against the clock.

6.7.4 AGILITY

6.7.4.1 THE TACTICAL ENVIRONMENT

Missile technology has progressed to the point where the pilot who gets the first shot off will probably win an air-to-air engagement. Following a head-on pass, the first shot will probably be fired within 5 to 10 seconds. In this environment, it's tactically sound to do whatever is necessary to be the first to point at the opponent, even if it means slowing down to take advantage of high instantaneous turn rates. Post-stall maneuvering technology, featuring vectored thrust for pitch and yaw control augmentation, is the focus of much recent interest. This technology is intended to exploit the first-shot constraint by employing extremely rapid decelerations to below the 1 g stall speed. A typical tactical scenario is depicted in figure 6.45.

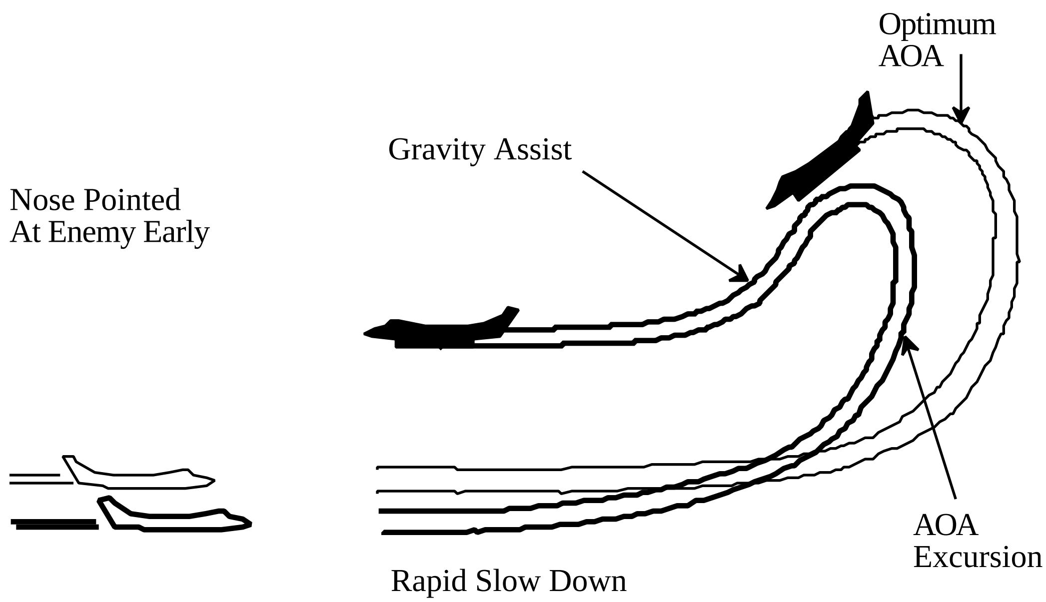

Figure 6.45
QUICK TURNAROUND USING POST-STALL TURN

At these post-stall conditions, very high instantaneous turn rates are possible using vectored thrust against very little aerodynamic damping. The nose is brought around using a combination of pitch and yaw rates to point at the opponent and fire the first shot. Rapid accelerations are performed to regain normal combat energy levels to engage other threats. The pilot uses instantaneous turn rate to rapidly point at his adversary, sacrificing energy to get the first shot, as illustrated in figure 6.46.

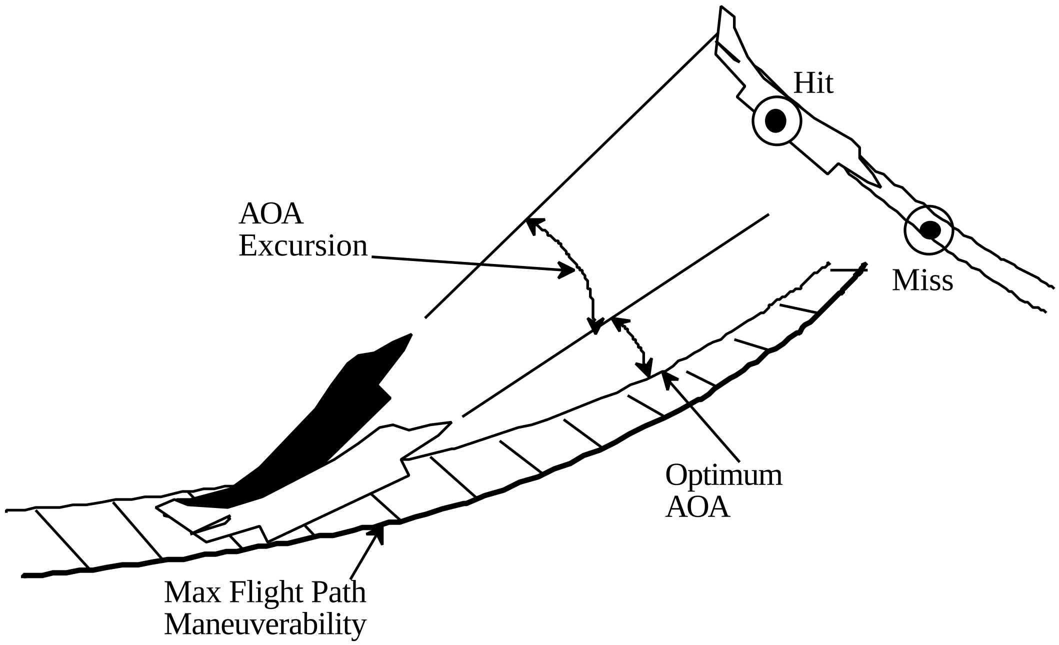

Figure 6.46
RAPID PITCH POINTING

The appeal of this technology is based on the capability to rapidly regain energy using a high thrust-to-weight ratio fighter design.

6.7.4.2 MISSILE PERFORMANCE

A big constraint in air-to-air combat is the requirement to point at the target before firing. This constraint is based largely upon missile capabilities. If the missiles are launched from a trail position at a reasonable range, the missile has very little maneuvering to do. On the other hand, to exploit the post-stall technology mentioned above, missiles have to be launched at very low speeds (high angle of attack), probably at a high angle-off. The missile has to accelerate from a very low speed and then perform a hard turn due to the high angle-off. Missile turn performance is a key issue for these tactics, since to a large extent, the missile is a mini-fighter with a slashing attack capability. As the fighter's requirement for close-in maneuvering diminishes, the demands on the missile increase.

6.7.4.3 DEFENSIVE AGILITY

Agility gives a defensive capability to generate rapid transients to confuse an enemy or to disrupt his attack. Such a defensive situation is depicted in figure 6.47.

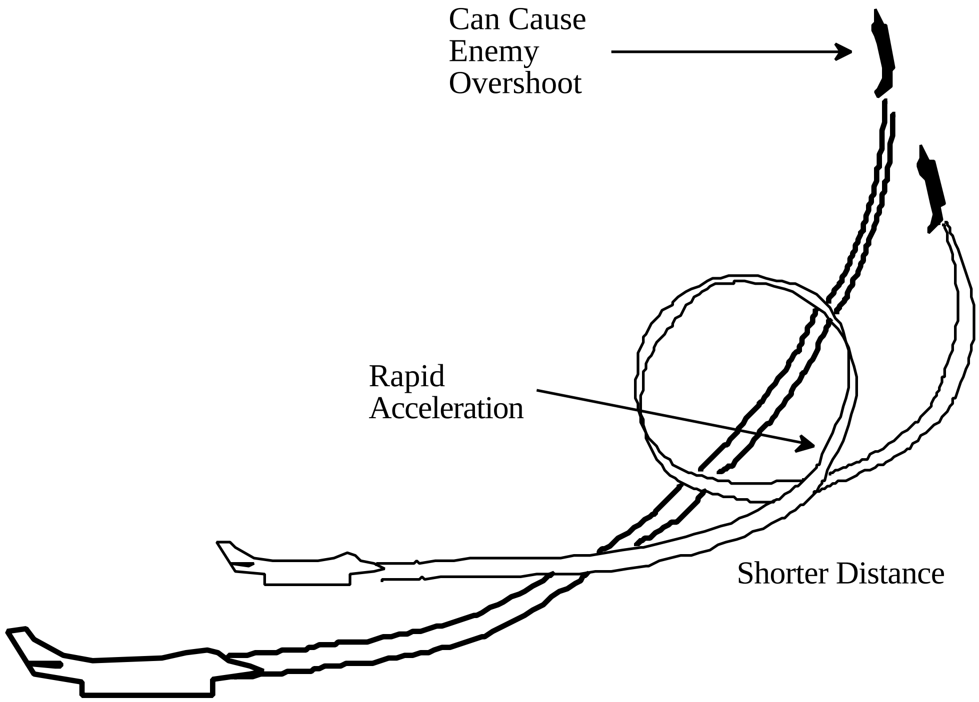

Figure 6.47
DEFENSIVE MANEUVER

This type of maneuver takes away the opponent's immediate offensive advantage, and a capability for rapid acceleration to maneuvering speed evens the odds.

6.7.4.4 CONTROLLABILITY

The previous discussions neglected an important aspect of agility, controllability. In this context, controllability means the ability to control the flight path geometry. The precise attitude control required for aiming is related more to flying qualities than performance. Here, the emphasis is on quick movements, like rapid 180 deg course reversals. From a mission evaluation viewpoint, the ability to start rapid changes in the flight path vector is not particularly useful if the change can't be stopped at the right place. There is no advantage to have a nimble airplane which can’t be controlled. Mission situations demanding more control force the pilot to be less aggressive with the controls. The classic case was the very maneuverable MiG-15 which lost repeatedly to the F-86 because of the Sabre's far superior controllability. Agility demands not only an enhanced maneuverability, but the ability to use it with accuracy.

6.8 SPECIFICATION COMPLIANCE

Standards for agility are in the developing stages, but a sample agility specification might contain turn rate and P_s minimum requirements within a tactical maneuvering corridor, such as:

At 15,000 ft, between 0.4 M and 0.8 M, for a given configuration and loading:

Sustained turn rate:	≥ 12 deg/s
Specific excess power:	≥ 75 ft/s

Another agility specification might address the minimum time to change states. Here, the relevant states are attitude, rate, and flight path acceleration. The specification might address the time from steady state to some threshold rate of change, and the time from initial steady state to final steady state.

6.9 GLOSSARY

6.9.1 NOTATIONS

a	Speed of sound	ft/s
AR	Aspect ratio	
a_R	Radial acceleration	ft/s^2
C_D	Drag coefficient	
C_L	Lift coefficient	
$C_{L_{max}}$	Maximum lift coefficient	
$C_{L_{max_{Test}}}$	Test maximum lift coefficient	
D	Drag	lb
$\Delta H_{P_{ic}}$	Altimeter instrument correction	ft
ΔH_{pos}	Altimeter position error	ft
$\Delta n_{z_{ic}}$	Normal acceleration instrument correction	G

$\Delta n_{z_{tare}}$	Accelerometer tare correction	g
D_{Std}	Standard drag	lb
ΔT	Change in thrust	lb
D_{Test}	Test drag	lb
ΔV_{ic}	Airspeed instrument correction	kn
ΔV_{pos}	Airspeed position error	kn
e	Oswald's efficiency factor	
E_h	Energy height	ft
F_R	Radial force	lb
F_Y	Sideforce	lb
g	Gravitational acceleration	ft/s^2
h	Tapeline altitude	ft
H_P	Pressure altitude	ft
H_{P_c}	Calibrated pressure altitude	ft
H_{P_i}	Indicated pressure altitude	ft
H_{P_o}	Observed pressure altitude	ft
K	Constant	
L	Lift	lb
L_{aero}	Aerodynamic lift	lb
M	Mach number	
M_o	Observed Mach number	
n_L	Limit normal acceleration	g
n_R	Radial load factor, $\frac{F_R}{W}$	g
n_Y	Sideforce load factor, $\frac{F_Y}{W}$	g
n_z	Normal acceleration	g
$n_{z\ sust}$	Sustained normal acceleration	g
$n_{z\ sust\ max}$	Maximum sustained normal acceleration	g
n_{z_i}	Indicated normal acceleration	g
$n_{z_{max}}$	Maximum normal acceleration	g
n_{z_o}	Observed normal acceleration	g
$n_{z_{Std}}$	Standard normal acceleration	g
$n_{z_{Test}}$	Test normal acceleration	g
$\frac{N}{\sqrt{\theta}}$	Referred engine speed	RPM
OAT	Outside air temperature	˚C or ˚K

P_a	Ambient pressure	psf
P_s	Specific excess power	ft/s
$P_{s\ 1\ g}$	Specific excess energy at 1 g	ft/s
P_{ssl}	Standard sea level pressure	2116.217 psf
q	Dynamic pressure	psf
R	Turn radius	ft
$R_{min\ V>V_A}$	Minimum turn radius for $V > V_A$	ft
R_{sust}	Sustained turn radius	ft
S	Wing area	ft^2
T	Thrust	lb
TE	Total energy	ft-lb
T_{ex}	Excess thrust	lb
T_G	Gross thrust	lb
THP_{avail}	Thrust horsepower available	hp
THP_{req}	Thrust horsepower required	hp
T_N	Net thrust	lb
T_{Std}	Standard thrust	lb
V_A	Maneuvering speed	ft/s
V_c	Calibrated airspeed	kn
V_i	Indicated airspeed	kn
V_{max}	Maximum airspeed	kn
V_{min}	Minimum airspeed	kn
V_{mrt}	Military rated thrust airspeed	kn
V_o	Observed airspeed	kn
V_s	Stall speed	kn or ft/s
V_T	True airspeed	ft/s
W	Weight	lb
W_{Std}	Standard weight	lb
W_{Test}	Test weight	lb
n_R	Radial load factor	g

6.9.2 GREEK SYMBOLS

α (alpha)	Angle of attack	deg
α_j	Thrust angle	deg
δ (delta)	Pressure ratio	
δ_h	Pressure ratio for selected altitude	
δ_{Test}	Test pressure ratio	
ϕ (phi)	Bank angle	deg
ϕ_E	Equivalent bank angle	deg
γ (gamma)	Flight path angle	deg
π (pi)	Constant	
ω (omega)	Turn rate	rad/s
$\omega_{max\ V>V_A}$	Maximum turn rate for $V > V_A$	rad/s
ω_{sust}	Sustained turn rate	deg/s

6.10 REFERENCES

1. Hoover, A.D., *Testing for Agility - a Progress Report,* Thirty-Second Symposium Proceedings, Society of Experimental Test Pilots, October, 1988.

2. McAtee, T.P., *Agility - Its Nature and Need in the 1990s*, Thirty-First Symposium Proceedings, Society of Experimental Test Pilots, September, 1987.

3. Naval Test Pilot School Flight Test Manual, *Fixed Wing Performance, Theory and Flight Test Techniques*, USNTPS-FTM-No.104, U. S. Naval Test Pilot School, Patuxent River, MD, July, 1977.

4. Powell, J., *Airplane Performance*, USNTPS Classroom Notes, USNTPS, Patuxent River, MD.

5. Rutowski, E.S., *Energy Approach to the General Aircraft Maneuverability Problem,* Journal of the Aeronautical Sciences, Vol 21, No 3, March 1954.

6. USAF Test Pilot School, *Performance Phase Textbook Volume I,* USAF-TPS-CUR-86-01, USAF, Edwards AFB, CA, April, 1986.

CHAPTER 7

CLIMB PERFORMANCE

CHAPTER 7

FIGURES

CHAPTER 7

EQUATIONS

Equation		PAGE
$E_h = h + \frac{V_T^2}{2\,g}$	(Eq 7.1)	7.2
$P_s = \frac{dE_h}{dt} = \frac{dh}{dt} + \frac{V_T}{g}\frac{dV_T}{dt}$	(Eq 7.2)	7.2
$\frac{dV}{dt} = \frac{dV}{dh}\frac{dh}{dt}$	(Eq 7.3)	7.2
$P_s = \frac{dh}{dt} + \frac{V}{g}\frac{dV}{dh}\frac{dh}{dt}$	(Eq 7.4)	7.3
$P_s = \frac{dh}{dt}\left[1 + \frac{V}{g}\frac{dV}{dh}\right]$	(Eq 7.5)	7.3
$\frac{dh}{dt} = P_s\left[\frac{1}{1 + \frac{V_T}{g}\frac{dV}{dh}}\right]$	(Eq 7.6)	7.3
$CCF = \frac{1}{1 + \frac{V_T}{g}\frac{dV}{dh}}$	(Eq 7.7)	7.3
$L - W\cos\gamma + T_G\sin\alpha_j = \frac{W}{g}\,a_z$	(Eq 7.8)	7.5
$T_G\cos\alpha_j - T_R - D - W\sin\gamma = \frac{W}{g}\,a_x$	(Eq 7.9)	7.5
$L = W\cos\gamma$	(Eq 7.10)	7.5
$T_G\cos\alpha_j - T_R - D - W\sin\gamma = \frac{W}{g}\frac{dV_T}{dt} = 0$	(Eq 7.11)	7.6
$T_{N_x} = T_G\cos\alpha_j - T_R$	(Eq 7.12)	7.6

$T_{N_x} - D = W \sin\gamma$	(Eq 7.13)	7.6
$\gamma = \sin^{-1}\left[\dfrac{T_{N_x} - D}{W}\right]$	(Eq 7.14)	7.6
$V \sin\gamma = \dfrac{\left[T_{N_x} - D\right]}{W} V = \dfrac{dh}{dt} = V_v$	(Eq 7.15)	7.6
$ROC = \dfrac{dh}{dt} = \dfrac{\left[T_{N_x} - D\right]}{W} V = \dfrac{T_{N_x} V - D V}{W} = \dfrac{P_A - P_{req}}{W}$	(Eq 7.16)	7.10
$t = \int_0^h \dfrac{1}{\frac{dh}{dt}} dh = \int_0^h \dfrac{1}{ROC} dh$	(Eq 7.17)	7.12
$V_v = V_T \sin\gamma$	(Eq 7.18)	7.14
$V_{hor} = V_T \cos\gamma$	(Eq 7.19)	7.14
$\text{Rate of Climb} = P_s \left(\dfrac{1}{1 + \frac{V}{g}\frac{dV_T}{dh}}\right)$	(Eq 7.20)	7.20
$\text{Time to Climb} = \int_{h_1}^{h_2} \dfrac{\left(1 + \frac{V}{g}\frac{dV_T}{dh}\right)}{P_s} dh$	(Eq 7.21)	7.20
$dt = \dfrac{dh + \frac{V}{g} dV_T}{P_s}$	(Eq 7.22)	7.21
$dE_h = dh + \dfrac{V}{g} dV$	(Eq 7.23)	7.21
$dt = \dfrac{dE_h}{P_s}$	(Eq 7.24)	7.21

$$\text{Time to Climb} = \int_{E_{h_1}}^{E_{h_2}} \frac{1}{P_s}\, dE_h$$ (Eq 7.25) 7.21

$$\frac{dE_h}{dW} = \frac{d}{dW}\left(h + \frac{V_T^2}{2\,g}\right) = \frac{dh}{dW} + \frac{V_T}{g}\frac{dV_T}{dW}$$ (Eq 7.26) 7.25

$$\text{Fuel to Climb} = \int_{W_1}^{W_2} dW = -\int_{E_{h_1}}^{E_{h_2}} \frac{1}{\frac{dE_h}{dW}}\, dE_h$$ (Eq 7.27) 7.25

$$-\frac{1}{\frac{dE_h}{dW}} = -\frac{dW}{dE_h} = -\frac{dW}{dt}\frac{dt}{dE_h} = \frac{\dot{W}_f}{P_s}$$ (Eq 7.28) 7.25

$$\text{Fuel to Climb} = \int_{E_{h_1}}^{E_{h_2}} \frac{\dot{W}_f}{P_s}\, dE_h = \int_{E_{h_1}}^{E_{h_2}} \frac{1}{\frac{P_s}{\dot{W}_f}}\, dE_h$$ (Eq 7.29) 7.26

$$E_{h_{Test}} = h_{Test} + \frac{V_{T_{Test}}^2}{2\,g}$$ (Eq 7.30) 7.37

$$\left(\frac{dh}{dt}\right)_{Test} = P_{s_{Test}}\left(\frac{1}{1 + \frac{V_{T_{ref}}}{g}\frac{dV_T}{dh}}\right)$$ (Eq 7.31) 7.38

$$P_{s_{Std}} = P_{s_{Test}}\frac{W_{Test}}{W_{Std}}\frac{V_{T_{Std}}}{V_{T_{Test}}} + \frac{V_{T_{Std}}}{W_{Std}}\left(\Delta T_{N_x} - \Delta D\right)$$ (Eq 7.32) 7.38

$$\Delta D = D_{Std} - D_{Test} = \frac{2\left(W_{Std}^2 - W_{Test}^2\right)}{\pi\, e\, AR\, S\, \gamma\, P_a\, M^2}$$ (Eq 7.33) 7.39

$$L = n_z W$$ (Eq 7.34) 7.40

$$n_z = \cos\gamma$$ (Eq 7.35) 7.40

$$\Delta D = \frac{2\left(W^2_{Std}\cos^2\gamma_{Std} - W^2_{Test}\cos^2\gamma_{Test}\right)}{\pi\, e\, AR\, \rho_{ssl}\, V_e^2\, S}$$ (Eq 7.36) 7.40

$$\Delta D = \frac{2\left(W^2_{Std} n^2_{z\,Std} - W^2_{Test}\, n^2_{z\,Test}\right)}{\pi\, e\, AR\, \rho_{ssl}\, V_e^2\, S}$$ (Eq 7.37) 7.40

$$\left(\frac{dh}{dt}\right)_{Std} = P_{s_{Std}}\left(\frac{1}{1 + \frac{V_T}{g}\frac{dV_T}{dh}}\right)$$ (Eq 7.38) 7.41

$$\gamma_{Std} = \sin^{-1}\left(\frac{\frac{dh}{dt}}{V_T}\right)$$ (Eq 7.39) 7.41

$$L = W\cos\gamma - T_G\,\sin\alpha_j$$ (Eq 7.40) 7.42

$$n_z = \frac{L}{W}$$ (Eq 7.41) 7.42

$$n_z = \cos\gamma - \frac{T_G}{W}\sin\alpha_j$$ (Eq 7.42) 7.42

$$\Delta T_N = f\left(\Delta H_P, \Delta T_a\right)$$ (Eq 7.43) 7.44

$$\text{Distance} = \int_{t_1}^{t_2} V_T\cos\gamma\, dt$$ (Eq 7.44) 7.46

$$\text{Fuel Used} = \int_{t_1}^{t_2} \dot{W}_f\, dt$$ (Eq 7.45) 7.47

$$^\circ C = {}^\circ K - 273.15$$ (Eq 7.46) 7.52

$OAT = f\left(T_a, M\right)$	(Eq 7.47)	7.52
$T_a = f\left(OAT, M\right)$	(Eq 7.48)	7.52
$V_T = f\left(OAT, M_T\right)$	(Eq 7.49)	7.53
$h = H_{P_{c\,ref}} + \Delta H_{P_c}\left(\frac{T_a}{T_{std}}\right)$	(Eq 7.50)	7.53

CHAPTER 7

CLIMB PERFORMANCE

7.1 INTRODUCTION

Climb performance is evaluated in various ways depending on the aircraft mission. An interceptor launching to take over a particular combat air patrol (CAP) station is primarily interested in climbing to altitude with the minimum expenditure of fuel. If launching on an intercept, the desire is to reach intercept altitude with the best fighting speed or energy in the minimum time. An attack aircraft launching on a strike mission is primarily interested in climbing on a schedule of maximum range per pound of fuel used. Different missions may require optimization of other factors during the climb. Primary emphasis in this chapter is on energy analysis since measuring climb performance in jet aircraft and determining climb performance for various climb schedules is best done through energy methods. This chapter also discusses the sawtooth climb as an alternate test method of determining specific excess power. However, the sawtooth climb method can be used successfully for lower performance aircraft during climb speed determination and is also suited for single engine climb performance evaluation in the takeoff or wave-off configuration.

7.2 PURPOSE OF TEST

The purpose of this test is to determine the following climb performance characteristics:

1. Conditions for best climb angle.
2. Conditions for best climb rate.
3. Conditions for the shortest time to climb.
4. Conditions for minimum fuel used to climb.
5. Climb schedules for the above conditions.
6. Evaluate the requirements of pertinent military specifications.

7.3 THEORY

7.3.1 SAWTOOTH CLIMBS

The primary method of determining specific excess power (P_S) is the level acceleration. Sawtooth climb is a secondary method of determining P_S. The sawtooth climb is more time consuming than the level acceleration run. There are conditions where the sawtooth climb is more applicable, especially in determining single engine wave-off for multiengine airplanes or climb in the approach configuration for a jet. The sawtooth climb is one method of obtaining the airspeed schedule for maximum rate of climb. The results of tests are derived from a series of short, timed climbs through the same altitude band. The test provides limited information on overall climb performance but does establish the best airspeed at which to climb at a specific altitude.

To express rate of climb potential in terms of P_S, true airspeed (V_T) must be evaluated in the climb. P_S is calculated by measuring energy height as in Eq 7.1 then taking the time derivative as in Eq 7.2.

$$E_h = h + \frac{V_T^2}{2\,g} \qquad \text{(Eq 7.1)}$$

$$P_s = \frac{dE_h}{dt} = \frac{dh}{dt} + \frac{V_T}{g}\frac{dV_T}{dt} \qquad \text{(Eq 7.2)}$$

The only time P_S is equal to rate of climb is when the climb is done at a constant true airspeed, which is rarely the case. If true airspeed is constant, then dV_T/dt in Eq 7.2 is zero. Climbing at constant indicated airspeed is not constant V_T. Climbing at constant Mach number is not constant V_T either, except when climbing in the stratosphere on a standard day.

From the chain rule, dV/dt can be expressed as in Eq 7.3 and substituted into Eq 7.1 to derive Eq 7.4 and Eq 7.5.

$$\frac{dV}{dt} = \frac{dV}{dh}\frac{dh}{dt} \qquad \text{(Eq 7.3)}$$

$$P_s = \frac{dh}{dt} + \frac{V}{g}\frac{dV}{dh}\frac{dh}{dt} \qquad \text{(Eq 7.4)}$$

$$P_s = \frac{dh}{dt}\left[1 + \frac{V}{g}\frac{dV}{dh}\right] \qquad \text{(Eq 7.5)}$$

Knowing P_S and the climb schedule, the rate of climb potential is:

$$\frac{dh}{dt} = P_s\left[\frac{1}{1 + \frac{V_T}{g}\frac{dV}{dh}}\right] \qquad \text{(Eq 7.6)}$$

Specific excess power is nearly independent of the climb or acceleration path for modest climb angles, but the actual rate of climb is adjusted by the velocity change along the climb path (dV_T/dh). A term called the climb correction factor (CCF) represents the values within the brackets of Eq 7.6 and is useful in evaluating rate of climb. CCF is defined as follows:

$$CCF = \frac{1}{1 + \frac{V_T}{g}\frac{dV}{dh}} \qquad \text{(Eq 7.7)}$$

Where:

CCF	Climb correction factor	
E_h	Energy height	ft
g	Gravitational acceleration	ft/s^2
h	Tapeline altitude	ft
P_s	Specific excess power	ft/s^2
t	Time	s
V	Velocity	ft/s
V_T	True airspeed	ft/s.

There are three cases to consider about the CCF.

1. If the aircraft is accelerating during the climb as in a constant indicated airspeed schedule, CCF < 1 and rate of climb is less than P_S.

2. If the aircraft is climbing at a constant true airspeed, CCF =1 and rate of climb equals P_S.

3. If the aircraft is decelerating while climbing, as in a constant Mach number through decreasing temperature, CCF > 1 and rate of climb is greater than P_S.

For a low speed aircraft the factor does not have much significance. For supersonic aircraft however, the influence of the CCF on rate of climb is significant. Figure 7.1 illustrates CCF as a function of Mach number.

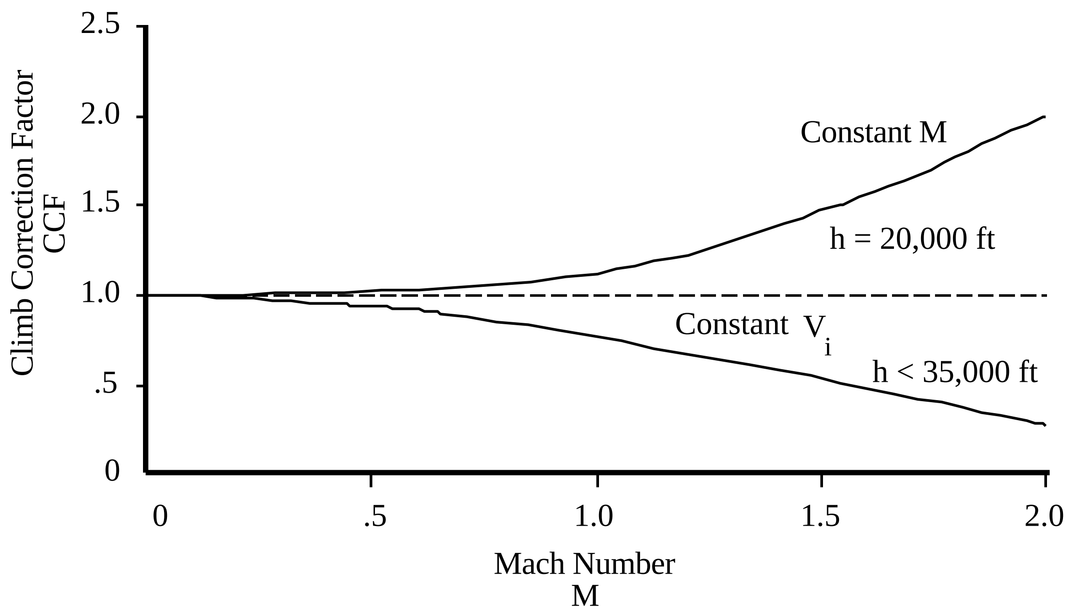

Figure 7.1
CLIMB CORRECTION FACTOR

7.3.2 STEADY STATE APPROACH TO CLIMB PERFORMANCE

The classical approach to aircraft climb performance problems was to use the static or steady state case. One major assumption was the aircraft had no acceleration along the flight path. True airspeed had to be held constant. This approach was derived before the total energy theory was developed, and is inadequate for analyzing climb profiles of supersonic aircraft where both true airspeed and altitude change rapidly. The following paragraphs are intended to present a quick overview of the classical approach.

7.3.2.1 FORCES IN FLIGHT

The forces acting on an aircraft in a climb are presented in figure 7.2 for review and can be resolved perpendicular and parallel to the flight path.

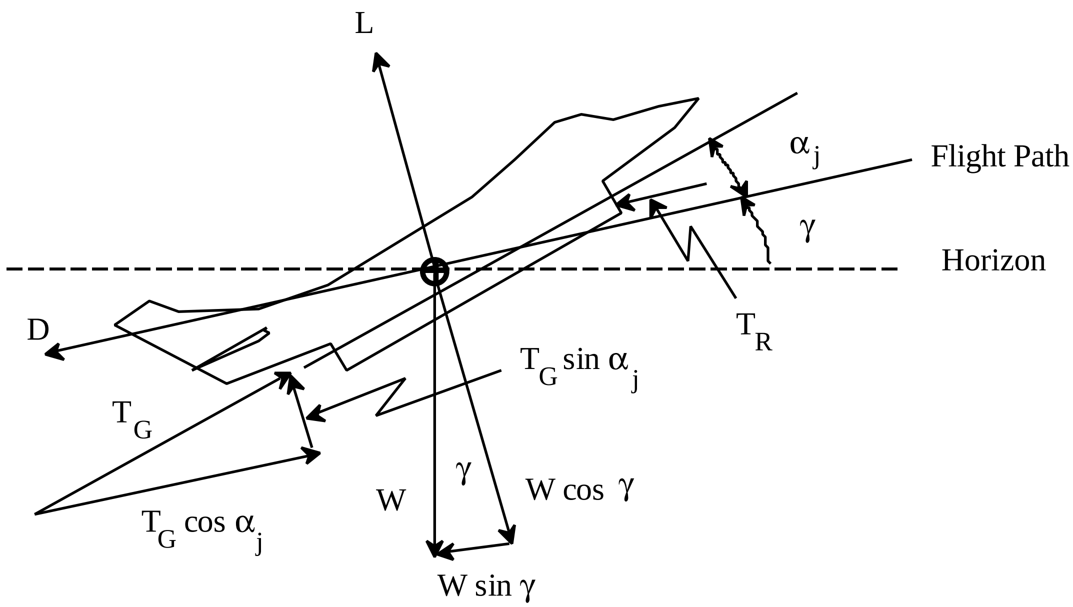

Figure 7.2
FORCES IN CLIMBING FLIGHT

Forces perpendicular to the flight path are:

$$L - W \cos \gamma + T_G \sin \alpha_j = \frac{W}{g} a_z \tag{Eq 7.8}$$

Forces parallel to the flight path are:

$$T_G \cos \alpha_j - T_R - D - W \sin \gamma = \frac{W}{g} a_x \tag{Eq 7.9}$$

By assuming angle of attack (α) is small, the engines are closely aligned with the fuselage reference line, and the aircraft is in a steady climb where acceleration parallel flight path (a_x) is zero, or at a constant true airspeed, the equations reduce to:

$$L = W \cos \gamma \tag{Eq 7.10}$$

$$T_G \cos \alpha_j - T_R - D - W \sin \gamma = \frac{W}{g} \frac{dV_T}{dt} = 0 \quad \text{(Eq 7.11)}$$

$$T_{N_x} = T_G \cos \alpha_j - T_R \quad \text{(Eq 7.12)}$$

$$T_{N_x} - D = W \sin \gamma \quad \text{(Eq 7.13)}$$

With true airspeed held constant, a useful expression for γ can be found:

$$\gamma = \sin^{-1}\left[\frac{T_{N_x} - D}{W}\right] \quad \text{(Eq 7.14)}$$

The term in brackets is specific excess thrust. By maximizing specific excess thrust, the climb angle is greatest. If both sides of Eq 7.13 are multiplied by V an expression for rate of climb is developed, as Eq 7.15, and is graphically shown in figure 7.3.

$$V \sin \gamma = \frac{\left[T_{N_x} - D\right]}{W} V = \frac{dh}{dt} = V_v \quad \text{(Eq 7.15)}$$

Where:

α	Angle of attack	deg
α_j	Thrust angle	deg
a_x	Acceleration parallel flight path	ft/s^2
a_z	Acceleration perpendicular to flight path	ft/s^2
D	Drag	lb
dh/dt	Rate of climb	ft/s
γ	Flight path angle	deg
L	Lift	lb
T_G	Gross thrust	lb
T_{N_x}	Net thrust parallel flight path	lb
T_R	Ram drag	lb
V	Velocity	ft/s
V_T	True airspeed	ft/s
V_v	Vertical velocity	ft/s
W	Weight	lb.

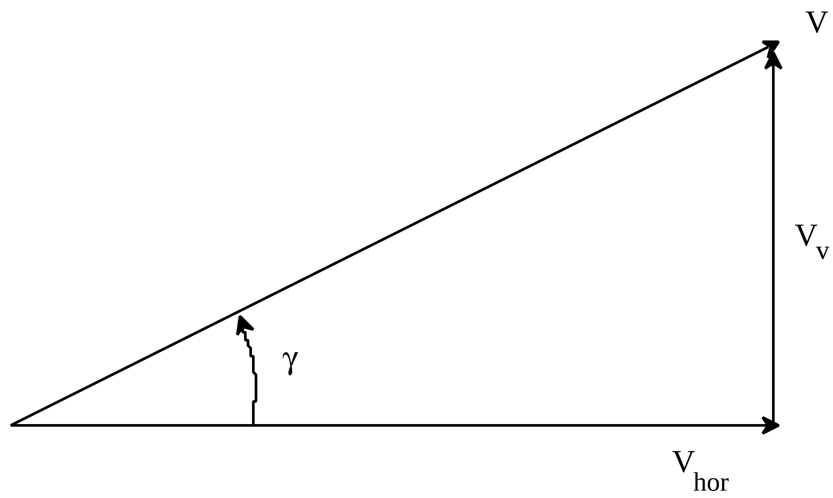

Figure 7.3
CLIMB VECTORS

Eq 7.15 shows if net thrust is greater than drag, dh/dt is positive and a climb results.

7.3.2.2 CLIMB ANGLE

As seen in Eq 7.14, the climb angle, γ, depends on specific excess thrust ($(T_{N_x}$ - D)/W. As the aircraft climbs, the propulsive thrust decreases. Drag remains essentially constant. There is an absolute ceiling where $T_{N_x} = D$ and $\gamma = 0$. Increasing altitude decreases specific excess thrust and the climb angle.

The effect of increasing weight on climb angle can be evaluated from Eq 7.14. Since climb angle is inversely proportional to weight, climb angle decreases as weight increases.

Wind is also a factor. A steady wind has no effect on the climb angle of the aircraft relative to the moving air mass. However, the maximum climb angle must give the most altitude gained for horizontal distance covered. The prime reason for optimizing climb angle might be to gain obstacle clearance during some portion of the flight. Winds do affect this distance and give apparent changes in γ as depicted in figure 7.4.

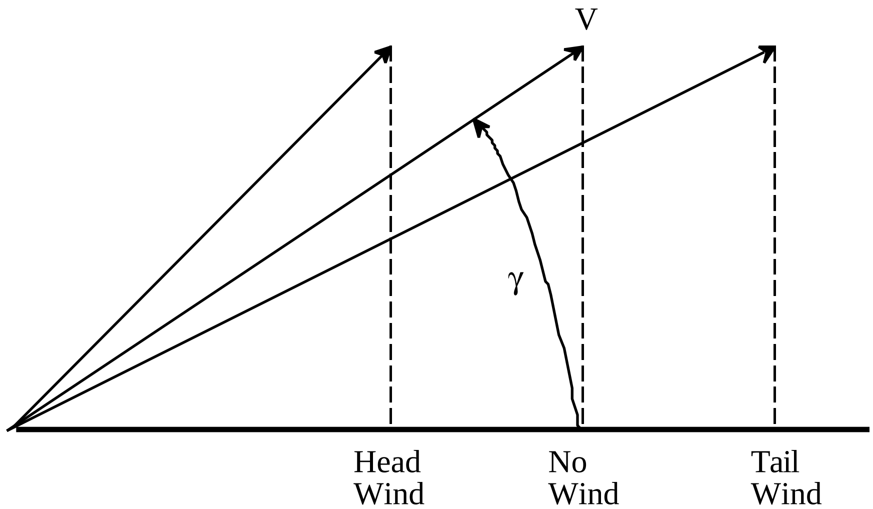

Figure 7.4
WIND EFFECT ON CLIMB ANGLE

Excess thrust, T_{N_x} - D, is a function of airspeed. The aircraft must be flown at the velocity where maximum excess thrust occurs to achieve the maximum climb angle. The net thrust available from a pure turbojet varies little with airspeed at a given altitude. In general, the same can be said for a turbofan. A jet lacking thrust augmentation usually climbs at the velocity for minimum drag or minimum thrust required to achieve the maximum climb angle. This is a classical result and leads to the assumption γ_{max} occurs at $V_{L/D_{max}}$. But, γ_{max} may occur over an airspeed band. In figure 7.5, the maximum excess thrust at military thrust occurs close to $V_{L/D_{max}}$. With thrust augmentation, thrust available varies with airspeed and γ_{max} occurs at other airspeeds.

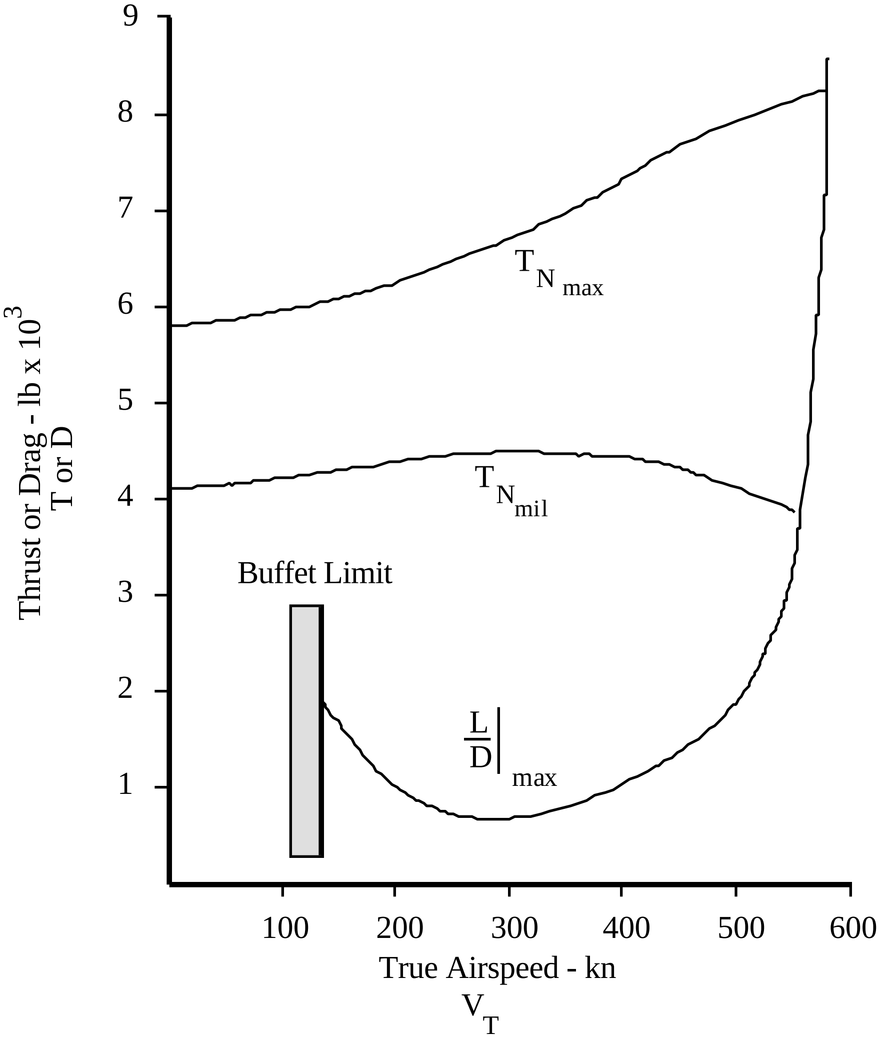

Figure 7.5

THRUST AND DRAG

Specific excess thrust determines climb angle, whether specific excess thrust is measured directly or calculated from independent estimates of thrust, drag, and weight.

7.3.2.3 CLIMB GRADIENT

Climb gradient is the altitude gained for the distance traveled. The gradient can be determined from figure 7.3 by dividing V_v by V_{hor} or by measuring tan γ. The gradient is usually expressed in percent where 100% occurs when $V_v = V_{hor}$, or tan $\gamma = 1$ (45 deg).

7.3.2.4 RATE OF CLIMB

Eq 7.2 shows rate of climb, dh/dt, depends upon specific excess power. This is similar to excess thrust, which was defined as the difference between net thrust available and drag (thrust required) at a specific weight. Excess power is also defined as the difference between the power available to do work in a unit of time and the work done by drag per unit time. Power available can be expressed as net thrust times velocity (T_{N_x} x V) and power lost to drag as drag times velocity (D x V). Then Eq 7.15 can be rewritten as Eq 7.16.

$$ROC = \frac{dh}{dt} = \frac{\left[T_{N_x} - D\right]}{W} V = \frac{T_{N_x} V - D V}{W} = \frac{P_A - P_{req}}{W} \qquad \text{(Eq 7.16)}$$

Where:

D	Drag	lb
dh/dt	Rate of climb	ft/s
T_{N_x}	Net thrust parallel flight path	lb
P_A	Power available	ft-lb/s
P_{req}	Power required	ft-lb/s
ROC	Rate of climb	ft/s
V	Velocity	ft/s, kn
W	Weight	lb.

In specific excess power, dh/dt is rate of climb at constant airspeed. Figure 7.6 depicts a typical curve of power available and required.

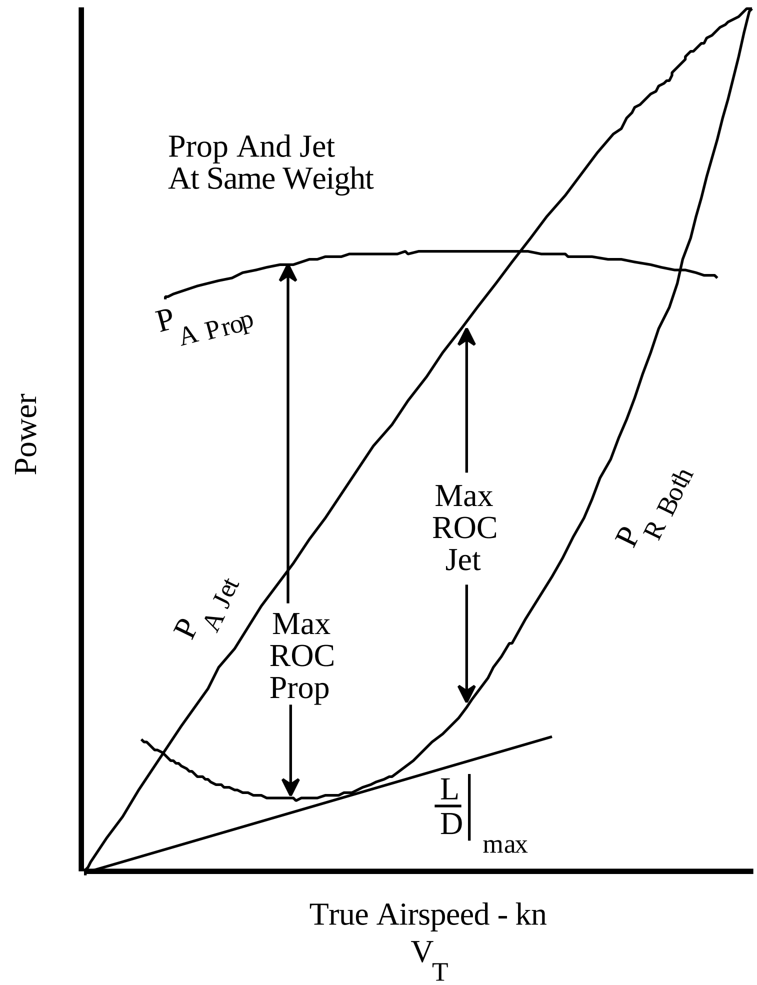

Figure 7.6
POWER AVAILABLE AND REQUIRED

The power required curve is derived by multiplying V by the drag at that speed. The power available curve is derived by multiplying V by the thrust at that speed. For the military power turbojet, the thrust is nearly constant so power available is a straight line originating at V=0. The slope of the curve is directly proportional to the magnitude of thrust.

For the turboprop, the thrust tends to decrease with an increase in velocity as also seen in figure 7.6. Depending on the exact shape of the turboprop thrust curve, the maximum value of excess thrust might occur at a speed less than $V_{L/D_{max}}$ and close to the speed for minimum thrust horsepower required. Propeller efficiencies also account for part of the curve shape. The slope of the curve for power available changes as the true airspeed changes.

Altitude has an effect on rate of climb similar to its effect upon climb angle. Rate of climb at the absolute ceiling goes to zero when $T_{N_x} = D$ and excess power is minimum. The service ceiling and combat ceiling, defined as the altitudes where 100 ft/min and 500 ft/min rates of climb can be maintained, are also finite altitudes.

Weight affects rate of climb directly and in the same manner as it does climb angle. Increasing weight with no change in excess power reduces rate of climb.

Wind affects rate of climb negligibly unless gradient and direction changes are large within the air mass.

True airspeed strongly affects rate of climb performance since thrust and drag are functions of velocity, and specific excess power directly depends upon true airspeed according to Eq 7.15. Maximum rate of climb for the jet occurs at much higher true airspeed than that for L/D_{max}.

7.3.2.5 TIME TO CLIMB

The rates of climb discussed are instantaneous values. At each altitude, there is one velocity which yields maximum rate of climb. That value pertains only to the corresponding altitude. Continuous variations in rate of climb must be attained through integration as in Eq 7.17.

$$t = \int_0^h \frac{1}{\frac{dh}{dt}} dh = \int_0^h \frac{1}{ROC} dh \qquad \text{(Eq 7.17)}$$

Where:

h	Tapeline altitude	ft
ROC	Rate of climb	ft/s
t	Time	s.

The term dh/dt in Eq 7.17 is not usually available as an analytical function of altitude. The determination of time to climb then can only be determined graphically as in figure 7.7.

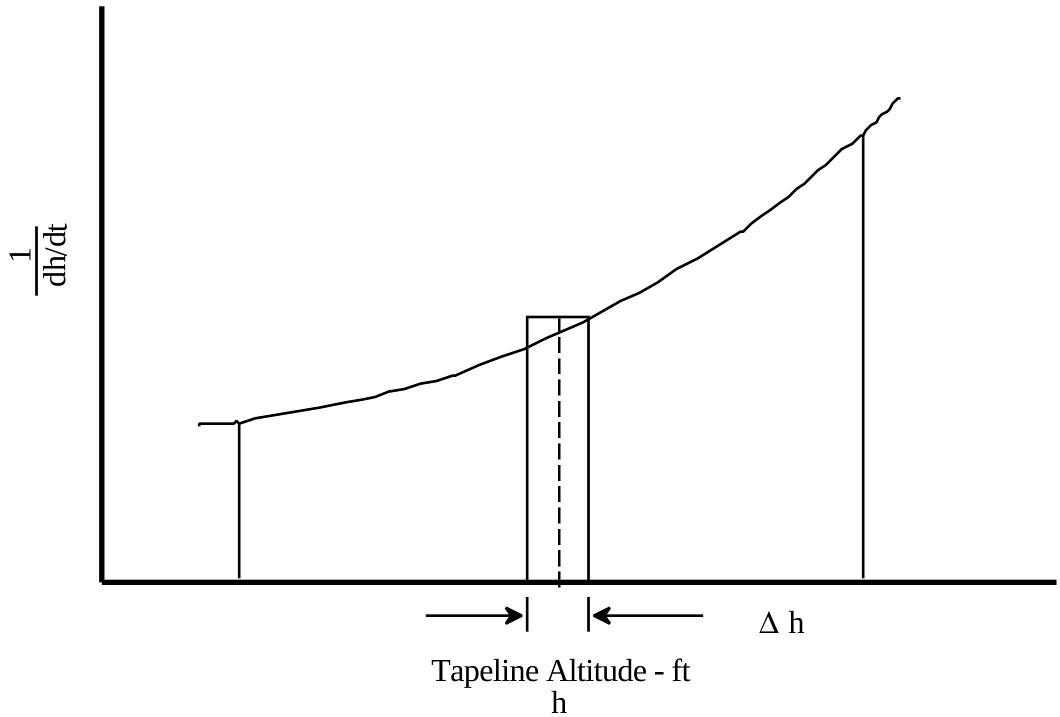

Figure 7.7
TIME TO CLIMB INTEGRATION

The method is limited by the fact that more information is needed than just the altitude change with time. Both altitude and airspeed must be specified, as well as the climb path itself and actual rate of climb at every point. A more accurate method to determine time to climb is discussed in section 7.3.3

7.3.2.6 SUMMARY OF STEADY STATE CLIMB

A curve of vertical velocity versus horizontal velocity can be used to summarize the steady state performance. A rate of climb curve is shown in figure 7.8.

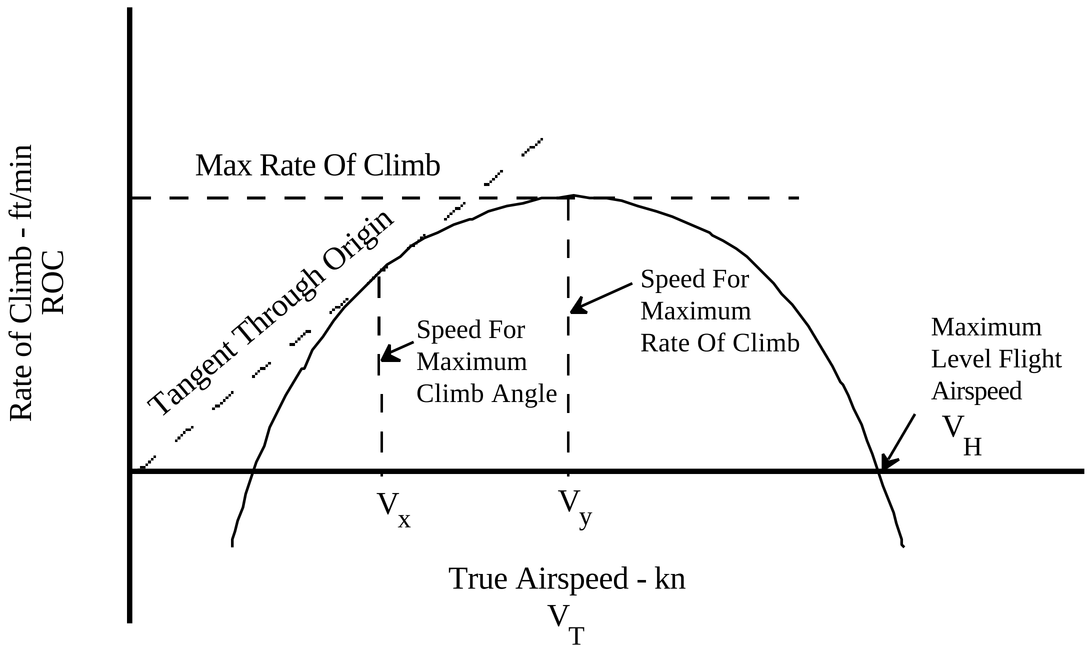

Figure 7.8
CLASSIC RATE OF CLIMB

If figure 7.8 is converted into vertical velocity versus horizontal velocity using Eqs 7.17 and 7.18, climb performance can be summarized graphically as in figure 7.9 for the same speed range.

$$V_v = V_T \sin \gamma \qquad \text{(Eq 7.18)}$$

$$V_{hor} = V_T \cos \gamma \qquad \text{(Eq 7.19)}$$

Where:

γ	Flight path angle	deg
V_{hor}	Horizontal velocity	ft/s
V_T	True airspeed	ft/s
V_v	Vertical velocity	ft/s.

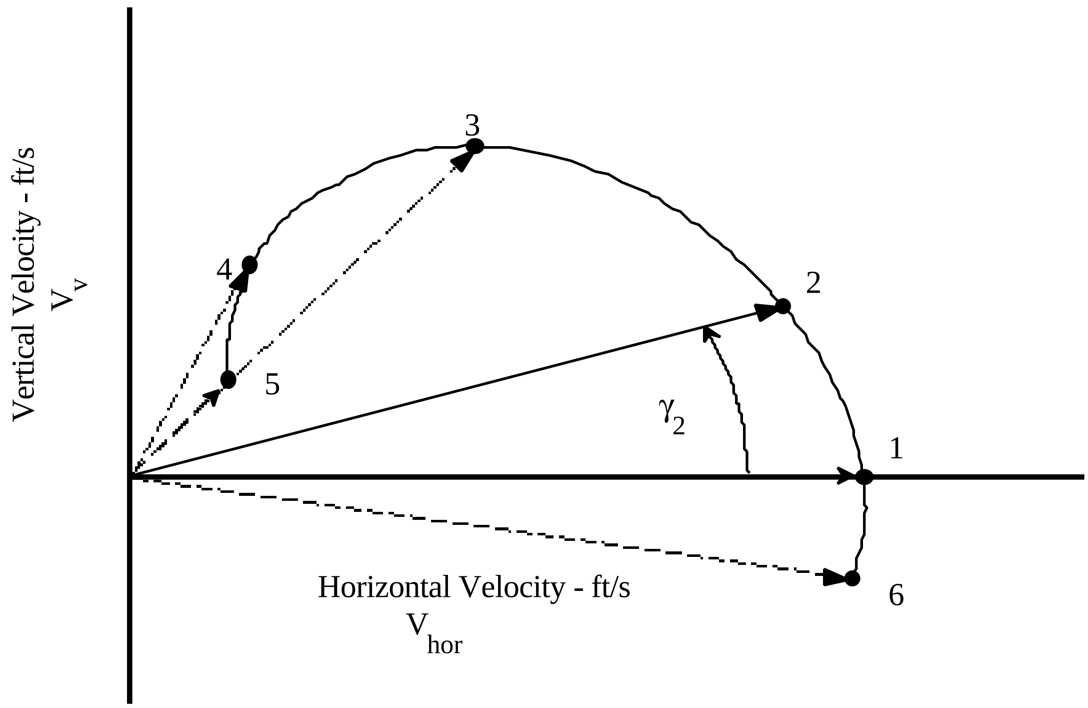

Figure 7.9
PERFORMANCE HODOGRAPH

A radius vector from the origin to any point on the plot represents the true airspeed and makes an angle to the horizontal equal to the actual climb angle at that speed. From figure 7.9:

Point 1	Maximum level flight airspeed	V_H
Point 2	Climb speed at the given rate of climb	V_T
Point 3	Speed for maximum rate of climb	V_y
Point 4	Speed for maximum climb angle	V_x
Point 5	Stall speed	V_s
Point 6	Descent	NA.

7.3.2.7 THRUST EFFECTS

The discussion to this point deals with one set of power parameters; however, rate of climb is calculated using Eq 7.16 and changes with throttle position or net thrust parallel to the flight path, T_{N_x}.

$$ROC = \frac{dh}{dt} = \frac{\left[T_{N_x} - D \right]}{W} V = \frac{T_{N_x} V - D V}{W} = \frac{P_A - P_{req}}{W} \qquad \text{(Eq 7.16)}$$

Where:

D	Drag	lb
T_{N_x}	Net thrust parallel flight path	lb
h	Tapeline altitude	ft
P_A	Power available	ft-lb/s
P_{req}	Power required	ft-lb/s
ROC	Rate of climb	ft/s
V	Velocity	ft/s
W	Weight	lb.

From a study of drag characteristics for jets, the maximum climb angle speed (V_X) occurs at $\left.\frac{C_L}{C_D}\right|_{max}$, which is the minimum drag condition. The speed is independent of power setting. The speed for best climb rate, V_y, increases with increasing thrust. Figure 7.10 illustrates the effects discussed.

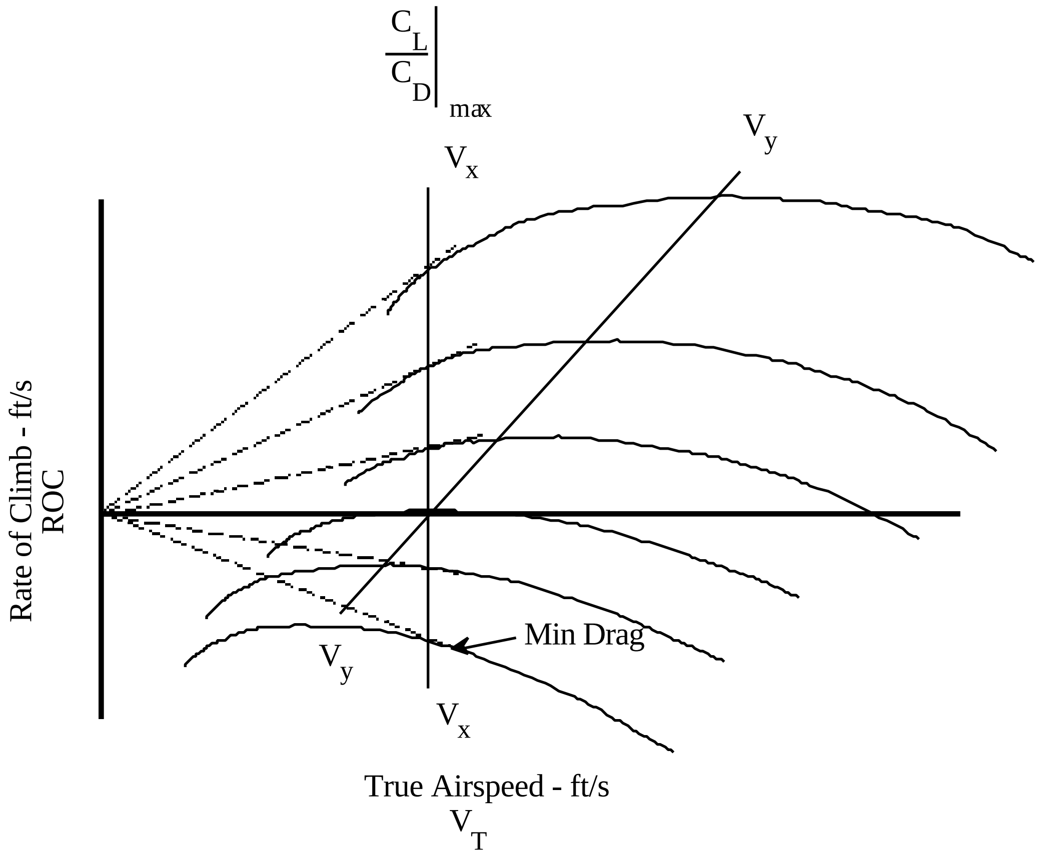

Figure 7.10
THRUST EFFECTS FOR JETS

For the propeller aircraft, the best rate of climb speed, V_y, does not change with increasing power. The speed for maximum climb angle, V_x decreases with the increased power setting as the climb progresses. Figure 7.11 shows the result.

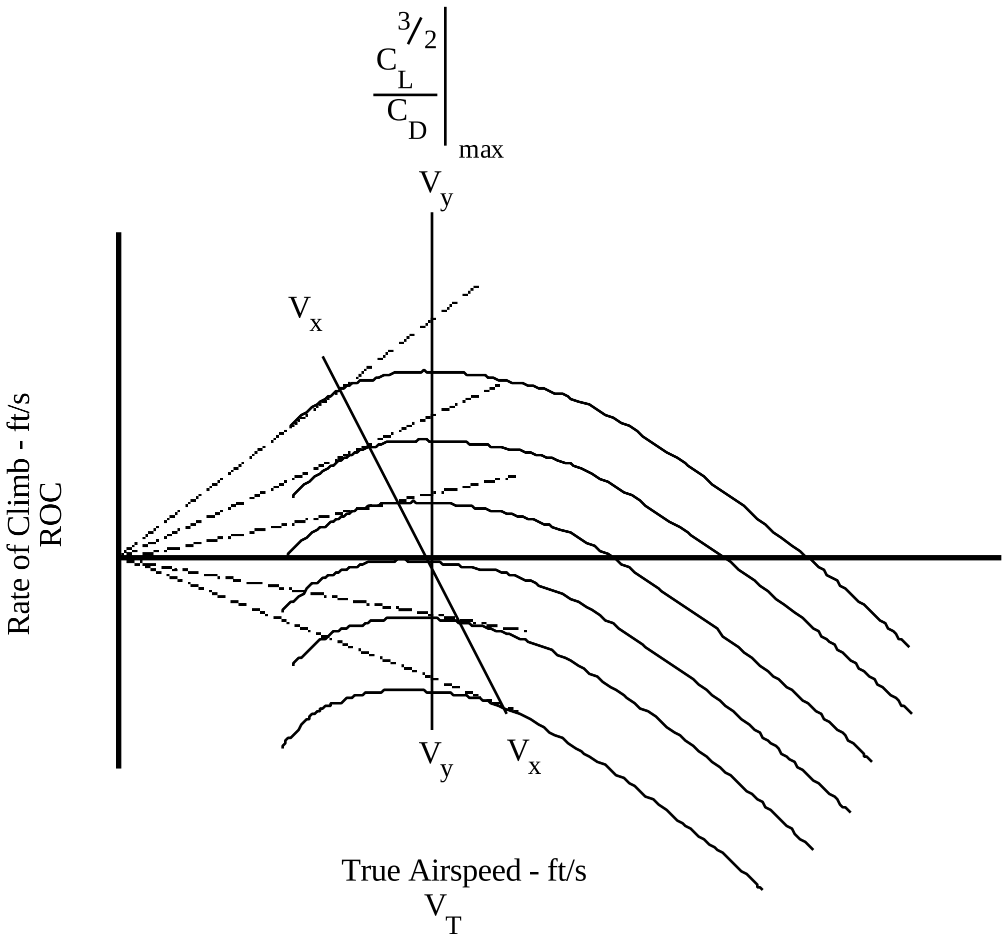

Figure 7.11

THRUST EFFECTS FOR PROPS

7.3.3 TOTAL ENERGY APPROACH TO CLIMB PERFORMANCE

Climb schedules can be determined by randomly flying a large number of climb schedules and picking the best schedule based on the flight results. Each flight requires a climb and if a schedule is selected based on measured P_S data, the results could be quite good. Schedules based on less information would yield poor results. There are more scientific approaches and this section uses the information attained from the excess power chapter to determine climb performance, and specifically climb schedules. The treatment starts with the subsonic jet and advances to supersonic speeds.

7.3.3.1 TIME BASED CLIMB SCHEDULE

P_S data taken from acceleration runs, sawtooth climbs, or other methods can be worked up on a cross-plot of altitude and Mach number, or true airspeed, with lines of constant energy height as shown in figure 7.12.

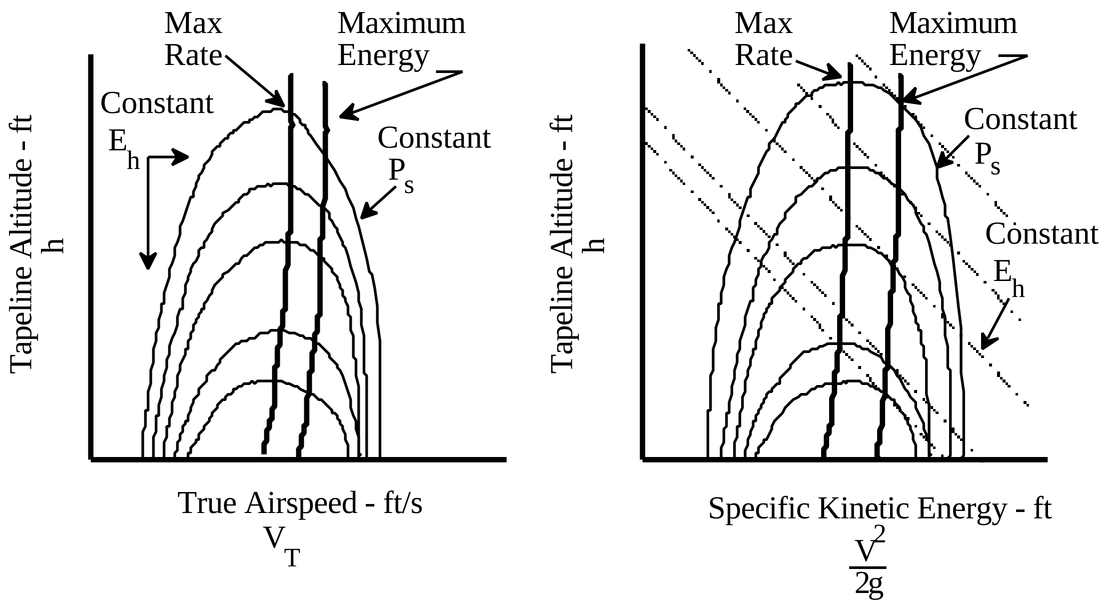

Figure 7.12
SUBSONIC CLIMB SCHEDULE

The peaks of the curves represent the speed at which the maximum specific excess power occurs at each altitude. Each peak is also the speed for maximum instantaneous rate of climb at that altitude for an aircraft flying at constant true airspeed. The maximum points occur at increasing airspeed; thus, as altitude increases, acceleration is required along the flight path. Excess power must be divided between the requirements of climbing and acceleration, which is seen as an increase in total energy as shown in Eq 7.1.

$$E_h = h + \frac{V_T^2}{2\,g} \qquad \text{(Eq 7.1)}$$

Where:

E_h	Energy height	ft
g	Gravitational acceleration	ft/s^2
h	Tapeline altitude	ft
V_T	True airspeed	ft/s.

By flying the points where the P_s contours are tangent to the lines of constant energy height, a schedule for the minimum time to achieve an energy state, or maximum rate of total energy addition, is developed as the optimum energy climb schedule.

The plot is also shown as a function of specific potential energy (h) and specific kinetic energy ($\frac{V^2}{2g}$). This curve may be useful if the points of tangency are not well defined.

7.3.3.1.1 SPECIFIC ENERGY VERSUS TOTAL ENERGY

Time to climb is given in Eq 7.17. The integration requires determining the actual rate of climb at every point, which cannot be easily obtained from figure 7.12. The integration will not work for any portion of the schedule where altitude is not increasing. To put Eq 7.17 in more useful terms the following equations are used:

$$P_s = \frac{dE_h}{dt} = \frac{dh}{dt} + \frac{V_T}{g}\frac{dV_T}{dt} \qquad \text{(Eq 7.2)}$$

$$\text{Rate of Climb} = P_s\left(\frac{1}{1 + \frac{V}{g}\frac{dV_T}{dh}}\right) \qquad \text{(Eq 7.20)}$$

$$\text{Time to Climb} = \int_{h_1}^{h_2} \frac{\left(1 + \frac{V}{g}\frac{dV_T}{dh}\right)}{P_s}\,dh \qquad \text{(Eq 7.21)}$$

$$dt = \frac{dh + \frac{V}{g}\,dV_T}{P_s} \tag{Eq 7.22}$$

Using the differential form of Eq 7.1 and substituting it into equation 7.21, time to climb can be expressed in terms which can be graphically integrated from figure 7.12.

$$dE_h = dh + \frac{V}{g}\,dV \tag{Eq 7.23}$$

$$dt = \frac{dE_h}{P_s} \tag{Eq 7.24}$$

$$\text{Time to Climb} = \int_{E_{h_1}}^{E_{h_2}} \frac{1}{P_s}\,dE_h \tag{Eq 7.25}$$

Where:

E_h	Energy height	ft
E_{h1}	Energy height at start of climb	ft
E_{h2}	Energy height at end of climb	ft
g	Gravitational acceleration	ft/s^2
h	Tapeline altitude	ft
h_1	Tapeline altitude start of climb	ft
h_2	Tapeline altitude end of climb	ft
P_s	Specific excess power	ft/s
ROC	Rate of climb	ft/s
t	Time	s
V	Velocity	ft/s
V_T	True airspeed	ft/s.

Results for both the maximum rate of climb schedule and the maximum energy climb schedule are shown in figure 7.13.

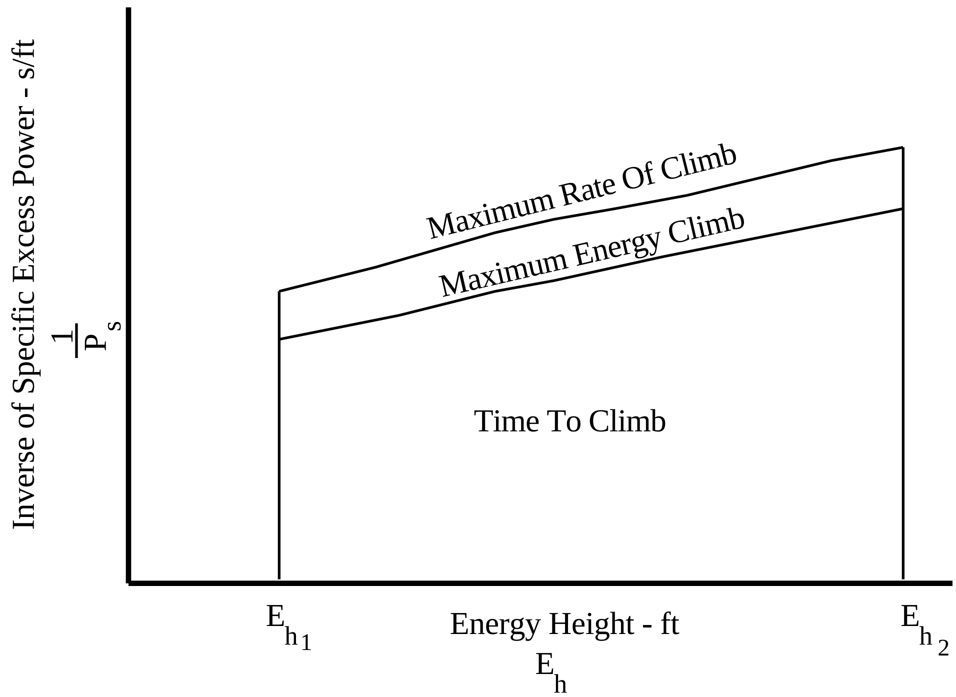

Figure 7.13
MINIMUM TIME TO CLIMB

The maximum energy climb schedule gives a path defined by altitude and Mach number for transitioning from one energy level to a higher level in the minimum time. Every point on the maximum energy climb schedule represents the maximum P_s for that energy height which will get the aircraft to an energy level faster than any other schedule. However, the potential energy is lower than in the maximum rate of climb with kinetic energy making up the difference. The maximum energy climb schedule will give the minimum time between two energy levels; however, the potential gains by flying this schedule can be negated by the real process of exchanging kinetic and potential energies. Theoretical treatments usually assume an ideal model in which the airplane can translate instantaneously, and without loss, along lines of constant energy height. The ideal model works well when the end points of the energy climb are near the maximum energy climb schedule, but breaks down when they are not, particularly if the energy levels are close together. For transitions between widely separated energy levels, the maximum energy climb schedule is nearly optimal and is recommended for jets climbing to high altitude. The climb schedule actually recommended is often a compromise between the theoretical maximum rate and maximum energy schedules, and may be further modified by considerations such as providing an airspeed or Mach number profile which is easy to fly, and/or providing a Mach number relative to maximum range or maximum endurance airspeed.

For a supersonic aircraft, the energy schedule becomes more significant. Figure 7.14 illustrates a typical climb schedule for a supersonic aircraft.

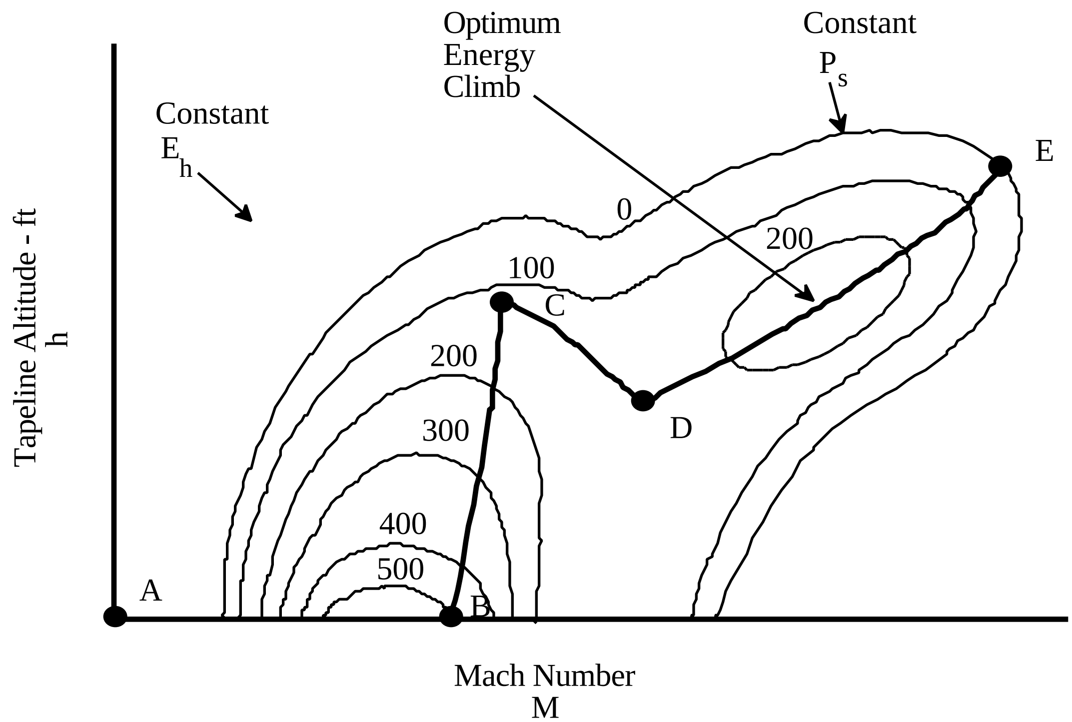

Figure 7.14

SUPERSONIC CLIMB SCHEDULE

If the final speed is near the aircraft's maximum speed, the large speed increase necessary renders the conventional method of using the peaks of the P_s curves useless. However, the energy method works well. Note in this example the optimum climb path includes an acceleration in a dive. This optimum energy climb path is also known as the Rutowski climb path, after its developer. The path (Figure 7.14) consists of four segments to reach energy state E in minimum time. Segment AB represents a constant altitude acceleration from V = 0 to climb speed at state B. The subsonic climb segment follows a path similar to the one illustrated to the tropopause at state C. This subsonic climb is usually a nearly constant Mach number schedule. An ideal pushover or dive is carried out at constant E_h from C to D. The acceleration in the dive is actually part of the optimum climb path. Segment DE is the supersonic climb to the final energy state desired at E. Note segments BC and DE pass through points on P_s contours which are tangent to lines of constant E_h. A climb schedule defined by the conventional method of the peaks of the P_s curves at each altitude is undesirable because of the large speed change involved if a speed near the maximum is desired at the end of the climb. However, the conventional schedule may still be useful if a profile is desired to reach maximum range airspeed at altitude.

When and how to transition from the subsonic segment to the supersonic segment may be an issue if the P_s contours near M = 1 are poorly defined. There is no complete agreement on when to start the pushover. Perhaps the most expeditious path is the one toward the highest P_s contour available without decreasing E_h. The assumption implies the climb should be subsonic until intercepting an E_h level tangent to two P_s contours of equal value, one in a subsonic region and the other in the supersonic region. Path CD in figure 7.14 illustrates a typical transition using this idea. Figure 7.15 illustrates the difficulty in choosing the transition paths when P_s contours become irregular in the transonic region.

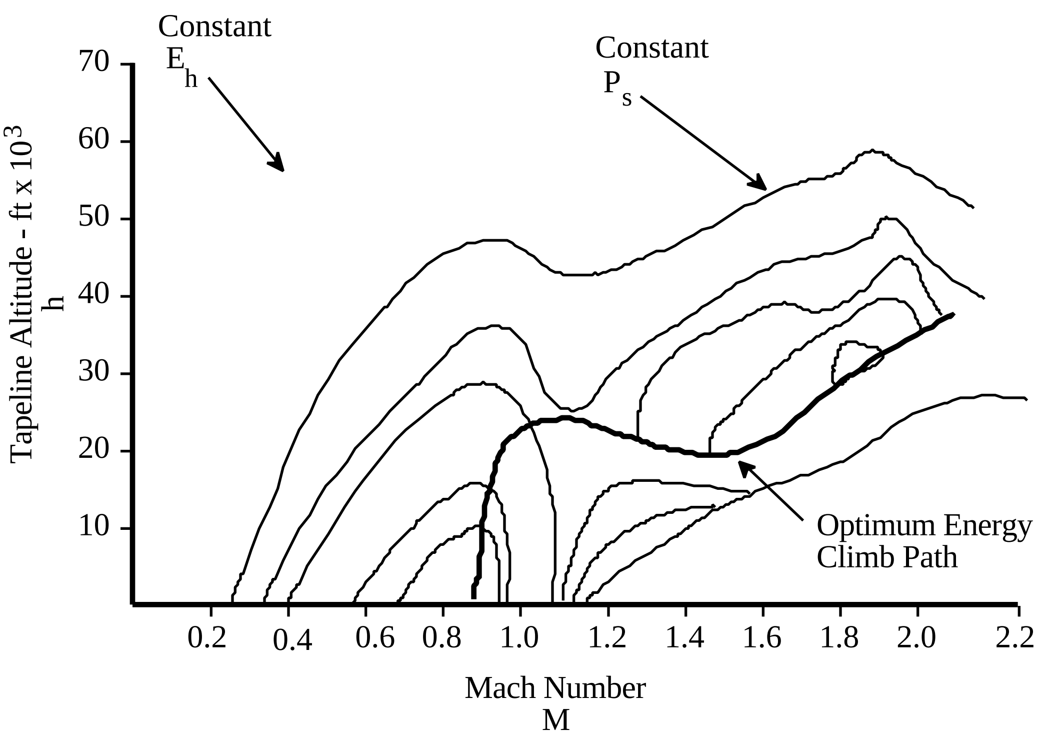

Figure 7.15
TYPICAL ENERGY LEVEL CLIMB PATH

Notice in figure 7.15, real transitions as opposed to ideal zooms and dives, where transitions are assumed to be instantaneous, result in a climb path with the corners rounded off. The abrupt discontinuities in angle of attack and attitude are avoided in the actual climb.

7.3.3.2 FUEL BASED CLIMB SCHEDULE

The aircraft mission may require the expenditure of minimum fuel to achieve a given energy level. The energy approach to climb performance can also be used to determine how much total energy is added per pound of fuel consumed. This requires specific energy to be differentiated with respect to the change in aircraft gross weight due to fuel used. Change in altitude per pound of fuel used is dh/dW in climbs, and the change in airspeed per pound of fuel in accelerations is dV/dW. The sum of both terms equals the change in specific energy with respect to fuel used as in Eq 7.26.

$$\frac{dE_h}{dW} = \frac{d}{dW}\left(h + \frac{V_T^2}{2\,g}\right) = \frac{dh}{dW} + \frac{V_T}{g}\frac{dV_T}{dW} \qquad \text{(Eq 7.26)}$$

Fuel burned in a climb can be determined by integrating Eq 7.26 as was done in determining time to climb.

$$\text{Fuel to Climb} = \int_{W_1}^{W_2} dW = -\int_{E_{h_1}}^{E_{h_2}} \frac{1}{\frac{dE_h}{dW}}\, dE_h \qquad \text{(Eq 7.27)}$$

A relationship of fuel flow to specific excess power can be written as Eq 7.28.

$$-\frac{1}{\frac{dE_h}{dW}} = -\frac{dW}{dE_h} = -\frac{dW}{dt}\frac{dt}{dE_h} = \frac{\dot{W}_f}{P_s} \qquad \text{(Eq 7.28)}$$

Eq 7.27 can be rewritten as follows:

$$\text{Fuel to Climb} = \int_{E_{h_1}}^{E_{h_2}} \frac{\dot{W}_f}{P_s}\, dE_h = \int_{E_{h_1}}^{E_{h_2}} \frac{1}{\frac{P_s}{\dot{W}_f}}\, dE_h \qquad \text{(Eq 7.29)}$$

Where:

E_h	Energy height	ft
g	Gravitational acceleration	ft/s^2
h	Tapeline altitude	ft
P_s	Specific excess power	ft/s
t	Time	s
V	Velocity	ft/s
V_T	True airspeed	kn
W	Weight	lb
$\dot{W}_f$	Fuel flow	lb/h.

Evaluating Eq 7.29 requires combining P_s and fuel flow data from other tests. From acceleration run data, the P_s curve similar to the solid line in figure 7.16, and referred fuel flow curve, similar to figure 7.17, can be generated.

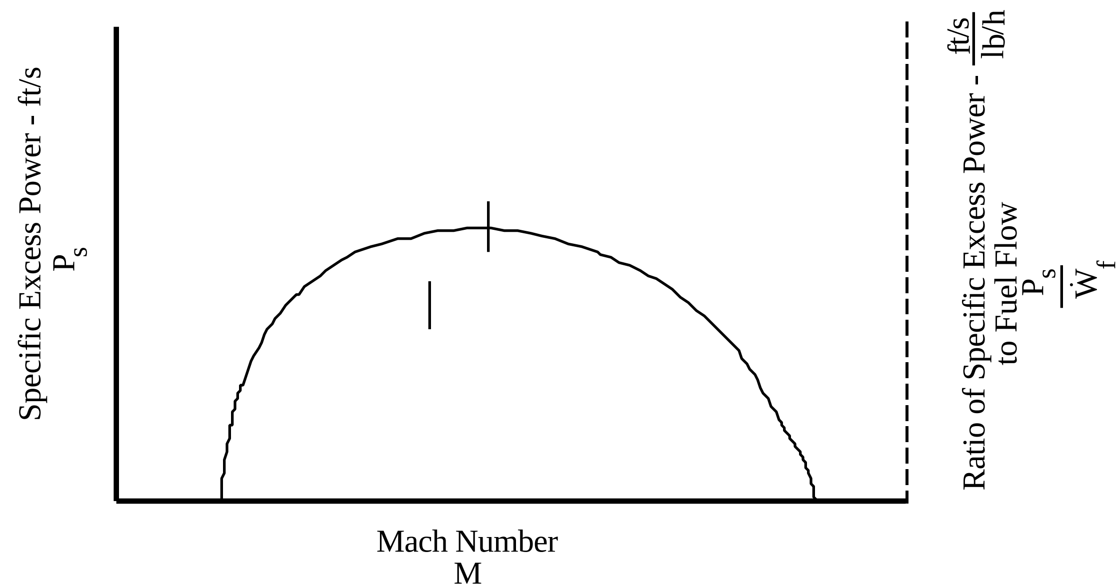

Figure 7.16

SPECIFIC EXCESS POWER CURVE

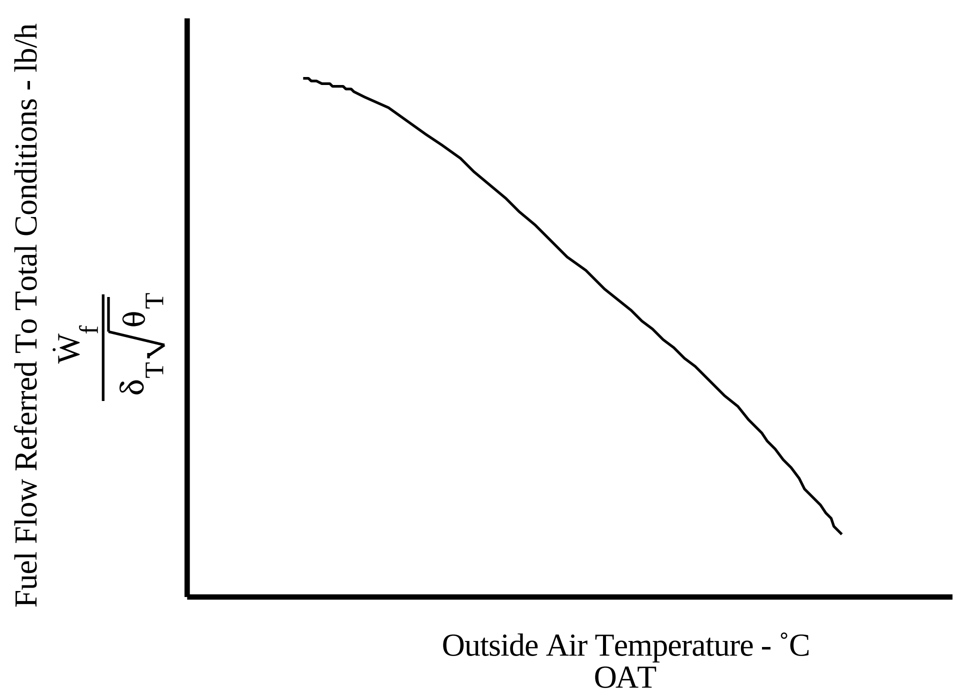

Figure 7.17

REFERRED FUEL FLOW

For a given altitude (δ) and temperature (θ), the outside air temperature (OAT) and referred fuel flow can be determined versus Mach number. For the same acceleration run, the actual fuel flow for standard conditions can be determined as shown in figure 7.18.

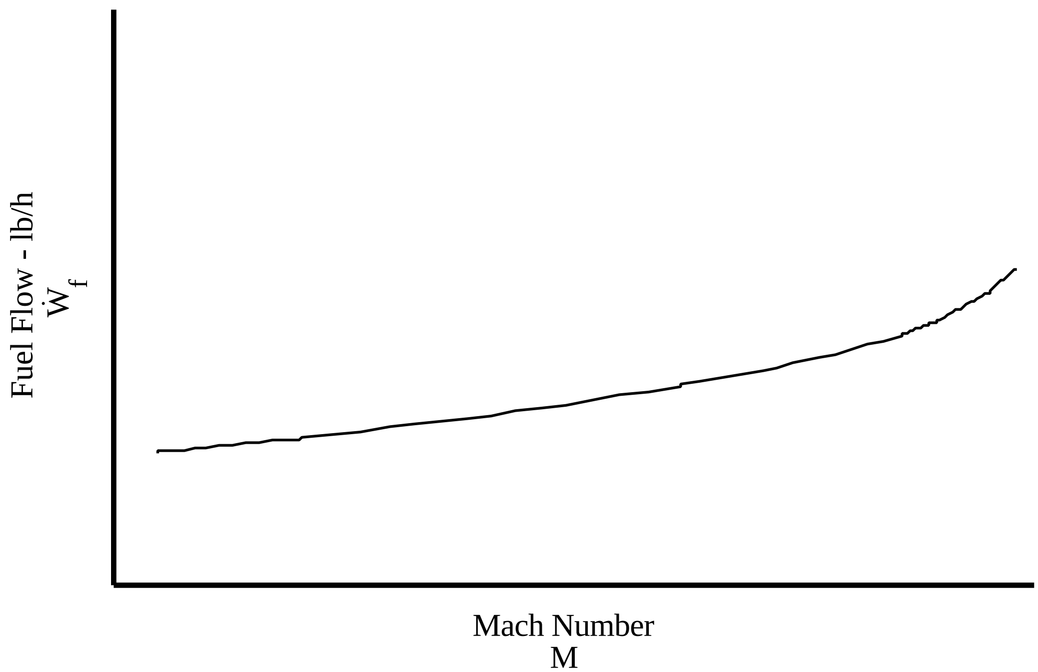

Figure 7.18
ACTUAL FUEL FLOW

The ratio of P_s to $\dot{W}_f$ can be determined by dividing each point on figure 7.16 by the corresponding points on figure 7.18 and plotting $\frac{P_s}{\dot{W}_f}$ versus Mach number as the dashed curve in figure 7.16. Since fuel flow increases with increasing speed, the peak of the $\frac{P_s}{\dot{W}_f}$ curve occurs at a slower speed than the peak of the P_s curve in figure 7.16.

To develop the minimum fuel climb schedule, all the $\frac{P_s}{\dot{W}_f}$ curves for each altitude are determined. The results are cross-plotted as shown in figure 7.19.

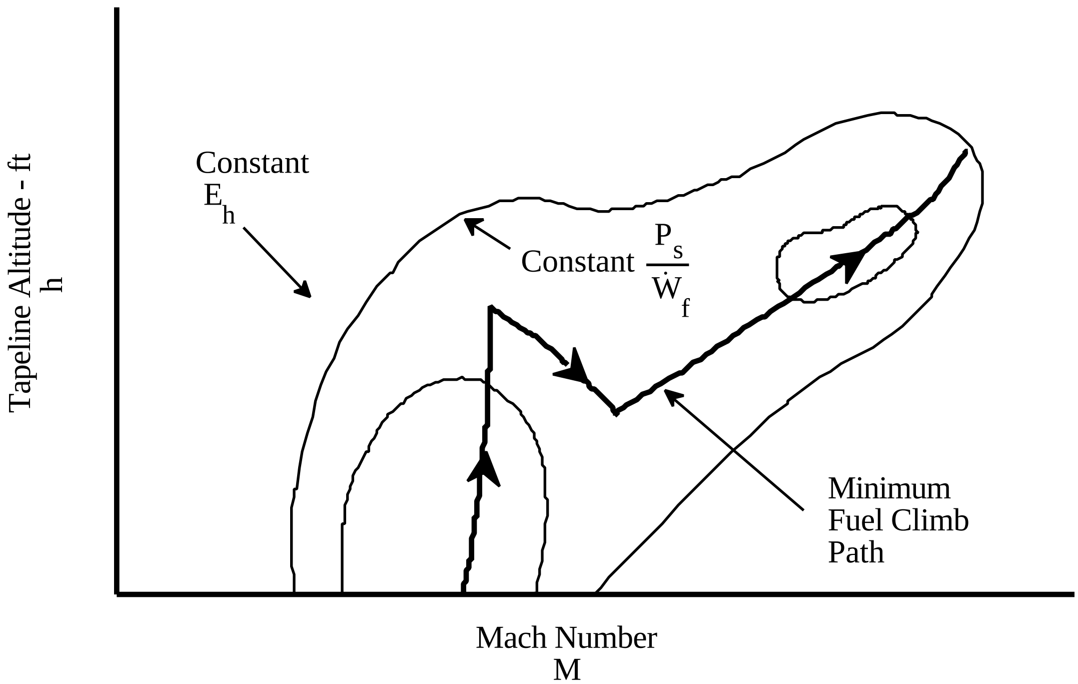

Figure 7.19
MINIMUM FUEL CLIMB SCHEDULE

7.3.3.2.1 TIME VERSUS FUEL BASED CLIMB

The climb path based on minimum fuel in figure 7.19 appears very much like the time based climb in figure 7.14. Figure 7.20 depicts a typical result given the same aircraft following an optimal time climb and an optimal fuel climb.

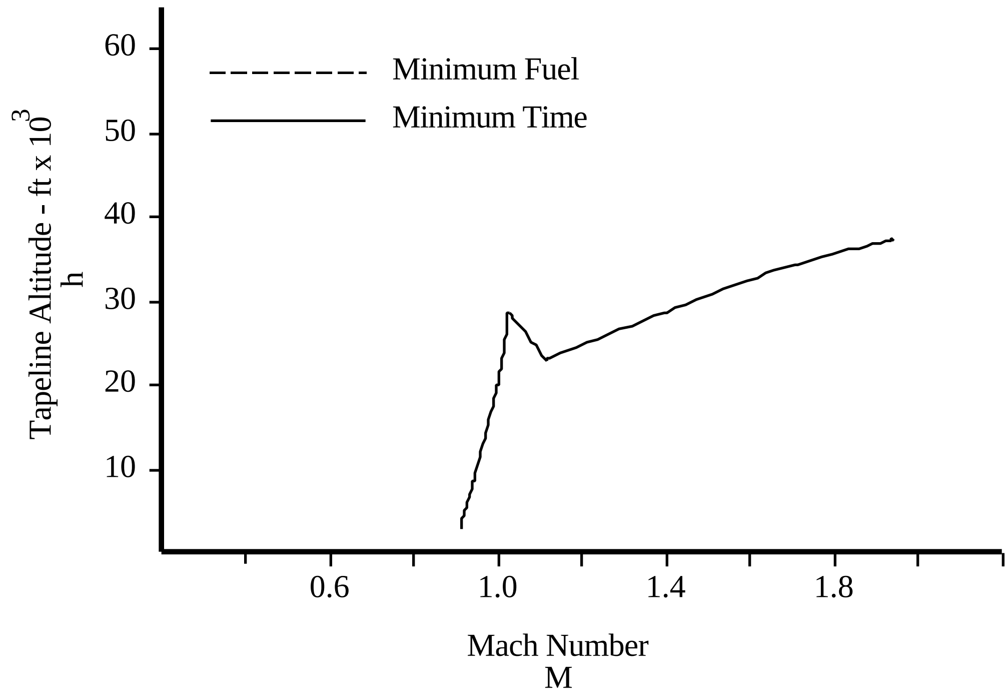

Figure 7.20
OPTIMAL TIME AND FUEL CLIMBS

The optimal minimum fuel climb path lies above, but roughly parallel, the optimal minimum time climb path. In reality, the optimal fuel path is easier to achieve since the optimal time case requires an ideal climb, an ideal dive, and an ideal zoom to reach the end point.

7.3.3.2.2 MAXIMUM RANGE CLIMB SCHEDULE

The maximum range climb schedule should achieve maximum range for fuel used during the climb to a desired altitude and cruise speed. There are sophisticated mathematical techniques which can be used to determine a theoretical solution. In practice, if the cruise speed is near the climb speed for an energy minimum fuel climb, the minimum fuel climb approximates the no-wind maximum range per pound of fuel.

The initial point of the cruise leg is defined by an altitude and an airspeed for a particular gross weight. The schedule which gets to that energy level with minimum fuel used, is close to the optimal time schedule. However, actual down range distance traveled in the climb is considered when optimizing the overall range problem which also includes cruise and descent.

As in the cruise phase, wind affects the range in a climb. For a head wind, an incremental increase in speed for the climb schedule slightly improves the range characteristic provided the peaks of the $\frac{P_s}{\dot{W}_f}$ curves, with respect to energy height, are not too sharp. For a tail wind, an incremental decrease in speed increases range over that obtained from the no-wind schedule.

7.4 TEST METHODS AND TECHNIQUES

7.4.1 SAWTOOTH CLIMB

A series of timed climbs are made at different speeds from a point below the test altitude to a point above it. Speeds are chosen to bracket the expected best climb speed of the aircraft. Power setting is defined by the scope of the test but is the same for each run. Normally, full power is used. A typical flight data card is shown in figure 7.21.

Target V_o	V_o	Initial H_P	Final H_P	Δt	Fuel	OAT	Misc

Figure 7.21
SAWTOOTH DATA CARD

Climbs are performed at the same power setting and aircraft configuration as used in the check climb (paragraph 7.4.3). The same altitude band is used for each climb, until P_s decreases and time, rather than altitude gain, becomes the test criterion. The altitude increment is about 1000 ft either side of a target altitude, or a height change attainable in two minutes, which ever is less. When time is the criterion, choose the climb band symmetrically about the target altitude.

The aircraft is first trimmed in the configuration desired while still well below the nominal altitude. Power is applied and final trim adjustments are made before reaching the lower limit of the altitude band being measured.

The exact time of entering and leaving the altitude band is recorded by a stopwatch or an instrumentation system.

Once through the altitude increment, data are recorded, and a descending turn is initialized to get the aircraft below the altitude band for another run. As many points as possible are flown at each altitude. In addition, a full power unaccelerated minimum speed point, and a maximum speed point are obtained at the test altitude in order to complete the curve.

Climb perpendicular to the prevailing winds to minimize the effects of wind shear. Confine the flights to the bounds of a limited geographical area since the primary concern is the shape of the curve obtained rather than the magnitude. For each altitude, a standard data card is prepared similar to figure 7.21 with the target indicated airspeed included for each point.

Record actual in-flight V_o, W, time, fuel counts or fuel remaining, and either outside air temperature or time of day so temperature can be obtained by other meteorological methods. The card can be expanded to record other parameters such as angle of attack, engine RPM, torque, etc. On the back of the data card, keep a running plot of observed time to climb versus V_o and before leaving the test altitude, examine the plot for points which need repeating.

The description above is only applicable when P_s is determined to be positive. If P_s is negative and the airplane is descending, then the same flight test technique applies, except in reverse. For a description of the sawtooth descent flight test technique, see paragraph 8.4.1.

7.4.1.1 DATA REQUIRED

1. Time: Record elapsed time from the beginning of the altitude band to the end, or two minutes whichever comes first.
2. Altitude: Record the observed pressure altitude H_{P_o} band for each point.

3. Velocity: Record observed airspeed, V_o.
4. OAT or T_a: Record ambient air temperature from on-board instrumentation at target altitude. (May be obtained from direct observation).
5. Fuel weight: Record the fuel remaining to determine aircraft gross weight.
6. Miscellaneous: Record other information desired such as RPM, angle of attack, and torque for a turboprop.

7.4.1.2 TEST CRITERIA

Allow sufficient altitude for the engine(s) to reach normal operating temperatures and the airplane to be completely stabilized at the desired airspeed before entering the data band. Smoothness is just as important as in acceleration runs and for the same reasons. If a small airspeed error is made while setting the airplane up, it is better to maintain the incorrect speed as accurately as possible, rather than try to correct it and risk aborting the entire run.

7.4.1.3 DATA REQUIREMENTS

1. Test altitude band ± 1000 ft about a target altitude.
2. V_o ± 1 kn with smooth corrections.
3. Normal acceleration ± 0.1 g.

7.4.1.4 SAFETY CONSIDERATIONS

There are no unique hazards or safety precautions associated with sawtooth climbs. Observe airspeed limits when in the powered approach configuration and engine limits at the selected thrust setting. Consider low altitude stall potential in slow speed climb tests and V_{mc} for multi-engine aircraft.

7.4.2 CHECK CLIMB TEST

The check climb test is flown to compare the standard day climb performance of an aircraft in a specific configuration to results predicted from sawtooth climbs or acceleration runs. The three main areas of investigation are:

1. Time to climb.
2. Distance traveled.
3. Fuel used.

In addition, data may be obtained on various engine parameters such as engine speed, exhaust gas temperature, engine pressure ratio, gross thrust, angle of attack, etc. These are useful to the analyst but are secondary to the three main parameters. The general method is to climb the aircraft to just below the maximum ceiling while maintaining precisely a predetermined climb schedule. This schedule may be a best climb schedule as obtained by flight test, a schedule recommended by the manufacturer, or some other schedule for which climb performance is of interest. Specify the schedule flown on each climb performance chart.

Record data at approximately equal increments of altitude and include time, speed, fuel flow, temperature, and any other desired parameters. For most jet aircraft, a mechanical recording means is necessary to obtain simultaneous reading of the many parameters of interest.

After the schedule to be flown is determined, data cards are prepared to record the climb data as in figure 7.22.

	t	Fuel temp	Fuel density	OAT or T_a	Fuel remaining	
Prior to Start	NA					
Start		NA	NA			
Taxi		NA	NA			
Takeoff		NA	NA			
t	H_{P_o}	V_o target	V_o actual	OAT or T_a	Fuel remaining	Misc

Figure 7.22
CHECK CLIMB

Adjust target points for instrument error and position error for both the airspeed indicator and altimeter. If the anticipated rate of climb is low, data are recorded every 1000 to 2000 ft. If the rate of climb is high, every 5000 ft is sufficient. The interval is adjusted as the rate of climb decreases with altitude.

An area of smooth air, light winds, and stable temperature gradients from ground level to the aircraft's maximum ceiling is desirable. The test area can be sampled via a survey balloon or another aircraft for wind and temperature data. Plan the flight to climb perpendicular to the wind direction.

Since gross weight, fuel weight, and fuel density are extremely important to climb tests, fuel and weigh the aircraft prior to commencement of tests. Fuel samples are taken and tested for temperature and density. Record fuel remaining and time for start, taxi, takeoff, and acceleration to climb schedule whenever conditions permit.

Establish level flight as low as possible on climb heading. If the rate of climb is high, the best entry is achieved by first stabilizing in level flight with partial power at some speed below the scheduled climb speed. Trim the aircraft for hands-off flight. When all preparations are complete and the data recorder is running, apply power, and as the climb speed is approached, rotate to intercept and maintain the climb schedule.

If rate of climb is fairly low, a better entry can be achieved by stabilizing on the target speed 1000 ft below entry altitude. When preparations are complete and the aircraft is trimmed, advance the power smoothly, and rotate the aircraft simultaneously to maintain airspeed. As the desired power setting is reached, stop the rotation, at which time the aircraft is approximately established on the climb schedule.

During the climb, trim the aircraft. Maintain the climb schedule to within 5 kn, if possible. A rapid cross-check between external horizon and the airspeed indicator is required. If the pitch attitude is very steep, it may be necessary to substitute the aircraft attitude indicator for the external horizon during initial portions of the climb.

Wind gradients appear as sudden airspeed changes. If these affect the climb speed schedule, the appropriate corrective action is a small, but immediate attitude correction. If the wind gradient effect subsides, apply an appropriate corrective action.

At high altitudes, maintaining a precise speed schedule becomes difficult. A slight rate of change of indicated airspeed implies a much larger rate of change of kinetic energy. Any undesirable trend is difficult to stop since the aerodynamic controls are less effective. The best way to cope is to avoid large corrections by a rapid cross-check, precise control, and constant attention to trim. If corrections become necessary, avoid over controlling due to the hysteresis in the airspeed indicator.

If the climb must be interrupted, stop the climb at a given pressure altitude, noting V_o, fuel, time, and distance if available. Descend below the altitude at which the climb was stopped. Maneuver as required and re-intercept the climb schedule as soon as possible to minimize gross weight change. Intercept the climb at the break off pressure altitude and airspeed after re-establishing attitude and stabilizing the climb.

The test for a turboprop aircraft is identical to the jet test. In this case however, engine torque and engine shaft horsepower (ESHP) are adjusted in the climb. The engine controls have to be managed to ensure optimum climb power is maintained.

7.4.2.1 DATA REQUIRED

Record the following data at each climb increment which should be as often as possible but no greater than each 5000 ft or 2 minutes for hand held data:

1. Time (t).
2. Observed airspeed (V_o).
3. Observed pressure altitude (H_{P_o}).
4. Temperature (OAT or T_a).
5. Fuel remaining (W_f), or start and end fuel weight.
6. Distance (d).
7. Miscellaneous as desired.

7.4.2.2 TEST CRITERIA

1. Maintain coordinated wings level flight.
2. Keep turns to a minimum and use less than 10 degrees bank to keep n_z near 1.0.
3. No more than 30 degrees heading change.

7.4.2.3 DATA REQUIREMENTS

1. Airspeed ± 5 kn or 0.01 M.
2. n_z ± 0.1 g.

7.5 DATA REDUCTION

7.5.1 SAWTOOTH CLIMB

The sawtooth climb data is reduced similar to the acceleration runs, but there are some additional correction factors necessitated by this test method.

Eq 7.20 expresses test day rate of climb in terms of P_s (which is independent of the climb path) and dV_T/dh (which defines the climb path).

$$\text{Rate of Climb} = P_s \left(\frac{1}{1 + \frac{V}{g} \frac{dV_T}{dh}} \right) \qquad \text{(Eq 7.20)}$$

Recall:

$$P_s = \frac{dE_h}{dt} = \frac{dh}{dt} + \frac{V_T}{g} \frac{dV_T}{dt} \qquad \text{(Eq 7.2)}$$

E_h for the end points of each sawtooth climb segment are determined from:

$$E_{h_{Test}} = h_{Test} + \frac{V_{T_{Test}}^2}{2\,g} \qquad \text{(Eq 7.30)}$$

The slope of E_h versus time as the climb passes through the reference altitude ($H_{P_{ref}}$) is $P_{s(Test)}$. In practice, since a small altitude band is chosen, the average slope is defined by E_h(end) - E_h(start) divided by elapsed time. In a similar way, dV_T/dh is computed from V_T(end) - V_T(start) divided by altitude change. True airspeed is obtained at the reference altitude ($V_{T_{Ref}}$) by linear interpolation between the end points. Substituting these values into Eq 7.20 yields:

$$\left(\frac{dh}{dt}\right)_{Test} = P_{s_{Test}} \left(\frac{1}{1 + \frac{V_{T_{ref}}}{g} \frac{dV_T}{dh}} \right) \qquad \text{(Eq 7.31)}$$

Where:

E_h	Energy height	ft
$E_{h_{Test}}$	Test energy height	ft
g	Gravitational acceleration	ft/s^2
h	Tapeline altitude	ft
h_{Test}	Test tapeline altitude	ft
P_s	Specific excess power	ft/s

$P_{s_{Test}}$	Test specific excess power	ft/s
t	Time	s
V	Velocity	ft/s
V_T	True airspeed	ft/s
$V_{T_{ref}}$	Reference true airspeed	ft/s
$V_{T_{Test}}$	Test true airspeed	ft/s.

7.5.1.1 SPECIFIC EXCESS POWER CORRECTION

$P_{s_{Test}}$ is next corrected to standard conditions, standard weight and temperature at $H_{P\ ref}$. The correction is carried out exactly as it was for the level acceleration data with the exception of the correction for the change in induced drag:

$$P_{s_{Std}} = P_{s_{Test}} \frac{W_{Test}}{W_{Std}} \frac{V_{T_{Std}}}{V_{T_{Test}}} + \frac{V_{T_{Std}}}{W_{Std}} \left(\Delta T_{N_x} - \Delta D\right) \quad \text{(Eq 7.32)}$$

Where:

ΔD	Standard drag minus test drag	lb
ΔT_{N_x}	Standard net thrust parallel flight path minus test net thrust	lb
$P_{s_{Std}}$	Standard specific excess energy	ft/s
$P_{s_{Test}}$	Test specific excess energy	ft/s
$V_{T_{Std}}$	Standard true airspeed	ft/s
$V_{T_{Test}}$	Test true airspeed	ft/s
W_{Std}	Standard weight	lb
W_{Test}	Test weight	lb.

7.5.1.2 DRAG CORRECTION

The drag correction used in the level acceleration data reduction is as follows:

$$\Delta D = D_{Std} - D_{Test} = \frac{2\left(W_{Std}^2 - W_{Test}^2\right)}{\pi\ e\ AR\ S\ \gamma\ P_a\ M^2} \quad \text{(Eq 7.33)}$$

The following assumptions are made:

1. $L = W$.
2. $T \sin \alpha_j = 0$ (no thrust lift).
3. $n_z = 1$ (level flight).

Figure 7.2 shows in a climb, even if the thrust vector is aligned with the flight path ($T_{N_x} \sin \alpha_j = 0$) the lift is not equal to the weight.

Summing the vertical forces:

$$L - W \cos \gamma + T_G \sin \alpha_j = \frac{W}{g} a_z \qquad \text{(Eq 7.8)}$$

For $T_G \sin \alpha_j = 0$, and zero acceleration:

$$L = W \cos \gamma \qquad \text{(Eq 7.10)}$$

Also, since:

$$L = n_z W \qquad \text{(Eq 7.34)}$$

For straight flight, the normal load factor is the cosine of the climb angle:

$$n_z = \cos \gamma \qquad \text{(Eq 7.35)}$$

The drag correction for a climb can now be written, assuming a parabolic drag polar, as:

$$\Delta D = \frac{2 \left(W_{Std}^2 \cos^2 \gamma_{Std} - W_{Test}^2 \cos^2 \gamma_{Test} \right)}{\pi \, e \, AR \, \rho_{ssl} \, V_e^2 \, S} \qquad \text{(Eq 7.36)}$$

Or:

$$\Delta D = \frac{2\left(W_{Std}^2 n_{z\,Std}^2 - W_{Test}^2 n_{z\,Test}^2\right)}{\pi\ e\ AR\ \rho_{ssl}\ V_e^2\ S} \quad \text{(Eq 7.37)}$$

In applying either Eq 7.36 or Eq 7.37, the requirement is to find the drag correction in order to compute the corrected rate of climb. However, in applying Eq 7.36, the corrected rate of climb is implicit in the γ_{Std} (standard flight path angle) term of the equation. In other words, the standard rate of climb is a function of itself. Therefore, an iterative method is necessary to solve Eq 7.36.

For the first approximation set $\gamma_{Std} = \gamma_{Test}$, where γ_{Test} is computed from the test results, and calculate the induced drag correction from Eq 7.36.

The induced drag correction obtained is substituted in Eq 7.32 to yield the first iteration of $P_{s_{Std}}$, which is in turn substituted in Eq 7.38 to give the first iteration value of rate of climb and the first iteration of standard day climb angle, γ_{Std} in Eq 7.39:

$$\left(\frac{dh}{dt}\right)_{Std} = P_{s_{Std}}\left(\frac{1}{1 + \frac{V_T}{g}\frac{dV_T}{dh}}\right) \quad \text{(Eq 7.38)}$$

$$\gamma_{Std} = \sin^{-1}\left(\frac{\frac{dh}{dt}}{V_T}\right) \quad \text{(Eq 7.39)}$$

Where:

α_j	Thrust angle	deg
AR	Aspect ratio	
a_z	Acceleration perpendicular to flight path	ft/s^2
D	Drag	lb
D_{Std}	Standard drag	lb
D_{Test}	Test drag	lb
e	Oswald's efficiency factor	
γ	Flight path angle	deg
	Ratio of specific heats	
g	Gravitational acceleration	ft/s^2

γ_{Std}	Standard flight path angle	deg
γ_{Test}	Test flight path angle	deg
L	Lift	lb
M	Mach number	
n_z	Normal acceleration	g
$n_{z_{Std}}$	Standard normal acceleration	g
$n_{z_{Test}}$	Test normal acceleration	g
π	Constant	
P_a	Ambient pressure	psf
ρ_{ssl}	Standard sea level air density	0.0023769 slug/ft^3
S	Wing area	ft^2
T_G	Gross thrust	lb
V_e	Equivalent airspeed	ft/s
V_T	True airspeed	ft/s
W	Weight	lb
W_{Std}	Standard weight	lb
W_{Test}	Test weight	lb.

This value of γ then becomes γ_{Std} in the induced drag correction and the iteration is repeated until γ_{Std} is no longer changing. For airplanes with modest climb capabilities, γ is small and the iteration closes quickly. For steep climb angles the situation is different and as γ approaches 90˚ the iteration may become unstable. However, this situation is not likely to occur under the conditions in which sawtooth climbs test techniques are chosen.

7.5.1.3 THRUST LIFT CORRECTION

All the previous corrections assumed no contribution to lift from the inclination of the thrust line to the flight path. This condition is not generally true, though the errors introduced by this assumption are small enough to be neglected for most cases. However, at low speed and high angle of attack, thrust lift must be taken into consideration, as shown in figure 7.2.

Eq 7.8 yields:

$$L = W \cos \gamma - T_G \sin \alpha_j \qquad \text{(Eq 7.40)}$$

Since induced drag depends on normal acceleration:

$$n_z = \frac{L}{W} \qquad \text{(Eq 7.41)}$$

$$n_z = \cos \gamma - \frac{T_G}{W} \sin \alpha_j \qquad \text{(Eq 7.42)}$$

The equation for the sum of the forces in the horizontal direction is affected since:

$$T_{N_x} = T_G \cos \alpha_j - T_R \qquad \text{(Eq 7.12)}$$

In Eq 7.32, both the ΔT_{N_x} and ΔD terms are affected by thrust lift.

$$P_{s_{Std}} = P_{s_{Test}} \frac{W_{Test}}{W_{Std}} \frac{V_{T_{Std}}}{V_{T_{Test}}} + \frac{V_{T_{Std}}}{W_{Std}} \left(\Delta T_{N_x} - \Delta D\right) \qquad \text{(Eq 7.32)}$$

Where:

α_j	Thrust angle	deg
ΔD	Standard drag minus test drag	lb
ΔT_{N_x}	Standard net thrust parallel flight path minus test net thrust	lb
γ	Flight path angle	deg
L	Lift	lb
n_z	Normal acceleration	g
$P_{s_{Std}}$	Standard specific excess power	ft/s
$P_{s_{Test}}$	Test specific excess power	ft/s
T_G	Gross thrust	lb
T_{N_x}	Net thrust parallel flight path	lb
T_R	Ram drag	lb
$V_{T_{Std}}$	Standard true airspeed	ft/s
$V_{T_{Test}}$	Test true airspeed	ft/s

W	Weight	lb
W_{Std}	Standard weight	lb
W_{Test}	Test weight	lb.

To apply this correction, the α_j variation from test day to standard day is needed. The climb angle, γ, and the thrust angle, α_j, both vary during the iteration process of determining standard day rate of climb. To simplify things, α_j is assumed to be small enough to neglect its effect.

7.5.1.4 ALTITUDE CORRECTION

The foregoing corrections allow P_s, in the form of rate of climb potential (i.e rate of climb corrected for increasing true airspeed) to be plotted for standard conditions. It may be necessary to refer these results to a new altitude. For example single-engine climb or wave-off performance at 5000 ft can be used to compute data for standard conditions at sea level. Constant weight and constant V_e correction are used to minimize the change in drag. An engine thrust model is used to calculate the change in net thrust due to changing altitude and temperature at constant V_e.

$$\Delta T_N = f\left(\Delta H_P, \Delta T_a\right) \qquad \text{(Eq 7.43)}$$

Where:

T_N	Net thrust	lb
H_P	Pressure altitude	ft
T_a	Ambient temperature	˚C.

The rate of climb is computed for the new altitude using this thrust correction. This will again involve the climb angle iteration since the changes in rate of climb and true airspeed will change the climb angle, which will in turn affect the induced drag. These analytical corrections to thrust, and the iterative corrections to drag, can be minimized by performing the tests as close to the reference altitude as safety and operational restrictions permit. The corrected results are presented as shown in figure 7.23.

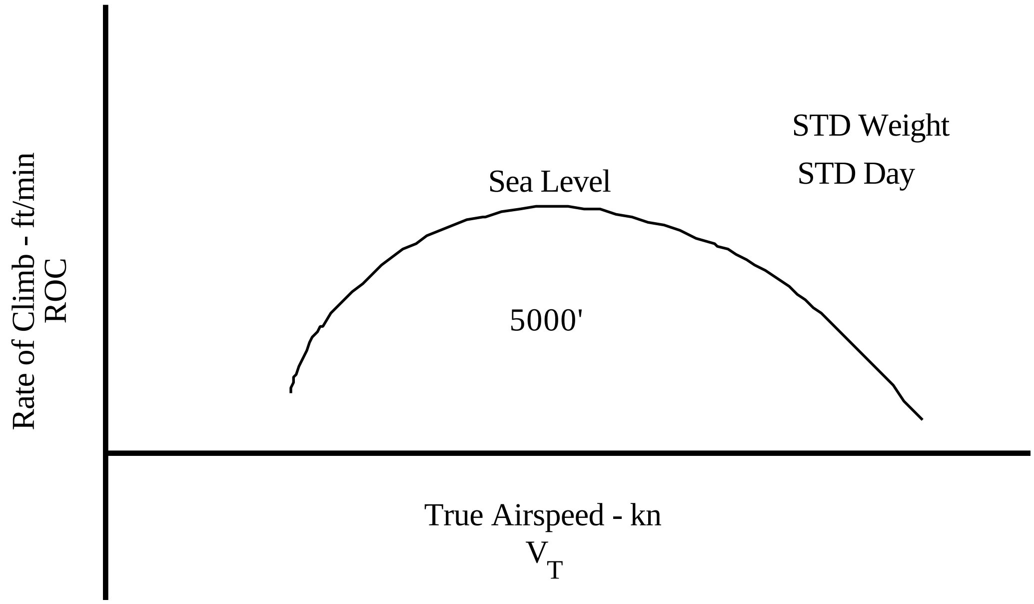

Figure 7.23
STANDARD DAY RATE OF CLIMB

7.5.2 COMPUTER DATA REDUCTION

Various computer programs are in existence to assist in reduction of performance data. This section contains a brief summary of the assumptions and logic which might be used. The treatment is purposefully generic as programs change over time or new ones are acquired or developed. Detailed instructions on the use of the particular computer or program are assumed to be available for the computer program. In any event, the operating system is invisible to the user. Data reduction from P_S level flight acceleration runs are in Chapter 5; however, energy analysis pertaining to climbs is reviewed.

7.5.2.1 ENERGY ANALYSIS

The purpose of the computer data reduction from energy analysis for climbs is to automatically calculate fuel, time and distance. This program is a subset to an energy analysis program which also calculates P_S from level acceleration runs. Basic data such as aircraft type, standard gross weight, etc. are entered.

Time to climb is calculated as follows:

$$\text{Time to Climb} = \int_{E_{h_1}}^{E_{h_2}} \frac{1}{P_s}\, dE_h$$

(Eq 7.25)

The program must know $\frac{1}{P_s}$ as a function of E_h, therefore the program plots the function and asks for a curve fit. The curve appears similar to figure 7.24.

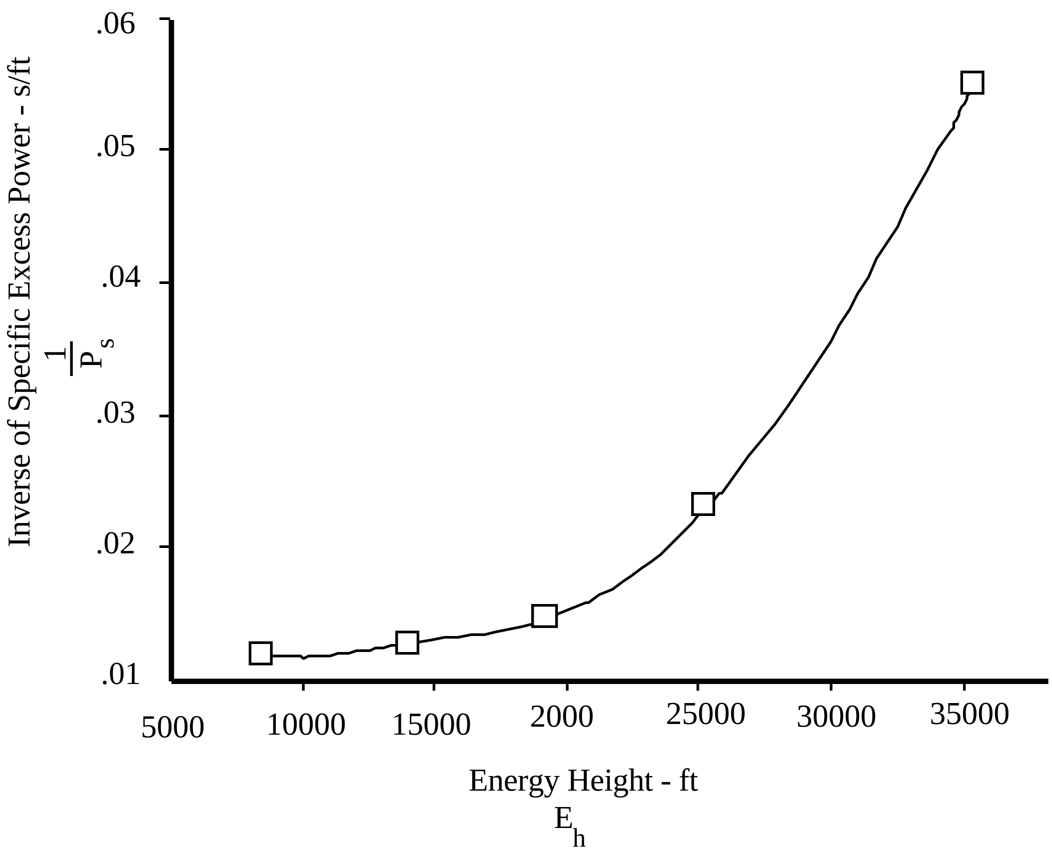

Figure 7.24
ENERGY RELATIONSHIP TO CLIMB

Distance flown in the climb is found by integration of the no wind ground speed with respect to time as in Eq 7.44.

$$\text{Distance} = \int_{t_1}^{t_2} V_T \cos\gamma \, dt$$

(Eq 7.44)

To perform the integration, the program must know $V_T \cos\gamma$. The plot should appear similar to figure 7.25

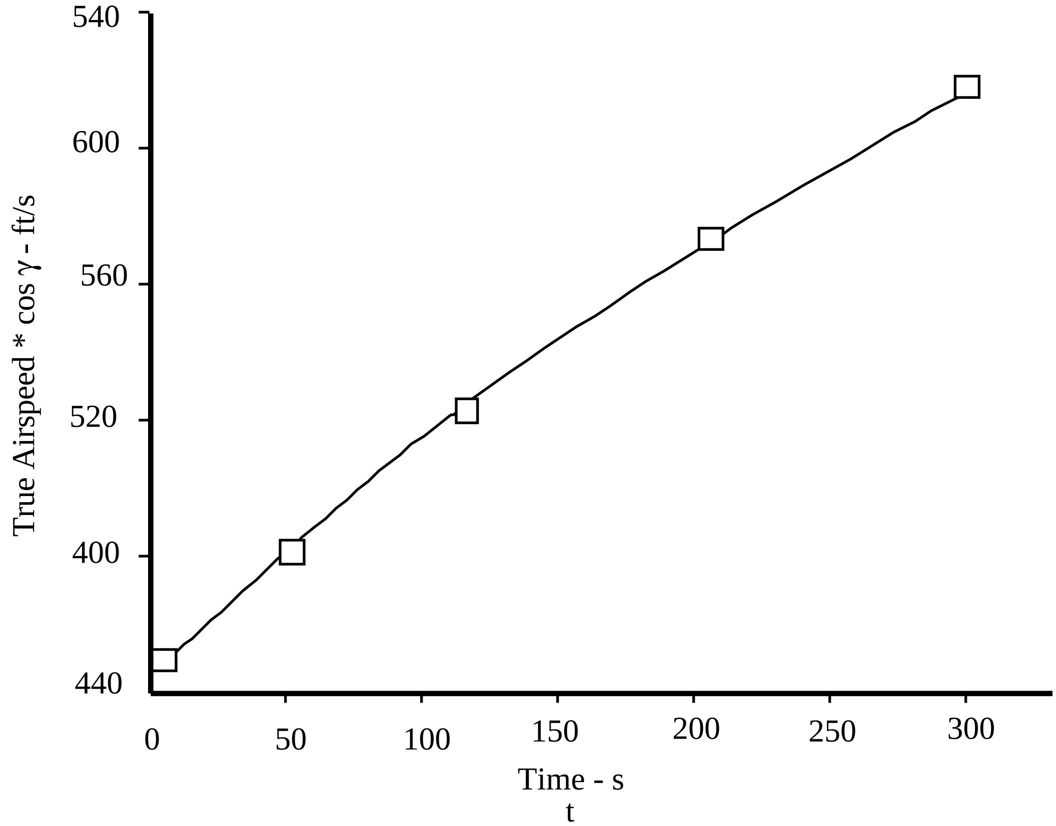

Figure 7.25
INTEGRATION RESULTS FOR DISTANCE

To calculate fuel used, the program must integrate standard day fuel flow with respect to time as in Eq 7.45.

$$\text{Fuel Used} = \int_{t_1}^{t_2} \dot{W}_f \, dt \qquad \text{(Eq 7.45)}$$

Where:

E_h	Energy height	ft
E_{h_1}	Energy height at start of climb	ft
E_{h_2}	Energy height at end of climb	ft
γ	Flight path angle	deg
P_s	Specific excess power	ft/s

t	Time	s
V_T	True airspeed	ft/s
$\dot{W}_f$	Fuel flow	lb/h.

The program first models the engine using referred fuel flow versus OAT, as in figure 7.26.

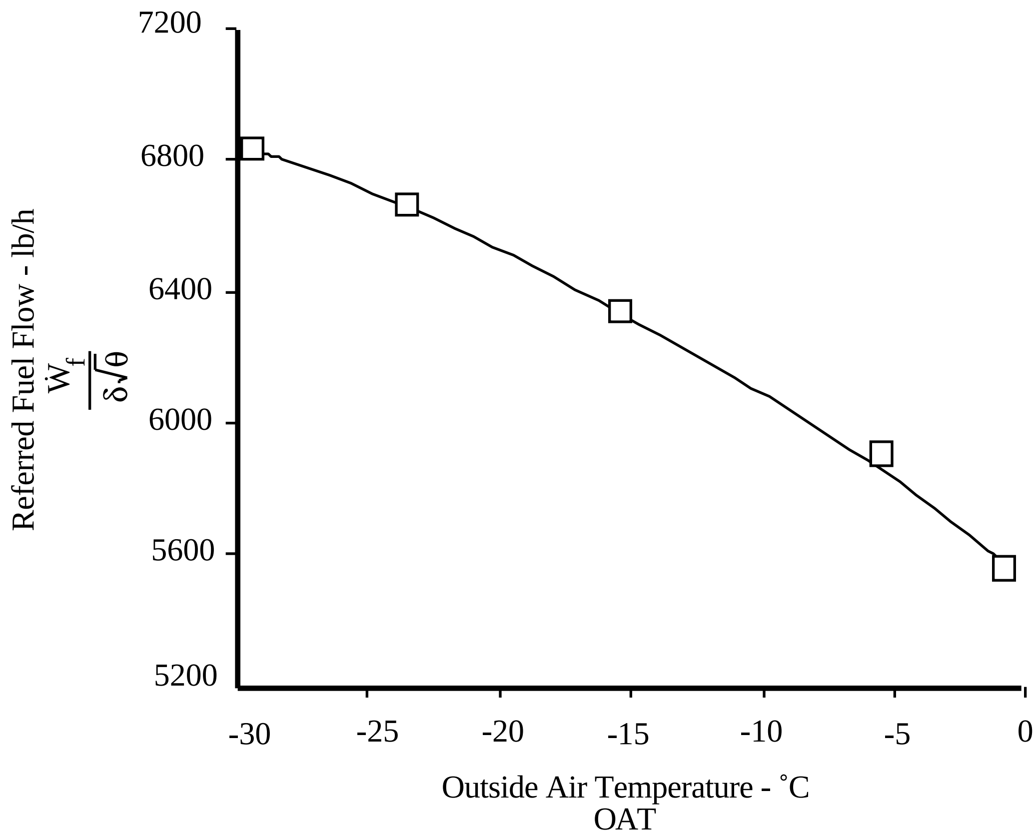

Figure 7.26
REFERRED FUEL USED

From figure 7.26, the program calculates standard day fuel flow and plots it versus time, as in figure 7.27.

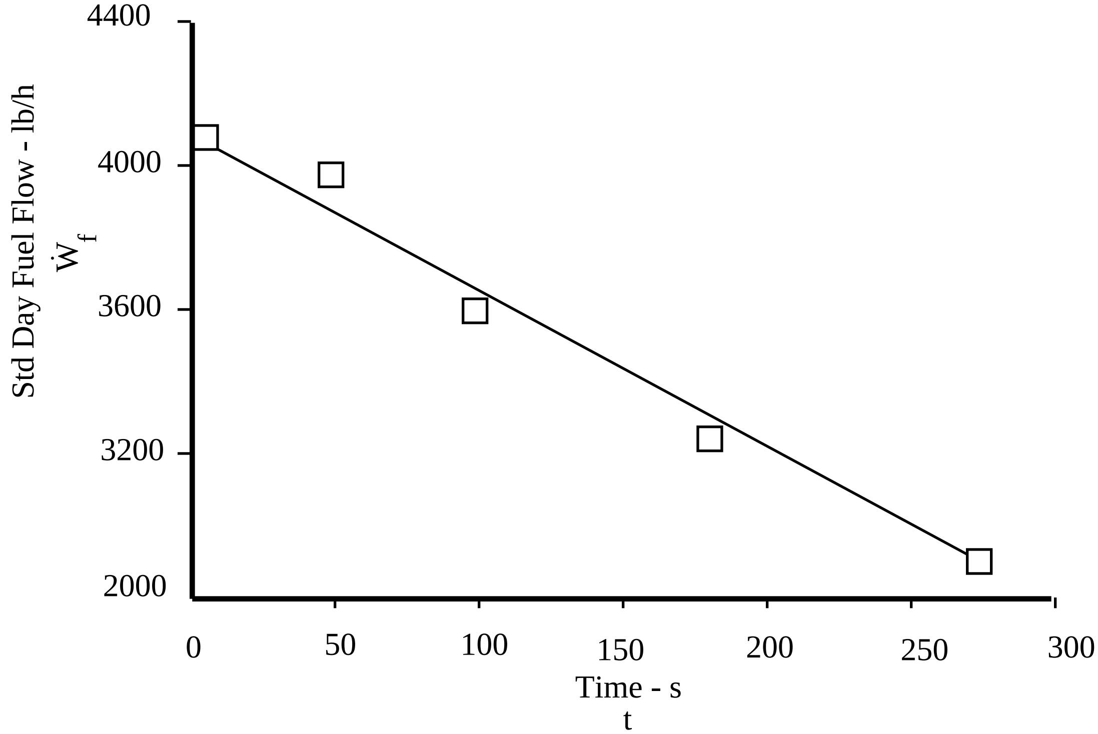

Figure 7.27

STANDARD DAY FUEL USED

The program then performs the three integrations using the curve fits determined, and plots altitude versus fuel used, time and distance in the climb. One possible example is shown in figure 7.28.

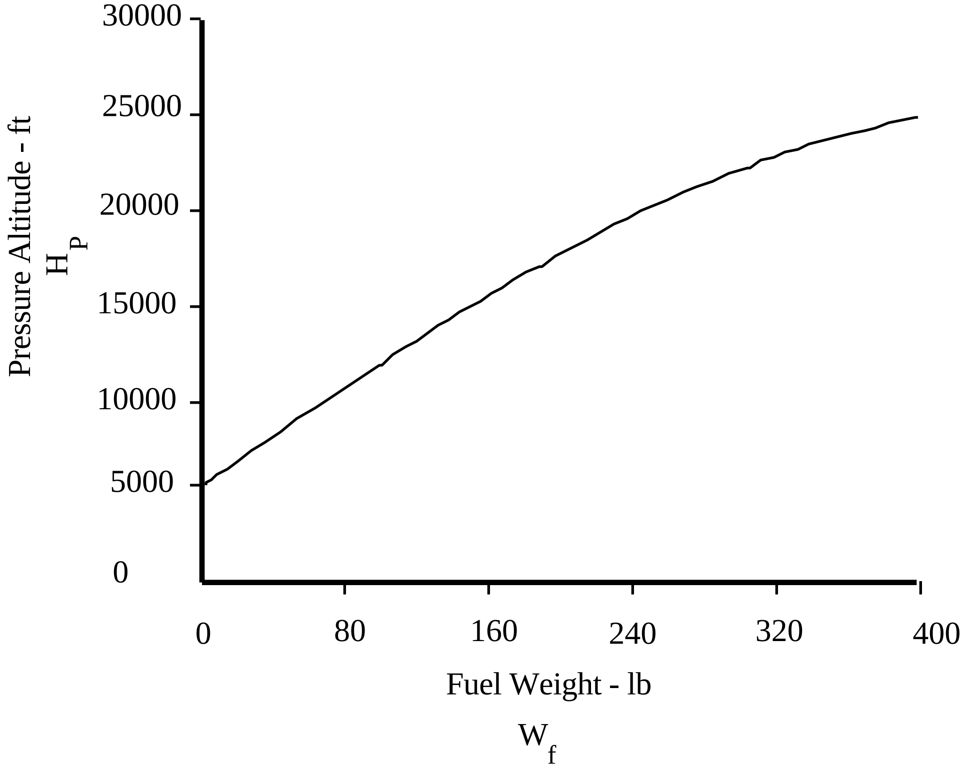

Figure 7.28
FUEL USED IN CLIMB

7.5.2.2 SAWTOOTH CLIMB

The purpose of the sawtooth climb data reduction program is to calculate rate and climb angle for any given gross weight, altitude and temperature, based on flight test data. From a menu selection, the appropriate choices are made to enter the sawtooth climb program. Data entry requirements for the program are as follows:

1. Basic data:
   a. Type of aircraft.
   b. Bureau number.
   c. Standard gross weight.
   d. Target altitude.
   e. Date of tests.
   f. Pilot’s name.
   g. Miscellaneous as allowed by the program.

2. For each data point:
   a. Initial indicated pressure altitude (ft).
   b. Final indicated pressure altitude (ft).
   c. Time required (s).
   d. Indicated airspeed (kn).
   e. OAT (˚C) or ambient temp (˚K).
   f. Fuel flow (lb/h).
   g. Gross weight (lb).
   h. Optional data as allowed by the program.

The program plots rate of climb and climb angle for the given altitude versus V_C, as in figures 7.29 and 7.30.

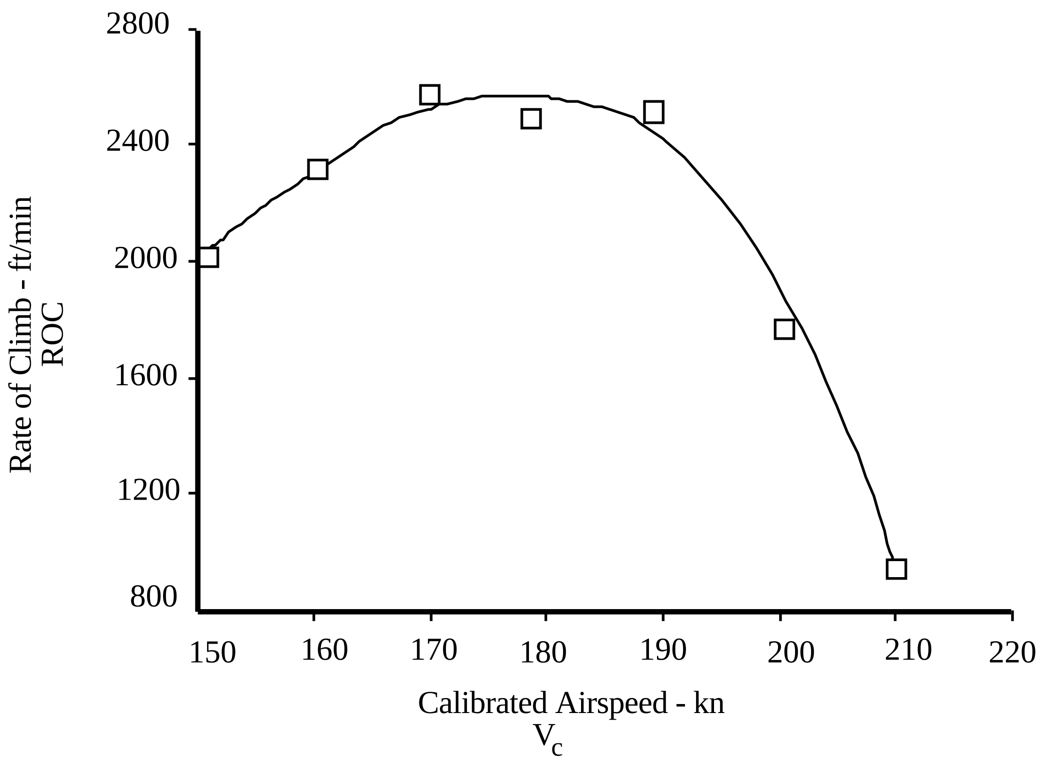

Figure 7.29
RATE OF CLIMB FROM SAWTOOTH CLIMBS

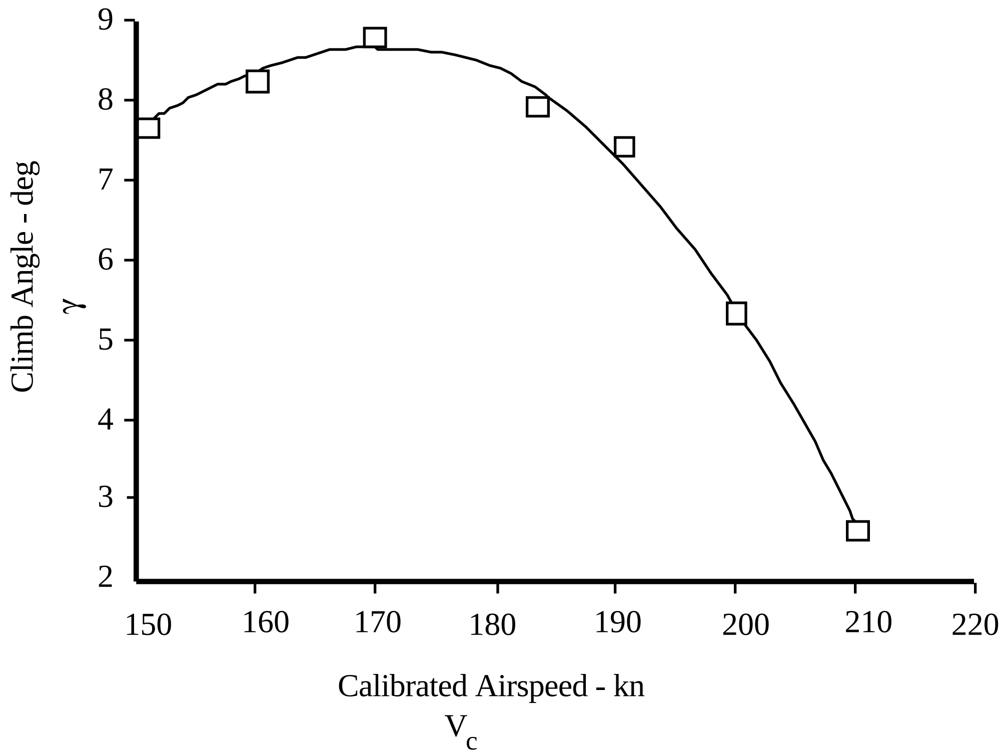

Figure 7.30

CLIMB ANGLE FROM SAWTOOTH CLIMBS

The following equations are used for the computer data reduction.

Obtain calibrated altitude (H_{P_c}) and calibrated airspeed (V_c) as in Chapter 2.

If ambient temperature (˚K) was entered:

$$^\circ C = {}^\circ K - 273.15 \qquad \text{(Eq 7.46)}$$

$$OAT = f\left(T_a, M\right) \qquad \text{(Eq 7.47)}$$

If OAT (˚C) was entered:

$$T_a = f\left(OAT, M\right) \qquad \text{(Eq 7.48)}$$

True airspeed:

$$V_T = f\left(OAT, M_T\right) \tag{Eq 7.49}$$

Altitude:

$$h = H_{P_{c\,ref}} + \Delta H_{P_c}\left(\frac{T_a}{T_{std}}\right) \tag{Eq 7.50}$$

Energy height:

$$E_h = h + \frac{V_T^2}{2g} \tag{Eq 7.1}$$

Test day P_S:

$$P_s = \frac{dE_h}{dt} = \frac{dh}{dt} + \frac{V_T}{g}\frac{dV_T}{dt} \tag{Eq 7.2}$$

Standard day P_S:

$$P_{s_{Std}} = P_{s_{Test}}\frac{W_{Test}}{W_{Std}}\frac{V_{T_{Std}}}{V_{T_{Test}}} + \frac{V_{T_{Std}}}{W_{Std}}\left(\Delta T_{N_x} - \Delta D\right) \tag{Eq 7.32}$$

Where:

D	Drag	lb
ΔD	Standard drag minus test drag	lb
ΔT_{N_x}	Standard net thrust parallel flight path minus test net thrust	lb
E_h	Energy height	ft
h	Tapeline altitude	ft
H_{P_c}	Calibrated pressure altitude	ft
$H_{P_{c\,ref}}$	Reference calibrated pressure altitude	Ft

M	Mach number	
M_T	True Mach number	
OAT	Outside air temperature	˚C
$P_{s_{Std}}$	Standard specific excess energy	ft/s
$P_{s_{Test}}$	Test specific excess energy	ft/s
T_a	Ambient temperature	˚K
T_{N_x}	Net thrust parallel flight path	lb
T_{Std}	Standard temperature	˚K
V_T	True airspeed	ft/s
$V_{T_{Std}}$	Standard true airspeed	ft/s
$V_{T_{Test}}$	Test true airspeed	ft/s
W_{Std}	Standard weight	lb
W_{Test}	Test weight	lb.

7.6 DATA ANALYSIS

The analysis of P_s data is directed towards determining the airplane optimum climb schedules. The theoretical optimum climb schedules are determined as described in section 7.3, by joining the points of maximum P_s (for a “minimum time” schedule) or points of maximum E_h (for a “maximum energy” schedule). The airspeed and Mach number schedules represented by these paths are then evaluated to determine whether they can be flown without undue difficulty, and are modified if necessary to make them flyable with the least penalty in climb performance. Finally, the climb schedules are flight-tested and the results, corrected to standard conditions, are compared with predictions.

The data from the sawtooth climb tests are intended to provide information for use in a far more restricted portion of the flight envelope than from level accelerations. The best climb speeds for the landing or single-engine wave-off configurations are unlikely to have much application above a few thousand feet, though they should certainly be determined for high elevation airports and should cover possible emergency diversion with the landing gear stuck down. The shape of these curves indicate the sensitivity of achieving the desired performance to airspeed errors. A peaked curve implies small inaccuracies in airspeed result in large performance penalties.

7.7 MISSION SUITABILITY

The mission requirements are the ultimate standard for climb performance. As stated in the beginning of the chapter, the mission of the airplane and specifically the mission of the flight to be flown determines the optimum condition for the climb. An interceptor is primarily interested in climbing to altitude with the minimum fuel if headed to a CAP station. An interceptor launching to intercept an incoming raid is primarily interested in arriving at the attack altitude with the best fighting speed and in the minimum time. An attack aircraft launching on a strike mission is primarily interested in climbing on a schedule of maximum range covered per pound of fuel burned. Still other types of mission may require, or desire, optimization of other factors during the climb.

In the case of single engine climb for multi engine aircraft or for wave-off, the test results in sawtooth climbs can develop the appropriate climb speeds to maximize obstacle clearance.

The specifications set desired performance in the production aircraft. These specifications are important as measures for contract performance. They are important in determining whether or not to continue the acquisition process at various stages of aircraft development.

As in all performance testing, the pure numbers cannot be the only determinant to acceptance of the aircraft. Mission suitability conclusions include the flying qualities associated with attaining specific airspeed schedules to climb. Consideration of the following items is worthwhile when recommending climb schedules or climb airspeeds:

1. Flight path stability.
2. Climb attitudes.
3. Field of view.
4. Mission profile or requirements.
5. Overall performance including climbing flight.
6. Compatibility of airspeeds / altitudes with the mission and location restrictions.
7. Performance sensitivities for schedule or airspeed deviations.

7.8 SPECIFICATION COMPLIANCE

Climb performance guarantees are stated in the detailed specification for the model and in Naval Air System Command Specification, AS-5263. The detail specification provides mission profiles to be expected and performance guarantees generically as follows:

1. Mission requirements.
   a. Land or sea based.
   b. Ferry capable.
   c. Instrument departure, transit, and recovery.
   d. Type of air combat maneuvering.
   e. Air to air combat (offensive and/or defensive) including weapons deployment.
   f. Low level navigation.
   g. Carrier suitability.

2. Performance guarantees are based on: type of day, empty gross weight, standard gross weight, drag index, fuel quantity and type at engine start, engine(s) type, loading, and configuration. The type of climb is specified, for example: Climb on course to optimum cruise altitude with military power (320 KIAS at sea level, 2 KIAS/1000 ft decrease to Mach number 0.72, Mach number 0.72 constant to level off).

Guarantees for climb likely include:

1. Instantaneous single engine climb in a given configuration.
2. A defined ceiling such as combat ceiling.
3. Wave-off rate of climb in a specific configuration.

AS-5263 further defines requirements for, and methods of, presenting characteristics and performance data for Naval piloted aircraft. Deviation from this specification are permissible, but in all cases must be approved by the procuring activity. Generally climb performance is presented as a function of altitude, plotting rate of climb at basic mission combat weight with maximum, intermediate, or normal thrust (power). Rates of climb for alternate loadings are presented to show the effects of drag changes with various external stores and/or weight changes. The effect of weight reduction during the climb is not considered. General provisions for the presentation of climb performance are as follows:

1. Performance is based on the latest approved standard atmospheric tables as specified by the Navy.
2. All speeds are presented as true airspeed in kn and Mach number; Mach number for jets, V_T for propeller aircraft.
3. Climb speed is the airspeed at which the optimum rate of climb is attained for the given configuration, weight, altitude, and power.
4. Service ceiling is that altitude at which the rate of climb is 100 ft/min at a stated loading, weight, and engine thrust (power).
5. Combat ceiling for subsonic vehicles is that altitude at which the rate of climb is 500 ft/min at the stated loading, weight, and engine thrust (power). Combat ceiling for supersonic vehicles is the highest altitude at which the vehicle can fly supersonically and have a 500 ft/min rate of climb at the stated loading, weight, and engine thrust (power).
6. Cruise ceiling for subsonic cruise vehicles is that altitude at which the rate of climb is 300 ft/min at normal (maximum continuous) engine ratting at stated weight and loading. Cruise ceiling for supersonic cruise vehicles is that altitude at which the rate of climb is 300 ft/min at normal (maximum continuous) engine ratting at stated weight and loading.
7. Cruise altitude is the altitude at which the cruise portion of the mission is computed.
8. Optimum cruise altitude is the altitude at which the aircraft attains the maximum nautical miles per pound of fuel for the momentary weight and configuration.
9. Combat altitude is the altitude at the target for the specific mission given.
10. Enroute climb data is based on the appropriate configuration, thrust (power) and weight. The aircraft has the landing gear and flaps retracted and the airspeed for best climb for the applicable condition is presented.
11. Enroute climb power for jet aircraft (fighter, attack, trainers) to cruise altitude is at intermediate (military) thrust. Propeller aircraft (patrol, transport) use maximum continuous power.
12. The time to climb to a specified altitude is expressed in minutes from start of enroute climb. Weight reduction as a result of fuel consumed is applied.
13. Combat climb is the instantaneous maximum vertical speed capability in ft/min at combat conditions; weight, configuration, altitude, and thrust (power).

14. The term thrust (power) is used to mean thrust (jet engine) and/or brake horsepower (shaft engines).

15. All fuel consumption data, regardless of source, is increased by 5 % for all engine thrust (power) conditions as a service tolerance to allow for practical operation, unless authorized otherwise. In addition, corrections or allowances to engine fuel flow is made for all power plant installation losses such as accessory drives, ducts, or fans.

7.9 GLOSSARY

7.9.1 NOTATIONS

AR	Aspect ratio	
a_x	Acceleration parallel flight path	ft/s^2
a_z	Acceleration perpendicular to flight path	ft/s^2
CAP	Combat air patrol	
CCF	Climb correction factor	
C_D	Drag coefficient	
C_L	Lift coefficient	
D	Drag	lb
d	Distance	ft
ΔD	Standard drag minus test drag	lb
dh/dt	Rate of climb	ft/s
D_{Std}	Standard drag	lb
D_{Test}	Test drag	lb
ΔT_{N_x}	Standard net thrust parallel flight path minus test net thrust	lb
e	Oswald's efficiency factor	
E_h	Energy height	ft
E_{h1}	Energy height at start of climb	ft
E_{h2}	Energy height at end of climb	ft
$E_{h_{Test}}$	Test energy height	ft
ESHP	Engine shaft horsepower	hp
g	Gravitational acceleration	ft/s^2
h	Tapeline altitude	ft
h_1	Tapeline altitude start of climb	ft
h_2	Tapeline altitude end of climb	ft

H_P	Pressure altitude	ft
H_{P_c}	Calibrated pressure altitude	ft
$H_{P_{c\ ref}}$	Reference calibrated pressure altitude	ft
H_{P_o}	Observed pressure altitude	ft
h_{Test}	Test tapeline altitude	ft
L	Lift	lb
M	Mach number	
M_T	True Mach number	
n_z	Normal acceleration	g
$n_{z_{Std}}$	Standard normal acceleration	g
$n_{z_{Test}}$	Test normal acceleration	g
OAT	Outside air temperature	˚C
P_A	Power available	ft-lb/s
P_a	Ambient pressure	psf
P_{req}	Power required	ft-lb/s
P_s	Specific excess power	ft/s
$P_{s_{Std}}$	Standard specific excess power	ft/s
$P_{s_{Test}}$	Test specific excess power	ft/s
ROC	Rate of climb	ft/s
S	Wing area	ft^2
t	Time	s
T_a	Ambient temperature	˚C
T_N	Net thrust	lb
T_{N_x}	Net thrust parallel flight path	lb
T_{Std}	Standard temperature	˚C
V	Velocity	ft/s
V_e	Equivalent airspeed	ft/s
V_H	Maximum level flight airspeed	kn
V_{hor}	Horizontal velocity	ft/s
V_i	Indicated airspeed	kn
V_{mc}	Airspeed for minimum control	kn
V_o	Observed airspeed	kn
V_s	Stall speed	kn
V_T	True airspeed	ft/s
$V_{T_{ref}}$	Reference true airspeed	ft/s
$V_{T_{Std}}$	Standard true airspeed	ft/s

$V_{T_{Test}}$	Test true airspeed	ft/s
V_v	Vertical velocity	ft/s
V_x	Speed for maximum climb angle	kn
V_y	Speed for maximum rate of climb	kn
W	Weight	lb
W_f	Fuel weight	lb
W_{Std}	Standard weight	lb
W_{Test}	Test weight	lb
$\dot{W}_f$	Fuel flow	lb/h

7.9.2 GREEK SYMBOLS

α (alpha)	Angle of attack	deg
α_j	Thrust angle	deg
δ (delta)	Pressure ratio	
γ (gamma)	Flight path angle	deg
	Ratio of specific heats	
γ_{Std}	Standard flight path angle	deg
γ_{Test}	Test flight path angle	deg
π (pi)	Constant	
θ (theta)	Temperature ratio	
ρ_{ssl} (rho)	Standard sea level air density	0.0023769 slug/ft^3

7.10 REFERENCES

1. Naval Air System Command Specification, *Guidelines For Preparation Of Standard Aircraft Characteristics Charts And Performance Data Piloted Aircraft (Fixed Wing), AS-5263,* 23 October, 1986.

2. Naval Test Pilot School Flight Test Manual, *Fixed Wing Performance, Theory and Flight Test Techniques,* USNTPS-FTM-No. 104, U. S. Naval Test Pilot School, Patuxent River, MD, July 1977.

3. Petersen, F.S., *Aircraft and Engine Performance,* Naval Air Test Center, Patuxent River, MD, 1958.

4. Powell, J.W., *Airplane Performance*, USNTPS Classroom Notes, USNTPS Patuxent River, MD.

5. Rutowski, E.S., "Energy Approach to the General Aircraft Maneuverability Problem", *Journal of the Aeronautical Sciences*, Vol 21, No 3, March 1954.

6. USAF Test Pilot School, *Performance Flight Test Phase*, Volume I, Chapter 9, USAF Test Pilot School, Edwards AFB, CA, August 1991.

7. USAF Test Pilot School, *Performance Planning Guide*, USAF Test Pilot School, Edwards AFB, CA, July 1987.

CHAPTER 8

DESCENT PERFORMANCE

CHAPTER 8

FIGURES

CHAPTER 8

EQUATIONS

Equation		PAGE
$\sum F_z = L = W \cos\gamma$	(Eq 8.1)	8.3
$\sum F_x = D = W \sin\gamma$	(Eq 8.2)	8.3
$\frac{L}{D} = \frac{\cos\gamma}{\sin\gamma} = \cot\gamma$	(Eq 8.3)	8.3
$V_{hor} = V_T \cos\gamma$	(Eq 8.4)	8.3
$V_v = V_T \sin\gamma$	(Eq 8.5)	8.3
$\frac{V_{hor}}{V_v} = \frac{V_T \cos\gamma}{V_T \sin\gamma} = \cot\gamma = \frac{L}{D}$	(Eq 8.6)	8.3
$\sin\gamma = \frac{V_v}{V_T}$	(Eq 8.7)	8.3
$\gamma = \sin^{-1}\left(\frac{V_v}{V_T}\right)$	(Eq 8.8)	8.4
$\gamma = \sin^{-1}\left(\frac{dh/dt}{V_T}\right)$	(Eq 8.9)	8.4
$\frac{L}{D} = \cot\left[\sin^{-1}\left(\frac{dh/dt}{V_T}\right)\right]$	(Eq 8.10)	8.4
$\text{Glide Ratio} = \frac{L}{D} = \frac{V_T \cos\gamma}{V_v}$	(Eq 8.11)	8.4
$GR = \frac{L}{D} \approx \frac{V_T}{V_v}$	(Eq 8.12)	8.4

$V_T = \sqrt{V_T^2 \sin^2 \gamma + V_T^2 \cos^2 \gamma} = \sqrt{V_T^2 \left(\sin^2 \gamma + \cos^2 \gamma \right)}$	(Eq 8.13)	8.5
$\sum F_x = W \sin \gamma - D = \frac{W}{g} \frac{dV_T}{dt}$	(Eq 8.14)	8.10
$\frac{D}{W} = \sin \gamma - \frac{1}{g} \frac{dV_T}{dt}$	(Eq 8.15)	8.10
$\frac{dV_T}{dt} = \frac{dV_T}{dh} \frac{dh}{dt}$	(Eq 8.16)	8.10
$\frac{D}{W} = \sin \gamma - \frac{1}{g} \frac{dV_T}{dh} \frac{dh}{dt}$	(Eq 8.17)	8.10
$\frac{dh}{dt} = V_T \sin \gamma$	(Eq 8.18)	8.11
$\frac{D}{W} = \sin \gamma - \frac{1}{g} \frac{dV_T}{dh} V_T \sin \gamma$	(Eq 8.19)	8.11
$\frac{L}{W} = \cos \gamma$	(Eq 8.20)	8.11
$\frac{L}{D} = \cot \gamma \left[\frac{1}{1 - \frac{V_T}{g} \frac{dV_T}{dh}} \right]$	(Eq 8.21)	8.11
$\frac{L}{D} = \cot \left[\sin^{-1} \left(\frac{(dh/dt)}{V_T} \right) \right] \left[\frac{1}{1 - \frac{V_T}{g} \frac{dV_T}{dh}} \right]$	(Eq 8.22)	8.11
$\frac{L}{D} = \left[\frac{GR}{1 - \frac{V_T}{g} \frac{dV_T}{dh}} \right]$	(Eq 8.23)	8.12
$GR = \frac{L}{D} \left[1 - \frac{V_T}{g} \frac{dV_T}{dh} \right]$	(Eq 8.24)	8.12
$V_c = V_i + \Delta V_{pos}$	(Eq 8.25)	8.29

$$H_{P_c} = H_{P_i} + \Delta H_{pos}$$ (Eq 8.26) 8.29

$$T_a(°C) = T_a\,(°K) - 273.15$$ (Eq 8.27) 8.29

$$OAT = f\left(T_a, M_T\right)$$ (Eq 8.28) 8.29

$$T_a = f\ \left(OAT, M_T\right)$$ (Eq 8.29) 8.29

$$V_{T_{Test}} = f\left(V_c, H_{P_c}, T_a\right)$$ (Eq 8.30) 8.29

$$V_{T_{Std}} = f\left(V_c, H_{P_c}, T_{Std}\right)$$ (Eq 8.31) 8.29

$$h = H_{P_{c\ ref}} + \Delta H_{P_c}\left(\frac{T_a}{T_{Std}}\right)$$ (Eq 8.32) 8.29

$$E_h = h + \frac{V^2_{T_{Test}}}{2g}$$ (Eq 8.33) 8.30

$$P_{s_{Test}} = \frac{dE_h}{dt}$$ (Eq 8.34) 8.30

$$P_{s_{Std}} = P_{s_{Test}}\left(\frac{W_{Test}}{W_{Std}}\right)\left(\frac{V_{T_{Std}}}{V_{T_{Test}}}\right) + \left(\frac{V_{T_{Std}}}{W_{Std}}\right)(\Delta T_{N_x} - \Delta D)$$ (Eq 8.35) 8.30

$$\gamma_{Test} = \sin^{-1}\left[\frac{dh/dt}{V_{T_{Test}}}\right]$$ (Eq 8.36) 8.30

$$DCF = 1+\left(\frac{V_{T_{Std}}}{g}\,\frac{dV_T}{dh}\right)$$ (Eq 8.37) 8.30

$$\left(\frac{dh}{dt}\right)_{Std} = \frac{P_{s_{Std}}}{DCF}$$ (Eq 8.38) 8.30

CHAPTER 8

DESCENT PERFORMANCE

8.1 INTRODUCTION

This chapter examines the theory and flight tests to determine aircraft descent performance. By definition, whenever an aircraft is in an unstalled descent, it is in either a glide or a dive. For purposes of this manual, a glide is defined as unaccelerated flight at a descent angle less than or equal to fifteen degrees, while a dive is defined as flight with a descent angle greater than fifteen degrees. Glides or dives may be either power-on or power-off maneuvers in different configurations, so a wide range of gliding and diving performance is possible with any given airplane.

Flight testing of an airplane's descent performance generally involves only the power-off case where the term power-off is used to define the idle thrust/minimum torque/minimum power glide performance.

While obtaining descent data in low drag configurations with power-off can be considered a rather benign flight test, the character of the testing changes dramatically for tests required to define the flameout landing pattern. And even the benign descent tests become exciting if an engine or other critical system fails.

8.2 PURPOSE OF TEST

The purpose of this test is to investigate aircraft descent performance characteristics to determine time, fuel used, and distance traveled. The tests are performed at different airspeeds and in different configurations to obtain data for the NATOPS manual including:

1. Optimum descent airspeed or Mach number/airspeed schedules.
2. Penetration descent schedules.
3. Precautionary approach patterns.
4. Flameout approach patterns.

8.3 THEORY

For stabilized, level flight, engine thrust or power is adjusted to balance the aircraft's drag. If the thrust or power is reduced to zero, the power required to maintain the aircraft's speed comes from the aircraft's time rate of change of kinetic and potential energy. The rate of energy expenditure varies directly with the rate of descent and linear acceleration.

For the discussion of gliding or power-off flight, the thrust or power is assumed to be negligible, and gliding performance is measured in terms of:

1. Minimum rate of descent (endurance).
2. Minimum glide angle (range).

With an aircraft in a steady power-off glide, the forces on the aircraft are lift, drag and weight as indicated in figure 8.1.

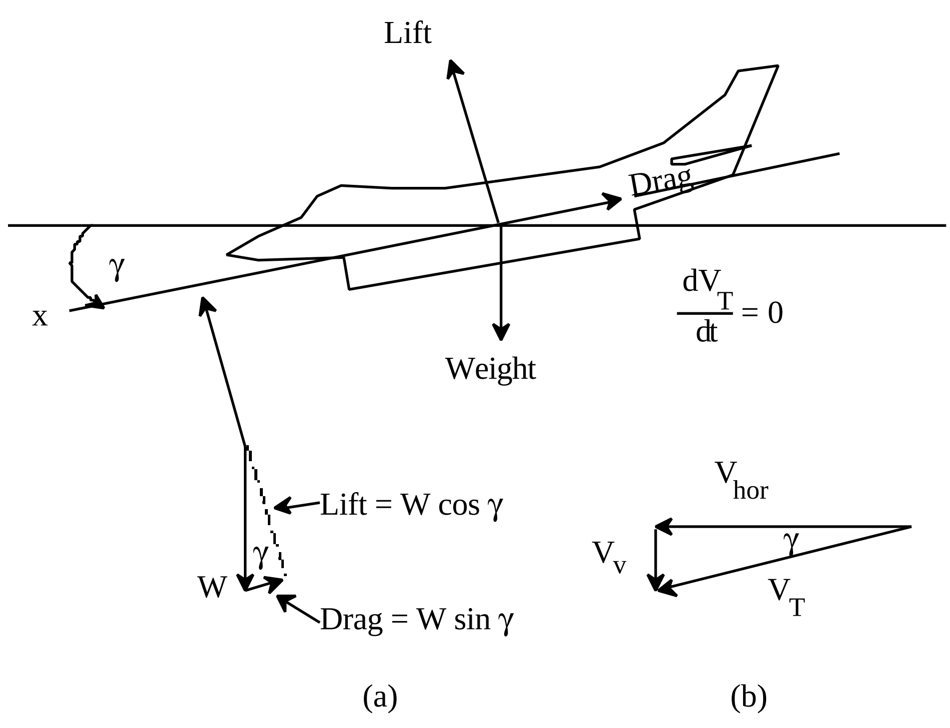

Figure 8.1
FORCES IN A STEADY GLIDE

The angle between the flight path and the horizon is called the flight path angle (γ); for a glide the flight path angle is negative. The descent (glide) angle is a function of both the descent rate (dh/dt) and true airspeed (V_T).

To evaluate descent performance, the true airspeed is assumed to be constant ($dV_T/dt = 0$).

In addition to glide angle, descent performance is described in terms of glide ratio (GR) defined as the ratio of horizontal to vertical velocity.

Since the condition is steady flight ($dV_T/dt = 0$), figure 8.1 (a) shows the forces are in equilibrium and resolving the forces perpendicular and parallel to the flight path gives:

$$\sum F_z = L = W \cos \gamma \tag{Eq 8.1}$$

$$\sum F_x = D = W \sin \gamma \tag{Eq 8.2}$$

$$\frac{L}{D} = \frac{\cos \gamma}{\sin \gamma} = \cot \gamma \tag{Eq 8.3}$$

The glide angle (γ) is a minimum when the ratio of lift to drag is a maximum.

Evaluating the vector diagram, figure 8.1 (b), where V_T = flight path speed produces:

$$V_{hor} = V_T \cos \gamma \tag{Eq 8.4}$$

$$V_v = V_T \sin \gamma \tag{Eq 8.5}$$

$$\frac{V_{hor}}{V_v} = \frac{V_T \cos \gamma}{V_T \sin \gamma} = \cot \gamma = \frac{L}{D} \tag{Eq 8.6}$$

$$\sin \gamma = \frac{V_v}{V_T} \tag{Eq 8.7}$$

$$\gamma = \sin^{-1}\left(\frac{V_v}{V_T}\right) \tag{Eq 8.8}$$

$$\gamma = \sin^{-1}\left(\frac{dh/dt}{V_T}\right) \tag{Eq 8.9}$$

$$\frac{L}{D} = \cot\left[\sin^{-1}\left(\frac{dh/dt}{V_T}\right)\right] \tag{Eq 8.10}$$

Generally measuring horizontal velocity directly is not convenient, so substituting $V_{hor} = V_T \cos\gamma$ into Eq 8.6, provides a more usable equation:

$$\text{Glide Ratio} = \frac{L}{D} = \frac{V_T \cos\gamma}{V_v} \tag{Eq 8.11}$$

When the glide ratio is greater than 7 to 1, $\cos\gamma$ is between 0.99 and 1.0. Since the glide ratio of most tactical aircraft fit this criteria in the low drag, clean configuration, the equation simplifies to:

$$GR = \frac{L}{D} \approx \frac{V_T}{V_v} \tag{Eq 8.12}$$

For small descent angles the horizontal speed (V_{hor}) is almost the same as the flight path speed (V_T). As the descent angle increases, this approximate identity is no longer valid.

Resolving the vertical and horizontal velocity components from figure 8.1 (b), and plotting V_{hor} against V_v yields a hodograph (Figure 8.2).

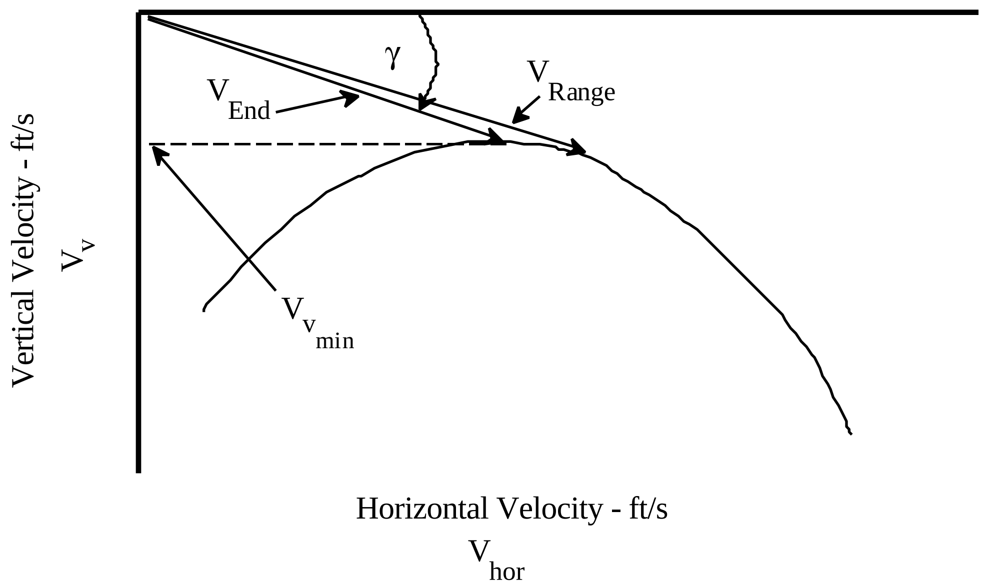

Figure 8.2
HODOGRAPH

On a hodograph, the radius vector from the origin to any part on the plot has a length proportional to the flight path speed and makes an angle to the horizontal equal to the actual descent angle (γ).

1. The vertical axis is: $dh/dt = V_v$ = rate of descent (ROD) = $V_T \sin \gamma$.
2. The horizontal axis is $V_{hor} = V_T \cos \gamma$.

Thus by the Pythagorean theorem, a line drawn from the origin to some point on the hodograph has a vector length:

$$V_T = \sqrt{V_T^2 \sin^2 \gamma + V_T^2 \cos^2 \gamma} = \sqrt{V_T^2 \left(\sin^2 \gamma + \cos^2 \gamma\right)} \qquad \text{(Eq 8.13)}$$

Where:

D	Drag	lb
F_Z	Force perpendicular to flight path	lb
F_X	Forces parallel to flight path	lb
γ	Flight path angle	deg
GR	Glide ratio	
h	Tapeline altitude	ft
L	Lift	lb
t	Time	s
V_{hor}	Horizontal velocity	kn or ft/s
V_T	True airspeed	kn or ft/s
V_v	Vertical velocity	ft/s
W	Weight	lb.

The angle made by the resultant velocity vector with the horizontal is γ. Therefore the hodograph representation gives the:

1. Rate of descent.
2. Horizontal speed.
3. Flight path speed.
4. Flight path angle.

8.3.1 WEIGHT EFFECT

As shown in Eq 8.3, for a given aircraft, the glide angle is determined solely by its lift-to-drag ratio, which is independent of weight. Note the higher the lift-to-drag ratio, the shallower the descent angle (assuming no wind). The hodograph in figure 8.3 shows an aircraft at two different weights.

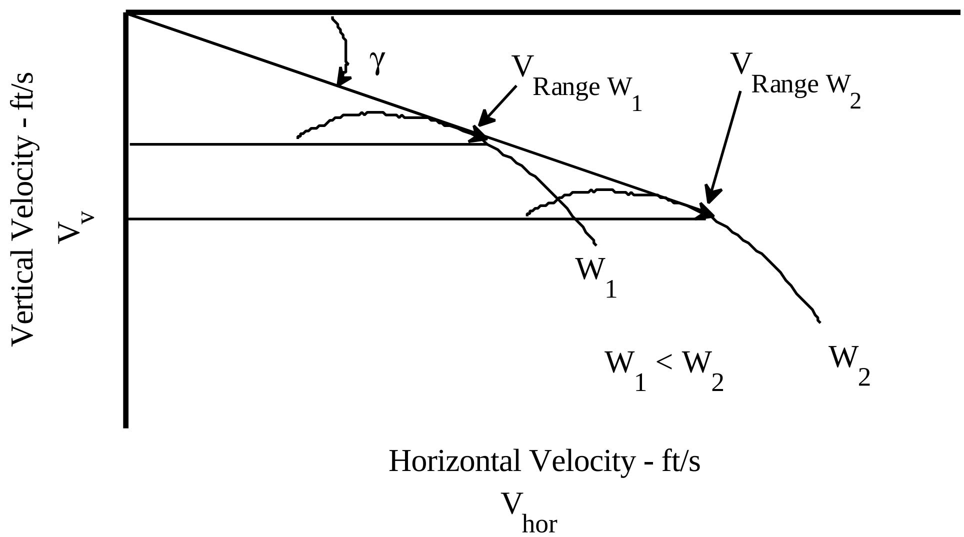

Figure 8.3
WEIGHT EFFECT ON DESCENT PERFORMANCE

To fly at the same $\left.\frac{L}{D}\right|_{max}$ (same descent angle) at a higher gross weight, the flight path airspeed increases and the rate of descent increases. At the higher airspeed for the higher gross weight, the increase in drag is offset by the increased weight component along the flight path.

8.3.2 WIND EFFECT

The effects of head wind or a tail wind can be resolved by displacing the origin of the hodograph by the amount of the head wind or tail wind component (Figure 8.4).

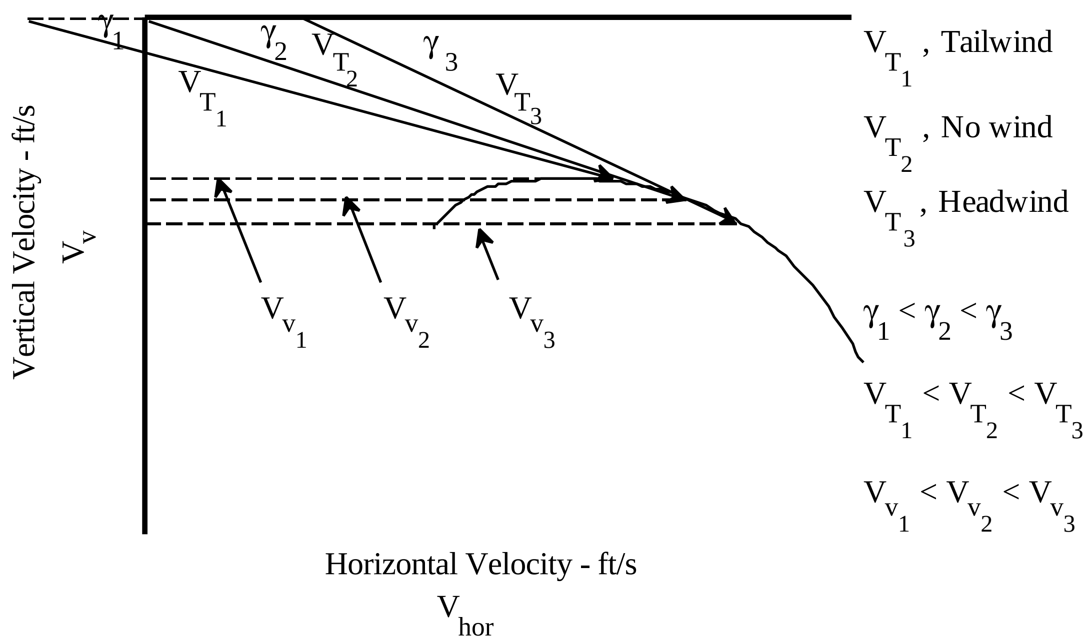

Figure 8.4

TAIL WIND / HEAD WIND EFFECT ON DESCENT PERFORMANCE

For maximum range in a tail wind, you must fly slower than when flying for range in the no wind case. The aircraft remains airborne for a longer time, taking advantage of the tail wind.

When gliding for maximum range in a tail wind jettisoning weight helps. This has the effect of increasing the endurance and allows the aircraft to gain more advantage from the tail wind.

In a head wind, the speed for optimum range is greater than the minimum drag speed and the time for which the aircraft is subject to the adverse wind effect is reduced.

When gliding for maximum range in a head wind, retaining weight helps because the wind affects the aircraft for a shorter time. To summarize:

1. No wind - weight has no effect on range.
2. Tail wind - jettison weight for best range.
3. Head wind - retain weight for best range.

8.3.3 DRAG EFFECT

As shown in figure 8.5, the effect of increasing drag is to move the hodograph plot to the left and down where the maximum glide speed occurs at a slower airspeed and at a higher rate of descent.

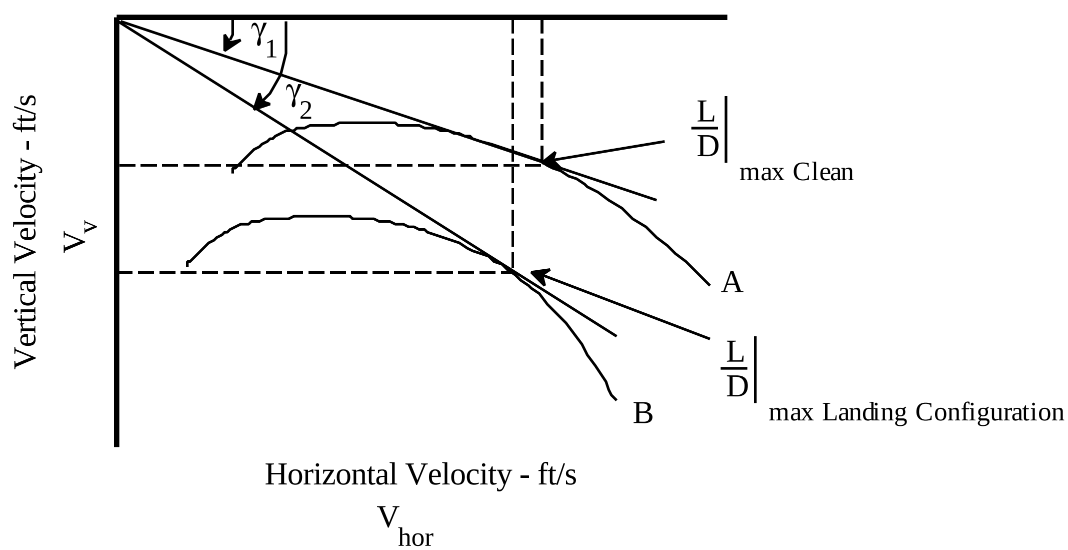

Figure 8.5
INCREASED DRAG EFFECT ON DESCENT PERFORMANCE

Understanding this relationship is most important when specifying a precautionary / flameout landing pattern. In preparing for landing when high drag items like gear, flaps, and speed brakes are extended, the descent performance of the aircraft jumps from figure 8.5 curve A to curve B. During the transition from the stabilized glide condition in curve B, to establish a flight path tangential to the runway during the landing flare, kinetic energy is traded for potential energy. However, once the deceleration is stopped, the rate of descent is fixed. As might occur with a flare which is too high above the runway, the aircraft would be at a point where a further decrease in airspeed is not possible due to stall, so the landing which results might be at an excessive rate of descent.

8.3.4 AIRSPEED EFFECT

Throughout the previous discussion, the aircraft was assumed to be descending at a constant true airspeed. Since many descents are done at a decelerating V_T (constant V_o) the effect of $dV_T/dt \neq 0$ is evaluated.

For an aircraft which is not accelerating, as in Eq 8.10, the L/D ratio for an aircraft in the power-off case could be calculated from measured flight parameters:

$$\frac{L}{D} = \cot\left[\sin^{-1}\left(\frac{dh/dt}{V_T}\right)\right] \tag{Eq 8.10}$$

In most cases a descent is flown with dV_T/dt decreasing. For the case where V_c = constant, the true airspeed is decreasing as the aircraft descends. Modifying Eq 8.1 and Eq 8.2 to account for the deceleration and summing the forces along the flight path:

$$\sum F_x = W \sin\gamma - D = \frac{W}{g}\frac{dV_T}{dt} \tag{Eq 8.14}$$

Re-arranging as:

$$\frac{D}{W} = \sin\gamma - \frac{1}{g}\frac{dV_T}{dt} \tag{Eq 8.15}$$

The flight path acceleration dV_T/dt can be expressed as:

$$\frac{dV_T}{dt} = \frac{dV_T}{dh}\frac{dh}{dt} \tag{Eq 8.16}$$

Substituting in Eq 8.15 gives:

$$\frac{D}{W} = \sin\gamma - \frac{1}{g}\frac{dV_T}{dh}\frac{dh}{dt} \tag{Eq 8.17}$$

Since:

$$\frac{dh}{dt} = V_T \sin\gamma \qquad \text{(Eq 8.18)}$$

Further substitution in Eq 8.17 gives:

$$\frac{D}{W} = \sin\gamma - \frac{1}{g}\frac{dV_T}{dh} V_T \sin\gamma \qquad \text{(Eq 8.19)}$$

The sum of the forces perpendicular to the flight path figure 8.1 (a) (regardless of flight path acceleration) can be resolved as:

$$\sum F_z = L = W\cos\gamma \qquad \text{(Eq 8.1)}$$

Or:

$$\frac{L}{W} = \cos\gamma \qquad \text{(Eq 8.20)}$$

Combining Eq 8.19 and Eq 8.20 produces:

$$\frac{L}{D} = \cot\gamma \left[\frac{1}{1 - \frac{V_T}{g}\frac{dV_T}{dh}} \right] \qquad \text{(Eq 8.21)}$$

Expressed in terms of flight parameters which can be measured:

$$\frac{L}{D} = \cot\left[\sin^{-1}\left(\frac{(dh/dt)}{V_T} \right) \right] \left[\frac{1}{1 - \frac{V_T}{g}\frac{dV_T}{dh}} \right] \qquad \text{(Eq 8.22)}$$

Eq 8.22 is Eq 8.10 modified by the flight path acceleration.

The instantaneous glide ratio, regardless of acceleration or deceleration ($dV_T/dh \neq 0$) is still the ratio of V_v/V_{hor} forming the descent angle γ where the glide ratio is cot γ:

$$\frac{L}{D} = \left[\frac{GR}{1 - \frac{V_T}{g} \frac{dV_T}{dh}} \right] \quad \text{(Eq 8.23)}$$

$$GR = \frac{L}{D} \left[1 - \frac{V_T}{g} \frac{dV_T}{dh} \right] \quad \text{(Eq 8.24)}$$

Where:

D	Drag	lb
F_z	Force perpendicular to flight path	lb
F_x	Force parallel to flight path	lb
γ	Flight path angle	deg
g	Gravitational acceleration	ft/s^2
GR	Glide ratio	
h	Tapeline altitude	ft
L	Lift	lb
t	Time	s
V_T	True airspeed	ft/s
W	Weight	lb.

The lift-to-drag ratio is a function of the drag polar and is independent of the descent path. The actual glide ratio is the lift-to-drag ratio modified by the path. In the example above where the aircraft is decelerating, the quantity $(1- \frac{V_T}{g} \frac{dV_T}{dh})$ is greater than 1, which results in the actual glide path angle being less than the aircraft L/D.

8.4 TEST METHODS AND TECHNIQUES

8.4.1 SAWTOOTH DESCENT

The sawtooth descent consists of a series of short descents at a constant observed airspeed (V_o) covering the range of desired test airspeeds. The altitude band for the descent is usually 1,000 ft either side of the target altitude for high L/D configurations or as much as 3,000 ft either side of the target altitude for low L/D configurations. Subsequent flights evaluate different target altitudes with the same test airspeeds.

Establish configuration and thrust/power setting above the desired start altitude. Allow sufficient altitude for the engine(s) to stabilize at the test thrust/power setting and stabilize at the desired airspeed before entering the data band.

Although the tolerance on V_o is ± 1 kn, this must not be achieved at the expense of a loss of smoothness. If a small airspeed error is made while establishing the descent, maintaining the off-target speed as accurately as possible is preferred rather than trying to correct to the target airspeed and risk aborting the entire run. While a photopanel or other automatic recording device can be used, good results may be obtained with a minimum number of hand-held data points using a stop watch.

To minimize wind shear, determine the wind direction and magnitude so all descent testing can be made perpendicular to the average wind in the altitude band being flown.

A typical flight data card is shown in figure 8.6.

Target V_o	V_o	Initial H_P	Final H_P	Δt	Fuel	OAT	Misc

Figure 8.6
SAWTOOTH DATA CARD

The exact time of entering and leaving the altitude band is recorded by a stopwatch or an instrumentation system.

Once through the altitude increment, record data, and a initiate climb above the altitude band for another run. As many points as possible are flown at each altitude.

Record actual in-flight V_o, W, time, fuel counts or fuel remaining, and either outside air temperature or time of day so temperature can be obtained by other meteorological methods. The card can be expanded to record other parameters such as angle of attack, engine RPM, torque, etc. On the back of the data card, keep a running plot of observed time to descend versus V_o and before leaving the test altitude, examine the plot for points which need repeating.

8.4.1.1 DATA REQUIRED

1. Time: Record elapsed time from the beginning of the altitude band to the end, or two minutes, whichever comes first.
2. Altitude: Record the observed pressure altitude (H_{P_o}) band for each point.
3. Velocity: Record observed airspeed, V_o.
4. OAT or T_a: Record ambient air temperature from on-board instrumentation at target altitude. (May be obtained from direct observation).
5. Fuel weight: Record the fuel remaining to determine aircraft gross weight.
6. Miscellaneous: Record other information desired such as RPM, angle of attack, and torque for a turboprop.

Additional data and information associated with the engine management criteria are important for the descent evaluation. For example:

1. Jet exhaust nozzle position at idle thrust and the minimum thrust setting to keep the nozzle closed.
2. Heating/air conditioning, pressurization, and anti-ice systems operation at low poser.
3. Engine and other aircraft systems operation limits at low power settings.

8.4.1.2 TEST CRITERIA

Allow sufficient altitude for the engine(s) to stabilize and the airplane to stabilize at the desired airspeed before entering the data band. Smoothness is just as important as in acceleration runs and for the same reasons. If a small airspeed error is made while establishing the test conditions, it is better to maintain the incorrect speed as accurately as possible, rather than try to correct it and risk aborting the entire run.

1. Balanced (ball centered) wings level, unaccelerated flight.
2. Engine bleed air system OFF, or operated in a normal flight mode.
3. Stabilized engine thrust/power setting.
4. Stabilize before the altitude band.
5. Altimeter: 29.92, standby.
6. Conduct test 90˚ to wind direction.
7. Bank angle ≤ 10˚.
8. Heading change ≤ 30˚.
9. Normal acceleration ± 0.1 g.

8.4.1.3 DATA REQUIREMENTS

1. Test altitude band ± 1000 ft about a target altitude.
2. V_o ± 1 kn with smooth corrections.

8.4.1.4 SAFETY CONSIDERATIONS

As with any descent, the field of view from most aircraft makes it difficult to clear the area in front and below the test track. This aircraft characteristic combined with the head down requirement to fly accurate data points may impact lookout doctrine. In multi-place aircraft, distinct responsibility should be assigned for maintaining an active lookout.

With prolonged operation at low thrust/power settings, the operation of the engine and other related systems should be evaluated before setting the minimum safety altitude where the descent testing will be terminated. For most aircraft this can be between 3,000 and 5,000 ft AGL.

8.4.2 CHECK DESCENT TEST

The check descent test is flown to compare the standard day descent performance of an aircraft in a specific configuration to results predicted from sawtooth descents. The three main areas of investigation are:

1. Time to descent.
2. Distance traveled.
3. Fuel used.

In addition, data may be obtained on various engine parameters such as engine speed, exhaust gas temperature, engine pressure ratio, gross thrust, angle of attack, etc. These are useful to the analyst but are secondary to the three main parameters. The general method is to descend the aircraft from just below the maximum ceiling to a minimum safety altitude while maintaining precisely a predetermined descent schedule. This schedule may be a minimum rate of descent, maximum range schedule, a schedule recommended by the manufacturer, or some other descent schedule of interest. Take care to specify the schedule flown on each descent performance chart.

Record data at approximately equal increments of altitude and include time, speed, fuel flow, temperature, and any other desired parameters. For most jet aircraft, a mechanical recording means is necessary to obtain simultaneous reading of the many parameters of interest.

After the schedule to be flown is determined, data cards are prepared to record the descent data as in figure 8.7.

	t	Fuel temp	Fuel density	OAT or T_a	Fuel remaining	
Prior to Start	NA					
Start		NA	NA			
Taxi		NA	NA			
Takeoff		NA	NA			
t	H_{P_o}	V_o target	V_o actual	OAT or T_a	Fuel remaining	Misc

Figure 8.7
CHECK DESCENT

Adjust target points for instrument error and position error for both the airspeed indicator and altimeter. If the anticipated rate of descent is low, data are recorded every 1000 to 2000 ft. If the rate of descent is high, every 5000 ft is sufficient.

An area of smooth air, light winds, and stable temperature gradients from ground level to the aircraft's maximum ceiling is desirable. The test area can be sampled via a survey balloon or another aircraft for wind and temperature data. Plan the flight to descend perpendicular to the wind direction.

Since gross weight, fuel weight, and fuel density are important, fuel and weigh the aircraft prior to commencement of tests. Fuel samples are taken and tested for temperature and density. Record fuel remaining and time for start, taxi, takeoff, and climb to descent schedule whenever conditions permit.

During the descent, trim the aircraft. Maintain the descent schedule to within 5 kn, if possible. A rapid cross-check between external horizon and the airspeed indicator is required. If the pitch attitude is very steep, it may be necessary to substitute the aircraft attitude indicator for the external horizon during initial portions of the descent.

Wind gradients appear as sudden airspeed changes. If these affect the descent speed schedule, a small but immediate attitude correction is necessary. If the wind gradient effect subsides, apply a counter correction to prevent a speed error in the opposite direction.

At high altitudes, the problem of maintaining a precise speed schedule is difficult. A slight rate of change of indicated airspeed involves a large rate of change of kinetic energy. Any undesirable trend is difficult to stop especially with relatively less effective aerodynamic controls. The best way to cope is to avoid errors by a rapid cross-check, precise control, and constant attention to trim. If corrections are necessary, avoid over controlling due to hysteresis in the airspeed indicator.

If the descent must be interrupted, stop the descent at a given pressure altitude, noting V_o, fuel, time, and distance if available. Climb above the altitude at which the descent was stopped. Maneuver as required and re-intercept the descent schedule as soon as possible to minimize gross weight change. Intercept the descent using a 1,000 ft overlap from the break off pressure altitude at the airspeed recorded when the interrupt occurred.

The test for a turboprop aircraft is identical to the jet test. In this case however, engine torque and engine shaft horsepower (ESHP) are adjusted in the descent.

8.4.2.1 DATA REQUIRED

Record the following data at each increment, which should be as often as possible, but no greater than each 5000 ft or 2 minutes, for hand held data:

1. Time (t).
2. Observed airspeed (V_o).
3. Observed pressure altitude (H_{P_o}).
4. Temperature (OAT or T_a).
5. Fuel remaining (W_f), or start and end fuel weight.
6. Distance (d).

8.4.2.2 TEST CRITERIA

1. Balanced (ball centered) wings level, unaccelerated flight.
2. Engine bleed air system OFF, or operated in a normal flight mode.
3. Stabilized engine thrust/power setting.
4. Stabilize before the altitude band.
5. Altimeter: 29.92, standby.
6. Conduct test 90˚ to wind direction.
7. Bank angle ≤ 10˚.
8. Heading change ≤ 30˚.
9. Normal acceleration ± 0.1 g.

8.4.2.3 DATA REQUIREMENTS

1. Airspeed ± 5 kn or 0.01 M.

8.4.2.4 SAFETY CONSIDERATIONS

As with the sawtooth descent, the check descent uses prolonged operation at low thrust/power settings. Therefore, the operation of the engine and other related systems has to be evaluated before setting the minimum safety altitude where the descent testing will be terminated. For most aircraft this can be between 3,000 and 5,000 ft AGL.

8.4.3 PRECAUTIONARY / FLAMEOUT APPROACH

A precautionary approach is a special approach profile flown when a malfunction makes the operation of critical aircraft systems questionable. Some of the circumstances when a precautionary approach might be appropriate are:

1. Low engine oil pressure.
2. Engine stall.
3. Engine instability (temperature/vibration).
4. Critically low fuel.
5. Engine fire indication.
6. Suspected FOD.
7. Main hydraulic pressure loss.
8. Flight control malfunction.

Generally, the precautionary approach profile is designed to keep the pilot within the ejection seat envelope as long as possible. Typically the last few seconds of the profile are out of the envelope, unless the pilot performs a pull up maneuver.

There are also situations during engine out testing or evaluation of new engine components when the re-light envelope is verified by flight test. Flameout landing pattern check points need to be identified. Also, in extreme conditions when impossible or impracticable to abandon the aircraft, a flameout approach may be the only alternative.

With the advent of high fidelity simulators, various precautionary/flameout patterns can be evaluated before the actual flight test work is done. The ultimate objective of a precautionary / flameout approach is to make a safe landing reasonably close to the desired touchdown point. Achieving this result is an iterative combination of a number of factors defined in figures 8.8 and 8.9. Working from the touchdown point backwards to define the approach parameters, the first step is to determine the desired touchdown speed. This speed is generally dictated by the margin of aircraft control in all axes. The touchdown speed is also a function of aircraft geometry. An aircraft may be controllable below an airspeed at which the empennage or tailpipe may contact the runway (F-16). Another constraint on touchdown speed is tire limit speed. Also, if reducing main gear loads on touchdown is a factor, a relatively high touchdown speed may be required to increase the control over the rate of descent at touchdown. Therefore, all these factors: controllability, aircraft geometry, tire speed, and rate of descent may determine the target touchdown speed.

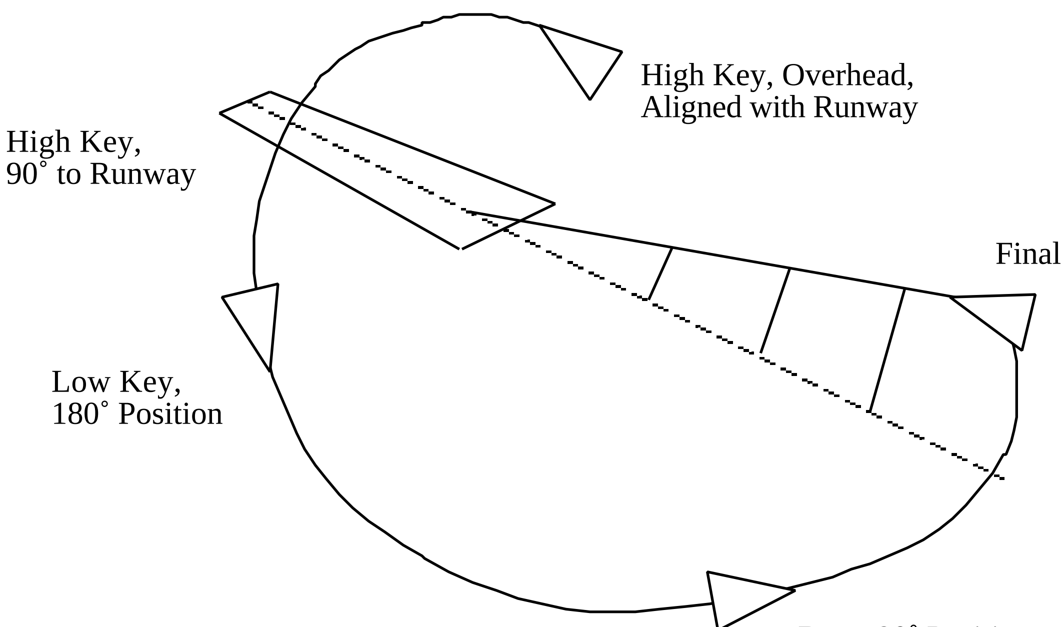

For High Key, Low Key, Base, And Final Define:

- Configuration
- Position with Respect to Runway
- Altitude
- Airspeed
- Wind Correction
- Weight Correction

Figure 8.8

OVERHEAD PRECAUTIONARY/FLAMEOUT PATTERN

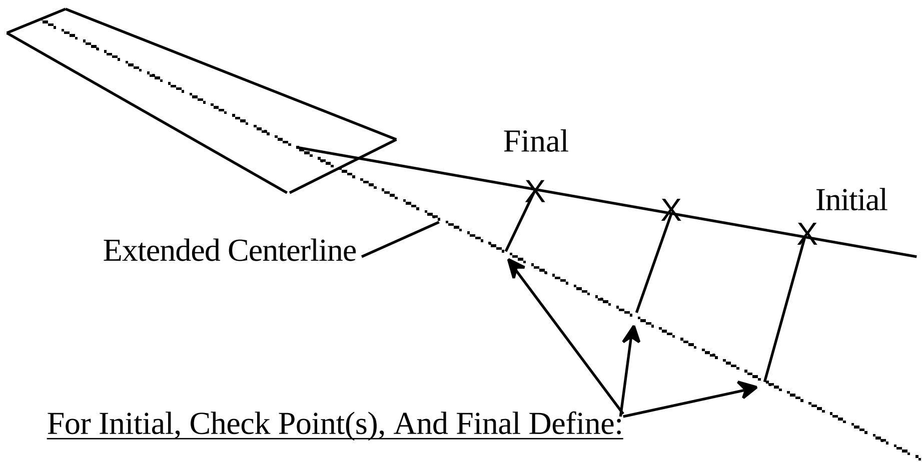

For Initial, Check Point(s), And Final Define:

- Configuration
- Distance From Runway
- Altitude
- Airspeed
- Wind Correction
- Weight Correction

Figure 8.9

STRAIGHT-IN PRECAUTIONARY/FLAMEOUT PATTERN

After determining the touchdown speed, determine the final approach speed. The minimum final approach speed may be dictated by the ability to flare, or by the ability to accurately fly to the pre-flare aim point and touchdown near the desired touchdown point. Approaches with the gear and flaps down can result in steep flight path angles and high rates of descent. Choose an airspeed which arrests the high rate of descent with some safety margin. The maximum final approach speed is often dictated by some aircraft structural or operating characteristic limit. Final approach speed may be limited by maximum gear down operating speed.

Another problem occurs when the aircraft is flown very close to its maximum L/D capability (assume L/D > 4). In this case, touchdown accuracy deteriorates because it becomes more difficult to account for winds and errors made earlier in the pattern prior to reaching final. For a given length final approach, the shorter time on final yields the better touchdown accuracy.

The distance and time from flare to touchdown can also define a maximum final approach airspeed because an extremely long time can adversely affect touchdown accuracy. The typical target final approach airspeed is roughly midway between the minimum and maximum airspeeds and allows about a 10% variance either way. This 10% adjustment factor allows for airspeed changes caused by gusts or wind shears and makes it possible to make fine adjustments to the glide slope in order to maintain a constant pre-flare aim point.

In summary, the final approach airspeed is largely dependent on the aircraft handling and performance characteristics during the flare, which is the time from the start of rotation to touchdown attitude. Final approach is flown at a constant, low angle of attack, which means airspeed is high relative to touchdown speed. At flare initiation, the angle of attack is increased and held approximately constant. The increased load factor reduces the rate of descent. The rate of descent is arrested typically by 100 to 200 ft AGL where another constant glide path is established to touchdown.

The flare attitude is established by determining the altitude required to arrest the rate of descent using a comfortable pitch rate and increase in load factor (moderate increase in angle of attack). Cross check altitude to start the flare then rotate the aircraft at a rate which arrests the descent at the desired altitude above the ground.

The final glide path is shallow, about 3 degrees, with the angle of attack and pitch attitude slowly increasing as the airspeed bleeds off to touchdown. Unless the aircraft has been configured prior to or at pattern entry, the final landing configuration is established at this time. If the landing gear are to be extended during the final glide, gear extension time and pitching moment changes are important considerations (Space Shuttle).

Other considerations during the final flare and touchdown are the deceleration rate, the ability to adjust the final sink rate, the changes in stability as the angle of attack increases, and the field of view (back seat of a trainer). All of these items contribute to the ease or difficulty in controlling the final touchdown. If the deceleration rate is too high, the adjustment of the touchdown rate of descent is possible only once. After this one attempt, any rotation to a higher angle of attack only increases the sink rate because of the large airspeed loss during the first rotation. This requires the aircraft be landed perfectly on the first rotation after entering the 3-degree glide slope. At the other extreme, if the deceleration rate is too low, a long flare covering excessive distance results.

Entry to final sets the minimum low key altitude and airspeed. From this minimum, a comfortable normal altitude and airspeed for the low key is established. Another consideration which can dictate a minimum time for the glide or pattern is battery life or other aircraft emergency system limitations.

The important concept in flying the pattern or gliding to the pattern is to understand the options for L/D control. These options are: the use of a drag device to dissipate energy, deviations from the speed for best L/D, and variations in ground track. In general, an approach is planned so extra altitude must be dissipated because it is much easier to dissipate extra energy than it is to conserve minimum energy. For example, if the pattern is entered with very low energy at low key, there is no choice but to fly at or near maximum L/D in order to reach final approach with enough altitude to push-over and accelerate to an acceptable flare airspeed. In summary, a pattern entered with enough altitude to require some energy dissipation is the most comfortable and the most accurate in terms of touchdown control.

8.4.3.1 DATA REQUIRED

For each of the key checkpoints in the pattern define:

1. Configuration.
2. Altitude.
3. Airspeed.
4. Position with respect to the intended point of landing.
5. Wind corrections.
6. Weight corrections.

8.4.3.2 TEST CRITERIA

1. Balanced (ball centered) wings level, unaccelerated flight.
2. Engine bleed air system OFF - or operated in a normal flight mode.
3. Stabilized engine thrust/power setting.
4. Altimeter: 29.92, standby.

8.4.3.3 DATA REQUIREMENTS

For each of the checkpoints in the pattern:

1. H_{P_o} ± 20 ft.
2. V_o ± 5 kn.

8.4.3.4 SAFETY CONSIDERATIONS

1. With a high rate of descent, plan for the point in the approach where a flare must be initiated to safely arrest the descent rate.
2. Don’t get slow (check deceleration).
3. Don’t get low (check rate of descent).
4. Maintain a good lookout.
5. Don’t exceed main gear loads on touchdown.
6. Watch structural loads (airspeed/g) in the landing configuration.
7. Don’t exceed tire speed limits.
8. Avoid operating characteristic limits.

Before testing precautionary/flameout approach patterns, review the current OPNAVINST 3710.7 Series (General Flight and Operating Instructions) and obtain a waiver if required.

Currently, Paragraph 542 of OPNAVINST 3710.7N states:

1. FLAMEOUT APPROACHES. Actual flameout approaches shall not be attempted unless it is impossible/impracticable to abandon the aircraft.
2. SIMULATED FLAMEOUT APPROACHES. Simulated flameout approaches are prohibited.

8.5 DATA REDUCTION

8.5.1 SAWTOOTH DESCENT

Various computer programs can assist in reducing performance data. This section contains a brief summary of the assumptions and logic which might be used. The treatment is purposefully generic as programs change over time and new ones are introduced. Detailed instructions for the particular computer or program are assumed to be available.

The purpose of the sawtooth descent data reduction program is to calculate rate and angle of descent for any given gross weight, altitude, and temperature based on flight test data.

From a menu selection, the appropriate choice is made to enter the sawtooth descent program. Data entry requirements for the program are as follows:

1. Basic data:
    a. Type of aircraft.
    b. Bureau number.
    c. Standard gross weight.
    d. Target altitude.
    e. Date of tests.
    f. Pilot’s name.
    g. Miscellaneous as allowed by the program.

2. For each data point:
    a. Initial indicated pressure altitude (ft).
    b. Final indicated pressure altitude (ft).
    c. Time required (s).
    d. Indicated airspeed (kn).
    e. OAT (˚C) or ambient temp (˚K).
    f. Fuel flow (lb/h).
    g. Gross weight (lb).
    h. Optional data as allowed by the program.

The program calculates rate and angle of descent for any weight, altitude and temperature condition. One method used is to calculate specific excess power (P_S) for each descent then correct P_S to the desired flight condition using the standard P_S correction formula.

The program calculates P_S for each data point (each descent), corrects P_S to the weight, altitude and temperature which was initially specified and calculates the resulting rate and angle of descent assuming constant calibrated airspeed (V_c) (Figures 8.10 and 8.11).

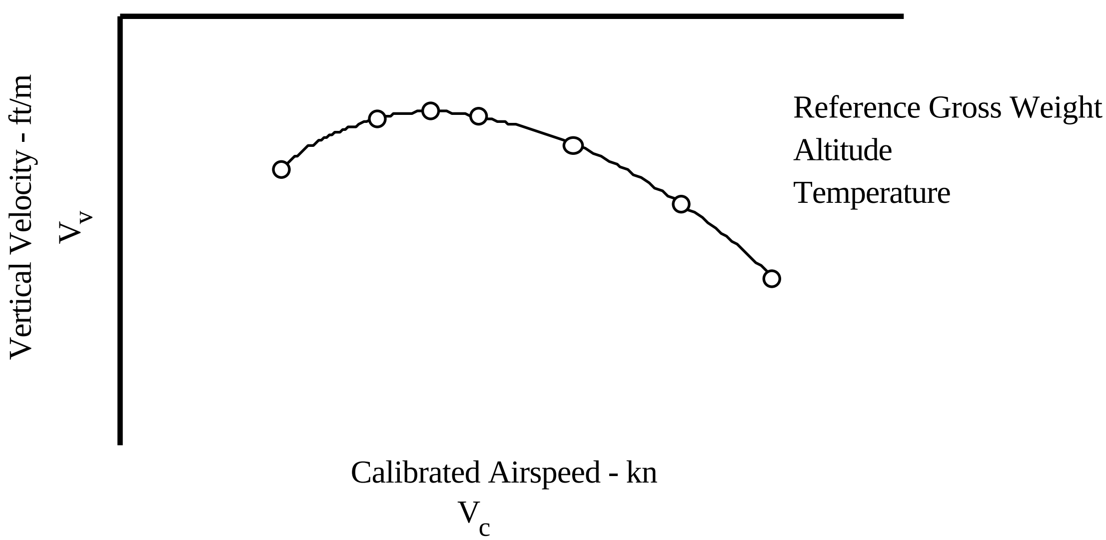

Figure 8.10
RATE OF DESCENT VERSUS CALIBRATED AIRSPEED

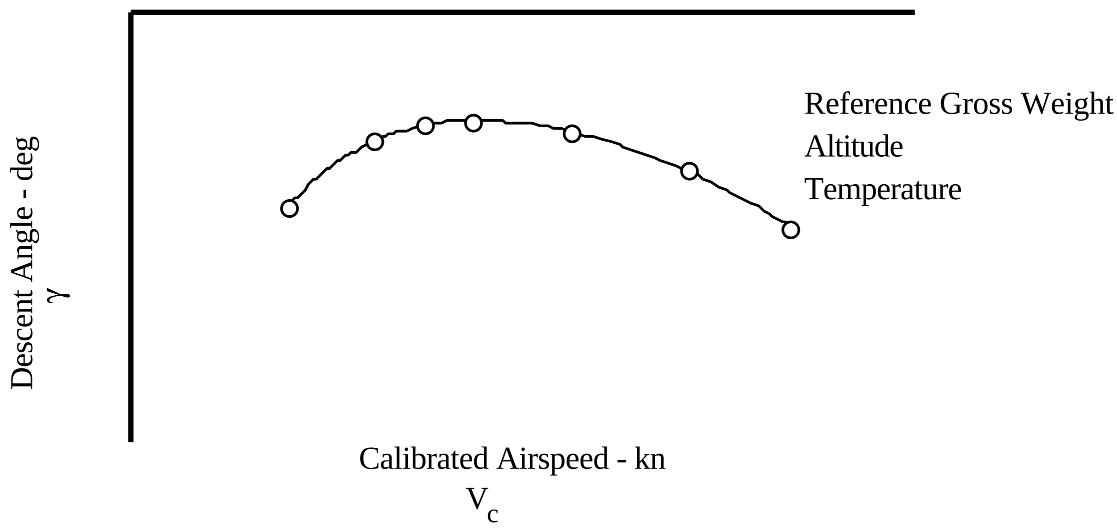

Figure 8.11
DESCENT ANGLE VERSUS CALIBRATED AIRSPEED

After these plots have been generalized, usually the ambient conditions can be changed (weight, altitude, temperature) and the data reduction can be repeated.

Another feature of the computer program is to correlate rate of descent and descent angle with angle of attack. Example figures 8.12 and 8.13 could be used to determine if there is an optimum angle of attack for the specified configuration. Generally also available from sawtooth descent data would be P_S plots vs Mach for the desired ambient conditions.

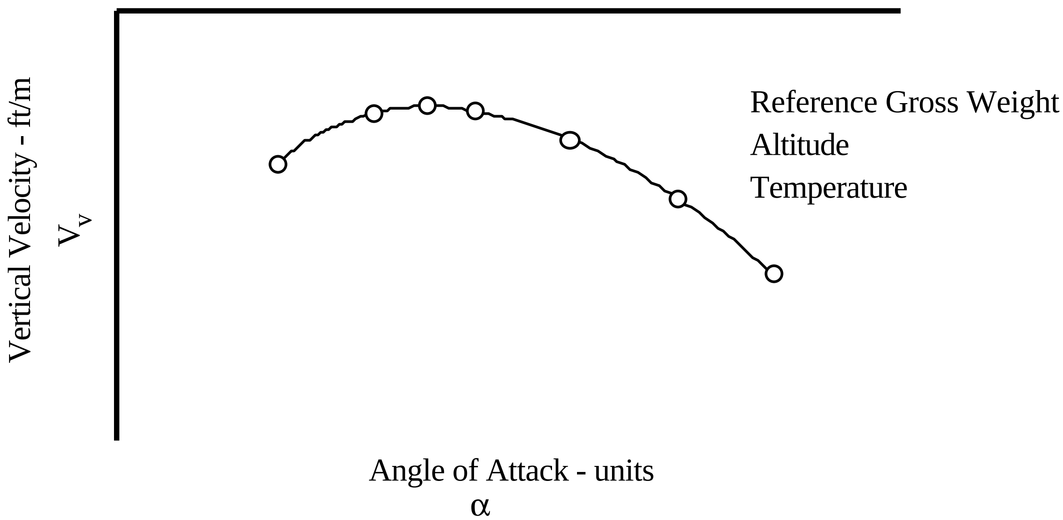

Figure 8.12
RATE OF DESCENT VERSUS ANGLE OF ATTACK

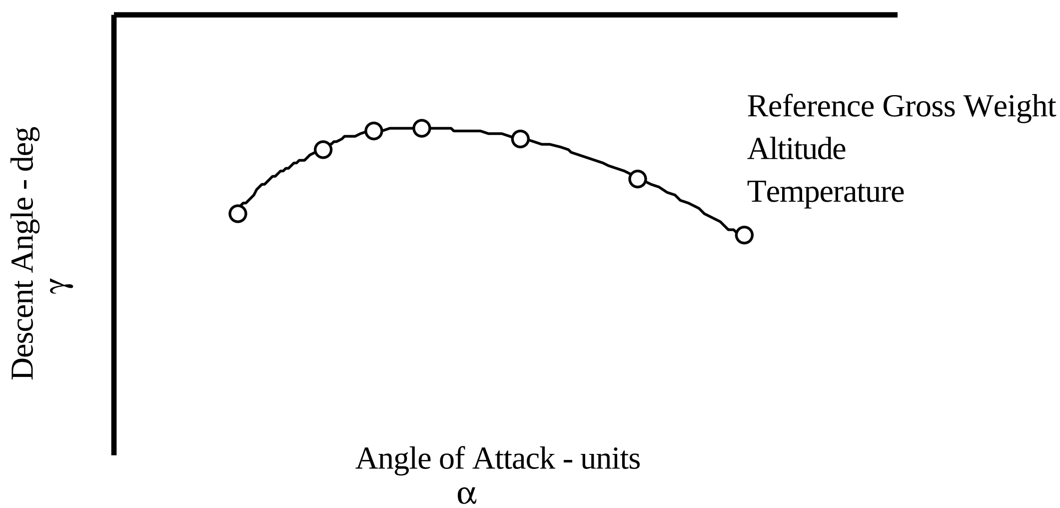

Figure 8.13
DESCENT ANGLE VERSUS ANGLE OF ATTACK

Equations used by the computer data reduction routine.

$$V_c = V_i + \Delta V_{pos} \tag{Eq 8.25}$$

$$H_{P_c} = H_{P_i} + \Delta H_{pos} \tag{Eq 8.26}$$

If ambient temperature (˚K) was entered:

$$T_a(\circ C) = T_a(\circ K) - 273.15 \tag{Eq 8.27}$$

$$OAT = f\left(T_a, M_T\right) \tag{Eq 8.28}$$

If ambient temperature (˚C) was entered:

$$T_a = f\left(OAT, M_T\right) \tag{Eq 8.29}$$

Test data true airspeed:

$$V_{T_{Test}} = f\left(V_c, H_{P_c}, T_a\right) \tag{Eq 8.30}$$

Standard day true airspeed:

$$V_{T_{Std}} = f\left(V_c, H_{P_c}, T_{Std}\right) \tag{Eq 8.31}$$

First data point as $H_{P_{c\,ref}}$:

$$h = H_{P_{c\,ref}} + \Delta H_{P_c}\left(\frac{T_a}{T_{Std}}\right) \tag{Eq 8.32}$$

Energy height:

$$E_h = h + \frac{V_{T_{Test}}^2}{2g} \qquad \text{(Eq 8.33)}$$

Test data P_s (from faired E_h versus time curve):

$$P_{s_{Test}} = \frac{dE_h}{dt} \qquad \text{(Eq 8.34)}$$

Standard day P_s:

$$P_{s_{Std}} = P_{s_{Test}} \left(\frac{W_{Test}}{W_{Std}} \right) \left(\frac{V_{T_{Std}}}{V_{T_{Test}}} \right) + \left(\frac{V_{T_{Std}}}{W_{Std}} \right) (\Delta T_{N_x} - \Delta D) \qquad \text{(Eq 8.35)}$$

Test day flight path angle (dh/dt from the curve of h versus time):

$$\gamma_{Test} = \sin^{-1} \left[\frac{dh/dt}{V_{T_{Test}}} \right] \qquad \text{(Eq 8.36)}$$

$(dh/dt)_{Std}$ is calculated from P_s based on (dV_T/dh) equivalent to constant V_c at standard conditions when $dV_T/dt \neq 0$. Apply descent correction factor (DCF):

$$DCF = 1 + \left(\frac{V_{T_{Std}}}{g} \frac{dV_T}{dh} \right) \qquad \text{(Eq 8.37)}$$

$$\left(\frac{dh}{dt} \right)_{Std} = \frac{P_{s_{Std}}}{DCF} \qquad \text{(Eq 8.38)}$$

Standard day flight path angle:

$$\gamma_{Std} = \sin^{-1} \left[\frac{(dh/dt)_{Std}}{V_{T_{Std}}} \right] \qquad \text{(Eq 8.39)}$$

Where:

ΔD	Standard drag minus test drag	lb
ΔH_{pos}	Altimeter position error	ft
ΔT_{N_x}	Standard net thrust parallel flight path minus test net thrust	lb
ΔV_{pos}	Airspeed position error	kn
DCF	Descent correction factor	
E_h	Energy height	ft
g	Gravitational acceleration	ft/s^2
γ_{Std}	Standard flight path angle	deg
γ_{Test}	Test flight path angle	deg
H_{P_c}	Calibrated pressure altitude	ft
$H_{P_{c\ ref}}$	Reference calibrated pressure altitude	ft
H_{P_i}	Indicated pressure altitude	ft
M_T	True Mach number	
OAT	Outside air temperature	˚C or ˚K
$P_{s_{Std}}$	Standard specific excess power	ft/s
$P_{s_{Test}}$	Test specific excess power	ft/s
t	Time	s
T_a	Ambient temperature	˚C or ˚K
T_i	Indicated temperature	˚C or ˚K
T_{Std}	Standard temperature	˚C or ˚K
V_c	Calibrated airspeed	kn
V_i	Indicated airspeed	kn
V_T	True airspeed	kn or ft/s
$V_{T_{avg}}$	Average true airspeed	kn or ft/s
$V_{T_{Std}}$	Standard true airspeed	kn or ft/s
$V_{T_{Test}}$	Test true airspeed	kn or ft/s
W_{Std}	Standard weight	lb
W_{Test}	Test weight	lb.

8.5.2 CHECK DESCENT

Descent data for an idle thrust descent is generally presented using test day weight and atmospheric conditions. For a more exact analysis, the rate of descent can be corrected to a standard gross weight. For tests conducted with all engines operating normally, corrections to thrust are generally not considered during the data reduction. However, for tests performed to establish the criteria for engine-out descents, a correction for thrust would be required.

The following equations are used in the data reduction:

$$V_i = V_o + \Delta V_{ic} \qquad \text{(Eq 8.40)}$$

$$V_c = V_i + \Delta V_{pos} \qquad \text{(Eq 8.25)}$$

$$H_{P_i} = H_{P_o} + \Delta H_{P_{ic}} \qquad \text{(Eq 8.41)}$$

$$H_{P_c} = H_{P_i} + \Delta H_{pos} \qquad \text{(Eq 8.26)}$$

$$T_i = T_o + \Delta T_{ic} \qquad \text{(Eq 8.42)}$$

$$V_T = 39.0\ M \sqrt{T_a\left(°K\right)} \qquad \text{(Eq 8.43)}$$

$$W_{f_{Used}} = W_{f_{Start}} - W_{f_{End}} \qquad \text{(Eq 8.44)}$$

$$\Delta d = V_{T_{avg}} \frac{\Delta t}{60} \qquad \text{(Eq 8.45)}$$

$$\text{Range} = \sum_{\text{Sea Level}}^{H_P} \Delta d \qquad \text{(Eq 8.46)}$$

Where:

d	Distance	nmi or ft
$\Delta H_{P_{ic}}$	Altimeter instrument correction	ft
ΔH_{pos}	Altimeter position error	ft
ΔT_{ic}	Temperature instrument correction	˚C or ˚K
ΔV_{ic}	Airspeed instrument correction	kn
ΔV_{pos}	Airspeed position error	kn
H_P	Pressure altitude	ft
H_{P_c}	Calibrated pressure altitude	ft
H_{P_i}	Indicated pressure altitude	ft
H_{P_o}	Observed pressure altitude	ft
M	Mach number	
θ	Temperature ratio	
t	Time	s
T_a	Ambient temperature	˚C or ˚K
T_i	Indicated temperature	˚C or ˚K
T_o	Observed temperature	˚C or ˚K
V_c	Calibrated airspeed	kn
V_i	Indicated airspeed	kn
V_o	Observed airspeed	kn
V_T	True airspeed	kn or ft/s
$V_{T_{avg}}$	Average true airspeed	kn or ft/s
$W_{f_{End}}$	End fuel weight	lb
$W_{f_{Start}}$	Start fuel weight	lb
$W_{f_{Used}}$	Fuel used	lb.

From the observed data compute as follows:

Step	Parameter	Notation	Formula	Units	Remarks
1	Indicated airspeed	V_i	Eq 8.40	kn	
2	Calibrated airspeed	V_c	Eq 8.25	kn	
3	Indicated pressure altitude	H_{P_i}	Eq 8.41	ft	
4	Calibrated pressure altitude	H_{P_c}	Eq 8.26	ft	
5	Mach number	M			From Appendix VI
6	Indicated temperature	T_i	Eq 8.42		
7	Ambient temperature	T_a			From Appendix VI
8	True airspeed	V_T	Eq 8.43	kn	
9	Fuel used	$W_{f_{Used}}$	Eq 8.44	lb	
10	Distance	d	Eq 8.45	nmi	
11	Range	Range	Eq 8.46	nmi	

Construct a graph of H_{P_c} versus time to descend. Fair a smooth curve through the data and extrapolate to sea level (Figure 8.14).

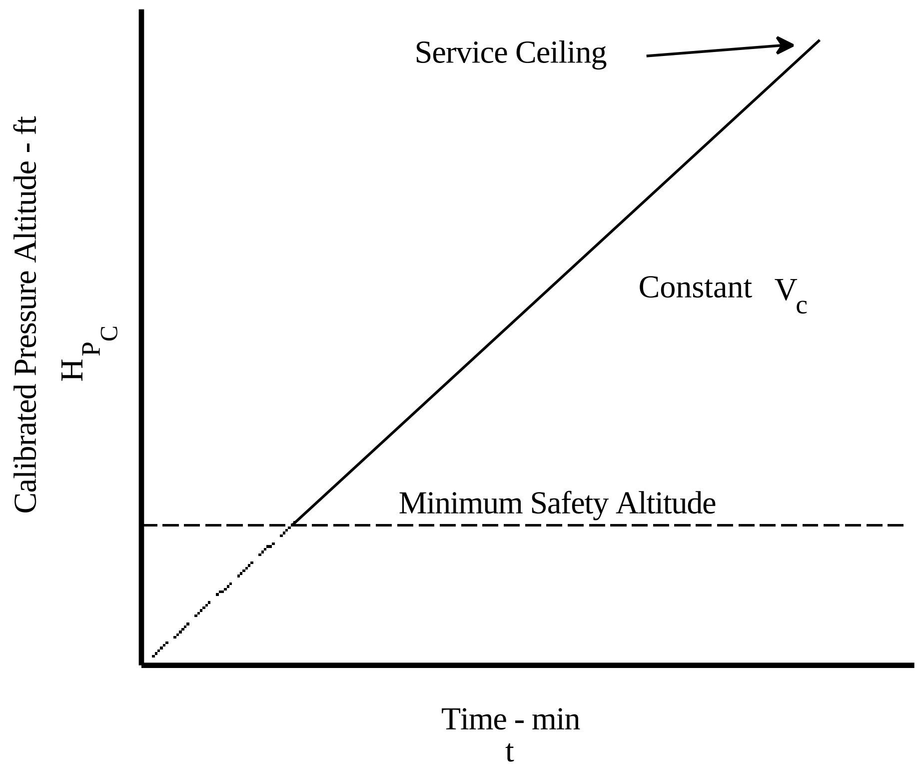

Figure 8.14
CALIBRATED PRESSURE ALTITUDE VERSUS TIME TO DESCEND

Construct a graph of H_{P_c} versus fuel used in the descent. Fair a smooth curve through the data and extrapolate to sea level (Figure 8.15).

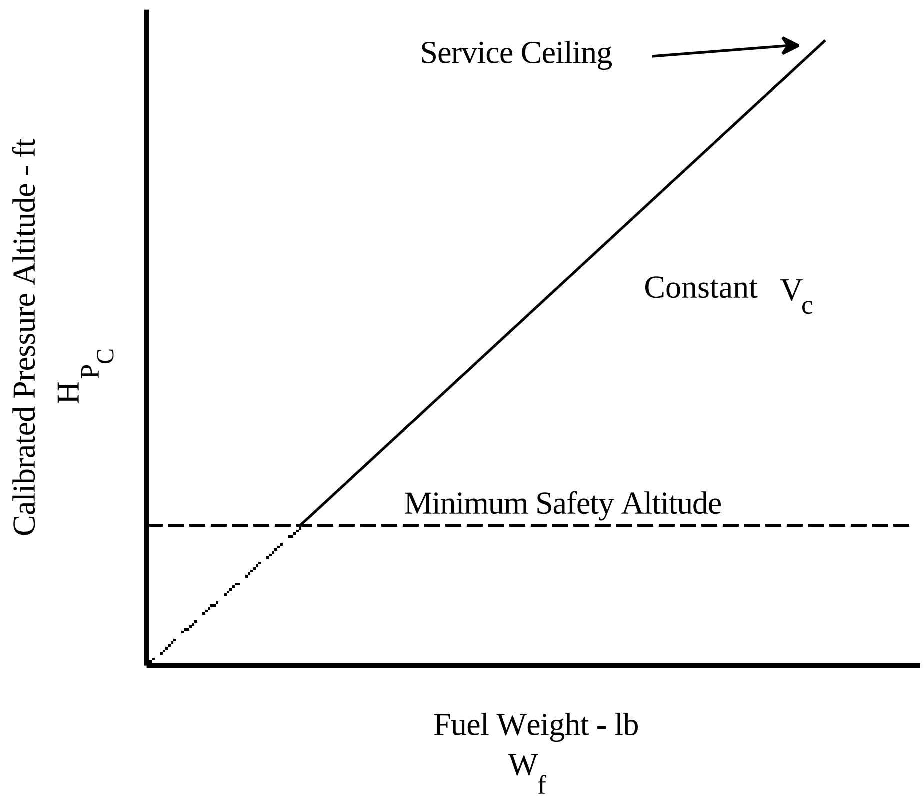

Figure 8.15
CALIBRATED PRESSURE ALTITUDE VERSUS FUEL USED IN THE DESCENT

From figure 8.14, graphically measure the indicated rate of descent (dH_{P_c}/dt) at appropriate intervals beginning at the service ceiling. Construct a table for each test airspeed and interval measured (Figure 8.16).

Altitude ft	Time, Δt s	dh/dt ft/s	V_T ft/s	Glide Ratio $\frac{V_T}{dh/dt}$
From top of test altitude (service ceiling) to minimum safe altitude in 2 to 5,000 ft increments				

Figure 8.16
RATE OF DESCENT AND GLIDE RATIO

Using figure 8.16, construct a graph of the variation of pressure altitude with distance traveled during the descent (Figure 8.17).

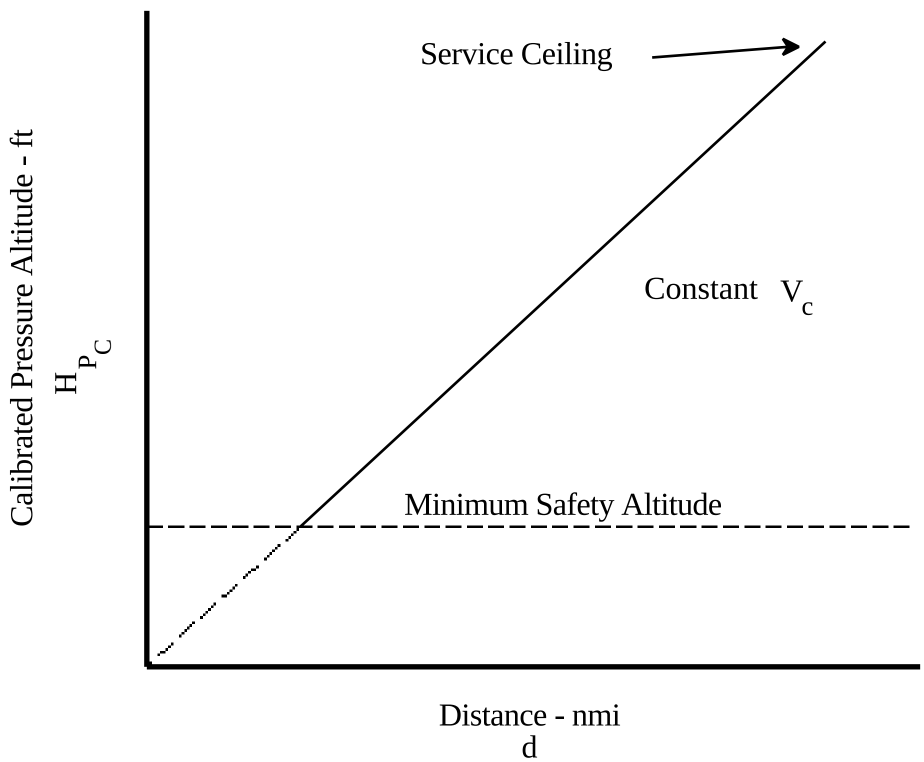

Figure 8.17

CALIBRATED PRESSURE ALTITUDE VERSUS DISTANCE TRAVELED DURING THE DESCENT

Combining figures 8.14, 8.15, and 8.17, the results can be presented either as a table or as a plot of time, fuel used, and distance for an idle descent from the service ceiling to sea level (Figure 8.18).

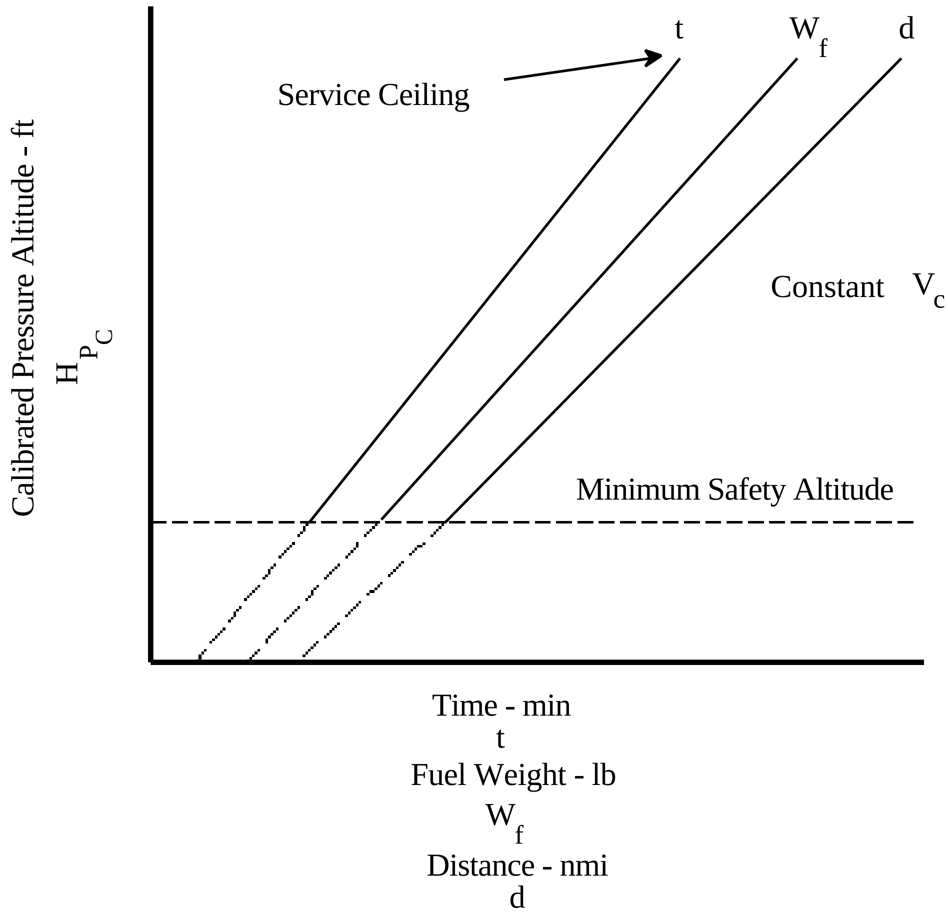

Figure 8.18

CALIBRATED PRESSURE ALTITUDE VERSUS TIME, FUEL USED, AND DISTANCE DURING THE DESCENT

Once this same data has been accumulated for several calibrated airspeeds (V_c), a family of V_c curves can be plotted (Figure 8.19).

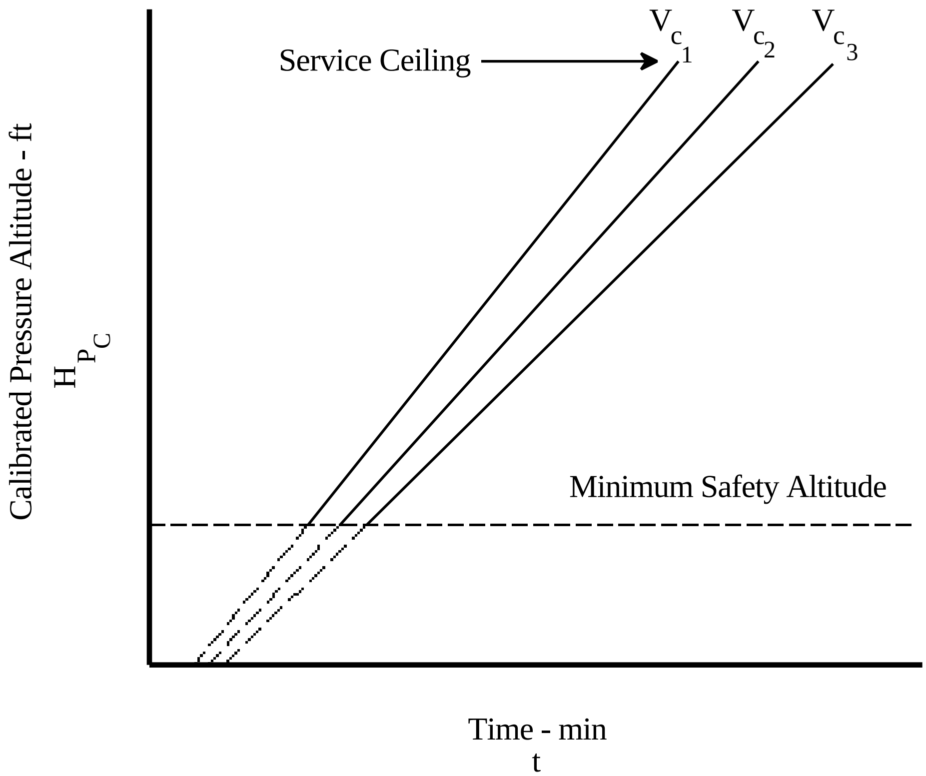

Figure 8.19
DESCENT PERFORMANCE, CALIBRATED PRESSURE ALTITUDE VERSUS TIME
FOR A FAMILY OF CALIBRATED AIRSPEEDS

Combining the glide ratio data from figure 8.16, obtained for each test V_C, and for each altitude, a plot of airspeed versus glide ratio can be made (Figure 8.20).

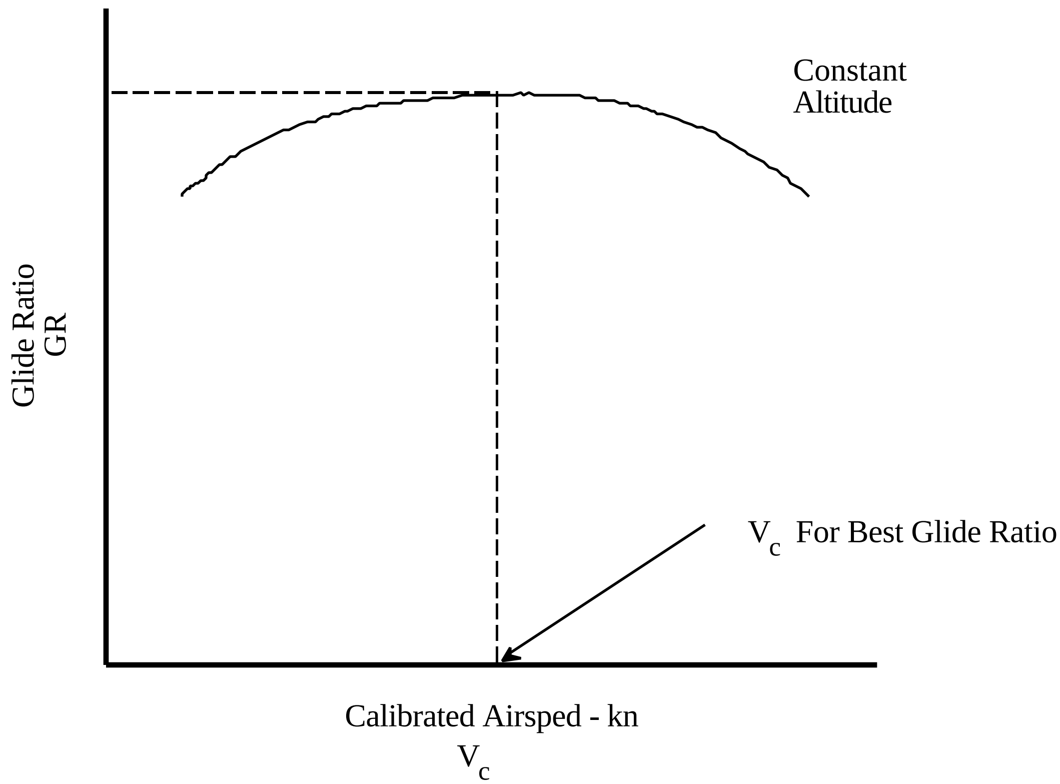

Figure 8.20
AIRSPEED VERSUS GLIDE RATIO

Taking the value for best glide ratio at each altitude, the plot in figure 8.21 is constructed to determine the optimum descent schedule.

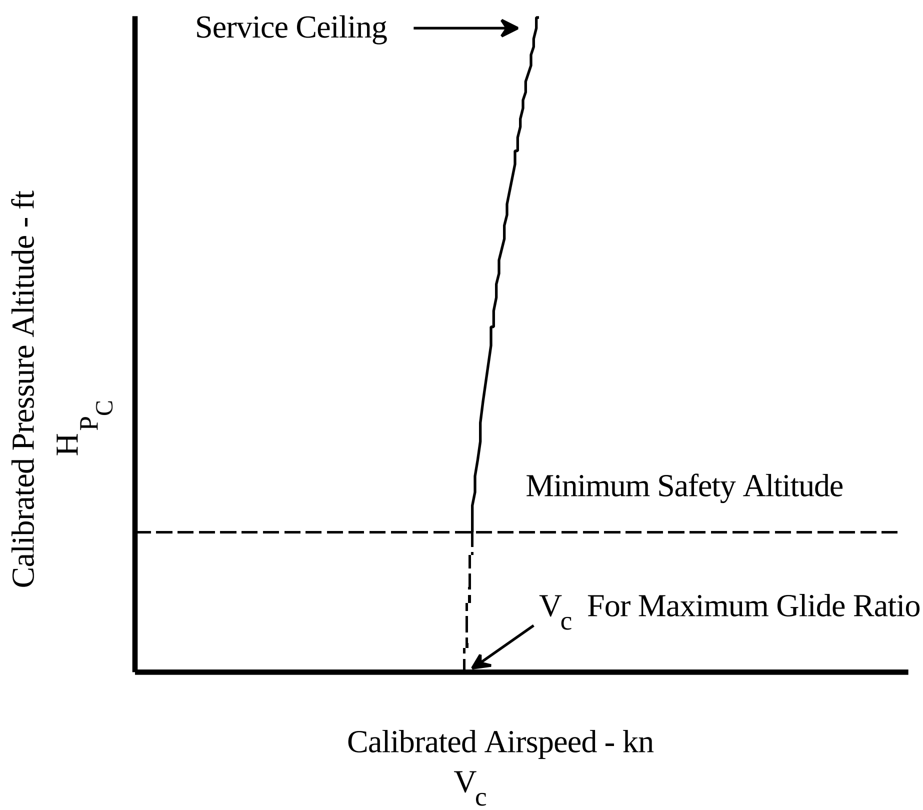

Figure 8.21
OPTIMUM DESCENT SCHEDULE

8.6 DATA ANALYSIS

The analysis of descent data is directed toward determining the optimum descent schedules to provide maximum range for fuel used for various configurations. Usually the difference in V_C is not great enough to warrant publishing a schedule; usually a best compromise V_C is specified.

Another aspect of the data analysis is to determine how sensitive the selected descent airspeed is to deviations on both the fast and slow side. For example, what percentage of the maximum range can be achieved if the aircraft is flown 20 kn faster than the recommended descent airspeed?

8.7 MISSION SUITABILITY

8.7.1 DESCENT PERFORMANCE

Mission suitability conclusions concerning descent performance are not restricted to optimum performance test results. Test results reflect the performance capabilities of the aircraft while mission suitability conclusions include the flying qualities and systems performance associated with specific airspeeds/thrust/power levels. Consideration of the following items is worthwhile when evaluating descent performance:

1. Field of view.
2. Mission profile requirement.
3. Compatibility of airspeed with the mission and location restrictions.
4. Performance sensitivity for altitude or airspeed deviation.
5. System performance:
    a. Pressurization.
    b. Anti-ice.
    c. Cockpit temperature.

8.7.2 PRECAUTIONARY/FLAME OUT APPROACH

Evaluating precautionary and flameout approaches depend upon the answers to the following questions:

1. Under what circumstances would a precautionary or flameout approach be recommended?
2. What training would be required for pilots to successfully complete the approach?
3. What is the pattern sensitivity to airspeed or altitude deviations?

8.8 SPECIFICATION COMPLIANCE

Generally, there are no specification compliance requirements against which the descent performance of an airplane must be demonstrated. Specifically, in NAVAIRSYSCOM Specification, AS-5263, which defines the requirements for performance data and mission profiles, the assumption used for the descent phase is no fuel is consumed and no distance is covered.

An exception exists for propeller airplanes with a published STOL performance achieved by using a beta range of propeller blade angle for the steep descent flight path. In this case, the rates of descent and correct beta blade angles need to be checked against the STOL performance guarantee.

8.9 GLOSSARY

8.9.1 NOTATIONS

AGL	Above ground level	
d	Distance	nmi or ft
ΔD	Standard drag minus test drag	lb
DCF	Descent correction factor	
$\Delta H_{P_{ic}}$	Altimeter instrument correction	ft
ΔH_{pos}	Altimeter position error	ft
ΔT_{ic}	Temperature instrument correction	˚C or ˚K
ΔT_{N_x}	Standard net thrust parallel flight path minus test net thrust	lb
ΔV_{ic}	Airspeed instrument correction	kn
ΔV_{pos}	Airspeed position error	kn
E_h	Energy height	ft
FOD	Foreign object damage	
F_x	Forces parallel to flight path	lb
F_z	Force perpendicular to flight path	lb
g	Gravitational acceleration	ft/s^2
GR	Glide ratio	
h	Tapeline altitude	ft
H_P	Pressure altitude	ft
H_{P_c}	Calibrated pressure altitude	ft
$H_{P_{c\,ref}}$	Reference calibrated pressure altitude	ft
H_{P_i}	Indicated pressure altitude	ft
H_{P_o}	Observed pressure altitude	ft
L	Lift	lb

M	Mach number	
M_T	True Mach number	
OAT	Outside air temperature	˚C or ˚K
$P_{s_{Std}}$	Standard specific excess power	ft/s
$P_{s_{Test}}$	Test specific excess power	ft/s
ROD	Rate of descent	ft/s
t	Time	s
T_a	Ambient temperature	˚C or ˚K
T_i	Indicated temperature	˚C or ˚K
T_o	Observed temperature	˚C or ˚K
T_{Std}	Standard temperature	˚C or ˚K
V_c	Calibrated airspeed	kn
V_{hor}	Horizontal velocity	kn or ft/s
V_i	Indicated airspeed	kn
V_o	Observed airspeed	kn
V_T	True airspeed	kn or ft/s
$V_{T_{avg}}$	Average true airspeed	kn or ft/s
$V_{T_{Std}}$	Standard true airspeed	kn or ft/s
$V_{T_{Test}}$	Test true airspeed	kn or ft./s
V_v	Vertical velocity	ft/s
W	Weight	lb
W_f	Fuel weight	lb
$W_{f_{End}}$	End fuel weight	lb
$W_{f_{Start}}$	Start fuel weight	lb
$W_{f_{Used}}$	Fuel used	lb
W_{Std}	Standard weight	lb
W_{Test}	Test weight	lb
$\dot{W}_f$	Fuel flow	lb/h

8.9.2 GREEK SYMBOLS

α (alpha)	Angle of attack	deg
γ (gamma)	Flight path angle	deg
γ_{Std}	Standard flight path angle	deg
γ_{Test}	Test flight path angle	deg
θ (theta)	Temperature ratio	

8.10 REFERENCES

1. Dommasch, D.O et al, *Airplane Aerodynamics*, 4th Edition, Pitman Publishing Company, N.Y., N.Y., 1967.

2. HP Model 9816 Computer System, “USNTPS Fixed Wing Aircraft Performance User Instructions”, March 1985.

3. NAVAIRSYSCOM Specification, AS-5263, “Guidelines for Preparation of Standard Aircraft Characteristics Charts and Performance Data, Piloted Aircraft (Fixed Wing)”, 23 October 1986.

4. Naval Test Pilot School Flight Test Manual, *Fixed Wing Performance, Theory and Flight Test Techniques*, USNTPS-FTM-No. 104, U.S. Naval Test Pilot School, Patuxent River, MD, July 1977.

5. OPNAVINST 3710.7N, “NATOPS General Flight and Operating Instructions”, 25 August, 1992.

6. Peterson, *Aircraft and Engine Performance*, USNTPS Textbook, USNTPS, Patuxent River, MD, 1958.

7. Powell, J.W., *Airplane Performance*, *Fixed Wing Flight Mechanics*, USNTPS Class Notes, USNTPS, Patuxent River, MD, undated.

8. Stinton, D., *The Design of the Aeroplane*, Van Nostrand Reinhold Company, N.Y.

9. USAF Test Pilot School Flight Test Manual, *Performance Flight Testing Phase*, Volume I, USAF Test Pilot School, Edwards AFB, CA, February 1987.

CHAPTER 9

TAKEOFF AND LANDING PERFORMANCE

CHAPTER 9

FIGURES

CHAPTER 9

TABLES

CHAPTER 9

EQUATIONS

$$D = \left(C_{D_p} + \frac{C_L^2}{\pi \; e \; AR} \right) q \; S$$ (Eq 9.13) 9.10

$$T_{ex} = T - \left(C_{D_p} + \frac{C_L^2}{\pi \; e \; AR} \right) q \; S - \mu \left(W - C_L \; q \; S \right)$$ (Eq 9.14) 9.10

$$\frac{dT_{ex}}{dC_L} = \left(\frac{2 \; C_L}{\pi \; e \; AR} \right) q \; S + \mu \left(q \; S \right)$$ (Eq 9.15) 9.10

$$C_{L_{Opt}} = \frac{\mu \; \pi \; e \; AR}{2}$$ (Eq 9.16) 9.10

$$S_2 = \int_{\text{Lift off}}^{50 \text{ ft}} (T - D) \; dS = \frac{W}{2g} \left(V_{50}^2 - V_{TO}^2 \right) + 50 \; W$$ (Eq 9.17) 9.12

$$S_2 = \frac{W \left(\frac{V_{50}^2 - V_{TO}^2}{2g} + 50 \right)}{(T - D)_{Avg}}$$ (Eq 9.18) 9.12

$$V_{TO_w} = V_{TO} - V_w$$ (Eq 9.19) 9.13

$$S_{1_w} = \frac{W \; V_{TO_w}^2}{2 \; g \; T_{ex_{Avg_w}}}$$ (Eq 9.20) 9.13

$$S_{1_{Std}} = \frac{W \left(V_{TO_w} + V_w \right)^2}{2 \; g \; T_{ex_{Avg}}}$$ (Eq 9.21) 9.13

$$S_{1_{Std}} = S_{1_w} \frac{T_{ex_{Avg_w}}}{T_{ex_{Avg}}} \left(1 + \frac{V_w}{V_{TO_w}} \right)^2$$ (Eq 9.22) 9.13

$$S_{1_{Std}} = S_{1_w}\left(1 + \frac{V_w}{V_{TO_w}}\right)^{1.85}$$ (Eq 9.23) 9.14

$$S_{2_{Std}} = S_{2_w} + \Delta S_2$$ (Eq 9.24) 9.14

$$T_{ex_{Avg}}\, S_{1_{SL}} = \frac{1}{2}\,\frac{W}{g}\,V_{TO}^2 - W\,S_{1_{SL}}\,\sin\theta$$ (Eq 9.25) 9.15

$$S_{1_{SL}} = \frac{W\,V_{TO}^2}{2\,g\left(T_{ex_{Avg}} + W\sin\theta\right)}$$ (Eq 9.26) 9.15

$$S_{1_{Std}} = \frac{S_{1_{SL}}}{\left(1 - \frac{2g\,S_{1_{SL}}}{V_{TO}^2}\,\sin\theta\right)}$$ (Eq 9.27) 9.15

$$S_{1_{Std}} = S_{1_{Test}}\left(\frac{W_{Std}}{W_{Test}}\right)^{2.3}\left(\frac{\sigma_{Test}}{\sigma_{Std}}\right)\left(\frac{T_{N_{Test}}}{T_{N_{Std}}}\right)^{1.3}$$ (Eq 9.28) 9.16

$$S_{2_{Std}} = S_{2_{Test}}\left(\frac{W_{Std}}{W_{Test}}\right)^{2.3}\left(\frac{\sigma_{Test}}{\sigma_{Std}}\right)^{0.7}\left(\frac{T_{N_{Test}}}{T_{N_{Std}}}\right)^{1.6}$$ (Eq 9.29) 9.16

$$S_{1_{Std}} = S_{1_{Test}}\left(\frac{W_{Std}}{W_{Test}}\right)^{2.6}\left(\frac{\sigma_{Test}}{\sigma_{Std}}\right)^{1.9}\left(\frac{N_{Test}}{N_{Std}}\right)^{0.7}\left(\frac{P_{a_{Test}}}{P_{a_{Std}}}\right)^{0.5}$$ (Eq 9.30) 9.17

$$S_{2_{Std}} = S_{2_{Test}}\left(\frac{W_{Std}}{W_{Test}}\right)^{2.6}\left(\frac{\sigma_{Test}}{\sigma_{Std}}\right)^{1.9}\left(\frac{N_{Test}}{N_{Std}}\right)^{0.8}\left(\frac{P_{a_{Test}}}{P_{a_{Std}}}\right)^{0.6}$$ (Eq 9.31) 9.17

$$S_3 = \frac{W\left(\frac{V_{TD}^2 - V_{50}^2}{2g} - 50\right)}{(T - D)_{Avg}}$$ (Eq 9.32) 9.19

$$S_4 = \int_{Touchdown}^{Stop} \left[T\text{-}D\text{-}\mu(W - L)\right] dS = \frac{1}{2}\ \frac{W}{g}\left(0 - V_{TD}^2\right)$$ (Eq 9.33) 9.19

$$S_4 = \frac{-W\ V_{TD}^2}{2g\left[\ T - D - \mu(W - L)\right]_{Avg}}$$ (Eq 9.34) 9.20

$$S_{3_{Std}} = S_{3_{Test}}\left(\frac{W_{Std}}{W_{Test}}\right)^{\left(2 + \frac{E_h}{E_h + 50}\right)}\left(\frac{\sigma_{Test}}{\sigma_{Std}}\right)^{\left(\frac{E_h}{E_h + 50}\right)}$$ (Eq 9.35) 9.23

$$E_h = \frac{V_{50}^2 - V_{TD}^2}{2g}$$ (Eq 9.36) 9.23

$$S_{4_{Std}} = S_{4_{Test}}\left(\frac{W_{Std}}{W_{Test}}\right)^2\left(\frac{\sigma_{Test}}{\sigma_{Std}}\right)$$ (Eq 9.37) 9.23

V_w = Wind Velocity cos (Wind Direction Relative To Runway) (Eq 9.38) 9.28

$$\sigma = 9.625\ \frac{P_a}{T_a}$$ (Eq 9.39) 9.29

$$V_{TD_w} = V_{TD} - V_w$$ (Eq 9.40) 9.30

$$S_{4_{Std}} = S_{4_w}\left(1 + \frac{V_w}{V_{TD}}\right)^{1.85}$$ (Eq 9.41) 9.30

$$S_{4_{Std}} = \frac{S_{4_{SL}}}{\left(1 - \frac{2\, g\, S_{4_{SL}}}{V_{TD}^{2}}\sin\theta\right)}$$

(Eq 9.42) 9.31

CHAPTER 9

TAKEOFF AND LANDING PERFORMANCE

9.1 INTRODUCTION

Field takeoff and landing tests are important portions of the flight test program for any aircraft. Generally, during the course of a flight test program, all takeoffs and landings are recorded for data purposes. Also, a number of test flights may be devoted entirely to takeoff and landing tests in various configurations including, aborted takeoffs, crosswind operations, wet/icy runway operations, landings in various configurations, and field arrested landings. All are accomplished at various gross weights.

The primary emphasis of this chapter is to discuss the conventional takeoff and landing (CTOL) performance of fixed wing aircraft supported primarily by aerodynamic forces rather than engine thrust. Discussion of short takeoff and landing (STOL) performance is limited to two sections of the chapter which discuss methods of shortening the takeoff and landing distance.

More than most other tests, takeoffs and landings are affected by factors which cannot be accurately measured nor properly compensated for. Only estimates of the capabilities of the aircraft are possible within rather broad limits, relying on a statistical average of numerous takeoffs and landings to minimize residual errors.

For purposes of this chapter, Naval Air Systems Command Specification, AS-5263, “Guidelines For Preparation Of Standard Aircraft Characteristics Charts And Performance Data Piloted Aircraft (Fixed Wing)”, is used to establish the criteria for takeoff and landing performance tests (Table 9.1).

Table 9.1
AS-5263 REQUIREMENTS

	Takeoff	Landing
Speeds [1]	V_{TO} at 1.1 times speed represented by 90% $C_{L_{max_{TO}}}$ $V_{CL_{50}}$ at ≥ 1.2 V_{s_T}	V_L at ≥ 1.1 V_{s_L} $V_{L_{50}}$ at ≥ 1.2 V_{s_L}
Distance	Takeoff ground roll plus distance to climb to 50 ft	Distance from 50 ft to touchdown plus landing roll
Rolling Coefficient	0.025	
Braking Coefficient		0.30

Note:
[1] Other criteria may apply also

Where:

$C_{Lmax_{TO}}$	Maximum lift coefficient, takeoff configuration	
$V_{CL_{50}}$	Climb speed at 50 ft	kn
V_L	Landing airspeed	ft/s, kn
$V_{L_{50}}$	Landing speed at 50 ft	kn
V_{s_L}	Stall speed, landing configuration, power off	kn
V_{s_T}	Stall speed, transition configuration, power off, flaps down, gear up	kn
V_{TO}	Takeoff ground speed	ft/s

The Federal Aviation Regulations (FAR) Part 23 and Part 25 establish different takeoff and landing criteria than AS-5263. With Department of the Navy acquiring off-the-shelf FAA certified aircraft, a review and understanding of the FAR is required before evaluating these aircraft for military missions.

9.2 PURPOSE OF TEST

The purpose of these tests include:

1. Development/verification of pilot takeoff and landing techniques appropriate for the test aircraft.

2. Develop flight manual data including:
    - a. Normal ground roll takeoff distance (time/fuel).
    - b. Distance, time, and fuel from liftoff to climb intercept.
    - c. Minimum (short field) ground roll takeoff distance (time/fuel).
    - d. Obstacle clearance takeoff distance (time/fuel).
    - e. Takeoff speed.
    - f. Speed/distances for checking takeoff acceleration.
    - g. Maximum refusal speed.
    - h. Emergency braking velocity.
    - i. Effects of runway condition.
    - j. Landing speed.
    - k. Landing ground roll distance.
    - l. Limit braking velocity for landing.

9.3 THEORY

9.3.1 TAKEOFF

The evaluation of takeoff performance can be examined in two phases, the ground and air phase. The ground phase begins at brake release, includes rotation, and terminates when the aircraft becomes airborne. The air phase is the portion of flight from leaving the ground until reaching an altitude of 50 ft. In the case where stabilizing at a constant climb speed before reaching 50 ft is possible, the air phase is divided into a transition phase and a steady state climb phase (Figure 9.1).

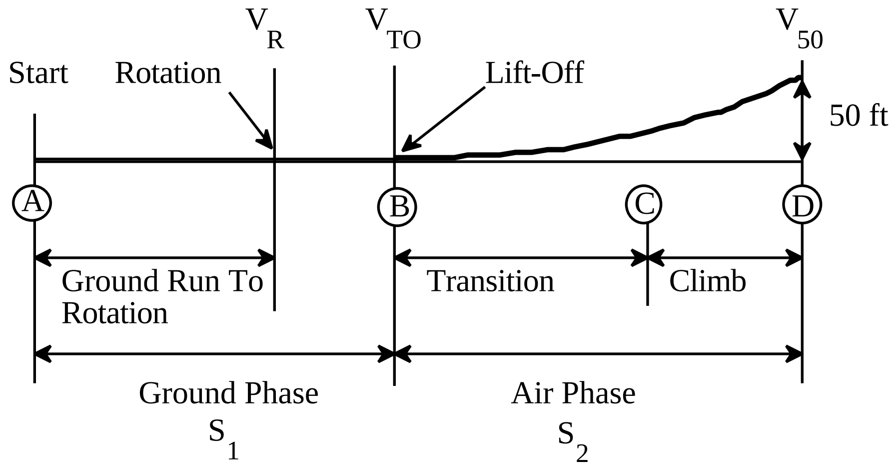

Figure 9.1

TAKEOFF PATH

Where:

S_1	Takeoff distance, brake release to lift off	ft
S_2	Takeoff distance, lift off to 50 ft	ft
V_{50}	Ground speed at 50 ft reference point	ft/s
V_R	Rotation airspeed	kn
V_{TO}	Takeoff ground speed	ft/s

Since lift off occurs almost immediately after or during rotation for most high performance aircraft, the ground phase is considered one distance (S_1) (Figure 9.1, A to B). Also, for most high performance aircraft, the transition to a steady climb speed is not completed before reaching 50 ft, even for a maximum climb angle takeoff. Therefore, the air phase is considered as one distance (S_2) (Figure 9.1, B to D).

9.3.1.1 FORCES ACTING DURING THE GROUND PHASE

The forces acting on the aircraft during the takeoff ground roll are shown in figure 9.2.

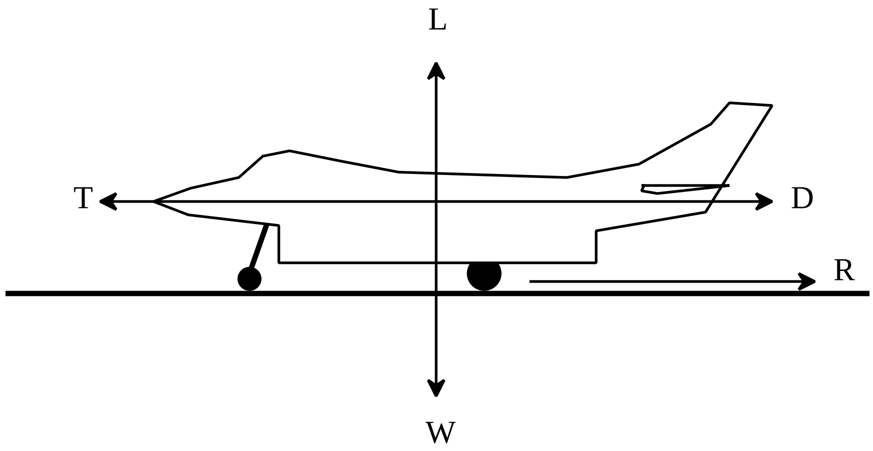

Figure 9.2
FORCES ACTING ON AN AIRCRAFT DURING TAKEOFF

In addition to the usual forces of lift, weight, thrust, and drag, an aircraft on takeoff roll is affected by an additional resistance force (R) which includes wheel bearing friction, brake drag, tire deformation, and energy absorbed by the wheels as they increase rotational speed. This force becomes smaller as lift increases and the weight-on-wheels is reduced. This resistance force can be expressed as:

$$R = \mu (W - L) \tag{Eq 9.1}$$

Typical values for the coefficient of friction (μ) are shown in Table 9.2.

Table 9.2
COEFFICIENT OF FRICTION VALUES

Surface	μ – Typical Values	
	Rolling, Brakes Off Ground Resistance Coefficient	Brakes On Wheel Braking Coefficient
Dry Concrete/Asphalt	0.02 – 0.05	0.3 – 0.5
Wet Concrete/Asphalt	0.05	0.15 – 0.3
Icy Concrete/Asphalt	0.02	0.06 – 0.1
Hard Turf	0.05	0.4
Firm Dirt	0.04	0.3
Soft Turf	0.07	0.2
Wet Grass	0.08	0.2

The arrangement of forces in figure 9.2 assumes engine thrust is parallel to the runway. For aircraft with engines mounted at an angle, the horizontal component of thrust is not reduced significantly until the angle becomes quite large. The vertical component of thrust from inclined engines reduces the effective weight of the aircraft. The mass of the aircraft, however, must be computed using the actual aircraft weight.

Setting the work done equal to the change in energy produces:

$$\int_0^{S_1} \left[T - D - \mu(W - L) \right] dS = \frac{1}{2}\frac{W}{g}\left(V_{TO}^2\right) \qquad \text{(Eq 9.2)}$$

Since none of the terms under the integral are constant during the takeoff roll, an exact evaluation is virtually impossible. The expression can be evaluated assuming the entire quantity remains constant at some average value. The integration is simplified and the expression becomes:

$$\left[T - D - \mu(W - L) \right]_{Avg} S_1 = \frac{1}{2}\frac{W}{g}\left(V_{TO}^2\right) \qquad \text{(Eq 9.3)}$$

Solving for S_1:

$$S_1 = \frac{W V_{TO}^2}{2g \left[T - D - \mu (W - L) \right]_{Avg}} \qquad \text{(Eq 9.4)}$$

Where:

D	Drag	lb
g	Gravitational acceleration	ft/s^2
L	Lift	lb
μ	Coefficient of friction	
R	Resistance force	lb
S_1	Takeoff distance, brake release to lift off	ft
T	Thrust	lb
V_{TO}	Takeoff ground speed	ft/s
W	Weight	lb.

Examination of the individual forces shows the assumption to be reasonable:

1. The engine thrust can be expected to decrease slightly as speed increases. A jet engine may enter ram recovery prior to lift off and realize an increase in thrust over that at lower speed. Propeller thrust will decrease throughout the takeoff roll.

2. Aerodynamic lift and drag increase during the roll in direct proportion to the square of the airspeed. If the aircraft attitude is changed considerably at rotation, both lift and drag increase sharply.

3. The coefficient of friction and the aircraft gross weight remain nearly constant.

The variations in these forces during the takeoff roll are shown graphically in figure 9.3.

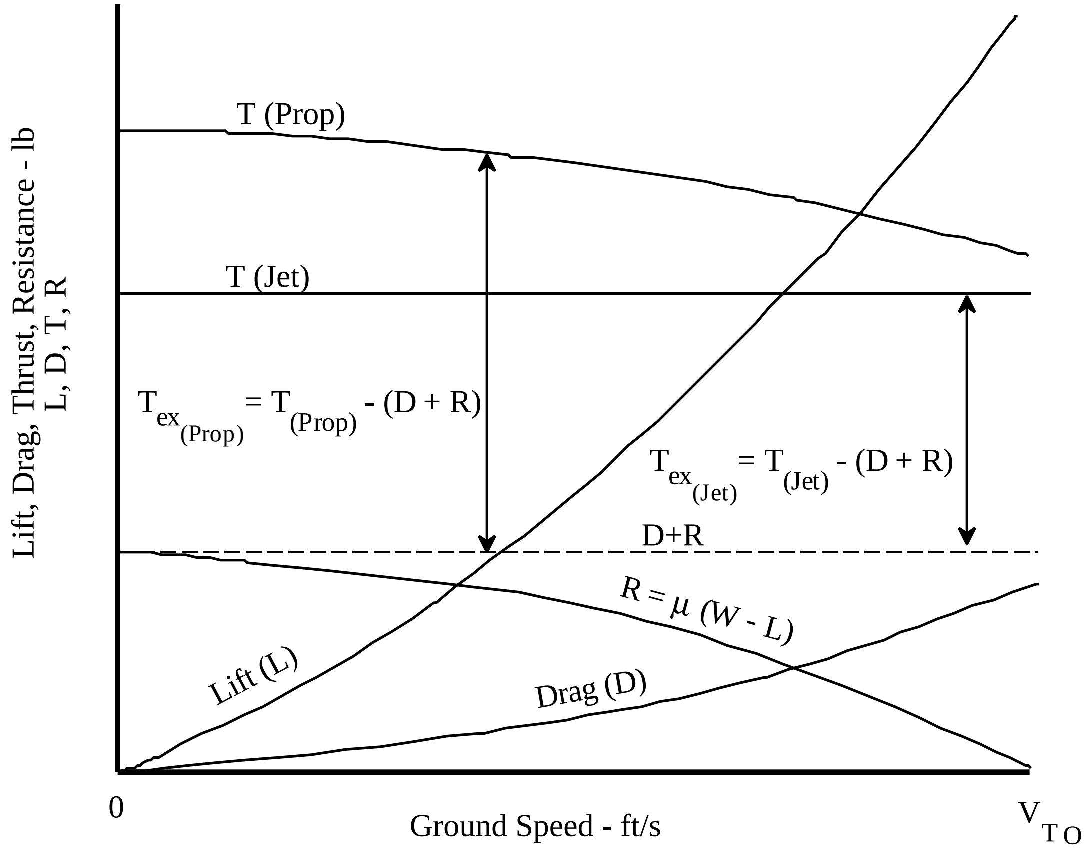

Figure 9.3
FORCE VERSUS VELOCITY

In general, the excess thrust (vector sum of T, D and R) at lift off is 80% of its initial value for a jet aircraft and 40% for a propeller aircraft. For both jets and props, test data has shown the use of the actual excess thrust at 0.75 V_{TO} as an average value for Eq 9.4 gives reasonable results.

9.3.1.2 SHORTENING THE TAKEOFF ROLL

Eq 9.4 shows ground roll can be shortened by lifting-off at a lower speed, since the distance increases with the square of the takeoff speed. Defining the takeoff test objectives as minimizing the ground roll, the aircraft should be lifted-off at $C_{L_{max}}$. However, the aerodynamic drag created by this technique may reduce excess thrust to an unacceptable level. In extreme cases, rotation to $C_{L_{max}}$ may reduce excess thrust with the result the aircraft will not accelerate or may even decelerate. If sufficient thrust is available to overcome the drag penalty, high lift slat and flap devices can provide a higher available lift coefficient.

A second approach to decreasing the takeoff distance (S_1) is increasing the thrust available either by operating the engine above its maximum rated power, such as by water injection or by use of an auxiliary engine such as JATO (Jet Assisted Takeoff). Thrust augmentation is of maximum value if it can be used throughout the takeoff roll. If augmentation is limited to a time shorter than required for takeoff, should the augmentation be used early or late in the ground roll? Since the energy gained equals the work done, limited augmentation is most efficient if used to maximize the work done. If the augmentation provides an increase in thrust (ΔT), for a fixed period of time (Δt), during which distance (ΔS) is traveled, then $\Delta S = V\Delta t$ and the work is:

$$\text{Work} = \Delta T \, V \, \Delta t \qquad \text{(Eq 9.5)}$$

Both ΔT and Δt are fixed by the limitations of the augmenting engine. The work done can be maximized if V is as large as possible. Therefore, for minimum ground roll, limited thrust augmentation should be used late, so it will burn out or reach its time limit just as the aircraft lifts-off.

Excess thrust during the takeoff roll is also dependent on aircraft angle of attack through both the drag term itself and the inclusion of lift in the wheel force term. If the optimum value of C_L is found, the best angle of attack to maximize excess thrust can be determined:

$$T_{ex} = T - D - \mu(W - L) \qquad \text{(Eq 9.6)}$$

$$q = \frac{1}{2}\rho V^2 \qquad \text{(Eq 9.7)}$$

$$D = C_D \, q \, S \qquad \text{(Eq 9.8)}$$

$$L = C_L \, q \, S \qquad \text{(Eq 9.9)}$$

$$C_D = C_{D_p} + C_{D_i} \qquad \text{(Eq 9.10)}$$

$$C_{D_i} = \frac{C_L^2}{\pi \, e \, AR} \qquad \text{(Eq 9.11)}$$

Substituting Eq 9.11 into Eq 9.10:

$$C_D = C_{D_p} + \frac{C_L^2}{\pi \, e \, AR} \qquad \text{(Eq 9.12)}$$

Substituting Eq 9.12 into Eq 9.8:

$$D = \left(C_{D_p} + \frac{C_L^2}{\pi \, e \, AR} \right) q \, S \qquad \text{(Eq 9.13)}$$

Substituting Eq 9.13 and Eq 9.9 into Eq 9.6:

$$T_{ex} = T - \left(C_{D_p} + \frac{C_L^2}{\pi \, e \, AR} \right) q \, S - \mu \left(W - C_L \, q \, S \right) \qquad \text{(Eq 9.14)}$$

Differentiating with respect to C_L:

$$\frac{dT_{ex}}{dC_L} = \left(\frac{2 \, C_L}{\pi \, e \, AR} \right) q \, S + \mu \left(q \, S \right) \qquad \text{(Eq 9.15)}$$

Setting the right side of Eq 9.15 equal to zero, the velocity term (q) drops out and the value of C_L for maximum excess thrust is constant and given by:

$$C_{L_{Opt}} = \frac{\mu \, \pi \, e \, AR}{2} \qquad \text{(Eq 9.16)}$$

Where:

AR	Aspect ratio	
C_D	Drag coefficient	
C_{D_i}	Induced drag coefficient	
C_{D_p}	Parasite drag coefficient	
C_L	Lift coefficient	
$C_{L_{Opt}}$	Optimum lift coefficient	
D	Drag	lb
e	Oswald's efficiency factor	
L	Lift	lb
μ	Coefficient of friction	
π	Constant	
q	Dynamic pressure	psf
ρ	Air density	slugs/ft^3
S	Wing area	ft^2
T	Thrust	lb
t	Time	s
T_{ex}	Excess thrust	lb
V	Velocity	ft/s
W	Weight	lb.

To achieve the shortest takeoff roll, a pilot establishes an angle of attack which corresponds to $C_{L_{Opt}}$ in Eq 9.16 and maintains $C_{L_{Opt}}$ until the speed permits rotation and lift off at $C_{L_{max}}$. In practice, however, this technique is seldom used because the dangers of over-rotating, lack of elevator or horizontal tail power, cross wind effects, or possible aircraft stability problems usually override any gain achieved. At the other extreme, since $C_{L_{Opt}}$ is quite small for most aircraft, an extremely long takeoff distance results if $C_{L_{Opt}}$ is held throughout the takeoff roll. As a practical matter, most aircraft are designed so that in the taxi attitude the wing is near the optimum angle of attack for minimizing the total resistance throughout takeoff. Therefore, most recommended takeoff techniques involve accelerating without changing attitude until the speed permits rotation and lift off at the maximum practical C_L available.

9.3.1.3 AIR PHASE

The equation for ground distance covered in climbing from lift off to 50 ft altitude is obtained in a manner similar to the ground roll equation except the resistance force no longer exists and a potential energy term must be included:

$$S_2 = \int_{\text{Lift off}}^{50\text{ ft}} (T - D)\, dS = \frac{W}{2g}\left(V_{50}^2 - V_{TO}^2\right) + 50\, W \qquad \text{(Eq 9.17)}$$

Assuming this quantity remains constant at some average value, the integration of Eq 9.17 becomes:

$$S_2 = \frac{W\left(\dfrac{V_{50}^2 - V_{TO}^2}{2g} + 50\right)}{(T - D)_{Avg}} \qquad \text{(Eq 9.18)}$$

Where:

D	Drag	lb
g	Gravitational acceleration	ft/s^2
S	Distance	ft
S_2	Takeoff distance, lift off to 50 ft	ft
T	Thrust	lb
V_{50}	Ground speed at 50 ft reference point	ft/s
V_{TO}	Takeoff ground speed	ft/s
W	Weight	lb.

To minimize the value of S_2 for a given weight, a constant speed climb is conducted at maximum excess thrust, while maximum excess thrust occurs at the speed for minimum drag, $\left.\frac{L}{D}\right|_{max}$, most aircraft lift off at an airspeed much slower than for $\left.\frac{L}{D}\right|_{max}$. As a practical matter, most high performance aircraft reach 50 ft within seconds while accelerating from lift off airspeed to climb airspeed.

9.3.1.4 TAKEOFF CORRECTIONS

9.3.1.4.1 WIND CORRECTION

The velocity in Eq 9.4 is ground speed at lift off, since this defines the energy level required. The aircraft flies according to the airspeed, which can be considerably different from ground speed in high winds. Since ground speed and true airspeed are equal in zero wind conditions, the ground speed required with wind, V_{TO_w} is:

$$V_{TO_w} = V_{TO} - V_w \tag{Eq 9.19}$$

V_w is positive for a head wind and includes only the component of wind velocity parallel to the takeoff direction. From Eq 9.4 and 9.6:

$$S_{1_w} = \frac{W\, V_{TO_w}^2}{2\, g\, T_{ex_{Avg_w}}} \tag{Eq 9.20}$$

The subscript, $_W$, indicates a parameter in the wind environment. Substituting Eq 9.19 into Eq 9.20:

$$S_{1_{Std}} = \frac{W\left(V_{TO_w} + V_w\right)^2}{2\, g\, T_{ex_{Avg}}} \tag{Eq 9.21}$$

Dividing Eq 9.21 by Eq 9.20 and rearranging gives:

$$S_{1_{Std}} = S_{1_w} \frac{T_{ex_{Avg_w}}}{T_{ex_{Avg}}} \left(1 + \frac{V_w}{V_{TO_w}}\right)^2 \tag{Eq 9.22}$$

The difference in excess thrust due to wind is difficult to determine but it does have a significant effect on takeoff roll. For steady state winds of less than 10 kn, an empirical relationship has been developed that provides the following equation for the correction for head wind/tail wind components:

$$S_{1_{Std}} = S_{1_w}\left(1 + \frac{V_w}{V_{TO_w}}\right)^{1.85} \qquad \text{(Eq 9.23)}$$

Eq 9.23 does not account for gusts, which may have considerable effect if they occur near lift off speed. This is one of the reasons wind speed below 5 kn is required before takeoff data is accepted.

For the air phase, an exact determination of wind velocity is more difficult. The correction is simple, however, based on the fact that change in distance by wind is:

$$S_{2_{Std}} = S_{2_w} + \Delta S_2 \qquad \text{(Eq 9.24)}$$

Where:

D	Drag	lb
ΔS_2	Change in S_2, equal to t V_w	ft
g	Gravitational acceleration	ft/s^2
L	Lift	lb
S_1	Takeoff distance, brake release to lift off	ft
$S_{1_{Std}}$	Standard takeoff distance, brake release to lift off	ft
S_{1_w}	Takeoff distance, brake release to lift off, with respect to wind	ft
S_2	Takeoff distance, lift off to 50 ft	ft
$S_{2_{Std}}$	Standard takeoff distance, lift off to 50 ft	ft
S_{2_w}	Takeoff distance, lift off to 50 ft, with respect to wind	ft
T	Thrust	lb
t	Time	s
T_{ex}	Excess thrust	lb
$T_{ex_{Avg}}$	Average excess thrust	lb
$T_{ex_{Avg\ w}}$	Average excess thrust, with respect to wind	lb
V_{TO}	Takeoff ground speed	ft/s

V_{TO_w}	Takeoff ground speed with respect to wind	ft/s
V_w	Wind velocity	ft/s
W	Weight	lb.

9.3.1.4.2 RUNWAY SLOPE

The runway slope adds a potential energy term to Eq 9.3:

$$T_{ex_{Avg}} S_{1_{SL}} = \frac{1}{2} \frac{W}{g} V_{TO}^2 - W S_{1_{SL}} \sin\theta \qquad \text{(Eq 9.25)}$$

The subscript, $_{SL}$, indicates a sloping runway parameter.

Solving for $S_{1_{SL}}$:

$$S_{1_{SL}} = \frac{W V_{TO}^2}{2 g \left(T_{ex_{Avg}} + W \sin\theta \right)} \qquad \text{(Eq 9.26)}$$

Solving Eq 9.4 and 9.26 for average excess thrust, equating the results, and solving for S_1 produces an expression for a standard S_1:

$$S_{1_{Std}} = \frac{S_{1_{SL}}}{\left(1 - \frac{2g\, S_{1_{SL}}}{V_{TO}^2} \sin\theta \right)} \qquad \text{(Eq 9.27)}$$

Where:

g	Gravitational acceleration	ft/s^2
θ	Runway slope angle	deg
S_1	Takeoff distance, brake release to lift off	ft
$S_{1_{SL}}$	Takeoff distance, brake release to lift off, sloping runway	ft
$S_{1_{Std}}$	Standard takeoff distance, brake release to lift off	ft
$T_{ex_{Avg}}$	Average excess thrust	lb

V_{TO}	Takeoff ground speed	ft/s
W	Weight	lb.

A fairly large slope is required before data is affected significantly. Low thrust-to-weight aircraft are affected more than high thrust-to-weight ratio aircraft.

9.3.1.4.3 THRUST, WEIGHT, AND DENSITY

Atmospheric conditions will affect the thrust available from the engine and will change the true airspeed required to fly a standard weight at a standard lift coefficient. As the weight changes, the airspeed required to fly at that C_L also changes. While an accurate analysis of these effects results in complex expressions, empirical relationships have been developed which provide reasonably accurate results.

For jet aircraft:

Ground phase:

$$S_{1_{Std}} = S_{1_{Test}} \left(\frac{W_{Std}}{W_{Test}}\right)^{2.3} \left(\frac{\sigma_{Test}}{\sigma_{Std}}\right) \left(\frac{T_{N_{Test}}}{T_{N_{Std}}}\right)^{1.3} \qquad \text{(Eq 9.28)}$$

Air phase:

$$S_{2_{Std}} = S_{2_{Test}} \left(\frac{W_{Std}}{W_{Test}}\right)^{2.3} \left(\frac{\sigma_{Test}}{\sigma_{Std}}\right)^{0.7} \left(\frac{T_{N_{Test}}}{T_{N_{Std}}}\right)^{1.6} \qquad \text{(Eq 9.29)}$$

The accuracy of Eq 9.28 and Eq 9.29 depends on the determination of net thrust, T_N. Normally values developed from thrust stand data are used.

For turboprop aircraft with constant speed propellers the correction equations are:

Ground phase:

$$S_{1_{Std}} = S_{1_{Test}} \left(\frac{W_{Std}}{W_{Test}}\right)^{2.6} \left(\frac{\sigma_{Test}}{\sigma_{Std}}\right)^{1.9} \left(\frac{N_{Test}}{N_{Std}}\right)^{0.7} \left(\frac{P_{a_{Test}}}{P_{a_{Std}}}\right)^{0.5} \qquad \text{(Eq 9.30)}$$

Air phase:

$$S_{2_{Std}} = S_{2_{Test}} \left(\frac{W_{Std}}{W_{Test}}\right)^{2.6} \left(\frac{\sigma_{Test}}{\sigma_{Std}}\right)^{1.9} \left(\frac{N_{Test}}{N_{Std}}\right)^{0.8} \left(\frac{P_{a_{Test}}}{P_{a_{Std}}}\right)^{0.6} \qquad \text{(Eq 9.31)}$$

Where:

N_{Std}	Standard propeller speed	rpm
N_{Test}	Test propeller speed	rpm
$P_{a_{Std}}$	Standard ambient pressure	psf
$P_{a_{Test}}$	Test ambient pressure	psf
$S_{1_{Std}}$	Standard takeoff distance, brake release to lift off	ft
$S_{1_{Test}}$	Test takeoff distance, brake release to lift off	ft
$S_{2_{Std}}$	Standard takeoff distance, lift off to 50 ft	ft
$S_{2_{Test}}$	Test takeoff distance, lift off to 50 ft	ft
σ_{Std}	Standard density ratio	
σ_{Test}	Test density ratio	
$T_{N_{Std}}$	Standard net thrust	lb
$T_{N_{Test}}$	Test net thrust	lb
W_{Std}	Standard weight	lb
W_{Test}	Test weight	lb.

9.3.1.5 PILOT TAKEOFF TECHNIQUE

Individual pilot technique can cause a greater variation in takeoff data than all other parameters combined. Some of the factors which significantly affect takeoff performance include:

1. Speed and sequence of brake release and power application.
2. The use of differential braking, nose wheel steering, or rudder deflection for directional control.
3. The number and amplitude of directional control inputs used.
4. Aileron/spoiler and elevator/horizontal tail position during acceleration.
5. Airspeed at rotation.
6. Pitch rate during rotation.
7. Angle of attack at lift off.

9.3.2 LANDING

The evaluation of landing performance can be examined in two phases, the air phase and the ground phase. The air phase starts at 50 ft above ground level and ends on touchdown. The ground phase begins at touchdown and terminates when the aircraft is stopped (Figure 9.4).

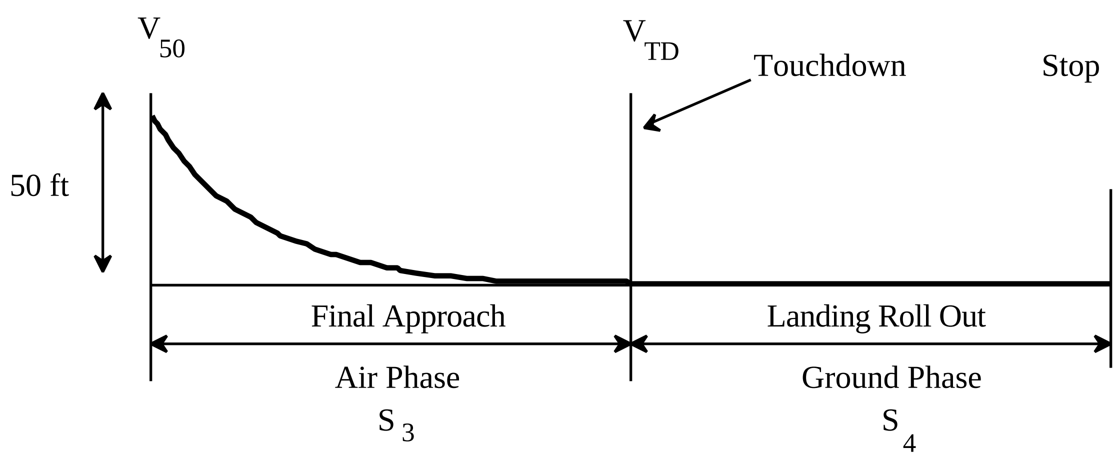

Figure 9.4
LANDING FLIGHT PHASES

Where:

S_3	Landing distance, 50 ft to touchdown	ft
S_4	Landing distance, touchdown to stop	ft
V_{50}	Ground speed at 50 ft reference point	ft/s
V_{TD}	Touchdown ground speed	ft/s

9.3.2.1 AIR PHASE

The equation governing the air distance on landing (S_3) is developed similarly to the takeoff equation:

$$S_3 = \frac{W\left(\frac{V_{TD}^2 - V_{50}^2}{2g} - 50\right)}{(T - D)_{Avg}} \qquad \text{(Eq 9.32)}$$

Where:

D	Drag	lb
g	Gravitational acceleration	ft/s^2
S_3	Landing distance, 50 ft to touchdown	ft
T	Thrust	lb
V_{50}	Ground speed at 50 ft reference point	ft/s
V_{TD}	Touchdown ground speed	ft/s
W	Weight	lb.

Examination of Eq 9.32 shows air distance is minimized if touchdown speed is maintained throughout the final descent (no flare) where $V_{TD} = V_{50}$ and a high drag/low thrust configuration (steep glide path) is used. The structural integrity of the aircraft becomes the limiting factor in this case.

9.3.2.2 FORCES ACTING DURING THE GROUND PHASE

The forces acting on an aircraft during the landing roll can be depicted similarly to those shown in figure 9.2 for takeoff. Low power settings and the increase in the coefficient of resistance due to brake application result in the excess thrust equation:

$$S_4 = \int_{Touchdown}^{Stop} \left[T\text{-}D\text{-}\mu(W - L) \right] dS = \frac{1}{2}\,\frac{W}{g}\left(0 - V_{TD}^2\right) \qquad \text{(Eq 9.33)}$$

When using an average value of the parameters the integration of Eq 9.33 becomes:

$$S_4 = \frac{-W\, V_{TD}^2}{2g\left[\,T - D - \mu(W - L)\,\right]_{Avg}} \qquad \text{(Eq 9.34)}$$

Where:

D	Drag	lb
g	Gravitational acceleration	ft/s^2
L	Lift	lb
μ	Coefficient of friction	
S	Distance	ft
S_4	Landing distance, touchdown to stop	ft
T	Thrust	lb
V_{TD}	Touchdown ground speed	ft/s
W	Weight	lb.

9.3.2.3 SHORTENING THE LANDING ROLL

Touchdown speed is one of the most important factors in the calculation of the distance required to stop. In addition to weight and speed at touchdown, landing roll can be influenced by all the factors in the excess thrust term. Thrust should be reduced to the minimum practical and, if available, reverse thrust should be employed as soon as possible after touchdown. The logic for early application of reverse thrust is the same as that for late use of time limited thrust augmentation on takeoff. Additional drag, whether from increased angle of attack (aerodynamic braking) or deployment of a drag chute, is most effective in the initial part of the landing roll for two reasons. Not only is a given force most effective at high speeds, but also the force itself is greater due to its dependence on V^2. Runway surface condition, as well as the mechanical design of the brakes themselves can cause the value of μ to vary over a considerable range. The assumption of an average excess thrust is reasonable as long as the attitude of the aircraft remains almost constant, but not if nose high aerodynamic braking is used after touchdown. Because aerodynamic braking is recommended to minimize landing roll for some aircraft, the question arises when is the most advantageous point to transition from one braking mode to the other. The relative magnitude of the forces involved are shown in figures 9.5 and 9.6.

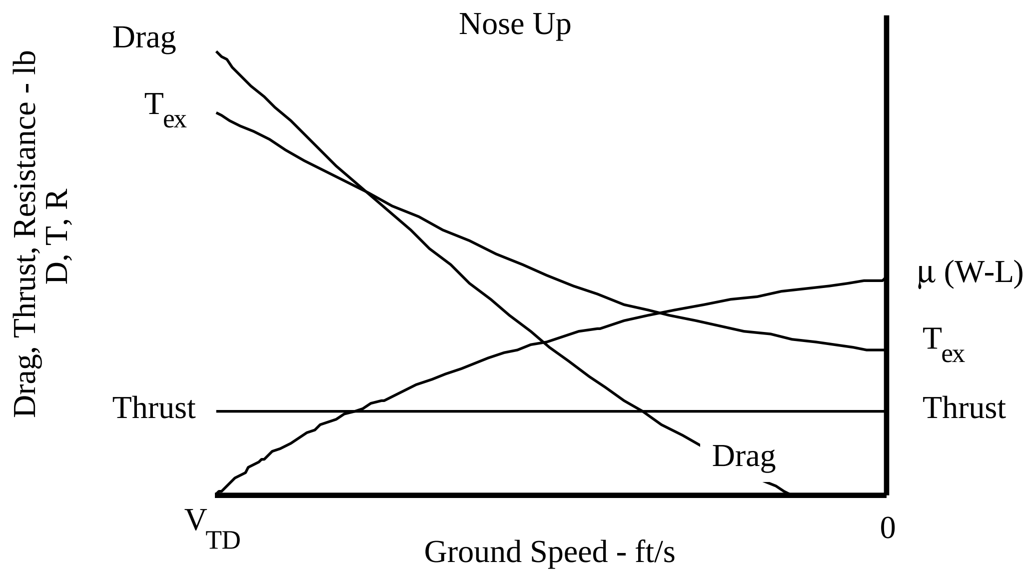

Figure 9.5

AERODYNAMIC BRAKING FORCES

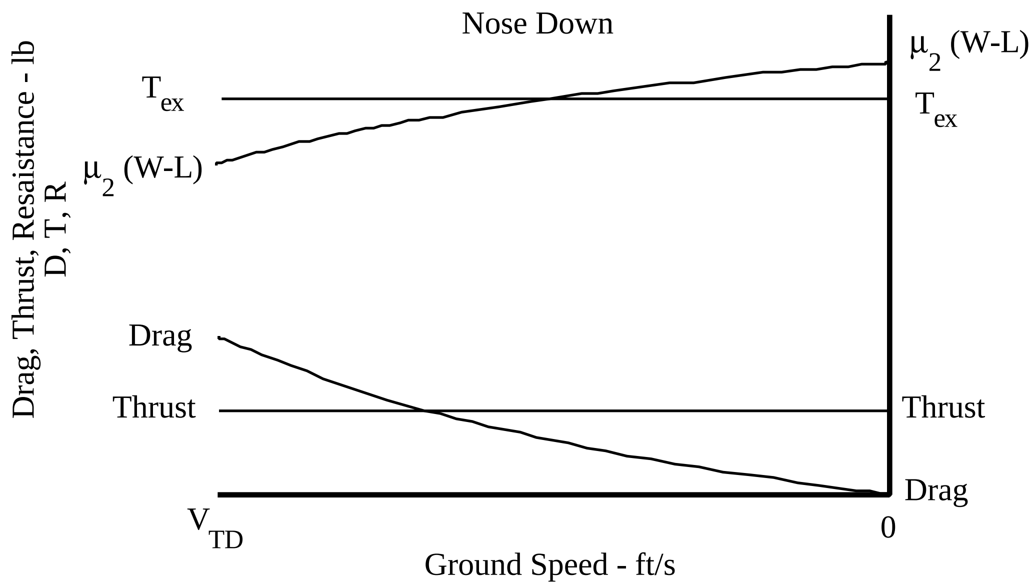

Figure 9.6

MAXIMUM WHEEL BRAKING FORCES

Notice that μ_2 (W-L) (where μ_2 is the coefficient of friction, brakes applied) is much greater than μ (W-L) which is the same as takeoff resistance. As shown in figure 9.7, the minimum stopping distance is achieved when aerodynamic braking is employed only as long as it provides a greater decelerating force than maximum wheel braking. An equation could be developed for the appropriate speed at which to make the transition using Eq 9.14 evaluated for both the aerodynamic braking and wheel braking condition. However, the resulting expression does not permit generalization of results.

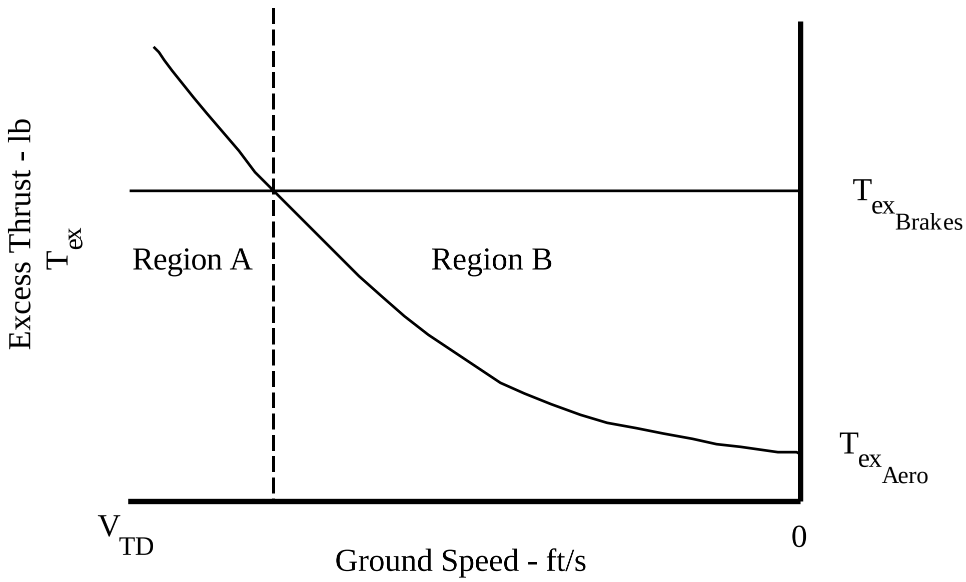

Region A: Aerodynamic Braking Better
Region B:Wheel Braking Better

Figure 9.7
AERODYNAMIC AND WHEEL BRAKING FORCES

9.3.2.4 LANDING CORRECTIONS

The corrections to standard day conditions for landing data are similar to the methods used in the takeoff. The wind correction equation and the runway slope correction equation are identical to those applied to the takeoff performance. The equation for thrust, weight, and density is the same if reverse thrust is used, but may be simplified if idle thrust is used by setting the test thrust equal to the standard thrust. The relationships are:

Air phase:

$$S_{3_{Std}} = S_{3_{Test}} \left(\frac{W_{Std}}{W_{Test}}\right)^{\left(2 + \frac{E_h}{E_h + 50}\right)} \left(\frac{\sigma_{Test}}{\sigma_{Std}}\right)^{\left(\frac{E_h}{E_h + 50}\right)} \qquad \text{(Eq 9.35)}$$

In Eq 9.35, E_h is the energy height representing the kinetic energy change during the air phase, expressed as follows:

$$E_h = \frac{V_{50}^2 - V_{TD}^2}{2g} \qquad \text{(Eq 9.36)}$$

Ground phase:

$$S_{4_{Std}} = S_{4_{Test}} \left(\frac{W_{Std}}{W_{Test}}\right)^2 \left(\frac{\sigma_{Test}}{\sigma_{Std}}\right) \qquad \text{(Eq 9.37)}$$

Where:

E_h	Energy height	ft
g	Gravitational acceleration	ft/s^2
$S_{3_{Std}}$	Standard landing distance, 50 ft to touchdown	ft
$S_{3_{Test}}$	Test landing distance, 50 ft to touchdown	ft
$S_{4_{Std}}$	Standard landing distance, touchdown to stop	ft
$S_{4_{Test}}$	Test landing distance, touchdown to stop	ft
σ_{Std}	Standard density ratio	
σ_{Test}	Test density ratio	
V_{50}	Ground speed at 50 ft reference point	ft/s
V_{TD}	Touchdown ground speed	ft/s
W_{Std}	Standard weight	lb
W_{Test}	Test weight	lb.

Past data has shown the weight correction to be valid for weights close to standard weight. In order to obtain data over a wide range of gross weights, a large number of tests must be conducted at carefully controlled weights at, or near, preselected standard values.

9.3.2.5 PILOT LANDING TECHNIQUE

Pilot technique is more important in the analysis of landing data than in takeoff data. Some of the factors which significantly affect landing performance include:

1. Power management during approach, flare, and touchdown.
2. Altitude of flare initiation.
3. Rate of rotation in the flare.
4. Length of hold-off time.
5. Touchdown speed.
6. Speed of braking initiation (aerodynamic and/or wheel) and brake pedal pressure.
7. Use of drag chute, spoilers, reverse thrust, or anti-skid.

9.4 TEST METHODS AND TECHNIQUES

9.4.1 TAKEOFF

9.4.1.1 TEST TECHNIQUE

To obtain repeatable takeoff performance data defining (and using) a repeatable takeoff technique is necessary.

1. Line up abeam a measured distance marker (runway remaining, Fresnel lens, etc.).
2. Ensure the nose wheel is straight.
3. Set takeoff power with engine stabilized (if possible), or establish throttle setting at/immediately after brake release.
4. Simultaneously release brakes and start clock or start clock and release brakes at a specified time.
5. Use rudder/nose wheel steering for alignment (no brakes).
6. Rotate at a prescribed airspeed to a specific attitude or angle of attack.

7. Once airborne, change configuration at specific altitude and airspeed.

While hand held data (stopwatch) can provide usable results, automatic recording devices are desired due to the dynamic nature of the tests.

9.4.1.2 DATA REQUIRED

1. Takeoff airspeed, V_{TO}.
2. Distance to lift off obtained by:
   a. Theodolite
   b. Runway camera.
   c. Paint gun.
   d. Observers.
   e. Laser.
   f. “Eyes right” - check runway marker.
3. Pitch attitude on rotation/initial climb.
4. Distance to 50 ft / distance to climb airspeed.
5. Time to lift off / 50 ft / climb airspeed.
6. Angle of attack at rotation/climb out.
7. Fuel used, brake release to climb airspeed.
8. Runway wind conditions.
9. Runway temperature.
10. Runway composition / runway condition reading (RCR).
11. Field elevation.
12. Altimeter.
13. Runway gradient.
14. Aircraft gross weight / center of gravity.
15. Power parameters: RPM, EGT.
16. Elevator/horizontal tail position.

9.4.1.3 TEST CRITERIA

1. Establish takeoff trim setting.
2. No brakes (limit use of rudder / nose wheel steering.).
3. Operate engine bleed air system OFF or in normal mode.

9.4.1.4 DATA REQUIREMENTS

1. Engine stabilized (if feasible).
2. Wind < 10 kn.
3. $W_{Test} \approx W_{Std}$.
4. Rate of climb from lift off to intercepting climb schedule < 500 ft/min.

9.4.1.5 SAFETY CONSIDERATIONS

1. Build up to define minimum lift off speeds / critical center of gravity etc.
2. Fly the aircraft first. Many parameters to observe/record. Set priorities.
3. Follow the course rules.
4. Don’t exceed the gear and flap speed limits.

9.4.2 LANDING

9.4.2.1 TEST TECHNIQUE

Use a repeatable defined technique for:

1. Approach (50 ft above the ground and flare point).
2. Flare (if required).
3. Touch down at a specific point (abeam Fresnel lens, etc.).
4. Aerodynamic braking (if appropriate) - specific attitude.
5. Braking (What speed? What pressure applied?).
6. Use of spoilers, thrust reverser(s), drag chute, anti-skid, etc.

While the landing distance can be measured by direct observation, automatic recording devices are desired (theodolite, runway camera etc.,) because of the dynamic nature of the tests.

9.4.2.2 DATA REQUIRED

1. Distance from 50 ft above the ground through the flare to touch down.
2. Glideslope angle.
3. Distance from touch down to full stop.
4. Runway wind conditions.
5. Runway temperature.
6. Runway composition / runway condition reading.
7. Field elevation.
8. Altimeter.
9. Runway gradient.
10. Aircraft gross weight / center of gravity.
11. Configuration.
12. Power parameters during landing and roll out: RPM, EGT.

9.4.2.3 TEST CRITERIA

Operate engine bleed air system OFF or in normal mode.

9.4.2.4 DATA REQUIREMENTS

1. Wind steady and < 10 kn.
2. $W_{Test} \approx W_{Std}$.

9.4.2.5 SAFETY CONSIDERATIONS

1. Build up to maximum effort stop landing (normally only demonstrated by the contractor).
2. Establish precautions against and procedures for:
   a. Hot brakes.
   b. Brake fire.
   c. Blown tire.
   d. Brake Failure.
3. Consider the geometry limit of aircraft for aerodynamic braking and sink rate at touch down.

9.5 DATA REDUCTION

The data for takeoff and landing performance is generally presented using test day weight and atmospheric conditions. The data reduction described below provides corrections to test day takeoff and landing distance to account for:

1. Wind.
2. Runway
3. Thrust, weight, and density.

9.5.1 TAKEOFF

From the pilot's data card and/or automatic recording device record:

1. Ground roll distance (brake release to lift off) (ft).
2. Wind velocity and direction relative to the runway (ft/s / degrees).
3. Lift off airspeed V_o (correct for position and instrument error (ft/s).
4. Temperature T_a (˚K).
5. Weight W (lb).
6. Pressure altitude H_P (ft).
7. Runway slope θ (deg).

The following equations are used in the data reduction:

$$V_w = \text{Wind Velocity } \cos \text{ (Wind Direction Relative To Runway)} \qquad \text{(Eq 9.38)}$$

$$V_{TO_w} = V_{TO} - V_w \qquad \text{(Eq 9.19)}$$

$$S_{1_{Std}} = S_{1_w}\left(1 + \frac{V_w}{V_{TO_w}}\right)^{1.85} \qquad \text{(Eq 9.23)}$$

$$S_{1_{Std}} = \frac{S_{1_{SL}}}{\left(1 - \frac{2g\, S_{1_{SL}}}{V_{TO}^2}\sin\theta\right)} \quad \text{(Eq 9.27)}$$

$$\sigma = 9.625\,\frac{P_a}{T_a} \quad \text{(Eq 9.39)}$$

$$S_{1_{Std}} = S_{1_{Test}}\left(\frac{W_{Std}}{W_{Test}}\right)^{2.3}\left(\frac{\sigma_{Test}}{\sigma_{Std}}\right)\left(\frac{T_{N_{Test}}}{T_{N_{Std}}}\right)^{1.3} \quad \text{(Eq 9.28)}$$

Where:

g	Gravitational acceleration	ft/s^2
P_a	Ambient pressure	psf
θ	Runway slope angle	deg
$S_{1_{SL}}$	Takeoff distance, brake release to lift off, sloping runway	ft
$S_{1_{Std}}$	Standard takeoff distance, brake release to lift off	ft
$S_{1_{Test}}$	Test takeoff distance, brake release to lift off	ft
S_{1_w}	Takeoff distance, brake release to lift off, with respect to wind	ft
σ_{Std}	Standard density ratio	
σ_{Test}	Test density ratio	
T_a	Ambient temperature	°K
$T_{N_{Std}}$	Standard net thrust	lb
$T_{N_{Test}}$	Test net thrust	lb
V_{TO}	Takeoff ground speed	ft/s
V_{TO_w}	Takeoff ground speed with respect to wind	ft/s
V_w	Wind velocity	ft/s
W_{Std}	Standard weight	lb
W_{Test}	Test weight	lb.

From the observed data compute as follows:

Step	Parameter	Notation	Formula	Units	Remarks
1	Wind component	V_w	Eq 9.38	ft/s	
2	Takeoff ground speed	V_{TO_w}	Eq 9.19	ft/s	
3	Ground roll	$S_{1_{Std}}$	Eq 9.23	ft	Wind corrected
4	Ground roll	$S_{1_{Std}}$	Eq 9.27	ft	Slope corrected
5	Density ratio	σ	Eq 9.39		
6	Ground roll	$S_{1_{Std}}$	Eq 9.28	ft	Thrust, weight, density corrected; T_N from thrust stand data

9.5.2 LANDING

From the pilot's data card and/or automatic recording device record:

1. Ground roll distance (touchdown to full stop) (ft).
2. Wind velocity and direction relative to the runway (ft/s / degrees).
3. Touchdown airspeed V_{TD} (correct for position and instrument error) (ft/s).
4. Temperature T_a (˚K).
5. Aircraft weight W (lb).
6. Pressure altitude H_P (ft).
7. Runway slope θ (deg).

The following equations are used in the data reduction.

$$V_w = \text{Wind Velocity } \cos(\text{Wind Direction Relative To Runway}) \qquad \text{(Eq 9.38)}$$

$$V_{TD_w} = V_{TD} - V_w \qquad \text{(Eq 9.40)}$$

$$S_{4_{Std}} = S_{4_w}\left(1 + \frac{V_w}{V_{TD}}\right)^{1.85} \qquad \text{(Eq 9.41)}$$

$$S_{4_{Std}} = \frac{S_{4_{SL}}}{\left(1 - \frac{2\,g\,S_{4_{SL}}}{V_{TD}^2}\,\sin\theta\right)} \qquad \text{(Eq 9.42)}$$

$$\sigma = 9.625\,\frac{P_a}{T_a} \qquad \text{(Eq 9.39)}$$

$$S_{4_{Std}} = S_{4_{Test}}\left(\frac{W_{Std}}{W_{Test}}\right)^2\left(\frac{\sigma_{Test}}{\sigma_{Std}}\right) \qquad \text{(Eq 9.37)}$$

Where:

g	Gravitational acceleration	ft/s^2
P_a	Ambient pressure	psf
θ	Runway slope angle	deg
$S_{4_{SL}}$	Landing distance, touchdown to stop, sloping runway	ft
$S_{4_{Std}}$	Standard landing distance, touchdown to stop	ft
$S_{4_{Test}}$	Test landing distance, touchdown to stop	ft
S_{4_w}	Landing distance, touchdown to stop, with respect to wind	ft
σ_{Std}	Standard density ratio	
σ_{Test}	Test density ratio	
T_a	Ambient temperature	˚K
V_{TD}	Touchdown ground speed	ft/s
V_{TD_w}	Touchdown ground speed with respect to wind	ft/s
V_w	Wind velocity	ft/s
W_{Std}	Standard weight	lb
W_{Test}	Test weight	lb.

From the observed data compute as follows:

Step	Parameter	Notation	Formula	Units	Remarks
1	Wind component	V_w	Eq 9.38	ft/s	
2	Touchdown ground speed	V_{TD}	Eq 9.40	ft/s	
3	Ground roll	$S_{4_{Std}}$	Eq 9.41	ft	Wind corrected
4	Ground roll	$S_{4_{Std}}$	Eq 9.42	ft	Slope corrected
5	Density ratio	σ	Eq 9.39		
6	Ground roll	$S_{4_{Std}}$	Eq 9.37	ft	Weight, density corrected

9.6 DATA ANALYSIS

The analysis of takeoff and landing data is directed toward determining the optimum technique(s) to maximize the capabilities of the test aircraft. Once the data has been incorporated into figures similar to figures 9.8 and 9.9, takeoff ground roll can be determined for a given aircraft weight, ambient temperature, pressure altitude, wind, and runway slope.

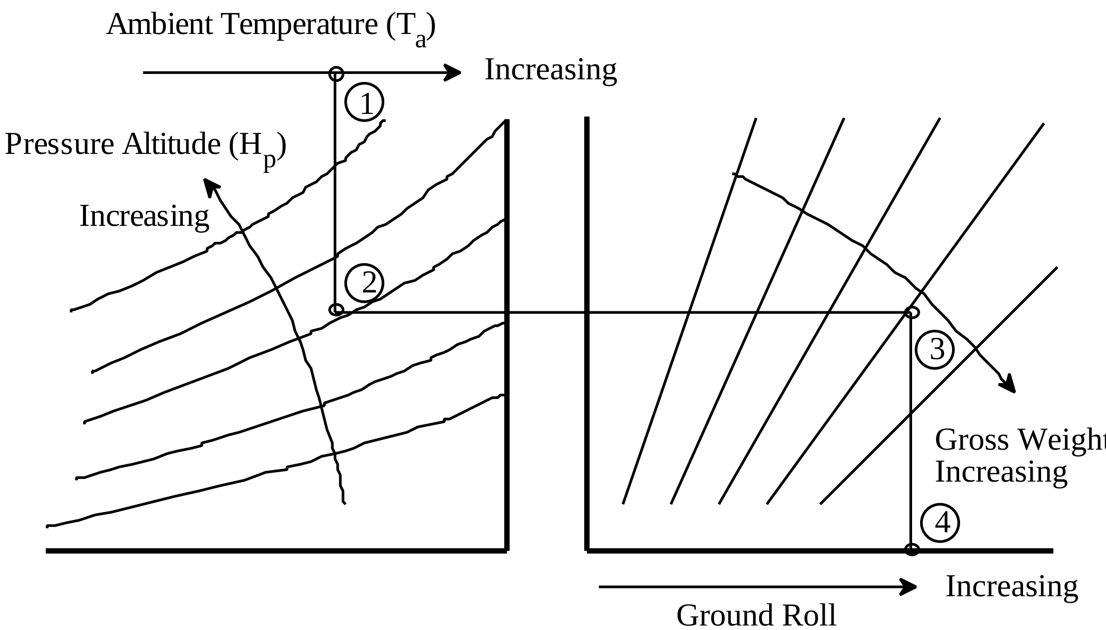

1 Ambient Temperature

2 Pressure Altitude

3 Gross Weight

4 Ground Roll Distance

Figure 9.8

GROUND ROLL DISTANCE AS A FUNCTION OF TEMPERATURE, PRESSURE ALTITUDE, AND WEIGHT

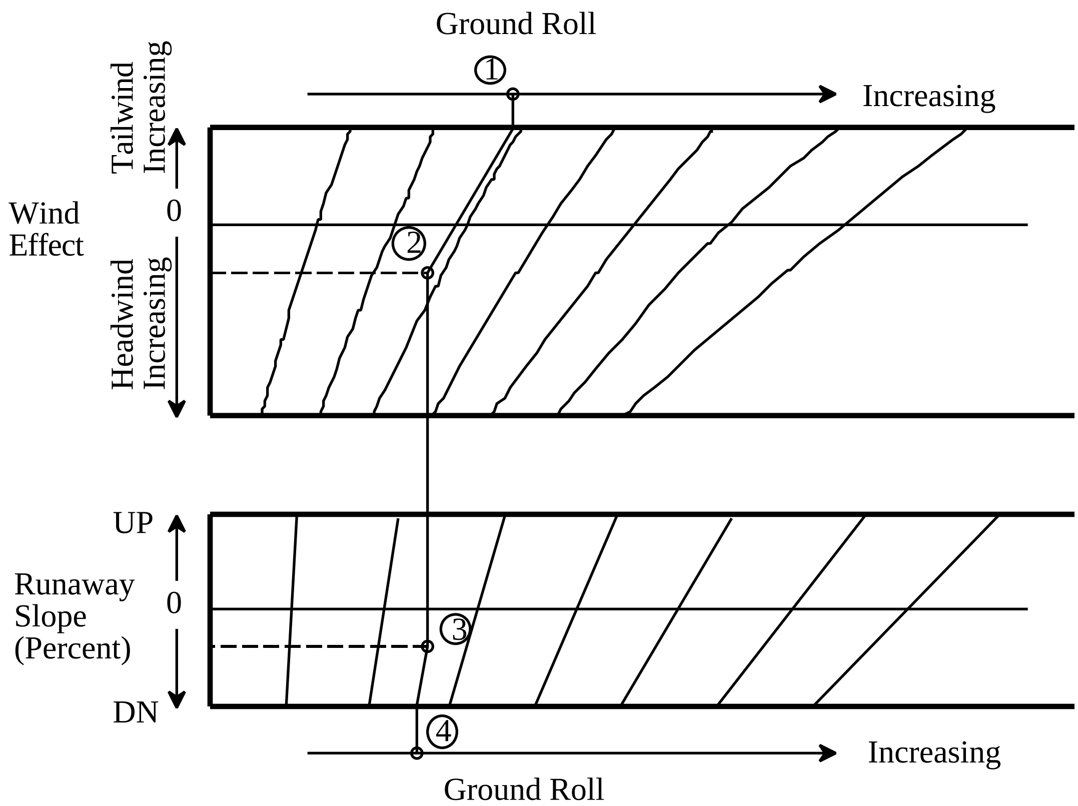

1 Ground Roll From Figure 9.8

1 To 2 Wind Correction

2 To 3 Slope Correction

4 Adjusted Ground Roll

Figure 9.9
GROUND ROLL CORRECTIONS FOR WIND AND RUNWAY SLOPE

9.7 MISSION SUITABILITY

The requirements for takeoff and landing performance are specified in the detail specification for the aircraft. The determination of mission suitability depends largely on whether the aircraft meets those requirements.

9.8 SPECIFICATION COMPLIANCE

The takeoff and landing performance is normally covered as a contract guarantee in the detail specification requirements of each aircraft. For example, based on a standard day, takeoff configuration, and a specific drag index, the takeoff distance is specified to be not greater than a certain number of feet. Similarly, for the guaranteed landing performance at a specified gross weight, configuration, and braking condition, a distance not greater than a certain number of feet is specified.

9.9 GLOSSARY

9.9.1 NOTATIONS

AR	Aspect ratio	
C_D	Drag coefficient	
C_{D_i}	Induced drag coefficient	
C_{D_p}	Parasite drag coefficient	
C_L	Lift coefficient	
$C_{L_{max}}$	Maximum lift coefficient	
$CL_{max_{TO}}$	Maximum lift coefficient, takeoff configuration	
$C_{L_{Opt}}$	Optimum lift coefficient	
D	Drag	lb
ΔS_2	Change in S_2, equal to t V_w	ft
e	Oswald’s efficiency factor	
E_h	Energy height	ft
g	Gravitational acceleration	ft/s^2
L	Lift	lb
N_{Std}	Standard propeller speed	rpm
N_{Test}	Test propeller speed	rpm
P_a	Ambient pressure	psf
$P_{a_{Std}}$	Standard ambient pressure	psf
$P_{a_{Test}}$	Test ambient pressure	psf
q	Dynamic pressure	psf
R	Resistance force	lb
S	Distance	ft
S	Wing area	ft^2

S_1	Takeoff distance, brake release to lift off	ft
$S_{1_{SL}}$	Takeoff distance, brake release to lift off, sloping runway	ft
$S_{1_{Std}}$	Standard takeoff distance, brake release to lift off	ft
$S_{1_{Test}}$	Test takeoff distance, brake release to lift off	ft
S_{1_w}	Takeoff distance, brake release to lift off, with respect to wind	ft
S_2	Takeoff distance, lift off to 50 ft	ft
$S_{2_{Std}}$	Standard takeoff distance, lift off to 50 ft	ft
$S_{2_{Test}}$	Test takeoff distance, lift off to 50 ft	ft
S_{2_w}	Takeoff distance, lift off to 50 ft, with respect to wind	ft
S_3	Landing distance, 50 ft to touchdown	ft
$S_{3_{Std}}$	Standard landing distance, 50 ft to touchdown	ft
$S_{3_{Test}}$	Test landing distance, 50 ft to touchdown	ft
S_4	Landing distance, touchdown to stop	ft
$S_{4_{SL}}$	Landing distance, touchdown to stop, sloping runway	ft
$S_{4_{Std}}$	Standard landing distance, touchdown to stop	ft
$S_{4_{Test}}$	Test landing distance, touchdown to stop	ft
S_{4_w}	Landing distance, touchdown to stop, with respect to wind	ft
T	Thrust	lb
t	Time	s
T_a	Ambient temperature	˚K
T_{ex}	Excess thrust	lb
$T_{ex_{Avg}}$	Average excess thrust	lb
$T_{ex_{Avg\ w}}$	Average excess thrust, with respect to wind	lb
T_N	Net thrust	lb
$T_{N_{Std}}$	Standard net thrust	lb
$T_{N_{Test}}$	Test net thrust	lb
V	Velocity	ft/s
V_{50}	Ground speed at 50 ft reference point	ft/s
$V_{CL_{50}}$	Climb speed at 50 ft	kn
V_L	Landing airspeed	ft/s, kn
$V_{L_{50}}$	Landing speed at 50 ft	kn

V_R	Rotation airspeed	kn
V_{s_L}	Stall speed, landing configuration, power off	kn
V_{s_T}	Stall speed, transition configuration, power off, flaps down, gear up	kn
V_{TD}	Touchdown ground speed	ft/s
V_{TD_w}	Touchdown ground speed with respect to wind	ft/s
V_{TO}	Takeoff ground speed	ft/s
V_{TO_w}	Takeoff ground speed with respect to wind	ft/s
V_w	Wind velocity	ft/s
W	Weight	lb
W_{Std}	Standard weight	lb
W_{Test}	Test weight	lb

9.9.2 GREEK SYMBOLS

μ (mu)	Coefficient of friction	
μ_2	Coefficient of friction, brakes applied	
π (pi)	Constant	
θ (theta)	Runway slope angle	deg
ρ (rho)	Air density	slugs/ft^3
σ_{Std} (sigma)	Standard density ratio	
σ_{Test}	Test density ratio	

9.10 REFERENCES

1. Clancy, L.J., *Aerodynamics*, A Halsted Press Book, John Wiley & Sons, New York 1975.

2. Departments of the Army, Navy, Air Force, Military Specification MIL-C-5011A, 5 November 1951.

3. Dommasch, D.O. et al, *Airplane Aerodynamics*, 4th Edition, Pitman Publishing Company, N.Y., N.Y., 1967.

4. Federal Aviation Regulations Part 23 and Part 25.

5. Kimberlin, R., "Takeoff and Landing Notes", The University of Tennessee Space Institute, undated.

6. "Military Standard Flying Qualities of Piloted Airplanes", MIL-STD-1797A 30 January 1990.

7. Naval Air Systems Command Specification, AS-5263, *Guidelines For Preparation Of Standard Aircraft Characteristics Charts And Performance Data Piloted Aircraft (Fixed Wing)*, 23 October, 1986.

8. Naval Test Pilot School Flight Test Manual, *Fixed Wing Performance, Theory and Flight Test Techniques*, USNTPS-FTM-No. 104, U.S. Naval Test Pilot School, Patuxent River, MD, July 1977.

9. Roberts, Sean C., *Light Aircraft Performance For Test Pilots and Flight Test Engineers*, Flight Research,. Inc. Mojave, CA, 9 July 1982.

10. Stinton, D., *The Design of the Aeroplane*, Van Nostrand Reinhold Company, N.Y.

11. USAF Test Pilot School Flight Test Manual, *Performance Flight Testing Phase, Volume I*, USAF Test Pilot School, Edwards AFB, CA, February 1987.

12. USAF Test Pilot School, *Performance Phase Planning Guide*, USAF Test Pilot School, Edwards, AFB, CA, July 1987.

CHAPTER 10

STANDARD MISSION PROFILES

CHAPTER 10

FIGURES

CHAPTER 10

STANDARD MISSION PROFILES

10.1 INTRODUCTION

From the beginning to the end of the flight test process, the flight test team must have a working knowledge of the mission and mission profiles against which the aircraft is to be evaluated. This knowledge at the start of the program enables the team to design the test program to concentrate on the mission specific altitudes, airspeeds, loadings, or other requirements which are representative of the mission(s).

The preceding chapters discuss in detail the testing required to evaluate specific performance characteristics. The final step for the flight test team is to assimilate all the performance data and determine if the aircraft can perform the required mission(s). This chapter looks at putting all of the performance characteristics together to enable the flight test team to evaluate an aircraft against a given mission profile (Figure 10.1).

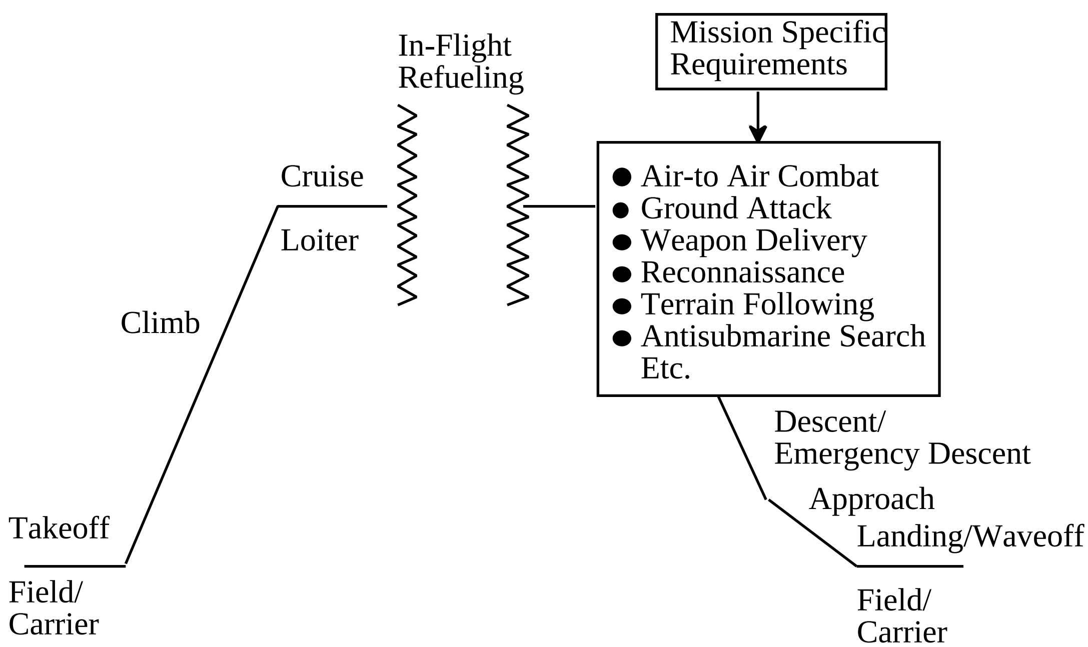

Figure 10.1
GENERIC MISSION PROFILE

10.2 PURPOSE OF TEST

The purpose of this chapter is to present standard mission profiles for:

1. General Navy Operational Missions.
2. Special Navy Operational Missions.
3. Naval Pilot Trainer Missions.
4. Naval Flight Officer Trainer Missions.

10.3 THEORY

Once the Navy has determined specific operational requirements, an aircraft design team takes this information to develop the aerodynamic, propulsion, and weight elements that ultimately give the flight test team an aircraft with certain performance characteristics (Figure 10.2).

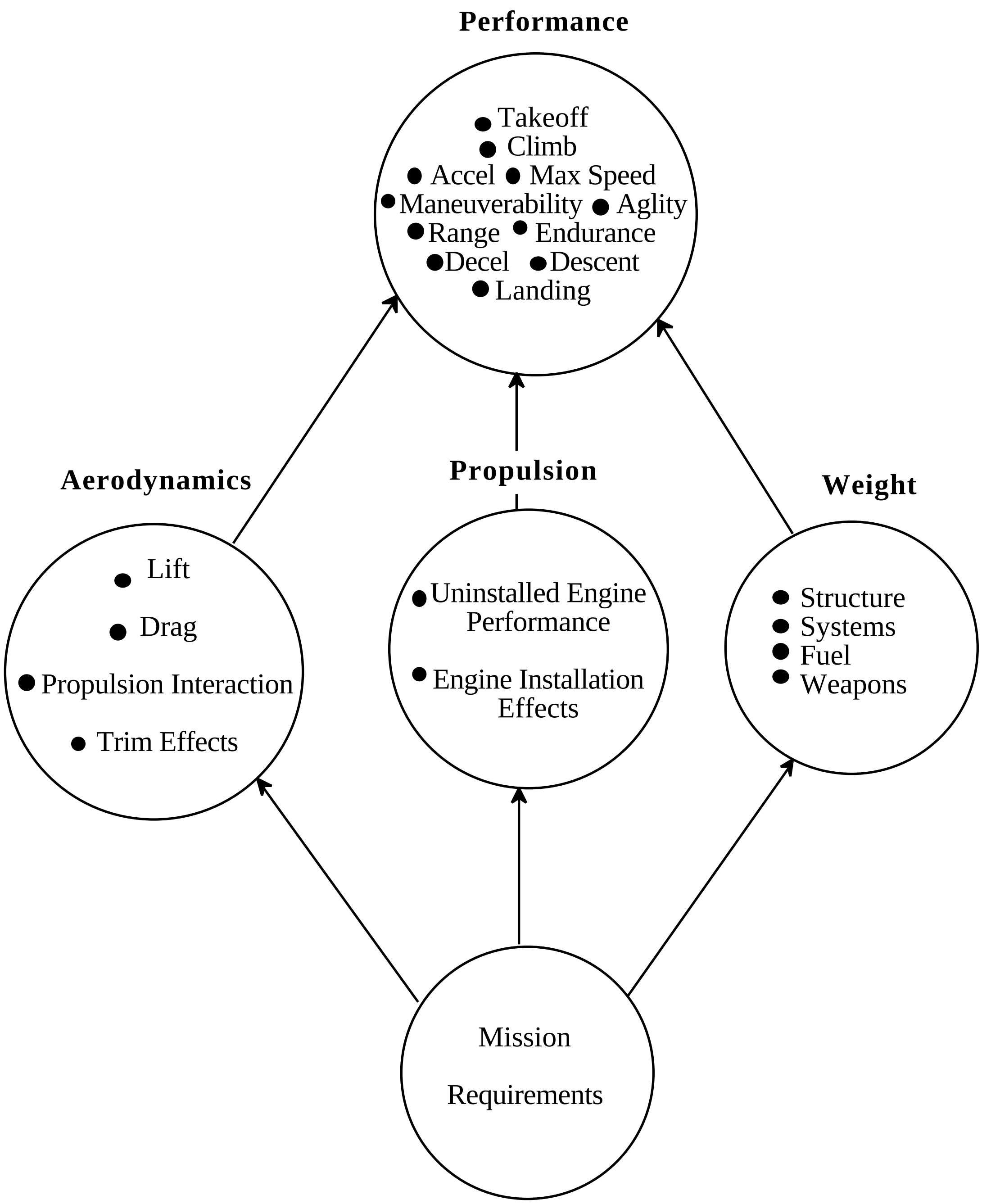

Figure 10.2
MISSION REQUIREMENTS WHICH DEFINE PERFORMANCE

Two important performance results determined by the flight test team are:

1. Performance guarantees.
2. Mission suitability.

Figure 10.3 illustrates the relationship of three key specifications dealing with an aircraft's performance test and evaluation program.

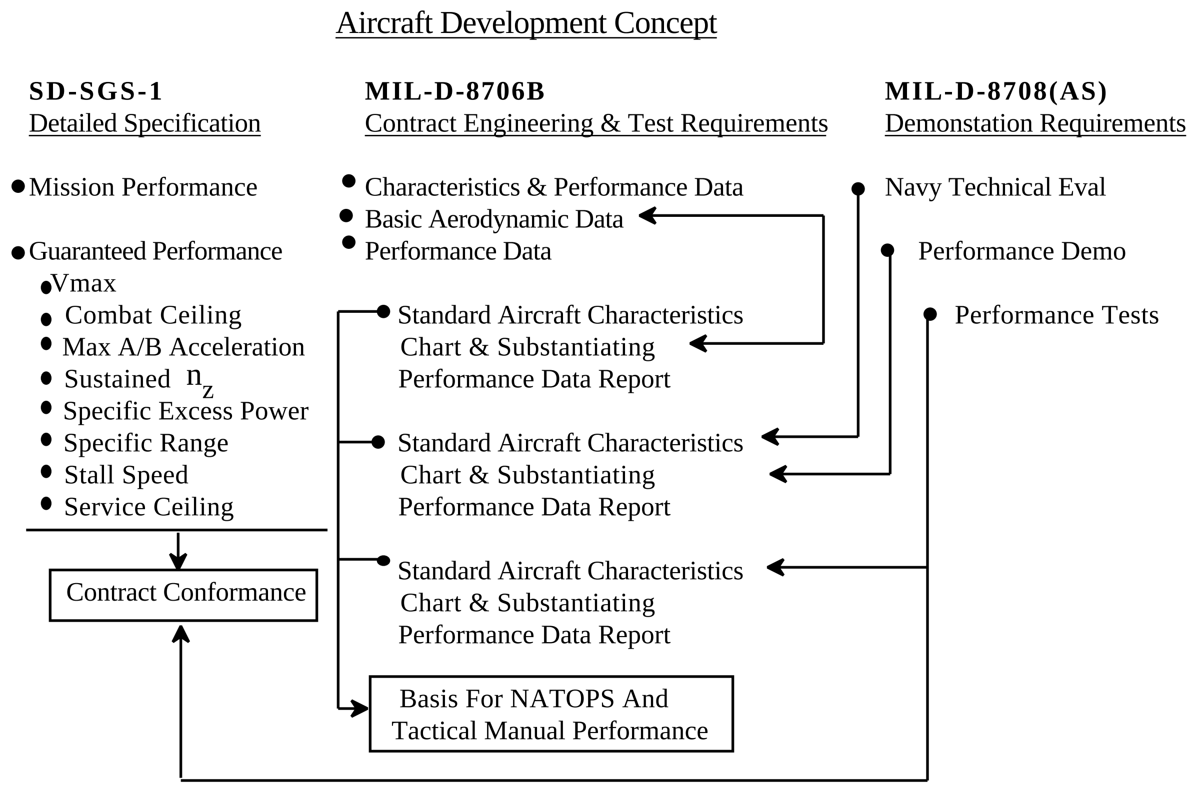

Figure 10.3
AIRCRAFT PERFORMANCE PROGRAM

As shown in figure 10.3, the data from the flight test program is used to develop the standard aircraft characteristics (SAC) charts, which in turn are used as the basis for NATOPS and Tactical Manual performance data. Also, through testing specific performance characteristics, the flight data verifies the contract performance guarantees.

While some data presented in flight manuals is based on flight test results, much of the data is calculated (estimated). It should be noted that the confidence level of these performance calculations is based on five sources. Since aircraft performance data are obtained from the marriage of aerodynamic, propulsion, and weight information, the confidence in the validity of the calculated results is dependent on the accuracy and validity of the individual components. The confidence level in the validity of the components is in turn dependent on a number of factors including the degree of development of the aircraft or weapons system, the availability of instrumented flight test data and/or the source of the data used for the calculations. For the most part, NAVAIRSYSCOM performance calculations are based on the best available data source in the following order of preference:

1. Formal government demonstration data used for showing conformance with contractual guarantees.
2. Government flight test data (Navy/Air Force evaluations).
3. Contractor flight test data.
4. Wind tunnel data.
5. Empirical estimates and state-of-the-art calculations.

Most performance calculations, especially mission calculation, are based on inputs from as many of the above sources as possible. It is impractical to obtain flight and wind tunnel data for all combinations of mission loadings (external stores) throughout the total aircraft flight envelope. However, the degree of confidence in the results can usually be assessed from the source of baseline aerodynamic, propulsion, and weight information used in the calculations.

While much of the performance planning data still exists only as paper charts, with the introduction of the Tactical Air Mission Planning System (TAMPS) each aircrew will soon have available computer access to the performance data base for their aircraft. During the transition from the paper charts to computer software the aircrew needs to know the source of the performance data and the assumptions made in establishing the computer data base.

10.4 MISSION PROFILES

10.4.1 BACKGROUND

For each aircraft the Navy flies, SAC charts are developed for at least four (4) mission types. The SAC charts are intended to provide a concise compilation of physical characteristics and performance capabilities of an aircraft or weapons system. The first SAC charts are developed for the clean mission which is intended to show the maximum capabilities of the aircraft (usually a high-high-profile). The second mission described is the ferry mission, where the greatest distance attainable on a practicable one-way mission with maximum authorized fuel and payload (external fuel tanks may be carried and must be retained for the duration of the flight). The third mission described by the SAC charts is the basic mission which takes the performance capabilities of the aircraft and applies the specific criteria of the mission profiles in AS-5263 (examples presented as sections 10.4.2 and 10.4.3 of this chapter). Finally, the fourth type of mission(s) described are the design mission(s), defined as the primary missions for which the aircraft was specifically procured (examples presented as sections 10.4.4 and 10.4.5). These missions are defined in procurement documents, such as the statement of work, and include the flight profiles, allowances, fuel (clean or external tanks) and payload. The mission profiles presented in sections 10.4.2, 10.4.3, 10.4.4, and 10.4.5 are extracted from the reference cited for each section.

10.4.2 GENERAL NAVY OPERATIONAL MISSIONS (REF 7)

10.4.2.1 HI-HI-HI (HIGH ALTITUDE SUBSONIC)

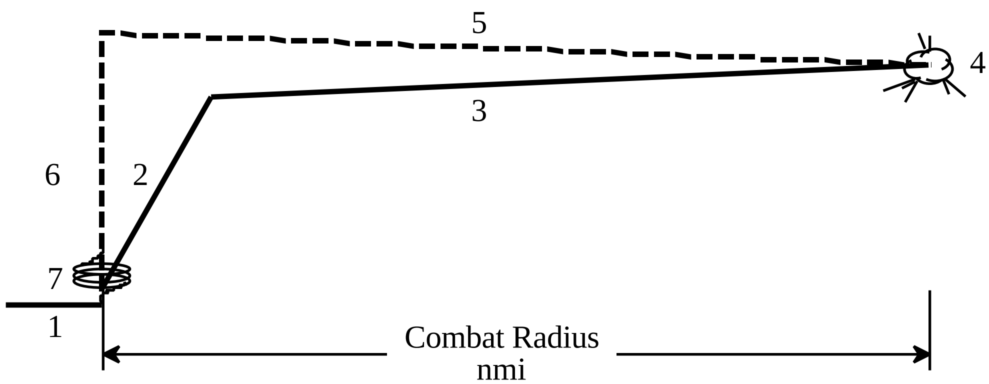

Figure 10.4
HI-HI-HI

1. Taxi, warm-up, takeoff, and acceleration to best climb speed: fuel allowance at sea level static equal to 4.6 min at intermediate thrust plus 30 seconds afterburner thrust if afterburner is used for takeoff.

2. Climb: on course at best climb speed at intermediate power to best cruise altitude (not to exceed cruise ceiling).

3. Cruise Out: to target at speeds and altitudes for best range, using a cruise climb flight path (not to exceed cruise ceiling).

4. Combat: fuel allowance equal to 5 min at maximum speed with intermediate thrust at best cruise altitude. No distance is credited (drop bombs, retain mounting hardware and missiles after combat).

5. Cruise Back: to base at speed and altitudes for best range, using a cruise climb flight path (not to exceed cruise ceiling).

6. Descent: descend to sea level (no fuel used, no distance gained).

7. Reserve: fuel allowance equal to 20 min loiter at sea level at speeds for maximum endurance with all engines operating plus 5% of initial total fuel (internal plus external).

a.	Mission Time:	Items 2 through 6.
b	Cycle Time:	Items 2 through 7.

10.4.2.2 FIGHTER ESCORT

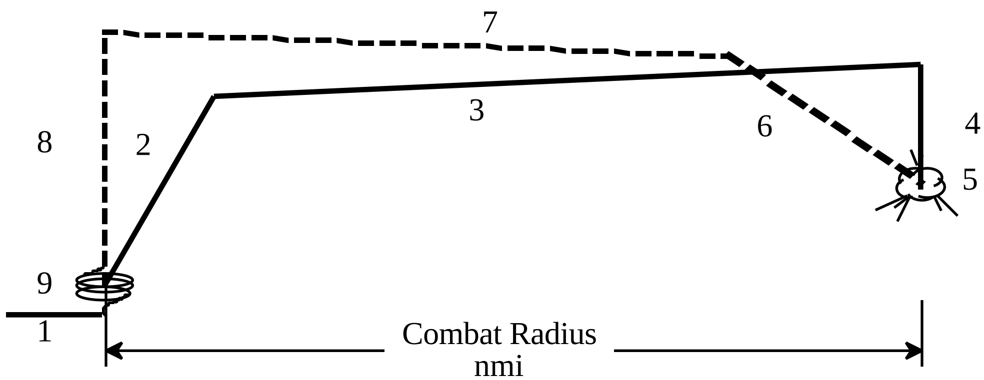

Figure 10.5
FIGHTER ESCORT

1. Taxi, warm-up, takeoff, and acceleration to best climb speed: fuel allowance at sea level static equal to 4.6 min at intermediate thrust plus 30 seconds afterburner thrusts if afterburner is used for takeoff.

2. Climb: on course at best climb speed at intermediate thrust to best cruise altitude (not to exceed cruise ceiling).

3. Cruise Out: to target at speeds and altitudes for best range, using a cruise climb flight path (not to exceed cruise ceiling).

4. Descent: descend to 10,000 ft (no fuel used, no distance gained).

5. Combat: fuel allowance equal to 2 min at maximum thrust, Mach 1.0 at 10,000 ft (no distance is credited, missiles are retained).

6. Climb: on course at best climb speed at intermediate thrust from 10,000 ft to best cruise altitude (not to exceed cruise ceiling).

7. Cruise Back: to base at speed and altitudes for best range, using a cruise climb flight path (not to exceed cruise ceiling).

8. Descent: descend to sea level (no fuel used, no distance gained).

9. Reserve: fuel allowance equal to 20 min loiter at sea level at speeds for maximum endurance with all engines operating plus 5% of initial total fuel (internal plus external).

a. Mission Time: Items 2 through 8.
b. Cycle Time: Items 2 through 9.

10.4.2.3 ALTERNATE FIGHTER ESCORT

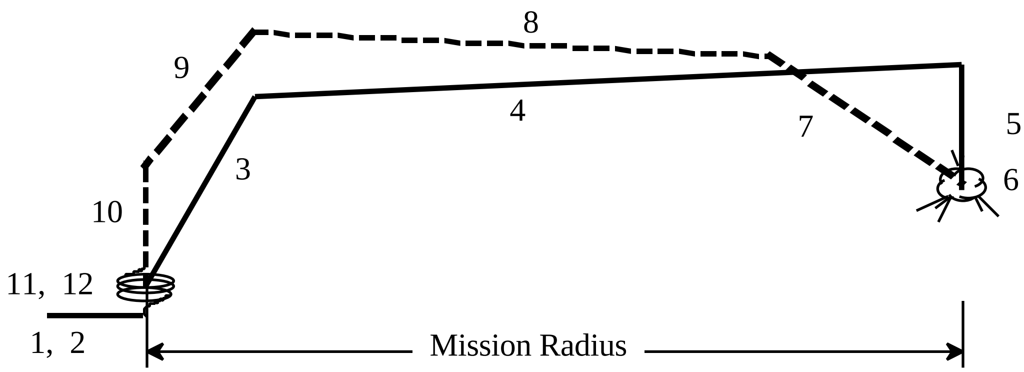

Figure 10.6
ALTERNATE FIGHTER ESCORT

1. Takeoff: start engines and takeoff allowance equal to 20 min at idle power and 30 seconds at intermediate power, sea level static.

2. Acceleration: intermediate power acceleration from 150 KCAS to best climb speed at sea level.

3. Climb: intermediate power climb from sea level to best cruise altitude.

4. Cruise Out: cruise climb at best conditions.

5. Descent: idle power descent to 20,000 ft at Mach 0.8 (credit time, fuel, and distance).

6. Combat: fuel allowance equal to 4 intermediate power sustained turns at Mach 0.9 at 20,000 ft and 3 maximum power sustained turns at Mach 0.9 at 20,000 ft.

7. Climb: intermediate power climb from 20,000 ft to best cruise altitude.

8. Cruise Back: cruise climb at best conditions.

9. Descent: idle power descent to 20,000 ft at 250 KCAS (credit time, fuel and distance).

10. Descent: idle power descent to 1,200 ft at 250 KCAS (credit time and fuel; no credit for distance).

11. Carrier Approach: cruise at 150 KCAS for a distance of 12 nmi at 1,200 ft (credit time and fuel; no credit for distance).

12. Reserve: 100 nmi bingo (no credit for distance). Intermediate power acceleration from 150 KCAS to best climb speed at sea level.

a. Intermediate power climb from sea level to best profile altitude.
b. Cruise at best profile altitude(s) at best conditions.
c. Idle power descent to 10,000 ft at 250 KCAS (credit time, fuel, and distance).
d. 10 min at 10,000 ft loiter at maximum endurance speed.
e. Mission Time: Items 3 through 11.
f. Cycle Time: Items 3 through 12.

10.4.2.4 DECK LAUNCHED INTERCEPT

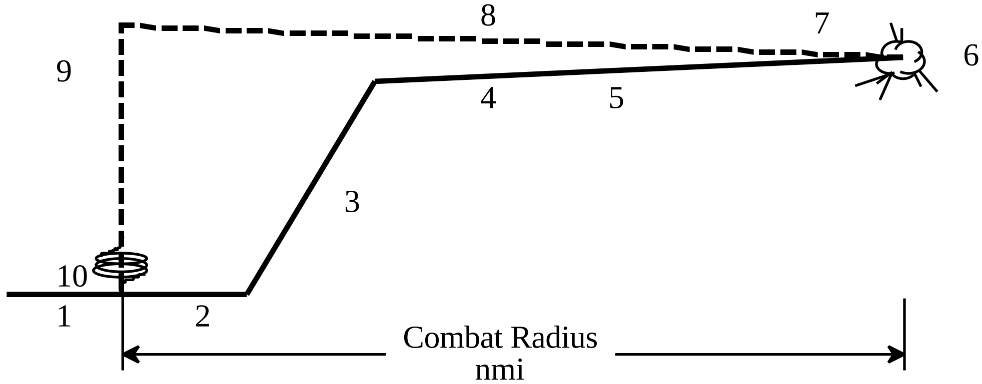

Figure 10.7
DECK LAUNCHED INTERCEPT

1. Taxi, warm-up, takeoff, and acceleration to Mach 0.3: fuel allowance at sea level static equal to 4.6 min at intermediate thrust plus 30 seconds afterburner thrust if afterburner is used for takeoff.

2. Acceleration: maximum power acceleration from Mach 0.3 to Mach 0.9 at sea level.

3. Climb: on course at Mach 0.9 at maximum power to 35,000 ft.

4. Acceleration: maximum power acceleration from Mach 0.9 to Mach 1.35 at 35,000 ft.

5. Dash Out: Mach 1.35 dash at 35,000 ft.

6. Combat: fuel allowance equal to 1 min at maximum power, Mach 1.35 at 35,000 ft (no distance is credited, missiles are retained).

7. Climb: on course at best climb speed at intermediate power to best cruise altitude (not to exceed cruise ceiling).

8. Cruise Back: to base at speed and altitudes for best range, using a cruise climb flight path (not to exceed cruise ceiling).

9. Descent: descend to sea level (no fuel used, no distance gained).

10. Reserve: fuel allowance equal to 20 min loiter at sea level at speeds for maximum endurance with all engines operating plus 5% of initial total fuel (internal plus external).

  a. Mission Time: Items 2 through 9.
  b. Cycle Time: Items 2 through 10.

Note: Dash Mach number and altitude variations should be considered for this mission.

10.4.2.5 COMBAT AIR PATROL

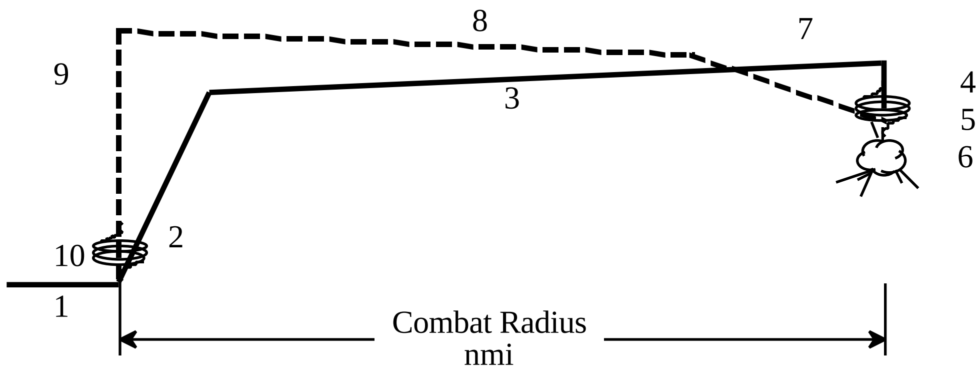

Figure 10.8
COMBAT AIR PATROL

1. Taxi, warm-up, takeoff, and acceleration to best climb speed: fuel allowance at sea level static equal 4.6 min at intermediate thrust plus 30 seconds afterburner thrust if afterburner is used for takeoff.

2. Climb: on course at best climb speed at intermediate thrust to best cruise altitudes (not to exceed cruise ceiling).

3. Cruise Out: to 150 nmi at speeds and altitudes for best range, using a climb flight path (not to exceed cruise ceiling).

4. Descent: descend to 35,000 ft (no fuel used, no distance gained).

5. Loiter: loiter at speed for maximum endurance at 35,000 ft (no distance is credited).

6. Combat: fuel allowance equal that used to accelerate from loiter speed at 35,000 ft to Mach 1.2 plus 2 min at maximum power, Mach 1.2 at 35,000 ft (no distance is credited, missiles are retained).

7. Climb: on course at best climb speed at intermediate power to best cruise altitude (not to exceed cruise ceiling).

8. Cruise Back: to base at speed and altitudes for best range, using a cruise climb flight path (not to exceed cruise ceiling).

9. Descent: descend to sea level (no fuel used, no distance gained).

10. Reserve: fuel allowance equal to 20 min loiter at sea level at speeds for maximum endurance with all engines operating plus 5% of initial total fuel (internal plus external).

a. Mission Time: Items 2 through 9.
b. Cycle Time: Items 2 through 10.

Note: Loiter altitude and combat variations should be considered for this mission.

10.4.2.6 CLOSE SUPPORT

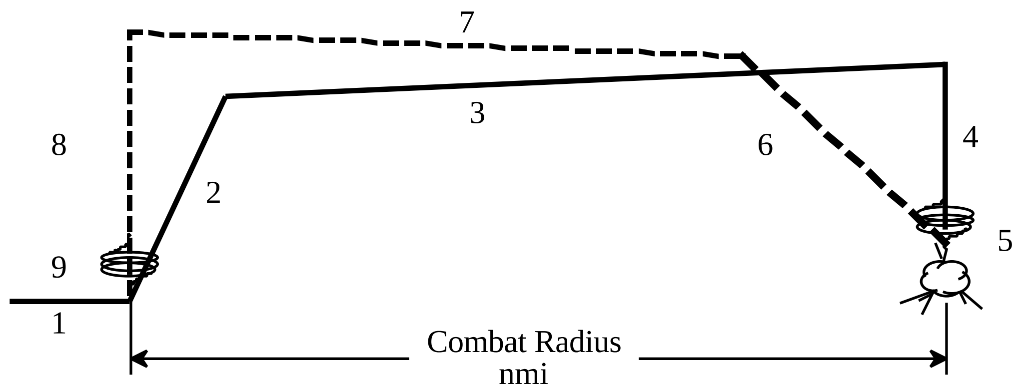

Figure 10.9
CLOSE SUPPORT

1. Taxi, warm-up, takeoff, and acceleration to best climb speed: fuel allowance at sea level static equal 4.6 min at intermediate thrust plus 30 seconds afterburner thrust if afterburner is used for takeoff.

2. Climb: on course at best climb speed at intermediate thrust to best cruise altitudes (not to exceed cruise ceiling).

3. Cruise Out: to target at speeds and altitudes for best range, using a climb flight path (not to exceed cruise ceiling).

4. Descent: descend to 5,000 ft (no fuel used, no distance gained).

5. Loiter: loiter for 1 hour at speed for maximum endurance at 5,000 ft (no distance is credited, drop bombs after loiter, retain mounting hardware and missiles).

6. Climb: on course at best climb speed at intermediate power from 5,000 ft to best cruise altitude (not to exceed cruise ceiling).

7. Cruise Back: to base at speed and altitudes for best range, using a cruise climb flight path (not to exceed cruise ceiling).

8 Descent: descend to sea level (no fuel used, no distance gained).

9. Reserve: fuel allowance equal to 20 min loiter at sea level at speeds for maximum endurance with all engines operating plus 5% of initial total fuel (internal plus external).

a. Mission Time: Items 2 through 8.

b. Cycle Time: Items 2 through 9.

10.4.2.7 FERRY/CROSS COUNTRY NAVIGATION

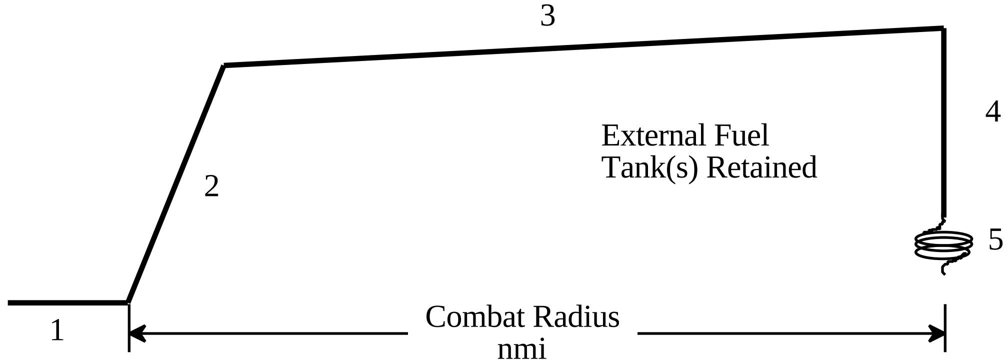

Figure 10.10
FERRY/CROSS COUNTRY NAVIGATION

1. Taxi, warm-up, takeoff, and acceleration to best climb speed: fuel allowance at sea level static equal to 4.6 min at intermediate thrust plus 30 seconds afterburner thrust if afterburner is used for takeoff.

2. Climb: on course at best climb speed at intermediate thrust to best cruise altitude (not to exceed cruise ceiling).

3. Cruise Out: to combat range at speeds and altitudes for best range, using a cruise climb flight path (not to exceed cruise ceiling).

4. Descent: descend to sea level (no fuel used, no distance gained).

5. Reserve: fuel allowance equal to 20 min loiter at sea level at speeds for maximum endurance with all engines operating plus 5% of initial total fuel (internal plus external).

   a. Mission Time: Items 2 through 4.
   b. Cycle Time: Items 2 through 5.

10.4.2.8 INTERDICTION

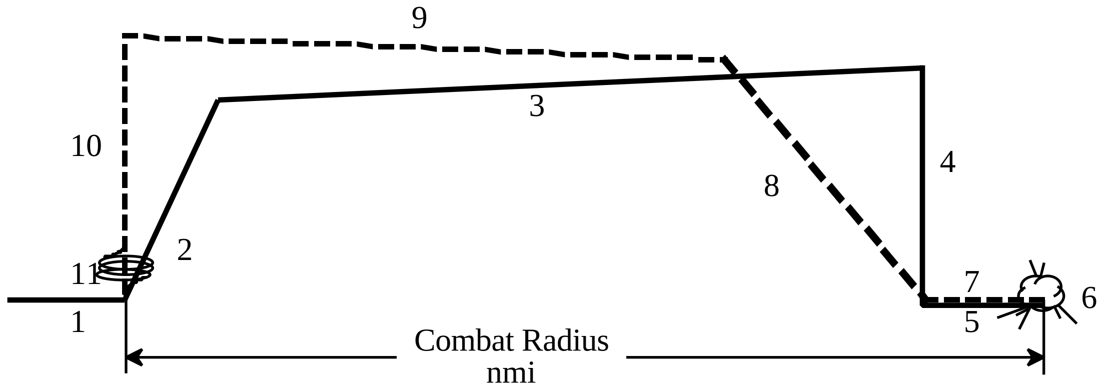

Figure 10.11
INTERDICTION

1. For taxi, warm-up, takeoff and acceleration to best climb speed: fuel allowance at sea level static equal 4.6 min at intermediate thrust plus 30 seconds afterburner thrust if afterburner is used for takeoff.

2. Climb: on course at best climb speed at intermediate thrust to best cruise altitudes (not to exceed cruise ceiling).

3. Cruise Out: at speeds and altitudes for best range, using a climb flight path (not to exceed cruise ceiling).

4. Descent: descend to sea level (no fuel used, no distance gained).

5. Run-in to target: sea level dash for 50 nmi at Mach 0.8 (or maximum speed at intermediate thrust if less than Mach 0.8).

6. Combat: fuel allowance equal to 5 min at intermediate thrust, Mach 0.8 (or maximum speed if less than Mach 0.8) at sea level. No distance is credited (drop bombs, retain mounting hardware and missiles after combat).

7. Run-out from target: sea level dash for 50 nmi at Mach 0.8 (or maximum speed at intermediate thrust if less than Mach 0.8).

8. Climb: on course at best climb speed at intermediate thrust from sea level to best cruise altitude (not to exceed cruise ceiling).

9. Cruise Back: at speeds and altitudes for best range, using a cruise climb flight path (not to exceed cruise ceiling).

10. Descent: descend to sea level (no fuel used, no distance gained).

11. Reserve: fuel allowance equal to 20 min loiter at sea level at speeds for maximum endurance with all engines operating plus 5% of initial total fuel (internal plus external).

   a. Mission Time: Items 2 through 10.
   b. Cycle Time: Items 2 through 11.

10.4.2.9 ALTERNATE INTERDICTION

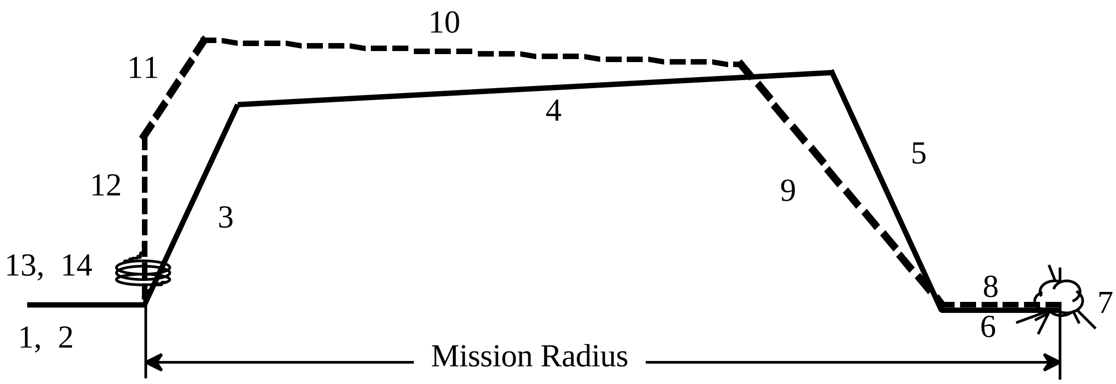

Figure 10.12
ALTERNATE INTERDICTION

1. Takeoff: start engines and takeoff allowance equal to 20 min idle power and 30 seconds intermediate power, sea level static.

2. Acceleration: intermediate power acceleration from 150 KCAS to best climb speed at sea level.

3. Climb: intermediate power climb from sea level to best cruise altitude.

4. Cruise Out: cruise climb at best conditions.

5. Descent: idle power descent to sea level at Mach 0.8 (credit time, fuel, and distance).

6. Dash Out: 50 nmi Mach 0.8 dash at sea level.

7. Combat: fuel allowance equal to 3 (4 g) sustained turns at Mach 0.8 at 5,000 ft (drop bombs; retain mounting hardware and missiles) and 1 maximum power (structural limit) sustained turn at Mach 0.8 at 5,000 ft.

8. Dash Back: 50 nmi Mach 0.8 dash at sea level.

9. Climb: intermediate power climb from sea level to best cruise altitude.

10. Cruise Back: cruise climb at best conditions.

11. Descent: idle power descent to 20,000 ft at 250 KCAS (credit time, fuel and distance).

12. Descent: idle power descent to 1,200 ft at 250 KCAS (credit time and fuel, no credit for distance).

13. Carrier Approach: cruise at 150 KCAS for a distance of 12 nmi at 1,200 ft (credit time and fuel; no credit for distance).

14. Reserve: 100 nmi bingo (no credit for distance). Intermediate power acceleration from 150 KCAS to best climb speed at sea level.

    a. Intermediate power climb from sea level to best profile altitude.
    b. Cruise at best profile altitude(s) at best conditions.
    c. Idle power descent to 10,000 ft at 250 KCAS (credit time, fuel, and distance).
    d. 10 min at 10,000 ft loiter at maximum endurance speed.
    e. Mission Time: Items 3 through 13.
    f. Cycle Time: Items 3 through 14.

10.4.2.10 HI-LO-HI

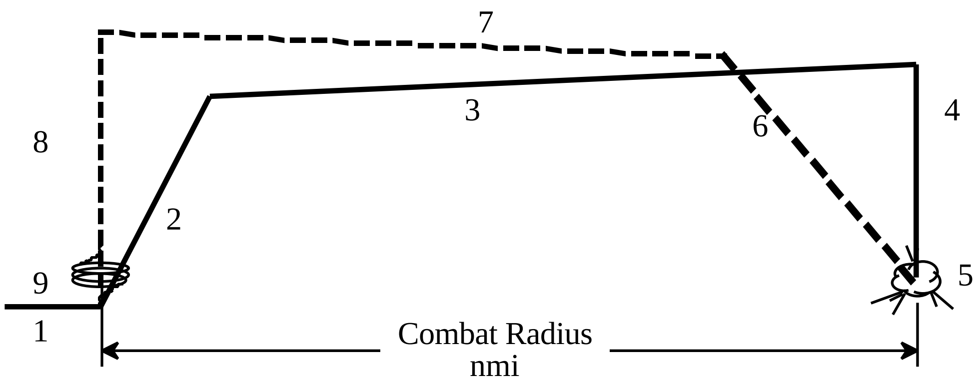

Figure 10.13
HI-LO-HI

1. Taxi, warm-up, takeoff, and acceleration to best climb speed: fuel allowance at sea level static equal to 4.6 min at intermediate thrust plus 30 seconds afterburner thrust if afterburner is used for takeoff.

2. Climb: on course at best climb speed at intermediate thrust to best cruise altitude (not to exceed cruise ceiling).

3. Cruise Out: at speeds and altitudes for best range, using a cruise climb flight path (not to exceed cruise ceiling).

4. Descent: descend to sea level (no fuel used, no distance gained).

5. Combat: fuel allowance equal to 5 min at maximum speed with intermediate thrust at sea level. No distance is credited (drop bombs, retain mounting hardware and missiles after combat).

6. Climb: on course at best climb speed at intermediate thrust from sea level to best cruise altitude (not to exceed cruise ceiling).

7. Cruise Back: at speeds and altitudes for best range, using a cruise climb flight path (not to exceed cruise ceiling).

8. Descent: descend to sea level (no fuel used, no distance gained).

9. Reserve: fuel allowance equal to 20 min loiter at sea level at speeds for maximum endurance with all engines operating plus 5% of initial total fuel (internal plus external).

a. Mission Time: Items 2 through 8.
b. Cycle Time: Items 2 through 9.

10.4.2.11 LO-LO-LO

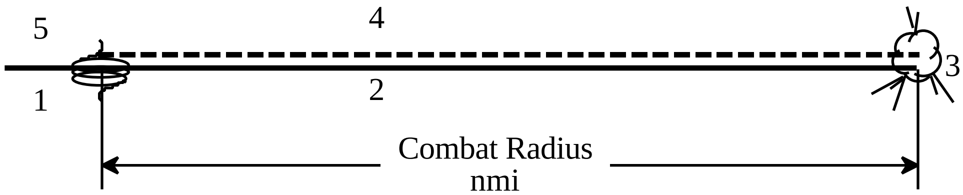

Figure 10.14
LO-LO-LO

1. Taxi, warm-up, takeoff, and acceleration to best cruise speed: fuel allowance at sea level static equal to 4.6 min at intermediate thrust plus 30 seconds afterburner thrust if afterburner is used for takeoff.

2. Cruise Out: at speed for best range at sea level.

3. Combat: fuel allowance equal to 5 min at maximum speed with intermediate thrust at sea level. No distance is credited (drop bombs, retain mounting hardware and missiles after combat).

4. Cruise Back: at speed for best range at sea level.

5. Reserve: fuel allowance equal to 20 min loiter at sea level at speeds for maximum endurance with all engines operating plus 5% of initial fuel (internal plus external).

a. Mission Time: Items 2 through 4.
b. Cycle Time: Items 2 through 5.

Note: An alternate LO-LO-LO mission would include a 50 nmi sea level dash to and from target at Mach 0.8 (or maximum speed at intermediate thrust if less than Mach 0.8).

10.4.2.12 LO-LO-LO-HI

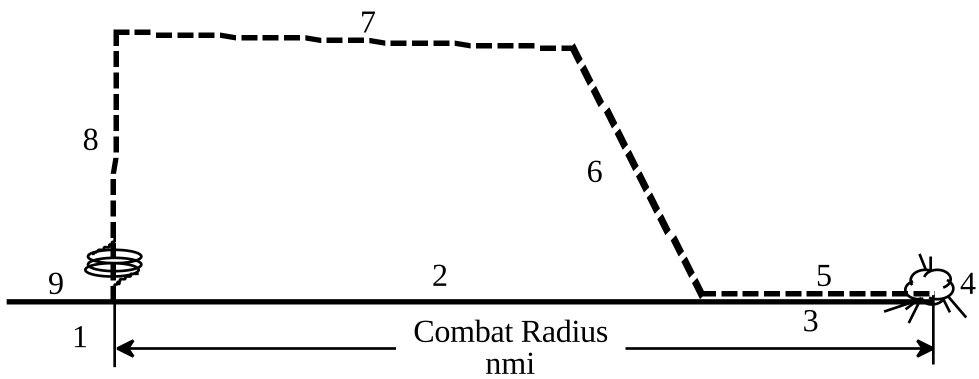

Figure 10.15
LO-LO-LO-HI

1. Taxi, warm-up, takeoff, and acceleration to best climb speed: fuel allowance at sea level static equal to 4.6 min at intermediate thrust plus 30 seconds afterburner thrust if afterburner is used for takeoff.

2. Cruise Out: at speed for best range at sea level.

3. Run-in to target: sea level dash for 50 nmi at Mach 0.8 (or maximum speed at intermediate thrust if less than Mach 0.8).

4. Combat: fuel allowance equal to 5 min at maximum speed with intermediate thrust at sea level. No distance is credited (drop bombs, retain mounting hardware and missiles after combat).

5. Run-out from target: sea level dash for 50 nmi at Mach 0.8 (or maximum speed at intermediate thrust if less than Mach 0.8).

6. Climb: on course at best climb speed at intermediate thrust from sea level to best cruise altitude (not to exceed cruise ceiling).

7. Cruise Back: at speeds and altitudes for best range, using a cruise climb flight path (not to exceed cruise ceiling).

8. Descent: descent to sea level (no fuel used, no distance gained).

9. Reserve: fuel allowance equal to 20 min loiter at sea level at speeds for maximum endurance with all engines operating plus 5% of initial total fuel (internal plus external).

a. Mission Time: Items 2 through 8.
b. Cycle Time: Items 2 through 9.

10.4.3 SPECIAL NAVY OPERATIONAL MISSIONS (REF 7)

10.4.3.1 CARGO AND TRANSPORT

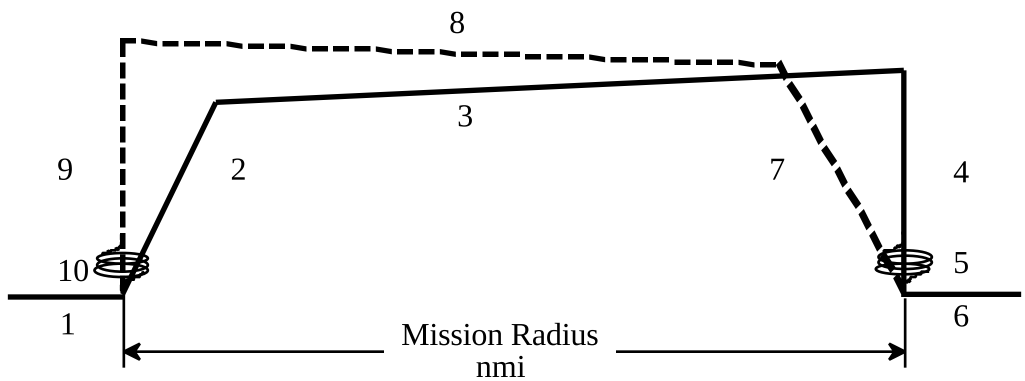

Figure 10.16
CARGO AND TRANSPORT

1. Taxi, warm-up, takeoff, and acceleration to best climb speed: fuel allowance at sea level static equal to 4.6 min at intermediate thrust (10 min for propeller aircraft at normal power) plus 30 seconds afterburner thrust if afterburner is used for takeoff.

2. Climb: on course at best climb speed at intermediate thrust (normal power for props) to best cruise altitude (not to exceed cruise ceiling).

3. Cruise Out: at speeds and altitudes for best range, using a cruise climb flight path (not to exceed cruise ceiling).

4. Descent: descend to sea level (no fuel used, no distance gained).

5. Land at remote base and unload passengers/cargo or pick-up passengers/cargo (specified by NAVAIRSYSCOM for the particular aircraft).

6. Repeat Step 1.

7. Repeat Step 2.

8. Cruise Back: at speeds and altitudes for best range, using a cruise climb flight path (not to exceed cruise ceiling).

9. Descent: descend to sea level (no fuel used, no distance gained).

10. Reserve: fuel allowance equal to 20 min (30 min for props) loiter at sea level at speeds for maximum endurance (maximum range for props) with all engines operating plus 5% of initial total fuel (internal plus external).

a. Mission Time: Items 2 though 9.
b. Cycle Time: Items 2 through 10.

10.4.3.2 ASW SEARCH

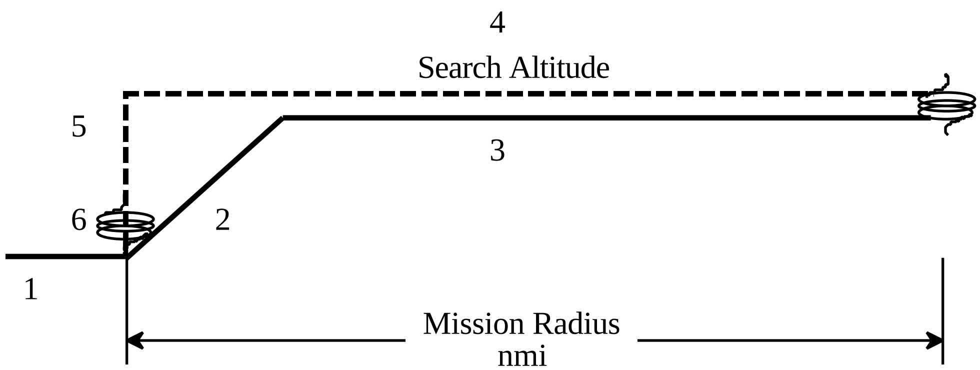

Figure 10.17
ASW SEARCH

1. Taxi, warm-up, takeoff, and acceleration to best climb speed: fuel allowance at sea level static equal to 4.6 min at intermediate thrust (10 min for propeller aircraft at normal power) plus 30 seconds afterburner thrust if afterburner is used for takeoff.

2. Climb: on course at best climb speed at intermediate thrust (normal power for props) to search altitude (not to exceed cruise ceiling).

3. Cruise Out: at search altitude at speed for maximum endurance (unless otherwise limited by handling qualities).

4. Cruise Back: at search altitude at speed for maximum endurance (unless otherwise limited by handling qualities).

5. Descent: descend to sea level (no fuel used, no distance gained).

6. Reserve: fuel allowance equal to 20 min (30 min for props) loiter at sea level at speeds for maximum endurance (maximum range for props) with all engines operating plus 5% of initial total fuel (internal plus external).

   a. Mission Time: Items 2 through 5.
   b. Cycle Time: Items 2 through 6.

10.4.3.3 AEW SEARCH

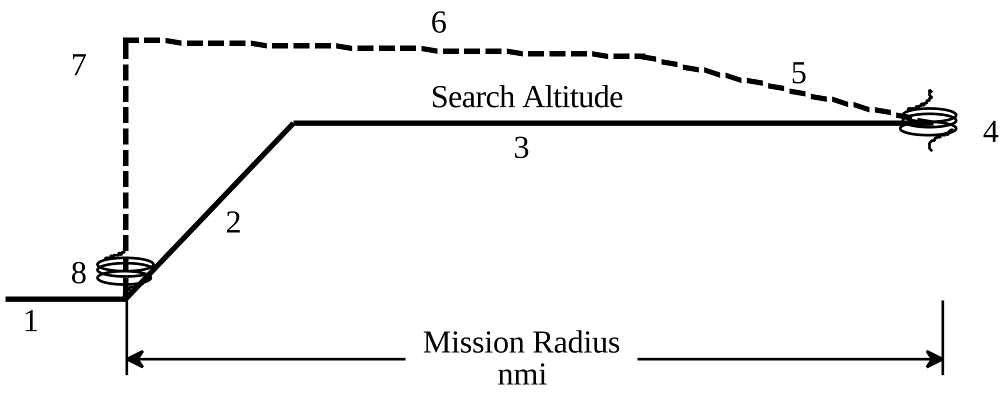

Figure 10.18
AEW SEARCH

1. Taxi, warm-up, takeoff, and acceleration to best climb speed: fuel allowance at sea level static equal to 4.6 min at intermediate thrust (10 min for propeller aircraft at normal power) plus 30 seconds afterburner thrust if afterburner is used for takeoff.

2. Climb: on course at best climb speed at intermediate thrust (normal power for props) to search altitude (not to exceed cruise ceiling).

3. Cruise Out: at speeds for best range at search altitude (not to exceed cruise ceiling) to distance specified by NAVAIRSYSCOM.

4. Loiter: loiter for 4 hours at speed for maximum endurance at search altitude (no distance is gained).

5. Climb: on course at best climb speed at intermediate thrust (normal power for props) to best cruise altitude (if higher than search altitude, but not to exceed cruise ceiling.

6. Cruise Back: at speeds and altitudes for best range, using a cruise climb flight path (not to exceed cruise ceiling).

7. Descent: descend to sea level (no fuel used, no distance gained).

8. Reserve: fuel allowance equal to 20 min (30 min for props) loiter at sea level at speeds for maximum endurance (maximum range for props) with all engines operating plus 5% initial total fuel internal plus external).

a. Mission Time: Items 2 through 7.
b. Cycle Time: Items 2 through 8.

10.4.3.4 ASW

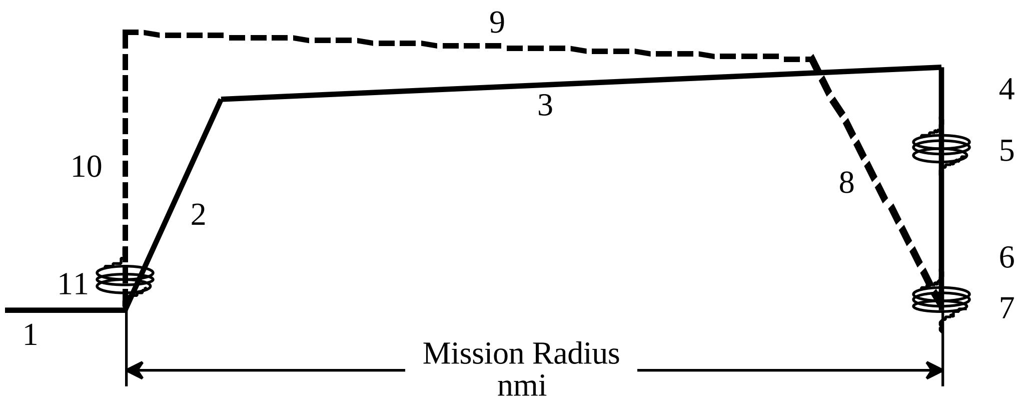

Figure 10.19
ASW

1. Taxi, warm-up, takeoff, and acceleration to best climb speed: fuel allowance at sea level static equal to 4.6 min at intermediate thrust (10 min for propeller aircraft at normal power) plus 30 seconds afterburner thrust if afterburner is used for takeoff.

2. Climb: on course at best climb speed at intermediate thrust (normal power for props) to best cruise altitude (not to exceed cruise ceiling).

3. Cruise Out: at speeds and altitudes for best range, using a cruise climb flight path (not to exceed cruise ceiling).

4. Descent: descend to 20,000 ft (no fuel used, no distance gained).

5. Search: search for 3 hours at speed for maximum endurance at 20,000 ft.

6. Descent: descend to 200 ft (no fuel used, no distance gained).

7. Search: search for 1 hour at speed for maximum endurance at 200 ft.

8. Climb: on course at best climb speed at intermediate thrust (normal power for props) to best cruise altitude (not to exceed cruise ceiling).

9. Cruise Back: at speeds and altitudes for best range, using a cruise climb flight path (not to exceed cruise ceiling).

10. Descent: descend to sea level (no fuel used, no distance gained).

11. Reserve: fuel allowance equal to 20 min (30 min for props) loiter at sea level at speeds for maximum endurance (maximum range for props) with all engines operating plus 5% of initial total fuel (internal plus external).

   a. Mission Time: Items 2 through 10.
   b. Cycle Time: Items 2 through 11.

10.4.3.5 RECONNAISSANCE

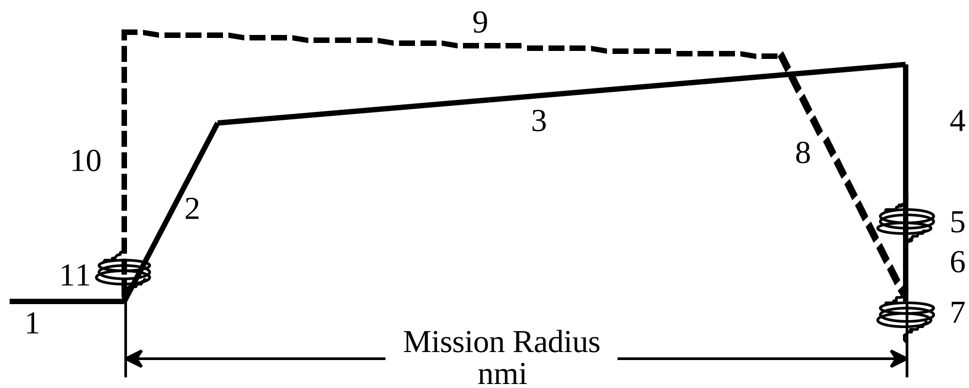

Figure 10.20
RECONNAISSANCE

1. Taxi, warm-up, takeoff, and acceleration to best climb speed: fuel allowance at sea level static equal to 4.6 min at intermediate thrust (10 min for propeller aircraft at normal power) plus 30 seconds afterburner thrust if afterburner is used for takeoff.

2. Climb: on course at best climb speed at intermediate thrust (normal power for props) to best cruise altitude (not to exceed cruise ceiling).

3. Cruise Out: at speeds and altitudes for best range, using a cruise climb flight path (not to exceed cruise ceiling).

4. Descent: descend to 5,000 ft (no fuel used, no distance gained).

5. Search: search for 3 hours at speed for maximum endurance at 5,000 ft.

6. Descent: descend to 200 ft (no fuel used, no distance gained).

7. Search: search for 1 hour at speed for maximum endurance at 200 ft.

8. Climb: on course at best climb speed at intermediate thrust (normal power for props) from 200 ft to best cruise altitude (not to exceed cruise ceiling).

9. Cruise Back: at speeds and altitudes for best range, using a cruise climb flight path (not to exceed cruise ceiling).

10. Descent: descend to sea level (no fuel used, no distance gained).

11. Reserve: fuel allowance equal to 20 min (30 min for props) loiter at sea level at speeds for maximum endurance (maximum range for props) with all engines operating plus 5% of initial total fuel (internal plus external).

a. Mission Time: Items 2 through 10.
b. Cycle Time: Items 2 through 11.

10.4.3.6 MINELAYING

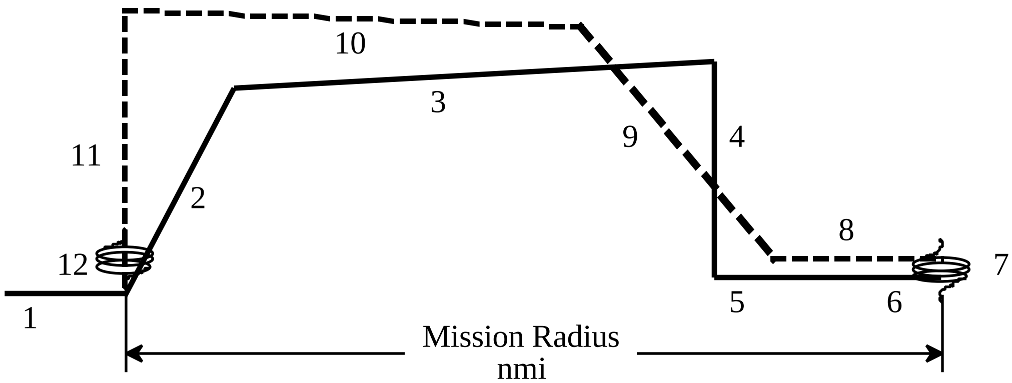

Figure 10.21
MINELAYING

1. Taxi, warm-up, takeoff, and acceleration to best climb speed: fuel allowance at sea level static equal to 4.6 min at intermediate thrust (10 min for propeller aircraft at normal power) plus 30 seconds afterburner thrust if afterburner is used for takeoff.

2. Climb: on course at best climb speed at intermediate thrust (normal power for props) to best cruise altitude (not to exceed cruise ceiling).

3. Cruise Out: at speeds and altitudes for best range, using a cruise climb flight path (not to exceed cruise ceiling).

4. Descent: descend to 200 ft (no fuel used, no distance gained).

5. Penetrate: at maximum continuous power for 300 nmi at 200 ft.

6. Attack: at maximum continuous power for 100 nmi at 200 ft.

7. Release Mines.

8. Escape: on course at maximum continuous power for 300 nmi.

9. Climb: on course at best climb speed at intermediate thrust (normal power for props) from 200 ft to best cruise altitude (not to exceed cruise ceiling).

10. Cruise Back: at speeds and altitudes for best range, using a cruise climb flight path (not to exceed cruise ceiling).

11. Descent: descend to sea level (no fuel used, no distance gained).

12. Reserve: fuel allowance equal to 20 min (30 min for props) loiter at sea level at speeds for maximum endurance (maximum range for props) with all engines operating plus 5% of initial total fuel (internal plus external).

a. Mission Time: Items 2 through 11.
b. Cycle Time: Items 2 through 12.

10.4.3.7 REFUEL/BUDDY TANKER

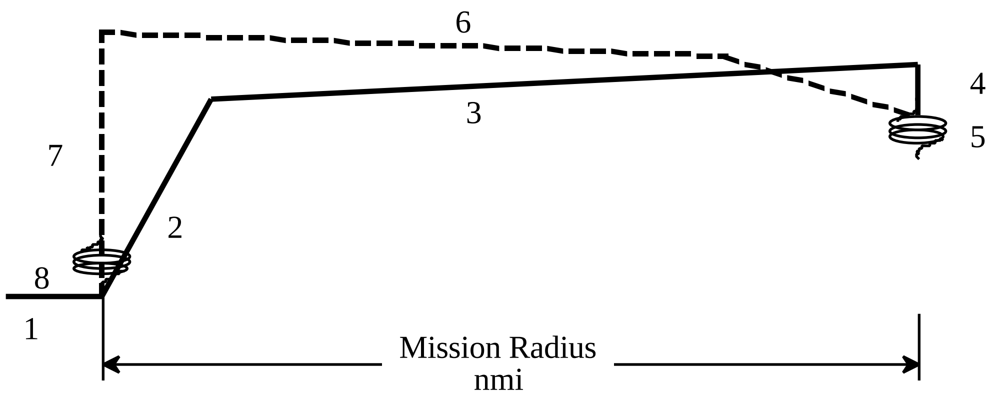

Figure 10.22
REFUEL/BUDDY TANKER

1. Taxi, warm-up, takeoff, and acceleration to best climb speed: fuel allowance at sea level static equal to 4.6 min at intermediate thrust (10 min for propeller aircraft at normal power) plus 30 seconds afterburner thrust if afterburner is used on takeoff.

2. Climb: on course at best climb speed at intermediate thrust (normal power for props) to best cruise altitude (not to exceed cruise ceiling).

3. Cruise Out: at speeds and altitudes for best range, using cruise climb flight path (not to exceed cruise ceiling) to point of rendezvous specified by NAVAIRSYSCOM.

4. Descent: descend to 20,000 ft (no fuel used, no distance gained).

5. Loiter: loiter for 1 hour at speed for maximum endurance to allow for rendezvous, hookup, and fuel transfer (no distance gained).

6. Climb: on course at best climb speed intermediate thrust (normal power for props) to best cruise altitude (not to exceed cruise ceiling).

7. Descent: descend to sea level (no fuel used, no distance gained).

8. Reserve: fuel allowance equal to 20 min (30 min for props) at sea level at speeds for maximum endurance (maximum range for props) with all engines operating plus 5% of initial total fuel (internal plus external).

a. Mission Time: Items 2 through 7.
b. Cycle Time: Items 2 through 8.

10.4.3.8 FAMILIARIZATION

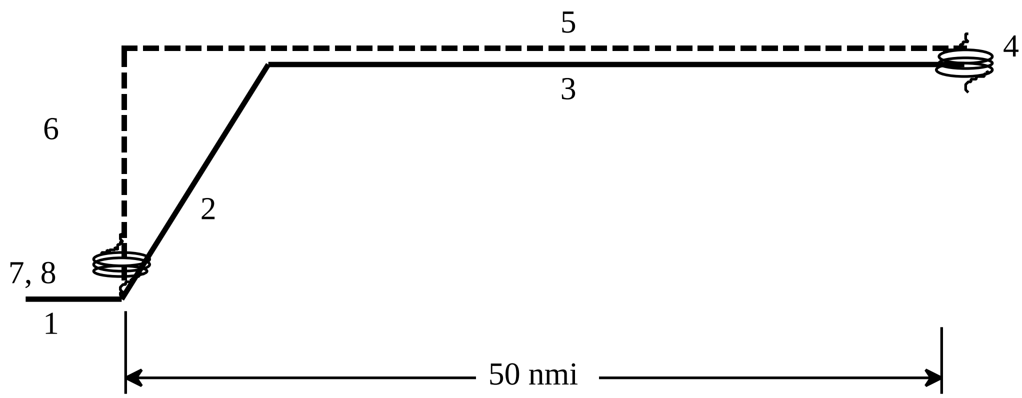

Figure 10.23
FAMILIARIZATION

1. Taxi, warm-up, takeoff, and acceleration to best climb speed: fuel allowance at sea level static equal to 4.6 min at intermediate thrust plus 30 seconds afterburner thrust if afterburner is used for takeoff.

2. Climb: on course at best climb speed at intermediate climb point at speed for best range at 20,000 ft.

3. Cruise Out: 50 nmi from initial climb point at speed for best range at 20,000 ft.

4. Air work at 20,000 ft: time for air work shall be allocated as follows: 35% at intermediate thrust (Mach equals corner speed), 45% at speed for maximum range, and 20% at flight idle (no distance gained).

5. Cruise Back: 50 nmi at speed for maximum range at 20,000 ft.

6. Descent: descend to sea level (no fuel used, no distance gained).

7. Six touch and go landings: fuel allowance equal to 30 min at approach airspeed in landing configuration and 2 min at intermediate thrust (sea level static).

8. Reserve: fuel allowance equal to 20 min loiter at sea level at speeds for maximum endurance with all engines operating plus 5% of initial total fuel (internal plus external).

a. Mission Time Items 2 through 7.
b. Cycle Time: Items 2 through 8.

10.4.3.9 CARRIER QUALIFICATION

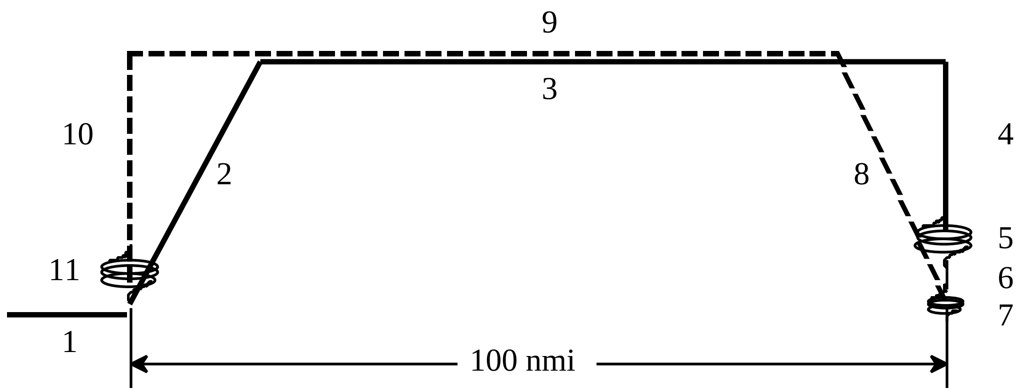

Figure 10.24
CARRIER QUALIFICATION

1. Taxi, warm-up, takeoff, and acceleration to best climb speed: fuel allowance at sea level static equal to 4.6 min at intermediate thrust plus 30 seconds afterburner thrust if afterburner is used to takeoff.

2. Climb: on course at best climb speed at intermediate thrust to 20,000 ft.

3. Cruise Out: 100 nmi from initial climb point at speed for best range at 20,000 ft.

4. Descent: descend to 5,000 ft (no fuel used, no distance gained).

5. Loiter: loiter for 15 min at speed for maximum endurance at 5,000 ft.

6. Descent: descend to sea level (no fuel used, no distance gained).

7. Carrier Work: fuel allowance (for each catapult launch and arrested landing cycle) equals 4.5 min at approach speed in landing configuration and 30 seconds at intermediate thrust (sea level static).

8. Climb: on course at best climb speed at intermediate thrust from sea level to 20,000 ft.

9. Cruise Back: 100 nmi at speed for maximum range at 20,000 ft.

10. Descent: descend to sea level (no fuel used, no distance gained).

11. Reserve: fuel allowance equal to 20 min loiter at sea level at speeds for maximum endurance with all engines operating plus 5% of initial total fuel (internal plus external).

a. Mission time: Items 2 through 10.
b. Cycle Time: Items 2 through 11.

10.4.3.10 AIR COMBAT MANEUVERING TRAINING

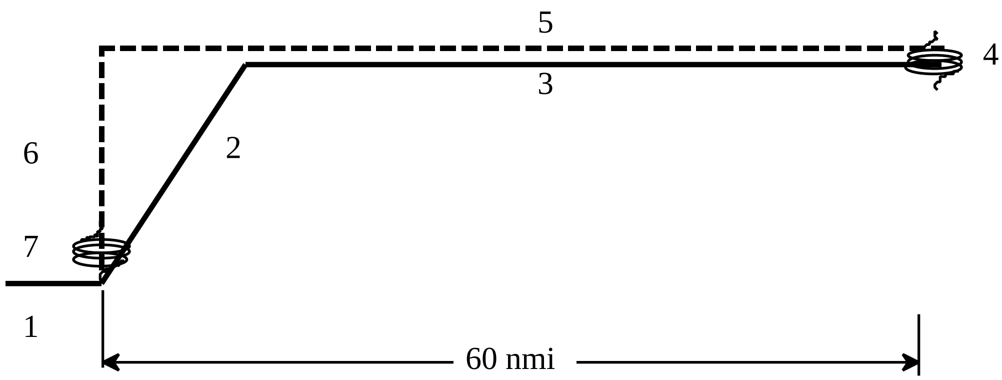

Figure 10.25
AIR COMBAT MANEUVERING TRAINING

1. Taxi, warm-up, takeoff, and acceleration to best climb speed: fuel allowance at sea level static equal to 4.6 min at intermediate thrust plus 30 seconds afterburner thrust if afterburner is used for takeoff.

2. Climb: on course at best climb speed at intermediate thrust to 25,000 ft.

3. Cruise Out: 60 nmi from initial climb point at speed for best range at 25,000 ft.

4. Air work at 25,000 ft: time for air work shall be allocated as follows: 55% at intermediate thrust (Mach equals corner speed), 30% at 80% intermediate thrust fuel flow (Mach equals corner speed), and 15% at speed for best range (no distance gained).

5. Cruise Back: 60 nmi at speed for best range.

6. Descent: descend to sea level (no fuel used, no distance gained).

7. Reserve: fuel allowance equal to 20 min loiter at sea level at speeds for maximum endurance with all engines operating plus 5% of initial total fuel (internal plus external).

a. Mission Time: Items 2 through 6.
b. Cycle Time: Items 2 through 7.

10.4.3.11 TACTICAL NAVIGATION

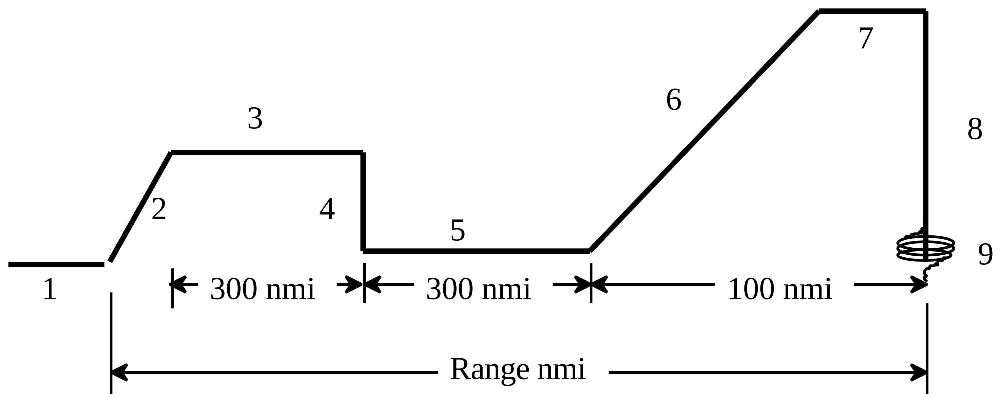

Figure 10.26
TACTICAL NAVIGATION

1. Taxi, warm-up, takeoff, and acceleration to best climb speed: fuel allowance at sea level static equal to 4.6 min at intermediate thrust plus 30 seconds afterburner thrust if afterburner is used for takeoff.

2. Climb: on course at best climb speed at intermediate thrust to 2,500 ft.

3. Cruise: 300 nmi at 300 KTAS at 2,500 ft.

4. Descent: descend to 500 ft (no fuel used, no distance gained).

5. Cruise: 300 nmi at 300 KTAS at 500 ft.

6. Climb: on course at best climb speed at intermediate thrust from 500 ft to 20,000 ft.

7. Cruise: 100 nmi from climb point at speed for best range at 20,000 ft.

8. Descent: descend to sea level (no fuel used, no distance gained).

9. Reserve: fuel allowance equal to 20 min loiter at sea level at speeds for maximum endurance with all engines operating plus 5% of initial total fuel (internal plus external).

a. Mission Time: Items 2 through 8.
b. Cycle Time: Items 2 through 9.

10.4.3.12 WEAPONS DELIVERY/GUNNERY

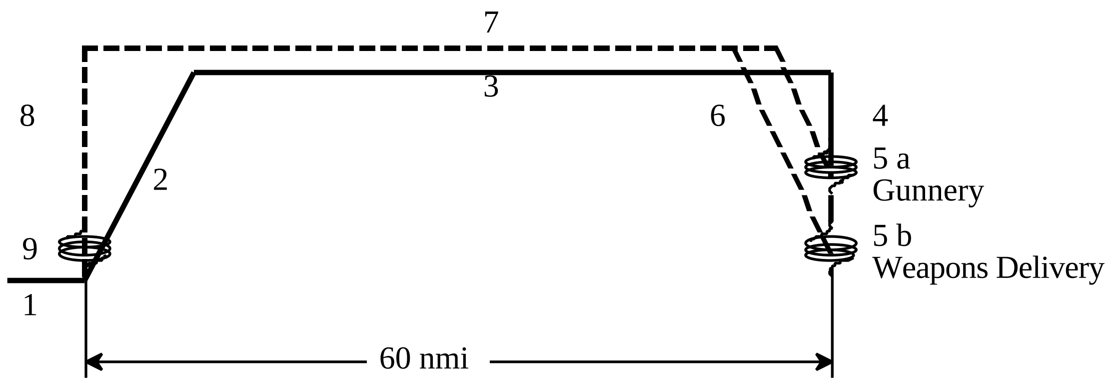

Figure 10.27
WEAPON DELIVERY/GUNNERY

1. Taxi, warm-up, takeoff, and acceleration to best climb speed: fuel allowance at sea level static equal to 4.6 min at intermediate thrust plus 30 seconds afterburner thrust if afterburner is used for takeoff.

2. Climb: on course at best climb speed at intermediate climb point at speed for best range at 20,000 ft.

3. Cruise Out: 60 nmi from initial climb point at speed for best range at 20,000 ft.

4. Descent: descend to gunnery altitude (10,000 ft) or weapons delivery altitude (sea level) (no fuel used, no distance gained).

5 a. Gunnery Option: time for gunnery shall be allocated as follows: 60% at intermediate thrust (Mach to be designated by NAVAIRSYSCOM), 25% at 80% intermediate thrust fuel flow (Mach to be designated by NAVAIRSYSCOM), and 15% at speed for best range (no distance gained).

5 b. Weapons Delivery Option: time for weapons delivery shall be allocated as follows: 50% at intermediate thrust (Mach to be designated by NAVAIRSYSCOM) and 50% at 80% intermediate thrust fuel flow (Mach to be designated by NAVAIRSYSCOM) (no distance gained).

6. Climb: on course at best climb speed at intermediate thrust from gunnery (10,000 ft) or weapons delivery (sea level) altitude.

7. Cruise Back: 60 nmi from climb point at speed for best range at 20,000 ft.

8. Descent: descend to sea level (no fuel used, no distance gained).

9. Reserve: fuel allowance equal to 20 min loiter at sea level at speeds for maximum endurance with all engines operating plus 5% of initial total fuel (internal plus external).

   a. Mission Time Items 2 through 8.
   b. Cycle Time: Items 2 through 9.

10.4.4 NAVY PILOT TRAINER MISSIONS (REF 6)

10.4.4.1 FAMILIARIZATION

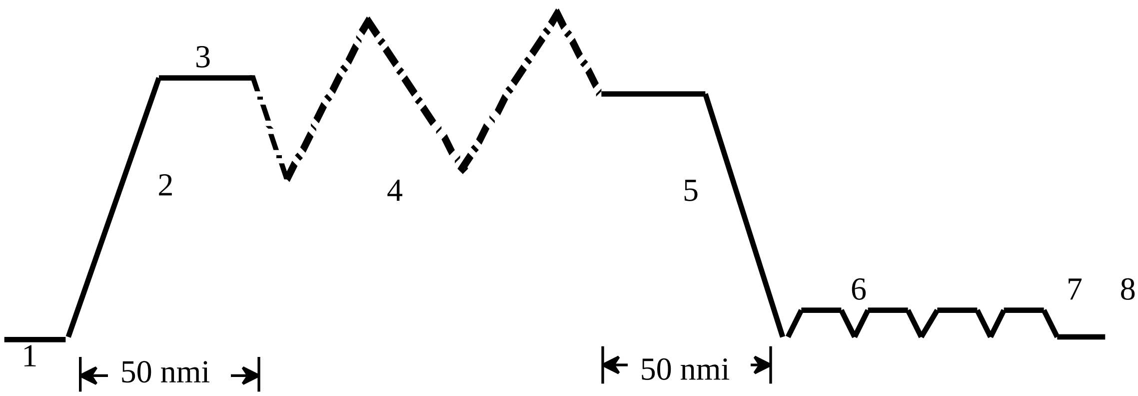

Figure 10.28
FAMILIARIZATION

1. Engine start, taxi, and takeoff: 15 min at idle thrust plus 1 min at maximum thrust (both at sea level static).

2. Climb to 20,000 ft with intermediate thrust.

3. Cruise to 50 nmi from initial climb point at 20,000 ft at airspeed for maximum specific range.

4. Basic Familiarization (FAM) Stage air work (at 20,000 ft):

   a. 10 min at maximum thrust (0.7 Mach).
   b. 8.7 min at airspeed for maximum specific range.
   c. 5.5 min at flight idle.
   d. Aerobatics.
   e. Stalls.
   f. Spins.
   g. Slow flight.
   h. Unusual attitude recoveries.

5. Cruise back at 20,000 ft at speed for maximum specific range and descend to field elevation (cruise back and descent distance 50 nmi).

6. Six touch and go landings with one full stop landing: 30 min at approach airspeed in landing configuration, 1.6 min at maximum thrust.

7. Taxi/shutdown: 3 min at sea level static idle.

8. Reserve: 20 min at sea level at airspeed for maximum specific endurance.

   a. Mission Time Items 2 through 6.
   b. Cycle Time: Items 2 through 8.

10.4.4.2 NIGHT FAMILIARIZATION

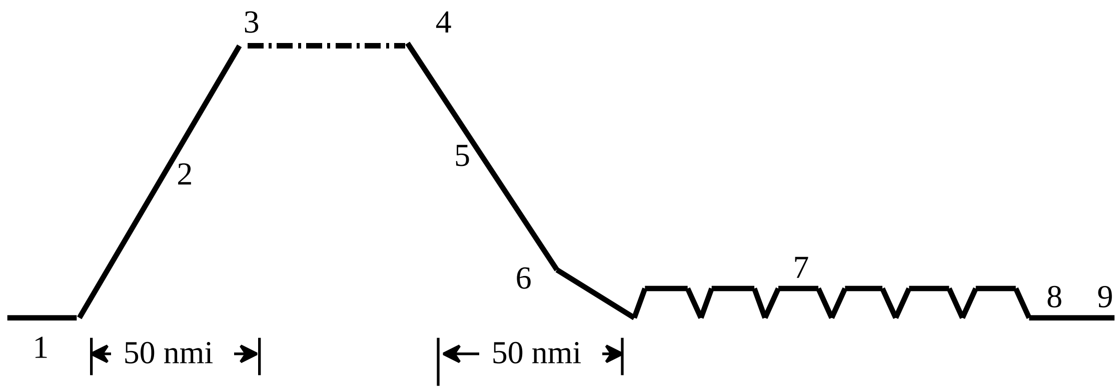

Figure 10.29
NIGHT FAMILIARIZATION

1. Engine start, taxi, and takeoff: 15 min as idle thrust plus 1 min at maximum thrust (both at sea level static).

2. Climb to 20,000 ft with maximum thrust.

3. Cruise to 50 nmi from initial climb point at 20,000 ft at airspeed for maximum specific range.

4. Night FAM training: 40.2 min at airspeed for maximum specific range at 20,000 ft, 2 min at maximum thrust at 20,000 ft (0.7 Mach).

5. Cruise back at 20,000 ft at airspeed for maximum specific range and descend to 3,000 ft (cruise and descent distance 50 nmi).

6. Precision approach (ground controlled approach/instrument landing system (GCA/ILS)) to touch and go: 2 min (flaps and gear-up) at airspeed for maximum specific endurance at 3,000 ft, 6 min at approach airspeed in landing configuration.

7. 6 visual flight rules (VFR) patterns; 5 touch and go, 1 full stop landing: 1.5 min at maximum thrust, 25.5 min at approach airspeed (all in landing configuration).

8. Taxi/shutdown: 3 min at sea level idle thrust.

9. Reserve Fuel: 20 min at sea level at airspeed for maximum specific endurance.

a.	Mission Time	Items 2 through 7.
b.	Cycle Time:	Items 2 through 9.

10.4.4.3 BASIC INSTRUMENTS

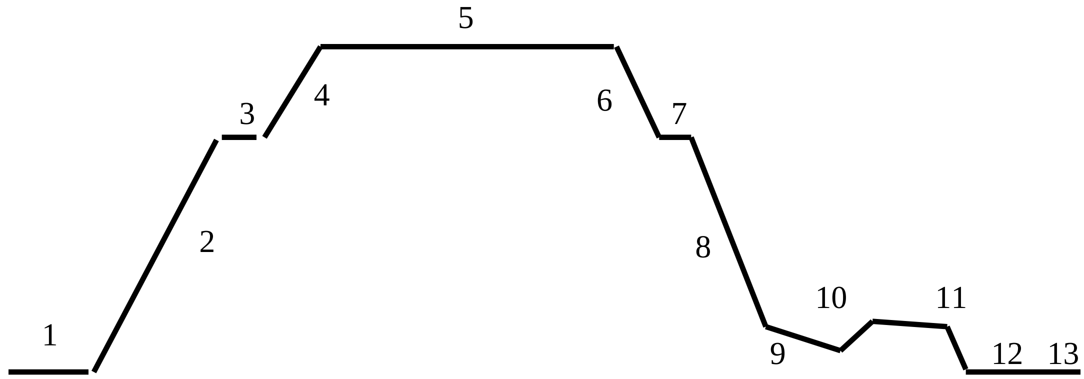

Figure 10.30
BASIC INSTRUMENTS

1. Engine start, taxi, and takeoff: 11 min at idle thrust plus 1 min at maximum thrust (both at sea level static).

2. Climb to 20,000 ft with maximum thrust.

3. 5 min at 20,000 ft at airspeed for maximum specific range.

4. Climb from 20,000 ft to 30,000 ft with maximum thrust.

5. Basic air work: 4 min at maximum thrust (0.7 Mach) plus 36.5 min at 30,000 ft at airspeed for maximum specific range.

6. Descend from 30,000 ft to 20,000 ft at 250 KCAS.

7. 6 min at 20,000 ft at airspeed for maximum specific endurance.

8. Descend from 20,000 to 1,500 ft at 250 KCAS.

9. Non-precision approach: 4 min at approach airspeed in landing configuration.

10. Missed approach: climb to 3,000 ft with maximum thrust.

11. GCA to touchdown: 2 min at airspeed for maximum specific range (gear and flaps up), 6 min at approach airspeed in landing configuration.

12. Taxi/shutdown: 3 min at sea level static idle.

13. Reserve fuel: 20 min at sea level at airspeed for maximum specific endurance.

a. Mission Time Items 2 through 11.
b. Cycle Time: Items 2 through 13.

10.4.4.4 RADIO INSTRUMENTS

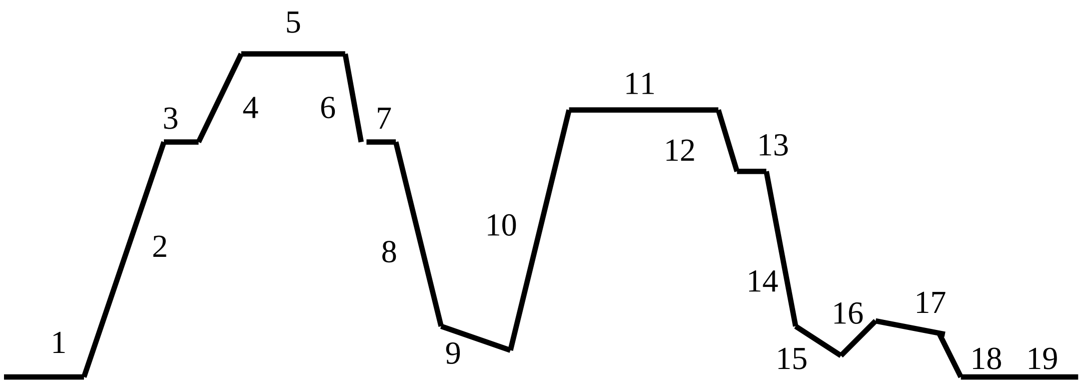

Figure 10.31
RADIO INSTRUMENTS

1. Engine start, taxi, and takeoff: 11 min at idle thrust plus 1 min at maximum thrust (both at sea level static).

2. Climb to 20,000 ft with maximum thrust.

3. 10 min at 20,000 ft at airspeed for maximum specific range.

4. Climb from 20,000 ft to 30,000 ft with intermediate thrust.

5. 19.3 min at 30,000 ft at airspeed for maximum specific range.

6. Descend from 30,000 ft to 20,000 ft at 250 KCAS.

7. 5 min at 20,000 ft at airspeed for maximum specific endurance.

8. High altitude (tactical air navigation/automatic direction finder (TACAN/ADF)) penetration to 1,500 ft.

9. Precision approach (GCA/ILS) in landing configuration: 4 min at approach airspeed.

10. Missed approach: climb to 25,000 ft.

11. 13 min at maximum specific range airspeed (enroute alternate).

12. Descend to 20,000 ft at 250 KCAS.

13. 5 min at 20,000 ft at maximum specific endurance airspeed.

14. High altitude penetration (TACAN/ADF) to 1,500 ft (250 KCAS).

15. Non-Precision final approach: 4 min at approach airspeed in landing configuration.

16. Missed approach: climb to 3,000 ft with maximum thrust.

17. GCA pattern to touchdown: 2 min at airspeed for maximum specific range (gear and flaps up), 6 min at approach airspeed in landing configuration.

18. Taxi/shutdown: 3 min at sea level static idle.

19. Reserve fuel: 20 min at seal level at airspeed for maximum specific endurance.

a. Mission Time Items 2 through 17.
b. Cycle Time: Items 2 through 19.

10.4.4.5 AIRWAYS NAVIGATION - 1

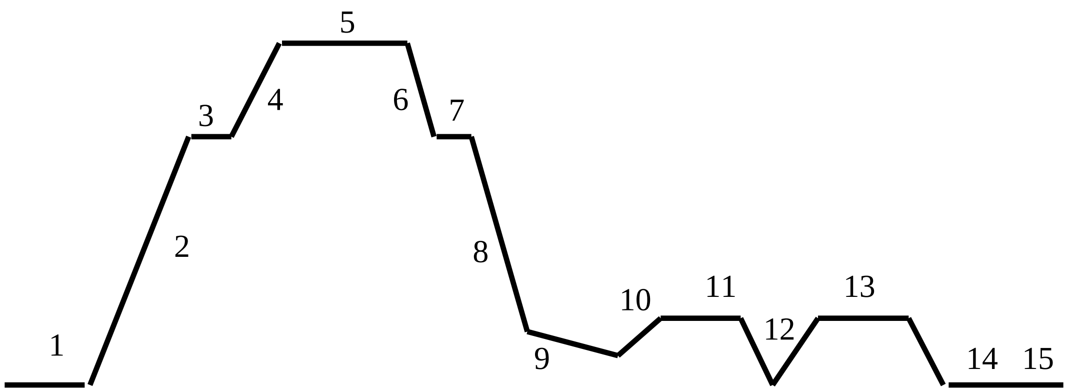

Figure 10.32
AIRWAYS NAVIGATION - 1

1. Engine start, taxi,and takeoff: 11 min at idle thrust plus 1 min at maximum thrust (both at sea level static).

2. Climb to 20,000 ft with maximum thrust.

3. 5 min at 20,000 ft at airspeed for maximum specific range.

4. Climb to 30,000 ft with maximum thrust.

5. Cruise at 30,000 ft at airspeed for maximum specific range.

6. Descend to 20,000 ft.

7. Hold at 20,000 ft for 6 min at airspeed for maximum specific endurance.

8. High altitude instrument penetration (TACAN/ADF) to 1,500 ft at 250 KCAS.

9. Non-precision final approach (TACAN): 4 min at approach speed in landing configuration.

10. Missed approach: climb to 3,000 ft with maximum thrust.

11. GCA pattern/precision approach (GCA/ILS) to low approach: 2 min at 3,000 ft (gear and flaps up), 6 min at approach speed in landing configuration.

12. Missed approach: climb to 3,000 ft with maximum thrust.

13. GCA pattern/precision approach (GCA/ILS) to full stop landing: 2 min at 3,000 ft (gear and flaps up), 6 min at approach speed in landing configuration.

14. Taxi/shutdown: 3 min at sea level static idle.

15. Reserve fuel: 20 min at sea level at airspeed for maximum specific endurance.

a.	Mission Time	Items 2 through 13.
b.	Cycle Time:	Items 2 through 15.

10.4.4.6 AIRWAYS NAVIGATION - 2

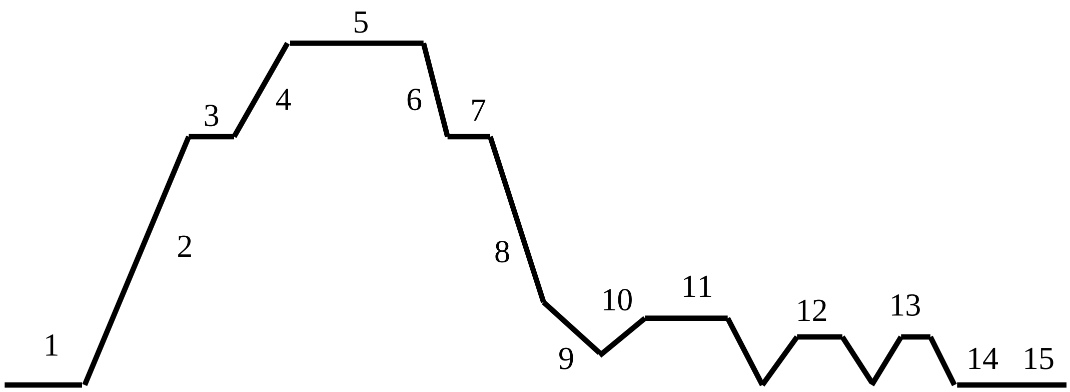

Figure 10.33
AIRWAYS NAVIGATION - 2

1. Engine start, taxi, and takeoff: 11 min at idle thrust plus 1 min at maximum thrust (both at sea level static).

2. Climb to 20,000 ft with maximum thrust.

3. Cruise for 10 min at 20,000 ft at airspeed for maximum specific range.

4. Climb from 20,000 to 35,000 ft with maximum thrust.

5. Cruise at 35,000 ft at airspeed for maximum specific range.

6. Descend from 35,000 to 20,000 ft.

7. Hold at 20,000 ft for one min at airspeed for maximum endurance.

8. High altitude penetration (TACAN/Radar Enroute Descent) 250 KCAS from 20,000 to 3,000 ft.

9. Non-precision final approach (TACAN): 4 min approach airspeed in landing configuration from 3,000 ft to minimum descent altitude (MDA).

10. Missed approach: climb to 3,000 ft with maximum thrust.

11. GCA Pattern, GCA approach to touch and go: 2 min at 3,000 ft (gear and flaps up), 6 min at approach speed in landing configuration.

12. VFR pattern to touch and go: 15 seconds at maximum thrust, 4.25 min at approach airspeed in landing configuration.

13. VFR pattern to full stop: 15 seconds at maximum thrust, 4.25 min at approach airspeed in landing configuration.

14. Taxi/shutdown: 3 min sea level static idle.

15. Reserve fuel: 20 min at sea level at airspeed for maximum specific endurance.

a. Mission Time Items 2 through 13.
b. Cycle Time: Items 2 through 15.

10.4.4.7 FORMATION

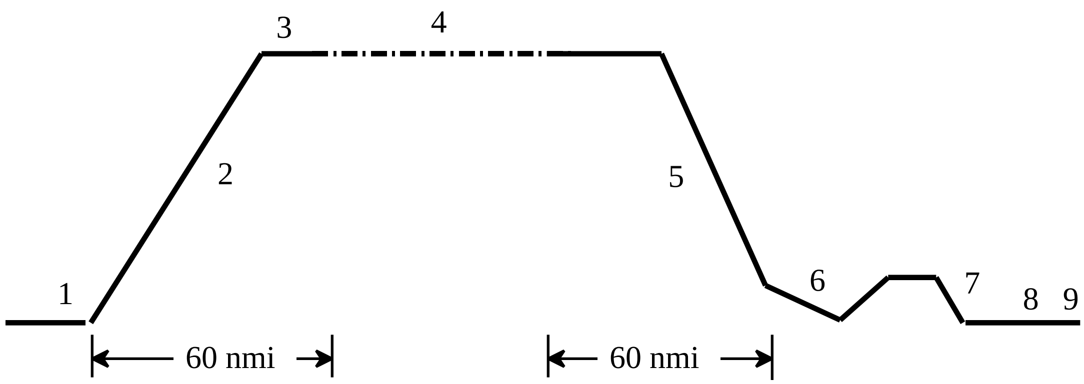

Figure 10.34
FORMATION

1. Engine start, taxi, and takeoff: 13 min at idle thrust plus 1 min at maximum thrust (both at sea level static).

2. Climb to 25,000 ft with maximum thrust.

3. Cruise to 60 nmi from initial climb point at 25,000 ft at airspeed for maximum specific range.

4. Formation Training: 8 min at maximum thrust, 14.8 min at maximum continuous thrust, 33.2 min at airspeed for maximum specific range:

   a. Break-up and rendezvous.
   b. Parade.
   c. Lead changes.
   d. Cruise.
   e. Column.

5. Cruise back at airspeed for maximum specific range at 25,000 ft and descend to 1,500 ft (cruise back & descent distance totals 60 nmi).

6. VFR field entry to touch and go landing: 4 min at 1,500 ft. 300 KCAS (gear and flaps up), 1 min at approach airspeed in landing configuration.

7. VFR landing pattern to full stop landing: 15 seconds at maximum thrust, 4.25 min at approach airspeed in landing configuration.

8. Taxi/shutdown: 3 min at sea level idle thrust.

9. Reserve fuel: 20 min at seal level at airspeed for maximum specific endurance.

   a. Mission Time — Items 2 through 7.
   b. Cycle Time: — Items 2 through 9.

10.4.4.8 NIGHT FORMATION

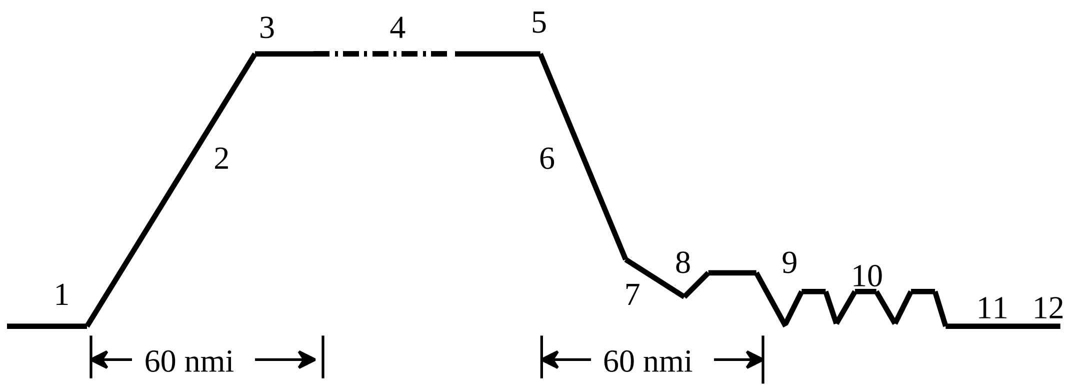

Figure 10.35
NIGHT FORMATION

1. Engine start, taxi, and takeoff: 15 min at idle thrust plus 1 min at maximum thrust (both at sea level static).

2. Climb to 25,000 ft with maximum thrust.

3. Cruise to 60 nmi from initial climb point at 25,000 ft at airspeed for maximum specific range.

4. Formation Maneuvers at 25,000 ft: 1.5 min at maximum thrust, 5.5 min at maximum continuous thrust, 30.9 min at maximum specific range airspeed.

5. Cruise back at 25,000 ft for return to field at airspeed for maximum specific range.

6. Section TACAN penetration from 25,000 ft to 1,500 ft at 250 KCAS (cruise back and TACAN penetration distance total 60 nmi).

7. Section non-precision final approach: 4 min at approach airspeed in landing configuration.

8. Missed approach: climb to 3,000 ft with maximum thrust.

9. GCA pattern/precision approach (GCA/ILS) to touch and go: 2 min at airspeed for maximum specific range (gear and flaps up), 6 min at approach airspeed in landing configuration.

10. 3 VFR landing patterns (2 touch and go's, 1 full stop): 12.75 min at approach airspeed in landing configuration, 45 seconds in landing configuration at maximum thrust.

11. Taxi/shutdown: 3 min at sea level static idle.

12. Reserve fuel: 20 min at sea level at airspeed for maximum specific endurance.

a.	Mission Time	Items 2 through 10.
b.	Cycle Time:	Items 2 through 12.

10.4.4.9 TACTICAL FORMATION

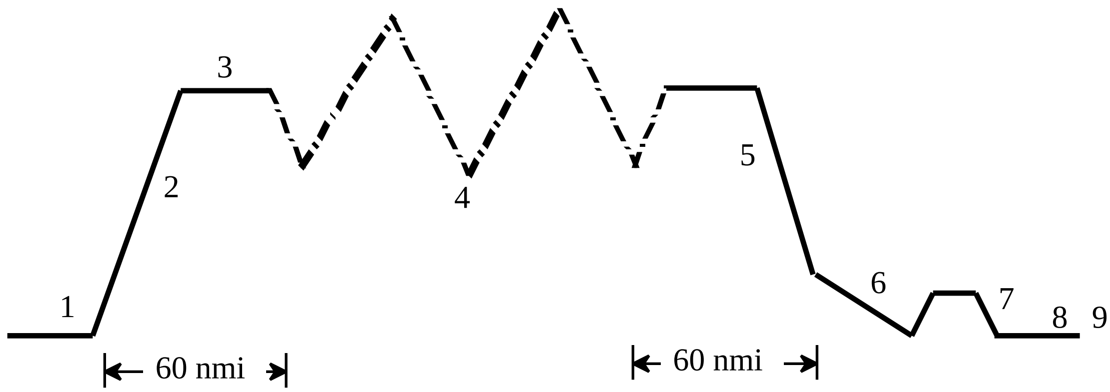

Figure 10.36
TACTICAL FORMATION

1. Engine start, taxi, ground marshall, and takeoff: 13 min at idle thrust plus 1 min at intermediate thrust (both at sea level static).

2. Climb to 25,000 ft with maximum thrust.

3. Cruise to 60 nmi from initial climb point at airspeed for maximum specific range.

4. Tactical Formation Maneuvers, 20,000 to 30,000 ft: 17 min at maximum thrust, 15 min at maximum continuous thrust, 22.1 min at airspeed for maximum specific range.

   a. Combat Spread/Loose Duece, called and uncalled turns, break turns, hard turns.
   b. Tactical wing.
   c. Vertical maneuvers, vertical reversals, high and lo and Yo-Yo’s.

5. Cruise back at 25,000 ft at airspeed for maximum specific range and descend to 1,500 ft (cruise back and descent distance total 60 nmi).

6. VFR field entry, break, and landing pattern to touch and go landing: 4 min at 1,500 ft 300 KCAS (gear and flaps up), 1 min at approach airspeed in landing configuration.

7. VFR pattern to full stop landing: 15 seconds at maximum thrust, 4.25 min to approach airspeed in landing configuration.

8. Taxi/shutdown: 3 min at sea level static idle.

9. Reserve fuel: 20 min at sea level at airspeed for maximum specific endurance.

   a. Mission Time Items 2 through 7.
   b. Cycle Time: Items 2 through 9.

10.4.4.10 AIR-TO-AIR GUNNERY

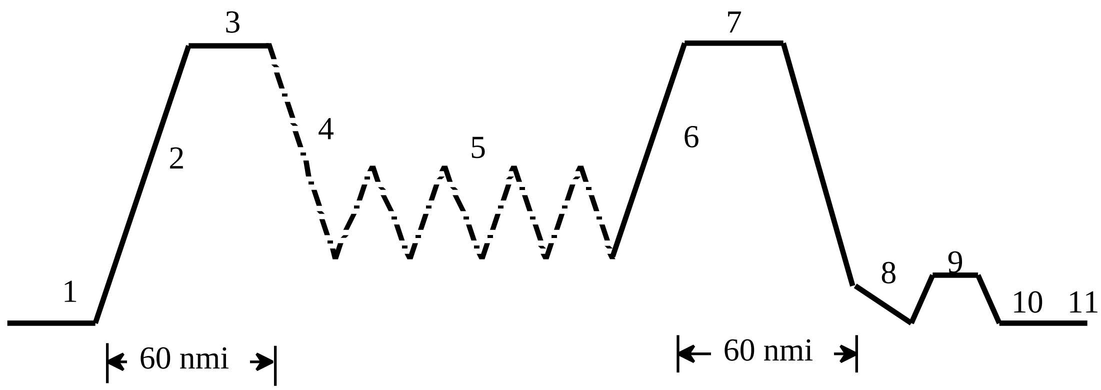

Figure 10.37
AIR-TO-AIR GUNNERY

1. Engine start, taxi, ground marshall,and takeoff: 25 min at idle thrust plus 1 min at intermediate thrust (both at sea level static).

2. Climb to 20,000 ft with maximum thrust.

3. Cruise to 60 nmi from initial climb point to gunnery range at airspeed for maximum specific range.

4. Descend from 20,000 ft to 10,000 ft (tractor altitude) at 325 KCAS.

5. Gunnery training; flatside gunnery, maneuvering target gunnery: 16.5 min at maximum thrust, 6 min at maximum continuous thrust, 9.7 min speed for maximum specific range.

6. Climb from 10,000 ft to 20,000 ft with maximum thrust.

7. Cruise back at 20,000 ft at airspeed for maximum specific range and descend to 1,500 ft (climb, cruise, and descent distance totals 60 nmi).

8. VFR field entry, break, and landing pattern to touch and go landing: 4 min at 1,500 ft 300 KCAS (gear and flaps up), 1 min at approach airspeed and landing configuration.

9. VFR pattern to full stop landing: 15 seconds at maximum thrust, 4.25 min at approach airspeed in landing configuration.

10. Taxi/Shutdown: 3 min at sea level static idle.

11. Reserve fuel: 20 min at sea level at airspeed for maximum specific endurance.

a.	Mission Time	Items 2 through 9.
b.	Cycle Time:	Items 2 through 11.

10.4.4.11 WEAPON DELIVERY

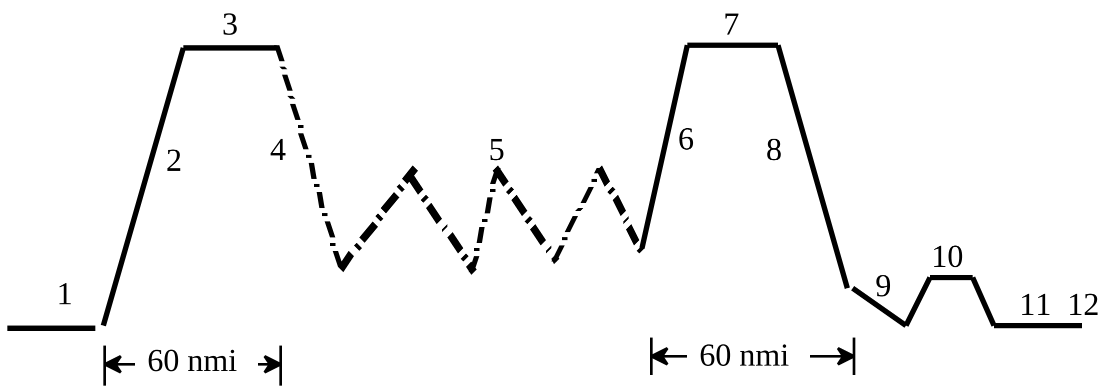

Figure 10.38
WEAPON DELIVERY

1. Engine start, taxi, ground marshall,and takeoff: 15 min at idle thrust plus 1 min at intermediate thrust (both at sea level static).

2. Climb to 20,000 ft with maximum thrust.

3. Cruise to 60 nmi from initial climb point to area at 20,000 ft at airspeed for maximum specific range.

4. Descend from 20,000 ft to 5,000 ft (release altitude) at 400 KCAS.

5. Bombing pattern maneuvers, 13,500 ft to 1,500 ft release speed 400 KCAS, pattern speed 250 KCAS, climb from 5,000 ft to 8,500 ft: 14 min at maximum thrust (0.45 Mach), 11.5 min at speed for maximum specific range, 5 min at in-flight idle thrust.

6. Climb from 4,000 ft to 20,000 ft with maximum thrust.

7. Cruise back at 20,000 ft at airspeed for maximum specific range.

8. Descend to 1,500 ft (climb, cruise, and descent distance total 60 nmi).

9. VFR field entry, break, and pattern to touch and go landing: 4 min at 1,500 ft 300 KCAS (gear and flaps up), 1 min at approach airspeed in landing configuration.

10. VFR pattern to full stop landing: 15 seconds at maximum thrust, 4.25 min at approach airspeed in landing configuration.

11. Taxi/shutdown: 3 min at sea level static idle.

12. Reserve fuel: 20 min at sea level at airspeed for maximum specific endurance.

a. Mission Time Items 2 through 10.
b. Cycle Time: Items 2 through 12.

10.4.4.12 WEAPONS DELIVERY - TAC NAV

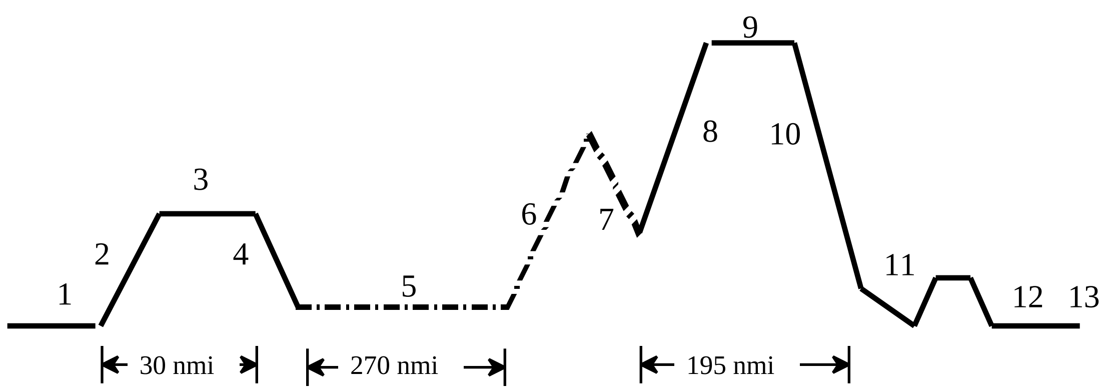

Figure 10.39
WEAPONS DELIVERY - TAC NAV

1. Engine start, taxi, ground marshall, and takeoff: 10 min at idle thrust plus 1 min at maximum thrust (both at sea level static).

2. Climb to 1,500 ft with maximum thrust.

3. Cruise at airspeed for maximum specific range.

4. Descend to 500 ft at 300 KCAS (climb, cruise, descent distance equal to 30 nmi).

5. Low Level Navigation (dead reckoning (D.R.) navigation) at 500 ft and 300 kn for 270 nmi.

6. “Pop-up Attack”, climb to 8,000 ft with maximum thrust.

7. “Roll-in Attack”, descend to 4,000 ft with maximum thrust.

8. Climb from 4,000 ft to 35,000 ft with maximum thrust.

9. Cruise back at 35,000 ft at airspeed for maximum specific range.

10. Radar descent to 3,000 ft at 250 KCAS (climb, cruise back and descent distance totals 195 nmi).

11. Precision Final Approach (GCA/ILS) to touch and go: 2 min at 3,000 ft (gear and flaps up) at airspeed for maximum specific endurance, 6 min at 1,500 ft (gear and flaps down) at airspeed for maximum specific endurance.

12. Taxi/shutdown: 3 min at sea level static idle.

13. Reserve fuel: 20 min at sea level at airspeed for maximum specific endurance.

a. Mission Time Items 2 through 11.
b. Cycle Time: Items 2 through 13.

10.4.4.13 AIR COMBAT MANEUVERING

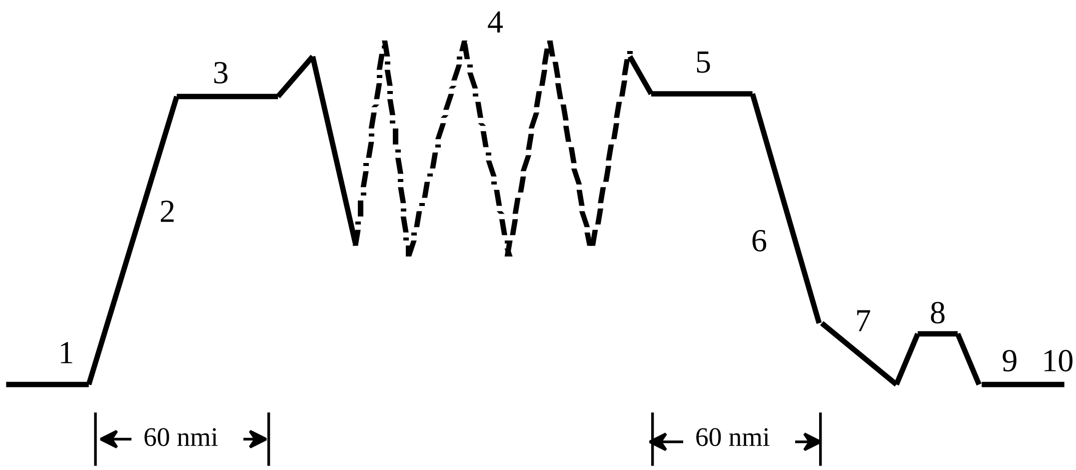

Figure 10.40
AIR COMBAT MANEUVERING

1. Engine start, taxi, ground marshall,and takeoff: 11 min at idle thrust plus 1 min at maximum thrust (both at sea level static).

2. Climb to 25,000 ft with maximum thrust.

3. Cruise to 60 nmi from initial climb point at 25,000 ft at airspeed for maximum specific range.

4. Air Combat Maneuvering, 10,000 ft to 30,000 ft:

   a. Gunsight tracking/high G maneuvering.
   b. Loose Duece/tactical wing maneuvering.
   c. Offensive ACM maneuvering.
   d. Defensive ACM maneuvering.
   e. Neutral ACM maneuvering.
   f. 19.8 min at maximum thrust (0.65 Mach).
   g. 10.1 min at maximum continuous thrust.
   h. 9.4 min at airspeed for maximum specific range.

5. Cruise back at 25,000 at airspeed for maximum specific range.

6. Descend from 25,000 to 1,500 ft at maximum specific range airspeed (cruise back and descent distance totals 60 nmi).

7. VFR field entry, break, and landing pattern to touch and go: 4 min at 1,500 ft. 300 KCAS (gear and flaps up), 1 min at approach airspeed in landing configuration.

8. VFR pattern to full stop landing: 15 seconds at maximum thrust, 4.25 min at approach airspeed in landing configuration.

9. Taxi/shutdown: 3 min at sea level static idle.

10. Reserve fuel: 20 min at sea level at airspeed for maximum specific endurance.

   a. Mission Time Items 2 through 8.
   b. Cycle Time: Items 2 through 10.

10.4.4.14 FIELD CARRIER LANDING PRACTICE (FCLP)

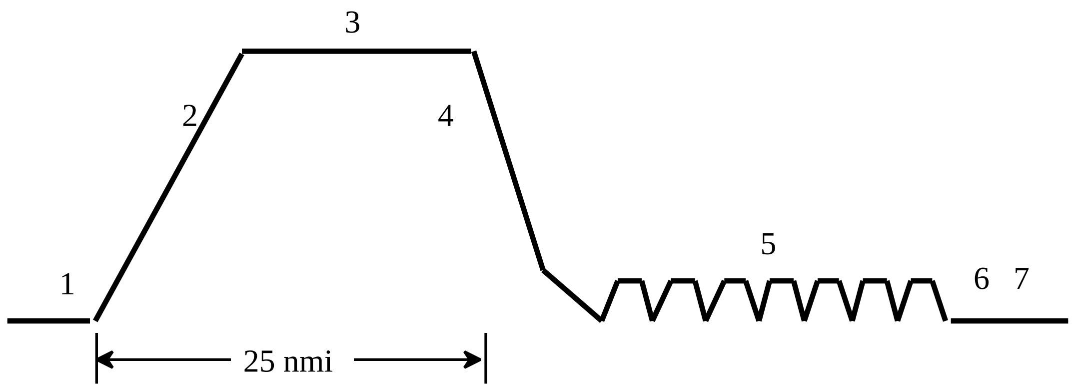

Figure 10.41
FIELD CARRIER LANDING PRACTICE (FCLP)

1. Engine start, taxi, and takeoff: 10 min at idle thrust plus 1 min at maximum thrust (both at sea level static).

2. Climb to 20,000 ft with maximum thrust.

3. Cruise to 25 nmi from initial climb point at 15,000 ft at airspeed for maximum specific range.

4. Descend from 15,000 ft to 1,500 ft at 250 KCAS.

5. FCLP: 34.8 min at approach airspeed in landing configuration at sea level, 2 min in landing configuration at sea level maximum thrust (final FCLP to full stop landing).
   a. 6 FCLPs to touchdown.
   b. 2 FCLPs to waveoffs.

6. Taxi/shutdown: 3 min at sea level idle thrust.

7. Reserve fuel: 20 min at sea level airspeed for maximum specific endurance.

   a. Mission Time Items 2 through 5.
   b. Cycle Time: Items 2 through 7.

10.4.4.15 CARRIER QUALIFICATION

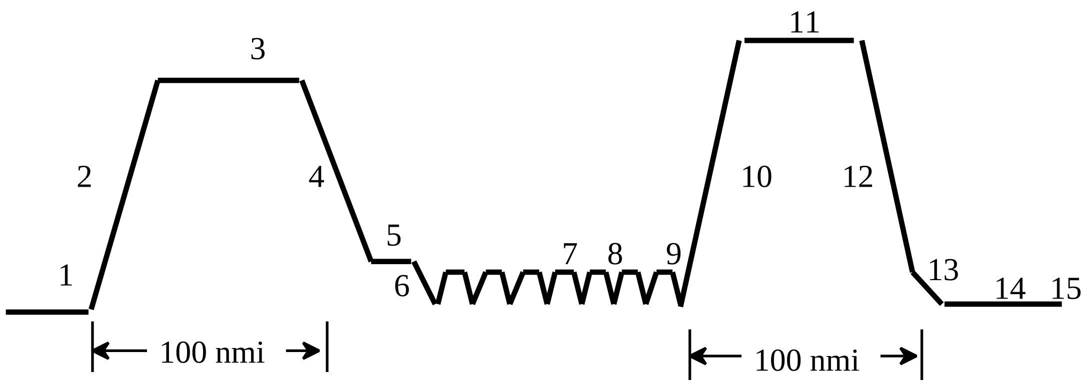

Figure 10.42
CARRIER QUALIFICATION

1. Engine start, taxi, and takeoff: 10 min at idle thrust plus 1 min at maximum thrust (both at sea level static).

2. Climb to 20,000 ft with maximum thrust.

3. Cruise at 20,000 ft at airspeed for maximum specific range.

4. Descend from 20,000 ft to 5,000 ft (climb, cruise and descent distance equals 100 nmi).

5. Hold at 5,000 ft at airspeed for maximum specific endurance for 15 min.

6. Descend from 5,000 ft to sea level at 250 KCAS.

7. 2 carrier (CV) touch and go landings: 10 min at approach airspeed in landing configuration, 5 min at maximum thrust in landing configuration (sea level).

8. 40 min at approach airspeed in landing configuration (sea level), 5.5 min at maximum thrust in landing configuration (sea level), 25 min at idle thrust (sea level). Refuel, add 1640 lb after 2 touch and go, 2 CV arrested landings, 1 CV bolter.

   a. 6 CV arrested landings.
   b. 5 CV catapult launches.
   c. 2 CV bolters/waveoffs.

9. Final CV catapult launch.

10. Climb to 27,000 ft with maximum thrust.

11. Cruise at 27,000 ft at airspeed for maximum specific range.

12. Descend from 27,000 ft to 1,500 ft at maximum specific range airspeed (climb, cruise back and descent distance totals 100 nmi).

13. VFR field entry, break, and landing: 2 min at sea level, 300 kn clean, 0.5 min at approach airspeed in landing configuration.

14. Taxi/shutdown: 3 min at sea level.

15. Reserve fuel: 20 min at sea level at airspeed for maximum specific endurance.

a.	Mission Time	Items 2 through 13.
b.	Cycle Time:	Items 2 through 15.

10.4.5 NAVAL FLIGHT OFFICER TRAINER MISSIONS (REF 2)

10.4.5.1 LOW LEVEL NAVIGATION - 1

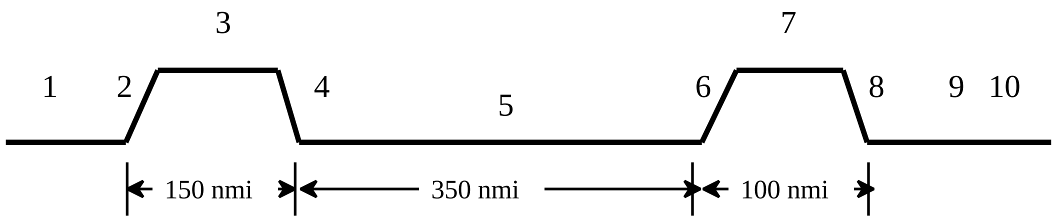

Figure 10.43
LOW LEVEL NAVIGATION - 1

1. Takeoff allowance for engine start, taxi, takeoff, and acceleration to climb speed: fuel consumed for 15 min at idle power, plus 1 min at takeoff power, sea level static conditions, all engines operating.

2. Climb at climb power from sea level to 10,000 ft altitude.

3. Cruise at 10,000 ft altitude at 250 KIAS.

4. Perform a 250 KIAS descent from 10,000 ft to 500 ft altitude (total distance traveled in 2, 3, and 4 shall be at least 150 nmi).

5. Cruise at 500 ft altitude at 300 KTAS for a distance of at least 350 nmi.

6. Climb at climb power from 500 ft to 8,000 ft altitude.

7. Cruise at 8,000 ft altitude at 250 KIAS.

8. Perform a 250 KIAS descent from 8,000 ft to sea level (total distance covered in segments 6, 7, and 8 shall be at least 100 nmi).

9. Instrument approach allowance: fuel equivalent to 8 min at approach power, approach configuration.

10. Reserve fuel requirement: the fuel required for a 150 nmi divert capability is defined as follows:

a. Climb at climb power from sea level to 10,000 ft.

b. Cruise 150 nmi from initial climb point at 10,000 ft altitude at speed for maximum range.

c. Loiter for 20 min at 10,000 ft at airspeed for maximum endurance (all engines operating).

d. Mission Time Items 2 through 9.

e. Cycle Time: Items 2 through 10.

10.4.5.2 LOW LEVEL NAVIGATION - 2

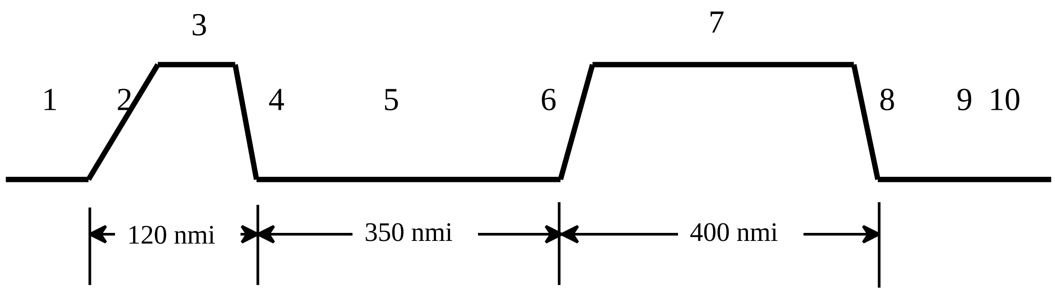

Figure 10.44
LOW LEVEL NAVIGATION - 2

1. Takeoff allowance for engine start, taxi, takeoff, and acceleration to climb speed: fuel consumed for 15 min at idle power, plus 1 min at takeoff power, sea level static conditions, all engines operating.

2. Climb at climb power from sea level to 10,000 ft altitude.

3. Cruise at 10,000 ft altitude at 250 KIAS.

4. Perform a 250 KIAS descent from 10,000 ft to 500 ft altitude (total distance traveled in segments 2, 3, and 4 shall be at least 120 nmi).

5. Cruise at 500 ft altitude at 300 KTAS for a distance of at least 350 nmi.

6. Climb at climb power from 500 ft to 40,000 ft altitude.

7. Cruise at 40,000 ft altitude at 400 KTAS.

8. Perform a 250 KIAS descent from 40,000 ft to sea level (total distance covered in segments 6, 7 and 8 shall be at least 400 nmi, cruise configuration).

9. Instrument approach allowance: fuel equivalent to 8 min at approach power, approach configuration.

10. Reserve fuel requirement: the fuel required for a 150 nmi divert capability is defined as follows:

a. Climb at climb power from sea level to 10,000 ft.

b. Cruise 150 nmi from initial climb point at 10,000 ft altitude at speed for maximum range.

c. Loiter for 20 min at 10,000 ft at airspeed for maximum endurance (all engines operating).

d. Mission Time Items 2 through 9.

e. Cycle Time: Items 2 through 10.

10.4.5.3 LOW LEVEL NAVIGATION - 3

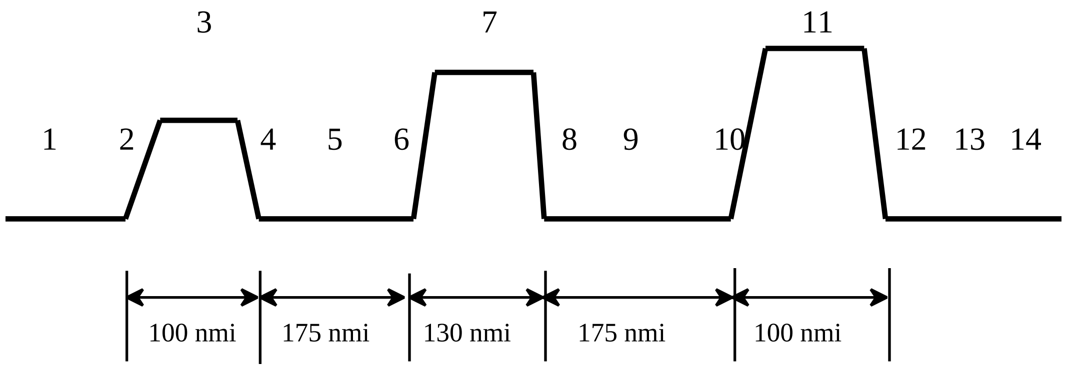

Figure 10.45
LOW LEVEL NAVIGATION - 3

1. Takeoff allowance for engine start, taxi, takeoff, and acceleration to climb speed: fuel consumed for 15 min at idle power, plus 1 min at takeoff power, sea level static conditions, all engines operating.

2. Climb at climb power from sea level to 10,000 ft altitude.

3. Cruise at 10,000 ft altitude at 250 KIAS.

4. Perform a 250 KIAS descent from 10,000 ft to 500 ft altitude (total distance traveled in segments 2, 3, and 4 shall be at least 100 nmi).

5. Cruise at 500 ft altitude at 300 KTAS for a distance of at least 175 nmi.

6. Climb at climb power from 500 ft to 16,500 ft altitude.

7. Cruise at 16,500 ft altitude at 350 KTAS.

8. Perform a 250 KIAS descent from 16,500 ft to 500 ft altitude.

9. Cruise at 500 ft altitude at 300 KTAS for a distance of at lease 175 nmi.

10. Climb at climb power from 500 ft to 20,000 ft altitude.

11. Cruise at 20,000 ft at 360 KTAS.

12. Perform a 250 KIAS descent from 20,000 ft altitude to sea level (total distance traveled in segments 10, 11 and 12 shall be at least 100 nmi).

13. TACAN approach allowance: fuel equivalent to 8 min at approach power, approach configuration.

14. Reserve fuel requirement: the fuel required for a 150 nmi divert capability is defined as follows:

a. Climb at climb power from sea level to 10,000 ft.

b. Cruise 150 nmi from initial climb point at 10,000 ft altitude at speed for maximum range.

c. Loiter for 20 min at 10,000 ft at airspeed for maximum endurance (all engines operating).

d. Mission Time Items 2 through 13.

e. Cycle Time: Items 2 through 14.

10.4.5.4 LOW LEVEL NAVIGATION - 4

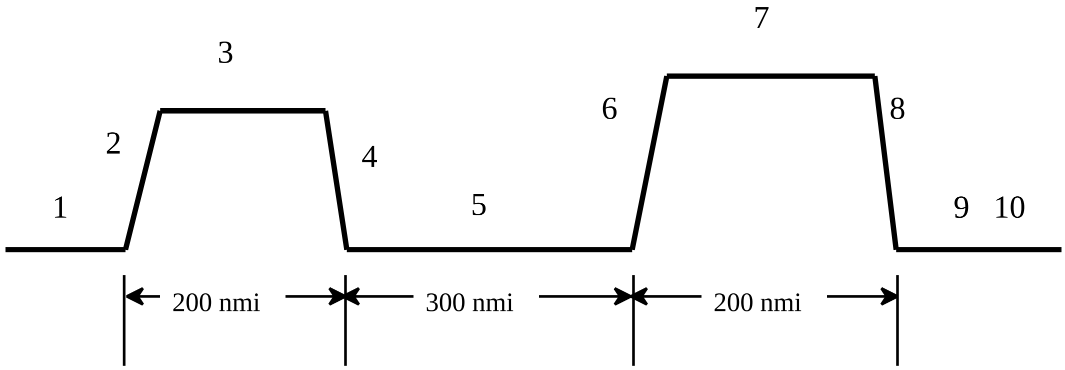

Figure 10.46
LOW LEVEL NAVIGATION - 4

1. Takeoff allowance for engine start, taxi, takeoff, and acceleration to climb speed: fuel consumed for 15 min at idle power, plus 1 min at takeoff power, sea level static conditions, all engines operating.

2. Climb at climb power from sea level to 18,000 ft altitude.

3. Cruise at 18,000 ft altitude at 330 KTAS.

4. Perform a 250 KIAS descent from 18,000 ft to 500 ft altitude (total distance traveled in segments 2, 3, and 4 shall be at least 200 nmi).

5. Cruise at 500 ft altitude at 300 KTAS for a distance of at least 300 nmi.

6. Climb at climb power from 500 ft to 18,000 ft altitude.

7. Cruise at 18,000 ft altitude at 360 KTAS.

8. Perform a 250 KIAS descent from 18,000 ft to sea level (total distance covered in segments 6, 7 and 8 shall be least 200 nmi).

9. TACAN approach allowance: fuel equivalent to 8 min at approach power, approach configuration.

10. Reserve fuel requirement: the fuel required for a 150 nmi divert capability is defined as follows:

a. Climb at climb power from sea level to 10,000 ft.

b. Cruise 150 nmi from initial climb point at 10,000 ft altitude at speed for maximum range.

c. Loiter for 20 min at 10,000 ft at airspeed for maximum endurance (all engines operating).

d. Mission Time Items 2 through 9.

e. Cycle Time: Items 2 through 10.

10.4.5.5 INSTRUMENT NAVIGATION - 1

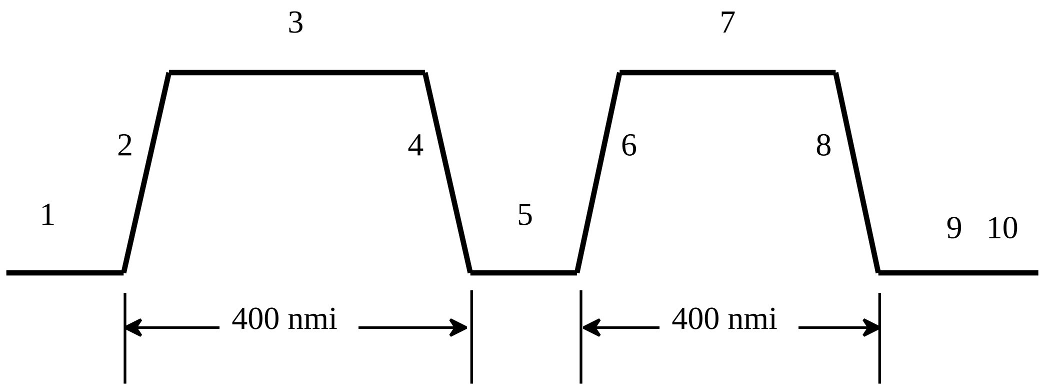

Figure 10.47
INSTRUMENT NAVIGATION - 1

1. Takeoff allowance for engine start, taxi, takeoff, and acceleration to climb speed: fuel consumed for 15 min at idle power, plus 1 min at takeoff power, sea level static conditions, all engines operating.

2. Climb at climb power from sea level to 40,000 ft altitude.

3. Cruise at 40,000 ft altitude at 400 KTAS.

4. Perform a 250 KIAS descent from 40,000 ft to sea level (total distance traveled in segments 2, 3, and 4 shall be at least 400 nmi).

5. TACAN approach allowance: fuel equivalent to 8 min at approach power, approach configuration.

6. Climb at climb power from sea level to 40,000 ft altitude.

7. Cruise at 40,000 ft altitude at 400 KTAS.

8. Perform a 250 KIAS descent from 40,000 ft to sea level (total distance covered in segments 6, 7 and 8 shall be at least 400 nmi).

9. TACAN approach allowance: fuel equivalent to 8 min at approach power, approach configuration.

10. Reserve fuel requirement: the fuel required for a 150 nmi divert capability is defined as follows:

a. Climb at climb power from sea level to 10,000 ft.

b. Cruise 150 nmi from initial climb point at 10,000 ft altitude at speed for maximum range.

c. Loiter for 20 min at 10,000 ft at airspeed for maximum endurance (all engines operating).

d. Mission Time Items 2 through 9.

e. Cycle Time: Items 2 through 10.

10.4.5.6 INSTRUMENT NAVIGATION - 2

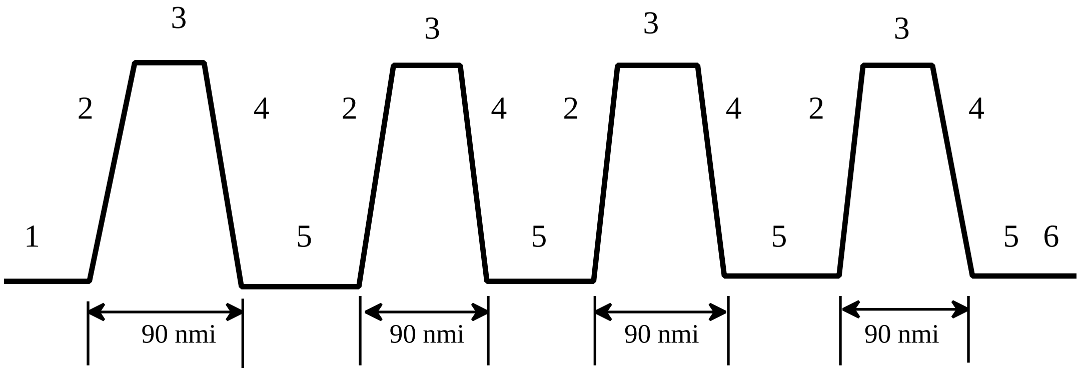

Figure 10.48
INSTRUMENT NAVIGATION - 2

1. Takeoff allowance for engine start, taxi, takeoff, and acceleration to climb speed: fuel consumed for 15 min at idle power, plus 1 min at takeoff power, sea level static conditions, all engines operating.

2. Climb at climb power from sea level to 18,000 ft altitude.

3. Cruise at 18,000 ft altitude at 360 KTAS.

4. Perform a 250 KIAS descent from 18,000 ft to sea level (total distance traveled in segments 2, 3, and 4 shall be at least 90 nmi).

5. TACAN approach allowance: fuel equivalent to 8 min at approach power, approach configuration.

6. Reserve fuel requirement: the fuel required for a 150 nmi divert capability is defined as follows:

a. Climb at climb power from sea level to 10,000 ft.

b. Cruise 150 nmi from initial climb point at 10,000 ft altitude at speed for maximum range.

c. Loiter for 20 min at 10,000 ft at airspeed for maximum endurance (all engines operating).

d. Mission Time Items 2 through 5.

e. Cycle Time: Items 2 through 6.

10.4.5.7 RADAR NAVIGATION - 1

Out (First Leg Of Out And In)

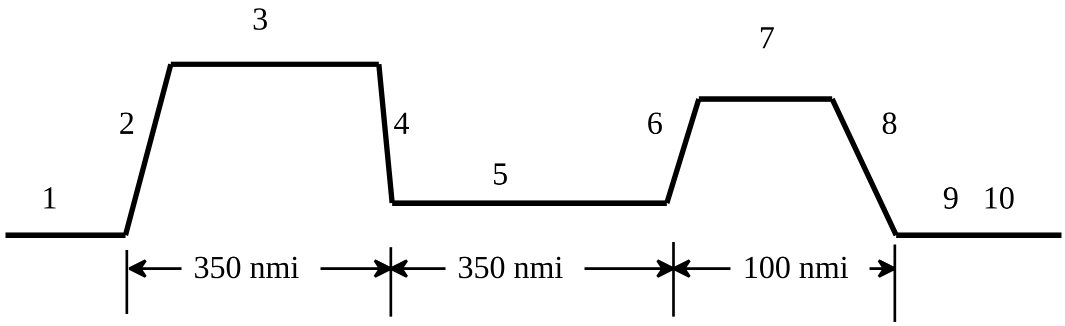

Figure 10.49
RADAR NAVIGATION - 1

1. Takeoff allowance for engine start, taxi, takeoff, and acceleration to climb speed: fuel consumed for 15 min at idle power, plus 1 min at takeoff power, sea level static conditions, all engines operating.

2. Climb at climb power from sea level to 35,000 ft altitude.

3. Cruise at 35,000 ft altitude at 360 KTAS.

4. Perform a 250 KIAS descent from 35,000 ft to 5,000 ft (total distance traveled in segments 2, 3, and 4 shall be at least 350 nmi).

5. Cruise at 5,000 ft altitude at 300 KTAS for a distance of at least 350 nmi.

6. Climb at climb power from 5,000 ft altitude to 18,000 ft altitude.

7. Cruise at 18,000 ft altitude at 360 KTAS.

8. Perform a 250 KIAS descent from 18,000 ft to sea level (total distance covered in segments 6, 7 and 8 shall be at least 100 nmi).

9. TACAN approach allowance: fuel equivalent to 8 min at approach power approach configuration.

10. Reserve fuel requirement: the fuel required for a 150 nmi divert capability is defined as follows:

a. Climb at climb power from sea level to 10,000 ft.

b. Cruise 150 nmi from initial climb point at 10,000 ft altitude at speed for maximum range.

c. Loiter for 20 min at 10,000 ft at airspeed for maximum endurance (all engines operating).

d. Mission Time Items 2 through 9.

e. Cycle Time: Items 2 through 10.

10.4.5.8 RADAR NAVIGATION - 2

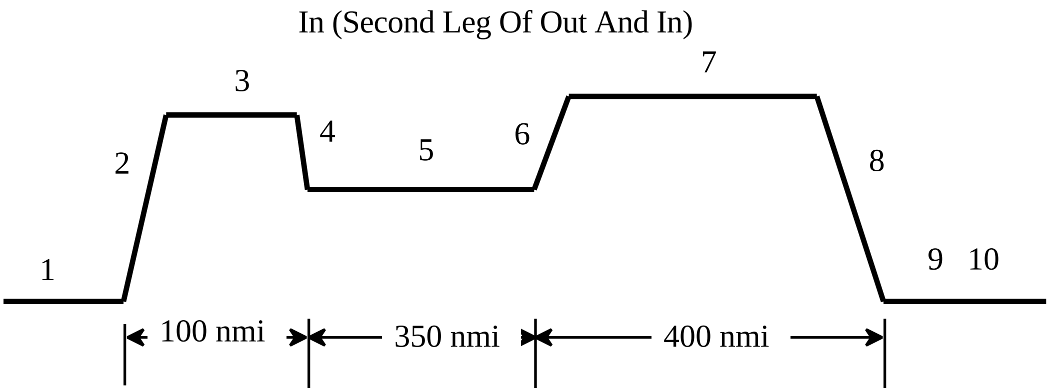

Figure 10.50
RADAR NAVIGATION - 2

1. Takeoff allowance for engine start, taxi, takeoff, and acceleration to climb speed: fuel consumed for 15 min at idle power, plus 1 min at takeoff power, sea level static conditions, all engines operating.

2. Climb at climb power from sea level to 18,000 ft altitude.

3. Cruise at 18,000 ft altitude at 360 KTAS.

4. Perform a 250 KIAS descent from 18,000 ft to 5,000 ft altitude (total distance traveled in segments 2, 3, and 4 shall be at least 100 nmi).

5. Cruise at 5,000 ft altitude at 300 KTAS for a distance of at least 350 nmi.

6. Climb at climb power from 5,000 ft altitude to 35,000 ft altitude.

7. Cruise at 35,000 ft altitude at 360 KTAS.

8. Perform a 250 KIAS descent from 35,000 ft to sea level (total distance covered in segments 6, 7 and 8 shall be at least 400 nmi).

9. TACAN approach allowance: fuel equivalent to 8 min at approach power approach configuration.

10. Reserve fuel requirement: the fuel required for a 150 nmi divert capability is defined as follows:

a. Climb at climb power from sea level to 10,000 ft.

b. Cruise 150 nmi from initial climb point at 10,000 ft altitude at speed for maximum range.

c. Loiter for 20 min at 10,000 ft at airspeed for maximum endurance (all engines operating).

d. Mission Time Items 2 through 9.

e. Cycle Time: Items 2 through 10.

10.4.5.9 LOCAL RADAR - 1

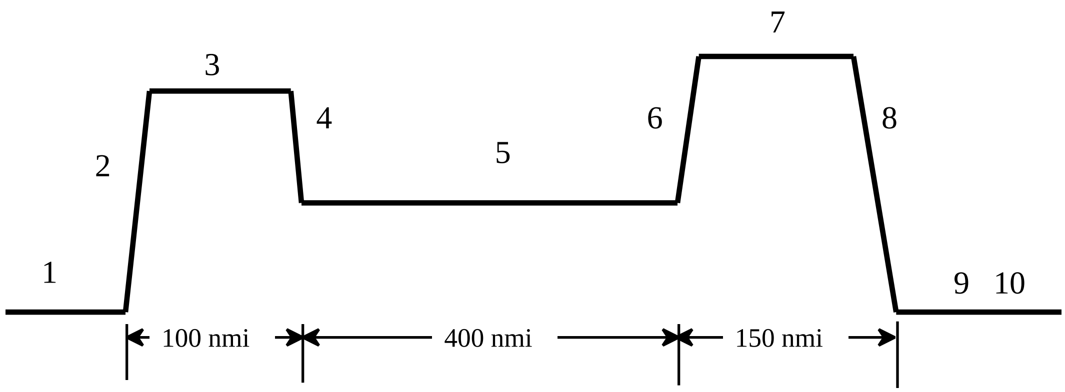

Figure 10.51
LOCAL RADAR - 1

1. Takeoff allowance for engine start, taxi, takeoff, and acceleration to climb speed: fuel consumed for 15 min at idle power, plus 1 min at takeoff power, sea level static conditions, all engines operating.

2. Climb at climb power from sea level to 10,000 ft altitude.

3. Cruise at 10,000 ft altitude at 250 KIAS.

4. Perform a 250 KIAS descent from 10,000 ft to 5,000 ft altitude (total distance traveled in segments 2, 3, and 4 shall be at least 100 nmi).

5. Cruise at 5,000 ft altitude at 300 KTAS for a distance of at least 400 nmi.

6. Climb at climb power from 5,000 ft altitude to 10,000 ft altitude.

7. Cruise at 10,000 ft altitude at 250 KIAS.

8. Perform a 250 KIAS descent from 10,000 ft to sea level (total distance covered in segments 6, 7 and 8 shall be at least 150 nmi).

9. Instrument approach allowance: fuel equivalent to 8 min at approach power approach configuration.

10. Reserve fuel requirement: the fuel required for a 150 nmi divert capability is defined as follows:

a. Climb at climb power from sea level to 10,000 ft.

b. Cruise 150 nmi from initial climb point at 10,000 ft altitude at speed for maximum range.

c. Loiter for 20 min at 10,000 ft at airspeed for maximum endurance (all engines operating).

d. Mission Time Items 2 through 9.

e. Cycle Time: Items 2 through 10.

10.4.5.10 LOCAL RADAR - 2

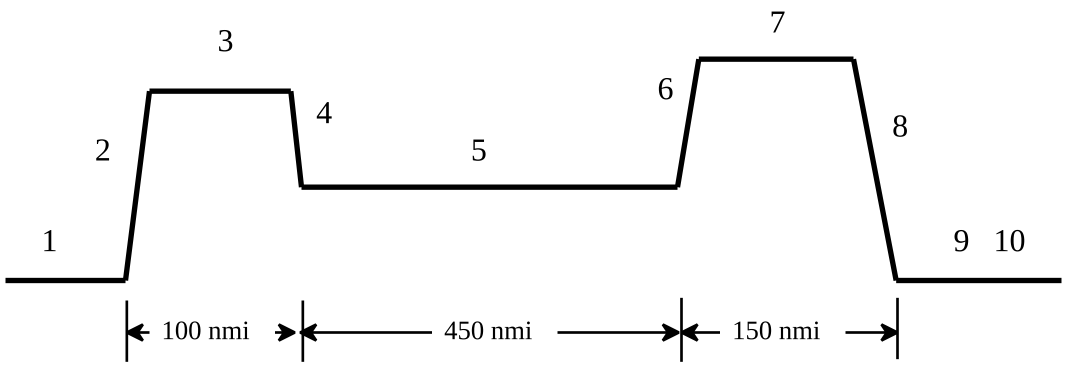

Figure 10.52
LOCAL RADAR - 2

1. Takeoff allowance for engine start, taxi, takeoff, and acceleration to climb speed: fuel consumed for 15 min at idle power, plus 1 min at takeoff power, sea level static conditions, all engines operating.

2. Climb at climb power from sea level to 10,000 ft altitude.

3. Cruise at 10,000 ft altitude at 250 KIAS.

4. Perform a 250 KIAS descent from 10,000 ft to 2,000 ft altitude (total distance traveled in segments 2, 3, and 4 shall be at least 100 nmi).

5. Cruise at 2,000 ft altitude at 300 KTAS for a distance of at least 450 nmi.

6. Climb at climb power from 2,000 ft altitude to 10,000 ft altitude.

7. Cruise at 10,000 ft altitude at 250 KIAS.

8. Perform a 250 KIAS descent from 10,000 ft to sea level (total distance covered in segments 6, 7 and 8 shall be at least 150 nmi).

9. Instrument approach allowance: fuel equivalent to 8 min at approach power, approach configuration.

10. Reserve fuel requirement: the fuel required for a 150 nmi divert capability is defined as follows:

a. Climb at climb power from sea level to 10,000 ft.

b. Cruise 150 nmi from initial climb point at 10,000 ft altitude at speed for maximum range.

c. Loiter for 20 min at 10,000 ft at airspeed for maximum endurance (all engines operating).

d. Mission Time Items 2 through 9.

e. Cycle Time: Items 2 through 10.

10.4.5.11 RIO PATTERN - INTERCEPTS - 1

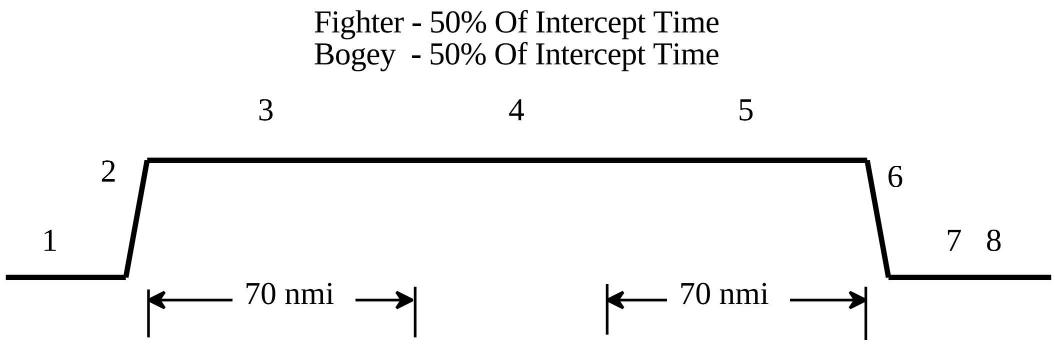

Figure 10.53
RIO PATTERN - INTERCEPTS - 1

INTERCEPT ALTITUDE/MACH NUMBER REQUIREMENTS

Block 1:	7,000 ft - 11,000 ft/0.45 Mach
Block 2:	13,000 ft - 17,000 ft/0.50 Mach
Block 3:	18,000 ft - 22,000 ft/0.55 Mach
15 intercepts for Block 1 only	
20 intercepts for Blocks 2 and 3	
Average flight duration:	2.3 hour for Block 1
	2.6 hour for Blocks 2 and 3
Capability to dash an additional 0.1 Mach for 15% of the profile	

1. Takeoff allowance for engine start, taxi, takeoff, and acceleration to climb speed: fuel considered for 15 min at idle power, plus 1 min at takeoff power, sea level static conditions, all engines operating.

2. Climb at climb power from sea level to 13,000 ft.

3. Cruise 70 nmi at 13,000 ft.

4. Perform 15 intercepts at intercept altitude for Block 1 and 20 intercepts at intercept altitude for Blocks 2 and 3: fuel allowance per intercept equivalent to 6 min at maximum airspeed. No distance gained during the intercepts.

5. Cruise back at 18,000 ft.

6. Perform a 250 KIAS descent from 18,000 ft to sea level.

7. TACAN approach allowance: fuel equivalent to 8 min at approach power approach configuration.

8. Reserve fuel requirement: the fuel required for a 150 nmi divert capability is defined as follows:

   a. Climb at climb power from sea level to 10,000 ft.
   b. Cruise 150 nmi from initial climb point at 10,000 ft altitude at speed for maximum range.
   c. Loiter for 20 min at 10,000 ft at airspeed for maximum endurance (all engines operating).
   d. Mission Time Items 2 through 7.
   e. Cycle Time: Items 2 through 8.

10.4.5.12 RIO PATTERN - INTERCEPTS - 2

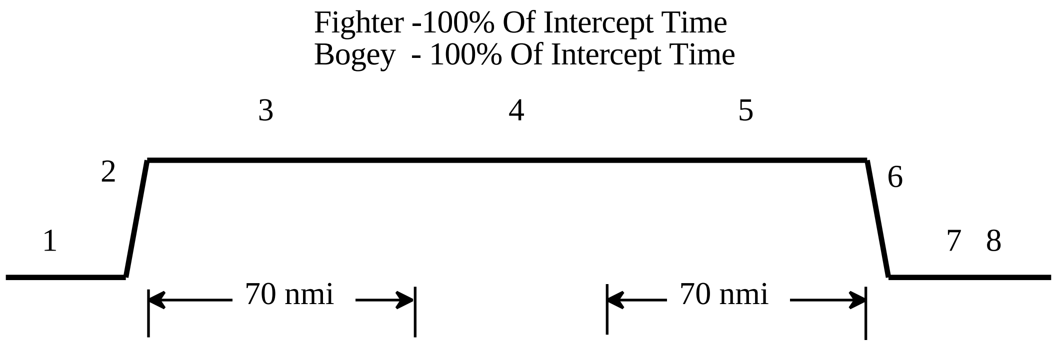

Figure 10.54
RIO PATTERN - INTERCEPTS - 2

INTERCEPT ALTITUDE/MACH NUMBER REQUIREMENTS

Block 1:	7,000 ft - 11,000 ft/0.45 Mach
Block 2:	13,000 ft - 17,000 ft/0.50 Mach
Block 3:	18,000 ft - 22,000 ft/0.55 Mach
15 intercepts for Block 1 only	
20 intercepts for Blocks 2 and 3	
Average flight duration:	2.3 hour for Block 1
	2.6 hour for Blocks 2 and 3
Capability to dash an additional 0.1 Mach for 15% of the profile	

1. Takeoff allowance for engine start, taxi, takeoff, and acceleration to climb speed: fuel considered for 15 min at idle power, plus 1 min at takeoff power, sea level static conditions, all engines operating.

2. Climb at climb power from sea level to 13,000 ft.

3. Cruise 70 nmi at 13,000 ft.

4. Perform 15 intercepts at intercept altitude for Block 1 and 20 intercepts at intercept altitude for Blocks 2 and 3: fuel allowance per intercept equivalent to 6 min at maximum airspeed. No distance gained during the intercepts.

5. Cruise back at 18,000 ft.

6. Perform a 250 KIAS descent from 18,000 ft to sea level.

7. TACAN approach allowance: fuel equivalent to 8 min at approach power approach configuration.

8. Reserve fuel requirements: the fuel required for a 150 nmi divert capability is defined as follows:

a. Climb at climb power from sea level to 10,000 ft.

b. Cruise 150 nmi from initial climb point at 10,000 ft altitude at speed for maximum range.

c. Loiter for 20 min at 10,000 ft at airspeed for maximum endurance (all engines operating).

d. Mission Time Items 2 through 7.

e. Cycle Time: Items 2 through 8.

10.5 CONCLUSION

Keep in mind the development of mission profiles is an evolutionary process. Advances in technology giving rise to high thrust to weight, low observables, smart weapons etc., all lead to changes in the way Navy aircraft missions will be defined and in a broader sense what the role of Naval aviation will be in the future.

10.6 GLOSSARY

10.6.1 NOTATIONS

ACM	Air combat maneuvering	
ADF	Automatic direction finder	
AEW	Airborne Early Warning	
ASW	Antisubmarine aircraft	
CV	Carrier	
Cycle time	Time of flight from the start of enroute climb (omitting takeoff time) to stopping engines after landing	
D.R.	Dead reckoning	
FAM	Familiarization	
FCLP	Field carrier landing pattern	
GCA	Ground controlled approach	
ILS	Instrument landing system	
MDA	Minimum descent altitude	
Mission time	Time in air (excluding time before start of initial climb and reserve)	
NATOPS	Naval Air Training and Operating Procedures Standardization Program	
NAVAIRSYSCOM	Naval Air System Command	
n_z	Normal acceleration	g
SAC	Standard aircraft characteristics	
TACAN	Tactical air navigation	
TAMPS	Tactical Air Mission Planning System	
VFR	Visual flight rules	

10.7 REFERENCES

1. "Aircraft Conceptual Design", Course Notes (#Y0606), Lockheed Technical Institute, Fall 1991.

2. "Functional Description For Training Services", Undergraduate Naval Flight Officer Training System Program, NASC, PMA 200, 3 April 1989.

3. Luter, M., NAVAIRSYSCOM (AIR-53012) Course Notes, (undated).

4. Military Specification (MIL-D-8708(AS)), "Demonstration Requirements for Airplanes", 31 January 1969.

5. Military Standard, MIL-STD-1797A, "Flying Qualities of Piloted Aircraft", 30 January 1990.

6. "Mission Profiles for Navy Pilot Trainer", (date unknown).

7. NAVAIRSYSCOM Specification, AS-5263, "Guidelines for Preparation of Standard Aircraft Characteristics Charts and Performance Data, Piloted Aircraft (Fixed Wing)", 23 October 1986.

8. Nicolai, L.M., *Fundamentals of Aircraft Design*, Fairborn, Ohio, E.P. Domicone Printing Services, 1975.

9. Raymer, D.P,. *Aircraft Design: A Conceptual Approach*, Washington, D.C., American Institute of Aeronautics and Astronautics, Inc., 1989.

10. Roskam, J., *Airplane Design* (Part I, II and VII), Ottawa, Kansas, Roskam Aviation and Engineering Corporation, 1988.

APPENDIX I

GLOSSARY

APPENDIX I

GLOSSARY

NOTATIONS

550	Conversion factor	$550 \frac{\text{ft-lb}}{\text{s}} = 1$ horsepower
a	Speed of sound	ft/s or kn
a	Temperature lapse rate	˚/ft
ACM	Air combat maneuvering	
ADF	Automatic direction finder	
AEW	Airborne Early Warning	
AFCS	Automatic flight control system	
AGL	Above ground level	
AR	Aspect ratio	
a_R	Radial acceleration	ft/s^2
ARDC	Arnold Research and Development Center	
a_{ssl}	Standard sea level speed of sound	661.483 kn
a_{ssl}	Standard sea level temperature lapse rate	0.0019812 ˚K/ft 0.0035662 ˚R/ft
ASW	Antisubmarine aircraft	
a_x	Acceleration parallel flight path	ft/s^2
a_z	Acceleration perpendicular to flight path	ft/s^2
BHP	Brake horsepower	hp
BLC	Boundary layer control	
c	Chord length	ft
$\frac{c}{2}$	Semi-chord length	ft
CAP	Combat air patrol	
CCF	Climb correction factor	
C_D	Drag coefficient	

C_{D_i}	Induced drag coefficient	
C_{D_M}	Mach drag coefficient	
C_{D_p}	Parasite drag coefficient	
$C_{D_{p\,(M)}}$	Parasite drag coefficient at high Mach	
C_{D_R}	Coefficient of ram drag	
CG	Center of gravity	% MAC
CG_{Std}	Standard CG	% MAC
CG_{Test}	Test CG	% MAC
CL	Confidence level	
C_L	Lift coefficient	
$C_{L_{aero}}$	Aerodynamic lift coefficient	
$\left(C_{L_{aero}\ Std\ \dot{V},\ CG,\ W}\right)_{Pwr\ OFF}$	Aerodynamic lift coefficient at standard deceleration rate, CG, and weight, power-off	
$\left(C_{L_{aero}\ Std\ \dot{V},\ CG,\ W}\right)_{Pwr\ ON}$	Aerodynamic lift coefficient at standard deceleration rate, CG, and weight, power-on	
$C_{L_{max}}$	Maximum lift coefficient	
$C_{L_{max\,(\Lambda = 0)}}$	Maximum lift coefficient at $\Lambda = 0$	
$C_{L_{max\,(\Lambda)}}$	Maximum lift coefficient at Λ wing sweep	
$C_{L_{max}\ Std\ \dot{V}}$	Maximum lift coefficient at standard deceleration rate	
$C_{L_{max}\ Std\ \dot{V},\ CG}$	Maximum lift coefficient at standard deceleration rate and CG	
$C_{L_{max}\ Std\ \dot{V},\ CG,\ W}$	Maximum lift coefficient at standard deceleration rate, CG, and weight	
$\left(C_{L_{max}\ Std\ \dot{V},\ CG,\ W}\right)_{Pwr\ ON}$	Maximum lift coefficient at standard deceleration rate, CG, and weight, power-on	
$C_{L_{max}\ Std\ \dot{V},\ CG,\ W,\ Hp}$	Maximum lift coefficient at standard deceleration rate, CG, weight, and altitude	
$C_{L_{max_{Test}}}$	Test maximum lift coefficient	
$CL_{max_{TO}}$	Maximum lift coefficient, takeoff configuration	

$C_{L_{Opt}}$	Optimum lift coefficient	
C_{L_s}	Stall lift coefficient	
$C_{L_{Test}}$	Test lift coefficient	
C_{T_G}	Coefficient of gross thrust lift	
CV	Carrier	
Cycle time	Time of flight from the start of enroute climb (omitting takeoff time) to stopping engines after landing	
D	Course length	nmi
D	Drag	lb
d	Distance	ft or nmi
d	Horizontal distance (Tower - aircraft)	ft
D.R.	Dead reckoning	
DCF	Descent correction factor	
ΔC_{L_E}	Coefficient of thrust-entrainment lift	
ΔC_{L_t}	Incremental tail lift coefficient	
ΔD	Standard drag minus test drag	lb
ΔD_i	Change in induced drag	lb
ΔD_p	Change in parasite drag	lb
deg	Degree	
Δh	Aircraft height above tower	ft
dh/dt	Rate of climb	ft/s
$\Delta H_{P_{ic}}$	Altimeter instrument correction	ft
$\Delta H_{P_{ic\ ref}}$	Reference altimeter instrument correction	ft
ΔH_{pos}	Altimeter position error	ft
D_i	Induced drag	lb
ΔL_t	Tail lift increment	lb
D_M	Mach drag	lb
ΔM_{pos}	Mach position error	
$\Delta n_{z_{ic}}$	Normal acceleration instrument correction	g
$\Delta n_{z_{tare}}$	Accelerometer tare correction	g
ΔP	Static pressure error	psf
D_p	Parasite drag	lb

$\frac{\Delta P}{q_c}$	Static pressure error coefficient	
$\frac{\Delta P}{q_{c_i}}$	Indicated static pressure error coefficient	
D_R	Ram drag	lb
ΔS_2	Change in S_2, equal to t V_w	ft
D_{Std}	Standard drag	lb
ΔT	Change in thrust	lb
DT IIA	Developmental Test IIA	
Δt	Elapsed time	s
ΔT_a	Temperature differential	
D_{Test}	Test drag	lb
ΔT_{ic}	Temperature instrument correction	˚C or ˚K
Δt_j	Time of each time interval	s
ΔT_{N_x}	Standard net thrust parallel flight path minus test net thrust	lb
ΔV_c	Compressibility correction	kn
ΔV_{ic}	Airspeed instrument correction	kn
ΔV_{pos}	Airspeed position error	kn
e	Base of natural logarithm	
e	Oswald's efficiency factor	
$e_{(M)}$	Oswald’s efficiency factor at high Mach	
EGT	Exhaust gas temperature	˚C
E_h	Energy height	ft
E_{h1}	Energy height at start of climb	ft
E_{h2}	Energy height at end of climb	ft
$E_{h_{Test}}$	Test energy height	ft
EPR	Engine pressure ratio	
ESHP	Engine shaft horsepower	hp
F/C	Fuel counter	lb
FAM	Familiarization	
FAR	Federal Aviation Regulations	
FCLP	Field carrier landing pattern	
FOD	Foreign object damage	
FPA	Flight path accelerometer	

F_R	Radial force	lb
ft/min	Foot per minute	
FTE	Flight test engineer	
FTM	Flight Test Manual	
F_X	Forces parallel flight path	lb
F_Y	Sideforce	lb
F_Z	Force perpendicular to flight path	lb
g	Gravitational acceleration	ft/s^2
g_c	Conversion constant	32.17 $lb_m/slug$
GCA	Ground controlled approach	
GR	Glide ratio	
GS	Ground speed	kn
g_{ssl}	Standard sea level gravitational acceleration	32.174049 ft/s^2
GW	Gross weight	lb
H	Geopotential	ft
h	Tapeline altitude	ft
h_1	Tapeline altitude start of climb	ft
h_2	Tapeline altitude end of climb	ft
H_P	Pressure altitude	ft
$H_{P\ ref}$	Reference pressure altitude	ft
H_{P_c}	Calibrated pressure altitude	ft
$H_{P_{c\ ref}}$	Reference calibrated pressure altitude	ft
$H_{P_{c\ twr}}$	Tower calibrated pressure altitude	ft
H_{P_i}	Indicated pressure altitude	ft
$H_{P_{i\ ref}}$	Reference indicated pressure altitude	ft
H_{P_o}	Observed pressure altitude	ft
$H_{P_{o\ ref}}$	Reference observed pressure altitude	ft
h_{Test}	Test tapeline altitude	ft
ICAO	International Civil Aeronautics Organization	
IFR	Instrument flight rules	
ILS	Instrument landing system	
INS	Inertial navigation system	
J	Propeller advance ratio	

K	Constant	
K_1	Parasite drag constant	
K_2	Induced drag constant	
K_3	Constant	
K_4	Constant	
K_c	Slope of $C_{L_{max}}{}_{Std\ \dot{V}}$ vs CG	
K_d	Slope of $C_{L_{max}}$ vs $\dot{V}$	
KE	Kinetic energy	ft-lb
K_o	Constant	
K_T	Temperature recovery factor	
K_W	Slope of $C_{L_{max}}{}_{Std\ \dot{V}\ ,\ CG}$ vs GW	lb^{-1}
L	Lift	lb
l	Length	ft
$L_{a/c}$	Length of aircraft	ft
L_{aero}	Aerodynamic lift	lb
l_t	Moment arm for tail lift	ft
L_{Thrust}	Thrust lift	lb
M	Mach number	
m	Mass	lb_m
MAC	Mean aerodynamic chord	
MAX	Maximum power	
MDA	Minimum descent altitude	
M_i	Indicated Mach number	
MIL	Military power	
Mission time	Time in air (excluding time before start of initial climb and reserve)	
M_{max}	Mach number at maximum thrust	
M_{mrt}	Mach number at military rated thrust	
M_o	Observed Mach number	
MSL	Mean sea level	
M_{Std}	Standard Mach number	
M_T	True Mach number	
M_{Test}	Test Mach number	
N	Engine speed	RPM
n	Number of time intervals	

NACA	National Advisory Committee on Aeronautics	
NATOPS	Naval Air Training and Operating Procedures Standardization Program	
NAVAIRSYSCOM	Naval Air System Command	
NAVAIRWARCENACDIV	Naval Air Warfare Center Aircraft Division	
n_L	Limit normal acceleration	g
n_R	Radial load factor, $\frac{F_R}{W}$	g
N_{Std}	Standard propeller speed	rpm
NTE	Navy Technical Evaluation	
N_{Test}	Test propeller speed	rpm
n_x	Acceleration along the X axis	g
n_Y	Sideforce load factor, $\frac{F_Y}{W}$	g
n_z	Normal acceleration	g
$n_{z\ sust}$	Sustained normal acceleration	g
$n_{z\ sust\ max}$	Maximum sustained normal acceleration	g
$n_z \frac{W}{\delta}$	Referred normal acceleration	g-lb
n_{z_i}	Indicated normal acceleration	g
$n_{z_{max}}$	Maximum normal acceleration	g
n_{z_o}	Observed normal acceleration	g
$n_{z_{Std}}$	Standard normal acceleration	g
$n_{z_{Test}}$	Test normal acceleration	g
$\frac{N}{\sqrt{\theta}}$	Referred engine speed	RPM
OAT	Outside air temperature	˚C or ˚K
P	Pressure	psf
P_A	Power available	ft-lb/s
P_a	Ambient pressure	psf
$P_{a_{Std}}$	Standard ambient pressure	psf
$P_{a_{Test}}$	Test ambient pressure	psf
PE	Potential energy	ft-lb
POPU	Push-over, pull-up	

P_{req}	Power required	ft-lb/s
P_S	Specific excess power	ft/s
P_S	Static Pressure	psf
$P_{S\ 1\ g}$	Specific excess energy at 1 g	ft/s
P_{ssl}	Standard sea level pressure	2116.217 psf 29.9212 inHg
$P_{s_{Std}}$	Standard specific excess power	ft/s
$P_{s_{Test}}$	Test specific excess power	ft/s
P_T	Total pressure	psf
P_T'	Total pressure at total pressure source	psf
q	Dynamic pressure	psf
q_c	Impact pressure	psf
q_{c_i}	Indicated impact pressure	psf
R	Engineering gas constant for air	96.93ft- lb_f/lb_m-˚K
R	Number of semi-chord lengths	
R	Resistance force	lb
R	Turn radius	ft
R.F.	Range factor	
$R.F._{Test}$	Test day average range factor	
R_e	Reynold's number	
$R_{min\ V>V_A}$	Minimum turn radius for $V > V_A$	ft
ROC	Rate of climb	ft/s
ROD	Rate of descent	ft/s
R_{Std}	Standard day cruise range	nmi
R_{sust}	Sustained turn radius	ft
R_T	Total range	nmi
R_{Test}	Test cruise range	nmi
S	Distance	ft
S	Wing area	ft^2
S.E.	Specific endurance	h/lb
S.R.	Specific range	nmi/lb
S_1	Takeoff distance, brake release to lift off	ft

$S_{1_{SL}}$	Takeoff distance, brake release to lift off, sloping runway	ft
$S_{1_{Std}}$	Standard takeoff distance, brake release to lift off	ft
$S_{1_{Test}}$	Test takeoff distance, brake release to lift off	ft
S_{1_w}	Takeoff distance, brake release to lift off, with respect to wind	ft
S_2	Takeoff distance, lift off to 50 ft	ft
$S_{2_{Std}}$	Standard takeoff distance, lift off to 50 ft	ft
$S_{2_{Test}}$	Test takeoff distance, lift off to 50 ft	ft
S_{2_w}	Takeoff distance, lift off to 50 ft, with respect to wind	ft
S_3	Landing distance, 50 ft to touchdown	ft
$S_{3_{Std}}$	Standard landing distance, 50 ft to touchdown	ft
$S_{3_{Test}}$	Test landing distance, 50 ft to touchdown	ft
S_4	Landing distance, touchdown to stop	ft
$S_{4_{SL}}$	Landing distance, touchdown to stop, sloping runway	ft
$S_{4_{Std}}$	Standard landing distance, touchdown to stop	ft
$S_{4_{Test}}$	Test landing distance, touchdown to stop	ft
S_{4_w}	Landing distance, touchdown to stop, with respect to wind	ft
SAC	Standard aircraft characteristics	
SAS	Stability augmentation system	
SHP	Shaft horsepower	hp
SHP_e	Equivalent shaft horsepower	hp
SHPSFC	Shaft horsepower specific fuel consumption	$\frac{lb/h}{hp}$
SS	Split-S	
STOL	Short take off and landing	

T	Temperature	˚C or ˚K
T	Thrust	lb
t	Time	s
T_a	Ambient temperature	˚C or ˚K
$T_{a\ ref}$	Reference ambient temperature	˚C or ˚K
TACAN	Tactical air navigation	
TAMPS	Tactical Air Mission Planning System	
$T_{a_{Std}}$	Standard ambient temperature	˚K
$T_{a_{Test}}$	Test ambient temperature	˚K
TE	Total energy	ft-lb
T_{ex}	Excess thrust	lb
$T_{ex_{Avg}}$	Average excess thrust	lb
$T_{ex_{Avg\ w}}$	Average excess thrust, with respect to wind	lb
T_G	Gross thrust	lb
THP	Thrust horsepower	hp
THP_{avail}	Thrust horsepower available	hp
THP_e	Equivalent thrust horsepower	hp
THP_i	Induced thrust horsepower	hp
THP_{min}	Minimum thrust horsepower	hp
THP_p	Parasite thrust horsepower	hp
THP_{req}	Thrust horsepower required	hp
THPSFC	Thrust horsepower specific fuel consumption	$\frac{lb/h}{hp}$
T_i	Indicated temperature	˚C or ˚K
Time	Time at the start of each segment	s
T_N	Net thrust	lb
$T_{N_{Std}}$	Standard net thrust	lb
$T_{N_{Test}}$	Test net thrust	lb
T_{N_x}	Net thrust parallel flight path	lb
$\frac{T_{N_x}}{\delta}$	Referred net thrust parallel flight path	lb
T_o	Observed temperature	˚C or ˚K
T_R	Ram drag	lb
TSFC	Thrust specific fuel consumption	$\frac{lb/h}{lb}$

T_{ssl}	Standard sea level temperature	15˚C, 288.15˚K; 59˚F, 518.67˚R
T_{Std}	Standard temperature	˚C or ˚K
T_{Std}	Standard thrust	lb
T_T	Total temperature	˚K
t_T	Total cruise time	s
T_{T_2}	Inlet total temperature (at engine compressor face)	˚K
T_{Test}	Test temperature (At tower)	˚K
T_{Test}	Test thrust	lb
USNTPS	U.S. Naval Test Pilot School	
V	Velocity	ft/s or kn
V_{50}	Ground speed at 50 ft reference point	ft/s
V_A	Maneuvering speed	ft/s
V_{APR}	Approach speed	kn
V_c	Calibrated airspeed	kn
$V_{CL_{50}}$	Climb speed at 50 ft	kn
$V_{c_{Std}}$	Standard calibrated airspeed	kn
$V_{c_{Test}}$	Test calibrated airspeed	kn
V_{c_W}	Calibrated airspeed corrected to standard weight	kn
V_e	Equivalent airspeed	ft/s or kn
V_{e_s}	Stall equivalent airspeed	kn
$V_{e_{Std}}$	Standard equivalent airspeed	kn
$V_{e_{Test}}$	Test equivalent airspeed	kn
VFR	Visual flight rules	
V_G	Ground speed	kn
V_H	Maximum level flight airspeed	kn
V_{hor}	Horizontal velocity	ft/s or kn
V_i	Indicated airspeed	kn
$V_{i_{Test}}$	Test indicated airspeed	kn
V_{i_W}	Indicated airspeed corrected to standard weight	kn
Vj	Avg true airspeed in time interval	kn

V_L	Landing airspeed	ft/s or kn
$V_{L_{50}}$	Landing speed at 50 ft	kn
V_{max}	Maximum airspeed	kn
V_{mc}	Airspeed for minimum control	kn
V_{min}	Minimum airspeed	kn
V_{mrt}	Military rated thrust airspeed	kn
V_o	Observed airspeed	kn
$V_{o\ ref}$	Reference observed airspeed	kn
$V_{PA_{min}}$	Minimum speed in the approach configuration	kn
V_R	Rotation airspeed	kn
V_s	Stall speed	ft/s or kn
V_{s_L}	Stall speed, landing configuration, power off	kn
V_{s_T}	Stall speed, transition configuration, power off, flaps down, gear up	kn
$V_{s_{Test}}$	Test stall speed	kn
V_T	True airspeed	ft/s or kn
$V_{T_{avg}}$	Average true airspeed	ft/s or kn
V_{TD}	Touchdown ground speed	ft/s
V_{TD_w}	Touchdown ground speed with respect to wind	ft/s
V_{TO}	Takeoff ground speed	ft/s
V_{TO_w}	Takeoff ground speed with respect to wind	ft/s
$V_{T_{ref}}$	Reference true airspeed	ft/s
$V_{T_{Std}}$	Standard true airspeed	ft/s or kn
$V_{T_{Test}}$	Test true airspeed	ft/s or kn
V_v	Vertical velocity	ft/s or fpm
V_w	Wind velocity	ft/s or kn
V_x	Speed for maximum climb angle	kn
V_y	Speed for maximum rate of climb	kn
$\dot{V}$	Acceleration/deceleration rate	kn/s
$\dot{V}_{Std}$	Standard acceleration /deceleration rate	kn/s

$\dot{V}_{Test}$	Test acceleration/deceleration rate	kn/s
W	Weight	lb
W/δ	Weight to pressure ratio	lb
W_1	Initial cruise weight	lb
W_2	Final cruise weight	lb
$W_{aircraft}$	Aircraft weight	lb
W_f	Fuel weight	lb
$W_{f_{End}}$	End fuel weight	lb
$W_{f_{Start}}$	Start fuel weight	lb
$W_{f_{Used}}$	Fuel used	lb
$\dot{W}_{f\ ref}$	Referred fuel flow	lb/h
W_{ref}	Referred aircraft weight	lb
W_{Std}	Standard weight	lb
W_{Std_1}	Standard initial cruise weight	lb
W_{Std_2}	Standard final cruise weight	lb
W_{Test}	Test weight	lb
WUT	Wind-up-turn	
$\dot{W}_f$	Fuel flow	lb/h
x	Scaled length of aircraft	
Y	Height of CG above ram drag	ft
y	Scaled height of aircraft above tower	
Z	Height of CG above gross thrust	ft
¢	Constant	

GREEK SYMBOLS

α (alpha)	Angle of attack	deg
α_i	Induced angle of attack	deg
α_j	Thrust angle	deg
β (beta)	Sideslip angle	deg
δ (delta)	Pressure ratio	
δ_h	Pressure ratio for selected altitude	
δ_{Test}	Test pressure ratio	
ϕ (phi)	Bank angle	deg
ϕ_E	Equivalent bank angle	deg

γ (gamma)	Ratio of specific heats	
γ	Flight path angle	deg
γ_{Std}	Standard flight path angle	deg
γ_{Test}	Test flight path angle	deg
η_P (eta)	Propeller efficiency	
Λ (Lambda)	Wing sweep angle	deg
λ (lambda)	Taper ratio	
λ	Lag error constant	
λ_s	Static pressure lag error constant	
λ_T	Total pressure lag error constant	
μ (mu)	Viscosity	lb-s/ft^2
μ	Coefficient of friction	
μ_2	Coefficient of friction, brakes applied	
π (pi)	Constant	
θ (theta)	Pitch attitude	deg
θ	Runway slope angle	deg
θ	Temperature ratio	
θ	Angle	deg
θ_{Std}	Standard temperature ratio	
θ_T	Total temperature ratio	
θ_{Test}	Test temperature ratio	
ρ (rho)	Air density	slug/ ft^3
ρ_a	Ambient air density	slug/ ft^3
ρ_{ssl}	Standard sea level air density	0.0023769 slug/ ft^3
σ (sigma)	Density ratio	
σ_{Std}	Standard density ratio	
σ_{Test}	Test density ratio	
τ (tau)	Inclination of the thrust axis with respect to the chord line	deg
ω (omega)	Turn rate	rad/s
$\omega_{max\ V>V_A}$	Maximum turn rate for V > V_A	rad/s
ω_{sust}	Sustained turn rate	deg/s

APPENDIX II

REFERENCES

APPENDIX II

REFERENCES

CHAPTER 1

1. NAVAIRTESTCEN Instruction 5213.3F, *Report Writing Handbook*, NAVAIRTESTCEN, Patuxent River, MD, 16 August 1984.

2. Naval Test Pilot School Flight Test Manual, *Fixed Wing Performance, Theory and Flight Test Techniques*, USNTPS-FTM-No.104, U. S. Naval Test Pilot School, Patuxent River, MD, July, 1977.

3. *U.S. Naval Test Pilot School Notice 1542*, Subj: Academic, Flight and Report Curriculum for Class --, U.S. Naval Test Pilot School, Patuxent River, MD.

4. USAF Test Pilot School, *Performance Phase Textbook Volume I*, USAF-TPS-CUR-86-01, USAF, Edwards AFB, CA, April, 1986.

CHAPTER 2

1. Dommasch, Daniel O. et al, *Airplane Aerodynamics*, 4th Edition, Pitman Publishing Corp., New York, NY, 1967.

2. Gracey, William, *Measurement of Aircraft Speed and Altitude*, A Wiley-Interscience Publication, New York, NY, 1981.

3. Gracey, William, *Measurement of Aircraft Speed and Altitude*, NASA Reference Publication 1046, May, 1980.

4. Houston, *Accuracy of Airspeed Measurements and Flight Calibration Procedures*, NACA Report No. 919, 1984.

5. McCue, J.J., *Pitot-Static Systems*, USNTPS Class Notes, USNTPS, Patuxent River, MD., June, 1982.

6. Military Specification, “Instrument Systems, Pitot Tube and Flush Static Port Operated, Installation of”, MIL-I-6115A, 31 December 1960.

7. Military Specification, MIL-I-5072-1, “Instrument Systems; Pitot Static Tube Operated, Installation of”, 17 October 1949.

8. Naval Test Pilot School Flight Test Manual, *Fixed Wing Performance, Theory and Flight Test Techniques*, USNTPS-FTM-No.104, U. S. Naval Test Pilot School, Patuxent River, MD, July, 1977.

9. USAF Test Pilot School, *Performance Phase Textbook Volume I*, USAF-TPS-CUR-86-01, USAF, Edwards AFB, CA, April, 1986.

CHAPTER 3

1. Branch, M., *Determination of Stall Airspeed at Altitude and Sea Level*, Flight Test Division Technical Memorandum, FTTM No. 3-72, Naval Air Test Center, Patuxent River, MD, November, 1972.

2. Federal Aviation Regulations, Part 23, *Airworthiness Standards: Normal, Utility, and Acrobatic Category Airplanes*, June 1974.

3. Lan, C. E., and Roskam, J., *Airplane Aerodynamics and Performance*, Roskam Aviation and Engineering Corp.,Ottawa, Kansas, 1981.

4. Lean, D., *Stalling and the Measurement of Maximum Lift*, AGARD Flight Test Manual, Vol II, Chap 7, Pergamon Press, Inc., New York, NY., 1959.

5. McCue, J.J., *Pitot-Static Systems*, USNTPS Class Notes, USNTPS, Patuxent River, MD., June, 1982.

6. Military Standard, “Flying Qualities of Piloted Aircraft”, MIL-STD-1797A, 30 January, 1990.

7. Naval Test Pilot School Flight Test Manual, *Fixed Wing Performance, Theory and Flight Test Techniques*, USNTPS-FTM-No.104, U. S. Naval Test Pilot School, Patuxent River, MD, July, 1977.

8. Powell, J., *Airplane Performance*, USNTPS Classroom Notes, USNTPS, Patuxent River, MD.

9. Strike Aircraft Test Directorate Flight Test Manual, *Carrier Suitability Testing Manual*, SA FTM-01, Strike Aircraft Test Directorate, Patuxent River, MD, March,1991.

10. USAF Test Pilot School, *Performance Phase Textbook Volume I*, USAF-TPS-CUR-86-01, USAF, Edwards AFB, CA, April, 1986.

CHAPTER 4

1. Department of the Army, *Operator's Manual for Army U-21A Aircraft*, TM 555-1510-209-10, Headquarters Department of the Army, Washington D.C., 26 September 1988.

2. Naval Air System Command Specification, *Guidelines For Preparation Of Standard Aircraft Characteristics Charts And Performance Data Piloted Aircraft (Fixed Wing), AS-5263,* 23 October, 1986.

3. Naval Test Pilot School Flight Test Manual, *Fixed Wing Performance, Theory and Flight Test Techniques*, USNTPS-FTM-No.104, U.S. Naval Test Pilot School, Patuxent River, MD, July 1977.

4. Powell, J.W., *Airplane Performance, Fixed Wing Flight Mechanics*, USNTPS Class Notes, USNTPS, Patuxent River, MD., no date.

5. Roberts, S.C., *Light Aircraft Performance for Test Pilots and Flight Test Engineers*, Flight Research, Inc, Mojave, CA., 9 July 1982.

6. USAF Test Pilot School Flight Test Manual, *Performance Flight Testing Phase*, Volume I, Chapter 11, USAF Test Pilot School, Edwards AFB, CA, February 1987.

7. USAF Test Pilot School, *Performance Phase Textbook Volume I*, USAF TPS-CUR-86-01, USAF, Edwards AFB, CA, April, 1986.

8. USAF Test Pilot School, *Performance Planning Guide*, USAF Test Pilot School, Edwards AFB, CA.,July 1987.

CHAPTER 5

1. Rutowski, E.S., *Energy Approach to the General Aircraft Maneuverability Problem,* Journal of the Aeronautical Sciences, Vol 21, No 3, March 1954.

2. Powell, J., *Airplane Performance*, USNTPS Classroom Notes, USNTPS, Patuxent River, MD.

3. USAF Test Pilot School, *Performance Phase Textbook Volume I*, USAF-TPS-CUR-86-01, USAF, Edwards AFB, CA, April, 1986.

CHAPTER 6

1. Hoover, A.D., *Testing for Agility - a Progress Report,* Thirty-Second Symposium Proceedings, Society of Experimental Test Pilots, October, 1988.

2. McAtee, T.P., *Agility - Its Nature and Need in the 1990s*, Thirty-First Symposium Proceedings, Society of Experimental Test Pilots, September, 1987.

3. Naval Test Pilot School Flight Test Manual, *Fixed Wing Performance, Theory and Flight Test Techniques,* USNTPS-FTM-No.104, U. S. Naval Test Pilot School, Patuxent River, MD, July, 1977.

4. Powell, J., *Airplane Performance*, USNTPS Classroom Notes, USNTPS, Patuxent River, MD.

5. Rutowski, E.S., *Energy Approach to the General Aircraft Maneuverability Problem,* Journal of the Aeronautical Sciences, Vol 21, No 3, March 1954.

6. USAF Test Pilot School, *Performance Phase Textbook Volume I*, USAF-TPS-CUR-86-01, USAF, Edwards AFB, CA, April, 1986.

CHAPTER 7

1. Naval Air System Command Specification, *Guidelines For Preparation Of Standard Aircraft Characteristics Charts And Performance Data Piloted Aircraft (Fixed Wing), AS-5263,* 23 October, 1986.

2. Naval Test Pilot School Flight Test Manual, *Fixed Wing Performance, Theory and Flight Test Techniques*, USNTPS-FTM-No. 104, U. S. Naval Test Pilot School, Patuxent River, MD, July 1977.

3. Petersen, F.S., *Aircraft and Engine Performance*, Naval Air Test Center, Patuxent River, MD, 1958.

4. Powell, J.W., *Airplane Performance*, USNTPS Classroom Notes, USNTPS Patuxent River, MD.

5. Rutowski, E.S., "Energy Approach to the General Aircraft Maneuverability Problem", *Journal of the Aeronautical Sciences*, Vol 21, No 3, March 1954.

6. USAF Test Pilot School, *Performance Flight Test Phase*, Volume I, Chapter 9, USAF Test Pilot School, Edwards AFB, CA, August 1991.

7. USAF Test Pilot School, *Performance Planning Guide*, USAF Test Pilot School, Edwards AFB, CA, July 1987.

CHAPTER 8

1. Dommasch, D.O et al, *Airplane Aerodynamics*, 4th Edition, Pitman Publishing Company, N.Y., N.Y., 1967.

2. HP Model 9816 Computer System, "USNTPS Fixed Wing Aircraft Performance User Instructions", March 1985.

3. NAVAIRSYSCOM Specification, AS-5263, "Guidelines for Preparation of Standard Aircraft Characteristics Charts and Performance Data, Piloted Aircraft (Fixed Wing)", 23 October 1986.

4. Naval Test Pilot School Flight Test Manual, *Fixed Wing Performance, Theory and Flight Test Techniques*, USNTPS-FTM-No. 104, U.S. Naval Test Pilot School, Patuxent River, MD, July 1977.

5. OPNAVINST 3710.7N, "NATOPS General Flight and Operating Instructions", 25 August, 1992.

6. Peterson, *Aircraft and Engine Performance*, USNTPS Textbook, USNTPS, Patuxent River, MD, 1958.

7. Powell, J.W., *Airplane Performance*, *Fixed Wing Flight Mechanics*, USNTPS Class Notes, USNTPS, Patuxent River, MD, undated.

8. Stinton, D., *The Design of the Aeroplane*, Van Nostrand Reinhold Company, N.Y.

9. USAF Test Pilot School Flight Test Manual, *Performance Flight Testing Phase*, Volume I, USAF Test Pilot School, Edwards AFB, CA, February 1987.

CHAPTER 9

1. Clancy, L.J., *Aerodynamics*, A Halsted Press Book, John Wiley & Sons, New York 1975.

2. Departments of the Army, Navy, Air Force, Military Specification MIL-C-5011A, 5 November 1951.

3. Dommasch, D.O. et al, *Airplane Aerodynamics*, 4th Edition, Pitman Publishing Company, N.Y., N.Y., 1967.

4. Federal Aviation Regulations Part 23 and Part 25.

5. Kimberlin, R., "Takeoff and Landing Notes", The University of Tennessee Space Institute, undated.

6. "Military Standard Flying Qualities of Piloted Airplanes", MIL-STD-1797A 30 January 1990.

7. Naval Air Systems Command Specification, AS-5263, *Guidelines For Preparation Of Standard Aircraft Characteristics Charts And Performance Data Piloted Aircraft (Fixed Wing)*, 23 October, 1986.

8. Naval Test Pilot School Flight Test Manual, *Fixed Wing Performance, Theory and Flight Test Techniques*, USNTPS-FTM-No. 104, U.S. Naval Test Pilot School, Patuxent River, MD, July 1977.

9. Roberts, Sean C., *Light Aircraft Performance For Test Pilots and Flight Test Engineers*, Flight Research,. Inc. Mojave, CA, 9 July 1982.

10. Stinton, D., *The Design of the Aeroplane*, Van Nostrand Reinhold Company, N.Y.

11. USAF Test Pilot School Flight Test Manual, *Performance Flight Testing Phase, Volume I*, USAF Test Pilot School, Edwards AFB, CA, February 1987.

12. USAF Test Pilot School, *Performance Phase Planning Guide*, USAF Test Pilot School, Edwards, AFB, CA, July 1987.

CHAPTER 10

1. “Aircraft Conceptual Design”, Course Notes (#Y0606), Lockheed Technical Institute, Fall 1991.

2. “Functional Description For Training Services”, Undergraduate Naval Flight Officer Training System Program, NASC, PMA 200, 3 April 1989.

3. Luter, M., NAVAIRSYSCOM (AIR-53012) Course Notes, (undated).

4. Military Specification (MIL-D-8708(AS)), “Demonstration Requirements for Airplanes”, 31 January 1969.

5. Military Standard, MIL-STD-1797A, “Flying Qualities of Piloted Aircraft”, 30 January 1990.

6. "Mission Profiles for Navy Pilot Trainer", (date unknown).

7. NAVAIRSYSCOM Specification, AS-5263, "Guidelines for Preparation of Standard Aircraft Characteristics Charts and Performance Data, Piloted Aircraft (Fixed Wing)", 23 October 1986.

8. Nicolai, L.M., *Fundamentals of Aircraft Design*, Fairborn, Ohio, E.P. Domicone Printing Services, 1975.

9. Raymer, D.P,. *Aircraft Design: A Conceptual Approach*, Washington, D.C., American Institute of Aeronautics and Astronautics, Inc., 1989.

10. Roskam, J., *Airplane Design* (Part I, II and VII), Ottawa, Kansas, Roskam Aviation and Engineering Corporation, 1988.

APPENDIX III

FIGURES

APPENDIX III

FIGURES

CHAPTER 4

CHAPTER 5

CHAPTER 6

CHAPTER 7

CHAPTER 8

CHAPTER 9

CHAPTER 10

APPENDIX IV

TABLES

APPENDIX IV

TABLES

APPENDIX V

EQUATIONS

APPENDIX V

EQUATIONS

CHAPTER 2

		PAGE
$P = \rho\, g_c\, R\, T$	(Eq 2.1)	2.4
$dP_a = -\rho\, g\, dh$	(Eq 2.2)	2.4
$g_{ssl}\, dH = g\, dh$	(Eq 2.3)	2.4
$\theta = \frac{T_a}{T_{ssl}} = \left(1 - 6.8755856 \times 10^{-6} H\right)$	(Eq 2.4)	2.5
$\delta = \frac{P_a}{P_{ssl}} = \left(1 - 6.8755856 \times 10^{-6} H\right)^{5.255863}$	(Eq 2.5)	2.5
$\sigma = \frac{\rho_a}{\rho_{ssl}} = \left(1 - 6.8755856 \times 10^{-6} H\right)^{4.255863}$	(Eq 2.6)	2.6
$P_a = P_{ssl}\left(1 - 6.8755856 \times 10^{-6} H_P\right)^{5.255863}$	(Eq 2.7)	2.6
$T_a = -56.50^\circ C = 216.65^\circ K$	(Eq 2.8)	2.6
$\delta = \frac{P_a}{P_{ssl}} = 0.223358\, e^{-4.80614 \times 10^{-5} (H - 36089)}$	(Eq 2.9)	2.6
$\sigma = \frac{\rho_a}{\rho_{ssl}} = 0.297069\, e^{-4.80614 \times 10^{-5} (H - 36089)}$	(Eq 2.10)	2.6
$P_a = P_{ssl}\left(0.223358\, e^{-4.80614 \times 10^{-5} \left(H_P - 36089\right)}\right)$	(Eq 2.11)	2.6

$$V_T = \sqrt{\frac{2}{\rho_a}\left(P_T - P_a\right)} = \sqrt{\frac{2q}{\rho_a}}$$ (Eq 2.12) 2.10

$$V_e = \sqrt{\frac{2q}{\rho_{ssl}}} = \sqrt{\frac{\sigma\, 2q}{\rho_a}} = \sqrt{\sigma}\, V_T$$ (Eq 2.13) 2.11

$$V_{e_{Test}} = V_{e_{Std}}$$ (Eq 2.14) 2.12

$$V_T^2 = \frac{2\gamma}{\gamma - 1}\frac{P_a}{\rho_a}\left[\left(\frac{P_T - P_a}{P_a} + 1\right)^{\frac{\gamma - 1}{\gamma}} - 1\right]$$ (Eq 2.15) 2.13

$$V_T = \sqrt{\frac{2\gamma}{\gamma - 1}\frac{P_a}{\rho_a}\left[\left(\frac{q_c}{P_a} + 1\right)^{\frac{\gamma - 1}{\gamma}} - 1\right]}$$ (Eq 2.16) 2.13

$$q_c = q\left(1 + \frac{M^2}{4} + \frac{M^4}{40} + \frac{M^6}{1600} + \ldots\right)$$ (Eq 2.17) 2.13

$$V_c^2 = \frac{2\gamma}{\gamma - 1}\frac{P_{ssl}}{\rho_{ssl}}\left[\left(\frac{P_T - P_a}{P_{ssl}} + 1\right)^{\frac{\gamma - 1}{\gamma}} - 1\right]$$ (Eq 2.18) 2.14

$$V_c = \sqrt{\frac{2\gamma}{\gamma - 1}\frac{P_{ssl}}{\rho_{ssl}}\left[\left(\frac{q_c}{P_{ssl}} + 1\right)^{\frac{\gamma - 1}{\gamma}} - 1\right]}$$ (Eq 2.19) 2.14

$$V_c = f\left(P_T - P_a\right) = f\left(q_c\right)$$ (Eq 2.20) 2.14

$$V_{c_{Test}} = V_{c_{Std}}$$ (Eq 2.21) 2.14

$$\frac{P'_T}{P_a} = \left[\frac{\gamma + 1}{2} \left(\frac{V}{a} \right)^2 \right]^{\frac{\gamma}{\gamma - 1}} \left[\frac{1}{\frac{2\gamma}{\gamma + 1} \left(\frac{V}{a} \right)^2 - \frac{\gamma - 1}{\gamma + 1}} \right]^{\frac{1}{\gamma - 1}}$$

(Eq 2.22) 2.15

$$\frac{q_c}{P_{ssl}} = \left[1 + 0.2 \left(\frac{V_c}{a_{ssl}} \right)^2 \right]^{3.5} - 1$$

(For $Vc \leq a_{ssl}$) (Eq 2.23) 2.15

$$\frac{q_c}{P_{ssl}} = \left[\frac{166.921 \left(\frac{V_c}{a_{ssl}} \right)^7}{\left[7 \left(\frac{V_c}{a_{ssl}} \right)^2 - 1 \right]^{2.5}} \right] - 1$$

(For $Vc \geq a_{ssl}$) (Eq 2.24) 2.15

$$V_e = \sqrt{\frac{2\gamma}{\gamma - 1} \frac{P_a}{\rho_{ssl}} \left[\left(\frac{q_c}{P_a} + 1 \right)^{\frac{\gamma - 1}{\gamma}} - 1 \right]}$$

(Eq 2.25) 2.17

$$V_e = V_T \sqrt{\sigma}$$

(Eq 2.26) 2.17

$$M = \frac{V_T}{a} = \frac{V_T}{\sqrt{\gamma g_c R T}} = \frac{V_T}{\sqrt{\gamma \frac{P}{\rho}}}$$

(Eq 2.27) 2.17

$$M = \sqrt{\frac{2}{\gamma - 1} \left[\left(\frac{P_T - P_a}{P_a} + 1 \right)^{\frac{\gamma - 1}{\gamma}} - 1 \right]}$$

(Eq 2.28) 2.17

$$\frac{P_T}{P_a} = \left(1 + \frac{\gamma - 1}{2} M^2 \right)^{\frac{\gamma}{\gamma - 1}}$$

(Eq 2.29) 2.18

$$\frac{q_c}{P_a} = \left(1 + 0.2\, M^2\right)^{3.5} - 1 \quad \text{for } M < 1$$ (Eq 2.30) 2.18

$$\frac{q_c}{P_a} = \left[\frac{166.921\, M^7}{\left(7M^2 - 1\right)^{2.5}}\right] - 1 \quad \text{for } M > 1$$ (Eq 2.31) 2.18

$$M = f\left(P_T - P_a\,,\, P_a\right) = f\left(V_c,\, H_P\right)$$ (Eq 2.32) 2.19

$$M_{Test} = M$$ (Eq 2.33) 2.19

$$\Delta H_{P_{ic}} = H_{P_i} - H_{P_o}$$ (Eq 2.34) 2.22

$$\Delta V_{ic} = V_i - V_o$$ (Eq 2.35) 2.22

$$H_{P_i} = H_{P_o} + \Delta H_{P_{ic}}$$ (Eq 2.36) 2.22

$$V_i = V_o + \Delta V_{ic}$$ (Eq 2.37) 2.22

$$\Delta P = P_s - P_a$$ (Eq 2.38) 2.27

$$\Delta V_{pos} = V_c - V_i$$ (Eq 2.39) 2.27

$$\Delta H_{pos} = H_{P_c} - H_{P_i}$$ (Eq 2.40) 2.27

$$\Delta M_{pos} = M - M_i$$ (Eq 2.41) 2.27

$$\frac{P_s}{P_a} = f_1\left(M, \alpha, \beta, R_e\right)$$ (Eq 2.42) 2.28

$$\frac{P_s}{P_a} = f_2\left(M, \alpha\right)$$ (Eq 2.43) 2.28

$$\frac{\Delta P}{q_c} = f_3\left(M, \alpha\right)$$ (Eq 2.44) 2.28

$\frac{\Delta P}{q_c} = f_4\left(M\right)$ (High speed)	(Eq 2.45)	2.28
$\frac{\Delta P}{q_c} = f_5\left(C_L\right)$ (Low speed)	(Eq 2.46)	2.28
$\frac{\Delta P}{q_{c_i}} = f_6\left(M_i\right)$ (High speed)	(Eq 2.47)	2.29
$\frac{\Delta P}{q_c} = f_7\left(W, V_c\right)$ (Low speed)	(Eq 2.48)	2.29
$V_{c_W} = V_{c_{Test}} \sqrt{\frac{W_{Std}}{W_{Test}}}$	(Eq 2.49)	2.30
$\frac{\Delta P}{q_c} = f_8\left(V_{c_W}\right)$ (Low speed)	(Eq 2.50)	2.30
$V_{i_W} = V_{i_{Test}} \sqrt{\frac{W_{Std}}{W_{Test}}}$	(Eq 2.51)	2.30
$\frac{\Delta P}{q_{c_i}} = f_9\left(V_{i_W}\right)$ (Low speed)	(Eq 2.52)	2.30
$\frac{T_T}{T} = 1 + \frac{\gamma - 1}{2} M^2$	(Eq 2.53)	2.32
$\frac{T_T}{T} = 1 + \frac{\gamma - 1}{2} \frac{V_T^2}{\gamma g_c R T}$	(Eq 2.54)	2.32
$\frac{T_T}{T} = 1 + \frac{K_T\left(\gamma - 1\right)}{2} M^2$	(Eq 2.55)	2.33
$\frac{T_T}{T} = 1 + \frac{K_T\left(\gamma - 1\right)}{2} \frac{V_T^2}{\gamma g_c R T}$	(Eq 2.56)	2.33
$\frac{T_T}{T_a} = \frac{T_i}{T_a} = 1 + \frac{K_T M^2}{5}$	(Eq 2.57)	2.33

$T_T = T_i = T_a + \dfrac{K_T\, V_T^2}{7592}$	(Eq 2.58)	2.33
$T_i = T_o + \Delta T_{ic}$	(Eq 2.59)	2.35
$K_T = \left(\dfrac{T_i\ (^\circ K)}{T_a\ (^\circ K)} - 1\right)\dfrac{5}{M^2}$	(Eq 2.60)	2.35
$V_{G_1} = 3600\left(\dfrac{D}{\Delta t_1}\right)$	(Eq 2.61)	2.50
$V_{G_2} = 3600\left(\dfrac{D}{\Delta t_2}\right)$	(Eq 2.62)	2.50
$V_T = \dfrac{V_{G_1} + V_{G_2}}{2}$	(Eq 2.63)	2.50
$\rho_a = \dfrac{P_a}{g_c\, R\, T_{a_{ref}}\ (^\circ K)}$	(Eq 2.64)	2.50
$\sigma = \dfrac{\rho_a}{\rho_{ssl}}$	(Eq 2.65)	2.51
$V_c = V_e - \Delta V_c$	(Eq 2.66)	2.51
$M = \dfrac{V_T}{38.9678\sqrt{T_{a_{ref}}\ (^\circ K)}}$	(Eq 2.67)	2.51
$q_c = P_{ssl}\left\{\left[1 + 0.2\left(\dfrac{V_c}{a_{ssl}}\right)^2\right]^{3.5} - 1\right\}$	(Eq 2.68)	2.51
$q_{c_i} = P_{ssl}\left\{\left[1 + 0.2\left(\dfrac{V_i}{a_{ssl}}\right)^2\right]^{3.5} - 1\right\}$	(Eq 2.69)	2.51

$$\Delta P = q_c - q_{c_i}$$ (Eq 2.70) 2.51

$$V_{i_W} = V_i \sqrt{\frac{W_{Std}}{W_{Test}}}$$ (Eq 2.71) 2.51

$$H_{P_{i_{ref}}} = H_{P_{o_{ref}}} + \Delta H_{P_{ic_{ref}}}$$ (Eq 2.72) 2.54

$$H_{P_i} = \frac{T_{ssl}}{a_{ssl}}\left[1 - \left(\frac{P_s}{P_{ssl}}\right)^{\frac{1}{\left(\frac{g_{ssl}}{g_c\, a_{ssl}\, R}\right)}}\right]$$ (Eq 2.73) 2.54

$$H_{P_{i_{ref}}} = \frac{T_{ssl}}{a_{ssl}}\left[1 - \left(\frac{P_a}{P_{ssl}}\right)^{\frac{1}{\left(\frac{g_{ssl}}{g_c\, a_{ssl}\, R}\right)}}\right]$$ (Eq 2.74) 2.55

$$\Delta h = d \tan\theta$$ (Eq 2.75) 2.57

$$\Delta h = L_{a/c} \frac{y}{x}$$ (Eq 2.76) 2.57

$$H_{P_c} = H_{P_{c_{twr}}} + \Delta h \frac{T_{Std}\ (^\circ K)}{T_{Test}\ (^\circ K)}$$ (Eq 2.77) 2.57

$$P_s = P_{ssl}\left(1 - 6.8755856 \times 10^{-6}\, H_{P_i}\right)^{5.255863}$$ (Eq 2.78) 2.57

$$P_a = P_{ssl}\left(1 - 6.8755856 \times 10^{-6}\, H_{P_c}\right)^{5.255863}$$ (Eq 2.79) 2.58

$$\text{Curve slope} = K_T \frac{\gamma - 1}{\gamma} T_a = 0.2\, K_T\, T_a\ (^\circ K)\ \text{(High speed)}$$ (Eq 2.80) 2.60

$$\text{Curve slope} = K_T \frac{0.2\, T_a\, (^\circ K)}{a_{ssl}^2} \text{ (Low speed)}$$ (Eq 2.81) 2.60

$$K_T = \frac{\text{slope}}{0.2\, T_a\, (^\circ K)} \text{ (High speed)}$$ (Eq 2.82) 2.60

$$K_T = \frac{\text{slope}\ a_{ssl}^2}{0.2\, T_a\, (^\circ K)} \text{ (Low speed)}$$ (Eq 2.83) 2.61

$$M_i = \sqrt{\frac{2}{\gamma - 1}\left[\left(\frac{q_{c_i}}{P_s} + 1\right)^{\frac{\gamma - 1}{\gamma}} - 1\right]}$$ (Eq 2.84) 2.62

$$\Delta P = \left(\frac{\Delta P}{q_{c_i}}\right) q_{c_i}$$ (Eq 2.85) 2.62

$$q_c = q_{c_i} + \Delta P$$ (Eq 2.86) 2.62

$$\Delta V_{pos} = V_c - V_{i_W}$$ (Eq 2.87) 2.63

$$P_a = P_s - \Delta P$$ (Eq 2.88) 2.63

$$H_{P_c} = \frac{T_{ssl}}{a_{ssl}}\left[1 - \left(\frac{P_a}{P_{ssl}}\right)^{\frac{1}{\left(\frac{g_{ssl}}{g_c\, a_{ssl}\, R}\right)}}\right]$$ (Eq 2.89) 2.63

CHAPTER 3

$$C_{L_{max\,(\Lambda)}} = C_{L_{max\,(\Lambda = 0)}} \cos(\Lambda)$$ (Eq 3.1) 3.7

$$V_{e_s} = \sqrt{\frac{n_z W}{C_{L_s}\, q\, S}}$$ (Eq 3.2) 3.10

$$\frac{V_{e_{s_1}}}{V_{e_{s_2}}} = \sqrt{\frac{C_{L_{s_2}}}{C_{L_{s_1}}}}$$

(Eq 3.3) 3.10

If $\frac{V_{e_{s_1}}}{V_{e_{s_2}}} = 0.8$, then $\frac{C_{L_{s_2}}}{C_{L_{s_1}}} = 0.64$

(Eq 3.4) 3.10

$$\frac{C_{L_{s_1}}}{C_{L_{s_2}}} = 1.56$$

(Eq 3.5) 3.10

$$\alpha_j = \alpha + \tau$$

(Eq 3.6) 3.17

$$L = L_{aero} + L_{Thrust}$$

(Eq 3.7) 3.17

$$L = n_z W$$

(Eq 3.8) 3.17

$$L_{Thrust} = T_G \sin \alpha_j$$

(Eq 3.9) 3.17

$$L = n_z W = L_{aero} + T_G \sin \alpha_j$$

(Eq 3.10) 3.17

$$C_L = \frac{L}{q\,S} = \frac{n_z W}{q\,S} = \frac{L_{aero}}{q\,S} + \frac{T_G \sin \alpha_j}{q\,S}$$

(Eq 3.11) 3.17

$$C_L = C_{L_{aero}} + \frac{T_G \sin \alpha_j}{q\,S}$$

(Eq 3.12) 3.17

$$C_L = C_{L_{aero}} + \frac{T_G \sin \alpha_j}{\frac{n_z W}{C_L}}$$

(Eq 3.13) 3.18

$$C_L = C_{L_{aero}} + C_L\left(\frac{T_G}{W}\,\frac{\sin \alpha_j}{n_z}\right)$$

(Eq 3.14) 3.18

$$C_L\left(1 - \frac{T_G}{W}\frac{\sin\alpha_j}{n_z}\right) = C_{L_{aero}}$$

(Eq 3.15) 3.18

$$C_L = \frac{C_{L_{aero}}}{\left(1 - \frac{T_G}{W}\frac{\sin\alpha_j}{n_z}\right)}$$

(Eq 3.16) 3.18

$$C_L = f\left(C_{L_{aero}}, \frac{T_G}{W}, \sin\alpha_j, n_z\right)$$

(Eq 3.17) 3.18

$$C_{L_{aero}} = f\left(\alpha, M, R_e\right)$$

(Eq 3.18) 3.19

$$C_{L_{aero}} = \frac{n_z W}{q\,S} = \frac{n_z W}{\frac{\gamma}{2} P_{ssl}\, S\, \delta\, M^2}$$

(Eq 3.19) 3.19

$$C_{L_{aero}} = \frac{n_z\left(\frac{W}{\delta}\right)}{\left(\frac{\gamma}{2} P_{ssl}\, S\right) M^2}$$

(Eq 3.20) 3.19

$$V_s = V_{s_{Test}}\sqrt{\frac{R + 2}{R + 1}} \text{ (For decelerations)}$$

(Eq 3.21) 3.21

$$C_{L_s} = C_{L_{Test}}\left(\frac{R + 1}{R + 2}\right) \text{ (For decelerations)}$$

(Eq 3.22) 3.21

$$V_s = V_{s_{Test}}\sqrt{\frac{R + 1}{R + 2}} \text{ (For accelerations)}$$

(Eq 3.23) 3.21

$$R = \frac{V_{s_{Test}}}{\frac{c}{2}\dot{V}}$$

(Eq 3.24) 3.21

$$C_{L_{max_{Std\,\dot{V}}}} = C_{L_{max}} + K_d\left(\dot{V}_{Std} - \dot{V}_{Test}\right)$$

(Eq 3.25) 3.22

$C_{L_{max_{Std\ \dot{V},\ CG}}} = C_{L_{max_{Std\ \dot{V}}}} + K_c \left(CG_{Std} - CG_{Test}\right)$	(Eq 3.26)	3.25
$\Delta L_t \left(l_t\right) = T_G\ (Z) - D_R\ (Y)$	(Eq 3.27)	3.26
$\Delta C_{L_t} = \frac{T_G}{q\ S}\left(\frac{Z}{l_t}\right) - \frac{D_R}{q\ S}\left(\frac{Y}{l_t}\right)$	(Eq 3.28)	3.26
$R_e = \frac{\rho\ V\ c}{\mu} = V_e \sqrt{\rho}\left(\frac{\sqrt{\rho_{ssl}}\ \ c}{\mu}\right)$	(Eq 3.29)	3.27
$C_{T_G} = \frac{T_G \sin \alpha_j}{q\ S}$	(Eq 3.30)	3.29
$C_{L_{max_{Std\ \dot{V},\ CG,\ W}}} = C_{L_{max_{Std\ \dot{V},\ CG}}} + K_W \left(W_{Std} - W_{Test}\right)$	(Eq 3.31)	3.31
$V_i = V_o + \Delta V_{ic}$	(Eq 3.32)	3.36
$V_c = V_i + \Delta V_{pos}$	(Eq 3.33)	3.36
$H_{P_i} = H_{P_o} + \Delta H_{P_{ic}}$	(Eq 3.34)	3.36
$H_{P_c} = H_{P_i} + \Delta H_{pos}$	(Eq 3.35)	3.36
$n_{z_i} = n_{z_o} + \Delta n_{z_{ic}}$	(Eq 3.36)	3.36
$n_z = n_{z_i} + \Delta n_{z_{tare}}$	(Eq 3.37)	3.36
$C_{L_{max_{Test}}} = \frac{n_z\ W_{Test}}{0.7\ P_{ssl}\ \delta_{Test}\ M^2\ S}$	(Eq 3.38)	3.37
$R = \frac{V_c}{\frac{c}{2}\ \dot{V}_{Test}}$	(Eq 3.39)	3.37

$$C_{L_{max_{Std\,\dot{V}}}} = C_{L_{max_{Test}}} \left(\frac{R + 1}{R + 2}\right)$$ (Eq 3.40) 3.37

$$\left(C_{L_{aero_{Std\,\dot{V},\,CG,\,W}}}\right)_{Pwr\ ON} = \left(C_{L_{max_{Std\,\dot{V},\,CG,\,W}}}\right)_{Pwr\ ON} - C_{T_G}$$ (Eq 3.41) 3.42

$$\left(C_{L_{aero_{Std\,\dot{V},\,CG,\,W}}}\right)_{Pwr\ OFF} = \left(C_{L_{aero_{Std\,\dot{V},\,CG,\,W}}}\right)_{Pwr\ ON} - \Delta C_{L_t} - \Delta C_{L_E}$$ (Eq 3.42) 3.42

$$V_{e_s} = \sqrt{\frac{841.5\, n_z\, W}{C_{L_{max}}\, S}}$$ (Eq 3.43) 3.44

CHAPTER 4

$$D_p = C_{D_p}\, qS$$ (Eq 4.1) 4.4

$$D_i = L\, \alpha_i = C_L\, q\, S\, \alpha_i$$ (Eq 4.2) 4.5

$$L = C_L\, qS$$ (Eq 4.3) 4.5

$$D_i = C_{D_i}\, qS$$ (Eq 4.4) 4.5

$$\alpha_i = \frac{C_L}{\pi\, AR}$$ (Eq 4.5) 4.5

$$C_{D_i} = \frac{C_L^2}{\pi\, AR}$$ (Eq 4.6) 4.6

$$C_{D_i} = \frac{C_L^2}{\pi\, e\, AR}$$ (Eq 4.7) 4.6

$$D = D_P + D_i + D_M$$ (Eq 4.8) 4.7

$C_D = C_{D_P} + C_{D_i} + C_{D_M}$	(Eq 4.9)	4.7
$D = C_D\, qS$	(Eq 4.10)	4.8
$C_D = C_{D_p} + \dfrac{C_L^2}{\pi\, e\, AR}$	(Eq 4.11)	4.8
$D = C_{D_P}\, q\, S + \dfrac{C_L^2}{\pi\, e\, AR}\, qS$	(Eq 4.12)	4.8
$L - W + T_G \sin\alpha_j = 0$	(Eq 4.13)	4.9
$L = W - T_G \sin\alpha_j$	(Eq 4.14)	4.9
$C_L = \dfrac{L}{qS}$	(Eq 4.15)	4.9
$C_L = \dfrac{W - T_G \sin\alpha_j}{qS}$	(Eq 4.16)	4.9
$D = C_{D_P}\, qS + \dfrac{\left(W - T_G \sin\alpha_j\right)^2}{\pi\, e\, AR\, qS}$	(Eq 4.17)	4.9
$D = C_{D_P}\, qS + \dfrac{W^2}{\pi\, e\, AR\, qS}$	(Eq 4.18)	4.9
$q = \dfrac{1}{2}\, \rho_{ssl}\, V_e^2$	(Eq 4.19)	4.9
$q = \dfrac{1}{2}\, \rho_a\, V_T^2$	(Eq 4.20)	4.9
$q = \dfrac{1}{2}\, \gamma\, P_a\, M^2$	(Eq 4.21)	4.10

$$D = \frac{C_{D_p} \rho_{ssl} V_e^2 S}{2} + \frac{2 W^2}{\pi e AR S \rho_{ssl} V_e^2} \qquad \text{(Eq 4.22)} \qquad 4.10$$

$$D = \frac{C_{D_p} \rho_a V_T^2 S}{2} + \frac{2 W^2}{\pi e AR S \rho_a V_T^2} \qquad \text{(Eq 4.23)} \qquad 4.10$$

$$D = \frac{C_{D_p} \gamma P_a M^2 S}{2} + \frac{2W^2}{\pi e AR S \gamma P_a M^2} \qquad \text{(Eq 4.24)} \qquad 4.10$$

$$D = \frac{C_{D_{p\ (M)}} \gamma P_a M^2 S}{2} + \frac{2W^2}{\pi e_{(M)} AR S \gamma P_a M^2} \qquad \text{(Eq 4.25)} \qquad 4.12$$

$$\frac{D}{\delta} = \frac{C_{D_{P(M)}} \gamma P_{ssl} M^2 S}{2} + \frac{2 \left(W/\delta\right)^2}{\pi e_{(M)} AR S \gamma P_{ssl} M^2} \qquad \text{(Eq 4.26)} \qquad 4.12$$

$$\frac{D}{\delta} = f\left(M, \frac{W}{\delta}\right) \qquad \text{(Eq 4.27)} \qquad 4.13$$

$$\dot{W}_f = f\left(P, \rho, \mu, V, L, N\right) \qquad \text{(Eq 4.28)} \qquad 4.14$$

$$\frac{\dot{W}_f}{\delta\sqrt{\theta}} = f\left(M, \frac{N}{\sqrt{\theta}}, R_e\right) \qquad \text{(Eq 4.29)} \qquad 4.14$$

$$\frac{\dot{W}_f}{\delta\sqrt{\theta}} = f\left(M, \frac{N}{\sqrt{\theta}}\right) \qquad \text{(Eq 4.30)} \qquad 4.15$$

$$\frac{T_{N_x}}{\delta} = f\left(M, \frac{N}{\sqrt{\theta}}\right) \qquad \text{(Eq 4.31)} \qquad 4.15$$

$$\frac{\dot{W}_f}{\delta\sqrt{\theta}} = f\left(M, \frac{T_{N_x}}{\delta}\right)$$ (Eq 4.32) 4.15

$$T_{N_x} = T_G \cos \alpha_j - T_R$$ (Eq 4.33) 4.15

$T_{N_x} = D$ (For small α_j, where $\cos \alpha_j \cong 1$) (Eq 4.34) 4.15

$$\frac{T_{N_x}}{\delta} = \frac{D}{\delta}$$ (Eq 4.35) 4.15

$$\frac{\dot{W}_f}{\delta\sqrt{\theta}} = f\left(M, \frac{D}{\delta}\right)$$ (Eq 4.36) 4.15

$$\frac{\dot{W}_f}{\delta\sqrt{\theta}} = f\left(M, \frac{W}{\delta}\right)$$ (Eq 4.37) 4.16

$$\theta = \frac{T_a}{T_{ssl}}$$ (Eq 4.38) 4.21

$$\theta_T = \frac{T_T}{T_{ssl}} = \frac{OAT}{T_{ssl}}$$ (Eq 4.39) 4.21

$$\frac{\dot{W}_f}{\delta\sqrt{\theta}} = f\left(M, OAT\right)$$ (Eq 4.40) 4.22

$$T_T = T_a\left(1 + \frac{\gamma - 1}{2} M^2\right)$$ (Eq 4.41) 4.22

$$P_T = P_a\left(1 + \frac{\gamma - 1}{2} M^2\right)^{\frac{\gamma}{\gamma - 1}}$$ (Eq 4.42) 4.22

$$\delta = \frac{P_a}{P_{ssl}}$$ (Eq 4.43) 4.23

$$\delta_T = \frac{P_T}{P_{ssl}}$$ (Eq 4.44) 4.23

$$\frac{\theta_T}{\theta} = \left(1 + 0.2\ M^2\right)$$ (Eq 4.45) 4.23

$$\frac{\delta_T}{\delta} = \left(1 + 0.2\ M^2\right)^{3.5}$$ (Eq 4.46) 4.23

$$\frac{\dot{W}_f}{\delta_T \sqrt{\theta_T}} = f\left(M, OAT\right)$$ (Eq 4.47) 4.23

$$TSFC = \frac{\dot{W}_f}{T_{N_x}}$$ (Eq 4.48) 4.25

$$T_{N_x} = D$$ (Eq 4.49) 4.26

$$\dot{W}_f \approx D$$ (Eq 4.50) 4.26

$$S.R. = \frac{nmi}{W_f}$$ (Eq 4.51) 4.28

$$S.R. = \frac{V_T}{\dot{W}_f}$$ (Eq 4.52) 4.28

$$S.E. = \frac{t}{W_{f_{Used}}}$$ (Eq 4.53) 4.28

$$S.E. = \frac{1}{\dot{W}_f}$$ (Eq 4.54) 4.29

$$Range = \left(S.R._{avg}\right)\left(Fuel\ Used\right)$$ (Eq 4.55) 4.31

$$nmi = \frac{nmi}{lb} \times lb$$ (Eq 4.56) 4.31

$$THP = \frac{T\ V_T}{550} = \frac{D\ V_T}{550}$$ (Eq 4.57) 4.33

$$THP = \frac{C_{D_P}\ \rho_a\ V_T^3\ S}{1100} + \frac{W^2}{275\ \pi\ e\ AR\ S\ \rho_a\ V_T}$$ (Eq 4.58) 4.33

$$THP = THP_p + THP_i$$ (Eq 4.59) 4.34

$$D = \frac{C_D}{C_L}\ W$$ (Eq 4.60) 4.35

$$THP = \frac{C_D\ W\ V_T}{C_L\ 550}$$ (Eq 4.61) 4.35

$$L = W = C_L\ \frac{1}{2}\ \rho_a\ V_T^2\ S$$ (Eq 4.62) 4.35

$$THP = \frac{\left(\frac{2}{S}\right)^{\frac{1}{2}} W^{\frac{3}{2}}\ C_D}{\rho_a^{\frac{1}{2}}\ C_L^{\frac{3}{2}}\ 550}$$ (Eq 4.63) 4.35

$$\rho_a = \rho_{ssl}\ \sigma$$ (Eq 4.64) 4.35

$$THP = \frac{\sqrt{2}\ W^{\frac{3}{2}}\ C_D}{\left(S\ \rho_{ssl}\right)^{\frac{1}{2}} \sqrt{\sigma}\ C_L^{\frac{3}{2}}\ 550}$$ (Eq 4.65) 4.35

$$THP_e = THP\ \sqrt{\sigma}$$ (Eq 4.66) 4.35

$$THP_e = \frac{\sqrt{2}\ W^{\frac{3}{2}}\ C_D}{\left(S\ \rho_{ssl}\right)^{\frac{1}{2}} C_L^{\frac{3}{2}}\ 550}$$ (Eq 4.67) 4.36

$THP = K_1 V_T^3 + K_2 V_T^{-1}$	(Eq 4.68)	4.37
$3 K_1 V_T^2 - K_2 V_T^{-2} = 0$	(Eq 4.69)	4.37
$3 K_1 V_T^3 = K_2 V_T^{-1}$	(Eq 4.70)	4.37
$3 THP_p = THP_i$	(Eq 4.71)	4.37
$3 D_p = D_i$	(Eq 4.72)	4.37
$3 C_{D_p} = C_{D_i}$	(Eq 4.73)	4.37
$THP = K_o \frac{C_D}{C_L^{\frac{3}{2}}}$	(Eq 4.74)	4.38
$V_T = \frac{V_e}{\sqrt{\sigma}}$	(Eq 4.75)	4.39
$THP = \frac{THP_e}{\sqrt{\sigma}}$	(Eq 4.76)	4.39
$\sigma = \frac{\rho_a}{\rho_{ssl}}$	(Eq 4.77)	4.40
$THP_e V_e = \frac{C_{D_P} \rho_{ssl} V_e^4 S}{1100} + \frac{W^2}{275 \pi e AR S \rho_{ssl}}$	(Eq 4.78)	4.40
$\eta_P = \frac{THP}{SHP}$	(Eq 4.79)	4.41
$THP = \eta_P SHP$	(Eq 4.80)	4.41
$THPSFC = \frac{\dot{W}_f}{THP}$	(Eq 4.81)	4.41

$SHPSFC = \frac{\dot{W}_f}{SHP}$	(Eq 4.82)	4.42
$\dot{W}_f = \frac{THP}{\eta_P}\ SHPSFC$	(Eq 4.83)	4.42
$\left(\frac{W}{\delta}\right)_{Target} = \frac{W + W_f}{\delta}$	(Eq 4.84)	4.47
$\left(\frac{W}{\delta}\right)_{Target} = \frac{W_{aircraft} + W_f}{\delta}$	(Eq 4.85)	4.48
$\delta = \frac{W_{aircraft}}{\left(\frac{W}{\delta}\right)_{Target}} + \frac{1}{\left(\frac{W}{\delta}\right)_{Target}} W_f$	(Eq 4.86)	4.48
$OAT = T_a \left(1 + \frac{\gamma - 1}{2} K_T M^2\right)$	(Eq 4.87)	4.48
$H_{P_c} = H_{P_o} + \Delta H_{P_{ic}} + \Delta H_{pos}$	(Eq 4.88)	4.59
$T_a = T_o + \Delta T_{ic}$	(Eq 4.89)	4.59
$V_c = V_o + \Delta V_{ic} + \Delta V_{pos}$	(Eq 4.90)	4.59
$V_T = \frac{V_c}{\sqrt{\sigma}}$	(Eq 4.91)	4.60
$M = \frac{V_T}{a_{ssl} \sqrt{\theta}}$	(Eq 4.92)	4.60
$\dot{W}_{f_{ref}} = \frac{\dot{W}_f}{\delta \sqrt{\theta}}$	(Eq 4.93)	4.60
$W_{ref} = \frac{W}{\delta}$	(Eq 4.94)	4.60

$$R_{Test} = \sum_{j=1}^{n} V_j \, \Delta t_j$$

(Eq 4.95) 4.63

$$R.F._{Test} = \frac{t_T}{\ln\left(\frac{W_1}{W_2}\right)}$$

(Eq 4.96) 4.63

$$R_{Std} = R.F._{Test} \ln\left(\frac{W_{Std_1}}{W_{Std_2}}\right)$$

(Eq 4.97) 4.63

$$M = f\left(V_c, H_{P_c}\right)$$

(Eq 4.98) 4.66

$$\delta = f\left(H_{P_c}\right)$$

(Eq 4.99) 4.67

$$\frac{W + W_f}{\delta} = \frac{W}{\delta}$$

(Eq 4.100) 4.67

$$\frac{W}{\delta}\,(\text{error}) = \frac{100\left[\frac{W}{\delta}\,(\text{test}) - \frac{W}{\delta}\,(\text{target})\right]}{\frac{W}{\delta}\,(\text{target})}$$

(Eq 4.101) 4.67

$$^\circ C = {}^\circ K - 273.15$$

(Eq 4.102) 4.67

$$OAT = f\left(T_a, M\right)$$

(Eq 4.103) 4.67

$$T_a = f\left(OAT, M\right)$$

(Eq 4.104) 4.67

$$S.R.\ \delta = \frac{661.483M}{\left(\frac{\dot{w}_f}{\delta\sqrt{\theta}}\right)}$$

(Eq 4.105) 4.68

$$V_e = \sqrt{\frac{2q}{\rho_{ssl}}} = \sqrt{\frac{\sigma 2q}{\rho_a}} = \sqrt{\sigma}\ V_T$$

(Eq 4.106) 4.73

$$SHP_e = SHP\sqrt{\sigma}$$

(Eq 4.107) 4.73

$$T_a = T_{a_{Std}} + \Delta T_a$$ (Eq 4.108) 4.78

$$S.R. = \frac{a_{ssl}\, M}{\left(\frac{\dot{W}_f}{\delta\sqrt{\theta}}\right)\delta}$$ (Eq 4.109) 4.78

$$V_{T_{Hot\,day}} = 661.483\, M \sqrt{\theta_{Std}} \left(\frac{\sqrt{\theta_{Hot\,day}}}{\sqrt{\theta_{Std}}}\right)$$ (Eq 4.110) 4.81

$$\dot{W}_{f_{Hot\,day}} = \dot{W}_{f_{Std}} \left(\frac{\sqrt{\theta_{Hot\,day}}}{\sqrt{\theta_{Std}}}\right)$$ (Eq 4.111) 4.82

$$\frac{\dot{W}_f}{\sqrt{\theta}} = ¢$$ (Eq 4.112) 4.82

$$\text{Range} = \int_0^{W_{f_{Used}}} (S.R.)\, dW_f$$ (Eq 4.113) 4.86

$$\text{Range} = \int_{W_1}^{W_2} (S.R.)\, dW$$ (Eq 4.114) 4.87

$$\text{Range} = \int_{W_1}^{W_2} (S.R.\ \delta) \left(\frac{W}{\delta}\right) \frac{1}{W}\, dW$$ (Eq 4.115) 4.87

$$\text{Range} = \int_{W_1}^{W_2} \left[\frac{661.483\, M}{\left(\frac{\dot{W}_f}{\delta\sqrt{\theta}}\right)} \frac{W}{\delta} \right] \frac{dW}{W}$$ (Eq 4.116) 4.87

$$\frac{D}{\delta} = K_3 + K_4 \left(\frac{W}{\delta}\right)^2$$ (Eq 4.117) 4.88

$$\text{R.F.} = \left[\left(\text{S.R. } \delta\right) \frac{W}{\delta} \right]$$ (Eq 4.118) 4.90

$$\text{R.F.} = \left[\frac{661.483\ M}{\left(\frac{\dot{W}_f}{\delta \sqrt{\theta}}\right)} \left(\frac{W}{\delta}\right) \right]$$ (Eq 4.119) 4.90

$$\text{Range} = \int_{W_1}^{W_2} \left(\text{R.F.}\right) \frac{dW}{W}$$ (Eq 4.120) 4.90

$$C_L = \frac{2\ W}{\gamma\ P_a\ M^2\ S} = \frac{2\ \frac{W}{\delta}}{\gamma\ M^2\ S\ P_{ssl}}$$ (Eq 4.121) 4.101

$$C_L = f\left(\frac{W}{\delta}, M^2\right)$$ (Eq 4.122) 4.101

$$\frac{\frac{W}{\delta}}{\frac{D}{\delta}} = \frac{W}{D} = \text{Constant}$$ (Eq 4.123) 4.101

$$\frac{661.483\ M}{\left(\frac{\dot{W}_f}{\delta\sqrt{\theta}}\right)} = \text{Constant}$$ (Eq 4.124) 4.102

$$\frac{\text{TSFC}}{\sqrt{\theta}} = \text{Constant}$$ (Eq 4.125) 4.102

$$\text{Range} = \text{R.F. } \ln \frac{W_1}{W_2}$$ (Eq 4.126) 4.105

CHAPTER 5

$TE = PE + KE$	(Eq 5.1)	5.2
$PE = \int_{o}^{h} W\, dh$	(Eq 5.2)	5.2
$PE = W\left(H_{P_c} + \Delta T \text{ correction}\right)$	(Eq 5.3)	5.2
$KE = \frac{1}{2}\frac{W}{g}V_T^2$	(Eq 5.4)	5.3
$TE = W\,h + \frac{1}{2}\frac{W}{g}V_T^2$	(Eq 5.5)	5.3
$\frac{TE}{W} = h + \frac{V_T^2}{2\,g}$	(Eq 5.6)	5.3
$E_h = h + \frac{V_T^2}{2\,g}$	(Eq 5.7)	5.3
$\frac{d}{dt}E_h = \frac{d}{dt}\left(h + \frac{V_T^2}{2\,g}\right)$	(Eq 5.8)	5.7
$\frac{d}{dt}E_h = \frac{dh}{dt} + \frac{V_T}{g}\frac{dV_T}{dt}$	(Eq 5.9)	5.7
$\sum F_x = \frac{W}{g}\frac{dV_T}{dt}$	(Eq 5.10)	5.8
$T_{N_x} = T_G \cos\alpha_j - T_R$	(Eq 5.11)	5.8
$T_{N_x} - D - W\sin\gamma = \frac{W}{g}\frac{dV_T}{dt}$	(Eq 5.12)	5.8
$\sin\gamma = \frac{V_T\text{ (vertical)}}{V_T\text{ (flight path)}} = \frac{\frac{dh}{dt}}{V_T}$	(Eq 5.13)	5.9

$$T_{N_x} - D - W\frac{dh}{dt}\frac{1}{V_T} = \frac{W}{g}\frac{dV_T}{dt}$$ (Eq 5.14) 5.9

$$\frac{V_T\left(T_{N_x} - D\right)}{W} - \frac{dh}{dt} = \frac{V_T}{g}\frac{dV_T}{dt}$$ (Eq 5.15) 5.9

$$\frac{V_T\left(T_{N_x} - D\right)}{W} = \frac{dE_h}{dt}$$ (Eq 5.16) 5.9

$$P_s = \frac{V_T\left(T_{N_x} - D\right)}{W}$$ (Eq 5.17) 5.9

$$P_s = \frac{dE_h}{dt}$$ (Eq 5.18) 5.10

$$P_s = \frac{dh}{dt} + \frac{V_T}{g}\frac{dV_T}{dt}$$ (Eq 5.19) 5.10

$$P_s = \frac{V_T\left(T_{N_x} - D - \Delta D_i\right)}{W}$$ (Eq 5.20) 5.13

$$P_s = \frac{V_T\left(T_{N_x} - D - \Delta D_i\right)}{W + \Delta W}$$ (Eq 5.21) 5.15

$$P_s = \frac{V_T\left(T_{N_x} - D - \Delta D_p\right)}{W}$$ (Eq 5.22) 5.16

$$P_s = \frac{V_T\,(T_{N_x} + \Delta T_{N_x} - D)}{W}$$ (Eq 5.23) 5.17

$$P_s = \frac{\left(P_A - \Delta P_A\right) - \left(P_{req} + \Delta P_{req}\right)}{W}$$ (Eq 5.24) 5.19

$$q_c = P_{ssl} \left\{ \left[1 + 0.2 \left(\frac{V_c}{a_{ssl}} \right)^2 \right]^{3.5} - 1 \right\}$$ (Eq 5.25) 5.28

$$P_a = P_{ssl} \left(1 - 6.8755856 \times 10^{-6} H_{P_c} \right)^{5.255863}$$ (Eq 5.26) 5.28

$$M = \sqrt{ \frac{2}{\gamma - 1} \left[\left(\frac{q_c}{P_a} + 1 \right)^{\frac{\gamma - 1}{\gamma}} - 1 \right] }$$ (Eq 5.27) 5.28

$$T_a = \frac{OAT + 273.15}{1 + \frac{\gamma - 1}{2} K_T M^2}$$ (Eq 5.28) 5.28

$$h = H_{P_c} \frac{T_{a_{Test}}}{T_{a_{Std}}}$$ (Eq 5.29) 5.28

$$V_T = M \sqrt{\gamma g_c R T_a}$$ (Eq 5.30) 5.28

$$\frac{W_{Test}}{W_{Std}}$$ (Eq 5.31) 5.31

$$\frac{V_{T_{Std}}}{V_{T_{Test}}} = \frac{M_{Std} \sqrt{\theta_{Std}}}{M_{Test} \sqrt{\theta_{Test}}}$$ (Eq 5.32) 5.32

$$\frac{V_{T_{Std}}}{V_{T_{Test}}} = \sqrt{\frac{T_{a_{Std}}}{T_{a_{Test}}}}$$ (Eq 5.33) 5.32

$$\Delta T = f \left(T_a \right)$$ (Eq 5.34) 5.32

$$\Delta D = D_{Std} - D_{Test} = \frac{2 \left(W_{Std}^2 - W_{Test}^2 \right)}{\pi \, e \, AR \, S \, \gamma \, P_a \, M^2}$$ (Eq 5.35) 5.32

$$P_{s_{Std}} = P_{s_{Test}} \frac{W_{Test}}{W_{Std}} \sqrt{\frac{T_{a_{Std}}}{T_{a_{Test}}}} + \frac{V_{T_{Std}}}{W_{Std}} \left(\Delta T_{N_x} - \Delta D\right)$$ (Eq 5.36) 5.32

$$V_c = V_i + \Delta V_{pos}$$ (Eq 5.37) 5.36

$$H_{P_c} = H_{P_i} + \Delta H_{pos}$$ (Eq 5.38) 5.36

$$M = f\left(V_c , H_{P_c}\right)$$ (Eq 5.39) 5.37

$$W_{Test} = \text{Initial W} - \int \dot{W}_f \; dt$$ (Eq 5.40) 5.37

$$°C = °K - 273.15$$ (Eq 5.41) 5.37

$$OAT = f\left(T_a , M_T\right)$$ (Eq 5.42) 5.37

$$T_a = f\left(OAT, M\right)$$ (Eq 5.43) 5.37

$$V_{T_{Test}} = f\left(V_c , H_{P_c} , T_a\right)$$ (Eq 5.44) 5.37

$$V_{T_{Std}} = f\left(V_c, H_{p_c}, T_{Std}\right)$$ (Eq 5.45) 5.37

$$h = H_{P_{c_{ref}}} + \Delta H_{P_c} \left(\frac{T_a}{T_{Std}}\right)$$ (Eq 5.46) 5.37

$$E_h = h + \frac{V_{T_{Test}}^2}{2g}$$ (Eq 5.47) 5.38

$$P_{s_{Test}} = \frac{dE_h}{dt}$$ (Eq 5.48) 5.38

$$\gamma_{Test} = \sin^{-1}\left(\frac{dh/dt}{V_{T_{Test}}}\right)$$ (Eq 5.49) 5.38

$$CCF = 1 + \left(\frac{V_{T_{Std}}}{g} \frac{dV}{dh} \right)$$ (Eq 5.50) 5.38

$$P_{s_{Std}} = P_{s_{Test}} \left(\frac{W_{Test}}{W_{Std}} \right) \left(\frac{V_{T_{Std}}}{V_{T_{Test}}} \right) + \left(\frac{V_{T_{Std}}}{W_{Std}} \right) (\Delta T_{N_x} - \Delta D)$$ (Eq 5.51) 5.38

$$\left(\frac{dh}{dt} \right)_{Std} = \frac{P_{s_{Std}}}{CCF}$$ (Eq 5.52) 5.38

$$\gamma_{Std} = \sin^{-1} \left(\frac{\left(\frac{dh}{dt} \right)_{Std}}{V_{T_{Std}}} \right)$$ (Eq 5.53) 5.39

$$\left| \gamma_{Test} - \gamma_{Std} \right| < 0.1$$ (Eq 5.54) 5.39

CHAPTER 6

$$n_z = \frac{L}{W}$$ (Eq 6.1) 6.3

$$L^2 = W^2 + (W \tan \phi)^2$$ (Eq 6.2) 6.3

$$n_z^2 = 1 + \tan^2 \phi$$ (Eq 6.3) 6.3

$$\tan \phi = \sqrt{\left(n_z^2 - 1 \right)}$$ (Eq 6.4) 6.4

$$L \cos \phi = W$$ (Eq 6.5) 6.4

$$n_z = \frac{1}{\cos \phi}$$ (Eq 6.6) 6.4

$$W \tan \phi = \frac{W}{g} a_R$$ (Eq 6.7) 6.4

$$a_R = g \tan \phi$$ (Eq 6.8) 6.4

$a_R = g\sqrt{\left(n_z^2 - 1\right)}$	(Eq 6.9)	6.4
$R = \dfrac{V_T^2}{a_R}$	(Eq 6.10)	6.5
$R = \dfrac{V_T^2}{g \tan\phi}$	(Eq 6.11)	6.5
$R = \dfrac{V_T^2}{g\sqrt{\left(n_z^2 - 1\right)}}$	(Eq 6.12)	6.6
$\omega = \dfrac{V_T}{R}$	(Eq 6.13)	6.6
$\omega = \dfrac{g}{V_T} \tan\phi$	(Eq 6.14)	6.6
$\omega = \dfrac{g}{V_T}\sqrt{\left(n_z^2 - 1\right)}$	(Eq 6.15)	6.6
$\phi = \tan^{-1}\left(\dfrac{F_Y}{W}\right)$	(Eq 6.16)	6.8
$L = \dfrac{W}{\cos\phi}$	(Eq 6.17)	6.8
$\Delta L = F_Y \tan\phi$	(Eq 6.18)	6.9
$F_R = W\tan\phi + \dfrac{F_Y}{\cos\phi}$	(Eq 6.19)	6.10
$n_R = \tan\phi + \dfrac{n_Y}{\cos\phi}$	(Eq 6.20)	6.10
$\phi_E = \tan^{-1}\left(\tan\phi + \dfrac{n_Y}{\cos\phi}\right)$	(Eq 6.21)	6.10

$$R = \frac{V_T^2}{g\left(\tan\phi + \dfrac{n_Y}{\cos\phi}\right)}$$
(Eq 6.22) 6.10

$$\omega = \frac{g\left(\tan\phi + \dfrac{n_Y}{\cos\phi}\right)}{V_T}$$
(Eq 6.23) 6.10

$$\Delta\omega = \frac{g\, n_Y}{V_T \cos\phi}$$
(Eq 6.24) 6.10

$$n_R = n_z - \cos\gamma$$
(Eq 6.25) 6.12

$$R_{(\text{wings level})} = \frac{V_T^2}{g\,(n_z - \cos\gamma)}$$
(Eq 6.26) 6.12

$$\omega_{(\text{wings level})} = \frac{g\,(n_z - \cos\gamma)}{V_T}$$
(Eq 6.27) 6.12

$$L = C_L q\, S + T_G \sin\alpha_j$$
(Eq 6.28) 6.16

$$n_z = \frac{C_L q}{W/S} + \frac{T_G}{W}\sin\alpha_j$$
(Eq 6.29) 6.16

$$n_{z_{max}} = \frac{C_{L_{max}}\, q}{(W/S)_{min}}$$
(Eq 6.30) 6.17

$$n_{z_{max}} = \frac{C_{L_{max}}}{(W/S)_{min}}\; 0.7\; P_a M^2$$
(Eq 6.31) 6.17

$$n_{z_{max}} = K M^2$$
(Eq 6.32) 6.17

$$K = \frac{0.7}{(W/S)}\; C_{L_{max}}\, P_a$$
(Eq 6.33) 6.17

$$\frac{1}{V_{s\,(1g)}^{2}} = \frac{n_L}{V_A^{2}}$$ (Eq 6.34) 6.18

$$V_A = V_{s\,(1g)}\sqrt{n_L}$$ (Eq 6.35) 6.18

$$R = \frac{a^2 M^2}{g\sqrt{K^2 M^4 - 1}}$$ (Eq 6.36) 6.20

$$\omega = \frac{g\sqrt{K^2 M^4 - 1}}{a\,M}$$ (Eq 6.37) 6.21

$$K = \frac{0.7}{(W/S)}\; C_{L_{max}}\, P_a$$ (Eq 6.38) 6.21

$$R_{min\;V>V_A} = \left(\frac{a^2}{g\sqrt{n_L^2 - 1}}\right) M^2$$ (Eq 6.39) 6.23

$$\omega_{max\;V>V_A} = \left(\frac{g\sqrt{n_L^2 - 1}}{a}\right)\frac{1}{M}$$ (Eq 6.40) 6.23

$$D = \frac{C_D}{C_L}\,L$$ (Eq 6.41) 6.29

$$T = \frac{C_D}{C_L}\,n_z W$$ (Eq 6.42) 6.29

$$n_z = \frac{T}{W}\,\frac{C_L}{C_D}$$ (Eq 6.43) 6.29

$$n_{z_{sust_{max}}} = \frac{T}{W}\left(\frac{C_L}{C_D}\right)_{max} \quad (\text{Jet})$$ (Eq 6.44) 6.29

$$n_z = \frac{T\left(V_T\right)}{W} \quad \frac{L}{D\left(V_T\right)}$$

(Eq 6.45) 6.29

$$n_{z_{sust_{max}}} = \frac{THP_{avail}}{W} \quad \frac{L}{\left(THP_{req}\right)_{min}} \qquad (\text{Propeller})$$

(Eq 6.46) 6.30

$$\omega_{sust} = \frac{57.3\ g}{V_T} \sqrt{n_{z_{sust}}^2 - 1} \qquad (\text{deg/s})$$

(Eq 6.47) 6.30

$$R_{sust} = \frac{V_T^{\ 2}}{g\sqrt{n_{z_{sust}}^2 - 1}}$$

(Eq 6.48) 6.30

$$\frac{T}{\delta} = f\left(M, \frac{\dot{W}_f}{\delta_T \sqrt{\theta_T}}\right)$$

(Eq 6.49) 6.32

$$\frac{\Delta D}{\delta} = \frac{\Delta T}{\delta}$$

(Eq 6.50) 6.33

$$\Delta D_{Std\text{-}Test} = \frac{1}{\pi eAR\ S\ (0.7)\ P_{ssl}\ \delta_{Test}\ M^2}\left[\left(n_z W\right)^2_{Std} - \left(n_z W\right)^2_{Test}\right]$$

(Eq 6.51) 6.34

$$n_{z_{Std}} = \sqrt{\frac{1}{W^2_{Std}}\left[\left(n_z W\right)^2_{Test} + \Delta T\ \pi\ e\ AR\left(0.7\right) S\ P_{ssl}\ \delta_{Test}\ M^2\right]}$$

(Eq 6.52) 6.34

$$n_{z_{Std}} = n_{z_{Test}}\left(\frac{W_{Test}}{W_{Std}}\right)$$

(Eq 6.53) 6.35

$$T_{ex} = T - D = \frac{W}{V_T}\frac{dh}{dt} + \frac{W}{g}\frac{dV_T}{dt}$$

(Eq 6.54) 6.38

$\frac{dV_T}{dt} = \frac{11.3\ P_s}{V_T}$	(Eq 6.55)	6.48
$n_z = n_{z_o} + \Delta n_{ic} + \Delta n_{z\ tare}$	(Eq 6.56)	6.57
$V_i = V_o + \Delta V_{ic}$	(Eq 6.57)	6.63
$V_c = V_i + \Delta V_{pos}$	(Eq 6.58)	6.63
$H_{P_i} = H_{P_o} + \Delta H_{P_{ic}}$	(Eq 6.59)	6.63
$H_{P_c} = H_{P_i} + \Delta H_{pos}$	(Eq 6.60)	6.63
$n_{z_i} = n_{z_o} + \Delta n_{z_{ic}}$	(Eq 6.61)	6.63
$n_{z_{Test}} = n_{z_i} + \Delta n_{z_{tare}}$	(Eq 6.62)	6.63
$C_{L_{max_{Test}}} = \frac{n_{z\ Test}\ W_{Test}}{0.7\ P_{ssl}\ \delta_{Test}\ M^2\ S}$	(Eq 6.63)	6.63
$V_T = a\ M$	(Eq 6.64)	6.64
$\Delta T = T_{Std} - T$	(Eq 6.65)	6.66
$n_{z_{sust}} = \sqrt{\frac{P_{s_{1g}}\ \pi\ e\ AR\ S\ 0.7\ P_{ssl}\delta\ M^2}{V_T W_{Std}} + 1}$	(Eq 6.66)	6.68
$T_{ex} = T - D = \frac{W_{Std}}{V_T}\ P_{s_{1g}}$	(Eq 6.67)	6.68
$n_{z_{sust}} = \sqrt{\left(\frac{n_z W_{Std}}{\delta\ M}\right)^2}\ \ \frac{\delta_h}{W_{Std}}\ M$	(Eq 6.68)	6.68

$$n_z = \left(\frac{\delta}{W}\right)\left(0.7 \ P_{ssl} \ S\right) \ C_L \ M^2$$ (Eq 6.69) 6.71

$$\left(n_z \frac{W}{\delta}\right)_{Test} = \left(0.7 \ P_{ssl} \ S\right) C_L \ M^2$$ (Eq 6.70) 6.71

CHAPTER 7

$$E_h = h + \frac{V_T^2}{2\,g}$$ (Eq 7.1) 7.2

$$P_s = \frac{dE_h}{dt} = \frac{dh}{dt} + \frac{V_T}{g}\frac{dV_T}{dt}$$ (Eq 7.2) 7.2

$$\frac{dV}{dt} = \frac{dV}{dh}\frac{dh}{dt}$$ (Eq 7.3) 7.2

$$P_s = \frac{dh}{dt} + \frac{V}{g}\frac{dV}{dh}\frac{dh}{dt}$$ (Eq 7.4) 7.3

$$P_s = \frac{dh}{dt}\left[1 + \frac{V}{g}\frac{dV}{dh}\right]$$ (Eq 7.5) 7.3

$$\frac{dh}{dt} = P_s\left[\frac{1}{1 + \frac{V_T}{g}\frac{dV}{dh}}\right]$$ (Eq 7.6) 7.3

$$CCF = \frac{1}{1 + \frac{V_T}{g}\frac{dV}{dh}}$$ (Eq 7.7) 7.3

$$L - W\cos\gamma + T_G \sin\alpha_j = \frac{W}{g} \ a_z$$ (Eq 7.8) 7.5

$$T_G \cos\alpha_j - T_R - D - W\sin\gamma = \frac{W}{g} \ a_x$$ (Eq 7.9) 7.5

$$L = W\cos\gamma$$ (Eq 7.10) 7.5

$$T_G \cos\alpha_j - T_R - D - W\sin\gamma = \frac{W}{g}\frac{dV_T}{dt} = 0$$ (Eq 7.11) 7.6

$$T_{N_x} = T_G \cos \alpha_j - T_R$$ (Eq 7.12) 7.6

$$T_{N_x} - D = W \sin \gamma$$ (Eq 7.13) 7.6

$$\gamma = \sin^{-1} \left[\frac{T_{N_x} - D}{W} \right]$$ (Eq 7.14) 7.6

$$V \sin \gamma = \frac{\left[T_{N_x} - D \right]}{W} V = \frac{dh}{dt} = V_v$$ (Eq 7.15) 7.6

$$ROC = \frac{dh}{dt} = \frac{\left[T_{N_x} - D \right]}{W} V = \frac{T_{N_x} V - D V}{W} = \frac{P_A - P_{req}}{W}$$ (Eq 7.16) 7.10

$$t = \int_0^h \frac{1}{\frac{dh}{dt}} dh = \int_0^h \frac{1}{ROC} dh$$ (Eq 7.17) 7.12

$$V_v = V_T \sin \gamma$$ (Eq 7.18) 7.14

$$V_{hor} = V_T \cos \gamma$$ (Eq 7.19) 7.14

$$\text{Rate of Climb} = P_s \left(\frac{1}{1 + \frac{V}{g} \frac{dV_T}{dh}} \right)$$ (Eq 7.20) 7.20

$$\text{Time to Climb} = \int_{h_1}^{h_2} \frac{\left(1 + \frac{V}{g} \frac{dV_T}{dh} \right)}{P_s} dh$$ (Eq 7.21) 7.20

$$dt = \frac{dh + \frac{V}{g} dV_T}{P_s}$$ (Eq 7.22) 7.21

$$dE_h = dh + \frac{V}{g} dV$$ (Eq 7.23) 7.21

$$dt = \frac{dE_h}{P_s}$$ (Eq 7.24) 7.21

$$\text{Time to Climb} = \int_{E_{h_1}}^{E_{h_2}} \frac{1}{P_s}\, dE_h$$ (Eq 7.25) 7.21

$$\frac{dE_h}{dW} = \frac{d}{dW}\left(h + \frac{V_T^2}{2\,g}\right) = \frac{dh}{dW} + \frac{V_T}{g}\,\frac{dV_T}{dW}$$ (Eq 7.26) 7.25

$$\text{Fuel to Climb} = \int_{W_1}^{W_2} dW = -\int_{E_{h_1}}^{E_{h_2}} \frac{1}{\frac{dE_h}{dW}}\, dE_h$$ (Eq 7.27) 7.25

$$-\frac{1}{\frac{dE_h}{dW}} = -\frac{dW}{dE_h} = -\frac{dW}{dt}\,\frac{dt}{dE_h} = \frac{\dot{W}_f}{P_s}$$ (Eq 7.28) 7.25

$$\text{Fuel to Climb} = \int_{E_{h_1}}^{E_{h_2}} \frac{\dot{W}_f}{P_s}\, dE_h = \int_{E_{h_1}}^{E_{h_2}} \frac{1}{\frac{P_s}{\dot{W}_f}}\, dE_h$$ (Eq 7.29) 7.26

$$E_{h_{Test}} = h_{Test} + \frac{V_{T_{Test}}^2}{2\,g}$$ (Eq 7.30) 7.37

$$\left(\frac{dh}{dt}\right)_{Test} = P_{s_{Test}}\left(\frac{1}{1 + \frac{V_{T_{ref}}}{g}\,\frac{dV_T}{dh}}\right)$$ (Eq 7.31) 7.38

$$P_{s_{Std}} = P_{s_{Test}}\,\frac{W_{Test}}{W_{Std}}\,\frac{V_{T_{Std}}}{V_{T_{Test}}} + \frac{V_{T_{Std}}}{W_{Std}}\,(\Delta T_{N_x} - \Delta D)$$ (Eq 7.32) 7.38

$$\Delta D = D_{Std} - D_{Test} = \frac{2\left(W_{Std}^2 - W_{Test}^2\right)}{\pi\, e\, AR\, S\, \gamma\, P_a\, M^2}$$ (Eq 7.33) 7.39

$L = n_z W$	(Eq 7.34)	7.40
$n_z = \cos\gamma$	(Eq 7.35)	7.40
$\Delta D = \dfrac{2\left(W_{Std}^2 \cos^2\gamma_{Std} - W_{Test}^2 \cos^2\gamma_{Test}\right)}{\pi\, e\, AR\, \rho_{ssl}\, V_e^2\, S}$	(Eq 7.36)	7.40
$\Delta D = \dfrac{2\left(W_{Std}^2 n_{z\,Std}^2 - W_{Test}^2\, n_{z\,Test}^2\right)}{\pi\, e\, AR\, \rho_{ssl}\, V_e^2\, S}$	(Eq 7.37)	7.40
$\left(\dfrac{dh}{dt}\right)_{Std} = P_{s_{Std}}\left(\dfrac{1}{1 + \dfrac{V_T}{g}\dfrac{dV_T}{dh}}\right)$	(Eq 7.38)	7.41
$\gamma_{Std} = \sin^{-1}\left(\dfrac{\frac{dh}{dt}}{V_T}\right)$	(Eq 7.39)	7.41
$L = W\cos\gamma - T_G \sin\alpha_j$	(Eq 7.40)	7.42
$n_z = \dfrac{L}{W}$	(Eq 7.41)	7.42
$n_z = \cos\gamma - \dfrac{T_G}{W}\sin\alpha_j$	(Eq 7.42)	7.42
$\Delta T_N = f\left(\Delta H_P, \Delta T_a\right)$	(Eq 7.43)	7.44
$\text{Distance} = \int_{t_1}^{t_2} V_T \cos\gamma\, dt$	(Eq 7.44)	7.46
$\text{Fuel Used} = \int_{t_1}^{t_2} \dot{W}_f\, dt$	(Eq 7.45)	7.47
$^\circ C = {}^\circ K - 273.15$	(Eq 7.46)	7.52

$$OAT = f\left(T_a, M\right)$$ (Eq 7.47) 7.52

$$T_a = f\left(OAT, M\right)$$ (Eq 7.48) 7.52

$$V_T = f\left(OAT, M_T\right)$$ (Eq 7.49) 7.53

$$h = H_{P_{c\,ref}} + \Delta H_{P_c} \left(\frac{T_a}{T_{std}}\right)$$ (Eq 7.50) 7.53

CHAPTER 8

$$\sum F_z = L = W \cos \gamma$$ (Eq 8.1) 8.3

$$\sum F_x = D = W \sin \gamma$$ (Eq 8.2) 8.3

$$\frac{L}{D} = \frac{\cos \gamma}{\sin \gamma} = \cot \gamma$$ (Eq 8.3) 8.3

$$V_{hor} = V_T \cos \gamma$$ (Eq 8.4) 8.3

$$V_v = V_T \sin \gamma$$ (Eq 8.5) 8.3

$$\frac{V_{hor}}{V_v} = \frac{V_T \cos \gamma}{V_T \sin \gamma} = \cot \gamma = \frac{L}{D}$$ (Eq 8.6) 8.3

$$\sin \gamma = \frac{V_v}{V_T}$$ (Eq 8.7) 8.3

$$\gamma = \sin^{-1}\left(\frac{V_v}{V_T}\right)$$ (Eq 8.8) 8.4

$$\gamma = \sin^{-1}\left(\frac{dh/dt}{V_T}\right)$$ (Eq 8.9) 8.4

$$\frac{L}{D} = \cot\left[\sin^{-1}\left(\frac{dh/dt}{V_T}\right)\right]$$ (Eq 8.10) 8.4

$\text{Glide Ratio} = \dfrac{L}{D} = \dfrac{V_T \cos\gamma}{V_v}$	(Eq 8.11)	8.4
$GR = \dfrac{L}{D} \approx \dfrac{V_T}{V_v}$	(Eq 8.12)	8.4
$V_T = \sqrt{V_T^2 \sin^2\gamma + V_T^2 \cos^2\gamma} = \sqrt{V_T^2\left(\sin^2\gamma + \cos^2\gamma\right)}$	(Eq 8.13)	8.5
$\sum F_x = W \sin\gamma - D = \dfrac{W}{g}\dfrac{dV_T}{dt}$	(Eq 8.14)	8.10
$\dfrac{D}{W} = \sin\gamma - \dfrac{1}{g}\dfrac{dV_T}{dt}$	(Eq 8.15)	8.10
$\dfrac{dV_T}{dt} = \dfrac{dV_T}{dh}\dfrac{dh}{dt}$	(Eq 8.16)	8.10
$\dfrac{D}{W} = \sin\gamma - \dfrac{1}{g}\dfrac{dV_T}{dh}\dfrac{dh}{dt}$	(Eq 8.17)	8.10
$\dfrac{dh}{dt} = V_T \sin\gamma$	(Eq 8.18)	8.11
$\dfrac{D}{W} = \sin\gamma - \dfrac{1}{g}\dfrac{dV_T}{dh} V_T \sin\gamma$	(Eq 8.19)	8.11
$\dfrac{L}{W} = \cos\gamma$	(Eq 8.20)	8.11
$\dfrac{L}{D} = \cot\gamma\left[\dfrac{1}{1 - \dfrac{V_T}{g}\dfrac{dV_T}{dh}}\right]$	(Eq 8.21)	8.11
$\dfrac{L}{D} = \cot\left[\sin^{-1}\left(\dfrac{(dh/dt)}{V_T}\right)\right]\left[\dfrac{1}{1 - \dfrac{V_T}{g}\dfrac{dV_T}{dh}}\right]$	(Eq 8.22)	8.11
$\dfrac{L}{D} = \left[\dfrac{GR}{1 - \dfrac{V_T}{g}\dfrac{dV_T}{dh}}\right]$	(Eq 8.23)	8.12

$$GR = \frac{L}{D}\left[1 - \frac{V_T}{g}\frac{dV_T}{dh}\right]$$ (Eq 8.24) 8.12

$$V_c = V_i + \Delta V_{pos}$$ (Eq 8.25) 8.29

$$H_{P_c} = H_{P_i} + \Delta H_{pos}$$ (Eq 8.26) 8.29

$$T_a(^\circ C) = T_a(^\circ K) - 273.15$$ (Eq 8.27) 8.29

$$OAT = f\left(T_a, M_T\right)$$ (Eq 8.28) 8.29

$$T_a = f\left(OAT, M_T\right)$$ (Eq 8.29) 8.29

$$V_{T_{Test}} = f\left(V_c, H_{P_c}, T_a\right)$$ (Eq 8.30) 8.29

$$V_{T_{Std}} = f\left(V_c, H_{P_c}, T_{Std}\right)$$ (Eq 8.31) 8.29

$$h = H_{P_{c\,ref}} + \Delta H_{P_c}\left(\frac{T_a}{T_{Std}}\right)$$ (Eq 8.32) 8.29

$$E_h = h + \frac{V_{T_{Test}}^2}{2g}$$ (Eq 8.33) 8.30

$$P_{s_{Test}} = \frac{dE_h}{dt}$$ (Eq 8.34) 8.30

$$P_{s_{Std}} = P_{s_{Test}}\left(\frac{W_{Test}}{W_{Std}}\right)\left(\frac{V_{T_{Std}}}{V_{T_{Test}}}\right) + \left(\frac{V_{T_{Std}}}{W_{Std}}\right)(\Delta T_{N_x} - \Delta D)$$ (Eq 8.35) 8.30

$$\gamma_{Test} = \sin^{-1}\left[\frac{dh/dt}{V_{T_{Test}}}\right]$$ (Eq 8.36) 8.30

$$DCF = 1 + \left(\frac{V_{T_{Std}}}{g} \frac{dV_T}{dh} \right)$$ (Eq 8.37) 8.30

$$\left(\frac{dh}{dt} \right)_{Std} = \frac{P_{s_{Std}}}{DCF}$$ (Eq 8.38) 8.30

$$\gamma_{Std} = \sin^{-1} \left[\frac{(dh/dt)_{Std}}{V_{T_{Std}}} \right]$$ (Eq 8.39) 8.30

$$V_i = V_o + \Delta V_{ic}$$ (Eq 8.40) 8.32

$$H_{P_i} = H_{P_o} + \Delta H_{P_{ic}}$$ (Eq 8.41) 8.32

$$T_i = T_o + \Delta T_{ic}$$ (Eq 8.42) 8.32

$$V_T = 39.0 \text{ M} \sqrt{T_a \left({}^\circ K \right)}$$ (Eq 8.43) 8.32

$$W_{f_{Used}} = W_{f_{Start}} - W_{f_{End}}$$ (Eq 8.44) 8.32

$$\Delta d = V_{T_{avg}} \frac{\Delta t}{60}$$ (Eq 8.45) 8.32

$$\text{Range} = \sum_{\text{Sea Level}}^{H_P} \Delta d$$ (Eq 8.46) 8.32

CHAPTER 9

$$R = \mu\,(W - L)$$ (Eq 9.1) 9.5

$$\int_0^{S_1} \left[T - D - \mu(W - L) \right] dS = \frac{1}{2}\,\frac{W}{g}\left(V_{TO}^2\right)$$ (Eq 9.2) 9.6

$$\left[T - D - \mu(W - L) \right]_{Avg} S_1 = \frac{1}{2}\,\frac{W}{g}\left(V_{TO}^2\right)$$ (Eq 9.3) 9.6

$$S_1 = \frac{W\,V_{TO}^2}{2g\left[T - D - \mu\,(W - L) \right]_{Avg}}$$ (Eq 9.4) 9.7

$$Work = \Delta T\,V\,\Delta t$$ (Eq 9.5) 9.9

$$T_{ex} = T - D - \mu(W - L)$$ (Eq 9.6) 9.9

$$q = \frac{1}{2}\rho V^2$$ (Eq 9.7) 9.9

$$D = C_D\,q\,S$$ (Eq 9.8) 9.9

$$L = C_L\,q\,S$$ (Eq 9.9) 9.9

$$C_D = C_{D_p} + C_{D_i}$$ (Eq 9.10) 9.9

$$C_{D_i} = \frac{C_L^2}{\pi\,e\,AR}$$ (Eq 9.11) 9.10

$$C_D = C_{D_p} + \frac{C_L^2}{\pi\,e\,AR}$$ (Eq 9.12) 9.10

$$D = \left(C_{D_p} + \frac{C_L^2}{\pi\,e\,AR} \right) q\,S$$ (Eq 9.13) 9.10

$$T_{ex} = T - \left(C_{D_p} + \frac{C_L^2}{\pi\, e\, AR} \right) q\, S - \mu\left(W - C_L\, q\, S \right)$$ (Eq 9.14) 9.10

$$\frac{dT_{ex}}{dC_L} = \left(\frac{2\, C_L}{\pi\, e\, AR} \right) q\, S + \mu\left(q\, S \right)$$ (Eq 9.15) 9.10

$$C_{L_{Opt}} = \frac{\mu\, \pi\, e\, AR}{2}$$ (Eq 9.16) 9.10

$$S_2 = \int_{\text{Lift off}}^{50\text{ ft}} (T - D)\, dS = \frac{W}{2g} \left(V_{50}^2 - V_{TO}^2 \right) + 50\, W$$ (Eq 9.17) 9.12

$$S_2 = \frac{W \left(\frac{V_{50}^2 - V_{TO}^2}{2g} + 50 \right)}{(T - D)_{Avg}}$$ (Eq 9.18) 9.12

$$V_{TO_w} = V_{TO} - V_w$$ (Eq 9.19) 9.13

$$S_{1_w} = \frac{W\, V_{TO_w}^2}{2\, g\, T_{ex_{Avg_w}}}$$ (Eq 9.20) 9.13

$$S_{1_{Std}} = \frac{W \left(V_{TO_w} + V_w \right)^2}{2\, g\, T_{ex_{Avg}}}$$ (Eq 9.21) 9.13

$$S_{1_{Std}} = S_{1_w} \frac{T_{ex_{Avg_w}}}{T_{ex_{Avg}}} \left(1 + \frac{V_w}{V_{TO_w}} \right)^2$$ (Eq 9.22) 9.13

$$S_{1_{Std}} = S_{1_w} \left(1 + \frac{V_w}{V_{TO_w}} \right)^{1.85}$$ (Eq 9.23) 9.14

$$S_{2_{Std}} = S_{2_w} + \Delta S_2$$ (Eq 9.24) 9.14

$$T_{ex_{Avg}} \; S_{1_{SL}} = \frac{1}{2} \; \frac{W}{g} \; V_{TO}^2 - W \; S_{1_{SL}} \; \sin\theta$$ (Eq 9.25) 9.15

$$S_{1_{SL}} = \frac{W \; V_{TO}^2}{2 \; g \left(T_{ex_{Avg}} + W \sin\theta \right)}$$ (Eq 9.26) 9.15

$$S_{1_{Std}} = \frac{S_{1_{SL}}}{\left(1 - \dfrac{2g \; S_{1_{SL}}}{V_{TO}^2} \; \sin\theta \right)}$$ (Eq 9.27) 9.15

$$S_{1_{Std}} = S_{1_{Test}} \left(\frac{W_{Std}}{W_{Test}} \right)^{2.3} \left(\frac{\sigma_{Test}}{\sigma_{Std}} \right) \left(\frac{T_{N_{Test}}}{T_{N_{Std}}} \right)^{1.3}$$ (Eq 9.28) 9.16

$$S_{2_{Std}} = S_{2_{Test}} \left(\frac{W_{Std}}{W_{Test}} \right)^{2.3} \left(\frac{\sigma_{Test}}{\sigma_{Std}} \right)^{0.7} \left(\frac{T_{N_{Test}}}{T_{N_{Std}}} \right)^{1.6}$$ (Eq 9.29) 9.16

$$S_{1_{Std}} = S_{1_{Test}} \left(\frac{W_{Std}}{W_{Test}} \right)^{2.6} \left(\frac{\sigma_{Test}}{\sigma_{Std}} \right)^{1.9} \left(\frac{N_{Test}}{N_{Std}} \right)^{0.7} \left(\frac{P_{a_{Test}}}{P_{a_{Std}}} \right)^{0.5}$$ (Eq 9.30) 9.17

$$S_{2_{Std}} = S_{2_{Test}} \left(\frac{W_{Std}}{W_{Test}} \right)^{2.6} \left(\frac{\sigma_{Test}}{\sigma_{Std}} \right)^{1.9} \left(\frac{N_{Test}}{N_{Std}} \right)^{0.8} \left(\frac{P_{a_{Test}}}{P_{a_{Std}}} \right)^{0.6}$$ (Eq 9.31) 9.17

$$S_3 = \frac{W \left(\dfrac{V_{TD}^2 - V_{50}^2}{2g} - 50 \right)}{(T - D)_{Avg}}$$ (Eq 9.32) 9.19

$$S_4 = \int_{\text{Touchdown}}^{\text{Stop}} \left[\text{T-D-}\mu(\text{W - L}) \right] dS = \frac{1}{2} \frac{W}{g} \left(0 - V_{TD}^2 \right)$$ (Eq 9.33) 9.19

$$S_4 = \frac{-W\, V_{TD}^2}{2g \left[\text{T - D -}\mu(\text{W - L}) \right]_{Avg}}$$ (Eq 9.34) 9.20

$$S_{3_{Std}} = S_{3_{Test}} \left(\frac{W_{Std}}{W_{Test}} \right)^{\left(2 + \frac{E_h}{E_h + 50} \right)} \left(\frac{\sigma_{Test}}{\sigma_{Std}} \right)^{\left(\frac{E_h}{E_h + 50} \right)}$$ (Eq 9.35) 9.23

$$E_h = \frac{V_{50}^2 - V_{TD}^2}{2g}$$ (Eq 9.36) 9.23

$$S_{4_{Std}} = S_{4_{Test}} \left(\frac{W_{Std}}{W_{Test}} \right)^2 \left(\frac{\sigma_{Test}}{\sigma_{Std}} \right)$$ (Eq 9.37) 9.23

V_w = Wind Velocity cos (Wind Direction Relative To Runway) (Eq 9.38) 9.28

$$\sigma = 9.625 \frac{P_a}{T_a}$$ (Eq 9.39) 9.29

$$V_{TD_w} = V_{TD} - V_w$$ (Eq 9.40) 9.30

$$S_{4_{Std}} = S_{4_w} \left(1 + \frac{V_w}{V_{TD}} \right)^{1.85}$$ (Eq 9.41) 9.30

$$S_{4_{Std}} = \frac{S_{4_{SL}}}{\left(1 - \frac{2\, g\, S_{4_{SL}}}{V_{TD}^2} \sin\theta \right)}$$ (Eq 9.42) 9.31

APPENDIX VI

STANDARD ATMOSPHERE

H ft	P_a psf	δ	T_a °K	θ	a kn	σ	ϕ	$\frac{\delta}{\phi\sqrt{\theta}}$
-1000	2193.818	1.0367	290.13	1.0069	663.753	1.0296	1.005	1.0276
-900	2185.956	1.0330	289.93	1.0062	663.526	1.0266	1.005	1.0249
-800	2178.117	1.0293	289.73	1.0055	663.300	1.0236	1.004	1.0221
-700	2170.300	1.0256	289.54	1.0048	663.073	1.0206	1.004	1.0193
-600	2162.506	1.0219	289.34	1.0041	662.846	1.0177	1.003	1.0165
-500	2154.735	1.0182	289.14	1.0034	662.619	1.0147	1.003	1.0137
-400	2146.986	1.0145	288.94	1.0028	662.392	1.0118	1.002	1.0110
-300	2139.260	1.0109	288.74	1.0021	662.165	1.0088	1.002	1.0082
-200	2131.557	1.0072	288.55	1.0014	661.938	1.0059	1.001	1.0055
-100	2123.876	1.0036	288.35	1.0007	661.710	1.0029	1.001	1.0027
0	2116.217	1.0000	288.15	1.0000	661.483	1.0000	1.000	1.0000
100	2108.581	0.9964	287.95	0.9993	661.256	0.9971	0.999	0.9973
200	2100.967	0.9928	287.75	0.9986	661.028	0.9942	0.999	0.9945
300	2093.375	0.9892	287.56	0.9979	660.800	0.9913	0.998	0.9918
400	2085.806	0.9856	287.36	0.9972	660.573	0.9883	0.998	0.9891
500	2078.259	0.9821	287.16	0.9966	660.345	0.9855	0.997	0.9864
600	2070.734	0.9785	286.96	0.9959	660.117	0.9826	0.997	0.9837
700	2063.231	0.9750	286.76	0.9952	659.889	0.9797	0.996	0.9810
800	2055.750	0.9714	286.57	0.9945	659.661	0.9768	0.996	0.9783
900	2048.291	0.9679	286.37	0.9938	659.433	0.9739	0.995	0.9756
1000	2040.854	0.9644	286.17	0.9931	659.205	0.9711	0.995	0.9729
1100	2033.438	0.9609	285.97	0.9924	658.977	0.9682	0.994	0.9703
1200	2026.045	0.9574	285.77	0.9917	658.748	0.9654	0.994	0.9676
1300	2018.673	0.9539	285.57	0.9911	658.520	0.9625	0.993	0.9649
1400	2011.324	0.9504	285.38	0.9904	658.292	0.9597	0.993	0.9623
1500	2003.995	0.9470	285.18	0.9897	658.063	0.9568	0.992	0.9596
1600	1996.689	0.9435	284.98	0.9890	657.834	0.9540	0.991	0.9570
1700	1989.404	0.9401	284.78	0.9883	657.606	0.9512	0.991	0.9543
1800	1982.141	0.9366	284.58	0.9876	657.377	0.9484	0.990	0.9517
1900	1974.899	0.9332	284.39	0.9869	657.148	0.9456	0.990	0.9490
2000	1967.678	0.9298	284.19	0.9862	656.919	0.9428	0.989	0.9464
2100	1960.479	0.9264	283.99	0.9856	656.690	0.9400	0.989	0.9438
2200	1953.301	0.9230	283.79	0.9849	656.461	0.9372	0.988	0.9412
2300	1946.145	0.9196	283.59	0.9842	656.232	0.9344	0.988	0.9386
2400	1939.010	0.9163	283.40	0.9835	656.003	0.9316	0.987	0.9360
2500	1931.896	0.9129	283.20	0.9828	655.773	0.9289	0.987	0.9334
2600	1924.803	0.9095	283.00	0.9821	655.544	0.9261	0.986	0.9308
2700	1917.731	0.9062	282.80	0.9814	655.314	0.9233	0.986	0.9282
2800	1910.680	0.9029	282.60	0.9807	655.085	0.9206	0.985	0.9256
2900	1903.651	0.8996	282.40	0.9801	654.855	0.9179	0.984	0.9230

H ft	P_a psf	δ	T_a °K	θ	a kn	σ	ϕ	$\frac{\delta}{\phi\sqrt{\theta}}$
3000	1896.642	0.8962	282.21	0.9794	654.625	0.9151	0.984	0.9205
3100	1889.654	0.8929	282.01	0.9787	654.396	0.9124	0.983	0.9179
3200	1882.687	0.8896	281.81	0.9780	654.166	0.9097	0.983	0.9153
3300	1875.741	0.8864	281.61	0.9773	653.936	0.9069	0.982	0.9128
3400	1868.816	0.8831	281.41	0.9766	653.706	0.9042	0.982	0.9102
3500	1861.911	0.8798	281.22	0.9759	653.475	0.9015	0.981	0.9077
3600	1855.027	0.8766	281.02	0.9752	653.245	0.8988	0.981	0.9051
3700	1848.164	0.8733	280.82	0.9746	653.015	0.8961	0.980	0.9026
3800	1841.321	0.8701	280.62	0.9739	652.784	0.8934	0.980	0.9001
3900	1834.499	0.8669	280.42	0.9732	652.554	0.8908	0.979	0.8976
4000	1827.697	0.8637	280.23	0.9725	652.323	0.8881	0.978	0.8950
4100	1820.915	0.8605	280.03	0.9718	652.093	0.8854	0.978	0.8925
4200	1814.154	0.8573	279.83	0.9711	651.862	0.8828	0.977	0.8900
4300	1807.414	0.8541	279.63	0.9704	651.631	0.8801	0.977	0.8875
4400	1800.694	0.8509	279.43	0.9697	651.400	0.8774	0.976	0.8850
4500	1793.993	0.8477	279.23	0.9691	651.169	0.8748	0.976	0.8825
4600	1787.314	0.8446	279.04	0.9684	650.938	0.8722	0.975	0.8801
4700	1780.654	0.8414	278.84	0.9677	650.707	0.8695	0.975	0.8776
4800	1774.014	0.8383	278.64	0.9670	650.476	0.8669	0.974	0.8751
4900	1767.395	0.8352	278.44	0.9663	650.245	0.8643	0.974	0.8726
5000	1760.795	0.8320	278.24	0.9656	650.013	0.8617	0.973	0.8702
5100	1754.216	0.8289	278.05	0.9649	649.782	0.8591	0.973	0.8677
5200	1747.656	0.8258	277.85	0.9642	649.550	0.8565	0.972	0.8653
5300	1741.116	0.8227	277.65	0.9636	649.319	0.8539	0.971	0.8628
5400	1734.596	0.8197	277.45	0.9629	649.087	0.8513	0.971	0.8604
5500	1728.096	0.8166	277.25	0.9622	648.855	0.8487	0.970	0.8579
5600	1721.616	0.8135	277.06	0.9615	648.623	0.8461	0.970	0.8555
5700	1715.155	0.8105	276.86	0.9608	648.391	0.8435	0.969	0.8531
5800	1708.714	0.8074	276.66	0.9601	648.159	0.8410	0.969	0.8507
5900	1702.292	0.8044	276.46	0.9594	647.927	0.8384	0.968	0.8482
6000	1695.890	0.8014	276.26	0.9587	647.695	0.8359	0.968	0.8458
6100	1689.508	0.7984	276.06	0.9581	647.463	0.8333	0.967	0.8434
6200	1683.145	0.7954	275.87	0.9574	647.230	0.8308	0.967	0.8410
6300	1676.802	0.7924	275.67	0.9567	646.998	0.8282	0.966	0.8386
6400	1670.477	0.7894	275.47	0.9560	646.765	0.8257	0.965	0.8362
6500	1664.173	0.7864	275.27	0.9553	646.533	0.8232	0.965	0.8338
6600	1657.887	0.7834	275.07	0.9546	646.300	0.8207	0.964	0.8315
6700	1651.621	0.7805	274.88	0.9539	646.067	0.8181	0.964	0.8291
6800	1645.374	0.7775	274.68	0.9532	645.834	0.8156	0.963	0.8267
6900	1639.146	0.7746	274.48	0.9526	645.601	0.8131	0.963	0.8244

H ft	P_a psf	δ	T_a °K	θ	a kn	σ	ϕ	$\frac{\delta}{\phi\sqrt{\theta}}$
7000	1632.937	0.7716	274.28	0.9519	645.368	0.8106	0.962	0.8220
7100	1626.747	0.7687	274.08	0.9512	645.135	0.8082	0.962	0.8196
7200	1620.576	0.7658	273.89	0.9505	644.902	0.8057	0.961	0.8173
7300	1614.424	0.7629	273.69	0.9498	644.669	0.8032	0.961	0.8150
7400	1608.291	0.7600	273.49	0.9491	644.435	0.8007	0.960	0.8126
7500	1602.177	0.7571	273.29	0.9484	644.202	0.7983	0.959	0.8103
7600	1596.082	0.7542	273.09	0.9477	643.968	0.7958	0.959	0.8080
7700	1590.006	0.7513	272.89	0.9471	643.735	0.7933	0.958	0.8056
7800	1583.948	0.7485	272.70	0.9464	643.501	0.7909	0.958	0.8033
7900	1577.909	0.7456	272.50	0.9457	643.267	0.7885	0.957	0.8010
8000	1571.889	0.7428	272.30	0.9450	643.033	0.7860	0.957	0.7987
8100	1565.887	0.7399	272.10	0.9443	642.799	0.7836	0.956	0.7964
8200	1559.904	0.7371	271.90	0.9436	642.565	0.7812	0.956	0.7941
8300	1553.939	0.7343	271.71	0.9429	642.331	0.7787	0.955	0.7918
8400	1547.993	0.7315	271.51	0.9422	642.097	0.7763	0.954	0.7895
8500	1542.066	0.7287	271.31	0.9416	641.863	0.7739	0.954	0.7872
8600	1536.156	0.7259	271.11	0.9409	641.628	0.7715	0.953	0.7849
8700	1530.265	0.7231	270.91	0.9402	641.394	0.7691	0.953	0.7827
8800	1524.393	0.7203	270.72	0.9395	641.159	0.7667	0.952	0.7804
8900	1518.538	0.7176	270.52	0.9388	640.925	0.7643	0.952	0.7781
9000	1512.702	0.7148	270.32	0.9381	640.690	0.7620	0.951	0.7759
9100	1506.884	0.7121	270.12	0.9374	640.455	0.7596	0.951	0.7736
9200	1501.084	0.7093	269.92	0.9367	640.220	0.7572	0.950	0.7714
9300	1495.303	0.7066	269.72	0.9361	639.985	0.7549	0.950	0.7691
9400	1489.539	0.7039	269.53	0.9354	639.750	0.7525	0.949	0.7669
9500	1483.793	0.7012	269.33	0.9347	639.515	0.7502	0.948	0.7647
9600	1478.066	0.6984	269.13	0.9340	639.280	0.7478	0.948	0.7624
9700	1472.356	0.6957	268.93	0.9333	639.044	0.7455	0.947	0.7602
9800	1466.664	0.6931	268.73	0.9326	638.809	0.7431	0.947	0.7580
9900	1460.990	0.6904	268.54	0.9319	638.573	0.7408	0.946	0.7558
10000	1455.333	0.6877	268.34	0.9312	638.338	0.7385	0.946	0.7536
10100	1449.695	0.6850	268.14	0.9306	638.102	0.7362	0.945	0.7514
10200	1444.074	0.6824	267.94	0.9299	637.866	0.7339	0.945	0.7492
10300	1438.471	0.6797	267.74	0.9292	637.630	0.7315	0.944	0.7470
10400	1432.885	0.6771	267.55	0.9285	637.394	0.7292	0.943	0.7448
10500	1427.317	0.6745	267.35	0.9278	637.158	0.7269	0.943	0.7426
10600	1421.767	0.6718	267.15	0.9271	636.922	0.7247	0.942	0.7404
10700	1416.234	0.6692	266.95	0.9264	636.686	0.7224	0.942	0.7383
10800	1410.718	0.6666	266.75	0.9257	636.450	0.7201	0.941	0.7361
10900	1405.220	0.6640	266.55	0.9251	636.213	0.7178	0.941	0.7339

STANDARD ATMOSPHERE

H ft	P_a psf	δ	T_a ˚K	θ	a kn	σ	ϕ	$\frac{\delta}{\phi\sqrt{\theta}}$
11000	1399.739	0.6614	266.36	0.9244	635.977	0.7156	0.940	0.7318
11100	1394.276	0.6589	266.16	0.9237	635.740	0.7133	0.940	0.7296
11200	1388.829	0.6563	265.96	0.9230	635.504	0.7110	0.939	0.7275
11300	1383.400	0.6537	265.76	0.9223	635.267	0.7088	0.938	0.7253
11400	1377.989	0.6512	265.56	0.9216	635.030	0.7065	0.938	0.7232
11500	1372.594	0.6486	265.37	0.9209	634.793	0.7043	0.937	0.7210
11600	1367.217	0.6461	265.17	0.9202	634.556	0.7021	0.937	0.7189
11700	1361.856	0.6435	264.97	0.9196	634.319	0.6998	0.936	0.7168
11800	1356.513	0.6410	264.77	0.9189	634.082	0.6976	0.936	0.7147
11900	1351.186	0.6385	264.57	0.9182	633.845	0.6954	0.935	0.7126
12000	1345.877	0.6360	264.38	0.9175	633.607	0.6932	0.935	0.7104
12100	1340.584	0.6335	264.18	0.9168	633.370	0.6910	0.934	0.7083
12200	1335.309	0.6310	263.98	0.9161	633.132	0.6888	0.933	0.7062
12300	1330.050	0.6285	263.78	0.9154	632.895	0.6866	0.933	0.7041
12400	1324.808	0.6260	263.58	0.9147	632.657	0.6844	0.932	0.7020
12500	1319.583	0.6236	263.39	0.9141	632.419	0.6822	0.932	0.7000
12600	1314.374	0.6211	263.19	0.9134	632.181	0.6800	0.931	0.6979
12700	1309.182	0.6186	262.99	0.9127	631.943	0.6778	0.931	0.6958
12800	1304.007	0.6162	262.79	0.9120	631.705	0.6757	0.930	0.6937
12900	1298.848	0.6138	262.59	0.9113	631.467	0.6735	0.930	0.6917
13000	1293.706	0.6113	262.39	0.9106	631.229	0.6713	0.929	0.6896
13100	1288.580	0.6089	262.20	0.9099	630.990	0.6692	0.928	0.6875
13200	1283.471	0.6065	262.00	0.9092	630.752	0.6670	0.928	0.6855
13300	1278.378	0.6041	261.80	0.9086	630.513	0.6649	0.927	0.6834
13400	1273.301	0.6017	261.60	0.9079	630.275	0.6627	0.927	0.6814
13500	1268.241	0.5993	261.40	0.9072	630.036	0.6606	0.926	0.6793
13600	1263.197	0.5969	261.21	0.9065	629.797	0.6585	0.926	0.6773
13700	1258.170	0.5945	261.01	0.9058	629.558	0.6564	0.925	0.6753
13800	1253.158	0.5922	260.81	0.9051	629.319	0.6542	0.925	0.6732
13900	1248.163	0.5898	260.61	0.9044	629.080	0.6521	0.924	0.6712
14000	1243.184	0.5875	260.41	0.9037	628.841	0.6500	0.923	0.6692
14100	1238.221	0.5851	260.22	0.9031	628.602	0.6479	0.923	0.6672
14200	1233.274	0.5828	260.02	0.9024	628.362	0.6458	0.922	0.6652
14300	1228.343	0.5804	259.82	0.9017	628.123	0.6437	0.922	0.6632
14400	1223.428	0.5781	259.62	0.9010	627.883	0.6416	0.921	0.6612
14500	1218.529	0.5758	259.42	0.9003	627.644	0.6396	0.921	0.6592
14600	1213.646	0.5735	259.22	0.8996	627.404	0.6375	0.920	0.6572
14700	1208.779	0.5712	259.03	0.8989	627.164	0.6354	0.919	0.6552
14800	1203.928	0.5689	258.83	0.8982	626.924	0.6334	0.919	0.6532
14900	1199.092	0.5666	258.63	0.8976	626.684	0.6313	0.918	0.6513

H ft	P_a psf	δ	T_a °K	θ	a kn	σ	ϕ	$\frac{\delta}{\phi\sqrt{\theta}}$
15000	1194.272	0.5643	258.43	0.8969	626.444	0.6292	0.918	0.6493
15100	1189.468	0.5621	258.23	0.8962	626.204	0.6272	0.917	0.6473
15200	1184.679	0.5598	258.04	0.8955	625.964	0.6251	0.917	0.6454
15300	1179.906	0.5576	257.84	0.8948	625.724	0.6231	0.916	0.6434
15400	1175.149	0.5553	257.64	0.8941	625.483	0.6211	0.916	0.6414
15500	1170.407	0.5531	257.44	0.8934	625.243	0.6190	0.915	0.6395
15600	1165.681	0.5508	257.24	0.8927	625.002	0.6170	0.914	0.6375
15700	1160.970	0.5486	257.05	0.8921	624.761	0.6150	0.914	0.6356
15800	1156.275	0.5464	256.85	0.8914	624.520	0.6130	0.913	0.6337
15900	1151.595	0.5442	256.65	0.8907	624.280	0.6110	0.913	0.6317
16000	1146.930	0.5420	256.45	0.8900	624.039	0.6090	0.912	0.6298
16100	1142.281	0.5398	256.25	0.8893	623.797	0.6070	0.912	0.6279
16200	1137.647	0.5376	256.05	0.8886	623.556	0.6050	0.911	0.6260
16300	1133.028	0.5354	255.86	0.8879	623.315	0.6030	0.910	0.6241
16400	1128.424	0.5332	255.66	0.8872	623.074	0.6010	0.910	0.6222
16500	1123.836	0.5311	255.46	0.8866	622.832	0.5990	0.909	0.6202
16600	1119.262	0.5289	255.26	0.8859	622.591	0.5970	0.909	0.6183
16700	1114.704	0.5267	255.06	0.8852	622.349	0.5951	0.908	0.6165
16800	1110.161	0.5246	254.87	0.8845	622.107	0.5931	0.908	0.6146
16900	1105.633	0.5225	254.67	0.8838	621.865	0.5911	0.907	0.6127
17000	1101.119	0.5203	254.47	0.8831	621.623	0.5892	0.907	0.6108
17100	1096.621	0.5182	254.27	0.8824	621.381	0.5872	0.906	0.6089
17200	1092.138	0.5161	254.07	0.8817	621.139	0.5853	0.905	0.6070
17300	1087.669	0.5140	253.88	0.8811	620.897	0.5834	0.905	0.6052
17400	1083.215	0.5119	253.68	0.8804	620.655	0.5814	0.904	0.6033
17500	1078.776	0.5098	253.48	0.8797	620.412	0.5795	0.904	0.6014
17600	1074.352	0.5077	253.28	0.8790	620.170	0.5776	0.903	0.5996
17700	1069.943	0.5056	253.08	0.8783	619.927	0.5756	0.903	0.5977
17800	1065.548	0.5035	252.88	0.8776	619.684	0.5737	0.902	0.5959
17900	1061.167	0.5014	252.69	0.8769	619.442	0.5718	0.901	0.5941
18000	1056.802	0.4994	252.49	0.8762	619.199	0.5699	0.901	0.5922
18100	1052.451	0.4973	252.29	0.8756	618.956	0.5680	0.900	0.5904
18200	1048.114	0.4953	252.09	0.8749	618.713	0.5661	0.900	0.5885
18300	1043.792	0.4932	251.89	0.8742	618.470	0.5642	0.899	0.5867
18400	1039.484	0.4912	251.70	0.8735	618.226	0.5623	0.899	0.5849
18500	1035.191	0.4892	251.50	0.8728	617.983	0.5605	0.898	0.5831
18600	1030.912	0.4871	251.30	0.8721	617.739	0.5586	0.897	0.5813
18700	1026.648	0.4851	251.10	0.8714	617.496	0.5567	0.897	0.5795
18800	1022.397	0.4831	250.90	0.8707	617.252	0.5548	0.896	0.5777
18900	1018.161	0.4811	250.71	0.8701	617.009	0.5530	0.896	0.5759

H ft	P_a psf	δ	T_a ˚K	θ	a kn	σ	ϕ	$\frac{\delta}{\phi\sqrt{\theta}}$
19000	1013.940	0.4791	250.51	0.8694	616.765	0.5511	0.895	0.5741
19100	1009.732	0.4771	250.31	0.8687	616.521	0.5493	0.895	0.5723
19200	1005.539	0.4752	250.11	0.8680	616.277	0.5474	0.894	0.5705
19300	1001.359	0.4732	249.91	0.8673	616.033	0.5456	0.893	0.5687
19400	997.194	0.4712	249.71	0.8666	615.788	0.5437	0.893	0.5669
19500	993.043	0.4693	249.52	0.8659	615.544	0.5419	0.892	0.5652
19600	988.906	0.4673	249.32	0.8652	615.300	0.5401	0.892	0.5634
19700	984.782	0.4654	249.12	0.8646	615.055	0.5383	0.891	0.5616
19800	980.673	0.4634	248.92	0.8639	614.810	0.5364	0.891	0.5599
19900	976.578	0.4615	248.72	0.8632	614.566	0.5346	0.890	0.5581
20000	972.496	0.4595	248.53	0.8625	614.321	0.5328	0.889	0.5563
20100	968.428	0.4576	248.33	0.8618	614.076	0.5310	0.889	0.5546
20200	964.374	0.4557	248.13	0.8611	613.831	0.5292	0.888	0.5529
20300	960.334	0.4538	247.93	0.8604	613.586	0.5274	0.888	0.5511
20400	956.308	0.4519	247.73	0.8597	613.341	0.5256	0.887	0.5494
20500	952.295	0.4500	247.54	0.8591	613.095	0.5238	0.887	0.5476
20600	948.296	0.4481	247.34	0.8584	612.850	0.5221	0.886	0.5459
20700	944.310	0.4462	247.14	0.8577	612.604	0.5203	0.885	0.5442
20800	940.338	0.4443	246.94	0.8570	612.359	0.5185	0.885	0.5425
20900	936.380	0.4425	246.74	0.8563	612.113	0.5167	0.884	0.5408
21000	932.435	0.4406	246.54	0.8556	611.867	0.5150	0.884	0.5390
21100	928.504	0.4388	246.35	0.8549	611.621	0.5132	0.883	0.5373
21200	924.586	0.4369	246.15	0.8542	611.375	0.5115	0.883	0.5356
21300	920.681	0.4351	245.95	0.8536	611.129	0.5097	0.882	0.5339
21400	916.790	0.4332	245.75	0.8529	610.883	0.5080	0.881	0.5322
21500	912.912	0.4314	245.55	0.8522	610.637	0.5062	0.881	0.5305
21600	909.047	0.4296	245.36	0.8515	610.391	0.5045	0.880	0.5289
21700	905.196	0.4277	245.16	0.8508	610.144	0.5028	0.880	0.5272
21800	901.358	0.4259	244.96	0.8501	609.897	0.5010	0.879	0.5255
21900	897.533	0.4241	244.76	0.8494	609.651	0.4993	0.879	0.5238
22000	893.721	0.4223	244.56	0.8487	609.404	0.4976	0.878	0.5222
22100	889.922	0.4205	244.37	0.8480	609.157	0.4959	0.877	0.5205
22200	886.137	0.4187	244.17	0.8474	608.910	0.4942	0.877	0.5188
22300	882.364	0.4170	243.97	0.8467	608.663	0.4925	0.876	0.5172
22400	878.604	0.4152	243.77	0.8460	608.416	0.4908	0.876	0.5155
22500	874.858	0.4134	243.57	0.8453	608.169	0.4891	0.875	0.5139
22600	871.124	0.4116	243.37	0.8446	607.921	0.4874	0.874	0.5122
22700	867.404	0.4099	243.18	0.8439	607.674	0.4857	0.874	0.5106
22800	863.696	0.4081	242.98	0.8432	607.426	0.4840	0.873	0.5089
22900	860.001	0.4064	242.78	0.8425	607.178	0.4823	0.873	0.5073

H ft	P_a psf	δ	T_a °K	θ	a kn	σ	ϕ	$\frac{\delta}{\phi\sqrt{\theta}}$
23000	856.319	0.4046	242.58	0.8419	606.931	0.4807	0.872	0.5057
23100	852.649	0.4029	242.38	0.8412	606.683	0.4790	0.872	0.5040
23200	848.993	0.4012	242.19	0.8405	606.435	0.4773	0.871	0.5024
23300	845.349	0.3995	241.99	0.8398	606.187	0.4757	0.870	0.5008
23400	841.717	0.3977	241.79	0.8391	605.938	0.4740	0.870	0.4992
23500	838.099	0.3960	241.59	0.8384	605.690	0.4724	0.869	0.4976
23600	834.493	0.3943	241.39	0.8377	605.442	0.4707	0.869	0.4960
23700	830.899	0.3926	241.20	0.8370	605.193	0.4691	0.868	0.4944
23800	827.318	0.3909	241.00	0.8364	604.945	0.4674	0.868	0.4928
23900	823.750	0.3893	240.80	0.8357	604.696	0.4658	0.867	0.4912
24000	820.194	0.3876	240.60	0.8350	604.447	0.4642	0.866	0.4896
24100	816.651	0.3859	240.40	0.8343	604.198	0.4625	0.866	0.4880
24200	813.120	0.3842	240.20	0.8336	603.949	0.4609	0.865	0.4864
24300	809.601	0.3826	240.01	0.8329	603.700	0.4593	0.865	0.4848
24400	806.094	0.3809	239.81	0.8322	603.451	0.4577	0.864	0.4833
24500	802.600	0.3793	239.61	0.8315	603.201	0.4561	0.863	0.4817
24600	799.119	0.3776	239.41	0.8309	602.952	0.4545	0.863	0.4801
24700	795.649	0.3760	239.21	0.8302	602.703	0.4529	0.862	0.4786
24800	792.192	0.3743	239.02	0.8295	602.453	0.4513	0.862	0.4770
24900	788.747	0.3727	238.82	0.8288	602.203	0.4497	0.861	0.4754
25000	785.314	0.3711	238.62	0.8281	601.953	0.4481	0.861	0.4739
25100	781.893	0.3695	238.42	0.8274	601.703	0.4465	0.860	0.4723
25200	778.484	0.3679	238.22	0.8267	601.453	0.4450	0.859	0.4708
25300	775.087	0.3663	238.03	0.8260	601.203	0.4434	0.859	0.4693
25400	771.702	0.3647	237.83	0.8254	600.953	0.4418	0.858	0.4677
25500	768.329	0.3631	237.63	0.8247	600.703	0.4403	0.858	0.4662
25600	764.969	0.3615	237.43	0.8240	600.452	0.4387	0.857	0.4647
25700	761.620	0.3599	237.23	0.8233	600.201	0.4371	0.856	0.4631
25800	758.283	0.3583	237.04	0.8226	599.951	0.4356	0.856	0.4616
25900	754.957	0.3567	236.84	0.8219	599.700	0.4340	0.855	0.4601
26000	751.644	0.3552	236.64	0.8212	599.449	0.4325	0.855	0.4586
26100	748.342	0.3536	236.44	0.8205	599.198	0.4310	0.854	0.4571
26200	745.053	0.3521	236.24	0.8199	598.947	0.4294	0.854	0.4556
26300	741.774	0.3505	236.04	0.8192	598.696	0.4279	0.853	0.4541
26400	738.508	0.3490	235.85	0.8185	598.445	0.4264	0.852	0.4526
26500	735.253	0.3474	235.65	0.8178	598.193	0.4248	0.852	0.4511
26600	732.010	0.3459	235.45	0.8171	597.942	0.4233	0.851	0.4496
26700	728.778	0.3444	235.25	0.8164	597.690	0.4218	0.851	0.4481
26800	725.558	0.3429	235.05	0.8157	597.438	0.4203	0.850	0.4466
26900	722.350	0.3413	234.86	0.8150	597.186	0.4188	0.849	0.4451

H ft	P_a psf	δ	T_a ˚K	θ	a kn	σ	ϕ	$\frac{\delta}{\phi\sqrt{\theta}}$
27000	719.153	0.3398	234.66	0.8144	596.935	0.4173	0.849	0.4436
27100	715.968	0.3383	234.46	0.8137	596.682	0.4158	0.848	0.4422
27200	712.793	0.3368	234.26	0.8130	596.430	0.4143	0.848	0.4407
27300	709.631	0.3353	234.06	0.8123	596.178	0.4128	0.847	0.4392
27400	706.479	0.3338	233.87	0.8116	595.926	0.4113	0.846	0.4378
27500	703.340	0.3324	233.67	0.8109	595.673	0.4099	0.846	0.4363
27600	700.211	0.3309	233.47	0.8102	595.421	0.4084	0.845	0.4349
27700	697.094	0.3294	233.27	0.8095	595.168	0.4069	0.845	0.4334
27800	693.987	0.3279	233.07	0.8089	594.915	0.4054	0.844	0.4320
27900	690.892	0.3265	232.87	0.8082	594.662	0.4040	0.844	0.4305
28000	687.809	0.3250	232.68	0.8075	594.409	0.4025	0.843	0.4291
28100	684.736	0.3236	232.48	0.8068	594.156	0.4011	0.842	0.4277
28200	681.675	0.3221	232.28	0.8061	593.903	0.3996	0.842	0.4262
28300	678.624	0.3207	232.08	0.8054	593.650	0.3981	0.841	0.4248
28400	675.585	0.3192	231.88	0.8047	593.396	0.3967	0.841	0.4234
28500	672.557	0.3178	231.69	0.8040	593.143	0.3953	0.840	0.4219
28600	669.540	0.3164	231.49	0.8034	592.889	0.3938	0.839	0.4205
28700	666.533	0.3150	231.29	0.8027	592.635	0.3924	0.839	0.4191
28800	663.538	0.3135	231.09	0.8020	592.381	0.3910	0.838	0.4177
28900	660.554	0.3121	230.89	0.8013	592.127	0.3895	0.838	0.4163
29000	657.580	0.3107	230.70	0.8006	591.873	0.3881	0.837	0.4149
29100	654.617	0.3093	230.50	0.7999	591.619	0.3867	0.836	0.4135
29200	651.665	0.3079	230.30	0.7992	591.365	0.3853	0.836	0.4121
29300	648.724	0.3065	230.10	0.7985	591.110	0.3839	0.835	0.4107
29400	645.794	0.3052	229.90	0.7979	590.856	0.3825	0.835	0.4093
29500	642.874	0.3038	229.70	0.7972	590.601	0.3811	0.834	0.4079
29600	639.965	0.3024	229.51	0.7965	590.346	0.3797	0.833	0.4066
29700	637.067	0.3010	229.31	0.7958	590.091	0.3783	0.833	0.4052
29800	634.180	0.2997	229.11	0.7951	589.836	0.3769	0.832	0.4038
29900	631.303	0.2983	228.91	0.7944	589.581	0.3755	0.832	0.4024
30000	628.436	0.2970	228.71	0.7937	589.326	0.3741	0.831	0.4011
30100	625.580	0.2956	228.52	0.7930	589.071	0.3728	0.830	0.3997
30200	622.735	0.2943	228.32	0.7924	588.815	0.3714	0.830	0.3983
30300	619.900	0.2929	228.12	0.7917	588.560	0.3700	0.829	0.3970
30400	617.076	0.2916	227.92	0.7910	588.304	0.3686	0.829	0.3956
30500	614.262	0.2903	227.72	0.7903	588.049	0.3673	0.828	0.3943
30600	611.458	0.2889	227.53	0.7896	587.793	0.3659	0.828	0.3929
30700	608.665	0.2876	227.33	0.7889	587.537	0.3646	0.827	0.3916
30800	605.882	0.2863	227.13	0.7882	587.281	0.3632	0.826	0.3903
30900	603.109	0.2850	226.93	0.7875	587.024	0.3619	0.826	0.3889

H ft	P_a psf	δ	T_a °K	θ	a kn	σ	ϕ	$\frac{\delta}{\phi\sqrt{\theta}}$
31000	600.347	0.2837	226.73	0.7869	586.768	0.3605	0.825	0.3876
31100	597.595	0.2824	226.53	0.7862	586.512	0.3592	0.825	0.3863
31200	594.853	0.2811	226.34	0.7855	586.255	0.3579	0.824	0.3849
31300	592.122	0.2798	226.14	0.7848	585.999	0.3565	0.823	0.3836
31400	589.400	0.2785	225.94	0.7841	585.742	0.3552	0.823	0.3823
31500	586.689	0.2772	225.74	0.7834	585.485	0.3539	0.822	0.3810
31600	583.988	0.2760	225.54	0.7827	585.228	0.3526	0.822	0.3797
31700	581.297	0.2747	225.35	0.7820	584.971	0.3512	0.821	0.3784
31800	578.616	0.2734	225.15	0.7814	584.714	0.3499	0.820	0.3771
31900	575.944	0.2722	224.95	0.7807	584.456	0.3486	0.820	0.3758
32000	573.283	0.2709	224.75	0.7800	584.199	0.3473	0.819	0.3745
32100	570.632	0.2696	224.55	0.7793	583.941	0.3460	0.819	0.3732
32200	567.991	0.2684	224.36	0.7786	583.684	0.3447	0.818	0.3719
32300	565.360	0.2672	224.16	0.7779	583.426	0.3434	0.817	0.3706
32400	562.739	0.2659	223.96	0.7772	583.168	0.3421	0.817	0.3693
32500	560.127	0.2647	223.76	0.7765	582.910	0.3408	0.816	0.3680
32600	557.525	0.2635	223.56	0.7759	582.652	0.3396	0.816	0.3667
32700	554.933	0.2622	223.36	0.7752	582.394	0.3383	0.815	0.3655
32800	552.351	0.2610	223.17	0.7745	582.135	0.3370	0.814	0.3642
32900	549.779	0.2598	222.97	0.7738	581.877	0.3357	0.814	0.3629
33000	547.216	0.2586	222.77	0.7731	581.618	0.3345	0.813	0.3617
33100	544.663	0.2574	222.57	0.7724	581.360	0.3332	0.813	0.3604
33200	542.120	0.2562	222.37	0.7717	581.101	0.3319	0.812	0.3591
33300	539.586	0.2550	222.18	0.7710	580.842	0.3307	0.811	0.3579
33400	537.062	0.2538	221.98	0.7704	580.583	0.3294	0.811	0.3566
33500	534.547	0.2526	221.78	0.7697	580.324	0.3282	0.810	0.3554
33600	532.042	0.2514	221.58	0.7690	580.065	0.3269	0.810	0.3541
33700	529.547	0.2502	221.38	0.7683	579.805	0.3257	0.809	0.3529
33800	527.061	0.2491	221.19	0.7676	579.546	0.3245	0.808	0.3517
33900	524.584	0.2479	220.99	0.7669	579.286	0.3232	0.808	0.3504
34000	522.117	0.2467	220.79	0.7662	579.026	0.3220	0.807	0.3492
34100	519.659	0.2456	220.59	0.7655	578.766	0.3208	0.807	0.3480
34200	517.211	0.2444	220.39	0.7649	578.506	0.3195	0.806	0.3468
34300	514.772	0.2433	220.19	0.7642	578.246	0.3183	0.805	0.3455
34400	512.342	0.2421	220.00	0.7635	577.986	0.3171	0.805	0.3443
34500	509.922	0.2410	219.80	0.7628	577.726	0.3159	0.804	0.3431
34600	507.511	0.2398	219.60	0.7621	577.465	0.3147	0.804	0.3419
34700	505.109	0.2387	219.40	0.7614	577.205	0.3135	0.803	0.3407
34800	502.716	0.2376	219.20	0.7607	576.944	0.3123	0.802	0.3395
34900	500.333	0.2364	219.01	0.7600	576.683	0.3111	0.802	0.3383

STANDARD ATMOSPHERE

H ft	P_a psf	δ	T_a °K	θ	a kn	σ	ϕ	$\frac{\delta}{\phi\sqrt{\theta}}$
35000	497.959	0.2353	218.81	0.7594	576.423	0.3099	0.801	0.3371
35100	495.593	0.2342	218.61	0.7587	576.162	0.3087	0.800	0.3359
35200	493.237	0.2331	218.41	0.7580	575.900	0.3075	0.800	0.3347
35300	490.890	0.2320	218.21	0.7573	575.639	0.3063	0.799	0.3335
35400	488.552	0.2309	218.02	0.7566	575.378	0.3051	0.799	0.3323
35500	486.223	0.2298	217.82	0.7559	575.116	0.3039	0.798	0.3311
35600	483.904	0.2287	217.62	0.7552	574.855	0.3028	0.797	0.3300
35700	481.593	0.2276	217.42	0.7545	574.593	0.3016	0.797	0.3288
35800	479.291	0.2265	217.22	0.7539	574.331	0.3004	0.796	0.3276
35900	476.997	0.2254	217.02	0.7532	574.069	0.2993	0.796	0.3264
36000	474.713	0.2243	216.83	0.7525	573.807	0.2981	0.795	0.3253
36100	472.424	0.2232	216.65	0.7519	573.573	0.2969	0.794	0.3241
36200	470.159	0.2222	216.65	0.7519	573.573	0.2955	0.794	0.3225
36300	467.905	0.2211	216.65	0.7519	573.573	0.2941	0.794	0.3210
36400	465.661	0.2200	216.65	0.7519	573.573	0.2927	0.794	0.3194
36500	463.429	0.2190	216.65	0.7519	573.573	0.2913	0.794	0.3179
36600	461.207	0.2179	216.65	0.7519	573.573	0.2899	0.794	0.3164
36700	458.996	0.2169	216.65	0.7519	573.573	0.2885	0.794	0.3148
36800	456.795	0.2159	216.65	0.7519	573.573	0.2871	0.794	0.3133
36900	454.605	0.2148	216.65	0.7519	573.573	0.2857	0.794	0.3118
37000	452.425	0.2138	216.65	0.7519	573.573	0.2843	0.794	0.3103
37100	450.256	0.2128	216.65	0.7519	573.573	0.2830	0.794	0.3089
37200	448.097	0.2117	216.65	0.7519	573.573	0.2816	0.794	0.3074
37300	445.949	0.2107	216.65	0.7519	573.573	0.2803	0.794	0.3059
37400	443.810	0.2097	216.65	0.7519	573.573	0.2789	0.794	0.3044
37500	441.682	0.2087	216.65	0.7519	573.573	0.2776	0.794	0.3030
37600	439.565	0.2077	216.65	0.7519	573.573	0.2763	0.794	0.3015
37700	437.457	0.2067	216.65	0.7519	573.573	0.2749	0.794	0.3001
37800	435.360	0.2057	216.65	0.7519	573.573	0.2736	0.794	0.2986
37900	433.272	0.2047	216.65	0.7519	573.573	0.2723	0.794	0.2972
38000	431.195	0.2038	216.65	0.7519	573.573	0.2710	0.794	0.2958
38100	429.128	0.2028	216.65	0.7519	573.573	0.2697	0.794	0.2944
38200	427.070	0.2018	216.65	0.7519	573.573	0.2684	0.794	0.2929
38300	425.023	0.2008	216.65	0.7519	573.573	0.2671	0.794	0.2915
38400	422.985	0.1999	216.65	0.7519	573.573	0.2658	0.794	0.2901
38500	420.957	0.1989	216.65	0.7519	573.573	0.2646	0.794	0.2888
38600	418.938	0.1980	216.65	0.7519	573.573	0.2633	0.794	0.2874
38700	416.930	0.1970	216.65	0.7519	573.573	0.2620	0.794	0.2860
38800	414.931	0.1961	216.65	0.7519	573.573	0.2608	0.794	0.2846
38900	412.941	0.1951	216.65	0.7519	573.573	0.2595	0.794	0.2833

H ft	P_a psf	δ	T_a °K	θ	a kn	σ	ϕ	$\frac{\delta}{\phi\sqrt{\theta}}$
39000	410.961	0.1942	216.65	0.7519	573.573	0.2583	0.794	0.2819
39100	408.991	0.1933	216.65	0.7519	573.573	0.2570	0.794	0.2805
39200	407.030	0.1923	216.65	0.7519	573.573	0.2558	0.794	0.2792
39300	405.078	0.1914	216.65	0.7519	573.573	0.2546	0.794	0.2779
39400	403.136	0.1905	216.65	0.7519	573.573	0.2534	0.794	0.2765
39500	401.203	0.1896	216.65	0.7519	573.573	0.2522	0.794	0.2752
39600	399.280	0.1887	216.65	0.7519	573.573	0.2509	0.794	0.2739
39700	397.365	0.1878	216.65	0.7519	573.573	0.2497	0.794	0.2726
39800	395.460	0.1869	216.65	0.7519	573.573	0.2485	0.794	0.2713
39900	393.564	0.1860	216.65	0.7519	573.573	0.2474	0.794	0.2700
40000	391.677	0.1851	216.65	0.7519	573.573	0.2462	0.794	0.2687
40100	389.799	0.1842	216.65	0.7519	573.573	0.2450	0.794	0.2674
40200	387.930	0.1833	216.65	0.7519	573.573	0.2438	0.794	0.2661
40300	386.070	0.1824	216.65	0.7519	573.573	0.2426	0.794	0.2648
40400	384.219	0.1816	216.65	0.7519	573.573	0.2415	0.794	0.2636
40500	382.377	0.1807	216.65	0.7519	573.573	0.2403	0.794	0.2623
40600	380.544	0.1798	216.65	0.7519	573.573	0.2392	0.794	0.2610
40700	378.719	0.1790	216.65	0.7519	573.573	0.2380	0.794	0.2598
40800	376.903	0.1781	216.65	0.7519	573.573	0.2369	0.794	0.2585
40900	375.096	0.1772	216.65	0.7519	573.573	0.2357	0.794	0.2573
41000	373.298	0.1764	216.65	0.7519	573.573	0.2346	0.794	0.2561
41100	371.508	0.1756	216.65	0.7519	573.573	0.2335	0.794	0.2548
41200	369.727	0.1747	216.65	0.7519	573.573	0.2324	0.794	0.2536
41300	367.954	0.1739	216.65	0.7519	573.573	0.2313	0.794	0.2524
41400	366.190	0.1730	216.65	0.7519	573.573	0.2301	0.794	0.2512
41500	364.434	0.1722	216.65	0.7519	573.573	0.2290	0.794	0.2500
41600	362.687	0.1714	216.65	0.7519	573.573	0.2279	0.794	0.2488
41700	360.948	0.1706	216.65	0.7519	573.573	0.2269	0.794	0.2476
41800	359.217	0.1697	216.65	0.7519	573.573	0.2258	0.794	0.2464
41900	357.495	0.1689	216.65	0.7519	573.573	0.2247	0.794	0.2452
42000	355.781	0.1681	216.65	0.7519	573.573	0.2236	0.794	0.2440
42100	354.075	0.1673	216.65	0.7519	573.573	0.2225	0.794	0.2429
42200	352.377	0.1665	216.65	0.7519	573.573	0.2215	0.794	0.2417
42300	350.688	0.1657	216.65	0.7519	573.573	0.2204	0.794	0.2406
42400	349.006	0.1649	216.65	0.7519	573.573	0.2193	0.794	0.2394
42500	347.333	0.1641	216.65	0.7519	573.573	0.2183	0.794	0.2383
42600	345.668	0.1633	216.65	0.7519	573.573	0.2172	0.794	0.2371
42700	344.010	0.1626	216.65	0.7519	573.573	0.2162	0.794	0.2360
42800	342.361	0.1618	216.65	0.7519	573.573	0.2152	0.794	0.2348
42900	340.720	0.1610	216.65	0.7519	573.573	0.2141	0.794	0.2337

STANDARD ATMOSPHERE

H ft	P_a psf	δ	T_a ˚K	θ	a kn	σ	ϕ	$\frac{\delta}{\phi\sqrt{\theta}}$
43000	339.086	0.1602	216.65	0.7519	573.573	0.2131	0.794	0.2326
43100	337.460	0.1595	216.65	0.7519	573.573	0.2121	0.794	0.2315
43200	335.842	0.1587	216.65	0.7519	573.573	0.2111	0.794	0.2304
43300	334.232	0.1579	216.65	0.7519	573.573	0.2101	0.794	0.2293
43400	332.629	0.1572	216.65	0.7519	573.573	0.2091	0.794	0.2282
43500	331.035	0.1564	216.65	0.7519	573.573	0.2081	0.794	0.2271
43600	329.447	0.1557	216.65	0.7519	573.573	0.2071	0.794	0.2260
43700	327.868	0.1549	216.65	0.7519	573.573	0.2061	0.794	0.2249
43800	326.296	0.1542	216.65	0.7519	573.573	0.2051	0.794	0.2238
43900	324.731	0.1534	216.65	0.7519	573.573	0.2041	0.794	0.2227
44000	323.174	0.1527	216.65	0.7519	573.573	0.2031	0.794	0.2217
44100	321.625	0.1520	216.65	0.7519	573.573	0.2021	0.794	0.2206
44200	320.083	0.1513	216.65	0.7519	573.573	0.2012	0.794	0.2196
44300	318.548	0.1505	216.65	0.7519	573.573	0.2002	0.794	0.2185
44400	317.021	0.1498	216.65	0.7519	573.573	0.1992	0.794	0.2175
44500	315.501	0.1491	216.65	0.7519	573.573	0.1983	0.794	0.2164
44600	313.988	0.1484	216.65	0.7519	573.573	0.1973	0.794	0.2154
44700	312.483	0.1477	216.65	0.7519	573.573	0.1964	0.794	0.2143
44800	310.984	0.1470	216.65	0.7519	573.573	0.1955	0.794	0.2133
44900	309.493	0.1462	216.65	0.7519	573.573	0.1945	0.794	0.2123
45000	308.010	0.1455	216.65	0.7519	573.573	0.1936	0.794	0.2113
45100	306.533	0.1448	216.65	0.7519	573.573	0.1927	0.794	0.2103
45200	305.063	0.1442	216.65	0.7519	573.573	0.1917	0.794	0.2093
45300	303.600	0.1435	216.65	0.7519	573.573	0.1908	0.794	0.2083
45400	302.145	0.1428	216.65	0.7519	573.573	0.1899	0.794	0.2073
45500	300.696	0.1421	216.65	0.7519	573.573	0.1890	0.794	0.2063
45600	299.254	0.1414	216.65	0.7519	573.573	0.1881	0.794	0.2053
45700	297.820	0.1407	216.65	0.7519	573.573	0.1872	0.794	0.2043
45800	296.392	0.1401	216.65	0.7519	573.573	0.1863	0.794	0.2033
45900	294.971	0.1394	216.65	0.7519	573.573	0.1854	0.794	0.2023
46000	293.556	0.1387	216.65	0.7519	573.573	0.1845	0.794	0.2014
46100	292.149	0.1381	216.65	0.7519	573.573	0.1836	0.794	0.2004
46200	290.748	0.1374	216.65	0.7519	573.573	0.1827	0.794	0.1994
46300	289.354	0.1367	216.65	0.7519	573.573	0.1819	0.794	0.1985
46400	287.967	0.1361	216.65	0.7519	573.573	0.1810	0.794	0.1975
46500	286.586	0.1354	216.65	0.7519	573.573	0.1801	0.794	0.1966
46600	285.212	0.1348	216.65	0.7519	573.573	0.1793	0.794	0.1956
46700	283.844	0.1341	216.65	0.7519	573.573	0.1784	0.794	0.1947
46800	282.484	0.1335	216.65	0.7519	573.573	0.1775	0.794	0.1938
46900	281.129	0.1328	216.65	0.7519	573.573	0.1767	0.794	0.1928

H ft	P_a psf	δ	T_a °K	θ	a kn	σ	ϕ	$\frac{\delta}{\phi\sqrt{\theta}}$
47000	279.781	0.1322	216.65	0.7519	573.573	0.1758	0.794	0.1919
47100	278.440	0.1316	216.65	0.7519	573.573	0.1750	0.794	0.1910
47200	277.105	0.1309	216.65	0.7519	573.573	0.1742	0.794	0.1901
47300	275.776	0.1303	216.65	0.7519	573.573	0.1733	0.794	0.1892
47400	274.454	0.1297	216.65	0.7519	573.573	0.1725	0.794	0.1883
47500	273.138	0.1291	216.65	0.7519	573.573	0.1717	0.794	0.1874
47600	271.828	0.1285	216.65	0.7519	573.573	0.1708	0.794	0.1865
47700	270.525	0.1278	216.65	0.7519	573.573	0.1700	0.794	0.1856
47800	269.228	0.1272	216.65	0.7519	573.573	0.1692	0.794	0.1847
47900	267.937	0.1266	216.65	0.7519	573.573	0.1684	0.794	0.1838
48000	266.653	0.1260	216.65	0.7519	573.573	0.1676	0.794	0.1829
48100	265.374	0.1254	216.65	0.7519	573.573	0.1668	0.794	0.1820
48200	264.102	0.1248	216.65	0.7519	573.573	0.1660	0.794	0.1812
48300	262.835	0.1242	216.65	0.7519	573.573	0.1652	0.794	0.1803
48400	261.575	0.1236	216.65	0.7519	573.573	0.1644	0.794	0.1794
48500	260.321	0.1230	216.65	0.7519	573.573	0.1636	0.794	0.1786
48600	259.073	0.1224	216.65	0.7519	573.573	0.1628	0.794	0.1777
48700	257.831	0.1218	216.65	0.7519	573.573	0.1620	0.794	0.1769
48800	256.595	0.1213	216.65	0.7519	573.573	0.1613	0.794	0.1760
48900	255.364	0.1207	216.65	0.7519	573.573	0.1605	0.794	0.1752
49000	254.140	0.1201	216.65	0.7519	573.573	0.1597	0.794	0.1743
49100	252.921	0.1195	216.65	0.7519	573.573	0.1590	0.794	0.1735
49200	251.709	0.1189	216.65	0.7519	573.573	0.1582	0.794	0.1727
49300	250.502	0.1184	216.65	0.7519	573.573	0.1574	0.794	0.1718
49400	249.301	0.1178	216.65	0.7519	573.573	0.1567	0.794	0.1710
49500	248.106	0.1172	216.65	0.7519	573.573	0.1559	0.794	0.1702
49600	246.916	0.1167	216.65	0.7519	573.573	0.1552	0.794	0.1694
49700	245.732	0.1161	216.65	0.7519	573.573	0.1544	0.794	0.1686
49800	244.554	0.1156	216.65	0.7519	573.573	0.1537	0.794	0.1678
49900	243.381	0.1150	216.65	0.7519	573.573	0.1530	0.794	0.1669
50000	242.215	0.1145	216.65	0.7519	573.573	0.1522	0.794	0.1661

APPENDIX VII

COMPRESSIBILITY CORRECTION

COMPRESSIBILITY CORRECTION

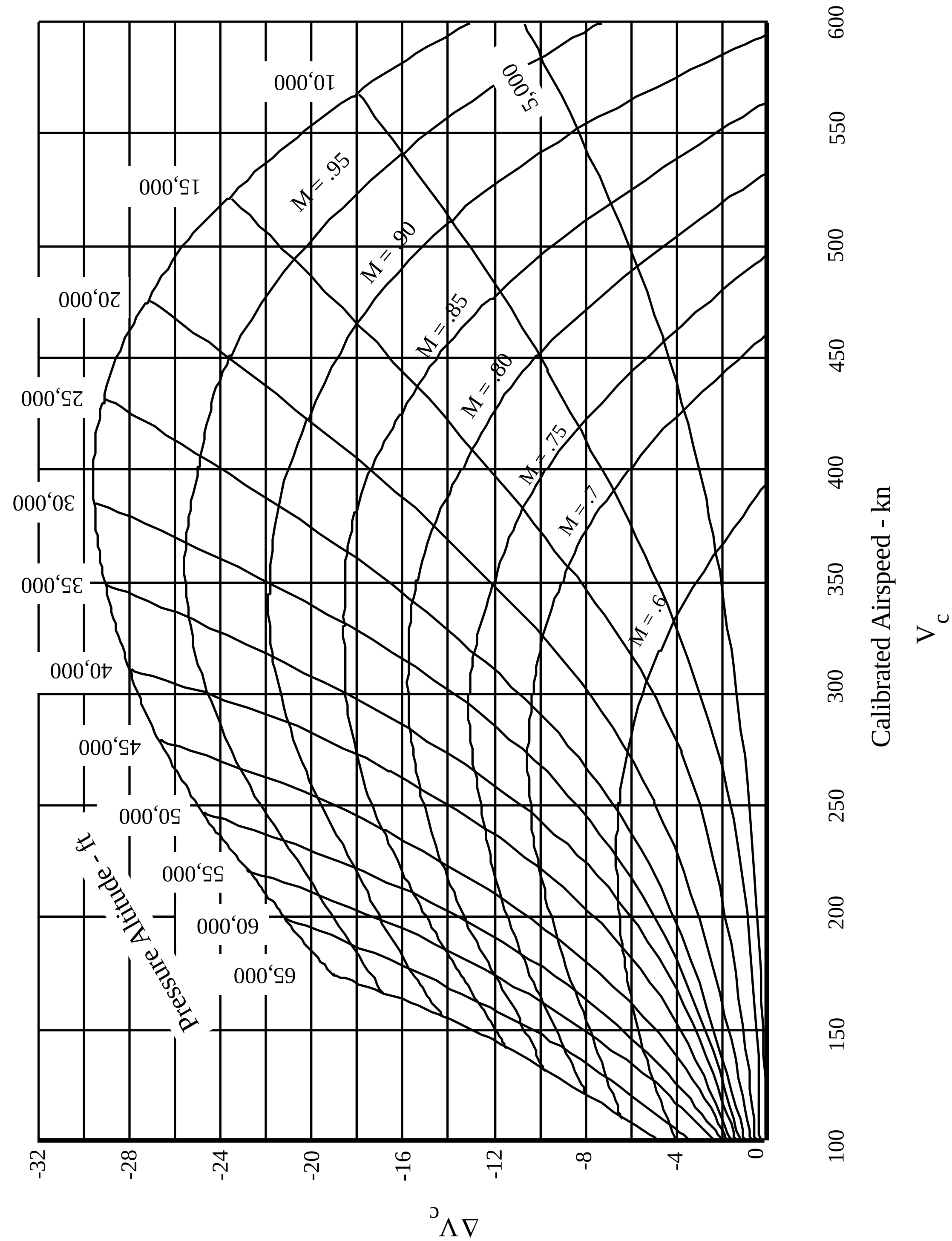

APPENDIX VIII

AIRSPEED, ALTITUDE, MACH NUMBER

AIRSPEED, ALTITUDE, MACH NUMBER

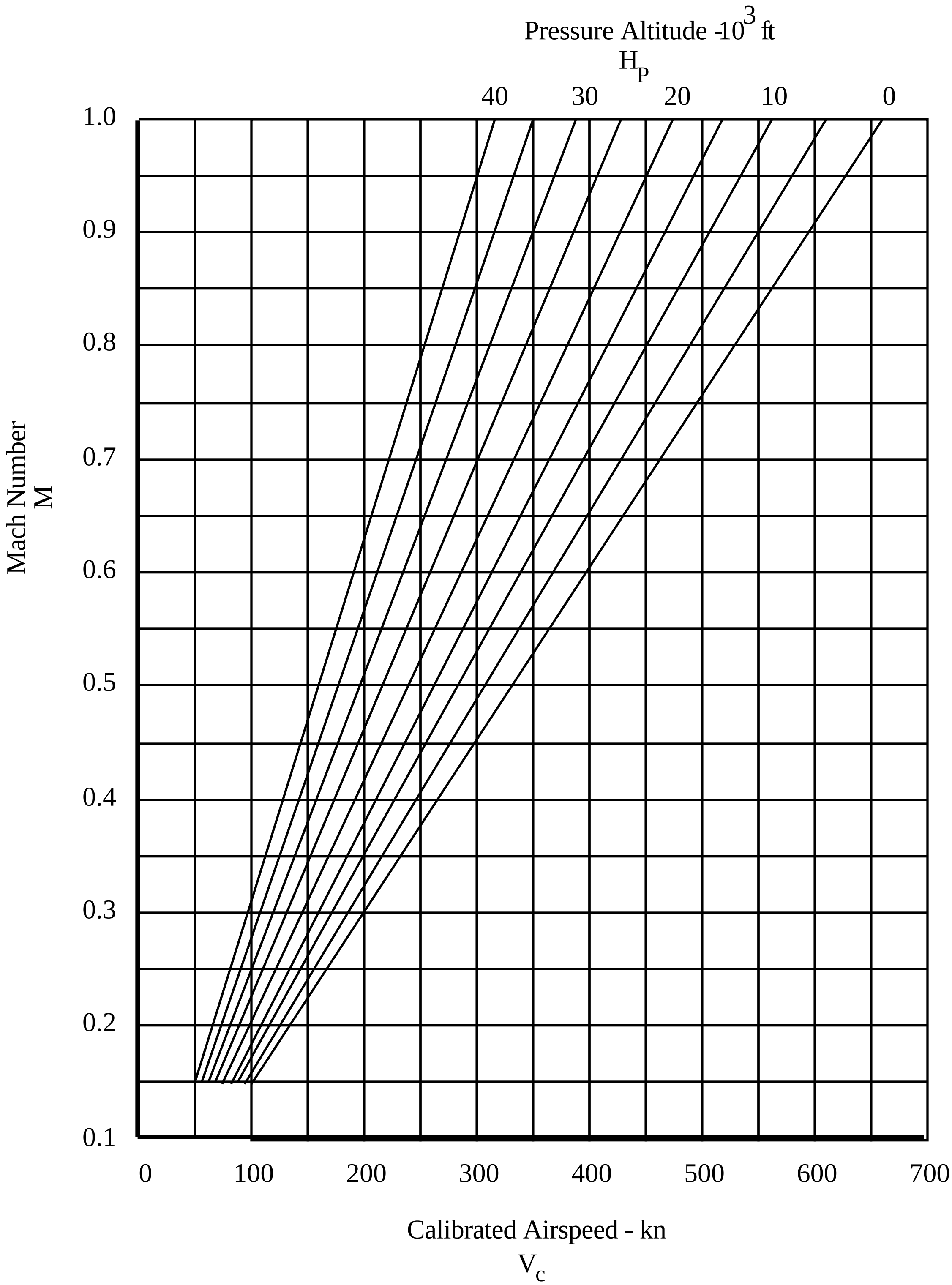

APPENDIX IX

ATMOSPHERIC AIR TEMPERATURE DETERMINATION

ATMOSPHERIC AIR TEMPERATURE DETERMINATION

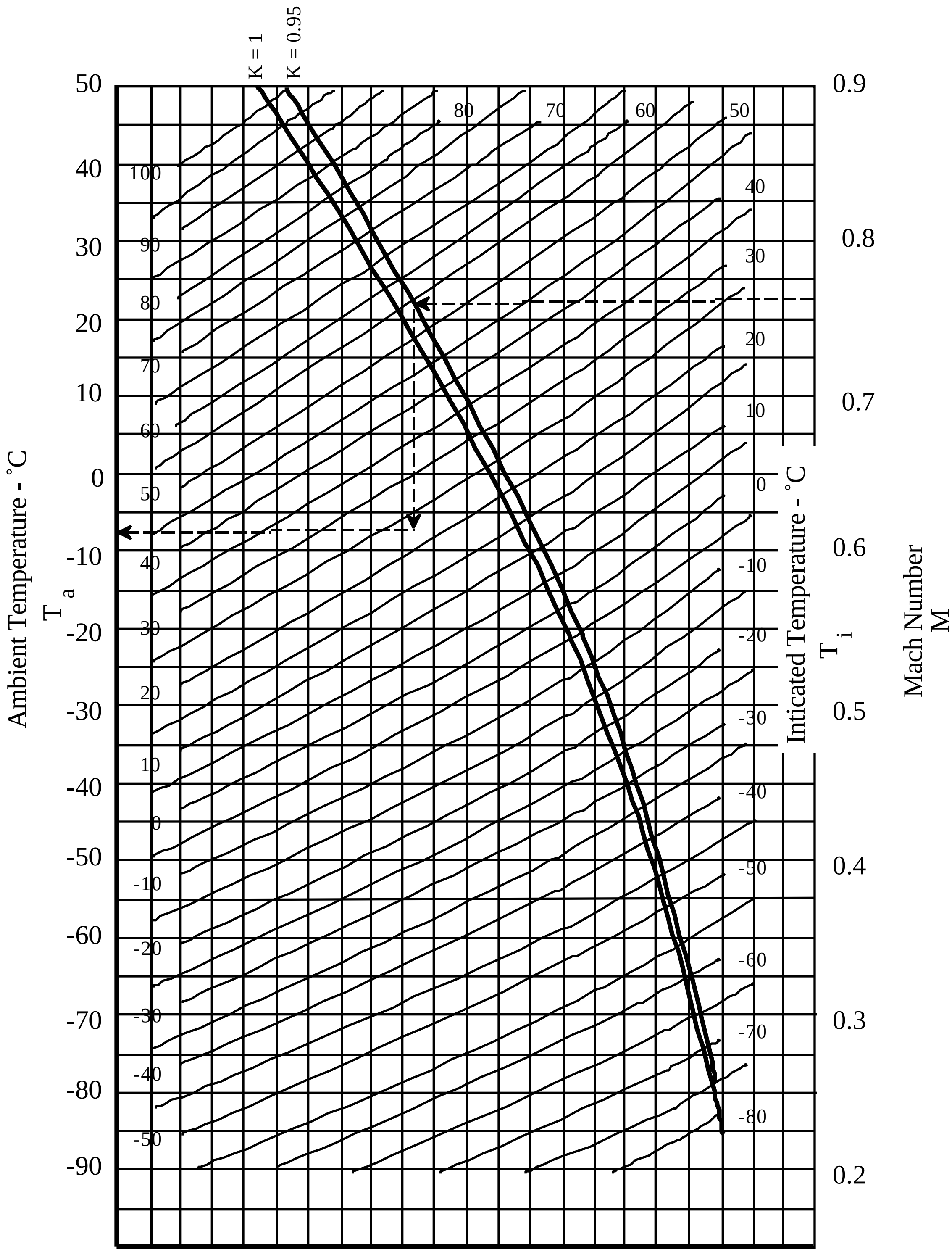

APPENDIX X

TEMPERATURE CONVERSION

TEMPERATURE CONVERSION

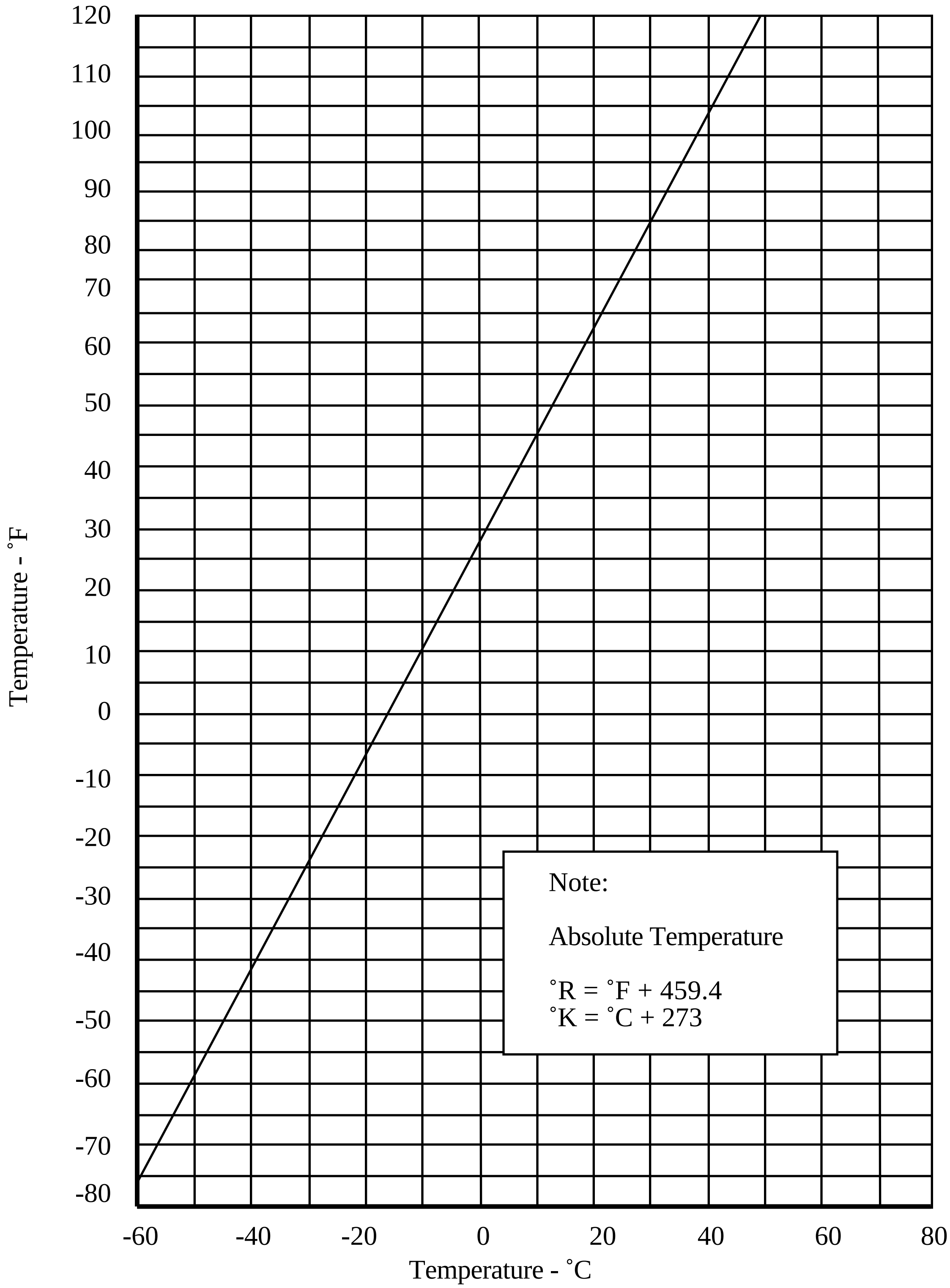

APPENDIX XI

STATIC PRESSURE, PRESSURE ALTITUDE

Pressure Altitude - ft H_P	Static Pressure - psf P_S 0	10	20	30	40	50	60	70	80	90
-1000	2193.8	2194.6	2195.4	2196.2	2197.0	2197.8	2198.5	2199.3	2200.1	2200.9
-900	2186.0	2186.7	2187.5	2188.3	2189.1	2189.9	2190.7	2191.5	2192.2	2193.0
-800	2178.1	2178.9	2179.7	2180.5	2181.2	2182.0	2182.8	2183.6	2184.4	2185.2
-700	2170.3	2171.1	2171.9	2172.6	2173.4	2174.2	2175.0	2175.8	2176.6	2177.3
-600	2162.5	2163.3	2164.1	2164.8	2165.6	2166.4	2167.2	2168.0	2168.7	2169.5
-500	2154.7	2155.5	2156.3	2157.1	2157.8	2158.6	2159.4	2160.2	2160.9	2161.7
-400	2147.0	2147.8	2148.5	2149.3	2150.1	2150.9	2151.6	2152.4	2153.2	2154.0
-300	2139.3	2140.0	2140.8	2141.6	2142.3	2143.1	2143.9	2144.7	2145.4	2146.2
-200	2131.6	2132.3	2133.1	2133.9	2134.6	2135.4	2136.2	2136.9	2137.7	2138.5
-100	2123.9	2124.6	2125.4	2126.2	2126.9	2127.7	2128.5	2129.2	2130.0	2130.8
0	2116.2	2115.5	2114.7	2113.9	2113.2	2112.4	2111.6	2110.9	2110.1	2109.3
100	2108.6	2107.8	2107.1	2106.3	2105.5	2104.8	2104.0	2103.2	2102.5	2101.7
200	2101.0	2100.2	2099.4	2098.7	2097.9	2097.2	2096.4	2095.7	2094.9	2094.1
300	2093.4	2092.6	2091.9	2091.1	2090.3	2089.6	2088.8	2088.1	2087.3	2086.6
400	2085.8	2085.1	2084.3	2083.5	2082.8	2082.0	2081.3	2080.5	2079.8	2079.0
500	2078.3	2077.5	2076.8	2076.0	2075.2	2074.5	2073.7	2073.0	2072.2	2071.5
600	2070.7	2070.0	2069.2	2068.5	2067.7	2067.0	2066.2	2065.5	2064.7	2064.0
700	2063.2	2062.5	2061.7	2061.0	2060.2	2059.5	2058.7	2058.0	2057.2	2056.5
800	2055.7	2055.0	2054.3	2053.5	2052.8	2052.0	2051.3	2050.5	2049.8	2049.0
900	2048.3	2047.5	2046.8	2046.1	2045.3	2044.6	2043.8	2043.1	2042.3	2041.6

	0	10	20	30	40	50	60	70	80	90
1000	2040.9	2040.1	2039.4	2038.6	2037.9	2037.1	2036.4	2035.7	2034.9	2034.2
1100	2033.4	2032.7	2032.0	2031.2	2030.5	2029.7	2029.0	2028.3	2027.5	2026.8
1200	2026.0	2025.3	2024.6	2023.8	2023.1	2022.4	2021.6	2020.9	2020.1	2019.4
1300	2018.7	2017.9	2017.2	2016.5	2015.7	2015.0	2014.3	2013.5	2012.8	2012.1
1400	2011.3	2010.6	2009.9	2009.1	2008.4	2007.7	2006.9	2006.2	2005.5	2004.7
1500	2004.0	2003.3	2002.5	2001.8	2001.1	2000.3	1999.6	1998.9	1998.1	1997.4
1600	1996.7	1996.0	1995.2	1994.5	1993.8	1993.0	1992.3	1991.6	1990.9	1990.1
1700	1989.4	1988.7	1987.9	1987.2	1986.5	1985.8	1985.0	1984.3	1983.6	1982.9
1800	1982.1	1981.4	1980.7	1980.0	1979.2	1978.5	1977.8	1977.1	1976.3	1975.6
1900	1974.9	1974.2	1973.5	1972.7	1972.0	1971.3	1970.6	1969.8	1969.1	1968.4
2000	1967.7	1967.0	1966.2	1965.5	1964.8	1964.1	1963.4	1962.6	1961.9	1961.2
2100	1960.5	1959.8	1959.0	1958.3	1957.6	1956.9	1956.2	1955.5	1954.7	1954.0
2200	1953.3	1952.6	1951.9	1951.2	1950.4	1949.7	1949.0	1948.3	1947.6	1946.9
2300	1946.1	1945.4	1944.7	1944.0	1943.3	1942.6	1941.9	1941.1	1940.4	1939.7
2400	1939.0	1938.3	1937.6	1936.9	1936.2	1935.5	1934.7	1934.0	1933.3	1932.6
2500	1931.9	1931.2	1930.5	1929.8	1929.1	1928.3	1927.6	1926.9	1926.2	1925.5
2600	1924.8	1924.1	1923.4	1922.7	1922.0	1921.3	1920.6	1919.9	1919.1	1918.4
2700	1917.7	1917.0	1916.3	1915.6	1914.9	1914.2	1913.5	1912.8	1912.1	1911.4
2800	1910.7	1910.0	1909.3	1908.6	1907.9	1907.2	1906.5	1905.8	1905.1	1904.4
2900	1903.7	1902.9	1902.2	1901.5	1900.8	1900.1	1899.4	1898.7	1898.0	1897.3

	0	10	20	30	40	50	60	70	80	90
3000	1896.6	1895.9	1895.2	1894.5	1893.8	1893.1	1892.4	1891.7	1891.1	1890.4
3100	1889.7	1889.0	1888.3	1887.6	1886.9	1886.2	1885.5	1884.8	1884.1	1883.4
3200	1882.7	1882.0	1881.3	1880.6	1879.9	1879.2	1878.5	1877.8	1877.1	1876.4
3300	1875.7	1875.0	1874.4	1873.7	1873.0	1872.3	1871.6	1870.9	1870.2	1869.5
3400	1868.8	1868.1	1867.4	1866.7	1866.1	1865.4	1864.7	1864.0	1863.3	1862.6
3500	1861.9	1861.2	1860.5	1859.8	1859.2	1858.5	1857.8	1857.1	1856.4	1855.7
3600	1855.0	1854.3	1853.7	1853.0	1852.3	1851.6	1850.9	1850.2	1849.5	1848.8
3700	1848.2	1847.5	1846.8	1846.1	1845.4	1844.7	1844.1	1843.4	1842.7	1842.0
3800	1841.3	1840.6	1840.0	1839.3	1838.6	1837.9	1837.2	1836.5	1835.9	1835.2
3900	1834.5	1833.8	1833.1	1832.5	1831.8	1831.1	1830.4	1829.7	1829.1	1828.4

APPENDIX XII

IMPACT PRESSURE, CALIBRATED AIRSPEED

Impact Pressure - psf
q_c

Calibrated Airspeed-kn V_c	0	1	2	3	4	5	6	7	8	9
50	8.48	8.82	9.17	9.53	9.89	10.26	10.64	11.02	11.41	11.81
60	12.21	12.62	13.04	13.47	13.90	14.34	14.78	15.24	15.70	16.16
70	16.64	17.12	17.60	18.10	18.60	19.10	19.62	20.14	20.67	21.20
80	21.75	22.30	22.85	23.41	23.98	24.56	25.15	25.74	26.33	26.94
90	27.55	28.17	28.79	29.43	30.07	30.71	31.37	32.03	32.69	33.37
100	34.05	34.74	35.43	36.13	36.84	37.56	38.28	39.01	39.75	40.50
110	41.25	42.01	42.77	43.55	44.33	45.11	45.91	46.71	47.52	48.33
120	49.15	49.98	50.82	51.66	52.51	53.37	54.24	55.11	55.99	56.88
130	57.77	58.67	59.58	60.49	61.42	62.35	63.28	64.23	65.18	66.14
140	67.10	68.07	69.06	70.04	71.04	72.04	73.05	74.06	75.09	76.12
150	77.16	78.20	79.26	80.32	81.38	82.46	83.54	84.63	85.73	86.83
160	87.94	89.06	90.19	91.32	92.46	93.61	94.77	95.93	97.10	98.28
170	99.47	100.66	101.86	103.07	104.28	105.51	106.74	107.98	109.22	110.47
180	111.74	113.00	114.28	115.56	116.85	118.15	119.46	120.77	122.09	123.42
190	124.76	126.10	127.45	128.81	130.18	131.55	132.94	134.33	135.72	137.13
200	138.54	139.96	141.39	142.83	144.27	145.72	147.18	148.65	150.13	151.61
210	153.10	154.60	156.10	157.62	159.14	160.67	162.21	163.75	165.31	166.87
220	168.44	170.02	171.60	173.19	174.80	176.41	178.02	179.65	181.28	182.92
230	184.57	186.23	187.89	189.57	191.25	192.94	194.63	196.34	198.05	199.78
240	201.51	203.24	204.99	206.75	208.51	210.28	212.06	213.85	215.64	217.44

	0	1	2	3	4	5	6	7	8	9
250	219.26	221.08	222.91	224.74	226.59	228.44	230.30	232.17	234.05	235.94
260	237.84	239.74	241.65	243.57	245.50	247.44	249.38	251.34	253.30	255.27
270	257.25	259.24	261.24	263.24	265.26	267.28	269.31	271.35	273.40	275.46
280	277.53	279.60	281.68	283.78	285.88	287.99	290.10	292.23	294.37	296.51
290	298.66	300.83	303.00	305.18	307.37	309.56	311.77	313.99	316.21	318.44
300	320.69	322.94	325.20	327.47	329.74	332.03	334.33	336.63	338.95	341.27
310	343.60	345.94	348.30	350.66	353.02	355.40	357.79	360.19	362.59	365.01
320	367.43	369.87	372.31	374.76	377.22	379.70	382.18	384.67	387.17	389.67
330	392.19	394.72	397.26	399.80	402.36	404.93	407.50	410.09	412.68	415.28
340	417.90	420.52	423.15	425.80	428.45	431.11	433.78	436.46	439.16	441.86
350	444.57	447.29	450.02	452.76	455.51	458.27	461.04	463.82	466.61	469.41
360	472.22	475.04	477.87	480.71	483.56	486.42	489.29	492.17	495.06	497.96
370	500.87	503.79	506.72	509.66	512.61	515.57	518.55	521.53	524.52	527.53
380	530.54	533.56	536.60	539.64	542.70	545.76	548.84	551.93	555.02	558.13
390	561.25	564.38	567.52	570.67	573.83	577.00	580.18	583.38	586.58	589.80
400	593.02	596.26	599.51	602.76	606.03	609.31	612.60	615.91	619.22	622.54
410	625.88	629.22	632.58	635.95	639.33	642.72	646.12	649.53	652.96	656.39
420	659.84	663.30	666.77	670.25	673.74	677.24	680.76	684.28	687.82	691.37
430	694.93	698.50	702.09	705.68	709.29	712.91	716.54	720.18	723.83	727.50
440	731.17	734.86	738.56	742.27	746.00	749.73	753.48	757.24	761.01	764.80

	0	1	2	3	4	5	6	7	8	9
450	768.59	772.40	776.22	780.05	783.90	787.75	791.62	795.50	799.39	803.30
460	807.21	811.14	815.09	819.04	823.01	826.98	830.98	834.98	839.00	843.02
470	847.07	851.12	855.19	859.26	863.36	867.46	871.58	875.71	879.85	884.01
480	888.17	892.35	896.55	900.75	904.97	909.21	913.45	917.71	921.98	926.27
490	930.57	934.88	939.20	943.54	947.89	952.25	956.63	961.02	965.42	969.84
500	974.27	978.71	983.17	987.64	992.13	996.62	1001.13	1005.66	1010.20	1014.75
510	1019.32	1023.90	1028.49	1033.10	1037.72	1042.35	1047.00	1051.66	1056.34	1061.03
520	1065.74	1070.46	1075.19	1079.94	1084.70	1089.47	1094.26	1099.06	1103.88	1108.71
530	1113.56	1118.42	1123.30	1128.19	1133.09	1138.01	1142.94	1147.89	1152.85	1157.83
540	1162.82	1167.83	1172.85	1177.89	1182.94	1188.00	1193.08	1198.18	1203.29	1208.41
550	1213.55	1218.71	1223.88	1229.07	1234.27	1239.48	1244.71	1249.96	1255.22	1260.50
560	1265.79	1271.10	1276.42	1281.76	1287.11	1292.48	1297.87	1303.27	1308.69	1314.12
570	1319.57	1325.03	1330.51	1336.01	1341.52	1347.04	1352.59	1358.15	1363.72	1369.31
580	1374.92	1380.54	1386.18	1391.84	1397.51	1403.20	1408.90	1414.62	1420.36	1426.11
590	1431.88	1437.67	1443.47	1449.29	1455.13	1460.98	1466.85	1472.74	1478.64	1484.56
600	1490.50	1496.46	1502.43	1508.42	1514.42	1520.44	1526.48	1532.54	1538.61	1544.70
610	1550.81	1556.94	1563.08	1569.24	1575.42	1581.61	1587.82	1594.05	1600.30	1606.57
620	1612.85	1619.15	1625.47	1631.81	1638.16	1644.53	1650.92	1657.33	1663.76	1670.20
630	1676.66	1683.14	1689.64	1696.16	1702.69	1709.25	1715.82	1722.41	1729.02	1735.65
640	1742.29	1748.96	1755.64	1762.34	1769.06	1775.80	1782.56	1789.34	1796.13	1802.95

	0	1	2	3	4	5	6	7	8	9
650	1809.78	1816.63	1823.51	1830.40	1837.31	1844.24	1851.19	1858.15	1865.14	1872.15
660	1879.18	1886.21	1893.27	1900.36	1907.46	1914.59	1921.73	1928.89	1936.07	1943.28
670	1950.50	1957.74	1964.99	1972.27	1979.57	1986.88	1994.22	2001.57	2008.94	2016.33
680	2023.74	2031.17	2038.61	2046.08	2053.56	2061.06	2068.58	2076.12	2083.67	2091.25
690	2098.84	2106.45	2114.08	2121.72	2129.39	2137.07	2144.77	2152.49	2160.23	2167.98
700	2175.75	2183.54	2191.35	2199.17	2207.01	2214.87	2222.75	2230.64	2238.55	2246.48
710	2254.43	2262.39	2270.37	2278.37	2286.38	2294.42	2302.47	2310.53	2318.62	2326.72
720	2334.83	2342.97	2351.12	2359.29	2367.47	2375.67	2383.89	2392.13	2400.38	2408.65
730	2416.93	2425.24	2433.55	2441.89	2450.24	2458.61	2466.99	2475.39	2483.81	2492.25
740	2500.70	2509.16	2517.64	2526.14	2534.66	2543.19	2551.74	2560.30	2568.88	2577.48